Environmental Earth Sciences

Américo Iadran Torres
Verena Agustina Campodonico *Editors*

Environmental Assessment of Patagonia's Water Resources

Springer

Environmental Earth Sciences

Series Editor

James W. LaMoreaux, Tuscaloosa, AL, USA

Environmental Earth Sciences encompass mulitdisciplinary studies of the Earth's atmosphere, biosphere, hydrosphere, lithosphere and pedosphere and humanity's interaction with them. This book series aims to provide a forum for this diverse range of studies, reporting on the very latest results and documenting our emerging understanding of the Earth's system and our place in it. The type of material published traditionally includes:

- proceedings that are peer-reviewed and published in association with a conference;
- post-proceedings consisting of thoroughly revised final papers; and
- research monographs that may be based on individual research projects.

The Environmental Earth Sciences series also includes various other publications, including:

- tutorials or collections of lectures for advanced courses;
- contemporary surveys that offer an objective summary of a current topic of interest; and
- emerging areas of research directed at a broad community of practitioners.

More information about this series at https://link.springer.com/bookseries/8394

Américo Iadran Torres ·
Verena Agustina Campodonico
Editors

Environmental Assessment of Patagonia's Water Resources

Springer

Editors
Américo Iadran Torres
Centro para el Estudio de Sistemas Marinos
CCT-CONICET CENPAT
Puerto Madryn, Chubut, Argentina

Verena Agustina Campodonico
Centro de Investigaciones en Ciencias de la Tierra
CONICET. Universidad Nacional de Córdoba
Córdoba, Argentina

ISSN 2199-9155 ISSN 2199-9163 (electronic)
Environmental Earth Sciences
ISBN 978-3-030-89675-1 ISBN 978-3-030-89676-8 (eBook)
https://doi.org/10.1007/978-3-030-89676-8

This Springer imprint is published by the registered company Springer Nature Switzerland AG
The registered company address is: Gewerbestrasse 11, 6330 Cham, Switzerland

Foreword

Without considering Antarctica, Patagonia is the world's only continental territory south of ~38º S. The vast region, spanning over one million square kilometers shared between Argentina and Chile, constitutes the whole southern tip of South America, naturally split by its Andean backbone. Sparsely populated, about 90% of this remote region is Argentinean. It comprises the southern section of the Andes, with lakes, fjords, and glaciers in the west, and displays contrasting deserts, tablelands, and steppes to the east. Patagonia is bounded by the Atlantic Ocean to the east and the Pacific Ocean on the west, both connected by the Strait of Magellan, the Beagle Channel, and the Drake Passage to the south.

This was the geographical setting that twenty-four years-old Charles Robert Darwin found when he arrived in Patagonia, in 1833. Addressing Patagonia's nature unavoidably leads to his citing because he was the first full-fledged naturalist who explored the region, recorded detailed biological and geological observations, collected specimens and samples, and described the striking scenario displayed before his inquisitive eyes. Darwin had taken his degree in 1831 at Christ's College, Cambridge, and the same year embarked on a five-year voyage on the HMS *Beagle*, as a companion to the captain, twenty-eight years-old Robert FitzRoy. The main aim of the voyage was to chart the coast of Patagonia and Tierra del Fuego and to record a series of chronometric readings around the world.

Darwin's early comments conveyed the image that Patagonia's barren landscape produced on him: "Everywhere the landscape wears the same sterile aspect; a dry gravelly soil supports tufts of brown withered grass, and low scattered bushes, armed with thorns."[1] He was particularly disturbed by the almost incessant gales and the rough seas. Notwithstanding, the excitement that the voyage of the HMS *Beagle* unleashed in young Darwin is evident in the intense correspondence that he exchanged with his sisters Caroline, Susan, and Catherine, with his university professor, John Stevens Henslow, other members of the family, and friends. The letters are full of scientific and personal comments, and descriptions; a real portrait

[1] Darwin C (1989) Voyage of the *Beagle.* Penguin Books, London, 432 p.

of Darwin's probing into nature and evidence that the voyage of the HMS *Beagle* was a turning point in his life, the commencement of a new, fruitful existence.[2]

Environmental Assessment of Patagonia's Water Resources is a book which seeks to contribute, not only to the early Darwinian legacy but also to the rich heritage left by distinguished naturalists and travelers that also surveyed the region, like Francisco Pascasio Moreno—a prolific scientist and explorer—among others. This book, ably edited by Américo Iadran Torres and Verena Campodonico, focuses on Argentine Patagonia's freshwater resources, mainly from hydrological, geochemical, and biological perspectives.

The editors of this book have accomplished a significant undertaking, collating fourteen chapters that tackle a wide spectrum of topics and case studies, addressing varied subjects in the natural as well as in the human-impacted domains. Themes such as the geothermal effect on freshwater bodies, and the geochemical characteristics of weathering-limited denudation, are found hand-in-hand with riverine biogeochemical assessments and nutrient dynamics. Clearly, attention has been distributed among the control imposed by a changing climate on riverine hydrological features, as well as in the environmental assessment of human-made disturbances in Patagonia's freshwaters.

As the title implies, the book will be highly appreciated, not only by all readers interested in probing into the environmental characteristics of Patagonia's freshwaters, but also by those particularly concerned in researching the processes governing the critical zone in a singular environment, such as Patagonia, the land that genuinely amazed Charles Darwin for its aggressive beauty.

Córdoba, Argentina Pedro José Depetris
June 2021

[2] Burkhardt F (ed) The Beagle letters. Cambridge U Press, Cambridge, 470 p.

Introduction

Continental Patagonia (between 36° and 54° S) covers an area of about 700,000 km^2 in southern South America. This austral region includes the Argentine provinces of Neuquén, Río Negro, Chubut, Santa Cruz, and Tierra del Fuego's Island. Its northern boundary in Argentina is defined by the Colorado River, whose headwaters are located at the Andes. Climate in the region is controlled by westerlies dynamics that blow from the Pacific Ocean, discharging most of their moisture on the Andes ranges and continuing as dry winds toward the East. Thus, climate is classified as humid cold at the Andes and arid in the steppe. Rainfall is mainly concentrated between the late austral winter and the early spring, and it ranges from 2700 mm $year^{-1}$ at the boundary between Argentina and Chile to 500 mm $year^{-1}$ at the steppe. Mean annual temperature ranges from 8 °C at high latitudes (above 2000 m a.s.l.) to 20 °C at the valleys, whereas it varies between 7.5 °C and 12.5 °C at the steppe.

The southernmost tip of South America (i.e., south of ca. 40° S) supplies important amounts of aeolian and fluvial terrigenous material to the South Atlantic Ocean. Besides, rivers transport nutritional material to the marine coastal zone, which benefit biological communities, contributing to the preservation of marine ecosystems. In this sense, the Patagonian coastline is well known for its biological diversity. Important breeding sanctuaries for whales, and other large and small marine mammals, seabirds, innumerable species of fish and crustaceans can be found here.

Eight main river systems (from north to south: Colorado, Negro, Chubut, Deseado, Chico, Santa Cruz, Coyle, and Gallegos), with their headwaters mainly located in the Andes, drain this region, and their combined drainage areas account for about 30% of the total Patagonian territory. The remaining 70% corresponds to closed basins and ephemeral smaller coastal drainage. Glacial dynamics are predominant in the Patagonian Andes, and the abundant fjords and lakes that characterize this region are geomorphologic relicts of Pleistocene glaciations. These lakes and drainage networks were largely created by glacial erosion and glacial and postglacial sediment accumulation such as moraines. Most modern Patagonian proglacial lakes drain through rivers to the Atlantic Ocean, although there are some systems that drain to the Pacific, like the Manso River. During the Late Pleistocene and Holocene, frequent volcanic eruptions occurred in the Andean region. Particularly, a natural acidic geothermal

system was developed at the Caviahue-Copahue volcanic complex (38° S, 71° W). It is characterized by an acidic hot lake located on the active crater of the Copahue volcano, two acid hot springs that seep out from the eastern flank of the volcanic edifice and merge downstream to form the Agrio River, and several hydrothermal manifestations nearby the volcano. Another geothermal system developed in the northwest of Neuquén Province is the Domuyo system (36°44′ S, 70°21′ W), where high-temperature waters from ascending convective circulation of groundwater reach the surface. Boiling water is conveyed to the main drainage system (Varvarco River) through its tributaries.

Patagonia is known worldwide for its pristine environments and wildlife biodiversity. Unfortunately, in the last decades, anthropic activities have increased, affecting the quantity and quality of Patagonian water resources. For instance, dams were constructed in the Colorado, Negro, and Chubut rivers. Furthermore, the main pollution sources are domestic and industrial sewage effluents due to growing population, agricultural runoff, oil extraction and transportation, and metal wastes located near harbors. The Negro and, to a lesser extent, the Chubut and Colorado basins are extensively farmed under irrigation (mainly with fruits and vegetables production and vineyards), interspersed with livestock breeding. For instance, the use of pesticides in agricultural areas is another serious problem of water pollution in rivers from northern Patagonia. These land-use practices impact on the ecological integrity of aquatic systems, leading to the deterioration of water quality, eutrophication, sedimentation, and changes or loss of biodiversity, among other problems. Additionally, non-native species such as the salmonids *Oncorhynchus tshawytscha* and *Salmo trutta* (among others), the microalgae *Didymosphenia geminata* and the beaver *Castor Canadensis*, which were introduced by humans, are nowadays producing significant changes in the functioning of Patagonian aquatic ecosystems. Mining is less important, and coal extraction in the headwaters of the Gallegos River (Río Turbio) in Santa Cruz Province is the main activity.

This book compiles 14 novel studies developed in different aquatic environments from Patagonia, which were selected by the editors for their scientific quality and thematic importance for the region. These contributions were performed by a group of Argentine scientists who specialize in different disciplines and have also been working in Patagonian environments for many years. The manuscripts included in this book detail the recent advances on the knowledge of different Patagonian freshwater environments, including the analysis of their hydrology, hydrogeology, and hydrochemistry, the isotopic signature, their relationship with the geomorphology, and the impact of the increasing anthropic activities on these water resources.

Chapter "Effects of Multiple Stressors Associated with Land-Use Practices in the Percy-Corintos Basin (Northwest Chubut): An Ecological Assessment" is devoted to the ecological assessment of the Percy-Corintos basin (north-western Patagonia) which is subjected to multiple stressors associated with changes in land-use practices such as urbanization, deforestation, extensive and intensive livestock breeding, pasture conversion and horticulture. These activities are altering the water quality and biodiversity of the main watercourses and associated wetlands, thus

management and restoration actions are needed. Specific actions are presented and discussed in order to conserve these ecosystem services.

The hydrological, hydrochemical, and nutrient dynamics in the Manso River drainage system (north-western Patagonia) is addressed in Chapter "The Manso River Drainage System in the Northern Patagonian Andes: Hydrological, Hydrochemical and Nutrient Dynamics," The hydrochemical signature of the Manso River is determined by the dominating geochemical processes along the basin. The upper basin is highly influenced by the Manso Glacier dynamics, whereas in the middle and lower basins silicate hydrolysis is the dominant process. Historical discharge data of the Upper Manso River indicates a positive trend due to meltwater discharge, favoring the growth of the proglacial lake. The Manso River appears to be highly sensitive to climate change, which affects not only the hydrological characteristics but also the geochemical signature.

Chapter "Geothermal Influence on the Hydrochemistry of Surface Streams in Patagonia Neuquina" is dedicated to the analysis of the geothermal influence on the hydrochemistry of streams in north-western Patagonia (36°44′ S; 70°21′ W) in the Domuyo geothermal system. In this region, there are several streams that run through an area of intense geothermal activity composed by aqueous solutions of high temperature which determine their hydrochemistry. They constitute the main sources of water supply for the local inhabitants, so the monitoring of changes in water quality results relevant.

Chapter "Hydrogeochemistry of an Acid River and Lake Related to an Active Volcano. The Case of Study: Agrio River—Copahue Volcano in Patagonia, Argentina" is devoted to the analysis of the hydrogeochemistry of the acid river and lake related to the active Copahue volcano, known as Agrio River-Caviahue Lake system. A compilation of 275 published analyses of water geochemistry is used to describe and revise the processes that control it. Besides, processes such as the incorporation of As, Tl, and Pb into waters through magmatic gases, and the absortion/adsortion of As, V, Cr and rare earth elements in hydroxysulfates precipitates are described for the first time.

An exhaustive study of the Negro River is presented in Chapter "Negro River Environmental Assessment." This drainage system is subjected to an increasing environmental pressure due to industrial activities, intensive agriculture production, and urban settlements. Human activities have led to the introduction of several contaminants such as persistent organic pollutants, pesticides, and heavy metals. Furthermore, anthropic activities have induced changes in the aquatic macroinvertebrate assemblages of the Negro River, where water quality and invasive species appear to be main drivers of change.

The main hydrological and geochemical characteristics of the Chubut River are addressed in Chapter "Patagonia's Chubut River: Overview of the Main Hydrological and Geochemical Features." The statistical tests (i.e., seasonal Kendall trend test) indicate that the discharge of the Chubut River during the low-water months has been significantly decreasing during the last decades. Silicate hydrolysis and limestone dissolution are the processes ruling chemical weathering. The Chubut's drainage basin is subjected to a weathering-limited denudation regime. Thus, erosion produces

mineral debris scarcely weathered and the mass of dissolved phases exported to the ocean is moderate.

The hydrochemical characteristics of the Negro, Colorado, and Chubut rivers are presented in Chapter "Hydrochemical Characteristics of Mid-Low Sections of North Patagonia Rivers, Argentina." The hydrochemical characteristics of the northern Patagonia rivers are a consequence of the weathering of silicate volcanic rocks located at the headwaters in the Andes, but strongly modified and conditioned by processes occurring during runoff in the extra-Andean zone. The determination of the main ion sources and the controlling factors are relevant for the effective management of water resources in arid and semiarid regions like Patagonia.

Chapter "Hydrochemistry of Patagonian Wet Meadows (*Mallines*) Under Different Geological Frames" is devoted to the assessment of the hydrochemistry of four areas with wet meadows in different geological frames located within Extra-Andean Patagonia. The most part of the Extra-Andean Patagonia without permanent watercourses has small springs that give rise to wetlands known as mallines, which are of great environmental relevance due to the ecosystem services they provide. These wet meadows are sustained by groundwater; thus, their hydrochemical characteristics vary as a result of groundwater interaction with rocks and sediments.

Chapter "The Main Hydrological Features of Patagonia's Santa Cruz River: An Updated Assessment" presents an updated assessment of the main hydrological features of the Santa Cruz River. This river exhibits the second largest discharge in the region and an important runoff. The analyses of discharge series show a positive trend, and the months with increased discharge suggest that the augmented water volume is supplied by snow/ice melt determined by the current global climate change. A remote connection with El Niño Southern Oscillation is suggested, which possibly influences river discharge by promoting the ice-dam rupture mechanism that periodically operates in the Perito Moreno glacier.

The relationship between sediments and phosphorous as a proxy in the evaluation of water resources quality in eleven Patagonian lakes (between 33º and 48º S) with different characteristics and degrees of anthropic impact is addressed in Chapter "The Role of Sediments and Phosphorus in the Evaluation of Water Resources Quality in Patagonia." It is demonstrated that pH controls the phosphorous exchange between sediment and the water column in the analyzed lakes and that the use of sediment bioassays with native algae is a particularly useful tool for rapidly evaluating the anthropic impact on water bodies. This study highlights that sediment analysis should be included in monitoring programs as they allow obtaining information on, for example, contaminated and uncontaminated areas and distribution patterns of contaminants.

A detailed hydrological and biogeochemical assessment of the Gallegos River is presented in Chapter "A Hydrological and Biogeochemical Appraisal of Patagonia's Río Gallegos." The Gallegos River is the southernmost river of continental Patagonia of Argentina. The Gallegos stands out among the remaining Patagonian rivers for its connection with the Southern Annular Mode, and due to its biogeochemistry, which appears to be affected by groundwater and debris, both associated with the Eocene bituminous coal beds.

The main hydrolithological features of the northern region of Tierra del Fuego Province, determined by means of geoelectrical analyses is presented in Chapter "Vertical Electrical Sounding Applied to Hydrolithological Interpretations in the Fuegian Steppe, Argentina." A conceptual model based on the correlation between layers of a similar resistivity and geological formations that occur in the area is elaborated, which is expected to contribute with the understanding of the hydrogeological system. The lithological and climatic characteristics mainly condition the hydrolithological system, and thus, the exploitation of groundwater resources must be properly planned in order to grant its sustainability.

Chapter "Water Quality Assessment in Urban Watersheds of Tierra del Fuego: A Perspective from the Integrated Water Resources Management" is devoted to the assessment of water quality of five relevant urban watersheds from Tierra del Fuego Province, by means of the evaluation of physicochemical and microbiological parameters. Several problems associated with the high anthropic pressure (i.e., land-use change such as urbanization) that these natural resources are subjected to are evident. The headwaters of the studied watersheds remain of good quality, whereas downstream poor-regular water quality is registered. This highlights the need to implement an integrated management plan of water resources with an ecosystem approach in order to preserve the environmental and population health.

Finally, chapter "Disturbances in Freshwater Environments of Patagonia: A Review" presents a detailed review on several disturbances affecting freshwater environments of Patagonia (between 36º and 55º S). This Chapter includes the analysis of the effects related to volcanism, invasive species, climate change, and land-use/land-cover changes, through a revision of the knowledge, and the discussion of the suitability of ecosystems for their recovery. The aquatic environments reflect a good recovery response to severe disturbances of natural origin, whereas irreversible changes of human origin tend to increase on ecosystems that are still healthy.

We believe that there is still much to know about these aquatic environments of Patagonia. Fortunately, more and more scientists of different disciplines are putting their effort to advance in the knowledge and understanding of these environments and to evaluate the effects of anthropic activities in order to propose mitigation and remediation programs. This book shows the wide variety of aquatic environments and stressors present in this region of South America and the art of our knowledge about them.

The editors are deeply grateful to Dr. James W. LaMoreaux, who during the V Argentinean Meeting of Surface Geochemistry (V RAGSU, its acronym in Spanish) held in La Plata, Buenos Aires, in June 2019, provided us the opportunity and facilities to produce this book. Also, the editors would like to express their gratitude to Dr. Pedro José Depetris for his guiding and support during the early stages of this process and for writing the preface of this book. Finally, the editors are very grateful to the colleagues who reviewed the different chapters. They were Dr. Silvana Halac (CICTERRA CONICET—National University of Córdoba, Argentina), Dr. Eduardo Kruse (National University of La Plata,

CITNOBA, Argentina), Dr. Carolina Tanjal (CIG CONICET—National University of La Plata, Argentina), Dr. María Gabriela García (CICTERRA CONICET—National University of Córdoba, Argentina), Dr. Luis Felipe Hax Niencheski (Fundação Universidade do Rio Grande, Brazil), Dr. Alfonso Vázquez Botello (National Autonomous University of Mexico), Dr. Javier Sánchez España (Geological and Mining Institute of Spain), Dr. Agostina Chiodi (National Universidad of Salta, CONICET, Argentina), Dr. Karla Pozo (Masaryk University, Czech Republic), Dr. Didier Gastmans (Paulista State University, Brazil), Dr. Vinicius Tavares Kütter (Federal University of Pará, Brazil), Dr. Carla Spetter (IADO CONICET, National University of the South, Argentina), Dr. Jorge Martinez (CICTERRA CONICET—National University of Córdoba, Argentina), Dr. Mónica Blarasin (National University of Río Cuarto, Argentina), and Dr. Lucas Ruiz (IANIGLA CONICET Mendoza, Argentina).

Patagonia, Argentina
June 2021

Américo Iadran Torres
Verena Agustina Campodonico

Contents

Effects of Multiple Stressors Associated with Land-Use Practices in the Percy-Corintos Basin (Northwest Chubut): An Ecological Assessment 1
María Laura Miserendino, Emilio Williams-Subiza, Luz M. Manzo, Cristina N. Horak, Cecilia Brand, Yanina A. Assef, and Luis B. Epele

The Manso River Drainage System in the Northern Patagonian Andes: Hydrological, Hydrochemical and Nutrient Dynamics 27
Karina L. Lecomte, Andrea I. Pasquini, Laura D. Sepúlveda, Pedro Temporetti, Fernando Pedrozo, and Pedro J. Depetris

Geothermal Influence on the Hydrochemistry of Surface Streams in Patagonia Neuquina 57
Esteban Villalba, Lucía Santucci, Guido Borzi, Andrea I. Pasquini, Gerardo Páez, and Eleonora Carol

Hydrogeochemistry of an Acid River and Lake Related to an Active Volcano. The Case of Study: Agrio River—Copahue Volcano in Patagonia, Argentina 75
Joaquín Llano, María Clara Lamberti, Daniel Sierra, and Mariano Agusto

Negro River Environmental Assessment 95
Andres H. Arias, Pablo A. Macchi, Mariza Abrameto, Patricio Solimano, Nathalia Migueles, Fredy G. Rivas, Aimé I. Funes, Graciela Calabrese, Mariano Soricetti, Adela Bernardis, Romina B. Baggio, Yeny Labaut, and Jorge E. Marcovecchio

Patagonia's Chubut River: Overview of the Main Hydrological and Geochemical Features 127
Pedro. J. Depetris and Andrea I. Pasquini

Hydrochemical Characteristics of Mid-Low Sections of North Patagonia Rivers, Argentina 153
Camilo Vélez-Agudelo, Daniel E. Martínez, Orlando M. Quiroz-Londoño, and Marcela A. Espinosa

Hydrochemistry of Patagonian Wet Meadows (*Mallines*) Under Different Geological Frames 179
María del Pilar Alvarez, Eleonora Carol, María Paz Pasquale Pérez, Edoardo Melendi, and Esteban Villalba

The Main Hydrological Features of Patagonia's Santa Cruz River: An Updated Assessment 195
Andrea I. Pasquini, Nicolás J. Cosentino, and Pedro J. Depetris

The Role of Sediments and Phosphorus in the Evaluation of Water Resources Quality in Patagonia 211
Pedro Temporetti, Guadalupe Beamud, José León, Leandro Rotondo, Mayra Cuevas, and Fernando Pedrozo

A Hydrological and Biogeochemical Appraisal of Patagonia's Río Gallegos 241
Pedro J. Depetris, Diego M. Gaiero, and Nicolás J. Cosentino

Vertical Electrical Sounding Applied to Hydrolithological Interpretations in the Fuegian Steppe, Argentina 261
Candela Gorza, Claudio Lexow, Juan F. Ponce, Andrea Coronato, Ramiro López, and María Laura Villarreal

Water Quality Assessment in Urban Watersheds of Tierra del Fuego: A Perspective from the Integrated Water Resources Management 275
Soledad Diodato, Yamila Nohra, Gerardo Noir, Julio Escobar, Romina Mansilla, and Alicia Moretto

Disturbances in Freshwater Environments of Patagonia: A Review 305
Rodolfo Iturraspe

Glossary 339

Effects of Multiple Stressors Associated with Land-Use Practices in the Percy-Corintos Basin (Northwest Chubut): An Ecological Assessment

María Laura Miserendino, Emilio Williams-Subiza, Luz M. Manzo, Cristina N. Horak, Cecilia Brand, Yanina A. Assef, and Luis B. Epele

Abstract Freshwater ecosystems are highly interactive with the processes that occur in the surrounding basin. Any alteration of either aquatic or terrestrial ecosystems can potentially impact the structure, composition and functioning of aquatic communities. The Percy-Corintos Basin (northwestern Chubut Province) is subjected to multiple land-uses including urbanization, deforestation, extensive and intensive livestock breeding, pasture conversion, and horticulture. These local processes have had profound effects on a regional scale, altering the water quality and biodiversity of the main watercourses and associated wetlands. Livestock breeding and wood collection have resulted in an important loss of forest cover in the upper Percy basin, which has in turn accelerated erosion processes, causing sedimentation at the lower section of the basin. Urbanization has resulted in strong organic pollution, habitat impoverishment, and has decreased macroinvertebrate biodiversity in Esquel Stream. In pre-urban areas, constructed wetlands for flood prevention, act as novel environments which increase spatial heterogeneity, and consequently enhance macrophyte and aquatic invertebrate diversity. While urbanization in the lower Percy basin has a moderate effect on the river, agricultural activities like confined livestock breeding and horticulture are increasingly affecting the environmental and biological quality of the Corintos River. Management and restoration actions are urgently needed in order to restore the ecosystem functioning. The present study details and discusses specific actions to conserve biodiversity and ecosystem services.

Keywords Organic pollution · Erosion · Macroinvertebrates · Macrophytes · Running waters · Wetlands

M. L. Miserendino (✉) · E. Williams-Subiza · L. M. Manzo · C. N. Horak · C. Brand · Y. A. Assef · L. B. Epele
Centro de Investigación Esquel de Montaña y Estepa Patagónica (CIEMEP-CONICET-UNPSJB), Roca 780 Esquel, Chubut, Argentina
e-mail: lauram@unpata.edu.ar

FCNyCS-Universidad Nacional de la Patagonia San Juan Bosco, Esquel, 9200 Chubut, Argentina

A. I. Torres and V. A. Campodonico (eds.), *Environmental Assessment of Patagonia's Water Resources*, Environmental Earth Sciences,
https://doi.org/10.1007/978-3-030-89676-8_1

1 Introduction

The disturbance of natural systems due to anthropogenic intervention has resulted in important modifications of landscape-catchment characteristics in almost all regions of the world (Allan 2004; Sabater et al. 2009). Specifically, changes in land use and land cover are strong drivers of environmental change and affect the functioning of aquatic ecosystems (Feld et al. 2016). In the river catchments of northwestern Patagonia, deforestation, pasture conversion, livestock breeding, crop production, and urbanization have been the dominant human activities that modified land cover parameters (Bertiller and Bisigato 1998; Miserendino and Pizzolón 2004; Gaitán et al. 2014; Peri et al. 2016).

Land uses that involve the widespread removal of vegetation alter flow characteristics and change the amount of sediment introduced into aquatic systems, particularly during flood events (Buendía et al. 2014). Loss of the riparian forest cover also decreases stream shading, causing fluctuations in water temperature regimes. Other effects on watercourses are directly linked to processes occurring at terrestrial–aquatic interface, such as wood and debris supply. The latter play a role in structuring instream habitat, and thus the loss of these materials can alter the physical habitat characteristics, leading to profound effects on trophic webs (Richardson et al. 2012).

Streams draining areas subjected to extensive cattle breeding also show a significant alteration of water quality. Riparian areas are vulnerable to impacts from livestock grazing, which include banks erosion, increased sedimentation, burial of spawning gravels, loss of vegetation cover and increased water temperatures (Herbst et al. 2012; O'Sullivan et al. 2019). In addition, nutrient enrichment (via urine and manure depositions), decreases dissolved oxygen and increases algal growth frequently resulting in **eutrophication** processes (Le Moal et al. 2019). All these changes reduce the habitat of riparian plant species, cold-water fish, and wildlife, thereby causing many native species to decline in number or go locally extinct (Smiley et al. 2011; Hill et al. 2016). The presence of pathogens in water has also been associated with farming activities (Poma et al. 2012), and high levels of faecal bacteria have been recorded **downstream** animal production systems (McKergow et al. 2012; Collins et al. 2013). In turn, increased faecal coliform counts and organic matter habitually results in low dissolved oxygen (Rizzo et al. 2012).

One of the most extreme agents of landscape change is urbanization. According to Paul and Meyer (2008), the increase in impervious surface cover within catchments is the most consistent and pervasive effect resulting from urban settlement. It has been demonstrated that imperviousness strongly alters the hydrology and geomorphology of streams and rivers. The runoff from urbanized surfaces as well as municipal and industrial discharges can result in increased loading of nutrients, metals, pesticides, and other contaminants into streams. The latter includes emergent contaminants, defined as either newer substances or known contaminants which are not commonly monitored or regulated in the environment (e.g. active pharmaceutical ingredients, personal-care-product additives, nanomaterials and microplastics).

These have garnered attention because of their unexpected or unknown biological activity and/or stability in aquatic environments (Reid et al. 2018).

From a historical perspective, the territorial organization and development of the Patagonian region have at some point been unplanned, with overlapping land-use practices and unsustainable forest management (Carabelli and Scoz 2008), in addition to accelerated urbanization (INDEC 2010). At the basin scale, several scientific studies have assessed the impact of land-use practices on aquatic resources (Miserendino and Pizzolón 2004; Serra et al. 2013; Mauad et al. 2015) whereas other approaches included spatial regional analysis with multiple sites being visited once (Miserendino 2001). Most research conducted on a temporal basis has been limited to one-year analysis (Miserendino and Pizzolón 2003; Miserendino 2009; Brand and Miserendino 2015), whereas long-term studies are infrequent. The availability of historical data is very significant to managers and key decision makers to conduct programs of biomonitoring, since a long-term vision of catchment processes and anthropogenic impacts would allow more accurate mitigation and rehabilitation actions.

The two main urban settlements of western Chubut province are Esquel and Trevelin, both of which are located within the Percy-Corintos basin. Water resources are exploited for drinking water supply, agricultural irrigation and livestock breeding, extraction of gravel for construction, recreation (e.g. swimming, fishing), and they also provide non-material benefits such as cultural values and educational opportunities.

The present study discusses the environmental and ecological consequences of different land-use practices in the Percy-Corintos basin, which have been a topic of research during the last three decades. These anthropogenic actions impact the ecological integrity of aquatic resources that provide numerous ecosystems services (Miserendino et al. 2010). As mentioned, long-term data are crucial to provide a solid background of knowledge to help authorities and managers in the protection of aquatic environments. In view of the documented results, mitigation and rehabilitation measures are proposed in order to help to increase water quality and decrease the loss of biodiversity in these important aquatic ecosystems.

2 Study Area Description

The present study focuses on three river systems: the Esquel Stream, the Percy River, and a series of small tributaries of the Corintos River, all of which are part of the Futaleufú-Yelcho binational hydric system (north-western Patagonia). The Futaleufú-Yelcho system flows from western Argentina into the Pacific Ocean through Chile and has an area of 7345 km^2. The study area encompasses part of the meridional precipitation gradient observed along the Andes region, with precipitation values ranging from 2600 mm $year^{-1}$ on the border between Argentina and Chile to 530 mm $year^{-1}$ 85 km eastward (Fig. 1). The reason for the precipitation gradient east of the Andes is the mountain range itself, which affects regional-scale

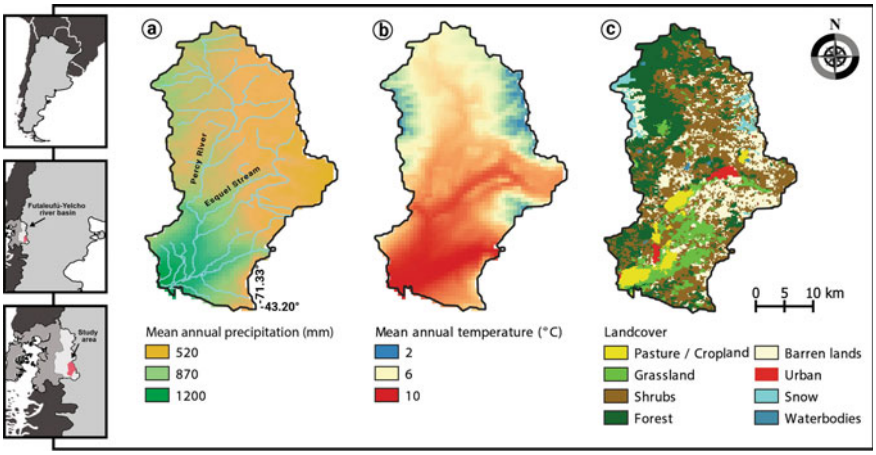

Fig. 1 Mean annual patterns of **a** Air temperature and **b** Rainfall and **c** Vegetation cover and land uses in the basin. Chubut Province, Argentina

climate by blocking the prevailing westerly winds. The orographic effect leads to precipitation occurring mostly along the western flanks of the Andes and decreasing eastwards (Insel et al. 2010).

Climatically, the region has been classified as temperate-cool; the mean annual temperature is 7 °C and precipitation occurs mainly from April to October, with snow falling in winter (June to September). Summers are dry and warm. Streams typically present two annual peak flows: one in autumn due to precipitation and another in spring due to snowmelt (Coronato and Del Valle 1988). Vegetation patterns vary mainly with precipitation. The study area is located in a transitional ecotone between the subantarctic forest and the Patagonian steppe. The subantarctic forest to the west is composed of, *Nothofagus dombeyi*, *N. antarctica*, *N. pumilio, Fitzroya cupressoides Drimys winteri*, *Ovidia andina*, and *Chusquea culeou*, among other species. To the east, the Patagonian steppe is characterized by xerophytic shrub-like species such as *Azorella prolifera* and *Colletia spinosissima* (Morello et al. 2012). Like most of the Patagonia region, the study area is sparsely populated. It encompasses only three settlements, of which the city of Esquel is the largest (population = 32,343 inhabitants).

2.1 Esquel Stream

The Esquel Stream is a third-order stream (discharge = 1.22 m^3 $s^{-1)}$ that has its origin approximately 1500 m a.s.l., on the south-eastern flank of the Esquel mountain range (Fig. 2). It flows down the side of the mountain, enters the city of Esquel, and flows through the 16 de Octubre Valley, finally joining the Percy River near the

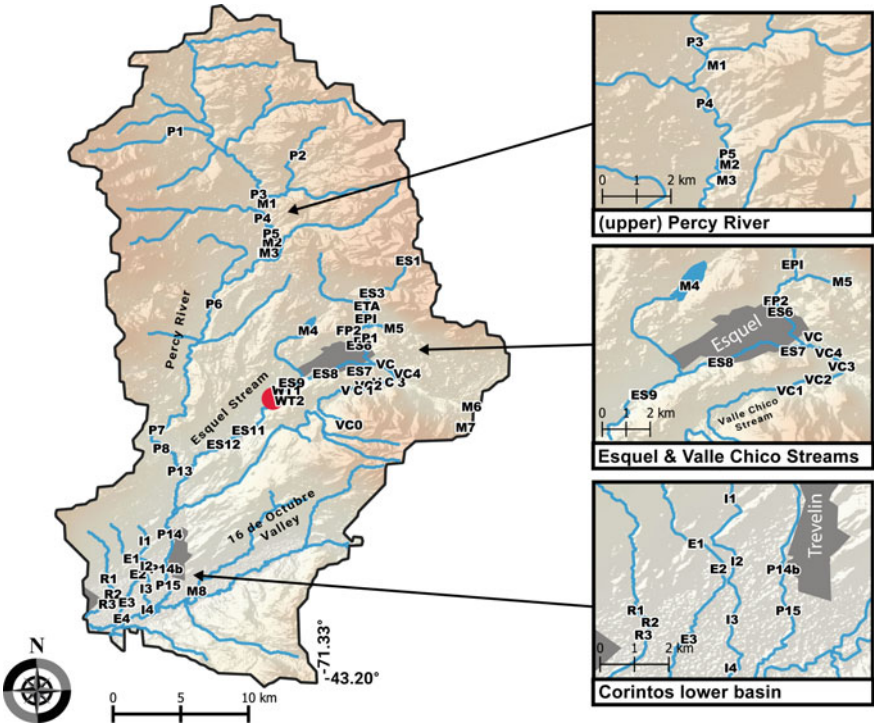

Fig. 2 Location of study sites in the Percy-Corintos system (Chubut Province, Patagonia, Argentina). P: Percy river, ES: Esquel stream, VC: Valle chico stream, E: Enna stream, R: Ruca stream, I: Ingram stream. M, FP and WT: wetlands. Grey areas: urbanizations. Red dot: Esquel waste water treatment plant. Codes and description of sites in Table 1

town of Trevelin (430 m a.s.l.). Volcanic igneous rocks compose the parental material and determine the chemical properties of running waters: circum-neutral pH, low conductivity, and low nutrient concentrations (Andrada de Palomera 2002). The Esquel Stream is fed by numerous small tributaries, among which the Valle Chico Stream is the most important in terms of discharge. It is also one of the most anthropically impacted, as it runs through rural and suburban areas. The Esquel Stream itself has also been subjected to several human disturbances and modifications. In 2008, a series of stabilization **ponds** were built **upstream** to the city with the goal of preventing the floods that affected some areas of Esquel. Around the same time, the middle portion of the Esquel Stream was channelized and straightened with concrete banks and beds. This channelization was extended during 2016 covering a total of 4000 m. These projects were successful in controlling floods, but have several negative effects that further aggravate other problems. For instance, the altered flow and sediment regime deposit thick layers of sediment in the channel bottom which need to be routinely removed with a hydraulic excavator.

2.2 Percy River

The Percy River is a fifth-order river (discharge = 11.99 m^3 s^{-1}) with a drainage basin of 1093 km^2. It originates on the western slopes of the Esquel mountain range (1100 m a.s.l.) and runs through the 16 de Octubre Valley as well as through the town of Trevelin, before joining the Corintos River at approximately 350 m a.s.l. Regional tectonic structures are characterized by grabens and horsts, originated by gravitational faults. They have a N-S direction and were reactivated by the Andean Orogeny. The Percy River flows partially along the bottom of a long tectonic graben. The oldest lithologies are marine and continental sedimentary rocks from the Carboniferous—Permian period (Cucchi 1980). In the upper catchment, the tributaries are comprised of small and medium-sized narrow courses, which are usually heavily shaded by *Nothofagus dombeyi* and *N. pumilio* trees. In contrast, the main channel which forms the middle and lower sections of the system has a width of 50 m and the riparian vegetation does not provide important shading. Below 700 m a.s.l., the river is flanked mostly by mixed and sparse riparian vegetation community, in which the exotic *Salix fragilis* is often present. Historically, the upper and middle sections of the basin have been used for extensive livestock production and wood fuel collection (Fig. 1). The occurrence of wildfires and pasture conversion has resulted in the loss of native vegetation cover and has hampered forest regeneration due to browsing and trampling. Other impacts include sedimentation, floodplain modification, and riparian clearing. In the lower basin, water is extracted from the river for irrigation through a network of small artificial channels. Dredging activities have resulted in bar and bank movements and riparian modification.

2.3 Corintos Lower Basin

The Corintos River has its headwaters southeast of the 16 de Octubre Valley and it is one of the main tributaries of the Rio Grande, the largest watercourse of the Futaleufú-Yelcho River basin. We will here discuss the three small tributaries of the Corintos River: the Enna, Ruca, and Ingram streams (0.8 to 0.73 m^3 s^{-1}). All three streams run through areas dedicated to livestock production, and present a degradation gradient which increases from the upper to the lower sections. The upper and middle reaches are generally affected by extensive livestock farms, some of which have mitigation measures (e.g. fenced enclosures). The lower reaches of the Ruca and Ingram streams are more heavily impacted, as they are located within confined animal production facilities where animals have free access to the stream all-year-round. In contrast, the lower Enna stream runs through a **wetland** area which supports livestock in a semi-intensive facility. The Ingram stream receives water from the Percy River through a man-made channel. This channel was constructed for irrigation purposes and is active mostly during the dry summer months.

3 Land Use Practices in the Catchment

3.1 Esquel Stream-Percy River System: Urbanization Effects

Understanding the impact of anthropogenic activities resulting from the urbanization of river catchments is an important challenge faced by resource managers. Authorities frequently demand scientific information in order to design remedial actions for aquatic resources. With this in mind, several studies have been conducted in the Esquel-Percy system, which have included extensive environmental and biological characterizations. Moreover, a considerable effort has been focused on obtaining tools for a rapid assessment, such as the macroinvertebrate-based biotic indexes that had been widely used in biological surveillance elsewhere (Rosenberg and Resh 1993; Barbour et al. 1999).

The physicochemical characteristic and the responses of **macrobenthic communities** to anthropogenic disturbances in the Esquel-Percy system have been previously assessed by Miserendino (1995) and Miserendino and Pizzolón (2000). The database included information on 14 sampling sites -along 51 km of the system– obtained from visits carried out on a monthly basis (November 1990 to October 1991) (Table 1, Fig. 2). These studies were conducted before the construction of the wastewater treatment plant (EWTP) in Esquel, whose population at that time was 23,000 inhabitants. Water quality variables were recorded along the system, and stream sections displayed strong pollution due to organic enrichment. Pizzolón and Miserendino (2001) identified a striking physicochemical gradient along the Esquel Stream and the Percy River that was likely explained by geomorphic, geochemical and anthropic factors. Headwater sites showed significantly lower water temperatures than the rest, which was associated with the marked altitudinal gradient occurring in the system (1000 m). A remarkable increase in conductivity (600%) was attributed to the particular ionic spectrum of the Willimanco Lake, whose composition is of the calcium-sulfate type instead of the more common calcium-bicarbonate type. Urbanization has a significant effect on the levels of several chemical compounds in the adjacencies of Esquel, with the maximum values recorded at site ES9, where untreated domestic sewage was discharged. Compared to pre-urban sites, the mean annual $\mathbf{BOD_5}$ at ES9, increased one order of magnitude, and the mean annual oxygen saturation decreased from 136 to 78% (Miserendino and Pizzolón 2000; Pizzolón and Miserendino 2001).

High levels of organic pollution explained most of the changes seen in the **macroinvertebrate community** in the middle reach of Esquel Stream. At sites receiving sewage discharges, the community was dominated by *Tubifex tubifex* and *Limnodrilus hoffmeisteri*, both of which are indicators of strong organic enrichment (Miserendino 1995). Nevertheless, stream self-depuration processes took place downstream of the sewage discharges and organic matter and oxygen values resembled those measured at pre-sewage discharges sites (e.g. ES12) (Pizzolón and Miserendino 2001). The macroinvertebrate community also displayed a recovery pattern, with species richness, diversity, and values of the biotic index (**BMPS**;

Table 1 Location, code and description of studied sites on the Percy-Corintos river basin, (Chubut Province, Patagonia, Argentina)

System	Site code	Type	Elevation m.a.s.l	Distance from the source km	Hydrology	Land use	Latitude	Longitude
Esquel stream	ES1	Stream	1444	0.91	P	Forest	−41.16296667	−70.7399611
	ES3	Stream	819	5.46	P	Forest/shrub	−41.14501389	−70.7103444
	ETA	Stream	729	7.31	P	Forest/shrub	−41.12393611	−70.7083222
	EPI	Stream	649	10.04	P	Forest/shrub	−41.10725278	−70.6981639
	ES6	Stream	610	11.23	SD	Forest/shrub	−41.10163611	−70.7002389
	VC	Stream	577	18.76	SD	Urban	−41.08216111	−70.7140306
	ES7	Stream	577	13.76	SD	Urban	−41.08202778	−70.7068556
	ES8	Stream	560	17.24	P	Urban	−41.07531667	−70.6726528
	ES9	Stream	540	21.72	P	Urban	−42.934916	−71.352461
	ES11[a]	Stream	497	26.62	P	Livestock	−41.02501944	−70.6031083
	ES12	Stream	465	30.68	P	Livestock	−42.98708333	−70.5457833
Percy river	P1	Stream	1021	7.27	P	Forest	−42.70547222	−71.4652778
	P2	River	900	6.01	P	Forest/shrub	−42.72744444	−71.3525
	P3	River	881	14.57	P	Forest/shrub	−42.76234722	−71.3891667
	P4	River	844	12.78	P	Forest/shrub	−42.783875	−71.3872222
	P5	River	839	21.74	P	Forest/shrub	−42.80238889	−71.3786111
	P6	River	719	32.37	P	Rural/urban	−42.86194444	−71.43
	P7	River	459	49.52	P	Forest	−42.97711111	−71.4825
	P8	River	459	52.18	P	Forest	−42.99258333	−71.4783333
	P13	River	433	56.35	P	Forest/shrub	−42.98053889	−70.5431194
	P14	River	387	63.26	P	Urban	−42.940125	−70.5271389

(continued)

Table 1 (continued)

System	Site code	Type	Elevation m.a.s.l	Distance from the source km	Hydrology	Land use	Latitude	Longitude
	P14b	River	368	65	P	Urban	−43.10325	−71.4747222
	P15[a]	River	358	69.28	P	Urban	−42.893475	−70.5255361
Corintos lower basin	I1	Stream	409	5.18	SD	Forest	−43.07781944	−71.4936111
	I2	Stream	366	8.698	SD	Horticulture	−43.10066111	−71.4927778
	I3	Stream	358	14.756	P	Livestock	−43.12125556	−71.4930556
	I4	Stream/Flood	351	23.35	P	Livestock	−43.13993611	−71.4925
	E1	Stream	395	7.1	P	Forest	−43.09275	−71.5005556
	E2	Stream	367	8.569	P	Horticulture	−43.10221111	−71.6619444
	E3	Stream	352	13.678	P	Livestock	−43.12830833	−71.5086111
	E4	Stream	342	21.54	P	Livestock	−43.14851667	−71.5152778
	R1	Stream	369	9.89	P	Forest	−43.11796944	−71.5275
	R2	Stream	354	10.57	P	Rural	−43.12230833	−71.5225
	R3	Stream	351	0.943	P	Livestock	−43.12455	−71.5227778
Valle Chico stream	VC0	Stream	768	10.23	P	Forest/shrub	−42.97780833	−71.3322222
	VC1	Stream	606	12.91	P	Rural	−42.93842222	−71.2944444
	VC2	Stream	588	16.33	P	Rural	−42.92822222	−71.2661111
	VC3	Stream	575	18.95	P	Urban	−42.93905556	−71.2791667
	VC4	Stream	575	19.6	P	Urban	−42.92663889	−71.2888889
Wetlands	M1	Pond	931	NA	T	Livestock	−42.77038889	−71.3825
	M2	Pond	847	NA	T	Livestock	−42.80568611	−71.3783333
	M3	Pond	829	NA	P	Livestock	−42.81128889	−71.3794444

(continued)

Table 1 (continued)

System	Site code	Type	Elevation m.a.s.l	Distance from the source km	Hydrology	Land use	Latitude	Longitude
	M4	Shallow lake	586	NA	P	Livestock	−42.88525	−71.3394
	M5	Shallow lake	704	NA	P	Livestock	−42.8879	−71.265
	M6	Pond	752	NA	T	Livestock	−42.961	−71.183
	M7	Pond	767	NA	T	Livestock	−42.977929	−71.17449
	M8	Pond	350	NA	T	Livestock	−43.123452	−71.447024
	FP1	Pond	634	NA	P	Flood attenuation	−42.89388889	−71.3016583
	FP2	Pond	629	NA	P	Flood attenuation	−42.89388889	−71.3016583
	WT1	Pond	537	NA	P	Waste water treat	−42.93944444	−71.3683639
	WT2	Pond	533	NA	P	Waste water treat	−42.93944444	−71.3683639

[a] Downstream effluent treatment plant. P: permanent, T: temporary, SD: summer disconnection, NA: not applicable

a measure of macroinvertebrate community that reflect water quality conditions), increasing from site ES9 to ES12 (Miserendino and Pizzolón 1999) (Table 2). Reports on bacterial counts indicated strong organic pollution at the urban and suburban sections of Esquel Stream and, to a lesser extent, at Trevelin (5000 inhabitants at the time of study).

According to Miserendino and Pizzolón (2000), the species composition, diversity, and density of macroinvertebrates in the Esquel-Percy system were mostly

Table 2 Average values (±SD) of taxa richness, diversity, and BMPS index, based on macroinvertebrate communities at 12 sites visited in a monthly basis (1991–1992) on the Esquel Stream and Percy River (Chubut Province, Patagonia)

Sampling sites	TAXA RICHNESS	DIVERSITY (Shannon Weaver H)	BMPS	Quality judgement
ES1	16.9 (2.2)	2.9 (0.5)	99.5 (14.6)	Non polluted waters
ES2	13.1 (2.3)	2.1 (0.5)	81.4 (20.4)	Probably incipient pollution or other kinds of perturbation
ES3	21.8 (3.2)	2.7 (0.3)	109.4 (24.8)	Non polluted waters
ES4	13.4 (3.1)	2.3 (0.6)	72.3 (16.6)	Probably incipient pollution or other kinds of perturbation
ES5	17.3 (3.3)	2.0 (0.6)	85.8 (16.4)	Probably incipient pollution or other kinds of perturbation
ES6	19.4 (4.1)	2.3 (0.5)	92.7 (29.8)	Probably incipient pollution or other kinds of perturbation
ES7	9.5 (2.2)	1.4 (0.3)	43.6 (18.7)	Probably pollution
ES8	13.0 (5.6)	1.6 (0.8)	53.1 (28.4)	Probably pollution
ES9	4.3 (1.5)	0.3 (0.3)	7.3 (12.2)	Strongly polluted
ES11	7.1 (3.3)	0.7 (0.6)	23.8 (25.1)	Polluted
ES12	13.5 (3.3)	2.3 (0.6)	64.4 (22.1)	Probably incipient pollution or other kinds of perturbation
P13	14.1 (4.0)	2.2 (0.5)	79.4 (19.9)	Probably incipient pollution or other kinds of perturbation
P14	17.0 (3.4)	1.9 (0.8)	80.9 (14.4)	Probably incipient pollution or other kinds of perturbation
P15	14.5 (3.5)	1.8 (0.8)	72.4 (12.3)	Probably incipient pollution or other kinds of perturbation

Adapted from Miserendino and Pizzolón (1999). Water quality judgement indicated on BMPS index. Code of sites in Table 1

explained by the topographic gradient, geochemical features (conductivity and total alkalinity) and anthropogenic factors (BOD_5 and oxygen saturation). Moreover, invertebrate communities also displayed differences which could be explained by a seasonal trend in climatic features.

After the construction of EWTP (Fig. 2), Miserendino et al. (2008) evaluated environmental variables, aquatic macroinvertebrate communities, as well as fish density and biomass at the pre-urban and post-urban reaches of the Esquel Stream. The study was conducted on a seasonal basis during 2005–2006 and water quality parameters were assessed including conductivity, major nutrients, total suspended solids (TSS) and dissolved oxygen. Among the main results, the authors found that nitrate and ammonium had significantly higher values at post-urban sites compared to reference sites. The maximum values of ammonium (271 $\mu g\ l^{-1}$) were coincident with summer, during the low water period. **Soluble reactive phosphorous (SRP)** was also significantly higher at ES11 than ES3. While fish density and biomass varied in a non-systematic manner, macroinvertebrate community displayed consistent responses to disturbance. At ES11, the pollution-intolerant taxa Plecoptera, Ephemeroptera, and Trichoptera were almost completely absent, total species richness was very low and the community was dominated by taxa tolerant to moderate organic pollution (*Hyalella* spp., *Helobdella* spp. and some Orthocladiinae), or to sedimentation (*Limnodrilus* spp.). Overall, assemblages were similar to those found before the construction of the EWTP (Miserendino 1995), when nutrients and a BOD_5 of 5.6 $mg\ l^{-1}$ indicated moderate pollution. None of the physicochemical and biological parameters assessed in the study suggested significant stream water recovery. Among the main factors explaining the poor ability of the EWTP to cope with the volume of waste produced were: the strong growth in population density (1992: 17,000 to 2006: 31,000 inhabitants) and a delay in the construction of the plant itself, resulting in an undersized facility. In addition, important increases in the impervious surfaces of the city most certainly contributed to runoff increased. Furthermore, it was also detected that the domestic sewage system was frequently flooded by stormwater, thus sewage and pluvial drainage systems were not always working as separate units.

In a later study, Assef et al. (2014) documented the deterioration in water quality downstream to the EWTP facilities (ES11). They found extreme values of total nitrogen (11,018.2 $\mu g\ l^{-1}$), ammonium (10,628.9 $\mu g\ l^{-1}$), and soluble reactive phosphorus (1,413.1 $\mu g\ l^{-1}$). In fact, the ammonium values found during the study in ES11 were 60 to 100 times higher than those previously reported by Miserendino et al. (2008) for the same season (Fig. 3). The impact of chlorination of domestic sewage (as part of the treatment process at the EWTP) on receiving surface waters (Esquel Stream) was investigated by García Sotillo (2011), who found that there was no evidence of significant trihalomethanes (THMs) formation. The obtained THMs values obtained were lower than permissible by national regulation for surfaces waters.

The Valle Chico Stream is one of the main tributaries of the Esquel Stream and runs through an area impacted by rural and urban land uses (Figs. 1c and 2). In addition, during several years the urban solids waste disposal plant of Esquel was settled in the middle area of the sub-catchment. The waste dump was shut down in 2009. In

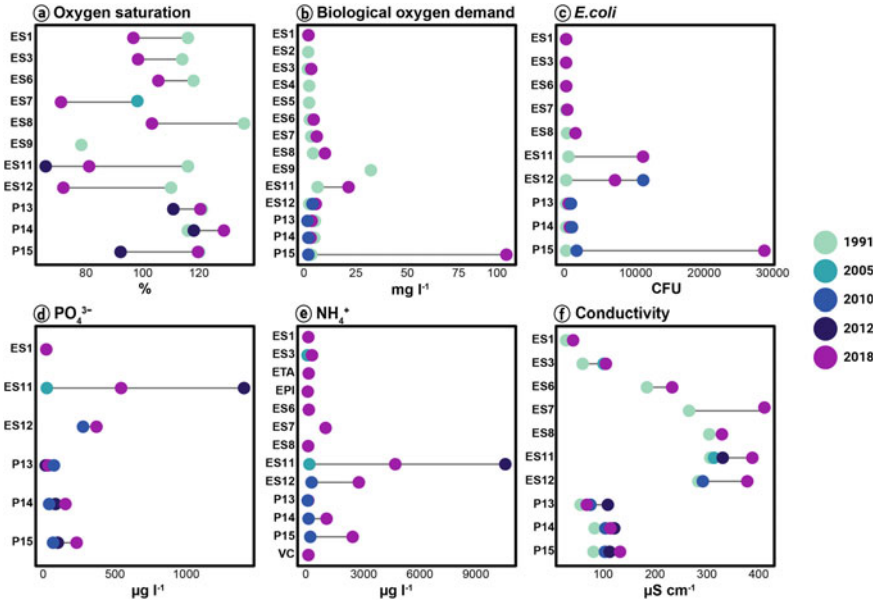

Fig. 3 Spatial and temporal patterns of environmental features at study sites in streams and rivers from the Percy-Corintos system (Chubut Province, Patagonia). Data from different studies conducted between 1991 and 2018 (see text). Code of sites in Table 1. Variables: **a** Oxygen saturation, **b** Biological oxygen demand, **c** Bacteria: *Escherichia coli*, **d** Soluble reactive phosphorous, **e** Ammonium and **f** Conductivity

a study conducted at five sites during high and low water periods, Manzo (2015) assessed the environmental changes and ecological responses of macroinvertebrates in the Valle Chico Stream (Table 1). The study reported changes in conductivity, alkalinity and turbidity at rural and urban sites, but trace metal levels were below the permissible values according to the recent normative (N° 25,051). Instead, levels of bacteria coliforms and BOD_5 exceeded critical values (EPA 2012 and DPN 2016). Several macroinvertebrate-based metrics indicated strong changes of water quality at urban sites. Bacteriological measures (*E. coli* and total coliforms) exceeded critical values during the low water period at sites affected by rural land-uses (DPN 2016). Other detected changes were due to channelization actions and dredging at pre-urban sites, resulting in increased water velocity and reduced habitat availability.

Nutrient and conductivity patterns through time can be seen in Fig. 3. More recent works (Williams-Subiza 2021) would indicate a general deterioration in water quality conditions at the urban (ES6, ES7 and ES8) and post-urban reaches (ES11 and ES12). In addition, the self-depuration processes downstream to the EWTP that were highlighted in earlier works by Pizzolón and Miserendino (2001) (see ES11-ES12 temporal sequence, Fig. 3) have been eroded, as accounted for in recent studies. Thus, in recent years, the high organic matter and nutrient loads released from treated

effluents into the Esquel Stream have negatively affected the natural purification of organic matter and nutrients.

Another important consequence of urbanization is the impact on the integrity of riparian stream corridors. Riparian ecosystems are crucial buffers of nutrients, sediments (erosion control), and materials that are transported into streams through runoff. Corridors are also an important factor in flood prevention, seed recruitment and provision of shelter; moreover, they play a role in increasing habitat heterogeneity and allochthonous input. Riparian areas are also key in maintaining and protecting aquatic biodiversity (Richardson et al. 2012). The extirpation of the riparian forest in the urbanized section of Esquel Stream occurred after channelization works, where different strata of vegetation (trees and shrubs) were replaced by concrete walls and riprapping structures. The replacement of the native *Nothofagus* species by the invasive *Salix* species (exotic) in the riparian forest at pre- and post-urban reaches has previously been documented by Miserendino (1995). Other works, through the use of the **QBRp** (**Index of Quality of Riparian Ecosystem for Patagonia**), also found a diminution in the quality of the riparian ecosystem (Miserendino et al. 2008; Kutschker et al. 2009). Furthermore, these studies detailed that the post-urban section in the Esquel Stream displayed poorly structured vegetation, with stream reaches being practically monopolized by the non-native *Salix fragilis.*

3.2 Lower Percy River: Sedimentation and Eutrophication Symptoms

The Percy River displays an ecological complexity that reflects the natural environmental gradient of elevation, temperature and precipitation; however, it is a watercourse affected by multiple anthropogenic impacts. In a study conducted in different sections of the Percy River, Miserendino et al. (2016) assessed the consequences of human pressures by using a set of environmental and biological measures. The study investigated physicochemical parameters, riparian ecosystem quality, habitat condition, riparian plants and macroinvertebrates at twelve sites along the Percy River's main channel (Fig. 1, Table 1). The main findings were that livestock and wood collection—the dominant activities in the upper and middle sections—have resulted in an important loss of forest cover. The authors also warned that if forest conversion continues to increase at current rates, the risk of soil erosion will increase to cover up to 28% of the total river basin. These results highlighted the vulnerability of the Percy **watershed**, and the potential ecological and economic implications of unsustainable land use. In the aforementioned scenario, the increase in the severity of fine sediment pulses could drastically impact macroinvertebrate survival. Compared to upper sites, nutrient levels in the lower Percy basin (P14, P14b, and P15) were several times higher; however, the impact on the macrobenthic community was not profound. Assemblages of sensitive Plecoptera (*Notoperlopsis femina*, *Antarctoperla michaelseni*, and *Potamoperla myrmidon*), Ephemeroptera (*Meridialaris laminata*,

Andesiops peruvianus and *A. torrens*) and Trichoptera (*Mastigoptila longicornuta*, *Cailloma pumida*, *Smicridea annulicornis* and *S. frequens*) species were still found at those urbanized sites. The most frequent changes in macroinvertebrate communities were the density increase of *Limnodrilus* sp. and *Glossiphoniidae* spp., which are taxa frequently associated with disturbed or polluted environments.

The main conclusion of Miserendino et al. (2016) was that the river had an adequate water flow, good levels of oxygen saturation, and available heterogeneous habitats given the present aquatic plants and algae. In addition, the impacts caused by the town of Trevelin were mostly local, and relatively small in comparison to the overall status of the watershed. Nevertheless, the authors recognized that the study was mostly focused on the spatial, rather than the temporal dimension, making these results of limited value. A study employing a temporal approach was carried out by Bauer (2010), who visited six sites on the lower Percy basin on a monthly basis (June 2009 to February 2010). The study examined 22 physicochemical and biological variables related to water quality. The author reported significant differences in terms of conductivity, nutrients, hardness, and alkalinity, with values being consistently higher at the outlet of Esquel Stream (P14, P15) into the Percy River (Figs. 2 and 3). Chlorophyll *a* and bacterial counts also increased at the same sites. In addition, treated effluents from Trevelin's wastewater treatment plant (TWTP), resulted in increased nutrient values. This study also indicated that the observed values of bacterial counts were higher than permissible for recreational use at the Percy River (P14b and P15). Values were particularly high during austral summer, coinciding with the low water period. Bauer (2010) also anticipated that some high nutrient values in rural areas were a consequence of livestock land use, with some forms of nitrogen and phosphorus probably having increased as a consequence of runoff during the wet period. Most nutrients increases resulted in high levels of periphyton at both rural and urban areas. This incipient eutrophication trend was also observed by Miserendino et al. (2016).

In a recent study (William-Subiza 2021), 13 sampling sites on the Esquel-Percy system previously studied by Miserendino (1995) were revisited. The survey was conducted on a seasonal basis during 2018 and revealed major deterioration in water quality at several sites, including those located on the lower Percy basin. Conductivity, BOD_5, PO_4^{-3}, NH_4^+ and bacterial counts (total coliforms) increased markedly at P14 and P15 compared to upper Percy basin sites. Mean values for these environmental variables were even higher than those reported by Bauer (2010) (Fig. 3). At P15, a site located downstream to the TWTP, the values of BOD_5 and bacteria reached 100 mg/l and 30,000 (CFU), respectively, indicating a malfunction in the treatment process of domestic effluent.

An evaluation of the status of the riparian corridor along 18 sampling sites at the main channel of the Percy River was conducted by Papazian (2009). According to QBRp scores, sites located at the lower Percy basin were the most affected. Scores ranged from 34.5 to 55 points and the judgment classes indicated poor quality in the riparian ecosystem. The quality reduction was attributed to the low complexity and loss of naturalness of the vegetation, poor structure and reduction in vegetation cover in the buffer zone. Other detected disturbances included anthropogenic intervention

on the channel and banks (dredging actions) at urbanized sites. As expected, the higher scores were documented in upper Percy basin sites (>82 points), where riparian ecosystems were well conserved or little disturbed.

3.3 *Effects of Agricultural Practices on the Corintos Lower Basin*

Following the trend in the intensification process of agricultural practices at the national level (Oesterheld 2008; Rizzo et al. 2012), semi-intensive or confined animal production systems are gaining a foothold in Patagonia. Due to demand and profitability increase, landowners have invested in infrastructure for food stocking (small grain silos, soft-silos, hay bales, etc.), and confined beef production systems are undoubtedly expanding (Iglesias et al. 2015). Different modalities of livestock feeding are been currently implemented in the lower Corintos basin (extensive cow-calf operations/finishing production systems). Meanwhile, governmental policies regarding protective measures for streams have been introduced in many regions, though the implementation of those regulations has been difficult (García et al. 2015). In Chubut Province, legislation regarding the waste management of agricultural production systems has recently been approved (DPNro/1540 Pcia. de Chubut 2016). This legislation defines and sets rules on the disposal of waste and manure, effluent treatment and the reuse of wastewater. However, it does not consider the implementation of off-stream watering systems and the restriction of livestock access to the watercourses (e.g. with electric fences) (Becerra and Antayhua 2017).

Horak et al. (2019) examined changes in water quality, **riparian integrity**, habitat conditions, and the macroinvertebrate community at three low order streams (Ruca, Enna and Ingram) that are tributaries of the Corintos River. The three streams had different modalities of animal production management. The sampling design included visits to 11 sites (including reference sites) on a bimonthly basis from July 2015 to April 2016 (Fig. 2, Table 1). They evaluated hydrological and physicochemical features, including oxygen, conductivity, nutrients (ammonium, nitrites plus nitrates and soluble reactive phosphorus), and TSS. In addition, epilithic chlorophyll *a* and bacteria (total coliforms and *E. coli*) were also measured.

According to the study, the most affected reaches were I4 and E4, which displayed increases in conductivity (twofold increase), and in soluble reactive phosphorus at E4 (twofold increase) (Fig. 4). At Ruca stream (R3), the animal operation did not result in substantial changes in most variables, although a marked increase in TSS (six-fold increase) was observed during austral summer (Fig. 4). Compared to other land uses, both intensive and semi-intensive confined animal production modalities had a low to moderate impact on oxygen, conductivity and nutrients. However, the recorded nutrient levels were markedly high compared with those reported for extensive livestock management at piedmont streams in the region (Miserendino et al. 2011), but similar to those documented at intensively grazed flooded wetland areas (Kutschker

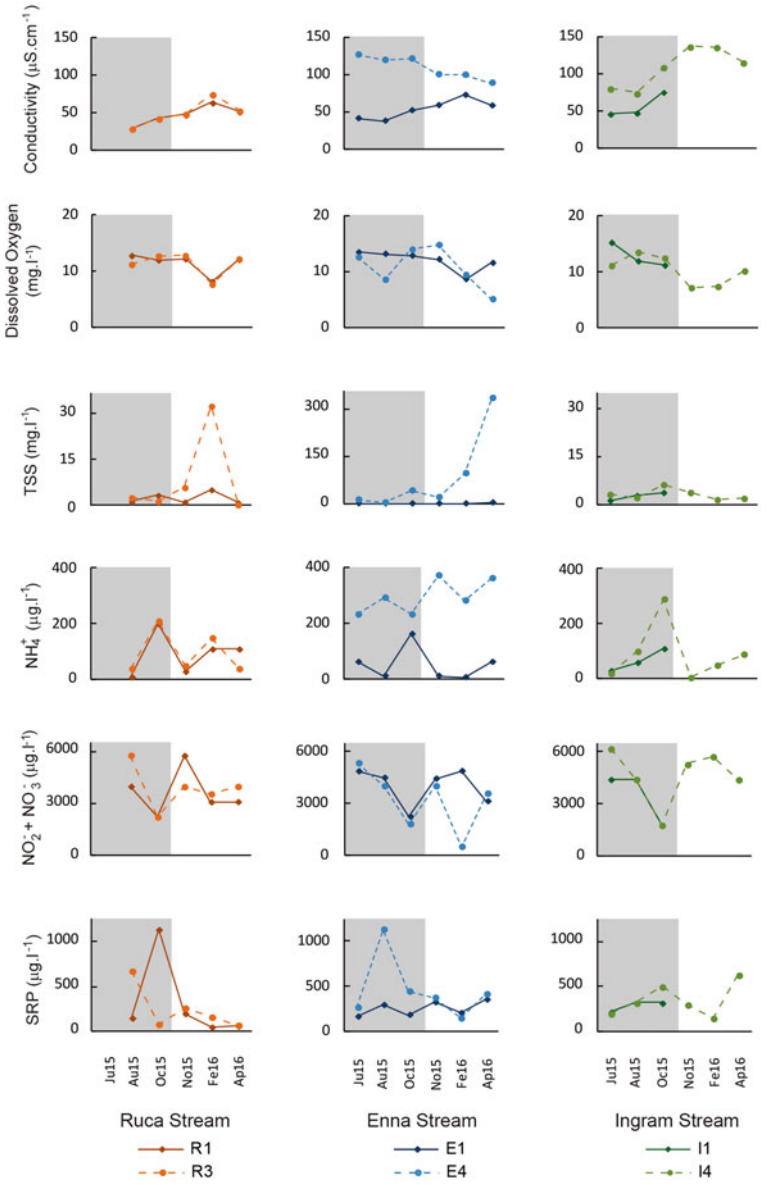

Fig. 4 Seasonal trend of environmental features at three tributaries of the low Corintos River (Chubut Province, Patagonia) during 2015–2016. Reference and disturbed sites at Ruca, Enna and Ingram streams. Code of sites, land use type in Table 1

et al. 2014; Epele and Miserendino 2015). Increases in organic matter and bacteria were also likely a result of livestock activity at Ingram and Enna impacted sites. The confined operation sites exceeded the recommended critical value for *E. coli* (320 CFU) according to the current normative for Chubut province (DPN°/1540 Pcia. de Chubut 2016; EPA 2012).

Regarding ammonium levels, extreme values occurred concurrently with livestock presence on the riverbanks, or during months in which stocking rates were at their highest (see E4, I4, Fig. 4). Livestock can significantly affect nutrient distribution, as animals tend to deposit more excreta in lounging areas near shade and water (Miller et al. 2010) and as observed in the study, when cattle access to the streams is unrestricted.

Using the same data, Horak et al. (2020), compared the composition of macroinvertebrate communities among sites (during high and low water periods) and established species-environmental relationships. They identified a gradient of disturbance defined by the variables: conductivity, oxygen, ammonium, soluble reactive phosphorus and bacteria, and species of macroinvertebrates were grouped accordingly. The paper also analyzed twelve metrics based on macroinvertebrate attributes and compared responses to environmental features. **EPT richness** (Ephemeroptera + Plecoptera + Trichoptera richness), number of insect families, density of tolerant taxa, abundance of collector-gatherers, and total invertebrate density all displayed significant responses to water quality changes. The overriding stressor explaining decreases of intolerant taxa (EPT) was ammonium.

The integrity of the studied reaches at Ruca, Enna and Ingram streams was also assessed using the QBRp and the **HA** (**habitat condition index**) (Horak et al. 2019). Confined animal operation modalities produced a significant impact on the riparian corridors, with most judgment classes from the QBRp index displaying strong riparian ecosystem alteration. Sites with extensive livestock breeding also showed lower QBRp scores, due to livestock foraging on grasses and herbaceous strata in the riparian corridor. Furthermore, the HA scores showed lower values at those stream reaches associated with confined animal operations. The most common habitat disturbances were those related to erosion processes and livestock trampling that in turn resulted in higher embeddedness, fine sediment deposition, and loss of channel sinuosity. At most impacted sites, the availability of epifaunal substrate was strongly reduced by the homogenization of the channel, the alteration in the riffle/pond sequence, and the monopolization of the substrate by one **macrophyte** species, among others.

3.4 Environmental and Ecological Functions of Wetlands in the Basin

Patagonian wetlands, colloquially known as "**mallines**", develop in association with particular conditions of the landscape where an unusual amount of water is available,

and are characterized by isolated small patches of hydrophytes included in a terrestrial matrix (Kandus et al. 2008). These azonal freshwater ecosystems provide the most productive soils for livestock breeding, a common land use at several mallines in the Percy-Corintos basin (Epele and Miserendino 2015).

The assessment of the basin's natural wetlands was incorporated as part of a different group of large-scale studies (Epele and Miserendino 2015; Epele et al. 2018, 2021), which included eight livestock-impacted ponds and shallow lakes (Table 1) that displayed particular characteristics regarding hydrological conditions and nutrient levels. Overall, those ponds exhibited medium nutrient values, limited by nitrogen, and a high (M5 and M6) or medium (M1-M4) regional priority for conservation (at a Patagonian scale).

Artificial or constructed wetlands (engineered ponds) are another component of the basin's aquatic environments. These were constructed for wastewater treatment (WT) and flood control (FP) in the Esquel urban area. A system of integrated wetlands (modules and ponds) was built in 1994 at the EWTP, in which domestic effluents and storm waters are processed before being discharged into Esquel Stream. Treated effluents are led towards two constructed ponds (sites WT1 and WT2; Fig. 2) for hydraulic retention. Flood prevention ponds were built in 2008, mainly to prevent the flooding that affected the lowland areas of Esquel (west part). Recently, Manzo et al. (2020) examined their water management function in the urban water cycle, analysed their role in enhancing local and regional biodiversity, and also assessed the functioning of the wastewater treatment plant. The authors found that the EWTP showed little success with regards to the processing of domestic effluent, with the nutrient values of treated effluents exceeding permissible standards for receiving surface waters in the region.

A comparison of the main environmental features of three types of ponds found in the basin (livestock, flood attenuation and wastewater treatments) is presented in Fig. 5. Wastewater treatment ponds displayed high values of soluble reactive phosphorus, nitrates plus nitrite and ammonium. An increasing conductivity gradient can be observed from flood attenuation ponds, to livestock ponds to wastewater treatment ponds. Oxygen levels were high at the flood attenuation ponds (both of which are connected to Esquel stream), and, as expected, values were lower at the wastewater treatment ponds. Invertebrate taxonomic richness per site exhibited a similar pattern, with the highest values recorded in FP ponds (mean of 29 taxa), followed by livestock wetlands (17 taxa), and WT (8 taxa). Livestock wetlands with 61 taxa, exhibited the highest taxonomic richness (Fig. 6), but included more sites than the FP (38 taxa) and WT sites (10 taxa). The EOT (Ephemeroptera, Odonata and Trichoptera) group dominated FP wetlands, whilst Chironomidae dominated livestock ponds. In contrast, WT ponds are dominated by *Psychoda* sp. and *Chironomus* sp., which are indicative of poor ecological conditions.

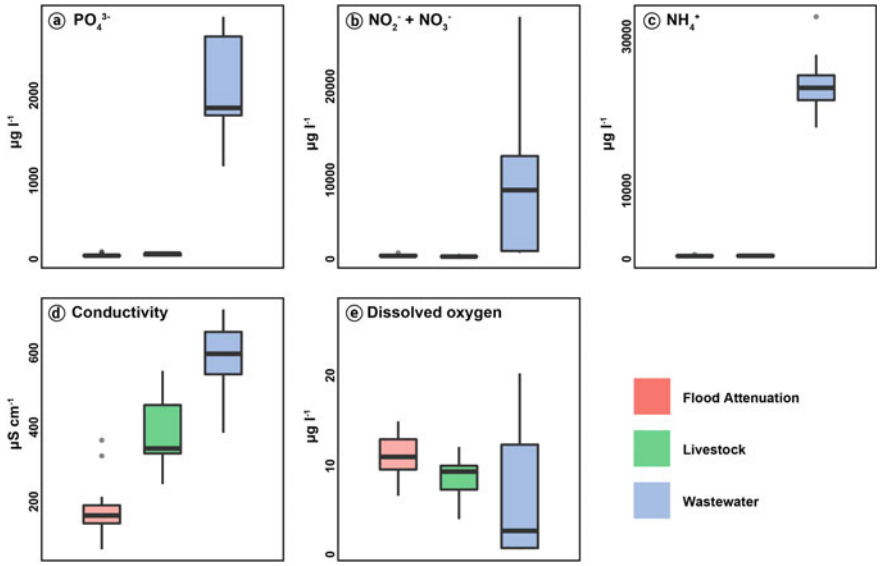

Fig. 5 Comparison of physicochemical features among three types of wetlands at Percy-Corintos system (Chubut Province, Patagonia) with different land uses: flood attenuation, livestock, and wastewater treatment ponds. **a** Soluble reactive phosphorus, **b** Nitrate, **c** Ammonium, **d** Conductivity, and **e** Dissolved oxygen (integrated data: 2016 and 2020)

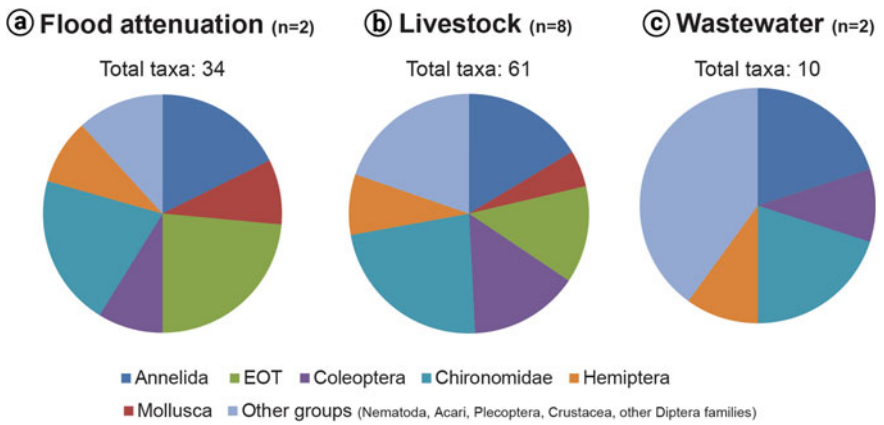

Fig. 6 Relative composition (Richness) of macroinvertebrates at three types of wetlands at the Percy-Corintos system (Chubut Province, Patagonia) with different land uses: **a** Flood attenuation, **b** Livestock, and **c** Wastewater treatment ponds (integrated data: 2016 and 2020)

3.5 *Water Quality and the Ecological Status of the Aquatic Systems in the Basin*

Worldwide experience has demonstrated that the most useful biological assessment methods for freshwater monitoring are based on **benthic macroinvertebrates** (Rosenberg and Resh 1993; Domínguez et al. 2020). Fortunately, these tools have previously been designed and adapted for Patagonian lotic environments. The BMPS **(Biotic Monitoring Patagonian Streams)** (Miserendino and Pizzolón 1999) is obtained from a table of 95 families of macroinvertebrates present in Patagonia which have different degrees of pollution sensitivity (scores 1–10). The total BMPS score ranges from 0 to > 150, with higher values corresponding to better water quality classes (see glossary). Another measure widely utilized in the area is the EPTr index.

In this biological assessment we compiled information from 36 sites in the Percy-Corintos system, using different studies conducted by Manzo (2015), Miserendino et al. (2016), Horak et al. (2019) and William-Subiza (2021) (Fig. 7). According to the BMPS biotic index and EPT richness scores, water quality conditions in the system varied from non-polluted to strongly polluted. As expected, analysis of the BMPS showed that only urban sites fall into the lower categories of water quality. This was the case at Esquel Stream's urban and post-urban reaches, Valle Chico Stream's urban sites, and in the reaches of the Percy River, nearby the town of Trevelin. The most affected reaches were ES11 to ES12 and VC3. This was coincident with higher values of nutrients, BOD_5 and bacteria counts.

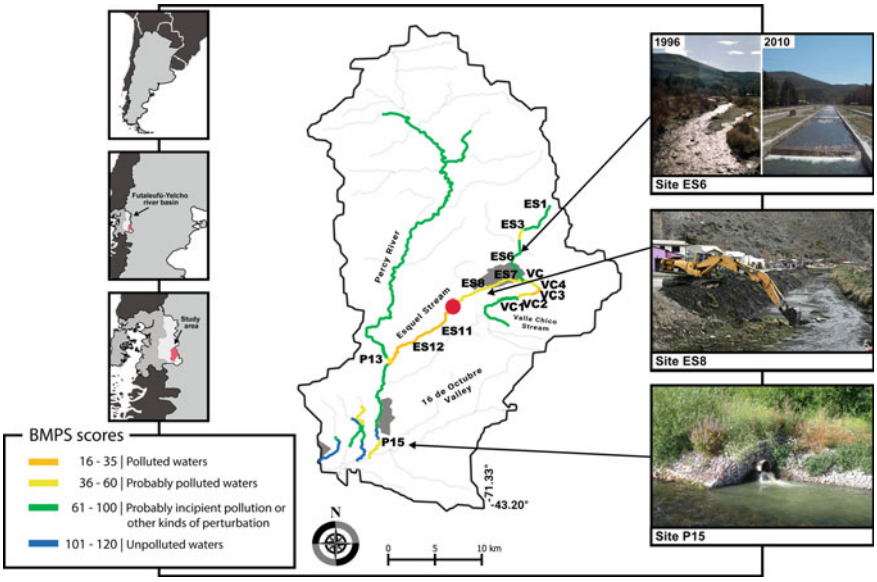

Fig. 7 Synthesis of water quality based on the BMPS scores. Pictures of the aquatic environments in the Percy-Corintos river system (integrated data: 2016 to 2020)

Several stream reaches were shown to be moderately impacted: at Esquel Stream (ES3, ES7, and ES8), Valle Chico Stream (VC, VC1, VC2 and VC4) and the Percy River (P13 and P15). Again, this corresponded to stretches associated mostly with urban sites.

A high number of sites in the Percy's upper basin, tributaries of the Corintos River, and some sections of Esquel stream (e.g. ES6) showed probable incipient pollution. It is possible that these results reflect some of the consequences of erosion, with evident symptoms of sedimentation in different stream segments. Nevertheless, in comparing these scores with those obtained by Miserendino and Pizzolón (1999), sites ES1 and ES3 showed lower judgment classes, indicating loss of macroinvertebrates sensitive species.

4 Mitigation Actions and Perspectives

Analyses in the present study have demonstrated an increased deterioration in water quality, eutrophication problems, sedimentation symptoms and the suppression of sensitive species or structural changes in biological communities, which have resulted in a progressive impact on the ecological integrity of the aquatic systems of the Percy-Corintos basin. Several stream and river segments appeared to be in worse environmental condition than those documented in earlier works. The riparian forest also changed in the middle and lower parts of the basin, where the replacement of the native *Nothofagus* with the exotic *Salix* species is rather striking. At present, several kilometers of the Esquel Stream are affected by channelization and realignment, and thus it lacks the natural sinuosity that mountain streams usually display. As a consequence of multiple land-use practices, the forest cover has been reduced. Other land-use practices, such as intensive livestock breeding, are taking place in the lower Corintos tributaries.

Given the current scenario, it is crucial that researchers help in the design of mitigation measures and recommendations to protect water resources and the numerous ecosystem services that they sustain. Government authorities, managers, and key decision-makers should have access to reliable information, in order to promote adequate measures for ecosystem rehabilitation (Domínguez et al. 2020).

Efforts for the restoration or mitigation of the ecological integrity of aquatic environments should be directed towards addressing the following issues:

(1) Erosion prevention: the protection of headwater forests and the restoration of altered riparian ecosystems. Territorial planning should be promoted and directed towards the conservation of certain areas, not only to protect the headwater forest, but also to regulate and supervise the practices allowed in the basin area. Resulting in moderate conservation of the forest which is currently mostly occupied by *N. antarctica.* It would be desirable to reestablish those native species which are missing from the riparian forest and bank vegetation, and to

maintain the connectivity of the corridors affected by fragmentation. Dredging should be avoided in river channels that results in excessive sedimentation.

(2) Control of water pollution and eutrophication: to adjust the functioning of wastewater treatment plants in order to reduce organic pollution and eutrophication processes. According to the current legislation, the EWTP is failing in nutrient load dissipation. It is crucial to find solutions for a better functioning of the wastewater treatment plant. Some feasible measures include: construction of new modules, enlargement of the primary treatment system, the completion of a water-storm network, and the reuse of treated effluents. Control of the eutrophication process in the lower part of the basin: these actions should involve the water authority commission from the adjacent urban centers, Esquel, (whose treated effluent flows into the Esquel Stream) and Trevelin. Both towns are experiencing an accelerated process of urban expansion.

(3) Reduction of the impact of agricultural practices: mitigation measures should be directed towards reducing livestock intrusion on streams, riparian areas, and wetlands. Riparian fencing and off-stream watering devices can be useful in mitigating these undesirable livestock impacts. The maintenance and restoration of buffer zones should be undertaken, and the application of fertilizers should be regulated. The creation of artificial wetlands can help to dissipate nutrients (urine and manure) from confined livestock developments. Riprap on water body shorelines and streams can safeguard against the impact of livestock trampling. Much of these tasks could be promoted through fiscal incentives to landowners that protect watercourses.

Acknowledgements This work has been funded by the PUE-0060/2017 CONICET, UNPSJB and PICT-2016/0180-ANPCYT, from Argentina. This is Scientific Contribution No. 163 from LIESA, CIEMEP.

References

Allan J (2004) Influence of land use and landscape setting on the ecological status of rivers. Limnética 23:187–198

Andrada de Palomera R (2002) Geomorfología del valle de Esquel y alrededores de las Lagunas Willimanco, Zeta y Carao, noroeste del Chubut. Actas del XV Congreso Geológico Argentino. El Calafate, Santa Cruz, Argentina (in Spanish)

Assef YA, Miserendino ML, Horak CN (2014) The multixenobiotic resistance mechanism in species of invertebrates associated to an urban stream in the patagonia mountain. Water Air Soil Pollut 225:1–13

Barbour MT, Gerritsen J, Snyder BD, Stribling JB (1999) Rapid bioassessment protocols for use in streams and wadeable rivers: periphyton, benthic macroinvertebrates, and fish. U.S. Environmental Protection Agency, Washington, DC

Bauer G (2010) Calidad del agua en el río Percy inferior en relación con las características naturales y de uso del suelo de la Cuenca. Tesis de grado. Facultad de Ciencias Naturales, sede Esquel, UNPSJB (in Spanish)

Becerra J, Antayhua MCC (2017) Plan Ganadero 2017–2021. Ministerio de la producción. Gobierno de la Provincia de Chubut (in Spanish)

Bertiller MB, Bisigato A (1998) Vegetation dynamics under grazing disturbance. the state-and-transition model for the Patagonian steppes. Ecol Austral 8:191–199

Brand C, Miserendino ML (2015) Testing the performance of macroinvertebrate metrics as indicators of changes in biodiversity after pasture conversion in Patagonian mountain streams. Water Air Soil Pollut 226:370

Buendia C, Gibbins CN, Vericat D, Batalla RJ (2014) Effects of flow and fine sediment dynamics on the turnover of stream invertebrate assemblages. Ecohydrology 7:105–1123

Carabelli F, Scoz R (2008) Human-Induced alterations in native forests of Patagonia, Argentina. In: Lafortezza R, Sanesi G, Chen J, Crow TR (eds) Patterns and processes in forest landscapes. Multiple use and sustainable management. Springer, Netherlands, pp 89–106

Collins KE, Doscher C, Rennie HG, Ross JG (2013) The effectiveness of riparian "restoration" on water quality-A case study of lowland streams in Canterbury, New Zealand. Restor Ecol 21:40–48

Coronato FR, Del Valle HF (1988) Caracterización hídrica de las cuencas hidrográficas de la provincia del Chubut. Cenpat-Conicet, Puerto Madryn (in Spanish)

DPN°, Decreto Provincial N°1540 (2016) Pcia de Chubut. Reglamentación Parcial de la Ley XI N° 35. Código Ambiental de la Provincia del Chubut. Disposición, N. 2010. Boletín Oficial, 19–21 (in Spanish)

Domínguez E, Giorgi A, Miserendino ML, Marchese M, Gómez N (2020) Problemáticas de cuencas en la Argentina. Recomendaciones para la gestión de cuencas. In: Domínguez E, Giorgi A, Gómez N (eds) La bioindicación en el monitoreo y evaluación de los sistemas fluviales de la Argentina: Bases para el análisis de la integridad ecológica (pp. 242–254). Eudeba, Buenos Aires (in Spanish)

EPA, Environmental Protection Agency (2012) Recreational water quality criteria. U. S. 1–69. 820-F-12-058

Epele LB, Grech MG, Manzo LM, Macchi P, Hermoso V, Miserendino ML et al (2021) Identifying high priority conservation areas for Patagonian wetlands biodiversity. Biodivers Conserv 30:1359–1374

Epele LB, Manzo LM, Grech MG, Macchi PA, Claverie AÑ, Lagomarsino L et al (2018) Disentangling natural and anthropogenic influences on Patagonian pond water quality. Sci Total Environ 613–614:866–876

Epele LB, Miserendino ML (2015) Environmental quality and aquatic invertebrate metrics relationships at patagonian wetlands subjected to livestock grazing pressures. PLoS ONE 10:1–19

Feld CK, Birk S, Eme D, Gerisc MH, Hering D, Kernan M et al (2016) Disentangling the effects of land use and geoclimatic factors on diversity in European freshwater ecosystems. Ecol Indic 60:71–83

Gaitán JJ, Oliva GE, Bran DE, Maestre FT, Aguiar MR, Jobbágy EG, Buono GG, Ferrante D, Nakamatsu VB, Ciari G, Salomone JM, Massara V (2014) Vegetation structure is as important as climate for explaining ecosystem function across Patagonian rangelands. J Ecol 102:1419–1428

García AR, Fleite SN, Ciapparelli I, Vázquez Pugliese D, Weigandt C, Fabrizio De Iorio A (2015) Observaciones, desafíos y oportunidades en el manejo de efluentes de feedlot en la provincia de Buenos Aires, Argentina. Ecol Austral 25:255–262 (in Spanish)

García Sotillo F (2011) Efectos de la cloración de efluentes cloacales tratados sobre la calidad del agua de ambientes lóticos naturales. Tesis de grado. Facultad de Ciencias Naturales, sede Esquel. UNPSJB (in Spanish)

Herbst DB, Bogan MT, Roll SK, Safford HD (2012) Effects of livestock exclusion on in-stream habitat and benthic invertebrate assemblages in montane streams. Freshw Biol 57:204–217

Hill MJ, Ryves DB, White JC, Wood PJ (2016) Macroinvertebrate diversity in urban and rural ponds: implications for freshwater biodiversity conservation. Biol Conserv 201:50–59

Horak CN, Assef YA, Grech MG, Miserendino ML (2020) Agricultural practices alter function and structure of macroinvertebrate communities in Patagonian piedmont streams. Hydrobiologia 847:3659–3676

Horak CA, Assef Y, Miserendino ML (2019) Assessing effects of confined animal production systems on water quality, ecological integrity, and macroinvertebrates at small piedmont streams (Patagonia, Argentina). Agric Water Manag 216:242–253

INDEC, Instituto Nacional de Estadísticas y Censos (2010) Censo Nacional de Población, Hogares y Viviendas 2010. https://www.indec.gob.ar/indec/web/Nivel4-CensoProvincia-999-999-26-035-2010. Accessed 01 March 2020 (in Spanish)

Iglesias R, Schorr A, Villa M, Vozzi A (2015) Situación actual y perspectiva de la ganadería en Patagonia sur. Centro Regional Patagonia Sur EEA Chubut, EEA Esquel y EEA Santa Cruz. INTA (in Spanish)

Insel N, Poulsen CJ, Ehlers TA (2010) Influence of the Andes mountains on South American moisture transport, convection, and precipitation. Clim Dyn 35(7–8):1477–1492

Kandus P, Minotti P, Malvárez AI (2008) Distribution of wetlands in Argentina estimated from soil charts. Acta Sci Biol Sci 30(4):403–409

Kutschker AM, Brand C, Miserendino ML (2009) Quality assessment of riparian corridors in streams of northwest Chubut affected by different land use. Ecol Austral 19:19–34

Kutschker AM, Epele LB, Miserendino ML (2014) Aquatic plant composition and environmental relationships in grazed Northwest Patagonian wetlands, Argentina. Ecol Eng 64:37–48

Le Moal M, Gascuel-Odoux C, Ménesguen A, Souchon Y, Étrillard C, Levain A et al (2019) Eutrophication: a new wine in an old bottle? Sci Total Environ 651:1–11

Manzo LM, Epele LB, Horak CN, Kutschker AM, Miserendino ML (2020) Engineered ponds as environmental and ecological solutions in the urban water cycle: a case study in Patagonia. Ecol Eng 154:105915

Manzo P (2015) Evaluación de la calidad del agua en el arroyo Valle Chico mediante el uso de bioindicadores y parámetros físico-químicos. Tesis de grado. Facultad de Ciencias Naturales, sede Esquel. UNPSJB (in Spanish)

Mauad M, Miserendino ML, Rizzo MA, Massaferro J (2015) Assessing the performance and the inter-annual variation of macroinvertebrate metrics in the Chalhuaco-Ñireco System (Northern Patagonia, Argentina). Iheringia, Série Zoologia

McKergow LA, Rutherford JC, Timpany GC (2012) Livestock-generated nitrogen exports from a pastoral wetland. J Environ Qual 41:1681

Miller J, Chanasyk D, Curtis T, Entz T, Willms W (2010) Influence of streambank fencing with a cattle crossing on riparian health and water quality of the Lower Little Bow river in Southern Alberta, Canada. Agric Water Manag 97:247–258

Miserendino ML (1995) Composición y distribución del macrozoobentos de un sistema lótico andino-patagónico. Ecol Austral 5:133–142 (in Spanish)

Miserendino ML (2001) Macroinvertebrate assemblages in Andean Patagonian rivers and streams: environmental relationships. Hydrobiologia 444:147–158

Miserendino ML (2009) Effects of flow regulation, basin characteristics and land-use on macroinvertebrate communities in a large arid Patagonian river. Biodivers Conserv 18:1921–1943

Miserendino ML, Brand C, Di Prinzio CY (2008) Assessing urban impacts on water quality, benthic communities and fish in streams of the Andes mountains, Patagonia (Argentina). Water Air Soil Pollut 194:91–110

Miserendino ML, Casaux R, Archangelsky M, Di Prinzio CY, Brand C, Kutschker AM (2011) Assessing land-use effects on water quality, in-stream habitat, riparian ecosystems and biodiversity in Patagonian northwest streams. Sci Total Environ 409:612–624

Miserendino ML, Epele LB, Brand C, Manzo LM (2020) Los indicadores biológicos en la patagonia. Calidad de agua e integridad ecológica: una mirada desde arroyos a mallines. In: Domínguez E, Giorgi A, Gómez N (eds) La bioindicación en el monitoreo y evaluación de los sistemas fluviales de la Argentina: bases para el análisis de la integridad ecológica. Eudeba, Buenos Aires (in Spanish), pp 148–155

Miserendino ML, Kutschker AM, Brand C, La Manna L, Di Prinzio C, Papazian G, Bava J (2016) Ecological status of a patagonian mountain river: usefulness of environmental and biotic metrics for rehabilitation assessment. Environ Manage 57:1166–1187

Miserendino ML, Pizzolón LA (1999) Rapid assessment of river water quality using macroinvertebrates: a family level biotic index for the Patagonic Andean zone. Acta Limnol Bras 11(2):137–148

Miserendino ML, Pizzolón LA (2000) Macroinvertebrates of a fluvial system in Patagonia: altitudinal zonation and functional structure. Arch Hydrobiol 150:55–83

Miserendino ML, Pizzolon LA (2003) Distribution of macroinvertebrate assemblages in the Azul-Quemquemtreu river basin, Patagonia, Argentina. N Z J Mar Freshwater Res 37:525–539

Miserendino ML, Pizzolón LA (2004) Interactive effects of basin features and land-use change on macroinvertebrate communities of headwater streams in the Patagonian Andes. River Res Appl 20:967–983

Morello J, Matteucci S, Rodriguez A, Silva M (2012) Ecorregiones y complejos ecosistémicos argentinos. Orientación Gráfica Editora, Buenos Aires (in Spanish)

Oesterheld M (2008) Impacto de la agricultura sobre los ecosistemas. Fundamentos ecológicos y problemas más relevantes. Ecol Austral 18:337–346 (in Spanish)

O'Sullivan M, Huallacháin DO, Antunes PO, Jennings E, Kelly-Quinn M (2019) The impacts of cattle access points on deposited sediment levels in headwater streams in Ireland. River Res Appl 35(2):146–158

Papazian G (2009) Evaluación de la calidad de los bosques de ribera en el Río Percy, Chubut (Argentina). Tesis de grado. Facultad de Ciencias Naturales, sede Esquel, UNPSJB (in Spanish)

Paul MJ, Meyer JL (2008) Stream in the Urban landscape. In: Marzluff JM et al (eds) Urban ecology. Springer, pp 207–231

Peri PL, Tejera L, Amico I, von Müller A, Martínez Pastur G, Bava J, et al (2016) Estado de situación del sector forestal en Patagonia Sur. Centro Regional Patagonia Sur, INTA (in Spanish)

Pizzolón L, Miserendino ML (2001) The performance of two regional biotic indices for running water quality in Northern Patagonian Andes. Acta Limnol Bras 13:11–27

Poma HR, Gutiérrez Cacciabue D, Garcé B, Gonzo EE, Rajal VB (2012) Towards a rational strategy for monitoring of microbiological quality of ambient waters. Sci Total Environ 433:98–109

Reid AJ, Carlson AK, Creed IF, Eliason EJ, Gell PA, Johnson PTJ et al (2018) Emerging threats and persistent conservation challenges for freshwater biodiversity. Biol Rev Camb Philos Soc 94(3):849–873

Richardson JS, Naiman RJ, Bisson PA (2012) How did fixed-width buffers become standard practice for protecting freshwaters and their riparian areas from forest harvest practices? Freshw Sci 31:232–238

Rizzo PF, Bres PA, Arreghini S, Crespo DE, Serafini RJM, de Iorio ARF (2012) Remediation of feedlot effluents using aquatic plants. Rev Fac Ciencias Agrar 44:47–64

Rosenberg DM, Resh VH (1993) Freshwater biomonitoring and benthic macroinvertebrates. Chapman Hall, New York

Sabater S, Donato JC, Giorgi A, Elosegi A (2009) El río como ecosistema. In: Elosegi A, Sabater S (eds) Conceptos y técnicas en ecología fluvial. Fundación BBVA, España (in Spanish), pp 23–37

Serra MN, Albariño R, Díaz Villanueva V (2013) Invasive *Salix fragilis* alters benthic invertebrate communities and litter decomposition in northern Patagonian streams. Hydrobiologia 701:173–188

Smiley PC, King KW, Fausey NR (2011) Influence of herbaceous riparian buffers on physical habitat, water chemistry, and stream communities within channelized agricultural headwater streams. Ecol Eng 37:1314–1323

Williams-Subiza E (2021) Efectos de la expansión urbana sobre la integridad ecológica de una cuenca patagónica: calidad del agua, hábitat y comunidades de macroinvertebrados. Tesis doctoral. UNPSJB. sede Esquel, Chubut (in Spanish)

The Manso River Drainage System in the Northern Patagonian Andes: Hydrological, Hydrochemical and Nutrient Dynamics

Karina L. Lecomte, Andrea I. Pasquini, Laura D. Sepúlveda, Pedro Temporetti, Fernando Pedrozo, and Pedro J. Depetris

Abstract The Manso River system is a mountainous basin fed by rain, snow and glacier meltwater from the Patagonian Andes. Glaciers located in the uppermost basin have shown a significant retreat though the last decades. Most of the annual precipitation occurs during austral winter and, together with meltwater, generates a bimodal annual hydrograph. Mean annual discharge increases from 12.5 m^3 s^{-1} in the upper basin, to ~80 m^3 s^{-1} in the lower basin. The historical discharge of the Manso Superior (i.e. Upper) River shows a significant positive trend due to meltwater discharge increase, generating the growth of the Proglacial lake. Lake Mascardi and the Manso Inferior (i.e. Lower) River show a negative statistical trend in their respective mean discharges. The hydrochemical signal of the Manso River is determined by dominating geochemical processes along the basin: the upper basin is highly influenced by the Manso Glacier dynamics, where pyrite oxidation generates sulfate-calcic waters, and it is responsible for the scavenging of phosphorous from the solution, causing a low soluble reactive phosphorous/total phosphorous ratio. The low N:P ratio indicates that nitrogen limits algal growth. In the middle and lower basin, the silicate hydrolysis is the dominant process, generating bicarbonate waters. The Manso River system appears to be highly sensitive to climate change, which is an attribute influencing both, the hydrological and geochemical signals.

K. L. Lecomte (✉) · A. I. Pasquini · L. D. Sepúlveda
Centro de Investigaciones en Ciencias de La Tierra. CONICET—Universidad Nacional de Córdoba, Av. Vélez Sarsfield, 1611, X5016CGA Córdoba, Argentina
e-mail: karina.lecomte@unc.edu.ar

K. L. Lecomte · A. I. Pasquini
Escuela de Geología, Facultad de Ciencias Exactas Físicas y Naturales, Universidad Nacional de Córdoba, Av. Vélez Sarsfield, 1611, X5016CGA Córdoba, Argentina

P. Temporetti · F. Pedrozo
Instituto de Investigaciones en Biodiversidad y Medioambiente, Universidad Nacional del Comahue—CONICET, Quintral 1250, 8400, San Carlos de Bariloche, Río Negro, Argentina

P. J. Depetris
Academia Nacional de Ciencias, Avenida Vélez Sarsfield 229–249, X5000WAA Córdoba, Argentina

A. I. Torres and V. A. Campodonico (eds.), *Environmental Assessment of Patagonia's Water Resources*, Environmental Earth Sciences,
https://doi.org/10.1007/978-3-030-89676-8_2

Keywords Patagonian hydrological systems · Glacial environment · Climate change · Biogeochemistry · Trend analysis · Dissolved trace elements

1 Introduction

Due to progressive melting and calving, glacial retreat is a process that is being documented worldwide (e.g. Hugonnet et al. 2021). Recent global calculations suggest that Andean glaciers are probably one of the highest contributors per unit area to sea level rise (e.g. Masiokas et al. 2020), and many scientific assessments have used the Andean ice mass loss as a clear indicator of climate change. Glacier retreat is currently mainly associated with global warming because there is an increasing glacial melting rate (since the second half of the twentieth century). Glaciers located in Argentina's Patagonian Andes, usually feed streams, rivers, groundwater and/or glacial/**proglacial lakes**. Increasing or decreasing meltwater discharge triggers modifications, which may be of varied nature (e.g. geochemical, Tranter 2003), in the riverine-proglacial lake system that is associated with receding glaciers.

The Manso River system is one of the mountainous river basins which has its **headwaters** in the eastern slope of the Patagonian Andes and is fed by snowmelt and glacier meltwater. Its singularity is that it flows to the Pacific Ocean on the western slopes of the Andes. This system is part of the southern Andes, particularly the Northern Patagonian Andes according to the glacio-climatological regions defined by Zalazar et al. (2020). In these latitudes, the Andes contain a wide variety of glaciers including permanent snowfields or **glacierets**, mountain glaciers, valley glaciers, and **icecaps**.

Focusing on different aspects, many contributions have looked into the Manso Glacier, Lake Mascardi, and Manso River area (e.g. Chillrud et al. 1994; Markert et al. 1997; Masiokas et al. 2008, 2010; Pasquini et al. 2008, 2013; Pedrozo et al. 1993; Pedrozo and Chillrud 1998; Rabassa et al. 1978, 1984; Rogora et al. 2008; Román-Ross et al. 2002; Ruiz et al. 2017; Worni et al. 2012). In this chapter, such glacial-proglacial area in Argentina's Northern Patagonian Andes is considered (Fig. 1), bringing forward aspects -mainly hydrological, hydrochemical and biogeochemical in nature- which may be related, directly or indirectly, to changes allocated to regional climate change. Particularly, Manso Glacier lost a volume of 0.085 ± 0.01 km^3 between the years 2000 and 2012 (Ruiz et al. 2017). In the present chapter, expanded information is used to analyze the hydrological response of a dying glacier, and an assessment on the hydrochemistry and nutrient dynamics is presented to complete the natural scenario.

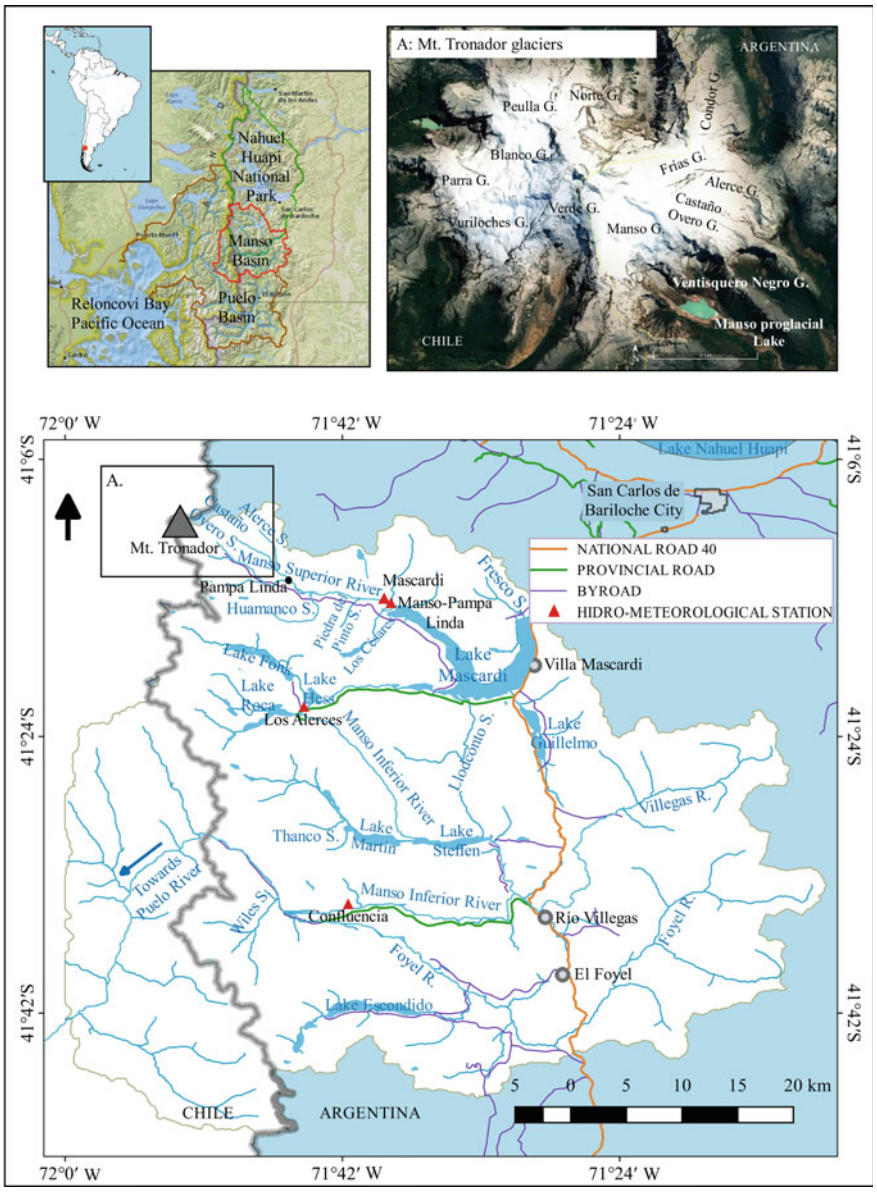

Fig. 1 Geographical location of the Manso River basin showing its main hydrographical features. Hydro-meteorological stations are also shown. Box A shows a detail of Mount Tronador glaciers

2 Geographical Framework

The Manso glacial and proglacial area, and the enclosing drainage basin (~2817 km^2) considered here are located in Argentina's Río Negro province, in Northern Patagonian Andes (Fig. 1). The area is an integral part of the Nahuel Huapi National Park, the oldest natural park and reserve in Argentina, established in 1934. Like many other similar Patagonian hydrological basins in the Andean region, the area was heavily glaciated during the Pleistocene; lakes and drainage basins were largely brought about by glacial erosion, moraines and other forms of glacial and post-glacial sediment accumulation. The region's highest peak is Mount Tronador (i.e. in the border between Argentina and Chile, with maximum elevation of 3554 m a.s.l.), which hosts four glaciers, which feed the Manso Superior River. The mountain's name (Tronador, Spanish for "thunderer") conveys the loud noise of ice and rock avalanches, and falling seracs that feed the glacier's lower level (Pasquini et al. 2013). Abundant rock debris in the Manso (Spanish for "tame") glacier's lower level conveys a dark aspect to the ice, giving birth to the name Ventisquero Negro (Spanish for "black snowdrift"), which is a debris covered glacier (Figs. 1 and 2a).

Masiokas et al. (2010) determined that the position of the glacial margin has varied relatively little between 1937 and 1991. However, during the next years a fast

Fig. 2 Photographs showing: **a** Panoramic view including Manso Glacier, Vestiquero Negro and the Manso proglacial Lake **b** View of the Manso Superior River near Pampa Linda; **c** Lake Mascardi **d** Manso Inferior Rriver downstream Lake Steffen

thinning and retreat of the glacial tongue was observed, resulting in the generation of a proglacial lake between the main moraine and the glacier margins. Glacier and snow meltwater (i.e. in spring and summer) and abundant wintertime precipitation give rise to the Castaño Overa and Alerce streams, which confluence with the Manso Superior River (Fig. 2b), and then flows into Lake Mascardi. Lower-order tributaries drain from both sides of the main valley with variable relief. A well-developed floodplain spreads **downstream**, reaching its mouth at Lake Mascardi.

Lake Mascardi (Fig. 2c) is a deep oligotrophic and **monomictic** lake with an area of ~39 km^2 and a mean depth of 218 m. In addition to the Manso Superior River it also receives Huamanco, Piedra del Pinto and Los Césares streams (from the S) and Fresco stream (from the N). Lake Guillelmo (850 m a.s.l. and 5.8 km^2) also drains to Lake Mascardi from the SE.

The river originating at the lake's outfall is named as Manso Inferior (i.e. Lower) River (Figs. 1 and 2d). It flows to the west crossing lakes Los Moscos and Hess (~1.5 km^2) and then its course swerves towards the SE and receives some tributaries before reaching Lake Steffen (~5.2 km^2, Fig. 1). The Manso Inferior River mean discharge increases significantly after leaving Lake Steffen and then its course turns westward. Before crossing the Andes, it is joined by the Villegas and Foyel rivers and towards the Puelo River, delivering its total discharge to the Pacific Ocean, at Chile's Reloncaví Bay.

In this chapter, the Manso's upper basin corresponds to Manso Superior River and its tributaries until Lake Mascardi. Downstream Lake Mascardi the river takes the name Manso Inferior River; this stretch is considered the middle basin until Lake Steffen. Finally, the **lower basin** is downstream Lake Steffen.

The geology of the region (e.g. Dalla Salda et al. 1991; Giacosa et al. 2001; González Bonorino 1979) involves three types of country rocks. (1) The meta-luminous granitoids of the Late Paleozoic-Tertiary forms the Cordilleran Patagonian Batholith. It is constituted by hornblendic and biotitic tonalites and granodiorites, amphibolitic granitic porphyries, andesitic dikes and tonalitic porphyries. (2) Breccias, andesitic lavas, hornfels, sandstones and conglomerates with limestones from the Cordilleran Volcanic Sedimentary Complex. (3) Thick Lower Tertiary volcanic sequence (Eocene–Oligocene), which constitutes the Tronador Formation. It is composed by olivine basalts, andesites, conglomerates and sandstones. Varves, tephras, and glacial-glaciofluvial deposits are widely disseminated throughout the region. Mount Tronador is a Miocene **stratovolcano** consisting of basaltic and basaltic andesite lavas and pyroclastic rocks.

Nahuel Huapi National Park's western half is covered profusely with temperate rain forests, whereas xerophytic Patagonian flora is dominant on the eastern half of the park. The dominant tree species in the park are *Nothofagus dombeyi* (cohiue), *Nothofagus pumilio* (lenga), and *Nothofagus antartica* (ñire). Also present is *Fitzroya cupressoides* or Patagonian larch, a slow-growing conifer. Other floras include *Luma apiculata* (arrayán) and *Austrocedrus chilensis* or Patagonian cedar (Brion et al. 1998).

3 Hydroclimatic Overview

The hydroclimatic characteristics, as well as the historical hydrological behavior of the Manso River system have been previously analyzed by Pasquini et al. (2008, 2013). A revisited analysis is presented here using updated information obtained from different hydro-meteorological stations located throughout the drainage basin.[1]

The mountainous climate in the region is cold and humid (Gallopin 1978; Villalba et al. 1990); the mean annual temperature near Lake Mascardi is 7.3 °C decreasing to the west along the valley, whereas the mean annual temperature for the entire drainage basin reaches about 12 °C. Mean annual temperatures of 17.4 °C and 3.8 °C have been recorded for January and July, respectively.

The hydrological behavior of the Manso River drainage system, as it happens in others glaciated Patagonian basins, is mainly governed by rainfall and snowfall regimes. The prevailing westerly winds supply all the moisture. Most of the annual precipitation in the region (i.e. rain and snow), occurs during the austral winter months and it is subjected to a marked west to east decreasing gradient. At Mount Tronador, the mean annual precipitation is 2700 mm, whereas at Lake Mascardi it reaches 1400 mm, decreasing progressively to the east up to 500 mm at the Patagonian steppe.

The updated data series (1991–2020 record period) recorded at Central Frey station (at Lake Mascardi, 41° 21′ 28.6″ S, 71° 33′ 46″ W), clearly shows a steep precipitation increase during the austral fall and winter (maximum mean precipitation in June), gradually decreasing until reaching minimum values during the austral summer (Fig. 3).

The mean annual hydrograph of the Manso Superior River (Fig. 4a) was arranged using an updated data series reconstructed correlating discharges at Mascardi station (41°15′ 03″S, 71°39′ 58″W, 1970–1991 record period) with gauge heights at Pampa Linda station (41° 15′ 18.60″S, 71° 39′ 07.10″W). The obtained data series (1970–2019) will be referred to as Mascardi station from now on. Manso Superior River shows a clear bimodal distribution in its monthly mean discharge (Fig. 4a) as a consequence of both, precipitation in winter and snowmelt during spring. Maximum mean discharge is registered in June, in coincidence with maximum precipitation, whereas the snowmelt signal is clearly discernible in November and December. The Manso River mean annual discharge at Mascardi station is 12.5 $m^3\ s^{-1}$, while the annual specific water yield is of 50.6 $L\ s^{-1}\ km^{-2}$. Mean annual discharge shows an increase compared with the 11 $m^3\ s^{-1}$ reported by Pasquini et al. (2013), when the last two decades of record are considered. The Manso River delivers at Mascardi station an annual water volume of 394 hm^3, with an annual mean runoff of 15 mm.

Downstream Lake Mascardi, the Manso Inferior River also receives water that flows from a number of lakes and streams located in the middle basin, which increase

[1] Dirección Nacional de Política Hídrica y Coordinación Federal, Sistema Nacional de Información Hídrica, Argentina, https://www.argentina.gob.ar/obras-publicas/hidricas/base-de-datos-hidrologica-integrada.

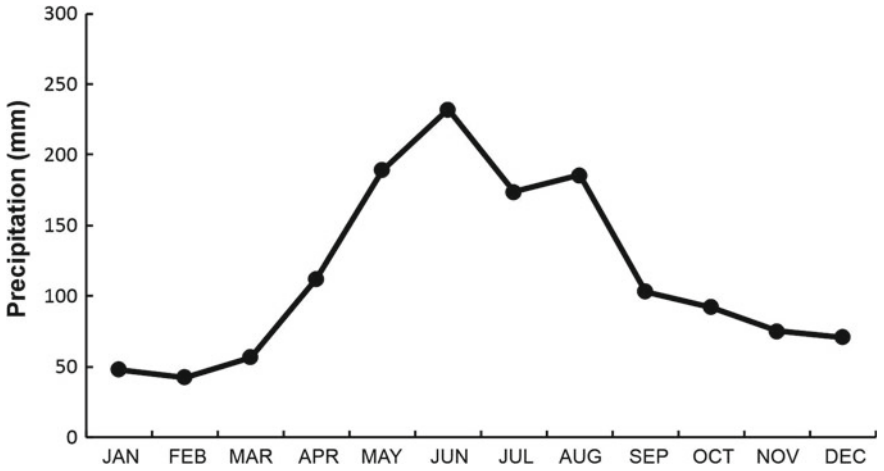

Fig. 3 Mean annual pluviograph at Lake Mascardi (Central Frey station) for the record period 1991–2020

its discharge considerably. At Los Alerces station (41°22′ 29″ S, 71° 44′ 53″ W, 1951–2020 record period), located downstream Lake Hess (Fig. 1), the Manso Inferior River discharges a mean annual flow of 43.6 $m^3\ s^{-1}$, with an annual specific water yield of 58.1 $L\ s^{-1}\ km^{-2}$. At this place the annual water volume supplied by the river is 1374 hm^3, whereas the annual mean runoff is 1832 mm. The annual mean hydrograph at Los Alerces (Fig. 4b) exhibits a bimodal pattern similar to the one recorded at Mascardi (i.e. in the upper basin), with maximum mean discharge occurring in July and November and minimum in March and April.

The Confluencia station (41°35′ 12.60″S–71°41′ 01.20″W, 1965–2020 record period) is located at the Manso River lower basin (i.e. downstream Lake Steffen). Here, the river also exhibits a considerable increase in its mean discharge resulting from the contribution of several lakes and streams that, in addition to the Manso River, also drain into Lake Steffen (e.g. Lake Martín and tributaries). The mean annual discharge at Confluencia is 79.3 $m^3\ s^{-1}$, whereas the specific water yield is 43.7 $L\ s^{-1}\ km^{-2}$. The annual water volume exported at Confluencia is 2500 hm^3, with an annual mean runoff of 1374 mm. Figure 4c shows the annual mean hydrograph at Confluencia, which also reflects a bimodal distribution in the annual flow variability, as it was observed **upstream**, although with a smoother pattern.

An analysis of the historical hydroclimatic variability in the Manso River system, using the updated time series, was performed by means of statistical trends analyses. The longest instrumental record of precipitation in the Manso River basin corresponds to the Los Alerces station (record period 1955–2019). Figure 5a shows the result of the Mann–Kendall trend test (Mann 1945; Kendall 1975) at Los Alerces, where a highly significant Sen's negative slope ($p < 0.001$) indicates an historical decrease in precipitation, which has also been pointed out earlier by other authors (e.g. Masiokas et al. 2008; Pasquini et al. 2008; and references therein). The linear trend in Fig. 5a

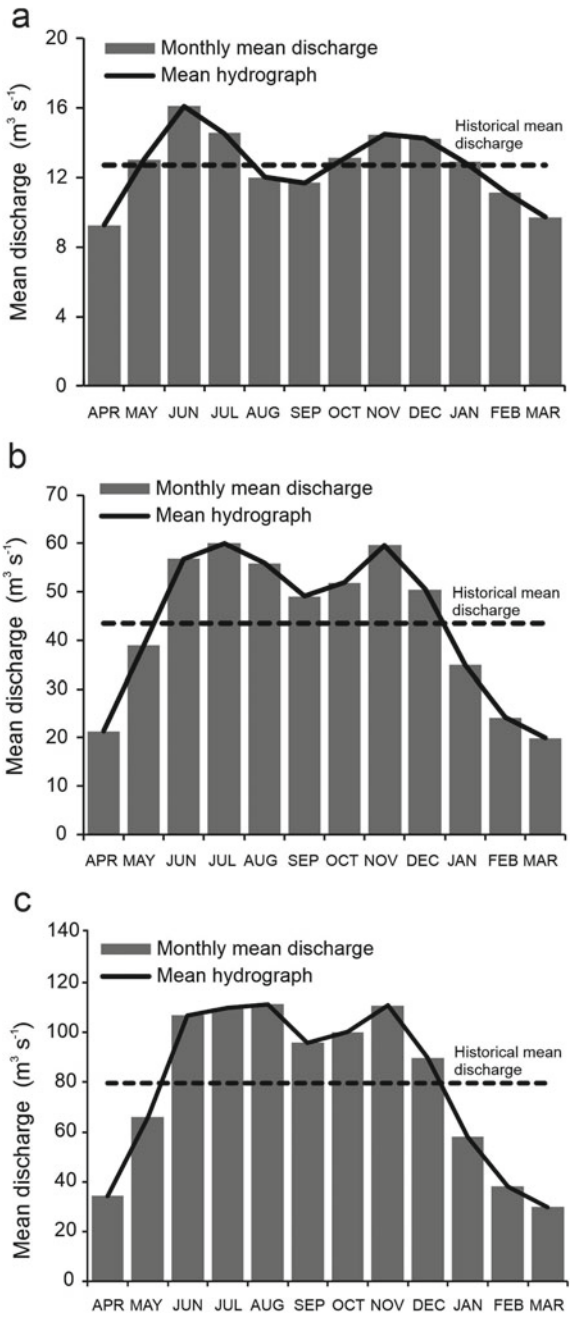

Fig. 4 **a** Mean annual hydrograph of the Manso Superior River at Mascardi station (1970–2020 record period, see text for explanation). **b** Idem for the Manso Inferior River at Los Alerces station (1951–2020 record period) in the middle basin. **c** Idem for the Manso Inferior River in the lower basin, at Confluencia station (1965–2020 record period)

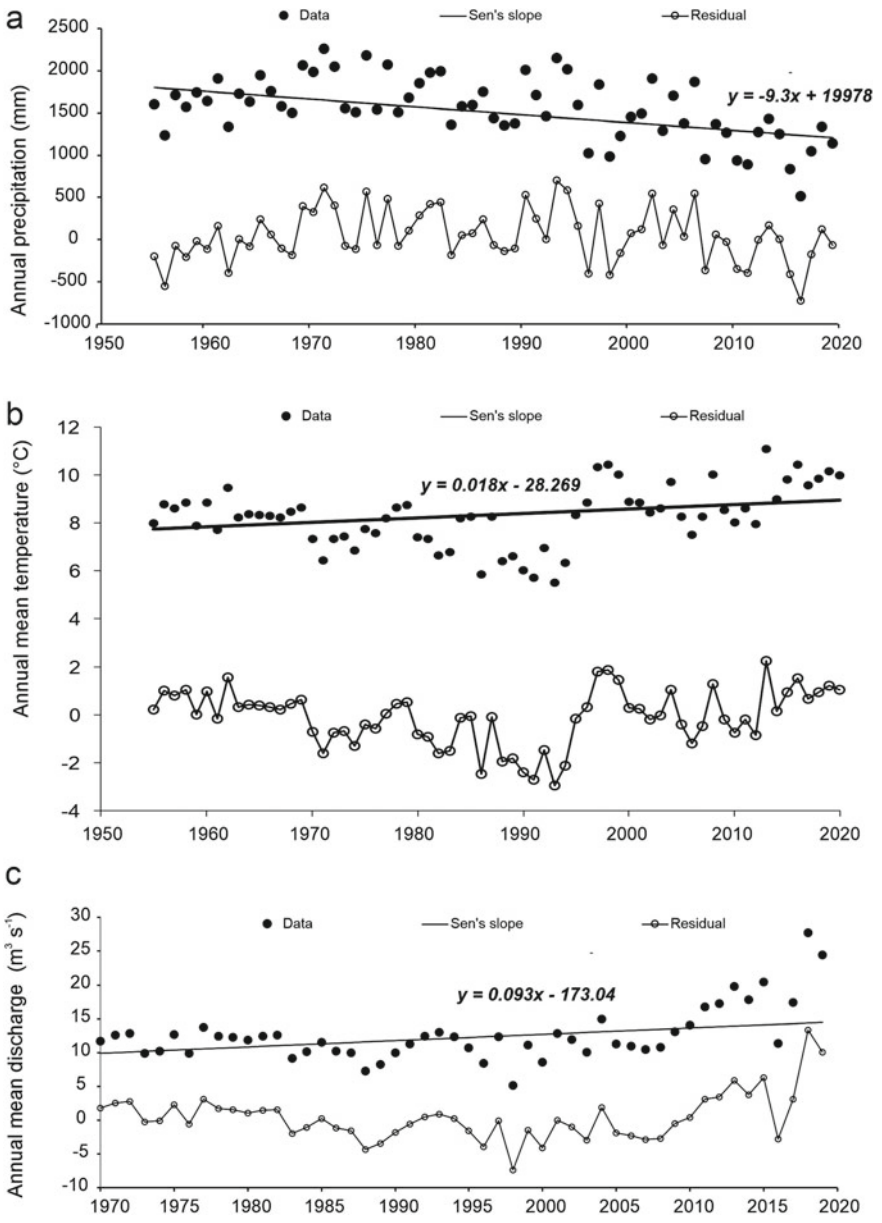

Fig. 5 **a** Mann–Kendall trend test for the annual precipitation time series at Los Alerces station (1955–2019 record period). **b** Idem **a** for the mean annual temperature time series at Los Alerces station (1955–2020 record period). **c** Mann–Kendall trend results for the mean annual discharge reconstructed time series of Manso Superior River at Mascardi station (1970–2020 record period)

indicates a decrease in the mean annual precipitation of ~9 mm y^{-1}. Along with the historical decreasing trend in precipitation, an increase in historical temperatures is also identified. Figure 5b shows the Mann Kendall test applied to the temperature time series at Los Alerces station (1955–2020 record period), where a significant ($p < 0.05$) positive trend indicates a regional warming. The Sen's slope shows an increase in temperature of > 1 °C in the last 6 decades. Such warming was also observed in previous works (e.g. Masiokas et al. 2008). Moreover, Pabón-Caicedo et al. (2020) pointed out that over the extratropical Andes, temperature reconstructions indicate that the twentieth century has been the warmest period during the last millennium in northern Patagonian, east of the Andes.

Historical trends in the mean annual discharge of the Manso River were analyzed in the upper and lower basin using the Mascardi (1970–2019) and Confluencia time series, respectively. Figure 5c shows a statistically significant positive trend of Manso Superior River discharge at Mascardi (i.e. in the upper basin). The Sen's slope (Fig. 5c) indicates that the mean annual discharge has increased about 2.8 m^3 s^{-1} in the last 40 years (i.e. ~70 L per year).

To better explore this substantial discharge increase in the Manso Superior River (upper basin), monthly trends were also performed by the **seasonal Kendall test** (Kendall 1975; Hirsch et al. 1982). The results (Table 1) show, for the same record period at Mascardi station, that the significant positive trend in river discharge occurs particularly in March, April, July, September, October and November. These results differ from those previously reported by Pasquini et al. (2013), who did not identify, a decade ago, positive trends in the Manso Superior River discharge. Taking in consideration that precipitation does not show a similar trend, it is possible to conclude that the increasing discharge of the Manso Superior River is a result of the increasing in

Table 1 Seasonal Kendall test of Manso Superior River monthly mean discharge

	N	Kendall *t*	p^a
January	50	0.971	0.16588
February	50	0.920	0.17869
March	50	3.573	**0.00018**
April	50	3.029	**0.00123**
May	50	1.079	0.14025
June	50	1.548	0.06085
July	50	2.125	**0.01680**
August	50	1.472	0.07046
September	50	3.037	**0.00120**
October	50	2.937	**0.00166**
November	50	1.757	**0.03945**
December	50	1.255	0.10470
Total	600	3.173	**0.00076**

[a] Statistically significant parameters in bold ($p < 0.05$)

the snow/ice melting during the last 15 years; moreover, considering that most of the statistically significant positive discharge trends are registered at the end of the austral winter and during the austral spring. This is coherent with the increase in size of the Manso proglacial Lake as a result of a shrinkage of the tongue, as reported by Paul and Mölg (2014) and Ruiz et al. (2017).

Lake Mascardi water level variability has been earlier analyzed by Pasquini et al. (2008) along with the variability of several Patagonian lakes, and it was later revisited by Pasquini et al. (2013) with a more extended record period. In such studies, the authors reported a significant decreasing trend in the water level in most months of the year. The new updated series of Mascardi Lake water level at Central Frey station (1970–2020 record period) shows a similar result since the historical monthly mean water level (Fig. 6a) clearly exhibits a negative trend. Moreover, the Sen's slope

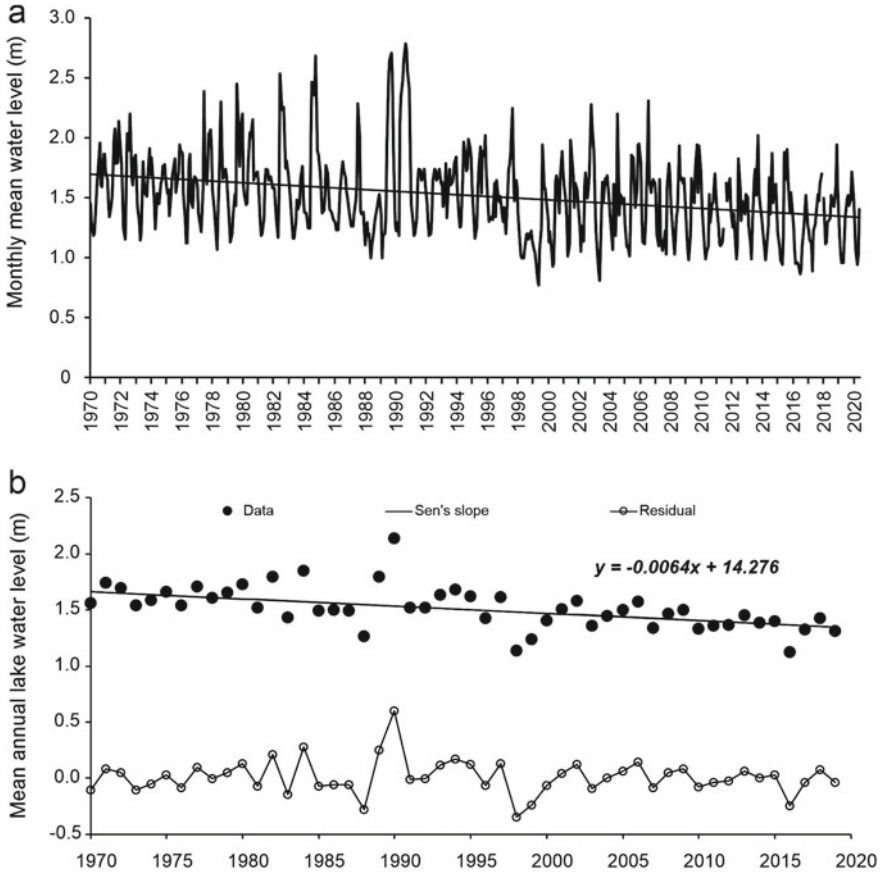

Fig. 6 **a** Monthly mean water level time series of Mascardi Lake at Central Frey station (1970–2020 record period). **b** Mann–Kendall trend test for the annual water level at the same place that in a)

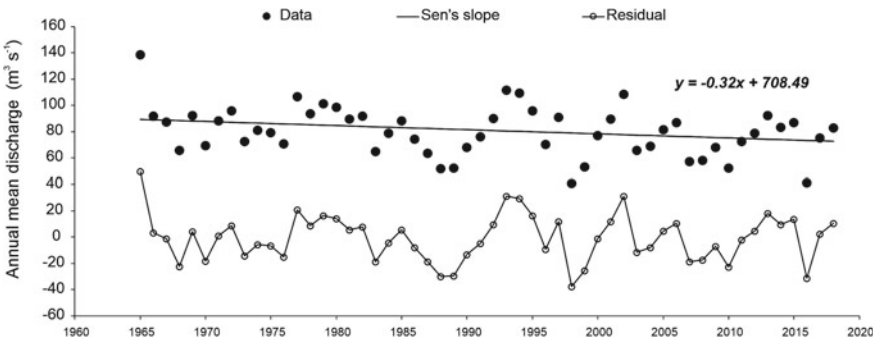

Fig. 7 Annual Mann–Kendall test applied to the Manso Inferior River discharge in the lower basin (i.e. downstream Lake Steffen), at Confluencia station (1965–2020 record period)

of the annual Mann Kendall trend test (Fig. 6b) evidences a statistically significant decreasing trend ($p < 0.001$) in Lake Mascardi water level, considering the last 50 years.

In the lower basin, Manso Inferior River discharge also shows a historical decreasing trend. The Mann–Kendall test applied on annual mean discharge series at Confluencia station (1965–2020 record period) shows a significant negative trend ($p < 0.05$) in the last 6 decades (Fig. 7). In this case, the Sen's slope denotes a decrease in mean annual river flow of 0.3 $m^3\ s^{-1}$ per year. This results also differs from those reported by Pasquini et al. (2013) who did not determine a significant trend in the Manso Inferior River discharge downstream Lake Steffen and, on the contrary, they found several months with a positive discharge trend in a gauging station close to the Argentina–Chile border.

In earlier studies Pasquini et al. (2008, 2013) also analyzed periodical signals in the Manso River basin. By means of harmonic analyses these authors found a clear inter-annual and near-decadal signature in Patagonia's proglacial lakes (including Lake Mascardi) which was associated with the **El Niño-Southern Oscillation** phenomena (**ENSO**). Moreover, these findings are supported by spectral coherence analysis, which shows a ~13-month time lag between ENSO occurrences and lake water level variability (Pasquini et al. 2008).

A more exhaustive analysis, which is beyond the scope of this chapter, would be necessary to better establish the subtle fluctuations in the hydrological behavior of the Manso River drainage system during the last decades. In the earlier study of Pasquini et al. (2008) a negative historical trend in the Manso Superior River basin (i.e. river discharge and lake water level) was interpreted as a consequence of decreasing melt water because the ice volume of the Manso Glacier was also markedly diminishing. Clearly, a different scenario is currently being observed, as the discharge of the Manso Superior River shows an increasing trend when the last 15 years of record are considered. Nevertheless, it is clear that the hydrological variability of the Manso River and associated lakes are highly sensitive to climatic changes occurring in the region since the last decades of the twentieth century, either

due to changes in atmospheric circulation, in the teleconnection with the ENSO events or even due to the influence of other modes of climatic variability such as the Antarctic Oscillation.

4 Hydrochemistry and Weathering Signature

Glaciers and icefields constitute the largest freshwater reservoirs on the planet, containing 28×10^6 km^3 of water (Tranter 2005). It is a widespread fact in the literature that a significant volume of sediment is transported by glacial systems to the oceans (e.g. Milliman and Farnsworth 2011), although the magnitude of the dissolved load transported by the ice **meltwater** is less known. Similarly, chemical **weathering** processes in these systems have been poorly documented (Sharp et al. 1995; Anderson et al. 2000), probably as a consequence of their apparent lower significance in relation to the products of physical erosion. However, Brown (2002) pointed out the significance of chemical weathering in these environments as an effective mechanism of CO_2 sequestration and its impact on climate change at an interglacial scale. On the other hand, the hydrology of glacial systems is closely linked to the dissolved geochemical signal produced, as it reflects the type and kinetics of the geochemical reactions that take place within the glacier, which are linked to the drainage system characteristics (Bennett and Glasser 2009). Thus, geochemical studies can provide information on the configuration and dynamics of glacial drainage systems (e.g. Brown 2002).

In glacial areas, streams and rivers flow with a mixed dissolved signal attributed to the snow and glacier meltwater, atmospheric precipitation and to the weathering of exposed rocks and sediments, which are continually changing the hydrochemistry. Weathering processes start when minerals, which were crystallized during high temperatures and pressures, reach surface conditions and become thermodynamically unstable. These new conditions plus physical and chemical weathering agents, as water, temperatures, wind, and biological impact, produces alteration in rocks and sediments (e.g. Depetris et al. 2014). In this way, initial solid phases are transformed to solutes, soils, and other sediments, controlling the global hydrogeochemical cycle of elements (White and Brantley 2003).

The Manso River system is controlled by the so-called **weathering-limited regime** (e.g. Stallard and Edmond 1983) due to its cold mountainous weather and the Andean active tectonics. Román-Ross et al. (2002) revealed that mineral hydrolysis in the region supplies a relatively reduced amount of dissolved material. Lake Mascardi's bottom sediments exhibit a low **chemical index of alteration** (**CIA,** Nesbitt and Young 1982) of ~55 (i.e. close to unaltered upper continental crust, UCC) and the modeling of the europium fractionation indicates little reworking of sediments, with a total loss of < 30% as soluble or weathered particulate material. In this kind of environment, the uppermost catchments usually preserve the atmospheric signal, with slightly acid pH and low total dissolved solids (TDS). Chillrud et al.

(1994) reported low concentrations of Cl^- (5.8 μM), and Na^+ (2.8 μM) in precipitation due to the orographic effect of the Andes Mountains, which generates that most of the cyclic marine salts discharge on the Chilean sector of the Andes Mountains. Downstream, the interaction between solid and dissolved phases, increases TDS values. Tranter et al. (2005) established that the dominant solutes in river waters that drain glacial areas are Ca^{2+} (regardless of the dominant lithology), HCO_3^- and SO_4^{2-} as a result of carbonate dissolution and sulfide oxidation as the main processes. On the other hand, some studies have shown that the rate of chemical weathering in the proglacial regions increases by a factor of 3 or 4 (e.g. Anderson et al. 2000; Wadham et al. 2001). Moreover, Anderson et al. (2000, 2003), Berry Lyons et al. (2003) and Hindshaw et al. (2011) highlight that solute fluxes and weathering rates in glacial regions are comparable to those in temperate zones.

The general aquatic geochemistry of **springs** and streams from the Manso River system has been previously defined (Chillrud et al. 1994; Pedrozo et al. 1993; Pedrozo and Chillrud 1998), but there was neither a discussion on trace element geochemistry in such aquatic system nor on the factors that control their dynamics. Other rivers of the Argentinian Patagonian Andes have been also described (Pedrozo et al. 1993; Diaz et al. 2007). In general, they present very dilute solutions, dominated by Ca^{2+}, HCO_3^- and dissolved Si.

In the present chapter, the Manso River hydrochemical analysis was made with data from samples collected during different field campaigns between 2000 and 2017, at different sampling sites along the entire hydrological basin. Moreover, data reported by Pedrozo et al. (1993) were also included. A total of 60 water samples were considered.

The physicochemical characteristics and dissolved major compounds are computed in Table 2. Data is divided into the Manso's upper stretch (i.e. Manso Superior River and tributaries) and the middle and lower ones (i.e. Manso Inferior River). Lakes' hydrochemistry is also represented (i.e. lakes Mascardi, Hess and Steffen) by means of mean values ± standard deviation (SD), minimum and maximum. In the entire hydrological basin, Manso River pH fluctuates from slightly acid to alkaline, varying between 5.7 and 8.3 with TDS between < 5 and ~75 mg L^{-1}. Clearly, the low intensity of weathering reactions results in the system's diluted waters. The relative abundance of anions is $HCO_3^- > SO_4^{2-} \geq Cl^-$, whereas the sequence for the main cations is $Ca^{2+} > Mg^{2+} > Na^+ > K^+$. Electrical conductivity varies between 9.6 and 115.6 μS cm^{-1}, with the highest values during the ice/snow melt season.

The hydrochemistry of lakes is quite constant. Similar to the Manso River, the TDS in lake waters are also low. The anions and major cations follow the same order of relative abundance as in the river; pH (~7.7) is also similar to those measured in the river. Redox potential reflects oxidant environments in both reservoirs (i.e. rivers and lakes).

The dissolved chemical signal can be defined by some diagrams. For instance, Piper diagram shows water classification with the major cation and anion compositions. In Fig. 8 the classification of the Manso River dissolved system is represented, divided into upper, middle and lower basin, and lakes. Manso proglacial Lake water

Table 2 Physicochemical characteristics and dissolved major composition of rivers and lakes from Manso system

Basin region		T	Eh	pH	EC	TDS	Ca^{2+}	Na^{+}	K^{+}	Mg^{2+}	Cl^{-}	SO_4^{2-}	HCO_3^{-}
		°C	mV		µS cm^{-1}	mg L^{-1}							
Upper (n=29)	mean ±	7.89 ±	352.56 ±	6.92 ±	51.90 ±	28.81 ±	5.73 ±	1.67 ±	0.54 ±	1.26 ±	0.49 ±	6.71 ±	15.88 ±
	SD	4.24	35.13	0.51	27.09	14.97	4.40	0.67	0.25	0.62	0.21	8.69	7.50
	Min	1.50	307.00	5.70	9.60	4.10	0.63	0.34	0.14	0.18	0.28	0.45	1.20
	Max	17.50	410.00	7.72	115.60	74.95	16.30	3.08	1.28	2.52	1.07	26.65	29.89
Middle (n=8)	mean ±	15.30 ±	308.20 ±	7.36 ±	57.24 ±	28.70 ±	5.56 ±	1.44 ±	0.40 ±	0.92 ±	0.74 ±	3.55 ±	19.74 ±
	SD	0.33	10.26	0.60	5.11	2.50	1.31	0.17	0.10	0.25	0.23	0.91	1.26
	Min	14.80	295.00	6.23	52.30	26.20	3.32	1.12	0.25	0.45	0.51	2.02	18.65
	Max	15.60	322.00	8.30	65.20	32.50	6.70	1.66	0.51	1.10	1.13	4.23	21.82
Lower (n=11)	mean ±	13.66 ±	406.73 ±	7.57 ±	59.35 ±	30.76 ±	7.71 ±	1.88 ±	0.44 ±	1.22 ±	0.63 ±	2.80 ±	26.33 ±
	SD	1.54	27.64	0.24	8.14	4.22	1.17	0.29	0.07	0.21	0.15	0.83	4.51
	Min	10.80	353.00	7.10	51.50	26.20	6.50	1.63	0.37	1.01	0.36	1.04	20.42
	Max	15.50	444.00	7.85	80.50	41.20	10.30	2.68	0.62	1.74	0.85	3.49	36.84
Lakes *(n=12)*	mean ±	12.48 ±	411.17 ±	7.67 ±	51.45 ±	26.53 ±	6.53 ±	1.62 ±	0.48 ±	1.12 ±	0.54 ±	2.90 ±	22.07 ±
	SD	3.00	37.98	0.11	0.85	0.67	0.88	0.22	0.12	0.17	0.12	1.04	3.86
	Min	7.70	306.00	7.54	49.85	25.20	5.40	1.42	0.39	0.85	0.35	1.29	19.40
	Max	15.90	441.00	7.89	52.45	27.40	9.10	2.14	0.80	1.53	0.70	4.36	33.74

Data is represented by the mean ± standard deviation, and minimum and maximum values of each upper, middle and lower basin, and the lakes. EC: electrical conductivity, TDS: total dissolved solids

is highlighted due to its influence in the upper basin hydrochemistry, presenting a clear sulfate–calcium type.

Along the Manso system, the classification shows a gradient from sodium/potassium type to calcium type, with respect to cations, and from sulfate to bicarbonate type with respect to anions. The uppermost catchments of the Manso Superior River, exhibit the Manso proglacial Lake influence (Fig. 8), as they present sulfate-type waters. Downstream, waters evolve towards a Ca^{2+} and HCO_3^- dominance due to the effect of **silicate hydrolysis**, as was proposed by Chillrud et al. (1994) and Pedrozo et al. (1993). The hydrochemical signal of the Manso Inferior River is less variable than in the upper basin, with a clear bicarbonate-calcium type. From a chemical point of view, lakes are similar to the Manso Inferior River. Finally, global mean runoff is added for comparison (Tranter 2003). It is quite similar, except for the chloride relative concentration, which is higher than in the analyzed system.

Table 3 shows dissolved trace element concentrations in the Manso River system, separated in upper, middle, lower basins and the lakes. It is evident again a great variation in the Manso Superior River, with both, the lowest and the highest concentrations of most of the trace elements. Figure 9a shows the multielemental extended normalized diagram (a.k.a. "spidergram") for the dissolved trace elements determined along the Manso River basins (rivers and lakes). Data was normalized against UCC (McLennan 2001) which is considered a common pattern in order to assess the

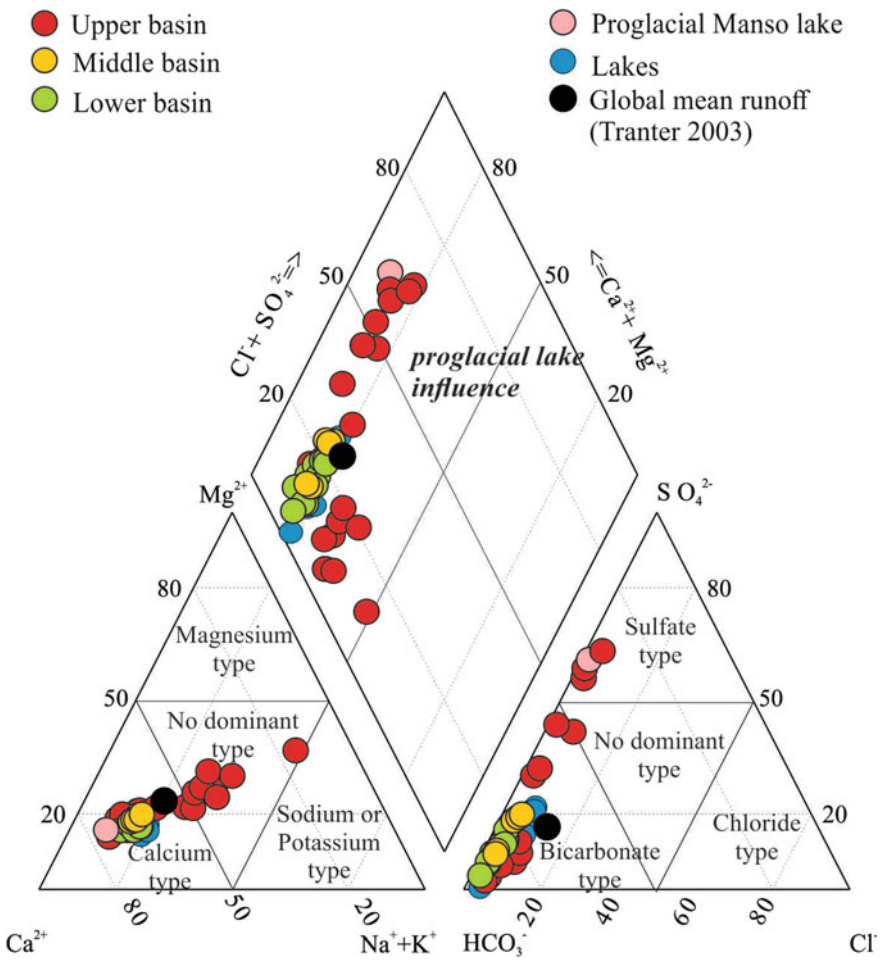

Fig. 8 Piper (1944) diagram showing the chemical classification of Manso River system's waters. Global mean runoff (Tranter 2003) is included for comparison

comparative concentration increase or decrease of different elements. The spidergram shows that the concentration of elements such as Al, Ti, Zr, Hf, and Th, known for their low mobility under normal surface conditions, are always the elements with the lowest normalized concentrations. In contrast, other elements such as Ni, Cu, As, Sr, Mo, Cd, and Sb are relatively enriched in this river waters, due to their higher mobility in comparison with the elements mentioned above.

The comparison between the Manso Superior and the Manso Inferior rivers, reveals that most of the elements have higher normalized concentrations in the uppermost stretch, which undergo a significant depletion after the passage through the Lake Mascardi. Such elements (Ti, V, Mn, Fe, Cu, Co, Y, Zr, Hf, and Pb) may be

Table 3 Trace dissolved elements (in μg L^{-1}) of rivers and lakes from Manso system

Basin region	Upper (n = 29)			Middle (n = 8)			Lower (n = 11)			Lakes (n = 12)		
	Mean ± SD	Min	Max	Mean ± SD	Min	Max	Mean ± SD	Min	Max	Mean ± SD	Min	Max
Si	4812.5 ± 2664.8	800.000	9300.000	4657.5 ± 682.5	3160.000	5440.000	5345.4 ± 796.7	4800.000	7500.000	4908.3 ± 844.7	3800.000	7400.000
Ti	2.371 ± 1.925	0.100	8.400	1.659 ± 1.806	0.100	4.047	0.236 ± 0.129	0.100	0.400	0.560 ± 0.381	0.200	1.200
V	0.771 ± 0.559	0.258	2.200	0.300 ± 0.089	0.112	0.400	0.391 ± 0.114	0.300	0.700	0.308 ± 0.029	0.300	0.400
Mn	20.013 ± 16.711	1.700	54.400	1.874 ± 1.186	0.582	4.200	2.209 ± 2.072	0.600	6.500	1.217 ± 0.805	0.400	2.900
Fe	103.755 ± 90.962	10.000	320.000	31.470 ± 13.385	18.342	60.000	21.818 ± 7.508	10.000	30.000	41.667 ± 44.484	10.000	150.0
Co	0.099 ± 0.073	0.002	0.255	0.017 ± 0.006	0.009	0.024	0.020 ± 0.007	0.011	0.035	0.042 ± 0.045	0.013	0.177
Ni	0.633 ± 0.458	0.300	1.700	0.340 ± 0.055	0.300	0.400	0.400 ± 0.195	0.300	0.900	0.542 ± 0.480	0.300	1.700
Cu	3.919 ± 5.802	0.200	23.900	1.111 ± 0.284	0.727	1.637	0.682 ± 0.125	0.500	0.900	1.158 ± 0.543	0.500	2.100
Ga	0.055 ± 0.044	0.010	0.140	0.024 ± 0.009	0.010	0.030	0.049 ± 0.018	0.040	0.100	0.077 ± 0.038	0.020	0.150
As	0.853 ± 1.737	0.130	7.660	0.360 ± 0.206	0.098	0.730	0.640 ± 0.297	0.340	1.400	0.611 ± 0.639	0.270	2.540
Rb	0.952 ± 0.324	0.459	1.680	0.851 ± 0.121	0.629	0.996	0.785 ± 0.103	0.599	0.944	0.818 ± 0.278	0.006	1.160
Sr	20.515 ± 11.664	1.390	39.300	19.315 ± 2.767	13.797	22.269	25.400 ± 4.972	20.500	38.100	20.333 ± 2.003	16.600	25.20
Y	0.078 ± 0.084	0.003	0.308	0.011 ± 0.002	0.008	0.016	0.016 ± 0.002	0.013	0.019	0.027 ± 0.010	0.011	0.041
Zr	0.051 ± 0.041	0.010	0.160	0.017 ± 0.004	0.010	0.020	0.028 ± 0.012	0.020	0.050	0.041 ± 0.031	0.020	0.130
Mo	0.293 ± 0.117	0.100	0.500	0.434 ± 0.351	0.200	1.291	0.582 ± 0.352	0.300	1.600	0.350 ± 0.183	0.200	0.900
Cd	0.042 ± 0.086	0.010	0.390	0.033 ± 0.022	0.010	0.067	0.010 ± 0.000	0.010	0.010	0.020 ± 0.012	0.010	0.050
Sb	0.017 ± 0.008	0.010	0.030	0.016 ± 0.005	0.010	0.021	0.018 ± 0.004	0.010	0.020	0.018 ± 0.006	0.010	0.030
Cs	0.019 ± 0.011	0.004	0.049	0.015 ± 0.006	0.003	0.021	0.018 ± 0.004	0.011	0.024	0.017 ± 0.003	0.014	0.023
Ba	3.586 ± 2.302	1.000	12.100	5.649 ± 2.695	2.300	10.300	4.300 ± 0.951	3.100	5.900	3.467 ± 0.812	2.400	4.800
Hf	0.005 ± 0.007	0.001	0.025	0.001 ± 0.000	0.001	0.001	0.001 ± 0.000	0.001	0.001	0.002 ± 0.001	0.001	0.002

(continued)

Table 3 (continued)

Basin region	Upper (n = 29)			Middle (n = 8)			Lower (n = 11)			Lakes (n = 12)		
	Mean ± SD	Min	Max	Mean ± SD	Min	Max	Mean ± SD	Min	Max	Mean ± SD	Min	Max
Tl	0.003 ± 0.001	0.001	0.005	0.002 ± 0.001	0.001	0.003	0.001 ± 0.000	0.001	0.002	0.002 ± 0.001	0.001	0.006
Pb	0.618 ± 0.624	0.040	2.290	0.506 ± 0.370	0.080	1.077	0.172 ± 0.228	0.050	0.850	0.250 ± 0.256	0.060	1.010
Th	0.009 ± 0.008	0.001	0.031	0.002 ± 0.001	0.001	0.004	0.005 ± 0.001	0.003	0.006	0.010 ± 0.005	0.005	0.019
U	0.018 ± 0.015	0.005	0.068	0.015 ± 0.004	0.005	0.020	0.028 ± 0.016	0.019	0.076	0.020 ± 0.006	0.014	0.035

Data is represented by the mean ± standard deviation, and minimum and maximum values in the upper, middle and lower basin, and lakes

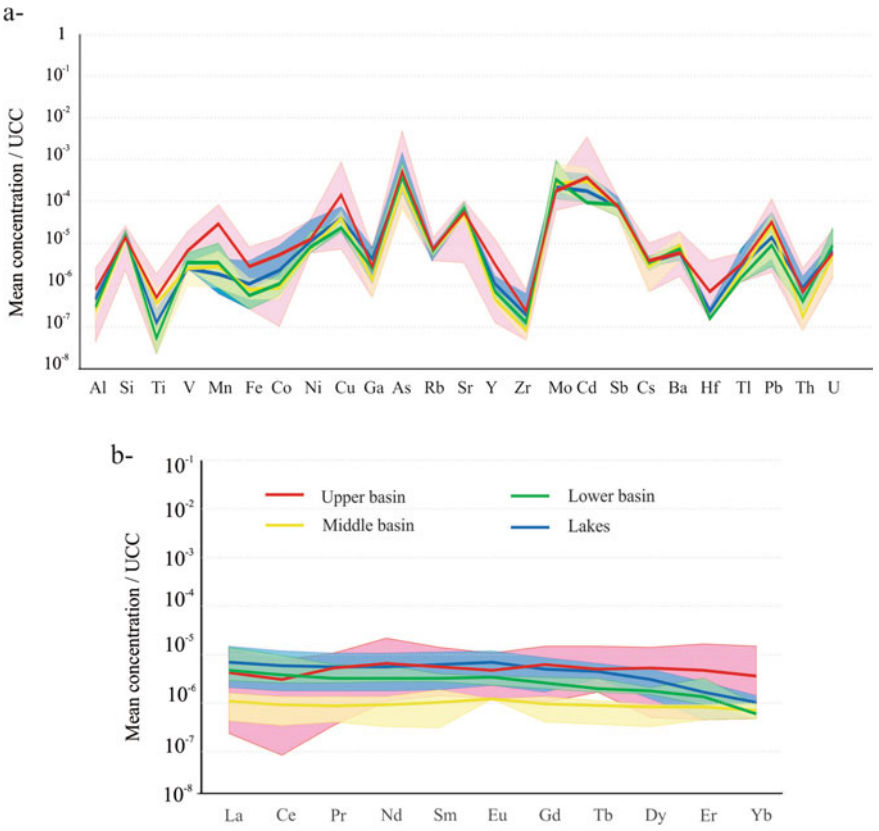

Fig. 9 Upper continental crust (UCC)-normalized spidergram for Manso River system divided into upper, middle, and lower basins, and lakes. Lines correspond to mean values, whereas shadow areas correspond to the total variation in each sector of the hydrological basin. **a** Trace elements and **b** rare earth elements

adsorbed by dissolved organic molecules, or into inorganic exchange sites, such as those supplied by iron oxides, clays or "glacial flour".

Concluding with the chemical comparison of the Manso's upper and lower stretches, there is a group of chemical elements which tend to increase their normalized concentrations in the downstream direction: Si, Sr, U, and some metal/oids that may form complexes (such as As, Mo). Figure 9a also includes data for lakes, which show a similar normalized pattern.

Of special interest among trace components are the group of **rare earth elements (REE)**, which are released during weathering but can be rapidly adsorbed onto colloids and thus constitute valuable tracers of the original rock (e.g. Elderfield et al. 1990; Sholkovitz 1995; García et al. 2007; Lecomte et al. 2016). REE have very similar chemical properties. They have been generally categorized into two groups based on their double-salt solubility: light rare earth elements (LREE) are called

the cerium sub-group elements (La to Eu) and heavy rare earth elements (HREE) are known as yttrium sub-group elements (Ga to Lu) (Henderson 1984; Krishnamurthy and Gupta 2015). The REE with lower atomic numbers (LREE) have larger ionic radii and hence are more incompatible, strongly concentrated in the continental crust compared to the REE with larger atomic numbers (HREE) (Krishnamurthy and Gupta 2015).

Table 4 includes mean REE dissolved concentrations in the Manso River system. Elements such as Ho, Tm and Lu are not included due to their concentrations below the detection limit. The total dissolved $\sum$REE concentrations range from 0.123 to 1.352 $\mu g\ L^{-1}$ in the upper basin, whereas they decrease noticeably in the middle basin (from 0.048 to 0.183 $\mu g\ L^{-1}$), after passing through Lake Mascardi. Lakes present the maximum total REE content, whereas the Manso River in the lower basin has intermediate concentrations. This behavior is more evident analyzing particularly the LREE. Moreover, LREE exhibit higher concentrations than HREE. Lanthanum concentrations range between 0.007 and 0.421 $\mu g\ L^{-1}$, while Yb concentrations just reach 0.031 $\mu g\ L^{-1}$ in the upper basin. The range of total REE concentrations is higher than those measured in other glacial areas draining comparable lithology (e.g. Tepe and Bou 2016).

REE concentrations measured in the Manso River system were also normalized to the UCC, and the obtained spidergram is shown in Fig. 9b. UCC-normalized mean river water in the upper, middle and lower stretches show relative flat patterns with some differences that are important to take into account. The highest mean values were measured in the upper basin and in lakes (Table 4). Moreover, in the upper basin REE concentrations also exhibit the highest variation (i.e. the lowest and the highest values when the entire system is considered). In the lower basin and in lakes, LREE are more enriched than HREE, whereas in the upper basin there is a slight predominance of HREE over LREE. The lowest values are documented in the middle basin, downstream Lake Mascardi, evidencing again adsorption and co-precipitation processes.

As was mentioned above, the rivers of the Argentinian Northern Patagonian Andes are dominated by Ca^{2+}, HCO_3^- and Si. However, the upper basin of the Manso Superior River, immediately after the Manso Glacier, has comparatively higher concentrations of dissolved Ca^{2+} and SO_4^{2-} in summer, with molar ratios of Ca^{2+}:SO_4^{2-} 1:1 which has been attributed to the oxidation of pyrite (Chillrud et al. 1994), that produces H_2SO_4. In such scenario, the formation of iron oxi-hydroxy substrates can occur as a by-product of precipitation due to a pH increase. The last process was very well described by Baffico et al. (2004) for the Agrio River, which in its upper basin has pH 3.0 (due to volcanic fluids of the Copahue volcano) and as it flows towards the Patagonian Plateau, becoming alkaline with the sequential precipitation of Fe and Al (Pedrozo et al. 2010).

The significance of sulfide oxidation in the upper basin can be analyzed by the relation of C_{ratio} versus TDS proposed by Brown et al. (1996). C_{ratio} is defined as $HCO_3^-/(HCO_3^- + SO_4^{2-})$, where a C_{ratio} ~1 indicates weathering dominated by carbonate reactions and a C_{ratio} value of ~0.5 indicates the coupling of sulfide oxidation and carbonate dissolution. In Fig. 10 it is plotted C_{ratio} versus TDS from the

Table 4 Dissolved rare earth elements (in $\mu g\ L^{-1}$) in rivers and lakes from Manso system

Basin region	Upper (n = 29)			Middle (n = 8)			Lower (n = 11)			Lakes (n = 12)		
	Mean ± SD	Min	Max	Mean ± SD	Min	Max	Mean ± SD	Min	Max	Mean ± SD	Min	Max
La	0.120 ± 0.097	0.007	0.356	0.031 ± 0.014	0.012	0.045	0.135 ± 0.092	0.084	0.395	0.193 ± 0.109	0.059	0.421
Ce	0.185 ± 0.156	0.005	0.459	0.055 ± 0.028	0.021	0.080	0.227 ± 0.121	0.157	0.575	0.349 ± 0.188	0.105	0.718
Pr	0.035 ± 0.021	0.002	0.072	0.006 ± 0.003	0.003	0.009	0.021 ± 0.007	0.018	0.041	0.037 ± 0.018	0.012	0.071
Nd	0.166 ± 0.119	0.026	0.526	0.023 ± 0.010	0.008	0.034	0.081 ± 0.021	0.067	0.142	0.140 ± 0.070	0.044	0.261
Sm	0.024 ± 0.019	0.006	0.060	0.004 ± 0.003	0.001	0.008	0.014 ± 0.002	0.012	0.017	0.026 ± 0.013	0.008	0.049
Eu	0.004 ± 0.003	0.001	0.009	0.001 ± 0.000	0.001	0.001	0.003 ± 0.000	0.002	0.003	0.006 ± 0.003	0.002	0.010
Gd	0.022 ± 0.016	0.004	0.054	0.004 ± 0.002	0.001	0.005	0.010 ± 0.001	0.007	0.012	0.018 ± 0.008	0.006	0.031
Tb	0.003 ± 0.003	0.001	0.009	bdl	bdl	bdl	0.001 ± 0.000	0.001	0.002	0.003 ± 0.001	0.002	0.004
Dy	0.017 ± 0.014	0.002	0.048	0.003 ± 0.001	0.001	0.003	0.006 ± 0.001	0.005	0.007	0.010 ± 0.005	0.004	0.017
Er	0.010 ± 0.010	0.001	0.036	0.002 ± 0.000	0.001	0.002	0.003 ± 0.001	0.002	0.007	0.004 ± 0.001	0.001	0.006
Yb	0.008 ± 0.009	0.001	0.031	0.002 ± 0.001	0.001	0.002	0.001 ± 0.000	0.001	0.002	0.002 ± 0.001	0.001	0.003
LREE	0.561	0.108	1.163	0.121	0.046	0.172	0.481	0.349	1.171	0.644	0.000	1.526
HREE	0.062	0.011	0.189	0.007	0.001	0.012	0.020	0.016	0.024	0.031	0.000	0.062
Total REE	0.623	0.123	1.352	0.128	0.048	0.183	0.502	0.365	1.193	0.788	0.242	1.588

Data is represented by the mean ± standard deviation and minimum and maximum values in the upper, middle and lower basin, and lakes. bdl: 0.001 $\mu g\ L^{-1}$

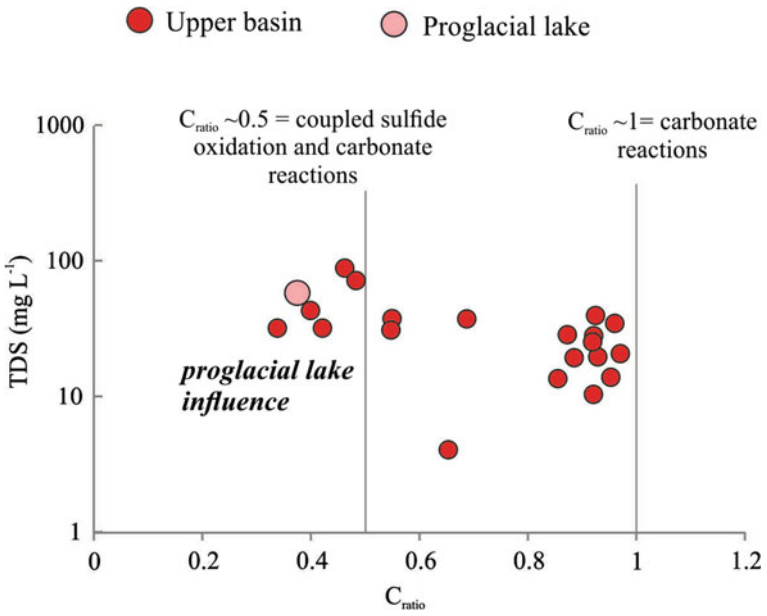

Fig. 10 C_{ratio} versus TDS in the upper basin of the Manso River

Manso Superior River waters. As it can be noted, both, carbonate dissolution and sulfide oxidation, are represented as dominant processes. Moreover, the pairing of sulfide oxidation and carbonate reactions control the chemistry of the waters that are directly influenced by the Manso proglacial Lake, whereas carbonation reactions mainly control the chemistry of the rest of the upper basin. On the other hand, in the middle and lower basins, waters have a predominant bicarbonate chemical signal, which indicates that the silicate hydrolysis is more relevant than in the uppermost catchments.

The computing yield of each major ionic species in the Manso Superior River **watershed** was analyzed by Pedrozo and Chillrud (1998). Their calculations supplied a significant weathering rate for the uppermost catchments (~16,000 mol km^{-2} d^{-1}), mainly due to the oxidation of pyrite (and the likely production of H_2SO_4) and a significant pCO_2. The rate is lower near the Manso River outfall at Lake Mascardi (~3700 mol km^{-2} d^{-1}). The difference is surely accounted for by the diluting effect of tributaries and/or groundwater flow, adsorption mechanisms onto particles, precipitation of solid phases, or biological consumption.

5 Suspended Sediments and Nutrient Dynamics

Data used for the following analysis correspond to samples collected during January and February (austral summer) between 1989 and 1991 in the Manso Superior River basin. Samples were taken from the Manso Superior River, Castaño Overo and Alerce streams, and several clear water type tributaries.

As mentioned above, the Manso Superior River, upstream its outflow into Lake Mascardi, shows a bimodal flow, with a minimum in July and the maximum in December, with an annual average of 12.5 $m^3\ s^{-1}$, strongly correlated with rain and snow precipitation. The monthly mean discharge at Mascardi (1970–2019 record period) varies in a wide range (2 to 60 $m^3\ s^{-1}$) with the floods that generally occur with spring and summer rains, which increase the glaciers melting. Such river behavior is coherent with the seasonal transport of suspended solids. In Fig. 11 the suspended solid concentrations from three different glacier meltwater discharges in the basin, i.e. Manso Superior River, Alerce and Castaño Overo streams, are represented. The figure shows that Manso Superior River is the one that contributes the most to the solid load (7–183 mg L^{-1}), while Alerce and Castaño Overo streams represent 7% and 45%, respectively. During the warm months, the glacial headwaters of the Manso River drainage basin and the river main channel (i.e. before reaching Lake Mascardi), are referred to as "**clear waters**". This "**milky water**" is determined by the high suspended solids load originating in the glaciers (i.e. "glacial flour"). In contrast, other tributaries in the basin, no directly related with glaciers, are of the "clear

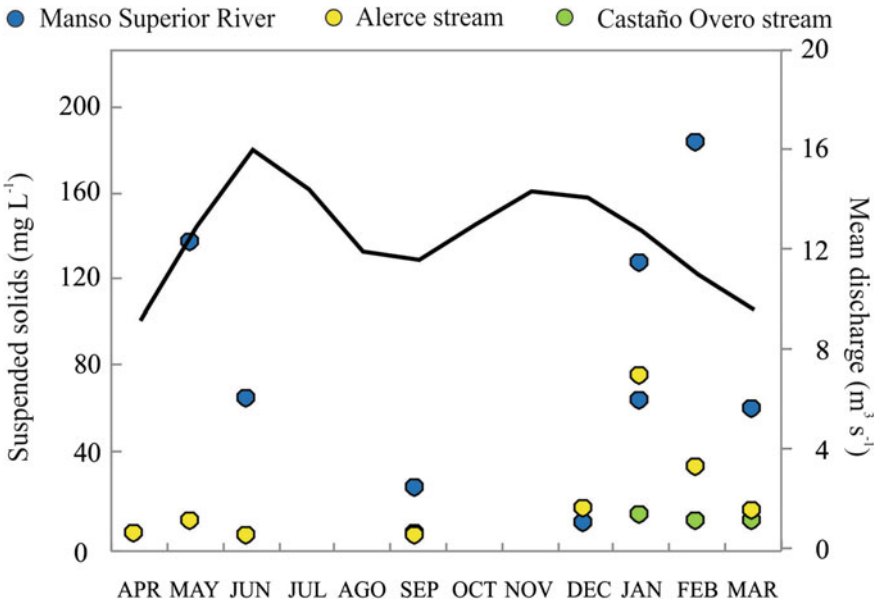

Fig. 11 Seasonal transport of suspended solids in the Manso Superior River basin

water" type (e.g. Huamanco and Los Cesares streams, Fig. 1, Pedrozo et al. 1993), with a very low suspended sediment load.

The role that P plays as an essential nutrient in water bodies has been widely studied (Larsen et al. 1981; Golterman et al. 1983; Horne and Goldman 1994; Wetzel 2001; Carpenter 2005). Dissolved P level in aquatic environments is controlled by the interaction with: (a) Fe and Al oxy-hydroxides and (b) Ca compounds (Tilman and Kilham 1976; Gunatilaka 1988; Sinke 1992). In both cases, these interactions occur because they have high affinity for the dissolved fraction of P. Depending on pH or redox potential, P can be adsorbed or desorbed onto Fe and Al oxy-hydroxides, and also P can be released to the solution by weathering of Ca-bearing minerals (Larsen et al. 1981; Boström et al. 1982; Koski-Vähälä et al. 2001; Katsev et al. 2006; Jin et al. 2006). The SRP:TP (**soluble reactive phosphorous**:total phosphorous) ratio shows again, the significance of **pyrite oxidation** as an important weathering reaction in the Manso Superior River basin. The precipitation of iron oxides removes SRP from solution and maintains a low SRP:TP ratio. This ratio is shown in Fig. 12 for the Manso Superior River, Castaño Overo and Alerce streams. These geochemical processes imply that, in the Manso Superior River, there is a high concentration of Fe controlling dissolved P, while in Castaño Overo and Alerce streams, the Fe content is lower and the SRP is larger than in the Manso River. The mechanism that operates in the Manso Superior River is opposite to that described for anoxic lake sediments with low or negative redox potential (Pedrozo and Chillrud 1998).

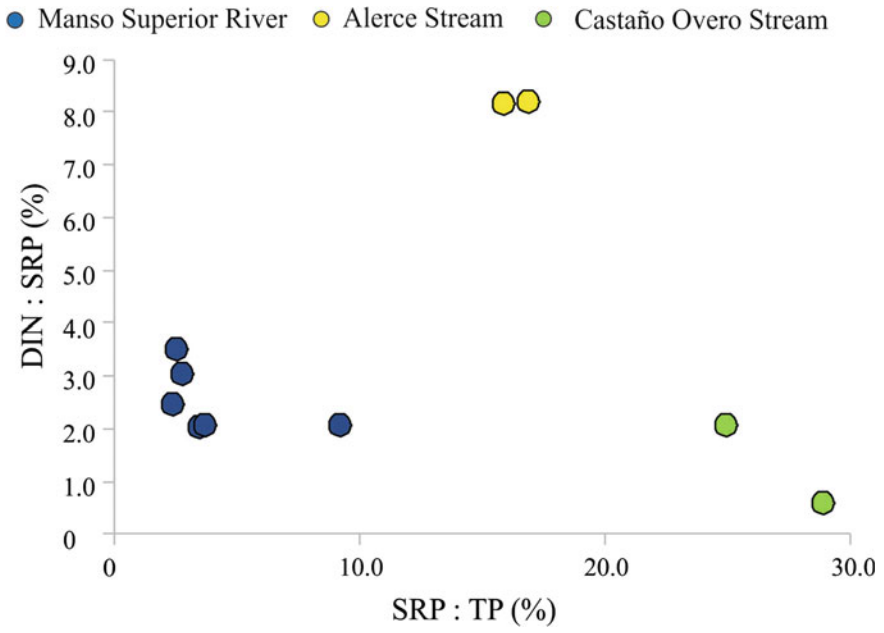

Fig. 12 DIN:SRP ratio versus SRP:TP ratio in the Manso Superior River basin

The inorganic N coming from the atmosphere is enough to explain the N content in the Manso Superior River water. The mean concentration of dissolved inorganic nitrogen (DIN) (1.78 μM; Pedrozo et al. 1993) in the precipitation (rain/snow) is higher than the mean range (0.44–1.17 μM) of DIN measured in the Manso Superior River throughout its entire basin. Moreover, these N concentrations are much lower than the values given by Meybeck (1982) for different environments worldwide (mean DIN = 28.57 μM). The relative concentration of NO_3^- (54%) in the Manso Superior River is higher than the NH_4^+ (27%), similarly to what is observed in other Patagonian rivers, and in agreement with values reported by Meybeck (1979) for world rivers. On the contrary, a set of Argentinian Andean Patagonian lakes present a similar NO_3^- and NH_4^+ percentages (53 and 47%, respectively) according to Pedrozo et al. (1993). The average DIN:SRP ratio allows to differentiate the three glacial sub-drains (Fig. 12). On the one hand, the lowest ratio is observed in the Castaño Overo stream (DIN:SRP = 0.55), along with its highest SRP:TP ratio (0.29). On the other hand, the Alerce stream is the one that has the highest DIN:SRP (8.13) ratio, and a low SRP concentration. Finally, the Manso Superior River presents the lowest SRP:TP ratio (mean of 0.04), whereas DIN:SRP decreases from 3.0 to 2.15 after the confluence with the Castaño Overo and Alerce tributaries. Most rivers are below the Redfield's ratio (N:P = 16:1; Wetzel 2001), suggesting that algal growth may be limited by nitrogen rather than phosphorus (Diaz et al. 2007).

6 Concluding Summary

The hydrological behavior of the Manso River drainage system is mainly governed by the rainfall and snowfall regimes, similarly to other glaciated Patagonian basins. Most of the annual precipitation in the region (rain and snow), occurs during the austral autumn–winter months (May–July) and it is subjected to a marked west to east decreasing gradient. Mean annual hydrograph shows a bimodal distribution as a consequence of atmospheric precipitations in winter and meltwater in spring and summer. Mean annual discharge in the upper basin is 12.5 $m^3\ s^{-1}$, whereas it increases downstream to 43.6 $m^3\ s^{-1}$, and reaches 79.3 $m^3\ s^{-1}$ in the lower basin. The annual water volume exported in the lower basin (at Confluencia) is of 2500 hm^3.

The Manso River is fed by several glaciers, and the homonymous glacier is the most important, showing a substantial retreat during the last decades. The trend test has shown a significant positive water yield in Manso Superior River, particularly during austral winter and spring. A significant increasing trend of temperatures during the last decades results in high shrinkage of glaciers which increases meltwater and then both, the Manso proglacial Lake's volume of water, and the discharge of the Manso Superior River. On the other hand, Lake Mascardi and the Manso Inferior River show a negative statistical trend. Harmonic analyses have shown clear inter-annual and near-decadal signals in Lake Mascardi, which were associated with the ENSO phenomena. Moreover, a lag of ~13-month between ENSO occurrences and lake water level variability was found by means of spectral coherence analysis. From

a hydrological point of view, the Manso River basin (including the associated lakes) has proven to be a highly sensitive system to climatic changes that occurred during the last decades.

High physical erosion, relatively high atmospheric precipitation along the Andes, and a restricted weathering rate define a weathering-limited denudation regime and the resulting diluted freshwater bodies. The dissolution of carbonates and the oxidation of pyrite occurring underneath the glacier are the key weathering reactions that supply HCO_3^-, SO_4^{2-}, and Ca^{2+}, the prevailing major ions in the upper basin, whereas in the rest of the basin (i.e. middle and lower basins), the hydrolysis of silicates also exerts its influence on the hydrochemistry. The concentration of dissolved minor and trace elements exhibit their own dynamics, mostly subjected to adsorption and/or complexation processes.

The oxidation of pyrite in the upper basin is also responsible for the formation of new substrates of iron oxi-hydroxide, controlling the concentration of dissolved P, which is scavenged from solution, resulting in a low SRP:TP ratio. Moreover, in the upper basin, the nitrate concentration is higher than the ammonium, similarly to other rivers in Patagonia and within the ranges for world rivers. The low N:P ratio indicates that algal growth in this environment is limited by nitrogen and not by phosphorus.

The suspended solids load determined in the upper basin, allows to differentiate two types of waters: “milky waters” with a high load of suspended solids in the Manso Superior River’s main channel, and “clear waters” with low suspended solids concentration in the tributaries.

From a geochemical point of view, an outstanding feature of the Manso River system, is the large variability in the concentration of major ions and trace elements (i.e. including REE), which is recorded in the upper basin (i.e. Manso Superior River). On the other hand, in the middle and lower basins, the chemical composition of water is less variable than in the upper basin. This particular characteristic reflects the great influence exerted by Manso Glacier’s meltwater on the hydrochemical signal of the Manso Superior River.

Acknowledgements This research was funded by the Agencia Nacional de Promoción Científica y Tecnológica (ANPCyT, PICT-2017-2026), the Consejo Nacional de Investigaciones Científicas y Técnicas (CONICET, Argentina, PIP 2017-2019 GI: 11220170100088CO, PUE CICTERRA-2016) and the Universidad Nacional de Córdoba (SeCyT, UNC 336-20180100385-CB). The authors also want to thank to Daniel Cielak for providing hydrological data.

References

Anderson SP, Drever JI, Frost CD, Holden P (2000) Chemical weathering in the foreland of a retreating glacier. Geochim Cosmochim Acta 64(7):1173–1189

Anderson SP, Longacre SA, Kraal ER (2003) Patterns of water chemistry and discharge in the glacier-fed Kennicott River, Alaska: evidence for subglacial water storage cycles. Chem Geol 202(3–4):297–312

Baffico GD, Diaz MM, Wenzel MT, Koschorreck M, Schimmele M, Neu TR, Pedrozo F (2004) Community structure and photosynthetic activity of epilithon from a highly acidic (pH $\leq$ 2) mountain stream in Patagonia, Argentina. Extremophiles 8(6):463–473

Bennett M, Glasser N (2009) Glacial geology: ice sheets and landforms. Wiley-Blackwell, United Kingdom

Berry Lyons W, Welch KA, Fountain AG, Dana GL, Vaughn BH, McKnight DM (2003) Surface glaciochemistry of Taylor Valley, southern Victoria land, Antarctica and its relationship to stream chemistry. Hydrol Process 17(1):115–130

Boström B, Jansson M, Forsberg C (1982) Phosphorus release from Lake Sediments. Arch Hydrobiol Beih Erg Limnol 18:5–59

Brion C, Puntieri J, Grigera D, Calvelo S (1998) Flora de Puerto Blest y sus alrededores. Centro regional Universitario Bariloche. Universidad Nacional del Comahue (in Spanish), p 201

Brown GH (2002) Glacier meltwater hydrochemistry. Appl Geochem 17:855–883

Brown GH, Sharp M, Tranter M (1996) Subglacial chemical erosion: seasonal variations in solute provenance, Haut Glacier d'Arolla, Valais, Switzerland. Ann Glaciol 22:25–31

Carpenter S (2005) Eutrophication of aquatic ecosystems: biostability and soil phosphorus. Proc Natl Acad Sci USA 102(29):10002–10005

Chillrud S, Pedrozo F, Temporetti P, Planas H, Froelich P (1994) Chemical weathering in glacial meltwater rivers: effects of pyrite oxidation on dissolved germanium and phosphate. Limnol Oceanogr 39(5):1130–1140

Dalla Salda LLH, Cingolani CA, Varela R (1991) El basamento cristalino de la región norpatagónica de los lagos Gutiérrez, Mascardi y Guillelmo Pcia. De Río Negro. RAGA 46:263–276 (in Spanish)

Depetris PJ, Pasquini AI, Lecomte KL (2014) Weathering and riverine denudation of continents. Springer, Netherlands

Diaz MM, Pedrozo FL, Reynolds C, Temporetti PF (2007) Chemical composition and the nitrogen-regulated trophic state of Patagonian lakes. Limnologica 37:17–27

Elderfield HR, Upstill-Goddard R, Sholkovitz ER (1990) The rare earth elements in rivers, estuaries and coastal sea waters: processes affecting crustal input of elements to the ocean and their significance to the composition of seawater. Geochim Cosmochim Acta 54:971–991

Gallopin GC (1978) Estudio ecológico integrado de la Cuenca del Río Manso Superior (Río Negro, Argentina). In Parques Nacionales De La República Argentina 14:161–230 (in Spanish)

García MG, Lecomte KL, Pasquini AI, Formica SM, Depetris PJ (2007) Sources of dissolved REE in mountainous streams draining granitic rocks, Sierras Pampeanas (Córdoba, Argentina). Geochim Cosmochim Acta 71:5355–5368

Giacosa RE, Heredia Carballo N, Zubía MA, González R, Faroux AJ, Césari O, Franchi M (2001) Hoja geológica 4172-IV San Carlos de Bariloche (in Spanish)

Golterman HL, Sly PG, Thoma RL (1983) Study of the relationship between water quality and sediment transport. UNESCO. Technical papers in Hydrology

González Bonorino F (1979) Esquema de la evolución geológica de la Cordillera norpatagónica. RAGA 34:184–202 (in Spanish)

Gunatilaka A (1988) Estimation of the available P-pool in a Large Freshwater Marsh. In sediment phosphorus group: working group summaries and proposals for future research. Arch Hydrobiol Beih Ergebn Limnol 30:15–24

Henderson P (1984) General geochemical properties and abundances of the rare earth elements. In: Henderson P (ed) Developments in geochemistry: 2. Rare earth element geochemistry. Elsevier, Amsterdam, pp 1–32

Hindshaw R, Tipper E, Reynolds B, Lemarchand E, Wiederhold JG, Magnusson J, Bourdon B (2011) Hydrological control of stream water chemistry in a glacial catchment (Damma Glacier, Switzerland). Chem Geol 285:215–230

Hirsch RM, Slack JR, Smith RA (1982) Techniques of trend analysis for monthly water quality data. Water Resour Res 18:107–121

Horne AJ, Goldman CR (1994) Limnology. MacGrawn-Hill Inc, New York

Hugonnet R, McNabb R, Berthier E, Menounos B, Nuth C, Girod L, Farinotti D, Huss M, Dussaillant I, Brun F, Kääb A (2021) Accelerated global glacier mass loss in the early twenty-first century. Nature 592(7856):726–731

Jin X, Wang S, Pang Y, Wu FC (2006) Phosphorus fractions and the effect of pH on the phosphorus release of the sediments from different trophic areas in Taihu Lake China. Environ Pollut 139(2):288–295

Katsev S, Tsandev I, L'Heureux I, Rancourt DG (2006) Factors controlling long-term phosphorus efflux from lake sediments: exploratory reactive-transport modelling. Chem Geol 234:127–147

Kendall MG (1975) Rank correlation methods. Griffin, London

Koski-Vähälä J, Hartikainen H, Tallberg P (2001) Phosphorus mobilization from various sediment poolin response to increased pH and silicate concentration. J Environ Qual 30:546–552

Krishnamurthy N, Gupta CK (2015) Extractive metallurgy of rare earths. CRC Press, Boca Raton

Larsen K, Shults L, Malneg A (1981) Summer internal phosphorus supplies in Shagawa lakes Minnesota. Limnol Oceanogr 26(4):740–754

Lecomte KL, Bicalho CC, Silva-Filho EV (2016) Geochemical characterization in karst basin tributaries of the San Franciscan depression: the Corrente river, western Bahia, NE-Brazil. J South Am Earth Sci 69:119–130

Mann HB (1945) Nonparametric tests against trend. Econometrica 13:245–259

Markert B, Pedrozo F, Geller W, Korhammer S, Friese K, Baffico G, Diaz M, Wolfl S (1997) A contribution to the study of the heavy-metal and nutritional element status of some lakes in the southern Andes of Argentina (Patagonia). Sci Total Environ 206:1–15

Masiokas MH, Luckman BH, Villalba R, Ripalta A, Rabassa J (2010) Little Ice Age fluctuation of Glaciar Río Manso in the north Patagonian Andes of Argentina. Quat Res 73:96–106

Masiokas MH, Rabatel A, Rivera Ibáñez A, Ruiz L, Pitte P, Ceballos JL, Barcaza G, Soruco A, Brown F, Berthier E, Dussaillant I, MacDonell S (2020) A review of the current state and recent changes of the Andean cryosphere. Front Earth Sci 8:99

Masiokas MH, Villalba R, Luckman BH, Lascano ME, Delgado S, Stepanek P (2008) 20th-century glacier recession and regional hydroclimatic changes in northwestern Patagonia. Global Planet Change 60(1):85–100

McLennan S (2001) Relationships between the trace element composition of sedimentary rocks and upper continental crust. Geochem Geophys Geosyst 2(4):2000GB0001009

Meybeck M (1979) Concentration des eaux fluviales en éléments majeurs et apports en solution aux océans. Rev Géol Dyn Géo Phys 21(3):215–246

Meybeck M (1982) Carbon, nitrogen, and phosphorus transport by world rivers. Am J Sci 282:401–450

Milliman JD, Farnsworth KL (2011) River discharge to the coastal ocean: a global synthesis. Cambridge University, Cambridge

Nesbitt HW, Young GM (1982) Early Proterozoic climates and plate motions inferred from major element chemistry of lutites. Nature 199:715–717

Pabón-Caicedo JD, Arias PA, Carril AF, Espinoza JC, Goubanova K, Lavado-Casimiro W, Masiokas M, Solman S, Villalba R (2020) Observed and projected hydroclimate changes in the Andes. Front Earth Sci 8:61

Pasquini AI, Lecomte KL, Depetris PJ (2008) Climate change and recent water level variability in Patagonian proglacial lakes Argentina. Global Planet Change 63(4):290–298

Pasquini AI, Lecomte KL, Depetris PJ (2013) The Manso Glacier drainage system in the northern Patagonian Andes: an overview of its main hydrological characteristics. Hydrol Process 27:217–224

Paul F, Mölg N (2014) Hasty retreat of glaciers in northern Patagonia from 1985 to 2011. J Glaciol 60:1033–1043

Pedrozo FL, Chillrud SN (1998) Relative water fluxes and silicate weathering from the Tributaries of a small Glaciated watershed in the Southern Patagonian Andes (Upper Manso Watershed, Argentina). Mitt Int Ver Theor Angew Limnol 26:935–939

Pedrozo F, Chillrud S, Temporetti P, Diaz M (1993) Chemical composition and nutrient limitation in rivers and lakes of Northern Patagonian Andes (39.5°–42°S; 71°W) (Rep. Argentina). Mitt Int Ver Theor Angew Limnol 25:207–214

Pedrozo FL, Díaz MM, Temporetti PF, Baffico GD, Beamud SG (2010) Características limnológicas de un sistema ácido: río Agrio-Lago Caviahue, Provincia del Neuquén Argentina. Ecol Austr 20(2):173–184 (in Spanish)

Rabassa J, Brandani A, Boninsegna JA, Cobos DR (1984) Cronología de la "Pequeña Edad de Hielo" en los galciares Río Manso y Castaño Overo, Co., Tronador, Pcia. de Río Negro. Actas IX Congreso De Geología Argentino 3:624–639 (in Spanish)

Rabassa J, Rubulis S, Suárez J (1978) Los glaciares del Monte Tronador. En Parques Nacionales De La República Argentina 14:259–318 (in Spanish)

Rogora M, Massaferro J, Marchetto A, Tartari G, Mosello R (2008) The water chemistry of some shallow lakes in Northern Patagonia and their nitrogen status in comparison with remote lakes in different regions of the globe. J Limnol 67:75–86

Román-Ross G, Depetris PJ, Arribére MA, Ribeiro Guevara S, Cuello GJ (2002) Geochemical variability since the Late Pleistocene in Lake Mascardi sediments, northern Patagonia, Argentina. J South Am Earth Sci 15:657–667

Ruiz L, Berthier E, Viale M, Pitte P, Masiokas MH (2017) Recent geodetic mass balance of Monte Tronador glaciers, northern Patagonian Andes. Cryosphere 11(1):619–634

Sharp M, Tranter M, Brown G, Skidmore M (1995) Rates of chemical denudation and CO_2 drawdown in a glacier-covered alpine catchment. Geology 23:61–64

Sholkovitz ER (1995) The aquatic chemistry of rare earth elements in rivers and estuaries. Aquat Geochem 1(1):1–34

Sinke JC (1992) Phosphorus dynamics in the sediment of an Eutrophic lake. Ph.D. Thesis, University of Wageningen

Stallard RF, Edmond JM (1983) Geochemistry of the Amazon 2. The influence of geology and weathering environment on the dissolved load. J Geophys Res 88:9617–9688

Tepe N, Bou M (2016) Behavior of rare earth elements and yttrium during simulation of arctic estuarine mixing between glacial-fed river waters and seawater and the impact of inorganic (nano-) particles. Chem Geol 438:134–145

Tilman D, Kilham SS (1976) Phosphate and silicate uptake and growth kinetics of the diatoms Asterionella formosa and Cyclotella meneghiniana in batch and semicontinuous culture. J Phycol 12:375–383

Tranter M (2003) Geochemical weathering in glacial and proglacial environments. In: Drever JI, Holland HD, Turekian KK (eds) Treatise on geochemistry. Elsevier, Amsterdam, pp 189–205

Tranter M (2005) Sediment and solute transport in glacial meltwater streams. In: Anderson MG (ed) Encyclopedia of hydrological sciences. Willey, pp 2633–2645

Tranter M, Skidmore M, Wadham J (2005) Hydrological controls on microbial communities in subglacial environments. Hydrol Process 19:995–998

Villalba R, Leiva JC, Rubulis S, Suarez J, Lenzano LE (1990) Climate, tree-ring, and glacial fluctuations in the Río Frías Valley, Río Negro Argentina. Arc Alp Res 22(3):215–232

Wadham JL, Cooper RJ, Tranter M, Hodgkins R (2001) Enhancement of glacial solute fluxes in the proglacial zone of a polythermal glacier. J Glaciol 47(158):378–386

Wetzel R (2001) Limnology. Academic Press, San Diego, USA

White AF, Brantley SL (2003) The effect of time on the weathering of silicate minerals: why do weathering rates differ in the laboratory and field? Chem Geol 202(3–4):479–506

Worni R, Stoffel M, Huggel C, Volz C, Casteller A, Luckman B (2012) Analysis and dynamic modeling of a moraine failure and glacier lake outburst flood at Ventisquero Negro, Patagonian Andes (Argentina). J Hydrol 444–445:134–145

Zalazar L, Ferri L, Castro M, Gargantini H, Gimenez M, Pitte P, Ruiz L, Masiokas M, Costa G, Villalba R (2020) Spatial distribution and characteristics of Andean ice masses in Argentina: results from the first National Glacier inventory. J Glaciol 1–12

Geothermal Influence on the Hydrochemistry of Surface Streams in Patagonia Neuquina

Esteban Villalba, Lucía Santucci, Guido Borzi, Andrea I. Pasquini, Gerardo Páez, and Eleonora Carol

Abstract The Domuyo System Natural Protected Area in the Patagonia neuquina presents a mountainous relief with steep valleys carved by both, glacial and fluvial processes, where the main water courses are the streams named Manchana Covunco, Aguas Calientes and Covunco, which are tributaries of the Varvarco River. These streams run through an area of intense geothermal manifestations composed by aqueous solutions of high temperature, which determine the chemistry of streams and springs. The surface water courses and springs located upstream the thermal springs are neutral to alkaline, of low temperature and electric conductivity, and Ca-HCO_3/Ca-HCO_3-SO_4 types, respectively. Downstream the thermal springs, an increase in pH, temperature, and electrical conductivity is registered, as well as changes towards Na-Cl facies, the dominant composition of the thermal springs. Also, thermal springs increase the As content limiting the water potability. The contribution from thermal springs to streams varies between 24 and 47%, while in springs it is close to 10%. In addition to the mixing water, carbonate, plagioclase, and pyroxene weathering processes are mainly evidenced in both, thermal springs and springs, while surface water is associated with carbonate and gypsum-anhydrite dissolution. The dissolved REE contents are 10^4–10^7 times lower than the Upper Continental Crust and show a decrease downstream the geothermal field. Understanding the processes that determine the hydrochemistry is of great relevance in this type of arid mountainous environments with scarce knowledge.

E. Villalba (✉) · L. Santucci · G. Borzi · E. Carol (✉)
Centro de Investigaciones Geológicas, Universidad Nacional de la Plata, Consejo Nacional de Investigaciones Científicas y Técnicas, La Plata, Argentina
e-mail: evillalba@cig.museo.unlp.edu.ar

E. Carol
e-mail: eleocarol@fcnym.unlp.edu.ar

A. I. Pasquini
Centro de Investigaciones en Ciencias de La Tierra, Universidad Nacional de Córdoba, Consejo Nacional de Investigaciones Científicas y Técnicas, Córdoba, Argentina

G. Páez
Instituto de Recursos Minerales, Universidad Nacional de la Plata, Consejo Nacional de Investigaciones Científicas y Técnicas, La Plata, Argentina

A. I. Torres and V. A. Campodonico (eds.), *Environmental Assessment of Patagonia's Water Resources*, Environmental Earth Sciences,
https://doi.org/10.1007/978-3-030-89676-8_3

Keywords Geothermal system · Chemistry signature · Water courses · Springs

1 Introduction

In the central-west and northwestern region of Argentina, there are a large number of **hydrothermal manifestations**. Particularly in Patagonia, the main hydrothermal manifestations, in terms of their magnitude, are found in the Neuquén province (Mas 2010; Burd et al. 2014; Monasterio et al. 2017). These manifestations are represented by the Copahue-Caviahue volcano-hydrothermal system in the center-west area of Patagonia and the Domuyo geothermal system in the northwest of the aforementioned province (e.g. Agusto 2011; Chiodini et al. 2014).

The Domuyo System Natural Protected Area comprises a region dominated by Cenozoic volcanism represented by pyroclastic rocks, lavas and extrusive **domes** of rhyolitic and andesitic compositions (Fig. 1a). This felsic volcanism is found on a pre-volcanic Mesozoic basement composed of conglomerates, sandstones and pelitic rocks, which in turn lies on top of granites and granodiorites of Paleozoic age (Zanettini et al. 2001; Miranda et al. 2006; Pesce 2013; Galetto et al. 2018). The Domuyo System Natural Protected Area hosts the Domuyo Geothermal Field, which is located in the western sector of the Chos Malal fold and thrust belt. It has been

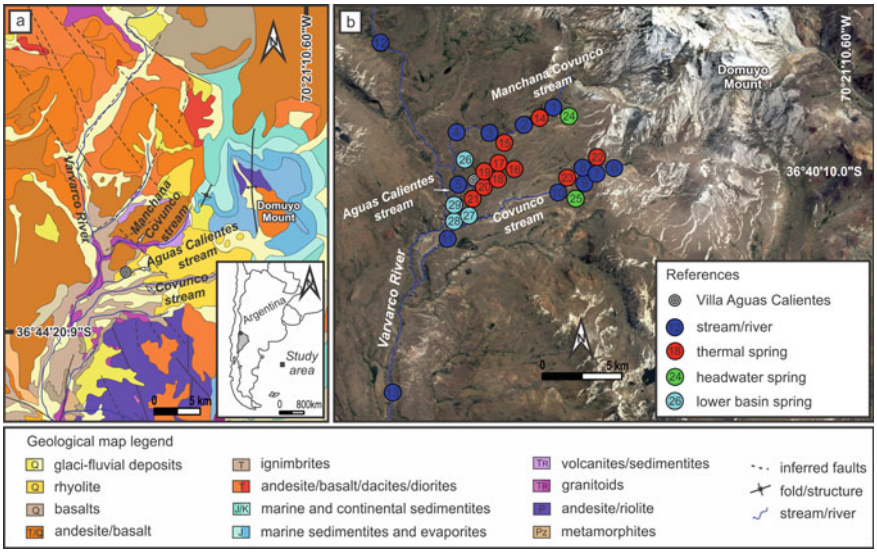

Fig. 1 **a** Regional geological map based on Zanettini et al. (2001), in the inset the Neuquén province is highlighted in grey color within the Argentina map and, **b** Satellite image from Google Earth Pro of the Domuyo system natural protected areas showing the location of sampling points from thermal springs (red points), surface water (blue points), and springs (green and light blue points). Capital letters are Quaternary (Q), Tertiary (T), Cretaceous (K), Jurassic (J), Triassic (TR), Permian (P) and Paleozoic age (Pz)

defined as a faulting-controlled **geothermal system**, where one of the most relevant tectonic structures is the Manchana Covunco Fault, whose location is close to the foot of the Domuyo Mount with a NNW-SSE direction (Galetto et al. 2018) and controls the location of the hydrothermal system. This region presents mountainous relief with steep valleys carved by both, glacial and fluvial processes (Zanettini et al. 2001). The main water courses are the streams named Manchana Covunco, Aguas Calientes and Covunco, which are tributaries of the Varvarco River (Fig. 1b). It is worth noting that small tributaries that drain through gullies and reach those streams are born in **springs**. At the same time, the area is characterized by the presence of **geothermal manifestations** composed of aqueous solutions of high temperature (from 40 to 97 °C), which result from ascending convective circulation of groundwater, mainly of **meteoric origin**, through fracture systems and permeable layers (Panarello et al. 1992; Chiodini et al. 2014; Tassi et al. 2016).

The climate is cold (annual average temperature close to 11 °C) and arid, with precipitation (200 mm per year) concentrated during austral winter, which occurs mainly in the form of snow (Pesce 2013; Cogliati et al. 2018). Therefore, in this region of arid characteristics, where water availability is scarce, streams and springs represent systems of high relevance as they constitute one of the main sources of water supply for the native fauna, livestock, and local inhabitants.

2 Field Methodology and Laboratory Analysis

In advance of carrying out field tasks for this study, antecedent information and satellite images were analyzed to design a monitoring network. Subsequently, samples of thermal water, springs and water courses were extracted underneath standardized norms of the American Public Health Association (APHA 2015) and analyzed in the Centro de Investigaciones Geológicas (CIG) laboratory. In the field, pH, electrical conductivity (EC), and temperature (T) of the water samples were measured with multiparameter equipment. Aliquots for Arsenic (As) and **rare earth elements (REE)** determinations (15 ml) were acidified to pH < 2 with ultrapure HNO_3 (>99.999%, redistilled) and stored in pre-cleaned polyethylene bottles. As and REE, from lanthanum (La) to lutetium (Lu), were determined by inductively coupled plasma-mass spectrometry (ICP-MS). Calibration curves were constructed from multi-element calibration standards (Perkin Elmer Inc. brand). All standard solutions and reagent blanks were prepared with deionized water and acidified with 1% HNO_3. The standard readings were repeated after measuring 5 samples. Aliquots of 1000 ml were stored in polyethylene bottles, without acidifying, at 4 °C for the determination of major ions.

Determinations of major ions (CO_3^{-2}, HCO_3^{-}, Cl^{-}, SO_4^{-2}, Ca^{+2}, Mg^{+2}, Na^{+}, K^{+}) were performed following standard methods outlined by APHA (2015). Carbonate (CO_3^{-2}), bicarbonate (HCO_3^{-}), calcium (Ca^{+2}), magnesium (Mg^{+2}), and chloride (Cl^{-}), were determined by volumetric methods (titration). The sodium (Na^{+}) and potassium (K^{+}) ions were determined by flame photometry, while sulfate (SO_4^{-2})

was precipitated in an acetic acid medium with $BaCl_2$ and its concentration was determined by turbidimetry. Ion balances were typically lower than 15% in all cases.

The chemical data of the waters were processed by into the Diagrammes Software (Smiler 2009), which was used to determine the different types of facies based on the major ion content and Piper (1944) diagram. Likewise, this software was used to estimate the saturation indices (SI) concerning different mineral phases using the Phreeqc Software (Parkhurst and Appelo 1999), which is incorporated into the program as an interface. In selected samples, the REE values obtained were normalized with respect to the concentration of the Upper Continental Crust (UCC) according to McLennan (2001). Finally, end-members mixing analyses were performed using Cl^- concentration in each type of sample because this is considered as a conservative ion and a useful tool to estimate, in this case, the contribution of **thermal springs** on the water courses and springs in the lower basin of the geothermal field.

3 Chemical Characteristics of Streams

The west flank of the Domuyo Mount presents a geothermal area that is crossed by the **watersheds** of the Manchana Covunco, Aguas Calientes, and Covunco (Figs. 1 and 2) which register an average low flow of 0.81 $m^3\ s^{-1}$. Table 1 shows the physicochemical parameters, the major composition, As content and relevant saturation indices of water samples. Springs in the headwater areas that contribute to the streams (samples 24 and 25; Fig. 1b) are characterized by an average pH, T, and EC of 7.2, 10.1 °C and 32 $\mu S\ cm^{-1}$ respectively, and Ca-HCO_3 facies (Fig. 3). At the **headwater** of the Manchana Covunco stream (sample 1; Figs. 1b and 2b), a pH of 8.1, temperature of 20.5 °C, and an EC of 1386 $\mu S\ cm^{-1}$ were recorded, and the chemical composition is dominated by Ca-HCO_3-SO_4 facies (Fig. 3). In the headwater of the Covunco stream (sample 6; Fig. 1b) pH values of 8.0, temperature of 15 °C and EC of 817 $\mu S\ cm^{-1}$ were registered, with Ca-HCO_3-SO_4-Cl facies (Fig. 3). In the middle watershed of the Manchana Covunco and Covunco streams and in the Aguas Calientes stream, numerous thermal springs are observed on the stream banks (Fig. 1b). These thermal springs have predominantly Na-Cl facies (Fig. 3), relatively high EC (from 1391 to 4394 $\mu S\ cm^{-1}$) and pH values between 7.2 and 9.3.

Downstream of the thermal springs, surface water of streams shows changes in the **chemical facies**, being predominantly Na-Cl (Fig. 3) and registering a strong increase of EC with respect to the values measured in the headwaters. The surface water collected from the Manchana Covunco stream (samples 2, 3, and 4; Figs. 1b and 2a) present average values of pH, temperature, and EC of 8.1, 28.7 °C and 3610 $\mu S\ cm^{-1}$ respectively. In the same way, waters from the Covunco stream (samples 7, 8, 9, 10 and 11; Figs. 1b and 2c, d) show a mean pH, temperature and EC of 8.4, 26.6 °C and 2856 $\mu S\ cm^{-1}$ respectively. In these areas of the low basin, several springs were also recognized, draining towards the streams (samples 26 to 29). These

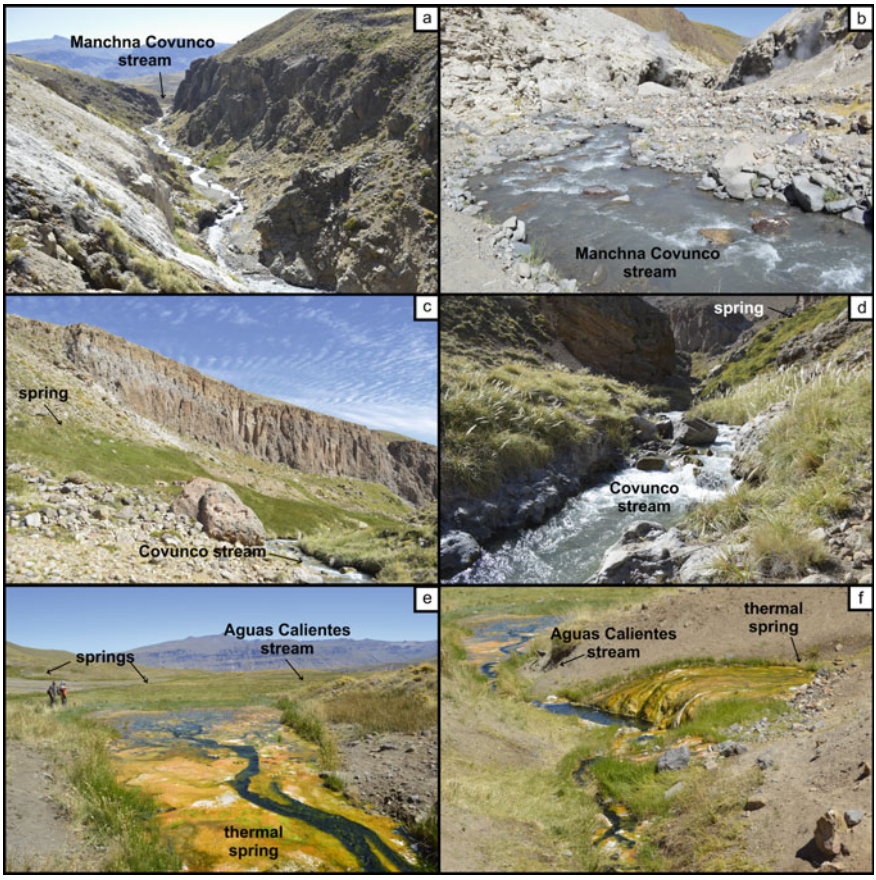

Fig. 2 Field photographs of surface water courses: Manchana Covunco stream in (**a**) and (**b**), Covunco stream in (**c**) and (**d**), Aguas Calientes stream in (**e**) and (**f**), springs in (**c**) to (**e**), and thermal springs in (**e**) and (**f**). Note headwaters are present in some water courses (white arrows)

waters present mean values of pH, temperature and EC of 7.1, 21.0 °C and 994 μS cm^{-1} respectively, while their chemical composition is Na-Cl (Table 1, Fig. 3).

The watersheds described above (Manchana Covunco and Covunco) drain towards the Varvarco River, which registers pH values of 7.94, temperature of 18.1 °C and EC of 320 μS cm^{-1} **upstream** the geothermal field (sample 12), while downstream the geothermal field (sample 13) the same parameters were of 7.80, 14.6 °C and 733 μS cm^{-1}, respectively. The chemical facies in Varvarco River is Ca-SO_4 in the upstream stretch and Na-SO_4-Cl after receiving the discharges from the geothermal field watersheds (Table 1, Fig. 3).

The joint analysis of all samples using the Piper (1944) diagram (Fig. 3) clearly shows the different evolution of chemical facies from the headwaters to the low basin, between surface water and springs (blue and green arrows, respectively, Fig. 3). In

Table 1 Physico-chemical parameters and major composition of water samples. Arsenic dissolved concentrations, as well as saturation indices (SI) of selected minerals are also included. Sample numbers are the same as in Fig. 1. lb = lower basin, hw = headwater

Sample	Composition	Type of sample	pH	T	EC	CO_3^{-2}	HCO_3^-	Cl^-	SO_4^{-2}	Ca^{+2}	Mg^{+2}	Na^+	K^+	As	SI cal	SI gyp	SI hal
				(°C)	(µS cm^{-1})	(mg L^{-1})									(Dimensionless)		
1	Ca-HCO_3-SO_4	Stream	8.09	20.5	1386	0	130.6	255.1	445.7	111.2	22.6	124.0	44.0	0.263	0.59	−0.98	−6.12
2	Na-Cl	Stream	8.11	39.2	3830	0	118.4	837.4	407.1	88.2	13.4	590.0	81.0	0.883	0.42	−1.2	−4.96
3	Na-Cl	Stream	8.03	19.3	3200	18.84	92.3	814.3	110.0	88.5	14.8	330.0	77.0	0.865	0.32	−1.66	−5.2
4	Na-Cl	Stream	8.19	27.5	3800	12.84	95.3	932.0	111.9	92.0	11.9	400.0	86.0	0.922	0.49	−1.65	−5.07
5	Na-Cl	Stream	7.99	39.4	1952	0	163.7	1033.5	45.9	26.7	9.6	720.0	69.0	0.939	0	−2.57	−4.77
6	Ca-HCO_3-SO_4-Cl	Stream	8.04	15	817	0	138.4	60.0	106.4	102.0	22.4	29.0	7.5	0.069	0.66	−1.48	−7.35
7	Na-Cl	Stream	8.43	31.5	2980	11.13	112.3	616.0	100.9	79.2	13.4	230.0	61.0	0.650	0.76	−1.7	−5.47
8	Na-Cl	Stream	8.37	27.9	2770	12.8	90.5	643.6	82.5	79.8	13.4	320.0	64.0	0.649	0.61	−1.79	−5.31
9	Na-Cl	Stream	8.61	30	3060	6.85	100.1	687.4	88.0	53.1	15.5	350.0	67.0	0.698	0.7	−1.94	−5.24
10	Na-Cl	Stream	8.32	23.4	3100	0	111.4	710.5	80.7	68.0	7.2	270.0	66.0	0.733	0.59	−1.85	−5.34
11	Na-Cl	Stream	8.29	20.4	2370	0	110.6	592.9	60.5	56.6	11.8	290.0	53.0	0.584	0.5	−2.04	−5.38
12	Ca-SO_4	River	7.94	18.1	320	0	90.5	1.4	161.4	51.6	12.4	4.1	1.9	0.009	0.11	−1.51	−9.81
13	Na-SO_4-Cl	River	7.8	14.6	733	0	95.8	141.4	161.4	41.6	18.7	121.0	9.0	0.144	−0.14	−1.67	−6.36
14	Na-Cl	Thermal	8.8	67	9610	17.1	77.5	1801.6	289.8	17.7	11.1	1030.0	160.0	1.969	0.14	−2.1	−4.41
15	Na-Cl	Thermal	8.54	92.4	5490	12.9	82.7	1584.8	201.7	30.1	11.6	810.0	79.0	1.793	0.21	−1.97	−4.56
16	Na-Cl	Thermal	7.25	62.4	1485	0	108.4	998.9	45.9	9.5	8.3	470.0	55.0	0.960	−1.32	−2.95	−4.96
17	Na-Cl	Thermal	7.17	57.3	2840	0	148.9	615.9	150.4	9.2	5.4	510.0	37.0	0.647	−1.3	−2.45	−5.13
18	Na-Cl	Thermal	7.68	59.7	4480	0	99.2	1130.3	67.7	15.5	7.1	550.0	60.0	0.944	−0.75	−2.61	−4.85

(continued)

Table 1 (continued)

Sample	Composition	Type of sample	pH	T	EC	CO_3^{-2}	HCO_3^-	Cl^-	SO_4^{-2}	Ca^{+2}	Mg^{+2}	Na^+	K^+	As	SI cal	SI gyp	SI hal
				(°C)	($\mu S\ cm^{-1}$)	($mg\ L^{-1}$)									(Dimensionless)		
19	Na-Cl	Thermal	8.3	56.2	1561	0	106.2	1065.8	172.4	14.3	1.9	820.0	59.0	0.894	−0.19	−2.3	−4.71
20	Na-Cl	Thermal	7.64	55.8	1391	0	120.1	959.6	49.5	6.5	10.0	470.0	60.0	0.910	−1.06	−3.08	−4.98
21	Na-Cl	Thermal	7.37	40	1866	0	123.6	777.4	34.9	4.7	11.1	380.0	49.0	1.969	−1.43	−3.33	−5.15
22	Na-Cl	Thermal	9.34	66.1	8850	46.2	20.0	2507.5	108.2	15.8	11.6	1170.0	190.0	2.271	−0.12	−2.59	−4.22
23	Na-Cl	Thermal	8.63	60.1	6370	24.0	104.5	1831.6	64.2	34.8	13	910.0	95.0	1.754	0.46	−2.41	−4.45
24	Ca-HCO_3	Spring (hw)	7.44	8.2	39	0	59.2	5.6	4.6	9.6	2.8	5.4	0.6	0.01	−1.15	−3.54	−9.05
25	Ca-HCO_3	Spring (hw)	6.95	12	25	0	42.7	0.9	1.1	8.9	0.8	1.1	0.2	0.001	−1.79	−4.15	−10.53
26	Na-Cl	Spring (lb)	7.02	19	347	0	77.0	70.1	5.5	11.9	4.5	38.0	7.5	0.102	−1.4	−3.45	−7.12
27	Na-Cl	Spring (lb)	7.55	21.4	893	0	58.8	244.8	47.7	13.0	7.7	118.0	19.0	0.103	−1.04	−2.6	−6.12
28	Na-Cl	Spring (lb)	7.12	22.6	1741	0	89.7	512.6	16.7	3.1	11.5	250.0	6.9	0.298	−1.94	−3.75	−5.49
29	Na-Cl	Spring (lb)	6.76	nd	nd	0	54.0	79.1	4.6	10.2	1.8	38.0	9.1	0.052	−1.88	−3.57	−7.07

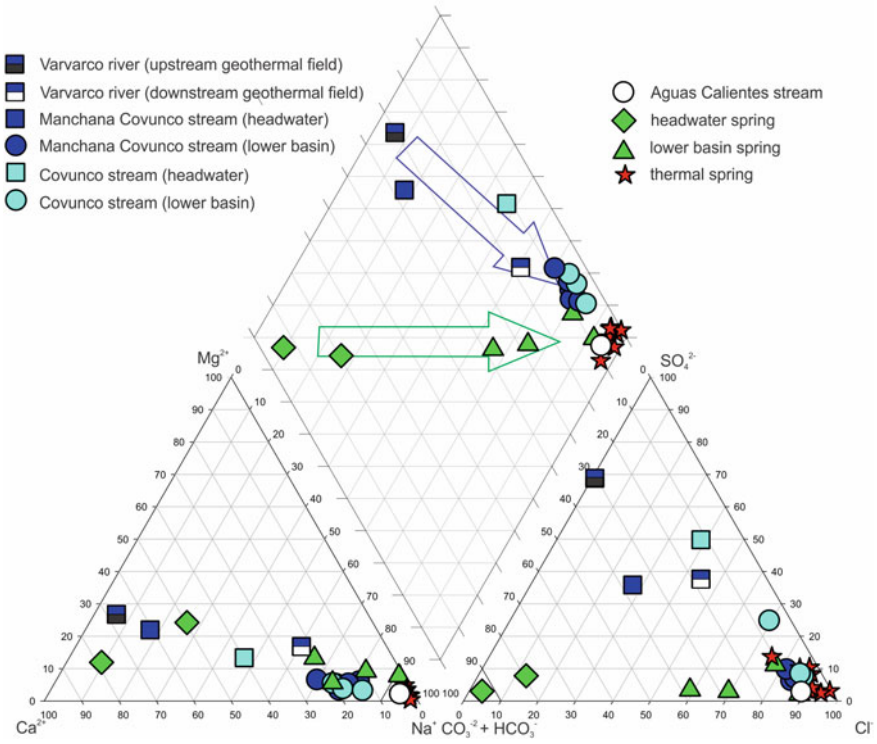

Fig. 3 Piper diagram showing the major composition and evolution of the studied waters. The blue arrow indicates the chemical evolution of stream water and the green arrow that of springs. Note that the symbol of the Aguas Calientes stream overlaps with thermal springs

both cases, the changing trend of chemical facies (towards Na-Cl compositions) is strongly controlled by the composition of the thermal springs.

On the other hand, thermal springs are characterized by high concentrations of As with values between 0.894 and 2.271 mg L^{-1} (Table 1). At headwaters low concentrations of As were measured (between 0.069 and 0.263 mg L^{-1}), while in the low basins, the streams present higher As values, between 0.584 and 0.939 mg L^{-1} (Table 1).

The analysis of the interaction between water and minerals (found in the rocks that compose the stream beds), performed by ionic relationships, allows the visualization of different behaviors (Fig. 4). The graph Na^+ versus Cl^- (Fig. 4a) shows that set of analyzed samples are grouped around the 1:1 ratio linear trend, which characterizes thermal springs, also showing higher concentrations of these ions. It is important to note that surface waters from Manchana Covunco and Covunco streams retrieved downstream and also the Aguas Calientes stream show a marked association with the thermal spring samples with respect to these ions. Besides, waters from the Varvarco River, although they are adjusted to the 1:1 ratio linear trend, they register low

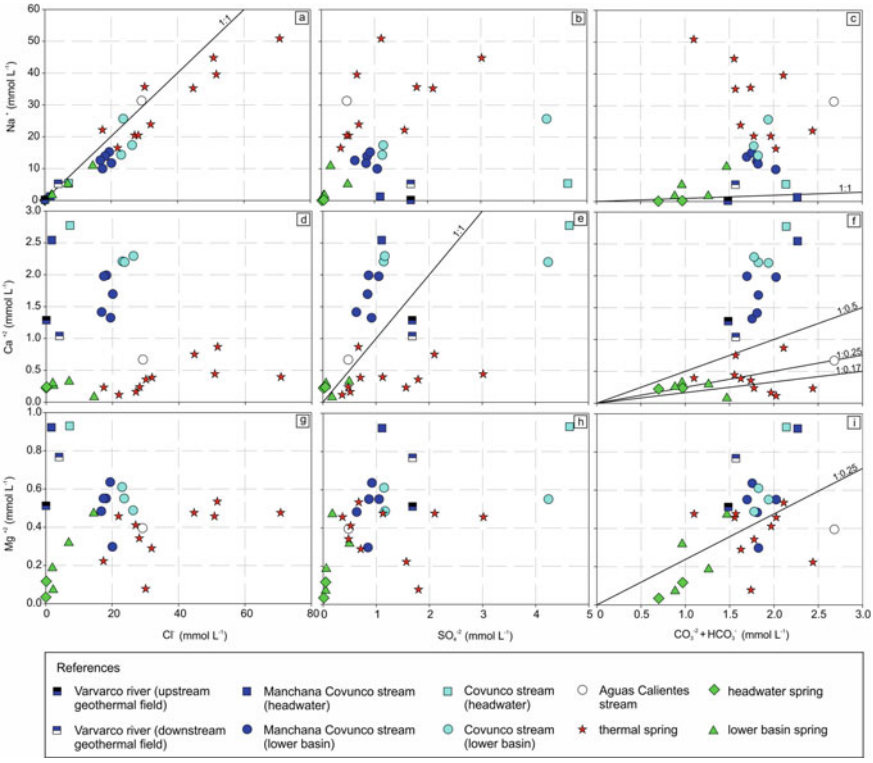

Fig. 4 Bivariate plots for each group of samples showing ionic relationships between anions and cations in mmol L^{-1}. The lines of theoretical dissolution of some minerals are also included

concentrations of these ions. The high Na^+ contents in the thermal springs determine that these samples (14–23, Fig. 1b) differ from the streams (with the exception of the Aguas Calientes sample) and the springs in the Na^+ versus SO_4^{-2} and Na^+ versus $CO_3^{-2} + HCO_3^-$ graphs (Fig. 4b–c).

The relationships Ca^{+2} versus Cl^-, Ca^{+2} versus SO_4^{-2} and Ca^{+2} versus $CO_3^{-2} + HCO_3^-$ show that thermal springs, springs, and the Aguas Calientes stream registered increases in its anionic contents associated with low concentrations of Ca^{+2} (Fig. 4d–f). Particularly, in the Ca^{+2} versus $CO_3^{-2} + HCO_3^-$ plot, the waters present ratios associated with the weathering of carbonates (1:0.5), oligoclase-type plagioclase (1:0.17), and pyroxenes (1:0.25). A different behavior is evidenced in samples from the Manchana Covunco and Covunco streams, where high Ca^{+2} concentrations are registered without observing a clear trend between the increase of this ion and the major anions. In the Ca^{+2} versus SO_4^{-2} graph, samples from the Varvarco River are close to the 1:1 ratio associated with the gypsum-anhydrite dissolution (Fig. 4e). Likewise, Mg^{+2} versus Cl^- and Mg^{+2} versus SO_4^{-2} graphs do not show trends in the different samples (Fig. 4g–h), whereas with respect to Mg^{+2} versus $CO_3^{-2} + HCO_3^-$ (Fig. 4i) the increase of these ions occurs in thermal springs, springs, and

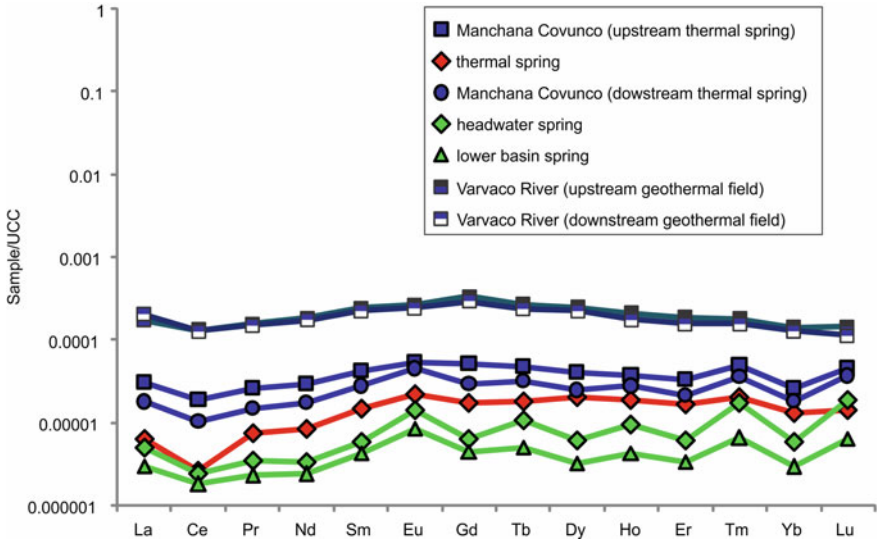

Fig. 5 Spider diagrams for dissolved rare earth elements (REE) normalized to Upper Continental Crust (UCC, McLennan 2001) for springs, streams, river and thermal spring from the studied system

Aguas Calientes stream with a ratio close to 1:0.25 corresponding to the weathering of pyroxenes.

The saturation indices (SI) with respect to calcite (Table 1) show subsaturated values for the springs waters, subsaturated to supersaturated for thermal springs and close to equilibrium to supersaturated in the streams and Varvaco River waters. The gypsum SI, although in all cases is negative (subsaturated), show a tendency towards equilibrium (less negative values) from springs to thermal springs and streams waters (Table 1). Regarding the halite SI, despite the high Cl^- and Na^+ concentrations registered in thermal springs, all samples presented subsaturated values, being more negative in springs and less negative in thermal springs waters (Table 1).

Some selected samples were analyzed in order to determine the concentration and variability of dissolved REE in the studied system. Five samples of the Manchana Covunco watershed, as well as, the two samples of the Varvaco River, were chosen for this purpose. Springs samples show the lowest total dissolved REE concentrations, with a ΣREE varying from 0.56 $\mu g\ L^{-1}$ at the headwaters to 0.36 $\mu g\ L^{-1}$ at the low basin. The analyzed thermal spring sample exhibits a ΣREE of 0.96 $\mu g\ L^{-1}$, whereas the Manchana Covunco stream shows a decreasing total dissolved REE content downstream the thermal spring, since in this river the ΣREE varies from 3.9 (upstream) to 2.3 $\mu g\ L^{-1}$ (downstream). On the other hand, the Varvarco River REE concentrations are of an order of magnitude higher than those of the other analyzed waters, and the river evidences almost no variation in the ΣREE from the headwaters to the low basin.

Figure 5 shows the spider diagram of the dissolved REE normalized to the Upper Continental Crust (UCC, McLennan 2001) for the studied system. The water samples

present REE concentrations of about 10^4 to 10^7 times lower that of the UCC. In the Manchana Covunco watershed the samples show, in general, similar UCC-normalized distribution, with relatively flat patterns and without evidence of significant fractionation between light (LREE, among La-Sm) and heavy (HREE, among Gd-Lu) rare earths elements ($La_N/Yb_N \sim 1$). An exception is given by the thermal spring that exhibits HREE-enriched UCC-normalized concentrations ($La_N/Yb_N = 0.48$). Besides, all samples of the Manchana Covunco basin present a negative Ce anomaly, and a positive Eu anomaly, the latter is more pronounced in springs. Positive $(Eu/Eu^*)_N$ in waters are usually attributed to the preferential weathering of plagioclase, because Eu^{+2} may substitute Sr^{+2} or Ca^{+2} in Ca-plagioclase (e.g. McLennan 1989). Meanwhile, negative Ce anomaly is due to the oxidation of Ce^{+3} to Ce^{+4} under alkaline conditions, which decreases its solubility and promotes its precipitation (e.g. Elderfield et al. 1990). The Varvaco River samples show a different UCC-normalized pattern, characterized by a barely enrichment in the LREE (mean $La_N/Yb_N = 1.41$) and a slightly negative Eu anomaly (mean $Eu/Eu^* = 0.93$).

4 Hydrogeochemical Processes and Geothermal Influence on Streams

The chemical characteristics of water along the streams highlight the clear influence that geothermal discharges have on them. Most of the **meltwater** infiltrates and recharges the groundwater which then forms the springs, and another part of this melting water drains feeding the streams (Tassi et al. 2016; Villalba et al. 2020). At the headwater area, upstream the geothermal field, the temperature of springs and streams (samples 1, 6, 24 and 25) are close to 13.9 °C. This value is strongly influenced by the climatic conditions, being similar to the average annual temperature recorded in the area (Pesce 2013). Streams and springs are characterized by neutral to slightly alkaline pH conditions, low EC, and Ca-HCO_3-SO_4 facies. The predominance of Ca^{+2}, HCO_3^- and SO_4^{-2} ions would be related mainly to the alteration of the mudstones and sandstones with a carbonate matrix, and gypsum that dominates headwaters area (Zanettini et al. 2001). In particular, stream waters present the highest Ca^{+2} concentrations and they are supersaturated with respect to calcite. The presence of gypsum that accompanies these sedimentary rocks would be an extra source of Ca^{+2}, and it would also contribute SO_4^{-2} ions, mainly in the Manchana Covunco stream (Fig. 4e). Although those waters are subsaturated with respect to gypsum, they show the least negative SI values regarding this mineral (Table 1). It is relevant to note that in this sector the high SO_4^{-2} contents in some samples could be also explain by the oxidation processes of H_2S at shallow depth (Tassi et al. 2016). At the springs, calcite and gypsum SI show subsaturation associated with low Ca^{+2} concentrations, despite this is the dominant cation. In the springs, the ionic relationships also indicate contributions of Ca^{+2}, Mg^{+2}, and HCO_3^- from the dissolution of silicates, such as plagioclase and pyroxenes (Figs. 4f and i). On the other hand, the

dissolution of albite (Fig. 4c) contributes Na^+ and HCO_3^- ions to both, springs and stream waters.

This hydrochemical signature of stream waters and springs in the headwaters sector strongly contrasts with that of the thermal springs. All thermal springs are characterized by high temperature (greater than 40.0 °C), relatively high EC (up to 1866.0 $\mu S\ cm^{-1}$) and by the dominance of Na-Cl facies. High concentrations of Na^+ and Cl^- are consistent with mature waters of geothermal systems at high temperatures. The concentrations of Na^+ and Cl^- were stoichiometrically equivalent as expected for typical geothermal brines (Giggenbach 1997; Vengosh et al. 2002). Gases such as SO_2 and HCl from the magmatic source dissolve within the hydrothermal groundwater to produce SO_4^{-2} and Cl^- (Tassi et al. 2016). As mentioned before, this SO_4^{-2} contribution would also explain the deviation of thermal spring waters in the graph of Ca^{+2} versus SO_4^{-2} (Fig. 4e). Likewise, it is expected that the contributions of Ca^{+2}, Mg^{+2} and HCO_3^- derive from the underlying igneous rocks (Zanettini et al. 2001). Given that aqueous emissions are the product of deep convective circulation of meteoric water (Panarello et al. 1992), most geochemical features of thermal springs would be acquired in depth. Extra contributions of HCO_3^- can also come from the dissolution of $CO_{2(g)}$ since this gas is one of the main components of the **fumaroles** (Tassi et al. 2016). However, saturated values in calcite are recorded, which would be the responsible of the precipitation of carbonatic terraces located in the vicinity of the thermal springs (Polk 1994; Villalba et al. 2020).

The low flow rates of streams (mean of 0.81 $m^3\ s^{-1}$) determine that the contributions from thermal springs strongly modified the chemical characteristics of stream waters. Downstream thermal springs, stream waters increase their EC and show the dominance of Na-Cl facies (Figs. 3 and 4). The contribution from thermal springs is registered not only in the facies change, but also in the Na^+ versus Cl^- ratio. With the purpose of estimating the contribution of thermal springs onto stream waters and springs downstream the geothermal field, an end-member mixing analysis was performed using chloride concentration as the dominant conservative ion of thermal springs. In the case of surface water streams, Cl^- concentration in the headwaters of the watershed and the average Cl^- concentration in thermal springs were considered as end members. As for springs, Cl^- concentration of the headwaters of the watershed and the average Cl^- concentration in thermal springs were considered.

The theoretical mixing model using Cl^- concentrations, allowed the estimation of the influence of thermal springs in the chemistry of stream and spring waters. The obtained results are schematically summarized in Fig. 6. For the Manchana Covunco watershed, the selected end-members were the sample from headwaters (sample 1) and the average concentration of Cl^- of the thermal springs (samples 14 and 15). It was estimated that downstream (sample 4), the contribution from thermal springs is of 47%. For the Covunco watershed case, the chosen end-members were a surface water sample located at the headwaters (sample 6) and the average concentration of Cl^- of thermal springs of the same water course (samples 22 and 23), estimating that downstream (sample 11), the water shows a 24% of geothermal contribution. At Aguas Calientes stream, no mixtures were calculated since, as it was observed in the chemical facies and ionic relationships, it has a chemical signature dominated

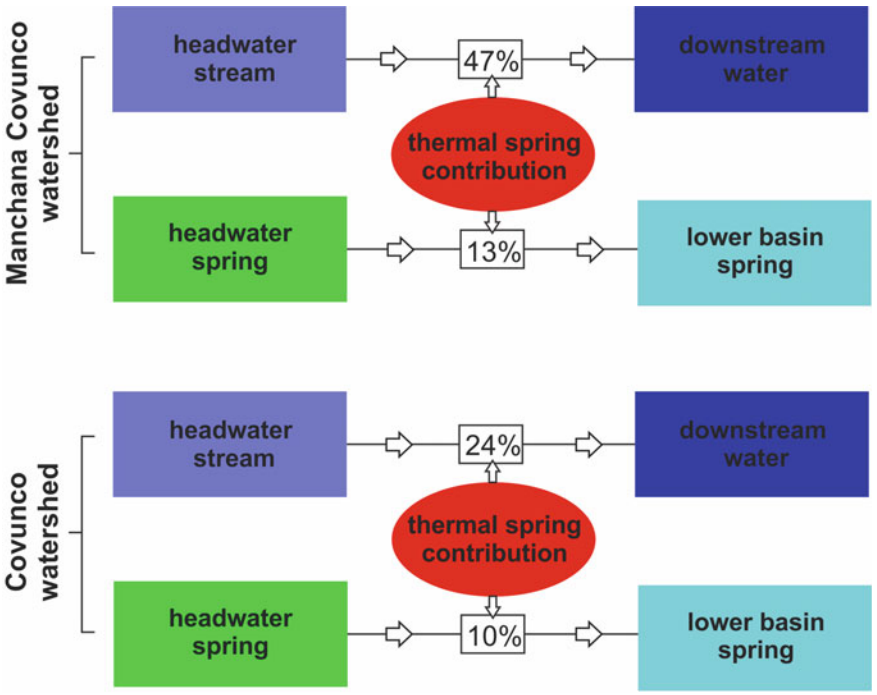

Fig. 6 Schematic diagram showing the estimated contributions of the thermal springs on the stream and spring waters in the downstream watershed of the Domuyo geothermal field

by thermal springs. In the case of springs, a mixture was computed between the Cl^- concentration of samples 24 and 25 (springs from headwaters) with the average concentration of Cl^- of thermal springs (samples 14 and 15, Manchana Covunco watershed) for the first case, and samples 22 and 23 (Covunco watershed) for the second one, estimating that downstream the springs, the geothermal contribution is between 10 and 13%.

The contribution from thermal springs with low Ca^{+2} concentrations produces an overall decrease in the Ca^{+2} contents from the headwaters to the lower basin due to the effect of dilution (Fig. 4d–f). In Manchana Covunco and Covunco streams there is an excess of Ca^{+2} which could be attributed to cation exchange processes, where the dominance of Na^+ would displace Ca^{+2} from the adsorption surface, constituting an extra contribution of this ion to the waters. The presence of adsorbent minerals such as clays and zeolites, associated with the adjacent areas to the geothermal field (Mas et al. 2000), would support the occurrence of this process.

Regarding trace elements concentrations that can limit the water quality for human consumption, it was observed that thermal springs also influence the concentrations of these elements. The elevated concentration of As recorded in thermal spring waters evidences how the interaction between rocks and waters at high temperature mobilizes As (Ellis and Mahon 1964, 1967). Considering the water quality standards

(WHO 2008), the geothermal contribution of As determines the potability of springs and stream waters located in the lower basin. Comparing the concentration of this trace element determined for headwaters and lower basin areas, it is evident that thermal springs deteriorate water quality for human supply. Thermal springs increase the As content to ~ 0.139 mg L^{-1} in the lower basin samples (Villalba et al. 2020).

The influence of thermal springs on the Manchana Covunco stream is also evidenced in the geochemistry of dissolved REE. Thermal spring waters have lower REE concentrations than stream surface waters at the headwaters, which are reflected in the decrease in total REE contents downstream. Moreover, the LREE/HREE fractionation as well as the positive Eu anomaly and negative Ce anomaly also show the influence of thermal springs on streams. On the other hand, the Aguas Calientes stream, which is mainly fed by thermal springs, has a major composition remarkably similar to that of thermal springs (Figs. 3 and 4). Note that the contribution from thermal springs is also recorded in springs, with an average percentage of 10% (Fig. 6). The influence of thermal springs on springs and water streams of the Domuyo System Natural Protected Area is outlined in Fig. 7. The aforementioned figure is a summarized diagram of the hydrothermal system behavior based on the models postulated by numerous works carried out in the area from geological, geochemical, geophysical, and satellite data (e.g. Panarello et al. 1992; JICA 1983–1984; Galetto et al. 2018; Tassi et al. 2016; Astort et al. 2019; Villalba et al. 2020).

The streams described above drain towards the Varvarco River, which has a higher flow, with discharges close to 94 m^3 s^{-1} (FAO 2015). This large difference in flow

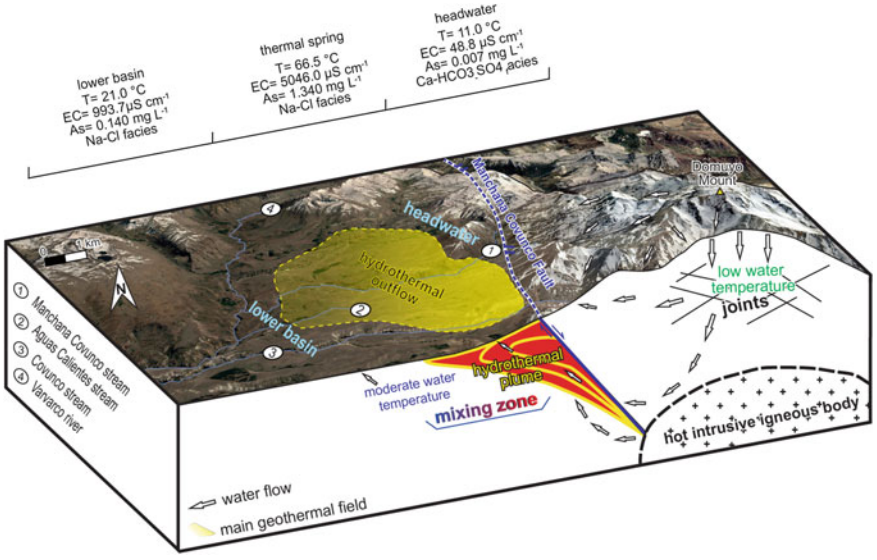

Fig. 7 Conceptual model summarizing the hydrochemical variations observed due to the interaction between the geothermal system studied and the different water streams and springs at the western slopes of the Domuyo Mount

rates, almost two orders of magnitude greater than the studied streams, may suggest that no significant variations in the chemical signature may be expected. However, a slight contribution of Na^+ and Cl^- ions can be detected in the Varvarco River downstream the geothermal field, which can be explained by the chemical facies observed in thermal springs (Figs. 3 and 4a). Upstream the geothermal field, the Varvarco River waters present Ca-SO_4 facies saturated in calcite and subsaturated in gypsum, whose composition would be mainly associated with the contribution of evaporitic rocks, like carbonates and gypsum, rocks outcropping in the upper basin (Zanettini et al. 2001). Downstream the geothermal field, the Varvarco River waters are of the Na-SO_4-Cl type, subsatured in calcite and gypsum and with a tendency to increase in Na^+ and Cl^- concentrations, similar to that of thermal springs, which may indicate its influence in the river chemistry. However, and possibly due to its low dissolved concentrations, both, the Na^+ and Cl^- contents and the distribution patterns of REE, do not show significant modifications in the Varvarco River downstream the geothermal field.

Despite the fact that there are no large populations in the study area, there are small family settlements and also nomadic people who raise livestock, as well as a small village that receives tourists (Aguas Calientes Village, Fig. 1). Thus, chemistry variations resulting from geothermal contribution acquire relevance in the area because stream waters and springs are the only source of water supply for local inhabitants. Although in this system changes associated with major ions and REE have been particularly analyzed, as it was stated above, thermal springs also provide trace elements such as As, which concentrations may cause geogenic contamination of water supply (Villalba et al. 2020), a characteristic that also affects other arid regions around the world (e.g. Ballantyne and Moore 1988; Smedley and Kinniburgh 2002; López et al. 2012).

5 Perspectives and Future Work

Streams and springs of the Domuyo geothermal field are the main sources of water supply for the local inhabitants (small family settlements and Aguas Calientes Village, Fig. 1) in this arid zone of northern Patagonia. In addition, these water courses are tributaries of the Varvarco River, from which small towns, such as Varvarco (60 km to the south) use water as a downstream supply. Therefore, a key aspect to analyze moving forward is the monitoring of changes in water quality over time due to changes in the dynamics of the Domuyo geothermal system and the variations of the recharge rate as a result of seasonal and long term climate changes. Additionally, further work is needed to articulate the research efforts with the local authorities in order to implement efficient water management policies in this remote area.

Acknowledgements This work was carried out thanks to the permits provided by Protected Natural Areas of the Province of Neuquén. Funding for this research was provided by the Agencia Nacional

de Promoción Científica y Tecnológica (PICT 2014-2206 and PICT 2019-4086) and the Consejo Nacional de Investigaciones Científicas y Técnicas (CONICET).

References

Agusto MR (2011) *Estudio geoquímico de los fluídos volcánicos e hidrotermales del Complejo Volcánico Copahue-Caviahue y su aplicación para tareas de seguimiento.* Doctoral thesis. Facultad de Ciencias Exactas y Naturales, Universidad de Buenos Aires (in Spanish)

Astort A, Walter TR, Ruiz F, Sagripanti L, Nacif A, Acosta G et al (2019) Unrest at Domuyo volcano, Argentina, detected by geophysical and geodetic data and morphometric analysis. Remote Sens 11(18):2175

APHA American Public Health Association (2015) Standard methods for the examination of water and wastewater. American Water Works Association, Water Environment Federation, Washington, DC

Ballantyne JM, Moore JN (1988) Arsenic geochemistry in geothermal systems. Geochim Cosmochim Acta 52(2):475–483

Burd AI, Booker JR, Mackie R, Favetto A, Pomposiello MC (2014) Three-dimensional electrical conductivity in the mantle beneath the Payún Matrú Volcanic Field in the Andean backarc of Argentina near 36.5 S: Evidence for decapitation of a mantle plume by resurgent upper mantle shear during slab steepening. Geophys J Int 198(2):812–827

Chiodini G, Liccioli C, Vaselli O, Calabrese S, Tassi F, Caliro S et al (2014) The Domuyo volcanic system: an enormous geothermal resource in Argentine Patagonia. J Volcanol Geotherm Res 274:71–77

Cogliati MG, Ostertag G, Caso M, Finessi FG, Groch D (2018) Análisis del balance hídrico medio mensual en la provincia del Neuquén (Argentina). Boletín Geográfico 40(2):26–44 (in Spanish)

Elderfield HR, Upstill-Goddard R, Sholkovitz ER (1990) The rare earth elements in rivers, estuaries and coastal sea waters: processes affecting crustal input of elements to the ocean and their significance to the composition of seawater. Geochim Cosmochim Acta 54:971–991

Ellis AJ, Mahon WAJ (1964) Natural hidrothermal systems and experimental hot-water/rock interactions. Geochim Cosmochim Acta 28:1324–1367

Ellis AJ, Mahon WAJ (1967) Natural hydrothermal systems and experimental hot-water/rock interactions. Geochim Cosmochim Acta 31:519–538

FAO Food and Agriculture Organization (2015) Documento de Trabajo N°7B: Balance Hídrico de la Cuenca del río Neuquén, Provincia del Neuquén. http://www.fao.org/fileadmin/user_upload/rlc/utf017arg/neuquen/DT_07B_Balance_HC3ADdrico_Cuenca_Neuquen.pdf. Accessed 13 July 2020 (in Spanish)

Galetto A, García V, Caselli A (2018) Structural controls of the Domuyo geothermal field, Southern Andes (36 38′ S), Argentina. J Struct Geol 114:76–94

Giggenbach WF (1997) The origin and evolution of fluids in magmatic-hydrothermal systems. In: Barnes HL (ed) Geochemistry of hydrothermal ore deposits. John Wiley and Sons, New York, pp 737–796

JICA Japan International Cooperation Agency (1983–1984) Ente Provincial de Energía de Neuquén, JICA-EPEN. Argentine Republic. Final Report on the Northern Neuquén Geothermal Development Project, 126

López DL, Bundschuh J, Birkle P, Armienta MA, Cumbal L, Sracek O et al (2012) Arsenic in volcanic geothermal fluids of Latin America. Sci Total Environ 429:57–75

Mas GR, Bengochea L, Mas LC (2000) Hydrothermal alteration at El Humazo Geothermal area, Domuyo Volcano, Argentina. In: Proceedings of the World Geothermal Congress, Kyushu, Tohoku, Japan, pp 1413–1418

Mas LC (2010) History and Present Situation of the Neuquén Geothermal Project. In: Proceedings of World Geothermal Congress. Bali, Indonesia

McLennan SM (1989) Rare earth elements in sedimentary rocks: influence of provenance and sedimentary processes. In: Lipin BR, McKay GA (eds) Geochemistry and mineralogy of rare earth elements, reviews in mineralogy, vol 21. Mineralogical Society of America, Washington D.C., pp 169–200

McLennan SM (2001) Relationships between the trace element sedimentary rocks and upper continental crust. Geochem Geophys Geosyst 2(4): 2000GC000109

Miranda F, Folguera A, Leal PR, Naranjo JA, Pesce A (2006) Upper Pliocene to lower Pleistocene volcanic complexes and upper Neogene deformation in the south-central Andes (36 ° 30 '-38 °S). Geol Soc Am Spec Pap 407:287

Monasterio AM, Armijo F, Hurtado I, Maraver F (2017) Análisis de las aguas minerales de la Provincia del Neuquén, República Argentina. Bol Soc Esp Hidrol Med 32(1):117–118

Panarello H, Sierra JL, Pedro G, D'Amore F (1992) Isotopic and geochemical study of the Domuyo Geothermal field. Neuquén, Argentina (N° IAEA-TECDOC-641)

Parkhurst DL, Appelo C (1999) User's guide to PHREEQC (Version 2): a computer program for speciation, batch-reaction, one-dimensional transport, and inverse geochemical calculations. Water-Resour Inv Rep 99(4259):312

Pesce AH (2013) The Domuyo Geothermal Area, Neuquén, Argentina. Geotherm Resour Council Trans 37:309314

Piper AM (1944) A graphic procedure in the geochemical interpretation of water analyses. Am Geophys Union Trans 25

Polk RE (1994) Interaction between bacteria, nanobacteria, and mineral precipitation in hot-springs in central Italy. Géogr Phys Quat 48:233–246

Smedley PL, Kinniburgh DG (2002) A review of the source, behaviour and distribution of arsenic in natural waters. J Appl Geochem 17(5):517–568

Smiler R (2009) Diagrammes software. Logiciel libre du laboratoired 'Hydrogéologie, universitéd' Avignon. http://www.lha.univavignon.fr/LHA-Logiciels.htm. Accessed 20 July 2020

Tassi F, Liccioli C, Agusto M, Chiodini G, Vaselli O, Calabrese S et al (2016) The hydrothermal system of the Domuyo volcanic complex (Argentina): a conceptual model based on new geochemical and isotopic evidences. J Volcanol Geotherm Res 328:198–209

Vengosh A, Helvacı C, Karamanderesi IH (2002) Geochemical constraints for the origin of thermal waters from western Turkey. J Appl Geochem 17(3):163–183

Villalba E, Tanjal C, Borzi G, Páez G, Carol E (2020) Geogenic arsenic contamination of wet-meadows associated with a geothermal system in an arid region and its relevance for drinking water. Sci Total Environ 137:571

WHO World Health Organization (2008) Guidelines for drinking-water quality: second addendum, vol 1, Recommendations

Zanettini JC, Santamaría GR, Leanza HA (2001) Hoja de la Carta Geológica de la República Argentina E. 1: 250.000 num. 3772-II (Las Ovejas) Provincia del Neuquén. Instituto de Geología y Recursos Minerales, Servicio Geológico Minero Argentino. Secretaría de Minería, Argentina. Boletín 263 (in Spanish)

Hydrogeochemistry of an Acid River and Lake Related to an Active Volcano. The Case of Study: Agrio River—Copahue Volcano in Patagonia, Argentina

Joaquín Llano, María Clara Lamberti, Daniel Sierra, and Mariano Agusto

Abstract During the last three decades, Copahue volcano has been one of the most studied volcanoes in Argentina and Chile. Extensive research has been devoted to studying the geochemistry of rocks and fluids of the Copahue-Caviahue volcanic complex, paying particular attention to the geochemical behavior of the water system. In this study, 275 published analyses of water geochemistry were compiled, in order to describe and revise the processes that control it. Thus, different processes that were previously described in the main volcanic-hydrological system were reanalyzed, such as ions and elements dilution along the Agrio River; alunite, jarosite and barite precipitation in the headwaters; schwertmannite and basaluminite precipitation in the Caviahue Lake and the lower Agrio River. Also, processes such as the incorporation of some elements (As, Tl and Pb) into waters through magmatic gases, and the absortion/adsortion of As, V, Cr and rare earth elements in the hydroxysulfates precipitates are described for the first time.

Keywords Acid waters · Copahue volcano · Schwertmannite · Basaluminite

1 Introduction

Hydrological systems related to active volcanoes around the world usually present characteristics that reflect the contribution of deep magmatic input (Giggenbach 1992; Rowe 1994; Deely and Sheppard 1996; Kusakabe et al. 2000; D'Alessandro

J. Llano (✉) · M. C. Lamberti · M. Agusto
Universidad de Buenos Aires, Facultad de Ciencias Exactas y Naturales, Buenos Aires, Argentina
e-mail: jllano@gl.fcen.uba.ar

J. Llano · M. C. Lamberti · D. Sierra · M. Agusto
Instituto de Estudios Andinos "Don Pablo Groeber", Universidad de Buenos Aires—CONICET, Buenos Aires, Argentina

D. Sierra
Instituto Geofísico de La Escuela Politécnica Nacional, Quito, Ecuador

A. I. Torres and V. A. Campodonico (eds.), *Environmental Assessment of Patagonia's Water Resources*, Environmental Earth Sciences,
https://doi.org/10.1007/978-3-030-89676-8_4

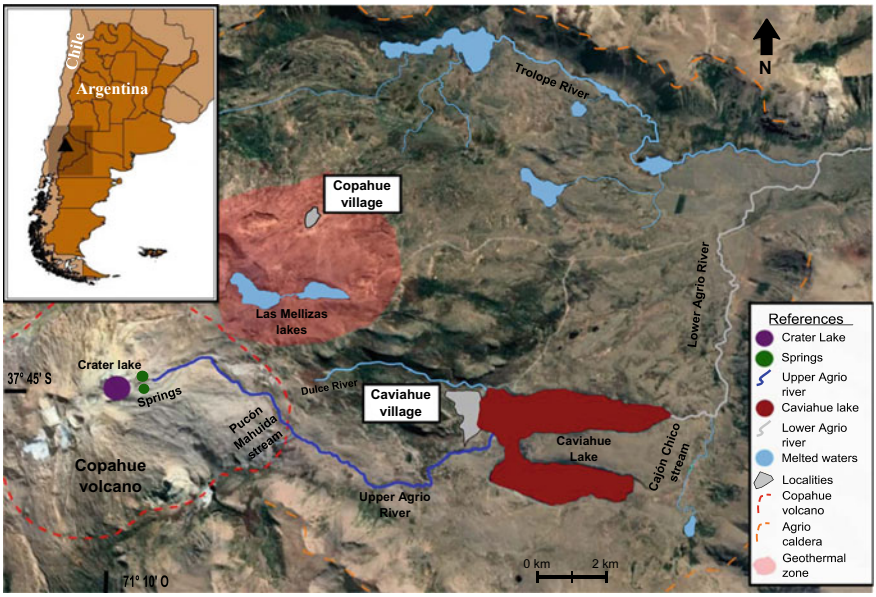

Fig. 1 Location of the Copahue-Caviahue Volcanic Complex. The volcanic hydrological system, melted waters and the geothermal zone are shown

et al. 2008; Varekamp 2015; Tassi et al. 2016). Particularly in the Argentinian Patagonia, the Copahue-Caviahue Volcanic Complex (CCVC) hosts a very uncommon hydrological system, conformed by an acidic river and lake: the Agrio River and the Caviahue Lake (Fig. 1). Copahue volcano (37°51′08″ S—71°10′03″ W), one of the most active volcanoes in the country, located inside the Agrio **caldera**, is constantly emitting volcanic gases. Also, during eruptive events it emits ashes from the eruptive center, affecting the main hydrological system in the area (Naranjo and Polanco 2004; Agusto et al. 2012, 2017). This volcano presented several recent eruptions in the last 30 years (Delpino and Bermúdez 1993; Naranjo and Polanco 2004; Petrinovic et al. 2014; Caselli et al. 2016; Agusto and Velez 2017), being this the reason why Copahue is one of the most studied volcanoes in Argentina (Mas et al. 1996; Linares et al. 1999; Folguera and Ramos 2000; Melnick et al. 2006; Varekamp et al. 2006; Ibáñez et al. 2008; Velez et al. 2011; Agusto et al. 2013; Chiodini et al. 2015; Tamburello et al. 2015; Balbis et al. 2016; Daga et al. 2016; Roulleau et al. 2016, 2017; Tassi et al. 2017; Albite et al. 2019; Barcelona et al. 2019; Lamberti et al. 2019; Báez et al. 2020; Cabrera et al. 2020). In the CCVC, acidic volcanic gases are constantly emitted from the deep **magmatic chamber**, reaching the surface and interacting with superficial meteoric waters. These gases heat and acidify the waters, developing an acidic shallow **hydrothermal system** which affects the surface water composition, that was widely studied for over three decades (Mas et al. 1996; Panarello 2002; Agusto et al. 2012, 2017; Varekamp 2008; Varekamp et al. 2009; Pedrozo et al. 2010; Farnfield

et al. 2012; Cabrera et al. 2016, 2020; Gaviria Reyes et al. 2016; Temporetti et al. 2019; Candela-Becerra et al. 2020).

In this work, all the available chemical analysis from different authors (Gammons et al. 2005; Parker et al. 2008; Chiacchiarini et al. 2010; Alexander 2014; Agusto and Varekamp 2016; Llano 2016; Rodriguez et al. 2016; Szentiványi 2018; Llano et al. 2020) were compiled, in order to revise the characteristics and processes previously described in the literature. Besides, interpretations of processes that have not been described yet in the system are provided here: such as the incorporation of some trace elements to waters through the gas emission, or the adsorption and absorption processes in the hydroxysulfates which precipitate in the Agrio River and Caviahue Lake.

2 Study Area

2.1 Geological Setting

The CCVC is comprised in the South Volcanic Zone (33° S—46° S) of the Andean range and it is located almost 30 km to the east of the actual volcanic arc front (Folguera et al. 2002; Melnick et al. 2006). The Agrio caldera is part of the CCVC, with Copahue volcano as the most distinctive geographical feature (Fig. 1). This is an active andesitic to basaltic **stratovolcano** of 1.2 Ma (Linares et al. 1999). It has 9 craters oriented N40°E. Nowadays, the active crater is the one located easternmost. **Phreatomagmatic** and **phreatic eruptions** have been constant during the last 250 years (Naranjo and Polanco 2004). The last eruptive cycles occurred in 1992, 1995, 2000 and from 2012-to nowadays (Delpino and Bermúdez 1993, 2002; Petrinovic et al. 2014; Agusto et al. 2017; OAVV 2021). The CCVC water geochemistry is modified by the gas emissions from the magmatic chamber (Agusto 2011; Agusto et al. 2012; Agusto and Varekamp 2016), evidenced by lower pH, higher conductivities and higher ion concentrations during eruptive periods.

Inside the CVCC there is a geothermal zone located in the northeast of the volcano (Fig. 1), that consist of five areas with fluid emissions of boiling, bubbling and mud pools with temperatures up to 96 °C and fumaroles with temperatures up to 160 °C (Agusto et al. 2013; Agusto and Velez 2017).

2.2 The Hydrological System of the Caviahue-Copahue Volcanic Complex

The water bodies inside the Agrio caldera have different geochemical characteristics. Agusto (2011) classified them into three distinct groups: waters from the volcanic hydrological system, steam heated waters of the geothermal zone and snow melted

waters. The first group corresponds to the **headwaters** at the volcano summit and the hydrological system that is originated at this site, being characterized by low pH (0.5–2.5) and high conductivity. High ionic concentrations are also distinctive features of this group, which are controlled by the interactions between the meteoric waters, the magmatic gases and host rock dissolution. The main acid magmatic gases (CO_2, SO_2, HCl, HF) interact with the aquifer producing the principal anions (SO_4^{2-}, Cl^-, F^-), not being in solution HCO_3^- due to the high water acidity (Agusto and Varekamp 2016). The major cations (Na^+, K^+, Ca^{2+}, Mg^{2+}), minor cations (Fe, Al), trace elements and **rare earth elements** (**REE**) are readily released from the host rock to solution. This process is favored by the low pH and the high temperatures of waters. The snow melted waters group is characterized by meteoric compositions with typical neutral pH and low conductivity values.

The main acidic waters constitute a hydrological system formed in the upper part of the Copahue volcano (Fig. 1). In addition, depending on the volcano activity, a high temperature and low pH volcanic crater lake is developed (Fig. 2a; Agusto and Velez 2017). During the volcano quiescent periods, the active crater usually presents a lake with diameters between 200 and 250 m and 35 m deep (Varekamp 2008). However, its appearance is highly variable depending on seasonal changes and volcanic state of activity (Agusto and Varekamp 2016; Llano et al. 2020). Its usual aspect is gray to green with permanent vapors emission and floating yellow sulfur (Varekamp 2008; Agusto 2011). The hot and acidic aquifer, a shallow volcanic-hydrothermal system developed below the top of the volcanic edifice, feds two springs (pH 1–2) which emerge from the eastern flank (Fig. 2b) and merge downstream to form the Upper Agrio River (Fig. 2c). This river flows from the eastern flank of the volcano for 18 km before reaching the Caviahue Lake (Fig. 2e), which has seasonally controlled temperature and pH values of 2–3. This lake has a horseshoe shape formed by glacial canyons or tectonovolcanic faults, with a maximum depth of approximately 90 m deep (Melnick et al. 2006; Varekamp 2008). It is stratified during summer season with a termocline around 35 m deep, while during winter season is fully mixed. Nevertheless, the lake does not present strong compositional stratification (Varekamp 2008). The only lake effluent is located in the northern arm, and it is called the Lower Agrio River, which merges with other rivers several kilometers outside the Agrio caldera. Along the Agrio River and the Caviahue Lake, the inflow of melted waters is constant (Fig. 2d). This contribution comes from permanent tributaries, such as the Pucón Mahuida stream, Dulce River, Trolope River, Cajón Chico stream and ephemeral tributaries developed during the spring and summer seasons.

3 Methodology

Many authors have studied the hydrological system related to Copahue volcano, providing a large amount of chemical analysis that we have compiled in this work. In this way, 275 water chemical analysis of the CVCC that have been published in the last twenty years (Gammons et al. 2005; Parker et al. 2008; Chiacchiarini

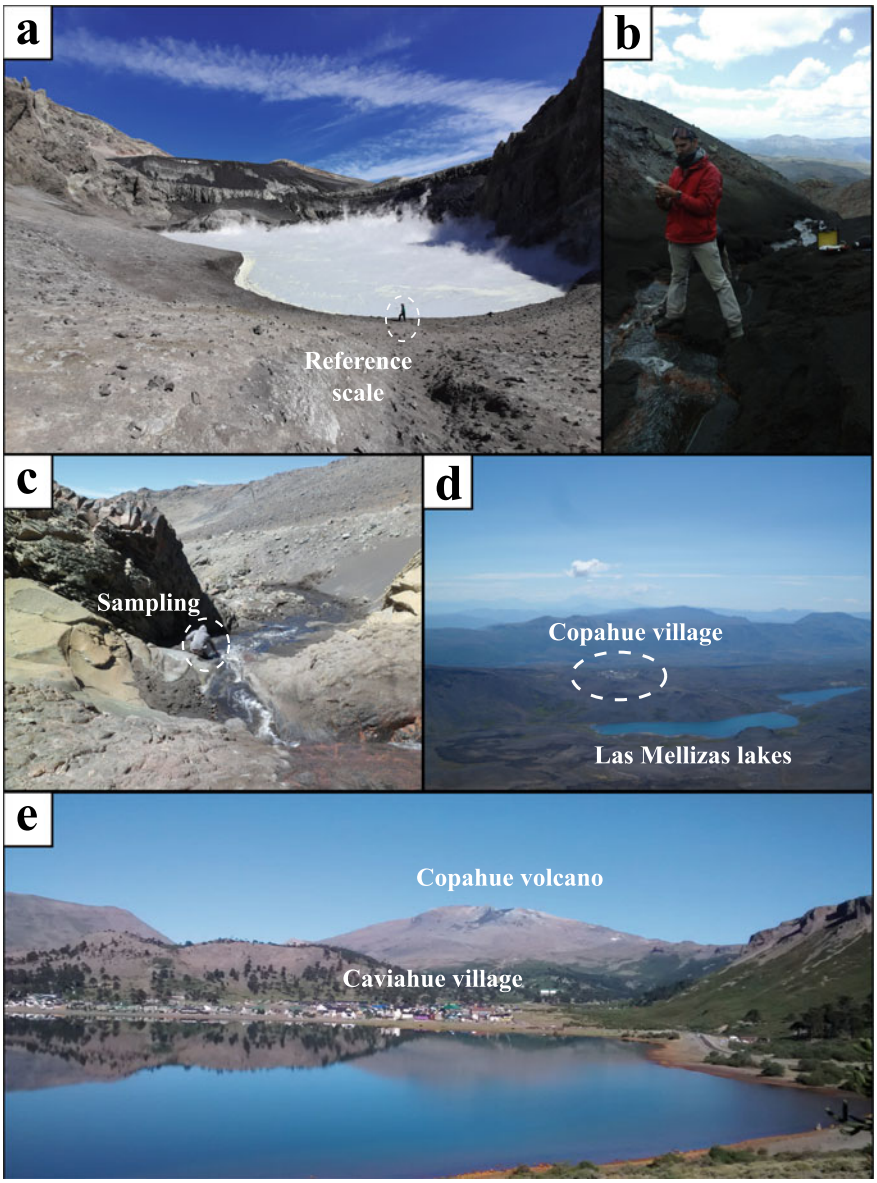

Fig. 2 **a** Crater Lake with reference scale, **b** sampling at the spring, **c** view of the Upper Agrio River near Caviahue village, **d** view from the Copahue volcano to Las Mellizas Lakes and the Copahue village, **e** view of Copahue volcano, Caviahue village and Caviahue Lake

et al. 2010; Alexander 2014; Agusto and Varekamp 2016; Llano 2016; Rodriguez et al. 2016; Szentiványi 2018; Llano et al. 2020) were used to describe the system and revise the processes that control water geochemistry. Of the total samples, 241 correspond to the volcanic hydrological system waters and 34 to melted waters. It is important to bear in mind that not all the chemical analyses are complete: most of them do not present trace elements and REE analyses, and there are many gaps in the physico-chemical parameters data.

For a better comparison between the different analyzed elements, a rock sample NV-30 from Las Mellizas formation (Roulleau et al. 2018) was used as reference for the host rock composition. Also, Cl^- and Na^+ were used as reference for all the binary diagrams, due to their condition of conservative elements (Agusto 2011).

4 Results

Although many of the cited authors have described the system chemistry, only a few have classified the waters using a ternary or a Langelier-Ludwing diagram (Agusto 2011; Agusto and Varekamp 2016; Szentiványi 2018; Llano et al. 2020). Figure 3 corresponds to the ternary diagram where major ionic composition is represented.

Waters from the main volcanic hydrological system are SO_4^{2-}–Cl^-, where samples from the upstream sector of the system, including the crater lake, springs and the Upper Agrio River, have SO_4^{2-}/Cl^- ratios that vary from 0.7 to 10, whereas the Caviahue Lake and the Lower Agrio River exhibit SO_4^{2-}/Cl^- ratios which are more homogeneous, closer to the sulfate corner, with an average of 5.3 (Fig. 3). This may be due to the significant input of melted waters to the lower part of the hydrological system, as this group has an average SO_4^{2-}/Cl^- ratio of 3.8. The reason why melted waters exhibit these ratio values is its null interaction with magmatic

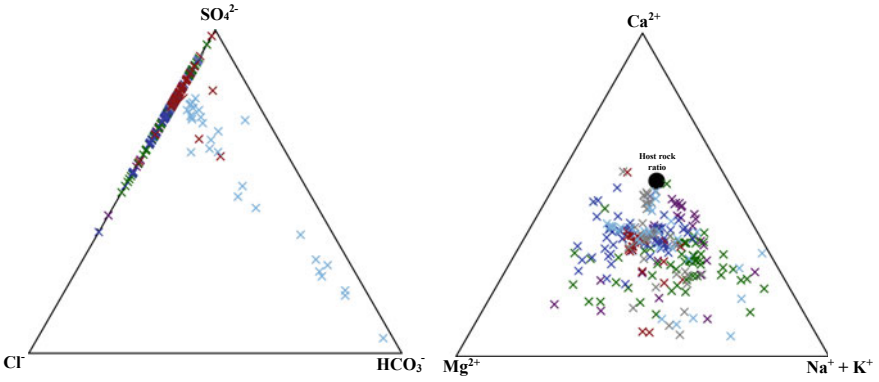

Fig. 3 Ternary diagrams for the different samples used in this study. Purple: Crater Lake; green: Springs; blue: Upper Agrio River; brown: Caviahue Lake; gray: Lower Agrio River; light blue: Melted waters; black circle: NV-30 rock sample (Roulleau et al. 2018)

gases. However, the interaction between some waters with volcanic ash might be a noteworthy process (Naranjo and Polanco 2004). An example of this is provided by the Pucón Mahuida stream (Fig. 1) where pH is usually below 6 and the F^- concentrations are above 2 ppm (Daga et al. 2016; Rodriguez et al. 2016; Szentiványi 2018; Llano et al. 2020). Nevertheless, melted waters composition varies from SO_4^{2-} to SO_4^{2-}–HCO_3^- and to strictly HCO_3^-.

The cations ternary diagram shows that almost all the samples are depleted on Ca^{2+} as compared to the NV-30 sample (Fig. 3). On the other hand, some samples show a Mg^{2+} enrichment, due to the input and dissolution of fresh magmatic material during eruptive events (Varekamp 2008; Agusto et al. 2012; Agusto and Varekamp 2016). All sampling sites show a spread plot, with no preferential cation ratios.

A common process in CCVC waters is the dilution of acidic waters all along the Agrio River due to the constant inflow of melted waters. This phenomenon can be inferred from the diagrams shown in Fig. 4, where a continuous decrease in the conductivity values together with the Cl^- concentrations is observed (Fig. 4a), as it happens with the SO_4^{2-} (Fig. 4b) and the F^- (Fig. 4c). Both, Cl^- and F^- have a conservative behavior, while SO_4^{2-} participates in the precipitation of different solids, such as **alunite** or anhydrite in the headwaters (Varekamp 2015; Agusto and Varekamp 2016). Nevertheless, no significant change in SO_4^{2-} concentrations is noticed, apart from the dilution along the system. Particularly, the pH (Fig. 4d) shows

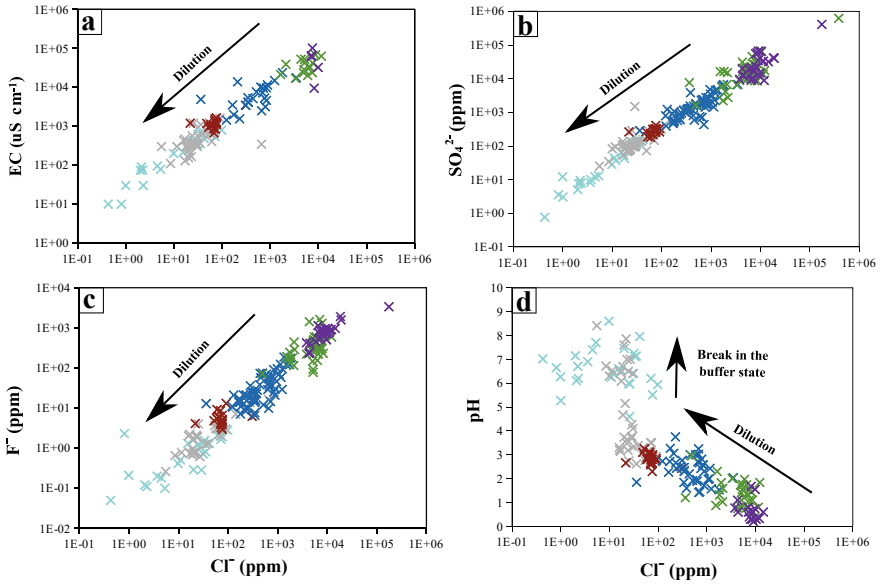

Fig. 4 **a** Electrical Conductivity, **b** SO_4^{2-}, **c** F^- and **d** pH versus Cl^-. The samples tendency is presented with the dilution process. In **d** its also recognized the change in the pH, breaking the buffer state. Purple: Crater Lake; green: springs; blue: Upper Agrio River; brown: Caviahue Lake; gray: Lower Agrio River; light blue: Melted waters

a continuous but more heterogeneous increase along the Agrio River watercourse, with a break around pH 3, particularly in the Lower Agrio River samples.

5 Discussion

5.1 Major Cations

The dilution process affects not only the physico-chemical parameters and the major ions, but also the contents of trace elements and REE. In Fig. 5, major cation

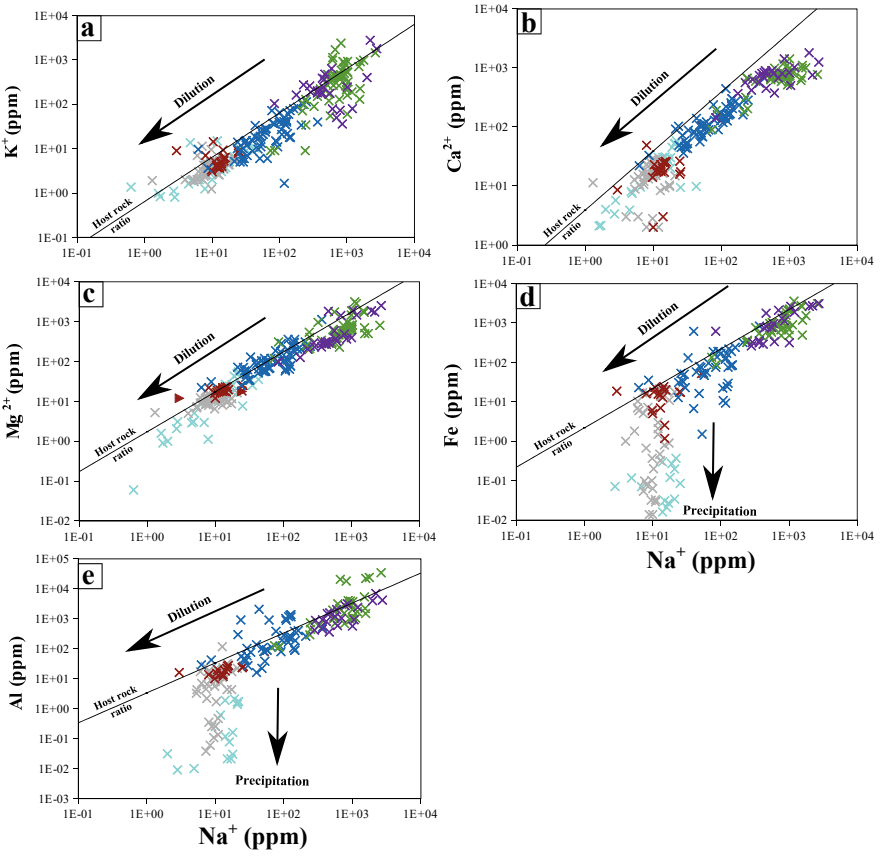

Fig. 5 **a** K^+, **b** Ca^{2+}, **c** Mg^{2+}, **d** Fe and **e** Al versus Na^+. It is presented the samples tendency with the dilution process. In **d** and **e** it is also recognized the hydroxysulfates precipitation due to pH increase. Purple: Crater Lake; green: Springs; blue: Upper Agrio River; brown: Caviahue Lake; gray: Lower Agrio River; light blue: Melted waters; black line: NV-30 rock sample ratio (Roulleau et al. 2018)

concentrations versus Na^+ concentrations in the hydrological system are plotted.

Potassium concentrations plot on the line defined by the host rock K-Na^+ ratios (Fig. 5a), showing that the incorporation of this element to waters is mainly through the dissolution of the host rock. Nevertheless, some samples of the crater lake and streams show an enrichment and also depletion in this element. This might be due to the precipitation and possibly redissolution of alunite at the hot and acidic headwaters (Gammons et al. 2005; Varekamp 2015; Agusto and Varekamp 2016). Downstream, K^+ is only affected by dilution along the hydrological system. Also at the headwaters, the precipitation of anhydrite or gypsum directly affects Ca^{2+} concentrations (Fig. 5b; Gammons et al. 2005; Varekamp 2008, 2015; Agusto and Varekamp 2016), but in this case the redissolution of these minerals does not occur. For this reason, all waters from the CCVC hydrological system show a depletion in the Ca^{2+} concentrations compared to the line defined by the host rock Ca-Na ratios. Mg^{2+} concentrations show a very similar trend to the ratios of NV-30 sample (Fig. 5c), although an enrichment of this element in waters previously and after a volcanic eruption was recognized, through the dissolution of fresh material incorporated to the system (Gammons et al. 2005; Varekamp 2008). Both Ca^{2+} and Mg^{2+} concentrations along the main system are affected by the dilution caused by melted waters input.

Regarding Fe concentrations (Fig. 5d), very similar values to the line defined by host rock ratios can be recognized, although precipitation of **jarosite** is described at the headwaters system (Gammons et al. 2005). Dilution is recognized along the main course of the Agrio River, until Na^+ concentrations of nearly 50 ppm are reached. At this point, in some samples from Caviahue Lake and Lower Agrio River, Fe concentrations reach values below 1 ppm, showing a slope break (Fig. 5d). This drop in Fe concentrations is directly related to the precipitation of **schwertmannite**, which occurs at approximately pH 3 in the study system (Caraballo et al. 2013; Alexander 2014; Agusto and Varekamp 2016; Llano 2016; Rodriguez et al. 2016; Llano et al. 2020). As the volcanic-hydrological system is very dynamic, the geographical position where the system reaches this pH continuously changes, therefore the schwertmannite precipitation occurs at different places through time. This occurs for two main reasons: the eruptive activity of Copahue volcano, which causes a decrease of pH during high activity periods (Agusto et al. 2012; Alexander 2014; Agusto and Varekamp 2016; Szentiványi 2018); and seasonal melted water inflows.

The Al presents a similar behavior to Fe. Along most of the system, Al-Na^+ ratios are close to the host rock ratios (Fig. 5e). Particularly, at the headwaters some samples show enriched values due to the redissolution of alunite (Varekamp 2015; Agusto and Varekamp 2016). When the system reaches concentrations near 10 ppm of Na^+, a break in the Al-Na^+ ratios slope is recognized showing samples with Al concentrations below 1 ppm. In this case, the Al hydroxysulfate precipitation occurs at pH between 4 and 5 (Bigham and Nordstrom 2000; Sánchez-España et al. 2011).

5.2 *Trace and Rare Earth Elements*

According to their behavior, trace elements in the CCVC hydrological system can be categorized into four different groups: (a) mobile elements; (b) relatively mobile elements; (c) immobile elements; (d) elements that are incorporated into waters through magmatic gases.

Mobile elements consist of Mn, Ni and Zn, and they are represented by Mn in Fig. 6a. Here, water Mn-Na^+ ratios are very close to the host rock ones, although a depletion of these trace elements at the headwaters of the system can be recognized. As it was described by Varekamp et al. (2009), Mn and Ni present high concentrations after the 90´s eruptive events. Particularly, Ni has been described as an element

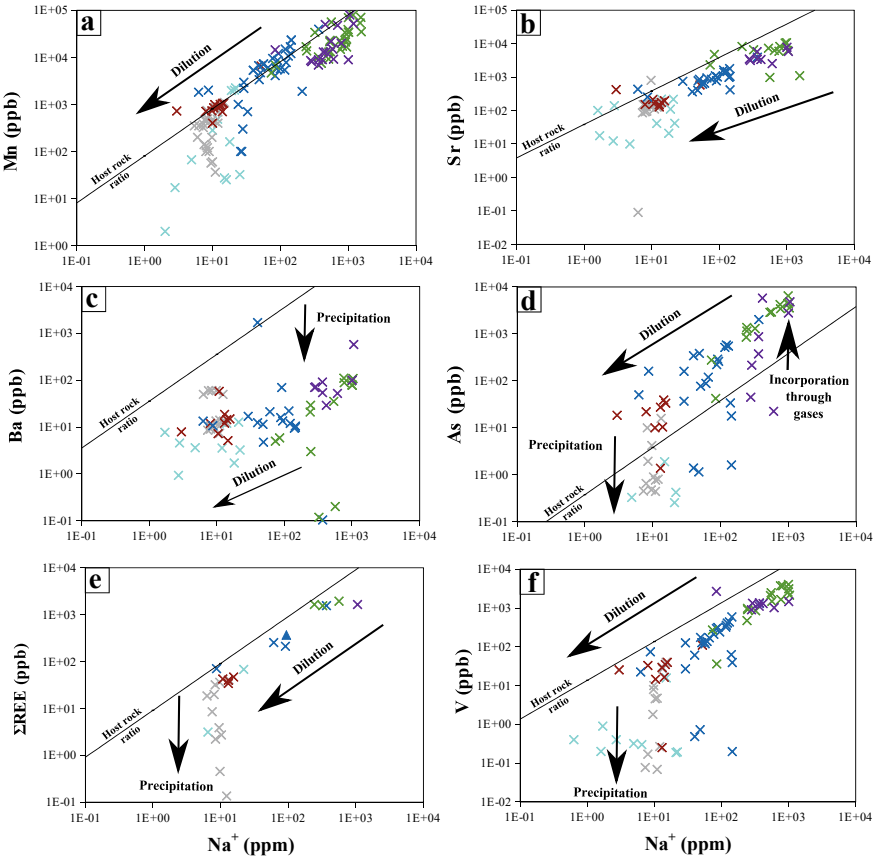

Fig. 6 **a** Mn, **b** Sr, **c** Ba, **d** As, **e** RRE and **f** V versus Na + . The samples tendency according to the dilution process is also presented. In **c**, **d**, **e** and **f** precipitation processes are also recognized. In **d** the incorporation of As into waters through magmatic gases is visualized. Purple: Crater Lake; green: Springs; blue: Upper Agrio River; brown: Caviahue Lake; gray: Lower Agrio River; light blue: Melted waters; black line: NV-30 rock sample ratio (Roulleau et al. 2018)

that can be incorporated into the shallow hydrothermal system by magmatic gases (Varekamp et al. 2009). However, this phenomenon was not recognized during the last eruptive period which started in 2012. The three elements of this group are affected by dilution process along the system. In melted waters, these elements can precipitate as secondary minerals (Stumm and Morgan 1996), as it is also recognized for some near-neutral Lower Agrio River samples (Fig. 6a).

Relatively mobile elements are Sr, Be, Co, Cr, Cs, Rb, Th, U, V and Y (not shown); the behavior of these elements is represented in Fig. 6b by Sr. All of them show ratios close to the line defined by the host rock ratio, but they are slightly more depleted than the mobile elements. Particularly, Rb and Sr can be enriched in waters after eruptive processes, as well as Co and Cr, due to olivine and sulfides dissolution. However, Co can precipitate as oxides or sulfides during non-eruptive periods (Varekamp et al. 2009). Relatively mobile elements concentrations are controlled by the dilution effect.

The group defined as immobile elements includes Ba, Bi, Cu, Hf, Mo, Sn, Ta, Ti and Zr. In Fig. 6c, Ba-Na^+ ratios from the water system are represented against the Ba-Na^+ ratio of NV-30 sample, showing that the former samples plot far from the latter. This decoupling respect to the host rock ratio is the consequence of Ba precipitation as baryte at the headwaters system (Gammons et al. 2005; Varekamp et al. 2009), while the rest of the elements can precipitate also at the headwaters as secondary minerals like **cassiterite** (SnO_2) or **molybdenite** (MoS_2), or they can be mostly retained in the host rock, as it occurs with Bi, Ti, Ta, Zr and Hf (Gammons et al. 2005; Varekamp et al. 2009).

The last group comprises the elements that are incorporated to the system through the magmatic gases, besides the water–rock interaction. It was recognized in other volcanic environments of the world that some elements (As, B, Cd, Pb, Sb and Tl) can be incorporated into the hydrological system by the gas phase or the aerosols (Aiuppa et al. 2003; Taran et al. 2008; Calabrese et al. 2011; Kaasalainen and Stefánsson 2012; Varekamp 2015). For this reason, these elements can constitute a precursor signal of volcanic activity, though more studies are needed to demonstrate this idea.

Being the As the representative of this group in Fig. 6d, it is recognized that the As-Na^+ ratios of most waters are above the As-Na^+ ratio of the host rock. The As enrichment is a consequence of its incorporation into waters through the magmatic gases contribution at the headwaters. The other elements that present the same behavior in the system are Tl and Pb.

It must be noted that the behavior evaluation of B, Cd and Sb could not be done due to the lack of data of these element concentrations in the rocks of this area.

In the case of REE, their behavior is similar to the relatively mobile elements, as they plot closely below the line defined by the REE-Na^+ ratio of the host rock (Fig. 6e). There is a remarkable break in the slope around Na^+ concentrations of 10 ppm, which can be related to hydroxysulfates precipitation. This process will be more discussed in the following section.

5.3 *Hydroxysulfates Precipitation*

The schwertmannite is an iron hydroxysulfate, very common in acidic waters mainly related to acid mine and rock drainage (Bigham et al. 1996; Yu et al. 1999; Bigham and Nordstrom 2000; Regenspurg et al. 2004; Jönsson et al. 2005; Regenspurg and Peiffer 2005; Sánchez-España 2007; Sánchez-España et al. 2011; Lecomte et al. 2017; Galván et al. 2018), but its occurrence is also recognized in environments related to active volcanic systems (Delmelle and Bernard 2000; Kawano and Tomita 2001; Palmer et al. 2011; Ohsawa et al. 2014). The mineral stoichiometry is $Fe_8O_8(OH)_x(SO_4)_y$ with $8 - x = 2y$ and $1 < y < 1.75$, it has a characteristic orange color (Fig. 7a) and its structure can vary from a low internal order to amorphous (Sánchez-España et al. 2011). In the Agrio River and Caviahue Lake, schwertmannite was recognized from XRD patterns (Fig. 7b) and from chemical analysis (Alexander 2014; Rodriguez et al. 2016). Llano et al. (2020) calculated the $\log(K_{Sch})$ in this particular system, as it was calculated for other systems in other regions of the world (Bigham et al. 1996; Yu et al. 1999; Kawano and Tomita 2001; Majzlan et al. 2004; Regenspurg and Peiffer 2005; Sánchez-España et al. 2011), obtaining two values with different methods. Using the Fe^{3+} activity versus pH a $\log(K_{Sch})$ of 17.17 ± 1.29 was calculated, whereas when using the ionic activity product (IAP) versus pH an average log(IAP) of 17.64 ± 3.42 was obtained. These values are in

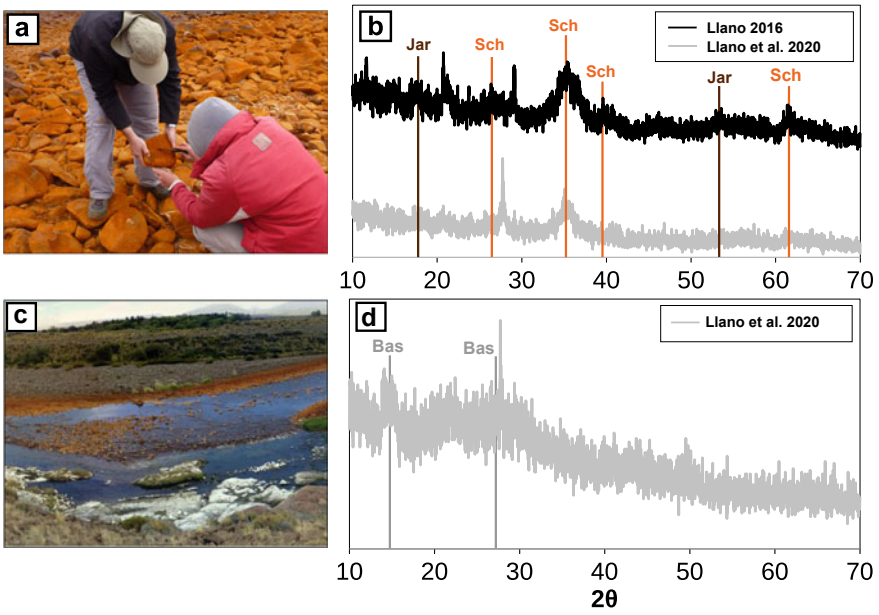

Fig. 7 **a** Schwertmannite precipitation at the Lower Agrio River; **b** XRD samples classified as schwertmannite; **c** basaluminite precipitation; **d** XRD sample classified as basaluminite. Sch: schwertmannite; Jar: jarosite; Bas: basalulminite (modified from Llano et al. 2020)

the same range than the ones calculated by Bigham et al. (1996) of 18 ± 2.5 and by Sánchez-España et al. (2011) of 18.8 ± 1.7 and 18.8 ± 3.5 for different acid mine drainage systems.

The Al case is different to that of Fe, as it is not well defined which precipitation is present in the Lower Agrio River. Some authors, such as Bigham and Nordstrom (2000) or Sánchez-España et al. (2011) have recognized different species of Al precipitation in other water systems, such as amorphous $Al(OH)_3$, **jurbanite** ($AlSO_4(OH)\cdot H_2O$), and hydrobasaluminite ($Al_4(SO_4)(OH)_{10}\cdot 12\text{-}36H_2O$) which recrystallizes to **basaluminite** ($Al_4(SO_4)(OH)_{10}$) when the precipitate gets dehydrated, therefore forming a continuous and diffuse sequence (Sánchez-España et al. 2011). These minerals have been less studied than schwertmannite, especially in the Agrio River system. The precipitate exhibits a white color, very amorphous solid phase (Fig. 7c) with a highly noisy XRD pattern (Fig. 7d) due to its low crystallinity structure (Sánchez-España et al. 2011). Llano et al. (2020) preliminary defined the mineral as basaluminite and a $\log(K_{Bas})$ was calculated, obtaining a value of 21.39 ± 2.05 using the Al activity and an average log(IAP) of 23.95 ± 1.26. These values are very similar to the ones obtained in acid mine drainage systems by Adams and Rawajfih (1977) of 21.7 to 24.1 and by Sánchez-España et al. (2011) of 23.9 ± 0.7 and 23.0 ± 2.7.

Analyzing the concentration distributions of the trace elements in the CCVC hydrological system, it is remarkable that most of them are only affected by dilution process. Nevertheless, in the Caviahue Lake and Lower Agrio River, it is recognized that As, Cr and V present a break in the slope in the same way as Fe and Al, being evidenced in Figs. 6d and 6f, with a high correlation between As and V ($R^2 = 0.99$; Farnfield et al. 2012).

The poorly crystalline schwertmannite and basaluminite structures cause the high specific surface area of these precipitates, favoring the adsorption of ions and complexes onto the precipitates surface as it was described by other authors (Sánchez-España et al. 2006, 2011; Wanner et al. 2018). As, V and Cr tend to form oxoanions with high negative charges (AsO_4^{3-}, VO_4^{3-} and CrO_4^{2-}, respectively), so they are favored to be adsorbed as they are attracted by the high density positive charges in the mineral surface. A similar process occurs in the system with P and its oxoanion PO_4^{3-} (Temporetti et al. 2019). While Cr has the same structure than SO_4^{2-} anion, therefore the absorption of this oxoanion into minerals internal structure is very common and has been experimentally demonstrated (e.g. Antelo et al. 2012). Many authors support the idea that As and V are adsorbed onto schwertmannite and basaluminite surface, preferentially over Cr (Bigham and Nordstrom 2000; Carlson et al. 2002; Fukushi et al. 2003; Jönsson et al. 2005; Regenspurg and Peiffer 2005; Antelo et al. 2012; Sánchez-España et al. 2016a; Wanner et al. 2018). Conversely, few authors have proposed the incorporation of these elements into the mineral structure (Fukushi et al. 2003; Regenspurg and Peiffer 2005; Antelo et al. 2012). In any case, high concentrations of As and V compared to the rest of trace elements were measured in Copahue schwertmannite (Alexander 2014; Rodríguez et al. 2016). Nevertheless, a significative abundance of Cr was not recognized in schwertmannite composition,

therefore it can be predominantly taken in the basaluminite structure at the Agrio River waters (Sánchez-España 2007; Sánchez-España et al. 2016b).

As it was mentioned above, the REE show a break in the slope concentrations along the Agrio River. The adsorption of this group of elements onto **colloid** surfaces has been described (Lewis et al. 1997; Verplanck et al. 2004), but in acidic systems REE have a conservative behavior until pH 5.5 (Gammons et al. 2005; Wood et al. 2006). Consequently, it is here proposed that neither schwertmannite nor basaluminite precipitation affects the REE concentrations below pH 5, but at higher pH the adsorption of REE onto basaluminite occurs.

In this system, the development of REE complexes diminishes downstream, as the REE are present mostly as free ions (Gammons et al. 2005). But when REE are found in complexes, they are mostly present as $LnSO_4^+$ (being Ln any REE), favoring the adsorption of these molecules onto the hydroxo surfaces (Moller 2002; Lozano et al. 2020), and therefore their concentrations are very dependent on the pH. Moreover, heavy REE are more easily adsorbed onto minerals surface than light REE when they interact with the hydroxysulfates precipitates (Gammons et al. 2005; Wood et al. 2006; Lozano et al. 2019). As a result, REE do not coprecipitate with hydroxysulfates at the CCVC hydrological system, but they tend to be adsorbed once the system reaches pH values near 5 to 5.5. Nevertheless, it is recommended a thoroughly analysis of the REE concentrations in schwertmannite and basaluminite to complement this study.

6 Conclusions

This work has compiled most of the available analytical data from studies made at the CCVC hydrological system, describing processes that control the chemistry of the headwaters and along the Agrio River and the Caviahue Lake. Furthermore, an analysis and classification of trace elements, based on their behavior in the system, is provided.

The main characteristics of the system are originated on top of the Copahue volcano, by the interaction between the snow melted waters in the summit and the acidic volcanic gases emitted from the deep magma chamber. These gases acidify and heat the waters of the volcanic-hydrothermal system that feed the crater lake and springs, favoring a more intense water–rock interaction, therefore enriching the elements concentrations in the headwaters of the Agrio River. Some ions and elements precipitate in this part of the system as different secondary minerals, but most of them are not affected by this process. Along the main river, dilution is recognized as the main process that controls all ions and element concentrations. Dilution is caused by the income of melted waters into the main river, affecting the physico-chemical parameters of the hydrological system.

Trace elements have been clustered into four groups, according to their behavior at the headwaters: mobile elements (Mn, Ni, Zn); relatively mobile elements (e.g. Be, Cr, Rb, Sr, etc.); immobile elements (e.g. Ba, Hf, Mo, Zr, etc.); and elements that

are incorporated into waters through magmatic gases (As, Tl and Pb, possibly B, Cd and Sb). Particularly, this last group of elements can provide valuable information about the volcanic activity, but further investigations must be carried out.

The other remarkable process that occurs in the hydrological system involves the precipitation of minerals of Fe and Al, which tends to precipitate as hydroxysulfates when water reaches pH values of 3 and 4–5 respectively. These processes also involve As, V and Cr, as they are adsorbed and/or absorbed by the precipitates. Something similar occurs with REE that are adsorbed onto basaluminite mineral surfaces at pH near 5.5.

This study contributes to the knowledge of the volcano-associated hydrological system, compiling most of the geochemical information of waters generated in the last 25 years and providing new interpretations about the processes controlling water characteristics of this area.

Acknowledgements The research leading to these results has received funding from the projects UBACyT 20020150200230BA, UBACyT 20020170200221BA, PICT-2015-3110, PICT-2016-2624 and Proyecto de Unidad Ejecutora (IDEAN) 22920160100051.

References

Adams F, Rawajfih Z (1977) Basaluminite and alunite: a possible cause of sulfate retention by acid soils. Soil Sci Soc Am J 41:686–692

Agusto M (2011) Estudio geoquímico de los fluidos volcánicos e hidrotermales del Complejo volcánico Copahue Caviahue y su aplicación para tareas de seguimiento. Ph.D. Thesis, University of Buenos Aires (in Spanish)

Agusto M, Caselli A, Tassi F, Dos Santos Afonso M, Vaselli O (2012) Seguimiento geoquímico de las aguas ácidas del sistema volcán Copahue-Río Agrio: Posible aplicación para la identificación de precursores eruptivos. RAGA 69:481–495 (in Spanish)

Agusto M, Tassi F, Caselli A, Vaselli O, Rouwet D, Capaccioni B, Caliro S, Chiodini G, Darrah T (2013) Gas geochemistry of the magmatic-hydrothermal fluid reservoir in the Copahue-Caviahue Volcanic Complex (Argentina). J Volcanol Geotherm Res 257:44–56

Agusto MR, Caselli A, Daga R, Varekamp J, Trinelli A, Dos Santos Afonso M, Guevara SR (2017) The crater lake of copahue volcano (Argentina): geochemical and thermal changes between 1995 and 2015. Geol Soc Lond Spec Publ 1:107–130

Agusto M, Varekamp J (2016) The copahue volcanic-hydrotermal system and applications for volcanic surveillance. In: Tassi F, Vaselli O, Caselli A (eds) Copahue volcano, active volcanoes of the world book series. Springer, Berlin, pp 1999–2038

Agusto M, Velez L (2017) Avances en el conocimiento del sistema volcánico-hidrotermal del Copahue: a 100 años del trabajo pionero de don Pablo Groeber. RAGA 74(1):109–124 (in Spanish)

Aiuppa A, Bellomo S, Brusca L, D'Alessandro W, Federico C (2003) Natural and anthropogenic factors affecting groundwater quality of an active volcano (Mt. Etna, Italy). Appl Geochem 18(6):863–882

Albite JM, Vigide NC, Caselli AT (2019) Caracterización de eventos glacivolcánicos en el Complejo volcánico Caviahue-Copahue y en la Formación Hualcupén, provincia del Neuquén. RAGA 76(3):183–198 (in Spanish)

Alexander E (2014) Aqueous geochemistry of an active magmato-hydrothermal system: Copahue Volcano, Río Agrio and Lake Caviahue, Neuquén, Argentina. Undergraduate Thesis, Wesleyan University

Antelo J, Fiol S, Gondar D, López R, Arce F (2012) Comparison of arsenate, chromate and molybdate binding on schwertmannite: Surface adsorption vs anion-exchange. J Colloid Interface Sci 386(1):338–343

Báez AD, Báez W, Caselli AT, Martini MA, Sommer CA (2020) The glaciovolcanic evolution of the Copahue volcano, Andean Southern Volcanic Zone, Argentina-Chile. J Volcanol Geotherm Res 396:106866

Balbis C, Petrinovic IA, Guzmán S (2016) A contribution to the hazards assessment at Copahue volcano (Argentina-Chile) by facies analysis of a recent pyroclastic density current deposit. J Volcanol Geotherm Res 327:288–298

Barcelona H, Yagupsky D, Vigide N, Senger M (2019) Structural model and slip-dilation tendency analysis at the Copahue geothermal system: inferences on the reservoir geometry. J Volcanol Geotherm Res 375:18–31

Bigham JM, Schwertmann U, Traina S, Winland R, Wolf M (1996) Schwertmannite and the chemical modeling of iron in acid sulfate waters. Geochim Cosmochim Acta 60:2111–2121

Bigham JM, Nordstrom DK (2000) Iron and aluminum hydroxusulfates from acid sulfate waters. Rev Mineral Geochem 40:351–403

Cabrera JM, Diaz MM, Schultz S, Temporetti P, Pedrozo F (2016) Iron buffer system in the water column and partitioning in the sediments of the naturally acidic Lake Caviahue, Neuquén, Argentina. J Volcanol Geotherm Res 318:19–26

Cabrera JM, Temporetti PF, Pedrozo FL (2020) Trace metal partitioning and potential mobility in the naturally acidic sediment of Lake Caviahue, Neuquén, Argentina. Andean Geol 47(1):46–60

Calabrese S, Aiuppa A, Allard P, Bagnato E, Bellomo S, Brusca L, D'Alessandro W, Parello F (2011) Atmospheric sources and sinks of volcanogenic elements in a basaltic volcano (Etna, Italy). Geochim Cosmochim Acta 75(23):7401–7425

Candela-Becerra LJ, Toyos G, Suárez-Herrera CA, Castro-Godoy S, Agusto M (2020) Thermal evolution of the Crater Lake of Copahue Volcano with ASTER during the last quiescence period between 2000 and 2012 eruptions. J Volcanol Geotherm Res 392:106752

Caraballo M, Rimstidt D, Macías F, Nieto JM, Hochella Jr M (2013) Metastability, nanocrystallinity and pseudo-solid solution effects on the undestanding of schwertmannite solubility. Chem Geol 360–361:22–31

Carlson L, Bigham JM, Schwertmann U, Kyek A, Wagner F (2002) Scavenging of as from acid mine drainage by schwertmannite and ferrihydrite: a comparison with synthetic analogues. Environ Sci Technol 36(8):1712–1719

Caselli A, Agusto M, Vélez ML, Forte P, Bengoa C, Daga R, Albite JM, Capaccioni B (2016) The 2012 eruption. In: Tassi F, Vaselli O, Caselli A (eds) Copahue volcano, active volcanoes of the world book series. Springer, Berlin, pp 61–77

Chiacchiarini P, Lavalle L, Giaveno A, Donati E (2010) First assessment of acidophilic microorganisms from geothermal Copahue-Caviahue system. Hydrometallurgy 104(3–4):334–341

Chiodini G, Cardellini C, Lamberti MC, Agusto M, Caselli A, Liccioli C, Tamburello G, Tassi F, Vaselli O, Caliro S (2015) Carbon dioxide diffuse emission and thermal energy release from hydrothermal systems at Copahue-Caviahue Volcanic Complex (Argentina). J Volcanol Geotherm Res 304:294–303

D'Alessandro W, Brusca L, Kyriakopoulos K, Michas G, Papadakis G (2008) Methana, the westernmost active volcanic system of the south Aegean arc (Greece): insight from fluids geochemistry. J Volcanol Geotherm Res 178(4):818–828

Daga R, Caselli A, Ribeiro Guevara S, Agusto M (2016) Tefras emitidas durante la fase inicial hidromagmática (julio de 2012) del ciclo eruptivo 2012-actual (2016) del volcán Copahue (Andes del sur). RAGA 74(2):191–206 (in Spanish)

Deely JM, Sheppard DS (1996) Whangaehu river, new Zealand: geochemistry of a river discharging from an active crater lake. Appl Geochem 11(3):447–460

Delmelle P, Bernard A (2000) Volcanic Lakes. In: Sigurdsson H (ed) Encyclopedia of volcanoes. Academic Press, California, pp 877–896

Delpino D, Bermúdez A (1993) La actividad del volcán Copahue durante 1992. Erupción con emisión de azufre piroclástico. Provincia de Neuquén. Dissertation, 12° Congreso Geológico Argentino (in Spanish)

Delpino D, Bermúdez A (2002) La erupción del volcán Copahue del año 2000. Impacto social y al medio natural. Provincia del Neuquén, Argentina. Dissertation, 15° Congreso Geológico Argentino (in Spanish)

Farnfield HR, Marcilla AL, Ward NI (2012) Arsenic speciation and trace element analysis of the volcanic río Agrio and the geothermal waters of Copahue, Argentina. Sci Total Environ 433:371–378

Folguera A, Ramos V (2000) Control estructural del volcán Copahue (38°S–71°O): implicancias tectónicas para el arco volcánico cuaternario (36°S–39°S). RAGA 55:229–244

Folguera A, Ramos VA, Melnick D (2002) Partición de la deformación en la zona del arco volcánico de los Andes neuquinos (36–39 S) en los últimos 30 millones de años. Rev Geol Chile 29(2):227–240

Fukushi K, Sasaki M, Sato T, Yanase N, Amano H, Ikeda H (2003) A natural attenuation of arsenic in drainage from an abandoned arsenic mine dump. Appl Geochem 18(8):1267–1278

Galván F, Murray J, Chiodi A, Pereyra R, Kirschbaum A (2018) Drenaje ácido natural en la caldera Negra Muerta y su influencia en las nacientes del río Calchaquí, provincia de Salta, NO Argentina. RAGA 75:80–94 (in Spanish)

Gammons CH, Wood SA, Pedrozo F, Varekamp J, Nelson BJ, Shope C, Baffico G (2005) Hydrogeochemistry and rare earth element behavior in a volcanically acidified watershed in Patagonia, Argentina. Chem Geol 222:249–267

Gaviria Reyes MA, Agusto M, Trinelli MA, Caselli A, Dos Santos Afonso M, Calabrese S (2016) Estudio hidrogeoquímico de las áreas termales del complejo volcánico Copahue-Caviahue. RAGA 73:256–269 (in Spanish)

Giggenbach WF (1992) Isotopic shifts in waters from geothermal and volcanic systems along convergent plate boundaries and their origin. Earth Planet Sci Lett 113:495–510

Ibáñez JM, Del Pezzo E, Bengoa C, Caselli A, Badi G, Almendros J (2008) Volcanic tremor and local earthquakes at Copahue volcanic complex, Southern Andes, Argentina. J Volcanol Geotherm Res 174(4):284–294

Jönsson J, Persson P, Sjöberg S, Lövgren L (2005) Schwertmannite precipitated from acid mine drainage: phase transformation, sulfate release and surface properties. Appl Geochem 20:179–191

Kaasalainen H, Stefánsson A (2012) The chemistry of trace elements in surface geothermal waters and steam, Iceland. Chem Geol 330:60–85

Kawano M, Tomita K (2001) Geochemical modeling of bacterially induced mineralization of schwertmannite and jarosite in sulfuric acid spring water. Am Min 86:1156–1165

Kusakabe M, Komoda Y, Takano B, Abiko T (2000) Sulfur isotopic effects in the disproportionation reaction of sulfur dioxide in hydrothermal fluids: implications for the $\delta^{34}S$ variations of dissolved bisulfate and elemental sulfur from active crater lakes. J Volcanol Geotherm Res 97(1–4):287–307

Lamberti MC, Vigide N, Venturi S, Agusto M, Yagupsky D, Winocur D, Barcelona H, Velez ML, Cardellini C, Tassi F (2019) Structural architecture releasing deep-sourced carbon dioxide diffuse degassing at the Caviahue-Copahue volcanic complex. J Volcanol Geotherm Res 374:131–141

Lecomte K, Maza S, Sarmiento A, Depetris P (2017) Geochemical behavior of an acid drainage system: the case of the Amarillo River, Famatina (La Rioja, Argentina). Environ Sci Pollut Res 24:1630–1647

Lewis AJ, Palmer MR, Sturchio NC, Kemp AJ (1997) The rare earth element geochemistry of acid-sulphate and acid-sulphate-chloride geothermal systems from Yellowstone National Park, Wyoming, USA. Geochim Cosmochim Acta 61(4):695–706

Linares E, Ostera H, Mas L (1999) Cronología K-Ar del complejo efusivo copahue-caviahue, provincia del neuquén. RAGA 54:240–247 (in Spanish)

Llano J (2016) Hidrogeoquímica de las aguas ácidas el río Agrio inferior, provincia de Neuquén. Undergraduate Thesis, University of Buenos Aires (in Spanish)
Llano J, Agusto M, Trinelli MA, Tufo A, García S, Velásquez G, Bucarey-Parra C, Delgado Huertas A, Litvak V (2020) Procesos hidrogeoquímicos vinculados a un ambiente volcánico activo: el caso del sistema río Agrio-Volcán Copahue. RAGA 77(4):490–504
Lozano A, Ayora C, Fernandez-Martinez A (2019) Sorption of rare earth elements onto basaluminite: the role of sulfate and pH. Geochim Cosmochim Acta 258:50–62
Lozano A, Ayora C, Fernández-Martínez A (2020) Sorption of rare earth elements on schwertmannite and their mobility in acid mine drainage treatments. Appl Geochem 113:104499
Majzlan J, Navrotsky A, Schwertmann U (2004) Thermodynamics of iron oxides: Part III. Enthalpies of formation and stability of ferrihydrite (~$Fe(OH)_3$), schwertmannite (~$FeO(OH)_{3/4}$ $(SO_4)_{1/8}$), and ε-Fe_2O_3. Geochim Cosmochim Acta 68(5):1049–1059
Mas GR, Mas LC, Bengochea L (1996) Alteración ácido-sulfática en el campo geotérmico copahue, provincia del neuquén. RAGA 51:78–86 (in Spanish)
Melnick D, Folguera A, Ramos V (2006) Structural control on arc volcanism: the caviahue-copahue complex, central to patagonian andes transition (38°S). J S Am Earth Sci 22:66–88
Möller P (2002) Rare earth elements and yttrium in geothermal fluids. Water Sci Technol 40:97–125
Naranjo J, Polanco E (2004) The 2000 AD eruption of Copahue volcano, southern Andes. Rev Geol Chile 31:279–292
OAVV, Observatorio Argentino de Vigilancia Volcánica (2021) Reporte de actividad volcánica: Volcán Copahue del 1 al 28 de febrero de 2021. In: https://mailchi.mp/c7eee1b239cd/reporte-de-actividad-volcanica-volcan-copahue-febrero-2021. Accessed 15 Feb 2021 (in Spanish)
Ohsawa S, Sugimori K, Yamauchi H, Koeda T, Inaba H, Kataoka Y, Kagiyama T (2014) Bownish discoloration of the summit crater lake of Mt. Shinmoe-dake, Kirichima Volcano, Japan: volcanic-microbial coupled origin. Bull Volcanol 76:809–819
Palmer S, Van Hinsberg V, McKenzie J, Yee S (2011) Characterization of acid river dilution and associated trace element behavior through hydrogeochemical modeling: a case study of the Banyu Pahit River in East Java, Indonesia. Appl Geochem 26:1802–1810
Panarello H (2002) Características isotópicas y termodinámicas de reservorio del campo geotérmico Copahue-Caviahue, provincia de Neuquén. RAGA 57:182–194 (in Spanish)
Parker S, Gammons C, Pedrozo F, Wood S (2008) Diel changes in metal concentrations in a geogenically acidic river: Río Agrio, Argentina. J Volcanol Geotherm Res 178:213–223
Pedrozo FL, Díaz MM, Temporetti PF, Baffico GD, Beamud SG (2010) Características limnológicas de un sistema ácido: río Agrio-Lago Caviahue, Provincia del Neuquén, Argentina. Ecol Austral 20(2):173–184 (in Spanish)
Petrinovic I, Villarosa G, D'Elia L, Guzman S, Paez G, Outes V, Manzoni C, Delmenico A, Balbis C, Carniel R, Hernando I (2014) La erupción del 22 de diciembre de 2012 del volcán Copahue, Neuquén, Argentina: Caracterización del ciclo eruptivo y sus productos. RAGA 71:161–173 (in Spanish)
Regenspurg S, Brand A, Peiffer S (2004) Formation and stability of schwertmannite in acidic pit lakes. Geochim Cosmochim Acta 68:1185–1197
Regenspurg S, Peiffer S (2005) Arsenate and chromate incorporation in schwertmannite. Appl Geochem 20:1226–1239
Rodriguez A, Varekamp J, Van Bergen M, Kading T, Oonk P, Gammons C, Gilmore M (2016) Acid rivers and lakes at caviahue-copahue volcano as potential terrestial analogues for aqueous paleo-envionments on mars. In: Tassi F, Vaselli O, Caselli A (eds) Copahue volcano, active volcanoes of the world book series. Springer, Berlin, pp 141–172
Roulleau E, Tardani D, Sano Y, Takahata N, Vinet N, Bravo F, Muñoz C, Sanchez J (2016) New insight from noble gas and stable isotopes of geothermal/hydrothermal fluids at Caviahue-Copahue Volcanic Complex: boiling steam separation and water-rock interaction at shallow depth. J Volcanol Geotherm Res 328:70–83
Roulleau E, Bravo F, Pinti DL, Barde-Cabusson S, Pizarro M, Tardani D, Muñoz C, Sanchez J, Sano Y, Takahata N, De la Cal F, Esteban C, Morata D (2017) Structural controls on fluid circulation at

the Caviahue-Copahue Volcanic Complex (CCVC) geothermal area (Chile-Argentina), revealed by soil CO_2 and temperature, self-potential, and helium isotopes. J Volcanol Geotherm Res 341:104–118

Roulleau E, Tardani D, Vlastelic I, Vinet N, Sanchez J, Sano Y, Takahata N (2018) Multi-element isotopic evolution of magmatic rocks from Caviahue-Copahue Volcanic Complex (Chile-Argentina): involvement of mature slab recycled materials. Chem Geol 476:370–388

Rowe Jr GL (1994) Oxygen, hydrogen, and sulfur isotope systematics of the crater lake system of Poas volcano, Costa Rica. Geochem J 28(3) 263–287

Sánchez-España J (2007) The behavior of iron and aluminum in acid mine drainage: speciation, mineralogy, and environmental significance. In: Lectcher TM (ed) Thermodynamics, solubility and environmental issues. Elsevier, Netherlands, pp 137–150

Sánchez-España JS, Pamo EL, Pastor ES, Andrés JR, Rubí JM (2006) The removal of dissolved metals by hydroxysulphate precipitates during oxidation and neutralization of acid mine waters, Iberian Pyrite Belt. Aquat Geochem 12(3):269–298

Sánchez-España J, Yusta I, Diez-Ercilla M (2011) Schwermannite and hydrobasaluminite: a re-evaluation of their solubility and control on the iron and aluminium concentration in acidic pit lakes. Appl Geochem 26:1752–1774

Sánchez-España J, Yusta I, Burgos WD (2016a) Geochemistry of dissolved aluminum at low pH: Hydrobasaluminite formation and interaction with trace metals, silica and microbial cells under anoxic conditions. Chem Geol 441:124–137

Sánchez-España J, Yusta I, Gray J, Burgos WD (2016b) Geochemistry of dissolved aluminum at low pH: Extent and significance of Al–Fe (III) coprecipitation below pH 4.0. Geochim Cosmochim Acta 175:128–149

Stumm W, Morgan JJ (1996) Aquatic chemistry: chemical equilibria and rates in natural waters. John Wiley and Sons Inc., New York

Szentiványi J (2018) Geología del sector NE del volcán Copahue y geoquímica de los fluidos volcánicos asociados. Undergraduate Thesis, University of Buenos Aires (in Spanish)

Tamburello G, Agusto M, Caselli A, Tassi F, Vaselli O, Calabrese S, Rouwet D, Capaccioni B, Di Napoli R, Cardellini C, Chiodini G, Bitetto M, Brusca L, Bellomo S, Aiuppa A (2015) Intense magmatic degassing through the lake of Copahue volcano, 2013–2014. J Geophys Res Solid Earth 120(9):6071–6084

Taran Y, Rouwet D, Inguaggiato S, Aiuppa A (2008) Major and trace element geochemistry of neutral and acidic thermal springs at El Chichón volcano, Mexico: implications for monitoring of the volcanic activity. J Volcanol Geotherm Res 178(2):224–236

Tassi F, Agusto M, Lamberti C, Caselli A, Pecoraino G, Caponi C, Szentiványi J, Venturi S, Vaselli O (2017) The 2012–2016 eruptive cycle at Copahue volcano (Argentina) versus the peripheral gas manifestations: hints from the chemical and isotopic features of fumarolic fluids. Bull Volcanol 79(10):1–14

Tassi F, Agusto M, Vaselli O, Chiodini G (2016) Geochemistry of the magmatic-hydrothermal fluid reservoir of Copahue volcano (Argentina): insights from the chemical and isotopic features of fumarolic discharges. In: Tassi F, Vaselli O, Caselli A (eds) Copahue volcano, active volcanoes of the world book series. Springer, Berlin, pp 119–139

Temporetti P, Beamud G, Nichela D, Baffico G, Pedrozo F (2019) The effect of pH on phosphorus sorbed from sediments in a river with a natural pH gradient. Chemosphere 228:287–299

Varekamp JC (2008) The volcanic acidification of glacial Lake Caviahue, province of Neuquén, Argentina. J Volcanol Geotherm Res 178(2):184–196

Varekamp JC (2015) The chemical composition and evolution of volcanic lakes. In: Rouwet D, Christenson B, Tassi F, Vandemeulebrouck J (eds) Volcanic lakes. Advances in volcanology. Springer, Berlin, pp 93–123

Varekamp JC, De Moor JM, Merrill MD, Colvin AS, Goss AR, Vroon PZ, Hilton DR (2006) Geochemistry and isotopic characteristics of the Caviahue-Copahue volcanic complex, Province of Neuquén, Argentina. Geol Soc Am Spec Pap 407:317–342

Varekamp JC, Ouimette AP, Herman SW, Flynn KS, Bermudez, A, Delpino D (2009) Naturally acid waters from Copahue volcano, Argentina. Appl Geochem 24(2):208–220

Velez ML, Euillades P, Caselli A, Blanco M, Díaz JM (2011) Deformation of copahue volcano: inversion of InSAR data using a genetic algorithm. J Volcanol Geotherm Res 202(1–2):117–126

Verplanck PL, Nordstrom DK, Taylor HE, Kimball BA (2004) Rare earth element partitioning between hydrous ferric oxides and acid mine water during iron oxidation. Appl Geochem 19(8):1339–1354

Wanner C, Pöthig R, Carrero S, Fernandez-Martinez A, Jäger C, Furrer G (2018) Natural occurrence of nanocrystalline Al-hydroxysulfates: insights on formation, Al solubility control and as retention. Geochim Cosmochim Acta 238:252–269

Wood SA, Gammons CH, Parker SR (2006) The behavior of rare earth elements in naturally and anthropogenically acidified waters. J Alloys Compd 418(1–2):161–165

Yu J, Heo B, Choi I, Chang H (1999) Apparent solubilities of schwertmannite and ferrihydrite in natural stream waters polluted by mine drainage. Geochim Cosmochim Acta 63:3407–3416

Negro River Environmental Assessment

Andres H. Arias, Pablo A. Macchi, Mariza Abrameto, Patricio Solimano, Nathalia Migueles, Fredy G. Rivas, Aimé I. Funes, Graciela Calabrese, Mariano Soricetti, Adela Bernardis, Romina B. Baggio, Yeny Labaut, and Jorge E. Marcovecchio

Abstract The Negro River comprises a multi compartmentalized environment which links Los Andes mountains with the Atlantic Ocean. Due to its relevance in terms of industries, intensive agriculture production and population is considered the second Argentinean river in importance; however, these economic activities have increased the environmental pressure, raising concerns. For instance, the intensive

A. H. Arias (✉) · J. E. Marcovecchio
Instituto Argentino de Oceanografía, CCT-CONICET, Bahía Blanca, Argentina
e-mail: aharias@iado-conicet.gov.ar

A. H. Arias
INQUISUR, Departamento de Química, Universidad Nacional del Sur, Bahía Blanca, Argentina

P. A. Macchi
Universidad Nacional de Río Negro, Instituto de Investigación en Paleobiología y Geología, Río Negro, Argentina

M. Abrameto · P. Solimano · F. G. Rivas · A. I. Funes · M. Soricetti · R. B. Baggio
Centro de Investigaciones y Transferencia de Río Negro, Rotonda Cooperación y Ruta Provincial N°1, Universidad Nacional de Río Negro, C.P. 8500 Viedma, Río Negro, Argentina

N. Migueles
Universidad Nacional de Río Negro, C.P. 8500 Viedma, Río Negro, Argentina

G. Calabrese
Instituto de Investigaciones en Recursos Naturales, Agroecología y Desarrollo Rural, Universidad Nacional de Río Negro, Bariloche, Río Negro, Argentina

A. Bernardis
Profesorado de Nivel Medio y Superior en Biología. General Roca, Universidad Nacional de Río Negro, Río Negro, Argentina

Y. Labaut
Universidad Nacional de Río Negro, Instituto de Investigación en Paleobiología y Geología, Río Negro, Argentina

J. E. Marcovecchio
Universidad Tecnológica Nacional-FRBB, Bahía Blanca, Argentina

Universidad FASTA, Mar del Plata, Argentina

A. I. Torres and V. A. Campodonico (eds.), *Environmental Assessment of Patagonia's Water Resources*, Environmental Earth Sciences,
https://doi.org/10.1007/978-3-030-89676-8_5

agriculture joint with urban settlements and industries have lead to the introduction of several Persistent Organic Pollutants, including legacy compounds (such as DDT and HCHs), new generation pesticides (endosulfan) and urban-industrial POPs (PCBs, PBDEs). In addition, several matrix have been shown to receive and accumulate heavy metal loads, including As, Cd, Cr, Co, Cu, Fe, Hg, Mn, Ni, Pb and Zn. Metal bioaccumulation and transference between environmental compartments (water, sediments, fish and mollusks) have been demonstrated to occur through the years. The anthropic activities have also induced changes in the aquatic macroinvertebrate assemblages of the Negro River, where both, water quality and invasive species, appear to be main drivers of the change. Added to this, from 17 fish species, only 9 are native, leading to a low zoogeographic integrity coefficient. Finally, the environmental quality threats, climate change and hydroelectric facilities pose synergistic new risks which are addressed in this chapter and further discussed.

Keywords Persistent organic pollutants · Heavy metals · Macroinvertebrates · Fish assemblages · Negro river · Patagonia

1 Introduction

The hydrographic system of the Negro River, along with the Limay and Neuquen rivers, is a set of water courses that form a natural environment, currently organized by different social, cultural and economic processes. Its headwaters are located at the west of Neuquén and Río Negro provinces. The area belongs to the Andes' lakes region and the main water source is precipitation occurring at the Andean zone, in the form of snow and rain. Water flows towards the main course, the Negro River, which outflows in the Atlantic coast. Once it leaves the **headwaters** area in the Andean region, there is a section that can be identified as the water catchment area outside the headwaters. This section is drained by two important water courses, one to the south, which is the Limay River and the other to the north, which is the Neuquén River. These rivers constitute the main tributaries of the Negro River (Fig. 1).

The Negro River is located in the third and last part of this hydrographic system, and it flows towards the Atlantic Ocean through the Upper, Middle and Low Valleys. It does not receive any tributary throughout its entire path to the Atlantic Ocean: it runs from the confluence point through the valley towards the east and crosses the entire Negro River province from west to east, including plateaus, fences, islands and plains throughout its extension. It is one of the main water courses in the country, and the most important in the province. Throughout its valleys, several economic activities are carried out, holding most of the population at its margins.

Three types of economic activities prevail throughout the Negro River catchment area. In the upper valley, intensive agricultural activities under irrigation are developed, such as fruits (especially apples and pears), grapes and other vegetables. The irrigated valley holds the largest concentration of population of the entire province along 100 km. The main cities include General Roca, Ingeniero Cipolletti, Villa

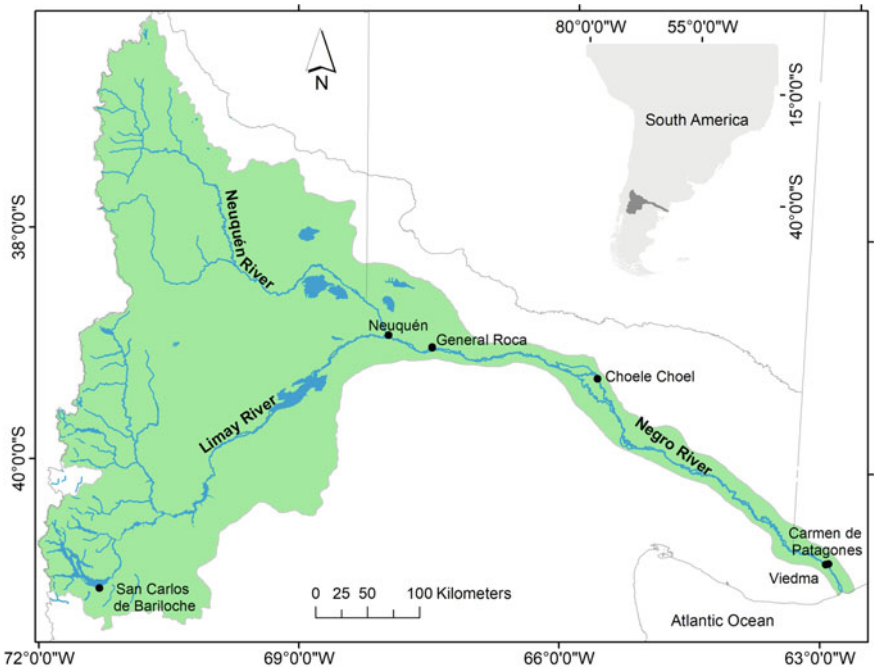

Fig. 1 The Negro River hydrographic scheme, including the Negro, Limay and Neuquén rivers, Patagonia, Argentina

Regina, Coronel Belisle, Darwin, Allen and Cinco Saltos. This area is followed by the middle valley, where the main activity is fruit and vegetables cultivation, interspersed with forages, vineyards and livestock breeding. Choele-Choel is one of the main cities in this area. Finally, the lower valley is emplaced the city of Viedma, which has a high public administration activity and several industries. Irrigated agriculture and livestock production are also developed in the area.

The growing population and the related economic activities have increased the environmental pressure over the freshwater ecosystems in the Argentinean Patagonia. While intensive agriculture is the second most important economic activity in region, the use of nonselective pesticides has significant implications to the environment quality (Loewy et al. 2011), particularly on aquatic macroinvertebrates assemblages (Macchi et al. 2014; Kohlmann et al. 2018). Extensive livestock farming, deforestation, wood and hydrocarbon extraction, flow regulation by dams, introduction of exotic species and the growth of unplanned urbanizations are also main threats currently impacting the area (Cazzaniga and Pérez 1999; Macchi 2008; Miserendino 2009; Miserendino and Brand 2009; Epele et al. 2018; Macchi et al. 2018).

Along the next sections a set of environmental impacts are revisited, aiming to review the Negro River environmental assessment from the past decades up to date. In this sense, along the first two sections both, persistent organic pollutants and heavy metal sources, occurrence, distribution and threats are explored. In the next section,

the macroinvertebrate assemblages of the Negro River are listed and analyzed as biological early warning sensors of the environmental status of the area. Finally, fish communities of the Negro River are revisited since they respond significantly and predictably to almost all kinds of anthropogenic disturbances. Their origin, current status and immediate and medium-term threats are addressed and discussed.

2 Persistent Organic Pollutants

Persistent Organic Pollutants (POPs) compounds belong to a group of substances of natural or anthropogenic origin, resistant to photolytic, chemical and biological degradation. They tend to bioaccumulate at different levels of the trophic web, with possible **upstream** biomagnification (Sangster 1989; Yalkoswky 2010). The consequent toxicity includes various alterations in the reproduction, development, and some immune functions of animals and plants (Langston et al. 2010). Among the persistent compounds, the organochlorine compounds include the known pesticides: hexachlorocyclohexanes (HCHs), hexachlorobenzene (HCB), dichlorodiphenyltrichloroethane (DDT), chlordanes and endosulphanes. Organochlorine pesticides have been banned or severely restricted by the sanitary or environmental Annexes in the III Rotterdam Convention (2004). Their use is also prohibited in Argentina, except for DDT which has a restricted use for certain applications (Table 1). For instance, HCHs are classified as carcinogenic to humans, DDT as probably carcinogenic to humans (2A) while HCB and chlordanes as possibly carcinogenic to humans (2B, IARC).

Table 1 Commonly used pesticides in the past at the Negro River catchment area

Compound	National Law	Resolution
Chlordane and Lindane	SAGPyA 513/98 Resolution	Prohibited for import, commercialization and use as phytosanitary products, as well as the products formulated based on these
DDT, Endrin, Aldrin	Law-ranking Decree No. 2121/90	Prohibited for import, manufacture, fractionation, commercialization and use of agricultural products formulated based on these active principles
Hexachlorobencene (H.C.B)	SAGPyA No. 750/2000 Resolution	Total prohibition
Hexachlorociclohexane (H.C.H), Dieldrin	National Law 22.289	Total Prohibition
Endosulfan	ENASA 511/11 Resolution	Total Prohibition. Only re-export or destruction as of July 1, 2013

The Negro River basin is not excluded from the input of persistent organic pollutants. As mentioned above, the upper valley region of Negro River and Neuquen produces the 80 and 90% of the apples and pears of Argentina, respectively. Besides, the production of fine fruit, olive trees, nuts, and horticulture has been incorporated in recent years (LIBIQUIMA-CITAAC 2016). This level of production involves the application of multiple families of pesticides during a period that extends from September to February. Most used pesticides include organophosphates (OF), carbamates (CB), pyrethroids (PIR) and neonicotinoids (NN). Due to the fact that pesticides such as organochlorine pesticides (OC; e.g. DDT and endosulfan) have been extensively used in the last century and until the beginning of the twenty-first century, the area shows an extensive occurrence of OF and OC residues in soils and groundwaters in rural areas (Comahue 2016). Methylazinphos and chlorpyrifos have been frequently detected in water and the main compounds include methylazinphos and carbaryl, with levels up to 22.5 ppb and 45.7 ppb, respectively (Loewy et al. 2011). With methylazinphos banning in 2016 this trend has changed over time, decreasing the environmental levels in about 30%. It has been also shown that approximately 50% of the applied pesticides are lost in the environment without reaching the intended targets, moving in a very high proportion to canals, lakes and streams due to drifting, runoff, washing by rain and irrigation (LIBIQUIMA-CITAAC 2016). Along 2006–2007, Isla et al. (2010) showed a decreasing trend of organochlorine compounds (OCs) contents in river sediments from the upper valley to the inlet, with an increment at the beginning towards the lower valley. The higher concentrations were found in the Neuquen River and Paso Cordova location, reaching 18.1 and 7.5 ng/g dry weight, respectively (summatory of 10 compounds). While Neuquén River showed a prevalence of parental DDT, which was already illegal use during that period (Isla et al. 2010), DDE dominated along the Negro River pointing to a past use, with a higher diversity of compounds, including endosulfans and HCHs. Among endosulfans, the parental isomers dominated, indicating a widespread current use during that period. In the same period, Miglioranza et al. (2013) demonstrated the occurrence and distribution of OCPs, PCBs and PBDEs in several environmental matrices (soils, sediments, suspended particle matter and **macrophytes**) along the Río Negro. Similarly to Isla et al. (2010), authors concluded that the soil can be considered a hot spot of DDTs in the area while the pp′-DDE was dominant in all samples. While the occurrence of endosulfans with a relation α-/β-isomers > 1 in all matrices denoted its current use in the region, their levels found in water are higher than the maximum values established for aquatic biota protection. During those years, DDTs, endosulfans, HCHs, chlordanes, PCBs and PBDEs were also detected at *Odontesthes hatchery* (patagonian silverside) from the Upper, Middle and Lower valleys of the Negro River (Ondarza et al. 2014). As a general outcome, all tissues showed decreasing levels from the upper to the lower regions. In agreement with another environmental matrix (Miglioranza et al. 2013), organochlorine pesticides were dominant (306–3449 ng g^{-1} lipid) followed by ΣPCBs (65–3102 ng g^{-1} lipid) and ΣPBDEs (22–870 ng g^{-1} lipid), pointing to agriculture as the main source. Regarding organochlorine pesticides, DDT was dominant (90% *pp′*-DDE) followed by endosulfan (α- > β- > sulfate), γ-HCH and γ-chlordane. This pattern was still

confirmed in 2018, showing the prevalence of this legacy POPs in the river and the growing awareness for endosulfan, which in occasions exceeded the chronic exposure limit of the CCME (Arias et al. 2019).

Polichlorinatedbiphenyls (PCBs) are a set of compounds of environmental concern as they have a high half-life (from 60 days to 27 years in water, and 3–38 years in sediments; Sinkkonen and Paasivirta 2000), they are resistant to degradation by physical, chemical and biological processes and they bioaccumulate through the food web (Muir et al. 1988; Thomann 1989), generating adverse effects on both, the environment and human health (Jones and De Voogt 1999). Despite their prohibition and the consequent decrease in their global levels (USEPA 1999), PCBs are widely distributed and are among the most problematic and important pollutants in the world due to their strong presence in the environment. Urban areas at the Negro River highly impact the river by the introduction of several POPs, including PCBs > cyclodienes > DDTs (Miglioranza et al. 2013). Besides a retention effect of riparian vegetation which was demonstrated for pesticides and macrophytes, the proximity to dumping sites often correlates with an increase in PBDE levels; the mechanistic paths of inputs includes leaching from dumping sites and eventual river flooding and land wash-up (Miglioranza et al. 2013). Particularly, in terms of PCBs, Isla et al. (2010) showed a relatively constant concentration as a consequence of chronic pollution, with the Limay River contributing with a higher PCB load in comparison to Neuquen River.

Recent data have shown that a major anthropogenic pressure over the river is still caused by the use of DDT (Arias et al. 2019). In comparison to previous reports such as those of Miglioranza et al. (2013) and Isla et al. (2010), there is a decrease in the current values of HCHs and endosulfans transported onto the Suspended Particulate Matter (SPM of the middle valley, while in the lower valley a slight increase in the contributions of HCHs and endosulfans were registered in comparison to 2006 (Fig. 2).

Regarding flame retardants (FRs), a set of compounds intended for thermal insulation, thermoplastics, textiles, plastic foams, etc., are based on chlorine and bromine. Bromine is currently used in a large number of products such as pesticides, gasoline additives, drilling fluids, and biocides, but currently the main application of bromine-based compounds is in the FRs production (Tombesi et al. 2017). In 2006, PBDE

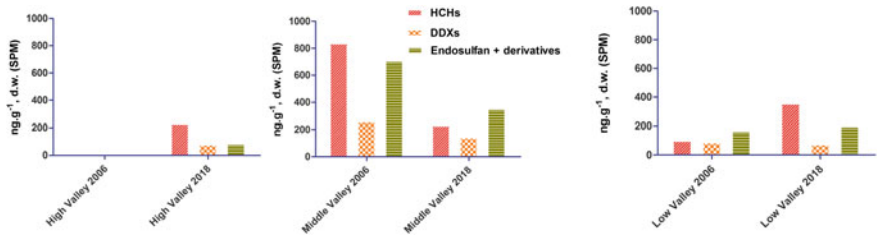

Fig. 2 HCHs, DDX and Endosulfans recorded at the Upper, Middle and Lower valleys of the Negro River in 2006 and 2018 (data from Miglioranza et al. 2013 and Arias et al. 2019)

could be associated to urban areas proximities and urban dumping sites (Miglioranza et al. 2013). Authors concluded that the proportion of PBDE congeners close to Viedma city would indicate a relatively recent use of penta-BDE mixtures due to the BDE-47/BDE-100 ratios. While BDE-100 is characterized by a high persistence, BDE-47 is one of the most ubiquitous BDE as a result of atmospheric transport. An air survey performed between 2010 and 2013 at the river basin can confirm the above mentioned patterns (Miglioranza et al. 2020). While endosulfan, trifluralin and DDT-related substances were the most prevalent pesticides in the Negro River **watershed**, low concentrations of industrial POPs were found (1.9 pg m^{-3} for Σ38 PCBs, and Σ5 PBDEs, respectively) and they were similar among sites.

3 Heavy Metal Pollution

Besides there are several essential metals which are commonly found in low concentrations and exhibit substantial implications to chemistry of natural ecosystems (e.g. Cu, Zn and Fe), some of them are toxic even in small concentrations (Cr, Pb, Cd, Hg, As) and pose a great concern due to their high acute and chronic effects and possible biomagnifications through the trophic web (Cai et al. 2011; Hu et al. 2013; Wang et al. 2015). This is the case for Negro River, where several research studies have been performed in this sense. In the next sections we describe the highlights of this research by matrix of study.

3.1 Water

Several challenges have been faced when comparing total or dissolved metals in the Negro River water (Phillips 1977); methods dispersion range from differences in sample pre concentration (filtration by membranes with several pore sizes) to the applied analytical methods (Inductively Coupled Plasma—optical spectrometry ICP-OES, ICP-Mass ICP-M, Graphite Furnace, etc.).

Regarding environmental levels, the most recent analysis based on the water soluble fraction showed low As, Cu and Zn levels, while traces of Cr, Ni, Cd, Pb were detected (Table 2; Abrameto 2019).

Historically, the Neuquén River has shown the maximum As levels (5.6 μg L^{-1}), which tend to diminish through the Upper and Middle valley of Negro River to reach a media concentration of 3.0 μg L^{-1} at the estuary zone. In many occasions, levels were shown to be above the water quality guidelines for aquatic life protection (Table 2) (CCME 2020). In general, the arsenic concentration is far from background levels and is remarkably close (or even higher) than the World Health Organization reference value for water sources destined to human consumption (WHO 2019; Table 2).

Table 2 Heavy metals and metalloids concentrations in freshwater of the Negro River

Authors	Location	Fraction	Concentration ($\mu g\ L^{-1}$)										
			Fe %	Hg	Mn	Co	Cr	Ni	Cd	Pb	Zn	As	Cu
Gaiero et al. (2002)	Conesa (MV)	Dissolved (0.22 μm)	11	–	1.6	0.08	0.9	1.7	–	03	1.6	–	1.4
		SPM (1996)	4.10	–	3.2	12	34	39	–	33	170	–	37
		SPM (1997–1998)	4.10	–	1.7	20	65	37	–	60	460	–	290
Abrameto et al. (2013)	GMitre (LV)	Total	–	–	–	–	–	–	–	–	n.d	2.42	2.4
	Drains (LV)		–	–	–	–	–	–	–	–	n.d	2.40	4.6
	Paloma Island-(LV)		–	–	–	–	–	–	–	–	n.d	1.16	4.9
	Maritime estuary		–	–	–	–	–	–	–	–	30	3.01	7.6
Abrameto et al. (2019)	Neuquén Vista Alegre	Dissolved (0.45 μm)	–	–	–	–	n.d	n.d	n.d	n.d	n.d	(3.16–4.32)	n.d
	Neuquén city		–	–	–	–	n.d	n.d	n.d	n.d	n.d	(6.63–8.36)	n.d
	Limay and Neuquén		–	–	–	–	n.d	n.d	n.d	n.d	n.d	n.d	n.d
	Cipoletti (UV)		–	–	–	–	n.d	n.d	n.d	n.d	n.d	(5.0–7.9)	n.d
	Fernandez Oro (UV)		–	–	–	–	n.d	n.d	n.d	n.d	n.d	(3.5–3.8)	n.d
	Allen Sewer (UV)		–	–	–	–	n.d	n.d	n.d	n.d	n.d	1.95	n.d
	Allen pipeline (UV)		–	–	–	–	n.d	n.d	n.d	n.d	n.d	3.5	n.d
	Allen Water catchment (UV)		–	–	–	–	n.d	n.d	n.d	n.d	n.d	4.5	n.d
	Roca (UV)		–	–	–	–	n.d	n.d	n.d	n.d	n.d	n.d	n.d
	Villa Regina (UV)		–	–	–	–	n.d	n.d	n.d	n.d	4.0	(3.2–14.7)	n.d

(continued)

Table 2 (continued)

Authors	Location	Fraction	Concentration ($\mu g\ L^{-1}$)										
			Fe %	Hg	Mn	Co	Cr	Ni	Cd	Pb	Zn	As	Cu
	Chichinales (UV)		–	–	–	–	n.d	n.d	n.d	n.d	n.d	8.9	n.d
	Chelforo (UV)		–	–	–	–	n.d	n.d	n.d	n.d	n.d	2.3	n.d
	Choele Choel (MV)		–	–	–	–	n.d	n.d	n.d	n.d	n.d	(4.4–8.6)	1.7
	Pomona (MV)		–	–	–	–	n.d	n.d	n.d	n.d	n.d	3.6	n.d
	Conesa (MV)		–	–	–	–	n.d	n.d	n.d	n.d	69.5	(3.7–5.3)	n.d
	Guardia Mitre (LV)		–	–	–	–	n.d	n.d	n.d	n.d	n.d	(3.4–8.9)	n.d
	Viedma (LV)		–	–	–	–	n.d	n.d	n.d	n.d	n.d	(3.8–7.5)	1.3
	Paloma Island—(LV)		–	–	–	–	n.d	n.d	n.d	n.d	n.d	(7.0–15.7)	8.5
	Patagones (LV)		–	–	–	–	n.d	n.d	n.d	n.d	n.d	11.4	n.d

Metal values are separated by different sectors and by sampling year, where (–) is Not analyzed
n.d not detected, *UV* upper valley, *MV* middle valley, *LV* lower valley

Regarding heavy metals transport mechanisms through the Negro River, Gaiero et al. (2002) showed that Cu would be mainly bonded to the particulate fraction and tends to increase its total concentration (dissolved + particulate) from the inland to the maritime estuary (Abrameto et al. 2013). In general, the partition coefficient (calculated among dissolved and suspended loads, Kd = HMdis/HMspm) shows a general decreasing tendency to the ocean for Zn, Cu and Pb, confirming the gradual adsorption increment on suspended particulate matter (Gaiero et al. 2002). Finally, in terms of Cr, the General Conesa City area showed a dissolved mean concentration of 0.9 $\mu g\ L^{-1}$; wide above the international aquatic life protection limits (CCME 2020).

3.2 Sediments

Sediments act as an end reservoir of metals that came into the aquatic system from several ways: through creeks, drainage systems, atmospheric deposition and leaching (Botté et al. 2010, 2013). While recording the past and present biogeochemical variability, they have an important role in the transport and storage of potentially dangerous metals (Zhang et al. 2014). The Negro River sediments have shown a set of heavy metals, including As, Cd, Cr, Co, Cu, Fe, Hg, Mn, Ni, Pb and Zn.

Firstly, Arribére et al. (2003) performed a study on heavy metals contents in the < 63 μm fraction of sediments and biota of the Upper Negro River. Recorded levels were higher at the coast of Neuquén city and the Limay confluence area, decreasing towards Allen and Regina City. Mercury maximum levels showed 0.28 $\mu g\ g^{-1}$ (d.w.) with a mean of 0.22 $\mu g\ g^{-1}$ (d.w.) in the river upper basin. Arsenic levels ranged from 12 to 5.2 $\mu g\ g^{-1}$ (d.w.) and Ni and Zn exhibited a media concentration of 29.2 and 106.3 $\mu g\ g^{-1}$ (d.w.) respectively, along the basin.

For the middle valley, Gaiero et al. (2002), showed that Ni and Zn values in a similar range to those (21 and 101 $\mu g\ g^{-1}$) reported by Arribére et al. (2003), while the mean concentrations of Co, Cr, Cu, Pb, Mn and Fe were the following: 20, 39, 36, 21, 1049 $\mu g\ g^{-1}$, 5.2% respectively. Considering the upper valley, Abrameto (2004) reported Hg, Ni and Zn levels which were preferably associated to the < 63 μm fraction, with remarkable Zn levels at Fernández Oro, which presented a maximum of 163.9 $\mu g\ g^{-1}$. Simultaneously, Cd, Mn and Ni showed constant mean concentrations throughout the area (0.2–0.97 $\mu g\ g^{-1}$; 0.14–0.19% and 5.6–9.43 $\mu g\ g^{-1}$, respectively) while Cu and Pb peaked at Fernández Oro site, with an average of 39.1 $\mu g\ g^{-1}$ and 29.9 $\mu g\ g^{-1}$, confirming a potential heavy metal hotspot in the area. Finally, Fe levels showed a mean value of 9.6% along the upper valley sediments.

Ward (2007) evaluated the occurrence of heavy metals in sediments of the upper Negro River valley (<63 μm). The mean Hg concentration was 0.06 $\mu g\ g^{-1}$ with peak levels ranging from 0.18 to 0.28 $\mu g\ g^{-1}$, exceeding the ISQG of 0.17 $\mu g\ g^{-1}$ (CCME 2020). Heavy metal levels were even higher at the confluence area, showing 6.3, 2.6, 35.9, 100.1, 79.9 and 46.8 $\mu g\ g^{-1}$ for As, Cd, Co, Cr, Pb and Zn, respectively. Abrameto et al. (2013) investigated the "total" content of heavy metals in bed

sediments from the Low Negro River Valley. In that occasion, hot spots were detected at "El Molino drainage", "Inlet maritime" and Patagones city coast (for As and Cu) and La Paloma island (Zn). The environmentally high levels for these metals raised a concern: 3–28.7 $\mu g\ g^{-1}$ for As, 6.4–37.5 $\mu g\ g^{-1}$ for Cu, and 17.1- 50.1 $\mu g\ g^{-1}$ for Zn. According to Ward (2007), mercury concentrations decrease towards the end of the upper valley, while higher Cd and As levels are detected at the lower valley.

Table 3 revises the heavy metals levels in Negro River bed sediments and other locations around the world. As shown, while Cr levels (Neuquén) were lower than those reported for other places, these levels were higher than those reported for the Bahía Blanca Estuary, Samborombón Bay, the Yangtze basin (China), and Río de La Plata sediments. A similar situation was observed for As: its levels at the upper basin and the coast of Neuquén were lower than those reported by Yi et al. (2008) for the Yangtze River. While Ni levels in bottom sediments of the Negro River were higher than those indicated for the Bahía Blanca Estuary, they were lower than those reported for the Samborombon Bay. Pb levels were comparable to the data recorded at Río de La Plata and the Bahía Blanca Estuary, but lower than those obtained in the Yangtze (China) and Dipsiz (Turkey) rivers. Regarding Hg levels, they were in the range of those registered within the Bahia Blanca Estuary (Argentina) and the middle basin of the Yangtze River, but higher than those indicated for the lower basin of the Yangtze River. Cu, Fe and Mn levels were at the same order of magnitude than those reported by other authors in rivers and estuaries worldwide.

3.3 Fish

There are three pathways by which fish can intake metals from the environment: by the tegument, gills or through diet. While the highest intake of metals occurs through the gills (Alam et al. 2002), they can also accumulate suspended particles from water by food ingestion. Abrameto (2004) investigated the levels of Ni, Cd, Hg, Pb, Zn, Fe and Mn in *O. hatcheri* and *P. colhuapiensis* collected in the upper and middle Negro River basin. Only Hg, Mn, Pb and Zn have been reported as bio accumulated heavy metals (Table 4). The Zn range for muscle tissue in the upper basin was from 5.49 to 7.08 $\mu g\ g^{-1}$ (w.w.) while fish samples from Beltran city averaged 10 $\mu g\ g^{-1}$ (w.w.). These values were lower than those reported by Arribere et al. (2003). Hg in the muscle of *O. hatcheri* showed similar levels throughout the upper and middle basin of the Negro River, with comparable levels to those reported by Arribere et al. (2003) and by Marcovecchio and Moreno (1993) on fish from the Río de la Plata estuary. Similarly to Zn patterns, Pb concentration in muscle tissues was higher in individuals collected from the Beltran city area (0.14 $\mu g\ g^{-1}$ w.w.) than those collected from Allen city area (0.05 $\mu g\ g^{-1}$ w.w., middle valley). Finally, Hg and Pb reported concentrations were lower than those contained in *O. bonariensis* in the Río de la Plata (Avigliano et al. 2015). Finally, Pb and Hg levels in Negro River fish could exceed the current daily recommended intake by the US Environmental Protection Agency (EPA 2020).

Table 3 Mean concentrations of heavy metals in sediments from Negro River basin compared to rivers and estuaries in Argentina and the world

Authors	Location	Concentration μg g^{-1} d.w.										
		Fe %	Hg	Mn %	Co	Cr	Ni	Cd	Pb	Zn	As	Cu
*Arribére et al. (2003)/Abrameto (2004)/ *Ward (2007)	Neuquén	13.63	0.07	23.10	–	17.93	13.56	0.34	7.53	53.88	6.56*	7.60
	Upper Valley	8.20	0.12	90.52	35.95	41.91	13.49	0.69	20.03	64.90	5.59*	12.58
*Gaiero et al. (2002)/Abrameto et al. (2012)	Middle Valley	5.20	–	0.10	20.00	39.00	21.00	8.30	21.00	74.25	15.97	22.63
Abrameto et al. (2012)	Lower Valley	–	–	–	–	–	–	3.46	13.46	36.00	–	21.34
Janiot et al. (2001)	Rio de la Plata	–	–	–	–	17.4/22.7	–	0.05/ 0.13	10.9/20.0	–	–	12.65/ 37.7
Demirak et al. (2006)	Dipsiz stream Yatagan basin	–	–	–	–	19.70	–	0.80	83.60	37.00	–	13.00
Yi et al. (2008)	Middle Yangtze River	–	0.16	–	–	61.38	–	0.11	37.38	109.1	14.38	38.25
Yi et al. (2008)	Lower reach of the Yangtze River	–	0.02	–	–	66.40	–	0.19	34.2	75.8	66.8	37.00
Tatone et al.(2015)	Río de la Plata	3.35	–	0.06	–	21.20	15.1	–	15.4	80.8	–	23.3
PMCA-EBB (2016)	Bahia Blanca Estuary	–	0.09	–	–	10.70	7.7	0.04	6.13	32.75	–	12.3

*Fractions < 63 μm

PMCA-EBB: Environmental Quality Monitoring Program of the Bahía Blanca Estuary

Table 4 List of studies in Negro River and other rivers reporting bioaccumulation of heavy metals and metalloids in fishes

Authors	Location	Species	Organ	Concentration μg g^{-1} w.w.										
				Fe	Hg	Mn	Co	Cr	Ni	Cd	Pb	Zn	As	Cu
Abrameto (2004)	Neuquén	*Odontesthes hatcheri*	Liver	14.2	–	4.38	n.d	n.d	n.d	n.d	n.d	27.9	–	n.d
			Muscle	2.44	–	3.42	–	–	–	–	n.d	7.08	–	–
		Percichtys colhuapiensis	Liver	60.99	–	3.79	–	–	–	n.d	n.d	26.60	–	–
			Muscle	3.25	–	3.12	–	–	–	–	n.d	5.49	–	–
	Allen (UV)	*Odontesthes hatcheri*	Liver	–	0.18	–	–	–	n.d	n.d	0.13	130	–	–
			Muscle	–	n.d	–	–	–	n.d	n.d	0.05	6.10	–	–
	Fernández Oro (UV)	*Odontesthes hatcheri*	Liver	–	0.36	–	–	–	–	n.d	1.43	91.2	–	–
			Muscle	–	0.13	–	–	–	n.d	n.d	–	–	–	–
	Beltrán (MV)	*Odontesthes hatcheri*	Liver	–	0.20	–	–	–	n.d	n.d	1.59	113	–	–
			Muscle	–	0.12	–	–	–	n.d	n.d	0.14	10	–	–
Arribéreet al. (2003)	Rio Negro (UV)	*Odontesthes hatcheri*	Muscle	–	0.077–0.384	–	0.016–0.025	–	<2	<0.3	–	12–39	0.056–0.118	–
Marcovecchio and Moreno (1993)	Río De La Plata	*Rhamdia*	Muscle	–	0.13	–	–	–	–	n.d	–	21.15	–	–
Avigliano et al. (2015)	Río De La Plata	*Odontesthes bonariensis*	Muscle	0.30	–	–	–	–	–	–	0.19	–	0.03	–

(–) Not analyzed; *n.d.* Not detected; *UV* upper valley; *MV* middle valley; *LV* lower valley

3.4 Mollusks

Abrameto et al. (2012) investigated the presence of Cd, Zn, As, Cu in *C. fluminea* collected from the middle and lower basins of the Negro River, and reported Cd concentrations from 0.7 to 0.13 $\mu g\ g^{-1}$, Zn levels between 10.5 and 29.2 $\mu g\ g^{-1}$, As concentrations from 0.16 to 0.87 $\mu g\ g^{-1}$, and Cu levels between 2.8 and 7.2 $\mu g\ g^{-1}$. Hünicken et al. (2019) reported lower concentrations of heavy metals, ranging from 3 to 3.68 $\mu g\ g^{-1}$ for Cu and from 10.5 to 11.9 $\mu g\ g^{-1}$ for Zn. Although spaced in time, there is solid evidence of the heavy metal impact in water, sediments, SPM and transference to the aquatic biota at the Negro River basin, including bioaccumulation and biomagnification processes (Table 5). This supports the urgent need for serial and tiered monitoring programs over the area.

4 Freshwater Macroinvertebrates Assemblages

Several studies have addressed the effects of anthropic activities (involving changes in the land use/cover) on the aquatic macroinvertebrate assemblages of Patagonian streams and rivers (Miserendino 2001; Macchi and Dufilho 2008; Miserendino and Masi 2010; Miserendino et al. 2011; Horak et al. 2020). As a result, biological criteria based on the analyses of aquatic macroinvertebrates have been added to the traditional physical–chemical monitoring methods to assess the quality of regional aquatic ecosystems (Miserendino and Pizzolón 1999; Brand and Miserendino 2015; Mauad et al. 2015; Kohlmann et al. 2018; Miserendino et al. 2020).

Despite an increase in the knowledge about the composition and structure of macroinvertebrate assemblages, the Negro River basin remains poorly studied in this way. The first documented survey was carried out by Wais (1990), who made a description of the macroinvertebrate assemblages at the Negro River, from the headwaters to the mouth, dividing it into the upper, middle and lower basin. A total of 63 families and 129 macroinvertebrate taxa were described, of which only 29 were recognized in the Negro River basin (lower valley). The richest taxa in the assessment were Mollusca and Diptera (Chironomidae family) and the analysis of functional groups showed a greater abundance of collector-gatherers throughout the basin, which were dominant along the entire basin (Wais 1990). Unfortunately, in that occasion, species-environment relationships were not analyzed.

In the following years, macroinvertebrate taxa received special attention: this was the case of the widespread Chironomidae (Paggi and Capítulo 2002; Paggi 2003) and the invasive mollusk species *Corbicula fluminea* (Archuby et al. 2015; Cazzaniga and Perez 1999; Martín and Estebenet 2002; Molina et al. 2015; Hünicken et al. 2019), particularly at the Limay and Negro rivers. Changes in the composition and structure of Chironomidae were related to water flow fluctuations due to the dams located upstream, in the Limay River. Main results showed the overlapping and return from

Table 5 List of some research in Negro River basin reporting bioaccumulation of heavy metals and metalloids in *Corbicula fluminea*

Authors	Location	Concentration μg g^{-1} w.w.										
		Fe	Hg	Mn	Co	Cr	Ni	Cd	Pb	Zn	As	Cu
Abrameto et al. (2012)	Conesa (MV)	–	–	–	–	–	–	0.11	–	19.10	0.16	4.30
	Zanjon de Oyuela-San Javier (LV)	–	–	–	–	–	–	0.13	–	29.20	0.24	5.80
	Isla La Paloma-Viedma (LV)	–	–	–	–	–	–	0.08	–	18.50	0.87	2.50
	Balneario-Viedma (LV)	–	–	–	–	–	–	0.07	–	23.90	0.69	7.20
Hünicken et al. (2019)	Dren El Molino-Viedma (LV)	–	–	–	–	–	–	–	–	11.68	–	3.68
	Puente Nuevo-Viedma (LV)	–	–	–	–	–	–	–	–	10.50	–	3.60
	Balneario-Viedma (LV)	–	–	–	–	–	–	–	–	11.40	–	3.00

(–) Not analyzed; *UV* upper valley; *MV* middle valley; *LV* lower valley

lotic environments with typical species (*Cricotopus*, *Thienemanniella*, *Limaya*) to more lentic species (*Ablabesmia*, *Dicrotendipes*) (Paggi and Capítulo 2002).

Invasive species are one of the main threats to freshwater biodiversity (Sala et al. 2000). For instance, *C. fluminea* population inhabiting the Negro River propagate in upstream direction to the Limay River at a rate of aprox. 8.8 km year^{-1} (Labaut 2021). This invasive bivalve causes biotic and structural changes influencing macroinvertebrates assemblages (Vaughn and Hakenkamp 2001; Gutiérrez et al. 2003; Werner 2008). Additionally, fishing with live incubators clams as bait could be an important potential vector for potential invasive species throughout Patagonian freshwater ecosystems (Belz et al. 2012).

There are several studies related to macroinvertebrates in upstream localities, including the Limay and Neuquén rivers, main tributaries of the Negro River. For instance, Luchini (1981) studied the assemblages and their relationships with temperature and water level fluctuations at the upper Limay River. Added to this, significant changes in the composition and decreased taxa richness of macroinvertebrate assemblages have been associated to poor water quality from the Duran stream, a tributary of the Limay River which flows through the city of Neuquén (Province of Neuquén) near to the confluence of Negro River. While in the upstream direction a high taxa richness (38 taxa) was correlated with high dissolved oxygen levels and the occurrence of particularly sensitive species to organic pollution (e.g. Leptoceridae -Tricoptera- and Leptophlebiidae -Ephemeroptera-), in the **downstream** direction, poor oxygenated waters-with values close to anoxia- were associated to low biodiversity (5 taxa). These last taxa belong to families tolerant to organic enrichment, such as Tubificidae, Glossiphoniidae and Chironomidae (Macchi 2008).

Macchi et al. (2018) recorded 43 taxa in the macroinvertebrate assemblages of irrigation and drainage system of Neuquén River basin, including Diptera (mainly Chironomidae), Ephemeroptera, Trichoptera and Gastropoda as the richest taxa. In this study, a decrease in biodiversity and abundance of macroinvertebrates (mainly the sensitive Baetidae -Ephemeroptera-) were associated with higher levels of chlorpyrifos and azinphosmethyl in surface waters. This coincided with an increase of tolerant species/groups such as *Hyalella curvispina* (Amphipoda), subfamily Chironominae and Gastropoda (Macchi et al. 2018). When comparing exposed sites to the insecticide with pristine ones (Anguiano et al. 2008) in Limay and Neuquén rivers, these species showed different levels of resistance to azinphosmethyl in non-target populations of *H. curvispina* and *Simulium* spp. (Diptera). Added to this, Lares et al. (2016) also found populations of *H. curvispina*, *Heleobia* sp. (Gastropoda) and *Girardia tigrina* (Tricladida) in sites with higher chlorpyrifos LC_{50} values than those previously reported.

River macroinvertebrates are influenced by both, habitat complexity and heterogeneity (Vinson and Hawkins 1998). In the Negro River the types of habitats varied according to the size of the substrate, with a predominance of boulders, cobble and pebbles upstream and higher content of gravel and sand downstream. Also, is common the presence of dense submerged macrophyte patches, generally monospecific, with a coverage close to 10% (Macchi et al. 2019). The most frequent species were *Myriophyllum aquaticum, Stuckenia pectinata, Stuckenia striata* and *Elodea*

callitrichoides. The substrate also showed litter and woody materials, which comes from riparian forest. The riparian forest patches in the floodplain of the regional rivers are dominated by exotics *Salix alba* and *Populus nigra,* next to *S. humboldtiana* (only native species), *S. rubens* and *P. deltoids,* as companion species (Datri et al. 2016).

Macchi et al. (2019) reported the first approach to establish the entire macroinvertebrate assemblages of Negro River basin, analyzing the relationships with other environmental variables. For the first time, the authors registered 72 macroinvertebrate taxa of 30 families along this river, with Diptera (30), Ephemeroptera (8) and Mollusca (8) as the richest taxa. The most abundant taxa were Chironomidae (mainly *Eukiefferiella*, *Pseudochironomus*, *Tanytarsus*, *Limaya longitarsis* and *Cricotopus*), Ephemeroptera (mainly *Americabaetis alphus* and *Meridialaris* spp.) and *H. curvispina* (Fig. 3). Results indicated that the size of the substrate, conductivity, nutrients and turbidity were the most important environmental variables driving the macroinvertebrate assemblages in the Negro River basin (Macchi et al. 2019).

Macroinvertebrates have been used for environmental monitoring in rivers and streams worldwide. The application of the **biotic index BMPS**-RN (Biological Monitoring Patagonian Streams Negro River; Miserendino and Pizzolón 1999 adapted by Macchi et al. 2019) has allowed to identify the hot spots in the Negro River (Fig. 4, sites in red and orange colors). These were often closely related to drains that collect excess irrigation from agriculture, containing pesticide and fertilizer residues. In some cases, these drains are also used by urban waste treatment plants as an effluent

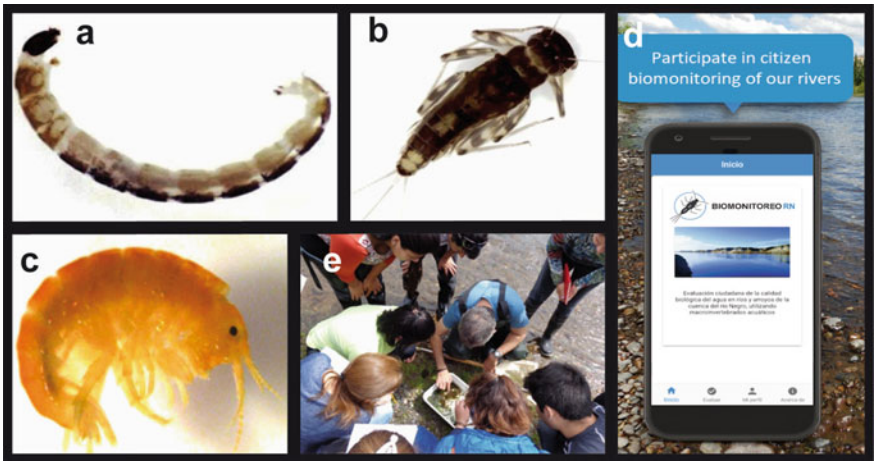

Fig. 3 **a**–**c**. Some of most abundant taxa in the Negro River. **a** *Cricotopus* (Chironomidae); **b** *Meridialaris chiloeensis* (Ephemeroptera); **c** *Hyalella curvispina* (Amphipoda). **d** Mobile application developed to enable involvement of the local population in the protection of the Negro River environment. **e** Using the app to provide data on biological water quality in participatory biomonitoring projects in the Negro River

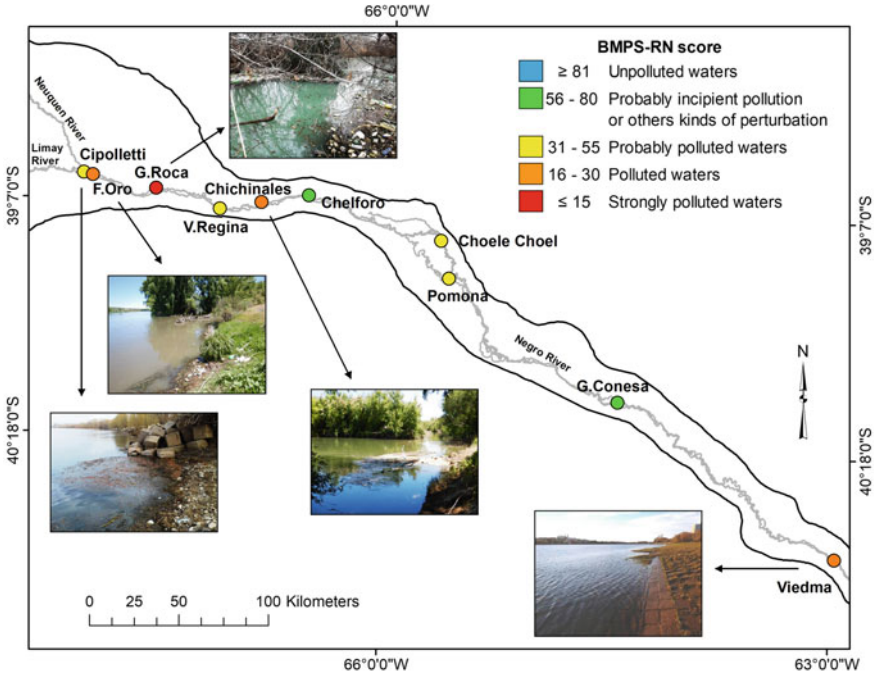

Fig. 4 Biological water quality monitoring based on BMPS-RN index at the Negro River

reception system, with little or no-treatment joint to industrial effluents and clandestine domestic sewage inputs. These contribute to a diffuse source of organic matter, nutrients, heavy metals and POPs into the Negro River. At impacted sites/locations, results showed a reduction in the taxonomic richness due to the elimination of sensitive species and an increase in the abundance of tolerant taxa such as Oligochatea and Chironominae. The increased numbers of these Rasmussen taxa at most of the degraded sites were consistent with those reported in worldwide moderately polluted rivers (Rasmussen et al. 2013; Horak et al. 2020).

The growing concern about the deterioration of water quality of the Negro River has led to a requirement for routine monitoring and the development of rapid testing that can be used by local governmental water management agencies. It is also important that citizens could get empowered towards sharing a sustainable environment and that all the community stakeholders take up the challenge of conserving and managing river water quality (Macchi and Maestroni 2020). Considering this, a mobile phone application (www.biomonitoreo.com.ar) has been developed by Macchi et al. (2019). This app, called RN Biomonitoring, is an initiative to allow the collective citizen participation in the monitoring of the biological quality of the water of the Negro River, oriented to enhance ownership and emphasize citizen responsibilities in the sustainable management of the national freshwaters (Fig. 3). These actions encourage the construction of a more active role for citizens in environmental monitoring of

natural resources, with greater commitments and reflective approaches to the problem of water.

5 Freshwater fish communities

5.1 Introduced Species: Status and Potential Problems

A total of 17 species have been identified in the Negro River; while 9 of these are native, 8 have been introduced from other Argentinean courses (Corydoras paleatus, Cnesterodon decemmaculatus, Cheirodon interruptus, Psalidodon pampa, and Odontesthes bonariensis) and other world regions (Oncorhynchus mykiss, Salmo trutta, and Cyprinus carpio) (Baigún et al. 2002, Casciotta et al. 2005, Alvear et al. 2007, Aigo et al. 2008, Solimano et al. 2019, Soricetti et al. 2020) (Table 6). This leads to a zoogeographic integrity coefficient of 0.52 (Elvira 1995). In the upper valley of the Negro River, the species assemblage is similar to those of the Andean zone of the Patagonia, including the Percichthyidae, Galaxiidae, Diplomystidae, and Salmonidae families. In particular, S. trutta is only found in the upper valley of the river. On the one hand, the abundance of O. mykiss, Galaxias maculatus, Diplomystes viedmensis and Percichthys trucha shows a decrease from west to east, with scarce catches in the lower valley (Soricetti et al. 2020). Conversely, Jenynsia lineata, Odontesthes hatcheri, and C. carpio are abundant throughout the entire river. The first report of C. carpio was documented at the lower valley by Alvear et al. (2007); after that, this species advanced to the upper valley in just a few years (Alvear et al. 2007, Solimano et al. 2019, Soricetti et al. 2020). Marine species can be found at the lower valley, such as Paralichtys orbignyanus, Mugil liza and Genidens barbus: while their abundance decrease from east to west, they are not present in the middle and upper valleys. On the other hand, Odontesthes bonariensis, freshwater specie, was probably introduced in the lower valley, but it presents a similar pattern of distribution of the marine species.

The two species of the Characidae family, Psalidodon pampa and Cheirodon interruptus, are rare in the upper valley of the Negro River, although they have been captured at irrigation channels at Allen city area (Solimano et al. 2019). These species are easily found in irrigation channels both in the middle and lower valleys, where they form shoals together with Corydoras paleatus (Baigún et al 2002, Soricetti et al. 2020). It is believed that C. interruptus has invaded the Negro River due to illegal releases by recreatinal fishers, since it is used as live bait for silverside fishing (Maiztegui et al. 2009). Shoals of C. paleatus are also very common and are distributed throughout the entire Negro River (Alvear et al. 2007, Solimano et al. 2019, Soricetti et al 2020). Finally, the species Cnesterodon decemmaculatus is rare and can be caught in flooded areas or low lagoons adjacent to the river (Soricetti et al. 2020). Table 6 shows the order, family, species, ordinary name, origin, and relative abundance of fish species at the different valleys of the Negro River.

5.1.1 Salmonids

Salmonids were stocked at the Negro River since 1904, for fishing purposes (Marini 1936). The first stocked species were *Coregonus cluppeaformis*, *Salvelinus fontinalis*, *Salvelinus namaychus*, *Salmo salar*, and *Onchorinchus mykiss*, while *Salmo trutta*, *C. clupeaformis*, and *S. namaycush* where not able to establish self-sustainable populations (Macchi et al. 2008; Macchi and Vigliano 2014). Up to date, only *S. truta* and *O. mykiss* can be found at the river. It is worth to mention that *O. mykiss* is the most abundant salmonid at the Negro River, mainly due to competition and the increase numbers of stocked individuals during the 40 s and 50 s (Macchi et al. 2008; Macchi and Vigliano 2014).

Salmonids are found in all freshwater environments of the Patagonia (Otturi et al. 2020) and their effect on native fauna has been difficult to assess due to the lack of data prior to their introduction (Casalinuovo et al. 2017). Besides, *O. mykiss* and *S. trutta* are on the list of the 100 most harmful invasive alien species in the world (Lowe et al. 2004). Several authors have stated that the introduction of salmonids produces large impacts on native communities (Aigo et al. 2008; Arismendi et al. 2009, 2014; Vigliano et al. 2009; Habit et al. 2010, 2012; Correa et al. 2012). At the Negro River, for instance, *O. mykiss* has been shown to compete for food with the native *P. trucha*, producing a decrease in the growth rate and abundance of the native species (Otturi et al. 2020). The effect of *O. myki ss* on *Galaxias* sp. occurs through two pathways, the first is by trophic competition between *Galaxias* ssp with *O. mykiss* juveniles (Tagliaferro et al. 2015), while the second is related to the predation by *O. mykiss* and *S. trutta* (Macchi et al. 2007; McDowall 2006). In addition, salmonids may be prone to feed on lamprey eggs or larvae (Arakawa and Lampman 2020).

5.1.2 Cyprinus Carpio

C. carpio is found almost everywhere in Argentina (Maiztegui 2016). It was introduced in the early twentieth century, for ornamental and aquaculture purposes (Mac Donagh 1948). Its introduction in the Negro River dates back to 2002 (Alvear et al. 2007) with not known rationale; however, there are some hypotheses by which they could have been used as an ecological answer to control the biomass of macrophytes in the irrigation channel systems. Table 6 shows the order, family, species, ordinary name, origin, and relative abundance of fish species at the different valleys of the Negro River.

The common carp is widely considered an ecosystem engineer (Crooks 2002) since it influences the availability of resources for other organisms (Jones et al. 1994), modifying the structure and functioning of the communities (McCollum et al. 1998; Usio and Townsend 2004). It represents one of the most damaging species for the aquatic systems and is listed between the eight worst invasive fish species in the world according to the IUCN (Lowe et al. 2004). It has a benthic feeding behaviour that produces alterations on the bottom (Tatrai et al. 1994); this sediment removal normally produces a suspension of solids and nutrients into the

Table 6 Order, Family, Species, Ordinary name, Origin, and relative abundance of fish species at the different valleys of the river

Order	Family	Species	Ordinary name	Origin	Relative Abundance		
					Upper valley	Middle valley	Lower valley
Petromyzontiformes	Geotriidae	*Geotria macrostoma*	Patagonian lamprey	Native	*	*	*
Characiformes	Characidae	*Psalidodon pampa*	Tetra	Exotic B	*	**	***
		Cheirodon interruptus	Tetra	ExoticB	*	**	***
Siluriformes	Diplomystidae	*Diplomystes viedmensis*	Velvet catfish	Native	*	*	*
	Callichthyidae	*Corydoras paleatus*	Peppered corydoras	Exotic B	**	**	***
	Ariidae	*Genidens barbus*	White sea catfish	Native			*
Cypriniformes	Cyprinidae	*Cyprinus carpio*	Common carp	Exotic C	***	***	***
Osmeriformes	Galaxiidae	*Galaxias maculatus*	Small puyen	Native	***	*	*
Salmoniformes	Salmonidae	*Salmo trutta*	Brown trout	Exotic C	*		
		Oncorhynchus mykiss	Rainbow trout	Exotic C	***	*	*
Atheriniformes	Atherinopsidae	*Odontesthes hatcheri*	Patagonic silverside	Native	***	***	***
		Odonteshes bonariensis	Silverside	Exotic B			***
Cyprinodontiformes	Poeciliidae	*Cnesterodon decemmaculatus*	Ten spotted live-bearer	Exotic B	*	*	*
	Anablepidae	*Jenynsia lineata*	Onesided livebearer	Native	***	***	***

(continued)

Table 6 (continued)

Order	Family	Species	Ordinary name	Origin	Relative Abundance		
					Upper valley	Middle valley	Lower valley
Perciformes	Percichthyidae	*Percichthys trucha*	Creole perch	Native	***	***	**
Mugiliformes	Mugilidae	*Mugil liza*	Mullet	Native			**
Pleuronectiformes	Paralichthydae	*Paralichtys orbignianus*	Flounder	Native			**

Built from Alvear et al. (2007), Aigo et al. (2008), Solimano et al. (2019), Soricetti et al. (2020)
* = Rare; ** = Common; *** = Abundant. B = Exotic of Brasilic origin C = Exotic from another continent

water column, thus generating a decrease in transparency and an increase in the algae population through "bottom-up" effects (Tatrai et al. 1990, 1996), modifying chlorophyll-a levels (Matsuzaki et al. 2007). It should be noted that the increase in the number of carp is directly proportional to the degree of river regulation (Gehrke 1997). Currently, *C. carpio* has showed a significant trophic overlap with *P. trucha* in summer and with *O. hatcheri* in spring (Alvear et al. 2007; Crichigno et al. 2013; Conte-Grand et al. 2015). Further impacts on endemic species will depend mostly on the carp biomass (Weber et al. 2010) and will range from decline to local extinction of native species (Crichigno et al. 2016; Koehn et al. 2000).

5.2 Native Species

5.2.1 Geotria Macrostoma

In recent years, its abundance has declined, a phenomenon which has been shown for several lamprey species worldwide (Maitland et al. 2015; Boulêtreau et al. 2020). Despite the fact that two decades ago it was common to observe large shoals of lampreys at the Negro River, recent studies have shown a scarcity or even absence of lamprey larvae. Alvear et al. (2007), Aigo et al. (2008), Solimano et al. (2019) and Soricetti et al. (2020) reported no captures, while Riva-Rossi et al. (2020) mentioned the capture of 3 juveniles of *G. macrostoma* in the lower valley. Hypotheses on the diminished abundance of this native species range from habitat modification by dams, climate change and the introduction of predators into the river (Mateus et al. 2012; Maitland et al. 2015; Hansen et al. 2016; Boulêtreau et al. 2020) such as the introduction of *C. carpio.* For instance, Arakawa and Lampman (2020) found that there is a high rate of consumption of ammocetes larvae by this species. Finally, the native species *G. macrostoma* has disappeared from the upper and middle reaches of the Limay River, upstream the dams (Pascual et al. 2007; Cussac et al. 2016).

5.2.2 Aplochiton Spp

On the one hand, the understanding of what has happened to the species of the genus *Aplochiton* in several Patagonian rivers, particularly in the Negro River, is extremely complex since there is no baseline knowledge or recorded population status prior to the entry of the salmonids (Casalinuovo et al. 2017). On the other hand, no individuals of this genus have been obtained in Patagonian rivers since 1945. *Aplochiton zebra* was reported for the Negro River by Pozzi (1945) and by Marini (1936) and Sorçaburu at Puerto Blest (captures performed in 1930 and 1933 respectively; Piacentino 1999; Cussac et al. 2020). In recent studies, no specimens of this species were caught (Alvear et al. 2007; Solimano et al. 2019; Soricetti et al. 2020) for both, the Negro and Limay rivers. In areas with still known occurrence, Patagonian rivers with Pacific catchments, it is commonly observed that they are

highly affected by salmonids (Lattuca et al. 2008; Arismendi et al. 2009). They are also abundant species at Chilean lakes where there is no presence of salmonids (Soto et al. 2006; Arismendi et al. 2009).

5.2.3 Dyplomistes Viedmensis

The family Diplomystidae is considered the first lineages to diverge from the ancestor of all living Siluriformes (Arratia 1987; Sullivan et al. 2006; Muñoz-Ramírez et al. 2014). Endemic from southern South America is distributed at both sides of the Andes (Muñoz-Ramírez et al. 2014) and consist of seven species, most of them facing conservation issues or extinct (Muñoz-Ramírez et al. 2010, 2014; Arratia and Quezada-Romegialli 2017). It is poorly known in Argentina (Bello and Ubeda 1998) where has been suggested the need of maximum conservation priority (Bello and Ubeda 1998; López et al. 2002). In the Negro River, *D. viedmensis* is still present but faces the anthropic use of the habitat and introduced species as relevant threats (Arratia 1987; López et al. 2002).

5.3 Environmental Threats for Fish Assemblages

Considering the current climate change predictions, two main processes can be expected to occur: the southward expansion of the Brazilian fauna and other introduced species (*P. pampa, Ch. interruptus, C. carpio*) and the extinction of southern fauna such as galaxids and salmonids (Cussac et al. 2020). An example of this type of displacement is the decrement of *G. barbus* communities in southeastern Brazil (Araújo et al. 2018) and its increment of the abundance of this species in the Negro River area, the southern part of its distribution (Solimano et al. 2019, Soricetti el al. 2020) and this may pose risks for the native *G. macrostoma*, a fact demonstrated to occur, with the interaction of predators siluriforms and lamprey, in southern France (Cucherousset et al. 2018) and Columbia River (Close et al. 1995).

Regarding future dams, while it is well known that flow fluctuations can generate biological effects on taxa that depend on flood or riparian habitats (Pringle et al. 2000), no reliable consequences on communities are still known (Macchi et al. 1999; Temporetti et al. 2001; Cussac et al. 2016).

Typically, the biodiversity crisis addresses species loss through extinction, although on a sub-global scale, the loss of populations through local extirpation and invasion by exotic species may be of most concern (Olden et al. 2011). Climate change is one of the main drivers of biotic homogenization, causing a change in species composition, but not in species richness (Magurran et al. 2015). If we take into account the studies conducted at the Negro River, the results show that the diversity is reduced and most of the inhabiting species are not native (Alvear et al. 2007; Solimano et al. 2019; Soricetti et al. 2020). Climate change and direct anthropic interventions such as live bait, recreational fishing, aquarium escapes or other uses

have led to a shift of the species transition zone to the south (Pérez and Cazorla 2008; Soricetti et al. 2020).

References

Abrameto M (2004) Distribución, especiación y biodisponibilidad de metales pesados en compartimientos abióticos y biológicos del Río Negro. Doctoral thesis. Universidad Nacional del Sur (in Spanish)

Abrameto M (2019) Heavy Metals at the Rio Negro. Environmental Monitoring Program of the Río Negro National University. http://rid.unrn.edu.ar/handle/20.500.12049/5300. Accessed 15 Apr 2021 (in Spanish)

Abrameto M, Barrio D, Banzato L, Fellenz N, Gibeli T (2012) Niveles de metales traza en invertebrados colectados en el Río Negro. In: Marcovecchio JE, Freije RH (eds) II Reunión de Geoquímica de la Superficie. Editorial UTN (in Spanish), Bahía Blanca, pp 1–5

Abrameto M, Dapeña C, Aldalur B, Caro A, Cecchini V, Fernandez C et al (2013) Marcadores de contaminación urbana y agrícola, en agua superficial y subterránea en el Valle inferior del río Negro, Argentina. In: Gonzales N, Kruse E, Trovatto M, Laurencena P (eds) Agua subterránea recurso estratégico Tomo II. Editorial ULP (in Spanish), La Plata, pp. 145–148

Ai YS, Koh HD, Seong WL, Aweng AL, Rak EH (2019) An Assessment of Heavy metals toxicity in asian clam, corbicula fluminea, from Mekong River, Pa Sak River, and Lopburi River, Thailand. Sci World J 4:1–5

Aigo J, Cussac V, Peris S, Ortubay S, Gómez S, López H et al (2008) Distribution of introduced and native fish in Patagonia (Argentina): patterns and changes in fish assemblages. Rev Fish Biol Fish 18(4):387–408

Alam MGM, Tanaka A, Allinson G, Laurenson LJB, Stagnitti F, Snowa ET (2002) Comparison of trace element concentrations in cultured and wild carp (*Cyprinus carpio*) of Lake Kasumigaura, Japan. Ecotoxicol Environ Saf 53:348–354

Alvear P, Rechencq M, Macchi PJ, Alonso MF, Lippolt GE, Denegri MA et al (2007) Composición, distribución y relaciones tróficas de la ictiofauna del río Negro, Patagonia Argentina. Ecol Austral 17:231–246 (in Spanish)

Arakawa H, Lampman RT (2020) An experimental study to evaluate predation threats on two native larval lampreys in the Columbia River Basin, USA. Ecol Freshw Fish 29:611–622

Araújo FG, Teixeira TP, Guedes APP, Costa de Azevedo MC, Machado Pessanha AL (2018) Shifts in the abundance and distribution of shallow water fish fauna on the southeastern Brazilian coast: A response to climate change. Hydrobiologia 814:205–218

Archuby FM, Adami M, Martinelli JC, Gordillo S, Boretto GM, Malvé ME (2015) Regional-scale compositional and size fidelity of rocky intertidal communities from the Patagonian Atlantic coast. Palaios 30(8):627–643

Arias AH, Ronda AC, Oliva AL, Tombesi NB (2019) Persistent organic compounds at the Río Negro. Environmental Monitoring Program of the Río Negro National University. http://rid.unrn.edu.ar/handle/20.500.12049/5300. Accessed 15 Apr 2021 (in Spanish)

Arismendi I, Penaluna BE, Dunham JB, García de Leaniz C, Soto D, Fleming IA et al (2014) Differential invasion success of salmonids in southern Chile: patterns and hypotheses. Rev Fish Biol Fish 24:919–941

Arismendi I, Soto D, Penaluna B, Jara C, Leal C, León-Muñoz J (2009) Aquaculture, non-native salmonid invasions and associated declines of native fishes in Northern Patagonian lakes. Freshw Biol 54(5):1135–1147

Arratia G (1987) Description of the primitive family Diplomystidae (Siluriformes, Teleostei, Pisces). Zoologisches Forschungsinstitut und Museum Alexander Koenig

Arratia G, Quezada-Romegialli C (2017) Understanding morphological variability in a taxonomic context in Chilean diplomystids (Teleostei: Siluriformes), including the description of a new species. Peer J 5:e2991

Arribére M, Guevara SR, Sánchez R, Gil M, Ross GR, Daurade L et al (2003) Heavy metals in the vicinity of a chlorine alkali factory in the upper Negro River ecosystem, Northern Patagonia Argentina. Sci Total Environ 301:187–203

Avigliano E, Schenone NF, Volpedo AV, Goessler W, Fernández Cirelli A (2015) Heavy metals and trace elements in muscle of silverside (*Odontesthes bonariensis*) and water from different environments (Argentina) aquatic pollution and consumption effect approach. Sci Total Environ 506–507:102–108

Bello M, Ubeda C (1998) Estado de conservación de los peces de agua dulce de la Patagonia Argentina. Aplicación de una metodología objetiva. Gayana Zool 62:45–60 (in Spanish)

Belz CE, Darrigran G, Netto OS, Boeger WA, Ribeiro PJ (2012) Analysis of four dispersion vectors in Inland waters: the case of the invading Bivalves in South America. J Shellfish Res 31(3):777–784

Botté S, Freije H, Marcovecchio JE (2010) Distribution of several heavy metals in tidal flats sediments within Bahía Blanca Estuary (Argentina). Water Air Soil Pollut 210:371–388

Botté S, Marcovecchio M, Fernández-Severini M, Negrin V, Panebianco MV, Simonetti P et al (2013) Ciclo de metales. In: Marcovecchio JE, Freije RH (eds) Procesos Químicos en Estuarios. Editorial UTN (in Spanish), Bahía Blanca, pp. 227–258

Boulêtreau S, Carry L, Meyer E, Filloux D, Menchi O, Mataix V et al (2020) High predation of native sea lamprey during spawning migration. Sci Rep 10:1–9

Brand C, Miserendino ML (2015) Testing the performance of macroinvertebrate metrics as indicators of changes in biodiversity after pasture conversion in Patagonian mountain streams. Water Air Soil Pollut 226(11):1–18

Cai MH, Lin J, Hong QQ, Wang Y, Cai MG (2011) Content and distribution of trace metals in surface sediments from the northern Bering Sea, Chukchi Sea, and adjacent Arctic areas. Mar Pollut Bull 63:523–527

Casalinuovo MA, Alonso MF, Macchi PJ, Kuroda JA (2017) Brown Trout in Argentina. In: Lobón-Cerviá J, Sanz CN (eds) Brown Trout: biology, ecology and management. Wiley, New Jersey, pp 599–621

Cazzaniga NJ, Pérez C (1999) Asiatic Clam, Corbicula fluminea, in Northwestern Patagonia (Argentina). J Freshw Ecol 14(4):551–552

CCME, Canadian Council of Ministers of the Environment (2020) http://st-s.ccme.ca/en/index.html?chems=4,9,12,15,16,20,21,61,63,62,65,71,123,129,131,138,139,226,229&chapters=1. Accessed 4 Feb 2021

Close DA, Fitzpatrick M, Li H, Parker B, Hatch D, James G (1995) Status report of the Pacific lamprey (*Lampetra tridentata*) in the Columbia River Basin. United States. Technical Report to Bonneville Power Administration DOE/BP-39067-1

Conte-Grand C, Sommer J, Ortí G, Cussac V (2015) Populations of Odontesthes (Teleostei: Atheriniformes) in the Andean region of Southern South America: body shape and hybrid individuals. Neotrop Ichthyol 13:137–150

Correa C, Bravo AP, Hendry AP (2012) Reciprocal trophic niche shifts in native and invasive fish: salmonids and galaxiids in Patagonian lakes. Freshw Biol 57:1769–1781

Crichigno S, Conte-Grand C, Battini M, Cussac V (2013) Cephalic morphological variation in freshwater silversides *Odontesthes hatcheri* and *Odontesthes bonariensis* in Patagonia: introgression and ecological relationships. J Fish Biol 83:542–559

Crichigno S, Cordero P, Blasetti G, Cussac V (2016) Dispersion of the invasive common carp Cyprinus carpio in southern South America: changes and expectations, westward and southward. J Fish Biol 89:403–416

Crooks JA (2002) Characterizing ecosystem level consequences of biological invasions: the role of ecosystem engineers. Oikos 97:153–166

Cucherousset J, Horky P, Slavík O, Ovidio M, Arlinghaus R, Boulêtreau S et al (2018) Ecology, behaviour and management of the European catfish. Rev Fish Biol Fish 28:177–190
Cussac VE, Barrantes ME, Boy CC, Górski K, Habit E, Lattuca ME et al (2020) New insights into the distribution, physiology and life histories of South American Galaxiid fishes, and potential threats to this unique Fauna. Diversity 12:178
Cussac VE, Habit E, Ciancio J, Battini MA, Riva Rossi C, Barriga JP et al (2016) Freshwater fishes of Patagonia: conservation and fisheries. J Fish Biol 89(1):1068–1097
Datri LA, Faggi AM, Gallo LA, Carmona F (2016) Half a century of changes in the riverine landscape of Limay River: the origin of a riparian neoecosystem in Patagonia (Argentina). Biol Invasions 18(6):1713–1722
Demirak A, Yilmaz F, Levent Tuna A, Ozdemir N (2006) Heavy metals in water, sediment, and tissues of Leuciscus Cephalus from a stream in southwestern Turkey. Chem 63:1451–1458
EPA, Environmental Protection Agency US (2020) https://www.epa.gov. Accessed 12 Mar 2021
Epele LB, Manzo LM, Grech MG, Macchi PA, Claverie AÑ, Lagomarsino L et al (2018) Disentangling natural and anthropogenic influences on Patagonian pond water quality. Sci Total Environ 613:866–876
Gaiero D, Probst J, Depetris P, Lelyter L, Kempe S (2002) Riverine transfer of heavy metals from Patagonia to the southwestern Atlantic Ocean. Reg Environ Change 3:51–64
Gehrke PC (1997) Differences in composition and structure of fish communities associated with flow regulation in New South Wales rivers. In: Harris JH, Gehrke PC (eds) Fish and rivers in stress: the NSW Rivers Survey. NSW Fisheries Office of Conservation and Cooperative Research Centre for Freshwater Ecol, Australia, pp. 185–215
Gutiérrez JL, Jones CG, Strayer DL, Iribarne OO (2003) Mollusks as ecosystem engineers: the role of shell production in aquatic habitats. Oikos 101(1):79–90
Habit E, Gonzalez J, Ruzzante DE, Walde SJ (2012) Native and introduced fish species richness in Chilean Patagonian lakes: inferences on invasion mechanisms using salmonid-free lakes. Divers Distrib 18:1153–1165
Habit E, Piedra P, Ruzzante DE, Walde SJ, Belk MC, Cussac VE, Gonzalez J, Colin N (2010) Changes in the distribution of native fishes in response to introduced species and other anthropogenic effects. Glob Ecol Biogeogr 19:697–710
Hansen MJ, Madenjian CP, Slade JW, Steeves TB, Almeida PR, Quintella BR (2016) Population ecology of the sea lamprey (*Petromyzon marinus*) as an invasive species in the Laurentian Great Lakes and an imperiled species in Europe. Rev Fish Biol Fish 26:509–535
Horak CN, Assef YA, Grech MG, Miserendino ML (2020) Agricultural practices alter function and structure of macroinvertebrate communities in Patagonian piedmont streams. Hydrobiologia 847(17):3659–3676
Hu B, Cui R, Li J, Wei H, Zhao J, Bai F, Song W, Ding X (2013) Occurrence and distribution of heavy metals in surface sediments of the Changhua River Estuary and adjacent shelf (Hainan Island). Mar Pollut Bull 76:400–405
Hünicken LA, Abrameto MA, Bonel N (2019) *Corbicula* at its southernmost invasion front in Patagonia: unusual low density and asymmetric trait responses to varying environmental conditions. J Moll Stud 85:143–153
Isla F, Miglioranza K, Ondarza P, Shimabukuro V, Menone M, Espinosa M, Moreno V (2010) Sediment and pollutant distribution along the Negro River: Patagonia, Argentina. Int J Riv Basin Manage 8:319–330
Janiot LJ, Sik E, Marcucci O, Gesino A, Molina D, Martínez L, Marcucci P (2001) Contaminantes orgánicos persistentes (COPs) y metales pesados en agua y sedimentos del río de la plata y su frente marítimo. https://www.dinama.gub.uy/oan/documentos/uploads/2016/12/COPs_y_metales_pesados_VJCM.pdf. Accessed 1 Mar 2021 (in Spanish).
Jones CG, Lawton JH, Shachak M (1994) Organisms as ecosystem engineers. In: Samson F, Knopf F (eds) Ecosystems management. Springer, New York, pp 130–147
Jones KC, De Voogt P (1999) Persistent organic pollutants (POPs): state of the science. Environ Pollut 100(1–3):209–221

Koehn J, Brumley A, Gehrke P (2000) Managing the impacts of carp. Bureau of Rural Sciences, Department of Agriculture. Australia: Fisheries and Forestry

Kohlmann B, Arroyo A, Macchi PA, Palma R (2018) Biodiversity and biomonitoring indexes. In: Maestroni B, Cavannan A (eds) Integrated analytical approaches for pesticide management. Academic Press, Viena, Austria, pp 83–106

Langston WJ, Pope ND, Jonas PJC, Nikitic C, Field MDR, Dowell B, Brown AR (2010) Contaminants in fine sediments and their consequences for biota of the Severn Estuary. Mar Poll Bull 61(1–3):68–82

Lattuca ME, Brown D, Castiñeira L, Renzi M, Luizon C, Urbanski J, Cussac V (2008) Reproduction of landlocked Aplochiton zebra Jenyns (Pisces, Galaxiidae). Ecol Freshw Fish 17:394–405

LIBIQUIMA-CITAAC, Laboratorio de Investigaciones Bioquímicas y Químicas del Medio Ambiente-Centro de Investigaciones en Toxicología Ambiental y Agrobiotecnología del Comahue (2016) Situación Ambiental por Agroquímicos e hidrocarburos en el Alto Valle del Río Negro y Neuquén (in Spanish)

Loewy RM, Monza LB, Kirs VE, Savini MC (2011) Pesticide distribution in an agricultural environment in Argentina. J Environ Sci Health B 46(8):662–670

López HL, Morgan CC, Montenegro M (2002) ProBiota. Serie Documentos. Ichthyological ecoregions of Argentina. http://sedici.unlp.edu.ar/handle/10915/10938. Accessed 15 Apr 2021

Lowe S, Browne M, Boudjelas S, De Poorter M (2004) 100 de las Especies Exóticas Invasoras más dañinas del mundo. Una selección del Global Invasive Species Database. UICN (in Spanish). https://portals.iucn.org/library. Accessed 5 Dec 2020

Luchini L (1981) Estudios Ecológicos en la Cuenca del Río Limay (Argentina). Natura Neotropicalis 1(12):44–58 (in Spanish)

Mac Donagh EJ (1948) Sobre la cría de carpas y pejerreyes en la provincia de San Luis. Notas Mus Plata 13:313–326 (in Spanish)

Macchi PA (2008) Degradación de la calidad del agua en el arroyo Durán. Dissertation, I Jornadas de Ciencias Naturales en la Patagonia. Biodiversidad y Conservación, Esquel, Chubut (in Spanish)

Macchi PA (2019) Biomonitoreo RN. https://biomonitoreo.com.ar. Accessed 11 Nov 2020 (in Spanish)

Macchi PA, Bernanrdis A, Saade I, Encina M, Navarro M, Baeza L, Mora GA (2019) Evaluación ecológica de la calidad de agua del río Negro utilizando macroinvertebrados acuáticos. Environmental Monitoring Program of the Río Negro National University. http://rid.unrn.edu.ar/handle/20.500.12049/5300. Accessed 15 Apr 2021

Macchi PA, Dufilho C (2008) Variación en la composición y organización funcional de macroinvertebrados bentónicos en una cuenca Patagónica. Dissertation, IV Congreso Argentino de Limnología. San Carlos de Bariloche. Río Negro (in Spanish)

Macchi PA, Loewy RM, Lares B, Latini L, Monza L, Guiñazú N, Montagna CM (2018) The impact of pesticides on the macroinvertebrate community in the water channels of the Río Negro and Neuquén Valley, North Patagonia (Argentina). Environ Sci Pollut Res 25(11):10668–10678

Macchi PA, Maestroni B (2020) Biomonitoring of freshwater ecosystems: research and citizen participation in the Upper Valley of Río Negro and Neuquén (Patagonia, Argentina). Food Env Prot News 23(2):28–30

Macchi PJ, Cussac VE, Alonso MF, Denegri MA (1999) Predation relationships between introduced salmonids and the native fish fauna in lakes and reservoirs in northern Patagonia. Ecol Freshw Fish 8:227–236

Macchi PJ, Pascual MA, Vigliano PH (2007) Differential piscivory of the native Percichthys trucha and exotic salmonids upon the native forage fish Galaxias maculatus in Patagonian Andean lakes. Limnol Temp S Am 37:76–87

Macchi PJ, Vigliano PH (2014) Salmonid introduction in Patagonia: the ghost of past, present and future management. Ecol Austr 24(2):162–172

Macchi PJ, Vigliano PH, Pascual MÁ, Alonso M, Denegri MA, Milano D, Asorey MG, Lippolt G (2008) Historical policy goals for fish management in northern continental Patagonia Argentina: A structuring force of actual fish assemblages? Am Fish Soc Symp 49:331–348

Magurran AE, Dornelas M, Moyes F, Gotelli NJ, McGill B (2015) Rapid biotic homogenization of marine fish assemblages. Nat Commun 6:8405
Maitland PS, Renaud CB, Quintella BR, Close DA, Docker MF (2015) Conservation of native lampreys. In: Docker MF (ed) Lampreys: biology conservation and control. Springer, The Netherlands, pp 375–428
Maiztegui T (2016) Ecología poblacional de Cyprinus carpio (teleostei) en los humedales de Ajó. Tesis Doctoral, Universidad Nacional de La Plata (in Spanish), Buenos Aires
Maiztegui T, Campanella D, Colautti DC (2009) Avances en el desarrollo del cultivo de la mojarra (Cheirodon interruptus) como alternativa a la explotación de poblaciones silvestres. *Biol Acuat,* pp 143–149 (in Spanish)
Marcovecchio JE, Moreno VJ (1993) Cadmium, Zinc and total mercury levels in the tissues of several fish species from La Plata river estuary, Argentina. Environ Monit Assess 25:119–130
Marini TL (1936) Los salmónidos en nuestro Parque Nacional Nahuel Huapi. Buenos Aires, Argentina: Anales de la Sociedad Científica Argentina (in Spanish)
Mateus CS, Rodríguez-Muñoz R, Quintella BR, Alves MJ, Almeida PR (2012) Lampreys of the Iberian Peninsula: distribution, population status and conservation. Endanger Species Res 16:183–198
Matsuzaki SS, Usio N, Takamura N, Washitani I (2007) Effects of common carp on nutrient dynamics and littoral community composition: roles of excretion and bioturbation. Fund App Limnol 168:27–38
Mauad M, Miserendino ML, Risso MA, Massaferro J (2015) Assessing the performance of macroinvertebrate metrics in the Challhuaco-Ñireco System (Northern Patagonia, Argentina). Iheringia Ser Zool 105(3):348–358
McCollum EW, Crowder LB, McCollum SA (1998) Complex interactions of fish, snails, and littoral zone periphyton. Ecology 79:1980–1994
McDowall R (2006) Crying wolf, crying foul, or crying shame: alien salmonids and a biodiversity crisis in the southern cool-temperate galaxioid fishes? Rev Fish Biol Fish 16:233–422
Miglioranza KS, Gonzalez M, Ondarza PM, Shimabukuro VM, Isla FI, Fillmann G, Moreno VJ (2013) Assessment of Argentinean Patagonia pollution: PBDEs, OCPs and PCBs in different matrices from the Río Negro basin. Sci Total Environ 452:275–285
Miglioranza KS, Ondarza PM, Costa PG, De Azevedo A, Gonzalez M, Shimabukuro VM, Fillmann G (2021) Spatial and temporal distribution of Persistent Organic Pollutants and current use pesticides in the atmosphere of Argentinean Patagonia. Chem 266:129015
Mirande JM, Koerber S (2015) Checklist of the freshwater fishes of Argentina. Ichthyological Contributions of Peces Criollos. https://ri.conicet.gov.ar/handle/11336/12893. Accessed 13 Sept 2020
Miserendino ML (2001) Macroinvertebrate assemblages in Andean Patagonian rivers and streams: environmental relationships. Hydrobiologia 444:147–158
Miserendino ML (2009) Effects of flow regulation, basin characteristics and land-use on macroinvertebrate communities in a large arid Patagonian river. Biodivers Conserv 18(7):1921–1943
Miserendino ML, Brand C (2009) Environmental effects of urbanization on streams and rivers in Patagonia (Argentina): the use of macroinvertebrates in monitoring. Adv Env Res 6:183–220
Miserendino ML, Casaux R, Archangelsky M, Di Prinzio CY, Brand C, Kutschker AM (2011) Assessing land-use effects on water quality, in-stream habitat, riparian ecosystems and biodiversity in Patagonian northwest streams. Sci Total Environ 409(3):612–624
Miserendino ML, Epele LB, Brand C, Manzo LM (2020) Los indicadores biológicos en la Patagonia. Calidad de agua e integridad ecológica: Una mirada desde arroyos a mallines. In: Domínguez E, Giorgi A, Gómez N (eds) La bioindicación en el monitoreo y evaluación de los sistemas fluviales de la Argentina: Bases para el análisis de la integridad ecológica. Eudeba (in Spanish), Argentina, pp. 148–155
Miserendino ML, Masi CI (2010) The effects of land use on environmental features and functional organization of macroinvertebrate communities in Patagonian low order streams. Ecol Indicators 10(2):311–319

Miserendino ML, Pizzolón LA (1999) Rapid assessment of river water quality using macroinvertebrates: a family level biotic index for the Patagonic Andean zone. Acta Limn Bras 11(2):137–148

Molina LM, Pereyra PJ, Molina Carrizo NG, Abrameto M (2015) Here come the clam: Southernmost record worldwide of the Asian clam *Corbicula fluminea* (Patagonia, Argentina). Russ J Biol Invasions 6:129–134

Mouthon J (2001) Life cycle and population dynamics of the Asian clam *Corbicula fluminea* (Bivalvia: Corbiculidae) in the Saone River at Lyon (France). Hydrobiology 452:109–119

Muir DC, Norstrom RJ, Simon M (1988) Organochlorine contaminants in Arctic marine food chains: accumulation of specific polychlorinated biphenyls and chlordane-related compounds. Environ Sci Tech 22(9):1071–1079

Muñoz-Ramírez C, Jara A, Beltrán-Concha M, Zuñiga-Reinoso A, Victoriano P, Habit E (2010) Distribución de la familia Diplomystidae (Pisces: Siluriformes) en Chile: nuevos registros. Bol Biodivers Chile, 6–17

Muñoz-Ramírez CP, Unmack P, Habit E, Johnson J, Cussac VE, Victoriano P (2014) Phylogeography of the ancient catfish family Diplomystidae: biogeographic, systematic, and conservation implications. Mol Phylogenet Evol 73:146–160

Olden JD, Kennard MJJ, Lawler JJ, Poff NL (2011) Challenges and ppportunities in implementing managed relocation for conservation of freshwater species. Conserv Biol 25:40–47

Ondarza PM, Gonzalez M, Fillman G, Miglioranza KSB (2014) PBDEs, PCBs and organochlorine pesticides distribution in edible fish from Negro River basin, Argentinean Patagonia. Chem 94:135–142

Otturi MG, Reggi PE, Battini MÁ, Barriga JP (2020) The effects of trophic interaction between the Patagonian native Percichthys trucha and the invasive oncorhynchus mykiss during the juvenile period. Biol Invasions 22:3293–3305

Paggi AC (2003) Los Quironómidos (Diptera) y su empleo como bioindicadores. Biol Acuat 21:50–57 (in Spanish)

Paggi AC, Capítulo AR (2002) Chironomid composition from drift: and bottom samples in a regulated north-Patagonian river (Río Limay, Argentina). SIL Proceedings, 1922–2010, 28(3):1229–1235

Pascual MA, Cussac V, Dyer B, Soto D, Vigliano P, Ortubay S, Macchi P (2007) Freshwater fishes of Patagonia in the 21st century after a hundred years of human settlement, species introductions, and environmental change. Aquat Ecosyst Health Manag 10:212–227

Pérez C, Cazorla AL (2008) Nuevos aportes al conocimiento de la ictiofauna del río Negro, provincia de río negro, Argentina. Nat Neotropicalis 1:83–87 (in Spanish)

Phillips DJH (1977) The use of biological indicator organisms to monitor trace metal pollution in marine and estuarine environments—a review. Environ Pollut 13:281–311

Piacentino GM (1999) New geographic localities of aplochiton species (Salmoniformes: Aplochitonidae) in the Argentinian Patagonia. Cybium Paris 23:209–211

Pozzi AJ (1945) Sistemática y distribución de los peces de agua dulce de la República Argentina. Gaea 7:239–292 (in Spanish)

Pringle CM, Freeman MC, Freeman BJ (2000) Regional effects of hydrologic alterations on riverine macrobiota in the new world: tropical-temperate comparisons. Bioscience 50:807–823

PMCA-EBB, Programa de monitoreo de la calidad ambiental de la zona interior del estuario de Bahía Blanca (2016). Instituto Argentino de Oceanografía. https://www.bahia.gob.ar/subidos/cte/informes/Informe-FINAL-Monitoreo-2015-2016.pdf. Accessed 4 Apr 2020 (in Spanish)

Rasmussen JJ, McKnight US, Loinaz MC, Thomsen NI, Olsson ME, Bjerg PL, Binning PJ, Kronvang B (2013) A catchment scale evaluation of multiple stressor effects in headwater streams. Sci Total Environ 442:420–431

Riva-Rossi C, Barrasso DA, Baker C, Quiroga AP, Baigún C, Basso NG (2020) Revalidation of the Argentinian pouched lamprey geotria macrostoma (Burmeister, 1868) with molecular and morphological evidence. PLoS ONE 15(5):1–26

Sangster J (1989) Octanol-water partition coefficients of simple organic compounds. J Phys Chem Ref Data 18(3):1111–1229

Solimano P, Guardiola Rivas FJ, Soricetti M, Morawicki S, Amestoy M, Garrido A, Quezada F (2019) Fish freshwater communities of the río Negro. Environmental Monitoring Program of the Río Negro National University. http://rid.unrn.edu.ar/handle/20.500.12049/5300. Accessed 15 Apr 2021

Soricetti M, Morawicki S, Guardiola Rivas FJ, Guidi C, Quezada F, Almirón AE, Solimano PJ (2020) Ichthyofauna of the lower course of the Negro river drainage, Patagonia Argentina. Check List 16:895–905

Soto D, Arismendi I, González JFG, Sanzana J, Jara F, Jara C, Guzman E, Lara A (2006) Sur de Chile, país de truchas y salmones: patrones de invasión y amenazas para las especies nativas. Rev Chil Hist Nat 79:97–117 (in Spanish)

Sullivan JP, Lundberg JG, Hardman M (2006) A phylogenetic analysis of the major groups of catfishes (Teleostei: Siluriformes) using rag1 and rag2 nuclear gene sequences. Mol Phylogenet Evol 41:636–662

Tagliaferro M, Arismendi I, Lancelotti J, Pascual M (2015) A natural experiment of dietary overlap between introduced rainbow trout (Oncorhynchus mykiss) and native puyen (Galaxias maculatus) in the Santa Cruz River, Patagonia. Environ Biol Fishes 98:1311–1325

Tatone LM, Bilos C, Skorupka CN, Colombo JC (2015) Trace metal behavior along fluvio-marine gradients in the Samborombón Bay, outer Río de la Plata estuary, Argentina. Cont Shelf Res 96:27–33

Tatrai I, Lammens E, Breukelaar A, Klein Breteler JP (1994) The impact of mature cyprinid fish on the composition and biomass of benthic macroinvertebrates. Arch Für Hydrobiol 131:309–320

Tatrai I, Oláh J, Józsa V, Kawiecka BJ, Mátyás K, Paulovits G, Pekár F, Szabó P (1996) Regulation of plankton and benthic communities and water quality by cyprinid fish. Lakes Reserv Res Manage 2:169–174

Tatrai I, Tóth G, Ponyi J, Zlinskzky J, Istvánovics V (1990) Bottom-up effects of bream (*Abramis brama* L.) in Lake Balaton. Hydrobiologia 200:167–175

Temporetti PF, Alonso MF, Baffico G, Diaz MM, Lopez W, Pedrozo FL, Vigliano PH (2001) Trophic state, fish community and intensive production of salmonids in Alicura reservoir (Patagonia, Argentina). Lakes Reserv Sci Policy Manage Sustain Use 6:259–267

Thomann RV (1989) Bioaccumulation model of organic chemical distribution in aquatic food chains. Environ Sci Tech 23(6):699–707

Tombesi N, Pozo K, Alvarez M, Přibylová P, Kukučka P, Audy O, Klánová J (2017) Tracking polychlorinated biphenyls (PCBs) and polybrominated diphenyl ethers (PBDEs) in sediments and soils from the southwest of Buenos Aires province, Argentina (South eastern part of the GRULAC region). Sci Total Environ 575:1470–1476

Usio N, Townsend CR (2004) Roles of crayfish: consequences of predation and bioturbation for stream invertebrates. Ecology 85:807–822

Vaughn CC, Hakenkamp CC (2001) The functional role of burrowing bivalves in freshwater ecosystems. Freshw Biol 46(11):1431–1446

Vigliano PH, Beauchamp DA, Milano D, Macchi PJ, Alonso MF, Asorey MIG, Denegri MA, Ciancio JE, Lippolt G, Rechencq M (2009) Quantifying predation on galaxiids and other native organisms by introduced rainbow trout in an ultraoligotrophic lake in northern Patagonia, Argentina: A bioenergetics modelling approach. Trans Am Fish Soc 138:1405–1419

Vinson MR, Hawkins CP (1998) Biodiversity of stream insects: variation at local, basin, and regional scales. Annu Rev Entomol 43(1):271–293

Wais I (1990) A checklist of the benthic macroinvertebrates of the Negro river basin, Patagonia, Argentina, including an approach to their functional feeding groups. Acta Limnol Bras 3:829–845

Wang Z, Wang Y, Zhao P, Chen L, Yan Ch, Yan Y, Chi Q (2015) Metal release from contaminated coastal sediments under changing pH conditions: implications for metal mobilization in acidified oceans. Mar Pollut Bull 101:707–715

Ward N (2007) Diario Río Negro. http://www1.rionegro.com.ar/diario/2007/01/08/20071v08a50.php. Accessed 10 Mar 2021 (in Spanish)

Weber M, Brown M, Willis D (2010) Spatial variability of common carp populations in relation to lake morphology and physicochemical parameters in the upper midwest United States. Ecol Freshw Fish 19:555–565

Werner S (2008) Effects of the invasive Asian clam *Corbicula fluminea* on the littoral communities of Lake Constance. Doctoral Dissertation, Universität Konstanz

WHO, World Health Organization (2019) https://www.who.int/en/news-room/fact-sheets/detail/arsenic. Accessed dia mes año

Yi Y, Wang-Zhang K, Yu G, Duan X (2008) Sediment pollution and its effect on fish through the food chain in the Yangtze river. Int J Sedim Res 23:338–347

Zhang C, Zhi-Gang Y, Guang-Ming Z, Min J, Zhong-Zhu Y, Fang C, Meng-Ying Z, Liu-Qing S, Liang H (2014) Effects of sediment geochemical properties on heavy metal bioavailability. Environ Int 73:270–281

Patagonia's Chubut River: Overview of the Main Hydrological and Geochemical Features

Pedro. J. Depetris and Andrea I. Pasquini

Abstract The Chubut River's mean annual discharge is ~1.1 km^3 (~35 $m^3\ s^{-1}$), contributes ~2% to Patagonia's total freshwater discharge, and ranks far behind the mighty Negro River (~32 $km^3\ y^{-1}$). In a semiarid scenario, the river has a mountainous active basin, low runoff (<3.5 mm y^{-1}), and a scanty specific water yield (1.1 L s^{-1} km^{-2}). The seasonal Kendall trend test shows that discharges during the low-water months (Jan.–Mar., May) have been significantly decreasing during the last decades. Ca^{2+}–HCO_3^- are the governing ions in the headwaters but the composition gradually shifts to a Na^+-type toward the lowermost reaches. Numerous Andean glaciers suggest that subglacial oxidation of pyrite may be an active solute-supplying mechanism. Silicate hydrolysis and limestone dissolution—implied by non-radiogenic $^{87}Sr/^{86}Sr$ ratios—are the processes ruling chemical weathering. The Chubut is a mesotrophic river, with a moderate organic load (mean TOC ~290 μmol L^{-1}, and mean yield ~10.5 mmol $m^{-2}\ y^{-1}$; ~60% accounted for by DOC). Suspended sediment yield at Los Altares (~14 T $km^2\ y^{-1}$) and in the lowermost reach (~25 T $km^2\ y^{-1}$) indicate a relatively low denudation. The alteration index of riverbed sediments (mean CIA ≈ 55) suggests scarce weathering; REE spider diagrams of sediments shows a signature compatible with continental island arcs.

Keywords Water chemistry · Geochemistry · Hydrology · Denudation · Solute provenance · River sediments

Pedro. J. Depetris
Academia Nacional de Ciencias, Córdoba, Argentina

A. I. Pasquini (✉)
Escuela de Geología, Facultad de Ciencias Exactas, Físicas y Naturales, Universidad Nacional de Córdoba, Córdoba, Argentina
e-mail: apasquini@unc.edu.ar

Centro de Investigaciones en Ciencias de La Tierra, Consejo Nacional de Investigaciones Científicas y Técnicas, and Universidad Nacional de Córdoba, Córdoba, Argentina

A. I. Torres and V. A. Campodonico (eds.), *Environmental Assessment of Patagonia's Water Resources*, Environmental Earth Sciences,
https://doi.org/10.1007/978-3-030-89676-8_6

1 Introduction

Due to the windy and arid characteristics ruling climate in southern South America's Atlantic seaboard plateau, Patagonia is considered among the unusual regions of the Earth. Several reasons make Patagonia an especially interesting expanse whose study could improve, for example, our understanding of climate change, particularly in connection with hydrological and geochemical issues. Its vast territory of over one million square kilometers consists of the southernmost stretch of the Andes, in the western part (with chains of about 2000–3000 m above the sea level (a.s.l.), and peaks that reach ~3700 m), and deserts, steppes and grasslands in the eastern plateau (~200–~600 m a.s.l.). The Colorado River (36º52′ S, 69º45′ W), with Andean **headwaters**, is usually considered Patagonia's northern boundary in the Argentine territory.

With ~1.1 km^3, the Chubut ranks, in terms of annual discharge, as the fourth largest Patagonian river, behind the Negro, Santa Cruz, and Colorado. Joined together, the drainage nets of the Chubut and Senguerr-Chico rivers occupy about 60% of the surface area of the Argentine province named after it, which was originally organized as the National Territory of Chubut in 1884, and colonized the following year by Welsh immigrants.

Several authors have studied varied aspects in connection with the hydrological features of the Chubut River (e.g. Moyano and Moyano 2013; Pasquini and Depetris 2007; Depetris and Pasquini 2008), and its geochemical/biogeochemical characteristics (e.g. Sastre et al. 1998; Pasquini 2000; Gaiero et al. 2002, 2003; Pasquini et al. 2005; Depetris et al. 2005).

Due to the dynamics of natural and/or anthropogenic factors, rivers tend to show modifications in their main characteristics (i.e. discharge regime, physicochemical and/or biological features, etc.). We are, hence, herein updating hydrological and geochemical information on Patagonia's Chubut River.

1.1 Physiographic and Climatic Features

The Chubut[1] River drainage basin is an east-flowing arid Patagonian fluvial system (Fig. 1). Its drainage area is ~53,200 km^2 (Subsecretaría de Recursos Hídricos 2002), and its main stem, the Chubut River, has an approximate length of ~800 km and headwaters in the Cerro de las Carreras (41º′ S, 71°19′ W)—at ~1800 m a.s.l.-, in Argentina's Río Negro Province. The main tributaries in the upper drainage are the Ñorquinco and Chico del Norte rivers, inflowing from the north, and the Tecka-Gualjaina River, joining the system from the south (Fig. 1). The Florentino Ameghino dam forms a reservoir lake (43°41′ S, 66°29′ W). The Chico del Sur River (i.e. a prolongation of the Senguerr River) used to join the Chubut River **upstream** from the

[1] Chubut comes from the aboriginal (i.e. tehuelche) word *chupat*, which means "transparent". Welsh settlers called the river "*Afon camwy*", meaning "twisting river".

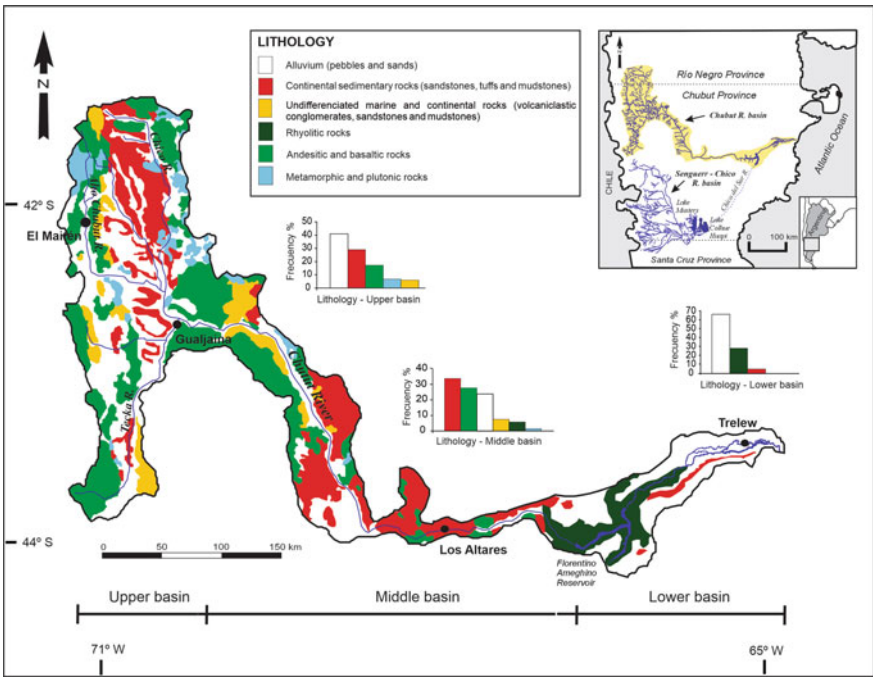

Fig. 1 Schematic map of Patagonia's Chubut River drainage basin showing an outline of the most abundant rock types. Histograms show the relative abundance (percent) of major rock types in the upper, middle, and lower river reaches

present location of the dam. Currently, this river, fed by the lakes Munster and Colhue Huapi, has been dammed by accumulated eolian debris which, almost permanently, obstruct its normal flow. The Chubut River reaches the Atlantic forming a small estuary at Bahía Engaño, near Rawson, the provincial capital.

The western headwaters of the Chubut River drainage basin are typified by mountainous north–south ranges (~500 and ~1800 m a.s.l.). The mean slope for the upper catchments is about 20%. The central drainage basin carves the Patagonian tableland (~200 and ~600 m a.s.l.), without receiving any significant tributary. An alluvial plain and fluvial terrace are the outstanding features in the lower drainage basin (~20 and ~150 m a.s.l.).

The Andes in Chubut's territory are separated by wide, deep, east–west transverse valleys. These valleys are occupied by glacial lakes and rivers that cross the Andes and flow east, to the Pacific Ocean.

The most distinctive climatic characteristics in the Chubut River drainage basin are scarce atmospheric precipitations and their marked negative gradient in short distances. In the headwaters, for example, mean annual rain- and snowfall is 500–600 mm, whereas 200 km to the east, near the confluence with the Gualjaina River

(Fig. 1), it barely reaches 100 mm. In the central basin, the mean annual rainfall is ~150 mm and in the coastal zone it increases up to ~250 mm.

Atmospheric precipitations have a marked seasonal character, with most of the water volume recorded in winter (73% occurring between April and September). In contrast, along the coastal zone, most atmospheric precipitations occur in (austral) autumn and spring. Mean evapotranspiration exhibits an increasing trend from the Andean region (500–600 mm y^{-1}) to the Atlantic coastal zone (700–800 mm y^{-1}).

Mean annual temperatures vary between 8 and 9 ºC in the west and center, and between 12 and 13 ºC in areas close to the coast. The prevailing vegetation is a bushy or herbaceous steppe, with a vegetation cover that varies between 20 and 50%. Due to aridity, soils are scarcely developed in most of the drainage basin, with dominant sandy fractions in the profile. Aridisols are by far the overriding soil-types in the drainage basin (e.g. Bouza et al. 2017).

1.2 Geological Setting

The Chubut River drainage basin is located at the southern boundary of the North Patagonian or Somún Curá Massif. It is a plateau, surrounded by sedimentary basins, which rise 500–700 m above the surrounding topography, and reaches a maximum of 1200 m a.s.l. With an area of approximately 100,000 km^2, it occupies most of the Argentine provinces of Río Negro and Chubut. An updated description of the continental crust of the northeastern region and, in general, Patagonia's main geological features, has been recently reported by Rapela and Pankhurst (2020) and in the references cited therein.

An abridged report of the geological setting of the Chubut River drainage basin has been described by Pasquini et al. (2005). Figure 1 shows a simplified geological scheme of the complex lithology of the Chubut River drainage basin which, for convenience, has been grouped into six major clusters. The dominant lithology in the upper basin are pebbles and sands, along with continental sedimentary rocks (sandstones, tuffs, and mudstones), which become dominant in the middle stretch (Fig. 1).

1.3 Methodology

The hydrological information was obtained from the data base operated by Argentina's *Secretaría de Infraestructura y Política Hídrica* (http://bdhi.hidricosargentina.gob.ar), and processed with standard statistical software.

The non-parametric **seasonal Kendall test** was employed to test for monotone trends in mean annual discharge time series. This test is a robust technique to detect and estimate linear trends and, also, was employed to seek significant trends in seasonal data with serial dependence (e.g. Hirsch and Slack 1984).

The chemical methodology employed to analyze water samples during the European Commission-funded PARAT Project (Contract CI1*-CT94-0030) was described in Pasquini et al. (2005). Other cited references must be consulted whenever methodological information is required for data from alternative sources.

2 Hydrological Aspects

The hydrological behavior of the Chubut River mainly dependents on rainfall and snowfall in the upper catchments. Most of the discharge is supplied by the upper Chubut River (i.e. 60–65% during the low-discharge period). There are indications, however, that the Chubut—as it probably happens with other Patagonian rivers—may receive groundwater supplies at different points along its middle and lower course. There is, for example, substantial evidence of submarine groundwater discharge in the coastal zone of Chubut and Santa Cruz provinces (42°–48° S) (Torres et al. 2018).

In the mountainous headwaters, atmospheric precipitations increase sharply in May (maximum mean precipitation) and June, during the austral fall and winter, and begin a gradual decrease that reaches its minimum in November (austral spring). The uppermost Chubut River gaging station (Estación Nacimiento, 41°43′ S, 71°08′ W) is operational since June 1967. During a period of over 50 years (i.e. until November 2019), the maximum recorded discharge (Q_{max}) was 29.17 $m^3\ s^{-1}$, whereas the minimum (Q_{min}) was 0.41 $m^3\ s^{-1}$.

Discharge data usually exhibit a log-normal statistical distribution. Therefore, the mathematical expectation is better approached by using the geometric mean discharge (Qg) (e.g. Davis 1986; Marsal and Merriam 2014). Q_g and the corresponding standard deviation (S_g) at the Estación Nacimiento for the analyzed period was $4.8 \pm 0.91\ m^3\ s^{-1}$. The highest discharges are usually recorded in July–August (i.e. austral winter), due to rainfall and in October–November, as a result of snowmelt.

Rainfall and snowfall at the El Maitén gaging station (42°06′ S, 71°10′ W) follows a pattern similar to the one recorded at Nacimiento, although maximum mean precipitation occurs in June, with the minimum also in November. The station is located at ~720 m a.s.l. and the available discharge time series for the period 1953–2019 includes over 6800 instantaneous discharge measurements, with $Q_{max} \approx 240\ m^3\ s^{-1}$ and $Q_{min} \approx 1.9\ m^3\ s^{-1}$. Q_g and the corresponding S_g is $16.2 \pm 2.23\ m^3\ s^{-1}$. Therefore, 95% of the compiled data is comprised within $Q_g \pm 2S_g$: $11.7\ m^3\ s^{-1} < Q_g < 20.7\ m^3\ s^{-1}$.

The Los Altares gaging station is placed in a semi-arid region, on the southern margin of the Chubut River, about 230 km from Trelew (to the E), and 323 km from Esquel (to the W). The wild landscape is known for its high cliffs and striking geomorphology. The Los Altares station (43°53′18.17″ S, 68°23′57.81″ W) is active since January 1943, record-keeping instantaneous discharges and other hydrometeorological variables. Chubut River's mean annual discharge time series have been plotted in Fig. 2. The linear trend in the figure ($p < 0.05$) shows that in 75 years, the mean annual discharge has decreased ~6 $m^3\ s^{-1}$ (~800 L per decade). Figure 3

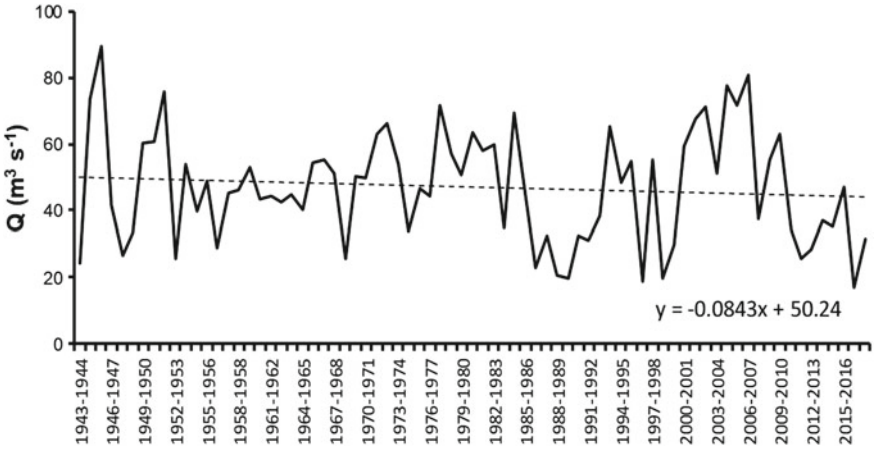

Fig. 2 Mean annual discharge time series (1943–2018) of the Chubut River (middle reach) at Los Altares gaging station. The regression equation ($p < 0.1$) suggests that the (arithmetic) mean annual discharge has decreased ~6 m^3 s^{-1} in 75 years

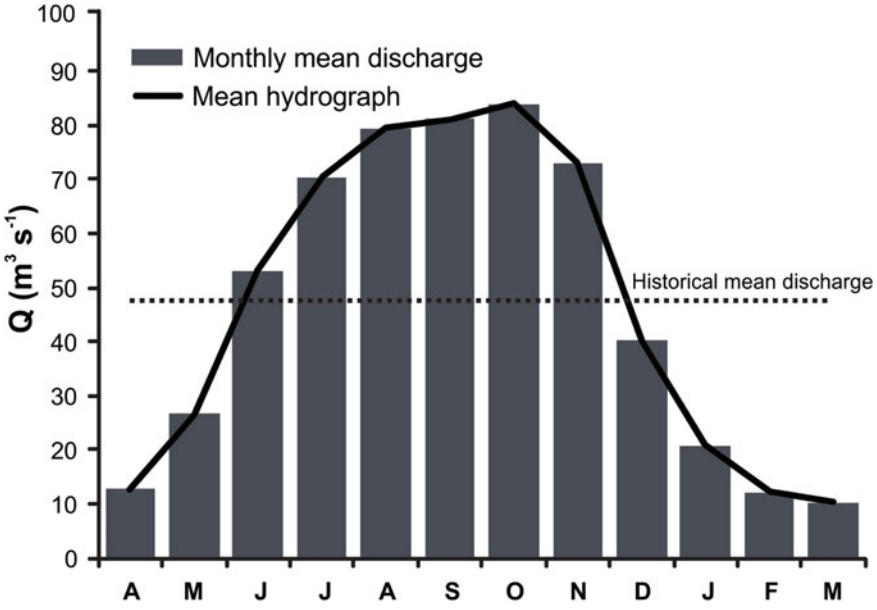

Fig. 3 Middle Chubut River's synthetic hydrograph at Los Altares (~270 km upstream the mouth; 625 m a.s.l.). The graph shows the (arithmetic) mean historical discharge (~47 m^3 s^{-1}) for 1943–2018, and the (arithmetic) mean monthly discharges for the average hydrological year

shows the mean annual hydrograph for the series of monthly mean discharges (i.e. period of 1943–2018), with maximum discharges occurring during austral spring. The average discharge (i.e. arithmetic mean) for the period was 47.04 $m^3\ s^{-1}$, whereas the annualized discharge was 14.84 km^3, the specific water yield was 2.87 $L\ s^{-1}\ km^{-2}$, and runoff exceeded 9 mm y^{-1}. In the studied time series, instantaneous Q_{max} was 524 $m^3\ s^{-1}$, and Q_{min} 2.1 $m^3\ s^{-1}$.

As it happens with the upstream discharge time series, the statistical distribution is markedly log-normal. The Chi-square test performed to verify log-normality (317.14) exceeds the critical value for 9 of freedom and $p < 0.001$. Hence, $Q_g \pm S_g$ at Los Altares is $35.9 \pm 2.72\ m^3\ s^{-1}$, which is lower than the arithmetic mean calculated above. The conversion to a Gaussian distribution of the discharge time series (1943–2018) allows to estimate that 95% of the data in the historical series falls within the range $30.5 < Q_g < 41.4\ m^3\ s^{-1}$.

The seasonal Kendall trend analysis (Kendall 1975; Hirsch and Slack 1984) is a non-parametric statistical tool that allows establishing monotonic trends in time series. The use of the technique at Los Altares shows a statistically significant discharge decrease ($p < 0.05$) during January-March and May (i.e. the months with low-water flow) (Table 1).

The Chubut's lower stretch originates at the reservoir lake formed by the Florentino Ameghino dam (Fig. 1), which became operative in 1963, 130 km west of the city of Trelew (i.e. Gaiman Department). The reservoir lake has a surface area of ~70 km^2, a mean maximum depth of ~25 m, and a storage capacity of ~16 km^3 of water, which is mostly used for irrigation, and power generation.

The Valle Inferior (43°17′35.13″ S, 65°29′54.72″ W) gaging station is located approximately 90 km **downstream** the Florentino Ameghino dam and less than

Table 1 Seasonal Kendall test: Chubut River monthly mean discharges at Los Altares

Month	N	Kendall t	p^*
January	75	−2.132	**0.01651**
February	75	−2.461	**0.00693**
March	75	−2.159	**0.01541**
April	75	−0.567	0.28527
May	75	−1.935	**0.02649**
June	75	−0.814	0.20776
July	75	−0.654	0.25651
August	75	−0.174	0.43100
September	75	0.897	0.18497
October	75	−0.851	0.19743
November	75	−1.505	0.06617
December	75	−1.606	0.05418
Total	900	−1.819	**0.03445**

*Statistically significant parameters in bold ($p < 0.05$)

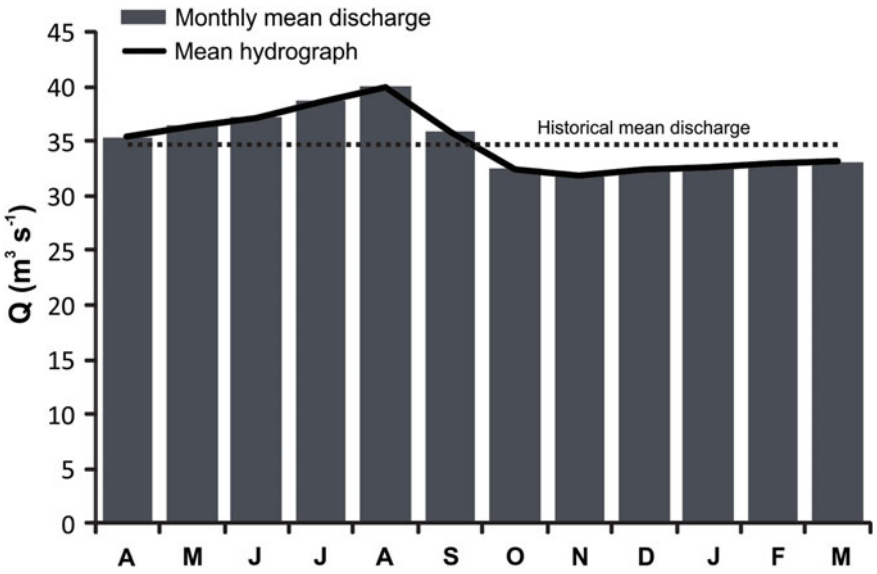

Fig. 4 Lower Chubut River's synthetic hydrograph at Valle Inferior. The graph shows the (arithmetic) mean historical discharge (~35 $m^3\ s^{-1}$) for the recorded period, and the (arithmetic) mean monthly discharges for the average hydrological year

50 km upstream from the Chubut's estuary in the Atlantic Ocean. It is in operation since 1993. The discharge time series (i.e. 1993–2018) is summarized in the synthetic hydrograph of Fig. 4, which shows the discharge modulation imposed by the dam. The annual mean discharge (i.e. arithmetic mean) at Valle Inferior is $34.9 \pm 14\ m^3\ s^{-1}$, and the mean annual flow is 1.1 km^3. The specific water yield is only 1.1 L s^{-1} km^{-2}, whereas runoff is slightly less than 3.5 mm y^{-1}. These parameters, considerably lower than those determined in the middle stretch, are mainly the joint consequence of evapotranspiration, consumptive use of water, and the conveyance of river water to the aquifers (Hernández et al. 1983). The negative trend of mean discharges is clearly exhibited in Fig. 5. In 25 years, annual mean discharges have decreased at a mean rate of ~7.8 m^3 per decade. This scenario of water loss can also be ascertained in lower graph of Fig. 5, which shows the discharge difference between Los Altares and Valle Inferior (delta Q) for the 1993–2018 record period.

3 Geochemical Perspective

Lithology, climate, biota, and relief are the key factors determining rock **weathering** on the Earth's surface (e.g. Depetris et al. 2014). The intensity of physical, biological and chemical weathering, on the other hand, determines the prevailing characteristics of dissolved and particulate byproducts that rivers transport to world oceans. In the

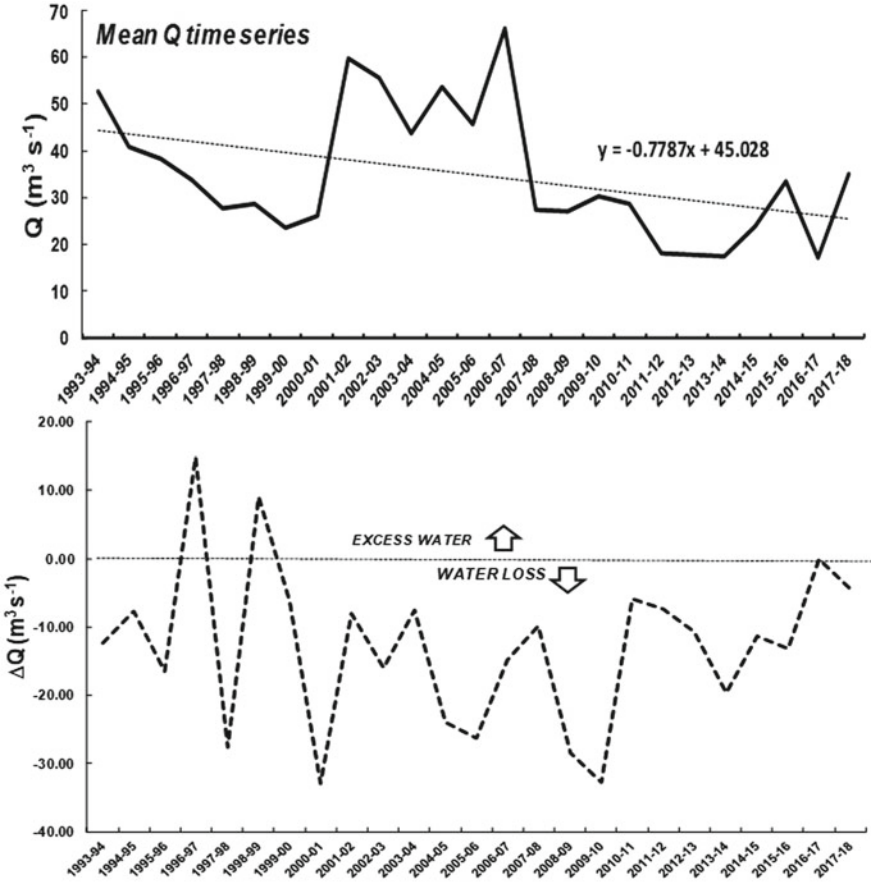

Fig. 5 Mean annual discharge time series of the Chubut River (lower reach) at Valle Inferior gaging station, for the 1993–2018 period (upper graph). The regression equation implies that the (arithmetic) mean annual discharge has decreased ~20 m^3 in 25 years. Q between Los Altares and Valle Inferior gaging stations, for the same period time (lower graph), showing a significant discharge decrease for Chubut's lower stretch during most of the time interval

Chubut River drainage basin, these three processes are significant in the mountainous headwaters, but it is clear that—considering extra-Andean Patagonia's prevailing arid characteristics—physical (or mechanical) weathering becomes more important than the other two processes in its middle and lower reaches. All things considered, the Chubut River is subjected to a ***weathering-limited regime*** (i.e. denudation remains limited by the rate of rock weathering) in the sense of Carson and Kirkby (1972).

3.1 Main Characteristics

In terms of chemical equivalents, the Chubut River upper catchments (i.e. tributaries and the main channel) are generally characterized by $Ca^{2+} > Na^{+} > Mg^{2+} > K^{+}$, and by $HCO_3^{-} > SO_4^{2-} > Cl^{-}$, among negatively charged species (Table 2). This chemical signature changes in the lower course, following the order of abundance $Na^{+} > Ca^{2+} > Mg^{2+} > K^{+}$, and $HCO_3^{-} > Cl^{-} \geq SO_4^{2-}$ (Table 3). The total dissolved solids (TDS) concentration in the Chubut River system usually fluctuates between 50 and 80 mg L^{-1} in the upper reaches, and between 110 and 160 mg L^{-1} at Los Altares. Typical TDS concentrations in the Gaiman–Rawson section (i.e. near the mouth) frequently oscillate in the 250–450 mg L^{-1} range. In the headwaters (i.e. Tecka-Gualjaina and Lepá rivers), TDS concentrations are usually logged in the 60–150 mg L^{-1} range. The TZ^{+} parameter [TZ^{+} (meq L^{-1}) = $(2Ca^{2+}) + (2Mg^{2+}) + (Na^{+}) + (K^{+})$] (e.g. Meybeck 2005) can be used with advantage to geochemically classify most Chubut River waters.

The Piper diagram (Fig. 6) shows a trend in the compositional triangle of major ions that begins in the Andean core—where lakes and rivers draining toward the Pacific Ocean are located-, revealing a dominant $Ca^{2+} > Mg^{2+}$ composition. The trend drifts towards a slight relative increase of Mg^{2+} in the upper Chubut and Senguerr rivers, which becomes increasingly dominated by $(Na^{+} + K^{+})$ in the Chubut's lower reaches. At the Musters and Colhué Huapi lakes begins the terminal phase of the Senguerr-Chico endorheic system which, in chemical terms, is characterized by a net dominance of $(Na^{+} + K^{+})$. In short, the chemical evolution originates as a Ca^{2+}-type, crosses the field where no particular cation is dominant, and ends as a Na^{+}-type (i.e. K^{+} is significantly less abundant).

The anions show a similar trend that begins in the Andean domain with a HCO_3^{-} control among the negatively charged species and shows, in the lower Chubut River and—more pronounced—in the Chico River, the increasing preeminence of Cl^{-}. Among anions, the series begins in the HCO_3^{-} type and ends in the no-dominant type realm (Fig. 6).

3.2 Provenance of Inorganic Dissolved Phases

Rock minerals have a variable susceptibility to weathering. The relative stability of the major rock-forming silicates during weathering is similar to Bowen's crystallization sequence (e.g. Langmuir 1997): the minerals that crystallize first in high-temperature magmas are those which are least stable when subjected to weathering. Thus mafic minerals (e.g. olivine, pyroxenes) usually weather more readily than felsic minerals (e.g. plagioclase, micas), and a Ca-rich plagioclase is generally weathered at a faster rate than a Na-rich plagioclase. Chemical weathering reactions fall into four

Table 2 Major chemical characteristics of the upper Chubut River and tributaries*

Date	E.C. ($\mu S\ cm^{-1}$)	pH	Cl^-	SO_4^{2-}	HCO_3^-	Ca^{2+} ($\mu mol\ L^{-1}$)	Mg^{2+}	Na^+	K^+	SiO_2	TZ^+ ($\mu eq\ L^{-1}$)
Dec '96[a]	166	8.6	83	158	1390	492	196	518	32	220	1926
Mar '97[b]	58.7	7.45	13	24	566	200	65	108	13	190	651
Dec '96[c]	193	8.53	149	92	1750	457	206	874	45	352	2245
Dec '96[d]	33.4	7.72	20	16	288	99	34	86	9	340	361
Mar '97[e]	178.2	7.97	195	147	1490	521	151	383	34	252	1761
Mar '97[f]	252	7.72	245	246	2039	692	256	594	41	270	2531

*Modified from Pasquini et al. (2005)
[a]Chubut (P. de Indios); [b]Chubut (El Maitén); [c]Mayo (R. Mayo); [d]Senguerr (RP 22); [e]Lepá (RN 40); [f]Gualjaina (Gualjaina)

Table 3 Major chemical characteristics of Chubut River at Trelew (~23 km from mouth)*

Date	E.C ($\mu S\ cm^{-1}$)	pH	Cl^-	SO_4^{2-}	HCO_3^-	Ca^{2+} ($\mu mol\ L^{-1}$)	Mg^{2+}	Na^+	K^+	SiO_2	TZ^+ ($\mu eq\ L^{-1}$)
Sep '95	284	8.11	544	229	1680	562	183	1190	27	180	2707
May '96	250	7.54	413	198	1700	542	178	1090	24	203	2554
Sep '96	247	6.75	504	219	1670	584	193	1170	30	195	2754
Dec '96	331	8.5	925	357	1830	694	251	1710	32	218	3632
Mar '97	190	7.67	82	223	1570	536	235	549	35	253	2126
Dec '97	285	7.2	724	277	1755	569	191	1600	29	226	3149
Apr '98	315	7.53	793	330	1990	649	220	1730	33	175	3501
Nov '98	459	7.94	1450	522	2300	815	295	2520	40	171	4780
Apr '98	405	8.43	1420	440	1990	664	196	2620	58	231	4398
GM[a]	298		600.5	294	1819.9	618	213	1436.4	33.2	204.1	3132.4
SD[b]	2.1		2.4	1.4	1.1	1.2	1.2	1.6	1.3	1.2	2.7

*Modified from Pasquini et al. (2005)
[a]Geometric mean; [b]Standard deviation

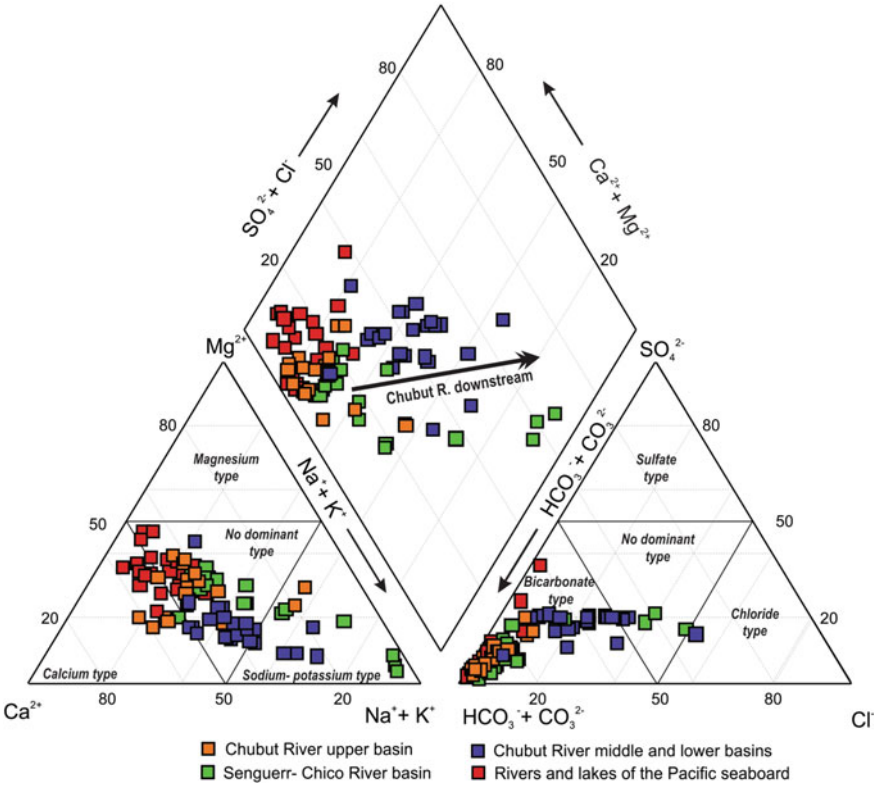

Fig. 6 Diagram (Piper 1944) showing the chemical evolution of Chubut River waters from the upper to the middle and lower stretches. Senguerr-Chico drainage basin, as well as rivers and lakes draining to the Pacific seaboard are also included

major clusters: hydrolysis reactions; dissolution/precipitation reactions; redox reactions; hydration/dehydration and transformation processes. Different combinations among these processes are also possible.

Before entering the characteristics of weathering in the Chubut River drainage basin it must be kept in mind that the lithology of the upper catchments (i.e. where physical erosion is intense and atmospheric precipitations are higher) is dominated by alluvium, followed by continental sedimentary rocks (sandstones, tuffs, and mudstones), and volcanic rocks (i.e. andesitic and basaltic rocks) (Pasquini et al. 2005). With these broad guidelines in mind, it is possible to approach the sources of dissolved inorganic components in the Chubut River system.

The mixing diagram in Fig. 7 shows the relationship of Ca^{2+} and HCO_3^- (in $\mu eq\ L^{-1}$), both normalized to Na^+, as measured in upper tributaries, and the upper and lower Chubut River (i.e. diagram after Gaillardet et al. 1999). Data of diluted lakes and rivers draining to the Pacific Ocean have been included for comparison (Scapini and Orfila 2001). The sampled rivers, lakes, and streams appear to have a

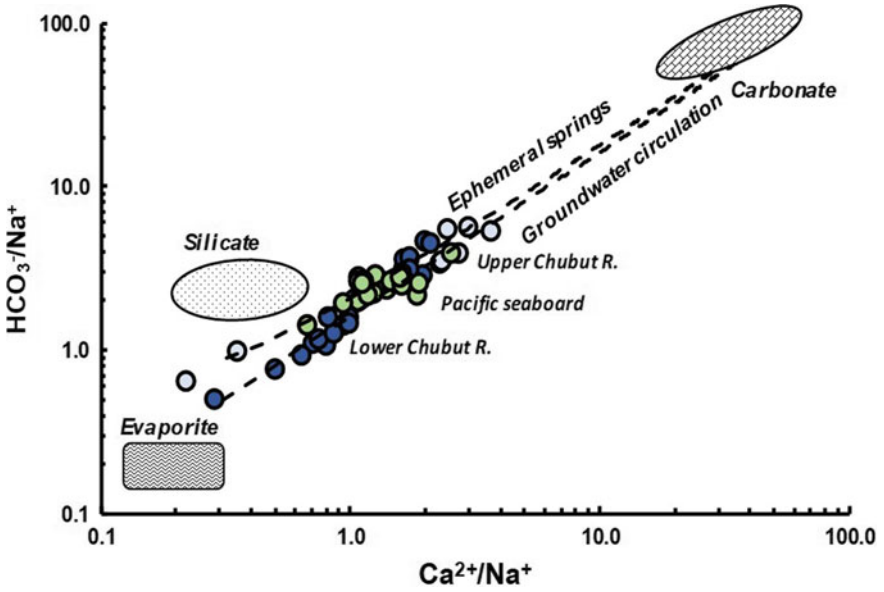

Fig. 7 Variability of Na^+-normalized Ca^{2+} and HCO_3^- concentrations (μeq L^{-1}) in the upper and lower Chubut River. Data from lakes and rivers draining to the Pacific Ocean included for comparison. Likewise, the evolution of weathering for Sierra Nevada (USA) rocks, as determined in ephemeral springs and deep groundwater (Garrels and Mackenzie 1967). Data uncorrected for rainfall; notice logarithmic axes. Diagram after Gaillardet et al. (1999)

more pronounced supply of weathering products from silicates and evaporites than of carbonates. It is also interesting to notice that some samples plot close to the line representing the composition of ephemeral springs, implying a relatively brief rock-water interaction, whereas other are closer to the composition of groundwater (i.e. longer rock-water contact time). The chemical data for springs and groundwater was collected in the Sierra Nevada (USA), and reflects the weathering of variable proportions of plagioclase, biotite, and K-feldspar (spring), and of plagioclase, biotite, and calcite (deep groundwater). The exercise (Garrels and Mackenzie 1967) was a reconstruction of source minerals, reproduced by Drever (1997). In ephemeral springs the overall reaction was:

$$\begin{aligned} &177 \text{ plagioclase} + 7.3 \text{ biotite} + 13 \text{ K - feldspar } (+H_2O + CO_2) \\ &= 133 \text{ kaolinite} + 110\ Na^+ + 68\ Ca^{2+} \\ &\quad + 22\ Mg^{2+} + 20\ K^+ + 270\ SiO_2 + 310\ HCO_3^- \end{aligned}$$

It appears, in terms of the Na^+-normalized Ca^{2+} and HCO_3^- concentrations, that the geochemical reconstruction computed by Garrels and Mackenzie (1967) fits reasonably well with both, springs with brief and groundwater with extended rock-water contact.

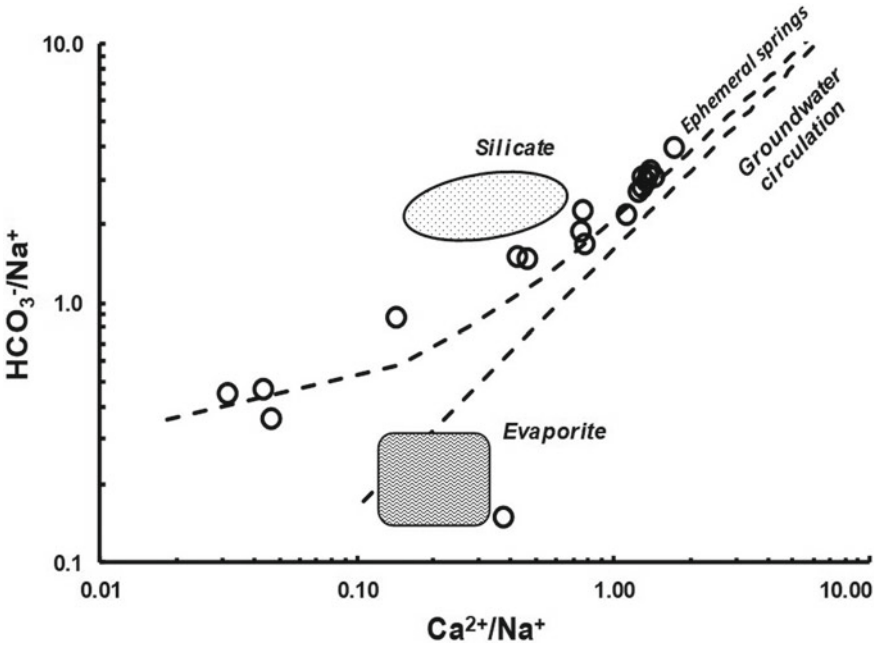

Fig. 8 Variability of Na^+-normalized Ca^{2+} and HCO_3^- concentrations (in μeq L^{-1}) in the Senguerr-Chico drainage basin. The geochemical signature of the flow-obstructed system contrasts markedly with the Chubut River. Other characteristics as in Fig. 7

In a similar albeit contrasting diagram, Fig. 8 shows the chemical composition of the Senguerr-Chico system. In this case, data falls close to the ephemeral spring composition of Garrels and Mackenzie (1967) (i.e. probably due to the deceptive effect of carbonate precipitation and the removal of Ca^{2+} and HCO_3^- from the solution). The system evolves towards a high ionic strength solution through the loss of water by evaporation that affects the Colhue-Huapi Lake and Chico River. A chemical divide, such as the one described by Drever (1997), surely functions and gypsum probably precipitates, leaving a solution which, in molar terms, is rich in Na^+, Cl^-, SO_4^{2-}, Ca^{2+}, Mg^{2+}, and CO_3^{2-} (Scapini and Orfila 2001).

The graph of Ca^{2+}/Na^+ versus Mg^{2+}/Na^+ (Fig. 9) shows a different scenario; where the weathering of Mg-bearing minerals seems to play a more important role in waters that probably undergo an extended rock-water contact. The reconstruction of weathering reactions during deeper circulation (Garrels and Mackenzie 1967), for example, show a more important character to Sierra Nevada's biotite and calcite as solute suppliers. In this case, the overall reaction was:

$$\begin{aligned} &175 \text{ plagioclase} + 14 \text{ biotite} + 115 \text{ calcite } (+H_2O + CO_2) \\ &= 81 \text{ smectite} + 33 \text{ kaolinite} + 109\ Na^+ + 167\ Ca^{2+} + 42\ Mg^{2+} + 12\ K^+ \\ &\quad + 539\ HCO_3^- + 137\ SiO_2 \end{aligned}$$

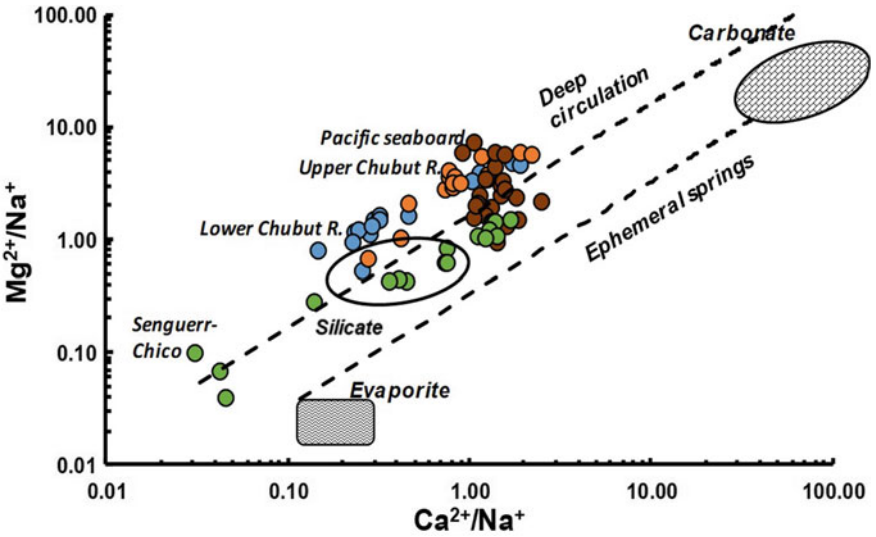

Fig. 9 Variability of Na^+-normalized Mg^{2+} and HCO_3^- concentrations (in μeq L^{-1}) in the upper and lower Chubut River. Data from the Senguerr-Chico system and the Pacific seaboard have been included for comparison. Other characteristics as in Fig. 7

Due to different geological conditions, there are minerals which are present in Chubut's drainage basin and absent or scarce in the Sierra Nevada and, hence, were not included in Garrels and Mackenzies' exercise. Such is the case, for example, of olivine, a mineral which hydrolyzes easily, common in mafic rocks, and a significant source of Mg and/or Fe:

$$(Fe, Mg)_2SiO_4 + 4\,H_2O = Fe^{2+} + Mg^{2+} + H_4SiO_4 + 4OH^-$$

In any event, it is important to look into the susceptibility of minerals to weathering, regardless of the rock involved.

In the Chubut River, SO_4^{2-} can be supplied by gypsum-bearing beds, by evaporites, or by redox reactions which involve sulfides, like pyrite. The latter is particularly important in glacial environments (e.g. Chillrud et al. 1994; Calmels et al. 2007). The reaction generates H_2SO_4, which assists in the dissolution of other minerals including carbonates, silicates and other sulfides:

$$4FeS_2 + 15O_2 + 14H_2O = 4Fe(OH)_3 + 16H^+ + 8SO_4^{2-}$$

This reaction is of particular importance in the subglacial and proglacial environments, where it is the dominant process producing solutes (Tranter 2005).[2] It must

[2] According to Argentina's glacier inventory (https://www.argentina.gob.ar/ambiente/agua/glaciares/inventario-nacional), there are over 1500 ice and rock glaciers and snow buildups in Chubut's Andean region, covering a surface area of ~225 Km^2.

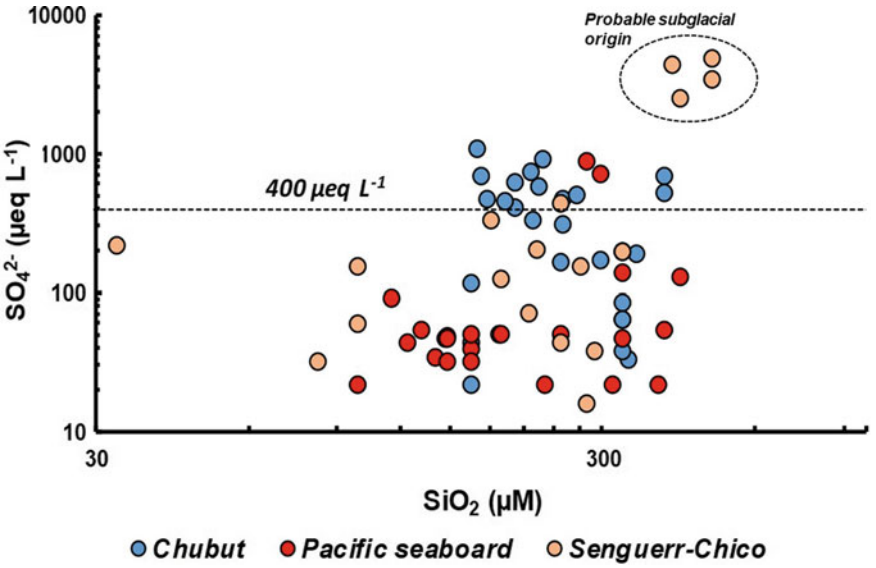

Fig. 10 SiO_2 versus SO_4^{2-} in the Chubut, Senguerr-Chico and in rivers and lakes of the Pacific seaboard. The graph shows the likely subglacial origin of Andean samples. Subglacial SO_4^{2-} may have contributed as well to the samples that plot above the 400 µeq L^{-1} line

be kept in mind, however, that the maximum SO_4^{2-} concentration resulting from sulfide oxidation in O_2-saturated surface waters is ~400 µeq L^{-1}. Subglacial waters triplicate this concentration (Tranter 2005).

Figure 10 shows the variability of SiO_2 and SO_4^{2-} concentrations in the Chubut River, in the neighboring Senguerr-Chico system, and in Andean lakes and rivers draining to the Pacific Ocean. High SiO_2 and SO_4^{2-} concentrations in lakes pertaining to the Senguerr-Chico drainage suggest, for some samples, a likely subglacial origin (e.g. Tranter 2005). The O_2-supersaturated subglacial environment is propitious for the dissolution of other minerals besides pyrite. The alteration of the Fe-olivine (i.e. fayalite) is another example of dissolution in an O_2-rich environment, producing silica and Fe oxide:

$$2Fe_2SiO_4 + O_2 + 4H_2O = 2Fe_2O_3 + 4H_4SiO_4$$

Sulfate determined in other samples plotting above the 400 µeq L^{-1} boundary may also be a mixture of subglacial SO_4^{2-}, outcropping salty groundwater, or from gypsum-rich beds and/or evaporites, whereas those falling below the boundary probably have a restricted SO_4^{2-} contribution from sulfide oxidation in surface waters saturated with O_2, along with other usual sources of SO_4^{2-}.

The Sr concentration and isotope composition of river waters are largely defined by the mixing of Sr derived from limestones and evaporites (i.e. low $^{87}Sr/^{86}Sr$, basically nonradiogenic), with Sr resulting from the weathering of silicate rocks (i.e.

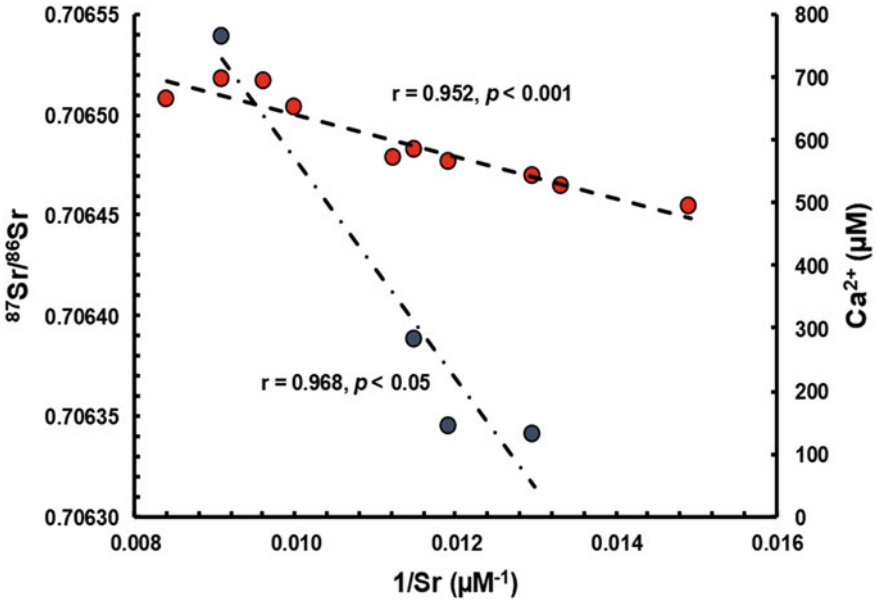

Fig. 11 $^{87}Sr/^{86}Sr$ ratio (red symbols) and Ca^{2+} concentrations (dark symbols) plotted against 1/Sr. The Sr isotopes suggest that Ca^{2+} is mostly supplied by limestone/carbonates

moderate to high $^{87}Sr/^{86}Sr$, radiogenic). In the Chubut River, the samples collected for isotopic analyses (Pasquini et al. 2005) showed low, nonradiogenic $^{87}Sr/^{86}Sr$ ratios, which fluctuated between 0.706340 ($Rb/Sr = 1.05 \times 10^{-3}$) and 0.706538 ($Rb/Sr = 6.06 \times 10^{-3}$), thus suggesting an origin associated with limestones and evaporites. Sr frequently replaces Ca in crystalline structures and in the Chubut River; Ca^{2+} shows a significant covariation with Sr, thus denoting a common source (Fig. 11).

3.3 The Organic Load

Dissolved organic carbon/matter (DOC or DOM) is the result of organic matter decay. Autochthonous DOC (i.e. originating from within the river or lake) usually comes from aquatic plants or algae, whereas it is known as allochthonous DOC when it has a source external to the water body (i.e. organic soils and decaying terrestrial plants or organisms supplying carbon). In water bodies, DOC is complemented by readily decomposable particulate organic carbon (POC),[3] which is separated in water samples by sieving or filtration. This fraction includes organic detritus and plant

[3] Also reported as particulate organic matter or POM.

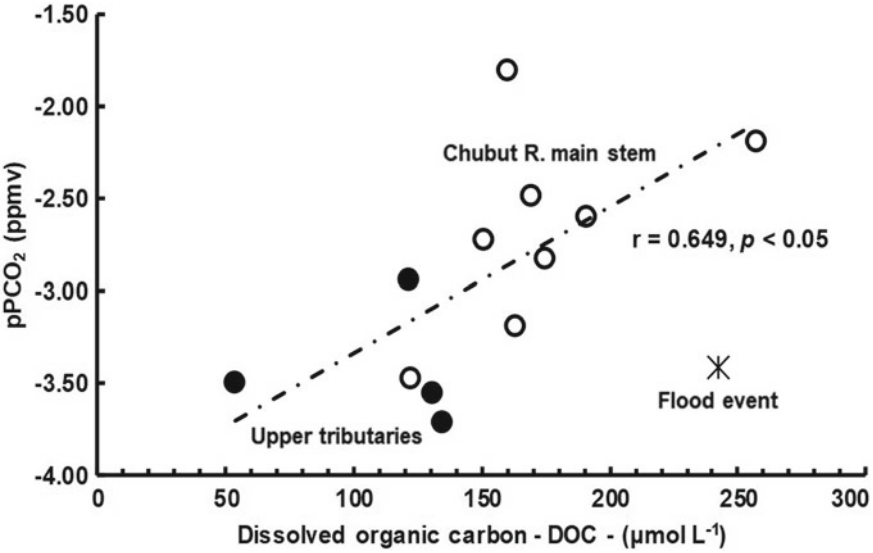

Fig. 12 Plot of DOC versus $pPCO_2$ in the Chubut River (Black symbols are tributaries). The correlation suggests that ~40% of the variability in the CO_2 partial pressure may be accounted for by the respiration of DOC by heterotrophic bacteria. The outlier symbol corresponds to an exceptional flood event

material, algae, and pollen, partly decomposed through heterotrophic consumption (e.g. Killops and Killops 2005).

DOC, POC, and nutrients were determined in an earlier exploratory investigation on the biogeochemical typology of Patagonian rivers (Depetris et al. 2005). The study showed low DOC concentrations,[4] between 164 and 258 μmol L^{-1} (i.e. mean concentration of 177 μmol L^{-1}), thus reflecting the scarcity of organic-rich soils in Chubut's drainage basin. These concentrations allow to compute a DOC specific yield of only ~6.3 mmol m^{-2} y^{-1}.

As stated above, DOC in rivers usually consist of amounts of biodegradable residues which are rapidly recycled, and more important quantities of a biological refractory residue (e.g. poorly biodegradable leftovers of organisms). Labile organic matter, when respired by heterotrophic bacteria, produces CO_2, in reactions like $(CH_2O)_n + nO_2 = nCO_2 + nH_2O$.

There is, therefore, a frequent association in water bodies between DOC and the CO_2 partial pressure (i.e. PCO_2). Figure 12 shows that in the Chubut River there is a significant positive correlation between DOC and $pPCO_2$ (i.e. $pPCO_2 = \log_{10} PCO_2$), implying that a part of DOC (i.e. the labile fraction) is respired by

[4] The global DOC average concentration fluctuates between ~400 and 480 μmol L^{-1} (Perdue and Ritchie 2005).

heterotrophs, increasing PCO_2 in the water and thus affecting the concentration of dissolved inorganic carbon (DIC).[5]

Chubut's POC average concentration was ~110 μmol L^{-1} (i.e. fluctuating between 91 and 141 μmol L^{-1}), also drastically below mean global values (i.e. 330–400 μmol L^{-1}, Perdue and Ritchie 2005). Therefore, POC's specific yield in the Chubut River was 4.2 mmol m^{-2} y^{-1} (Depetris et al. 2005). Accordingly, mean total organic carbon (TOC) in the Chubut River was ~290 μmol L^{-1} (i.e. ~60% accounted for by DOC), with a mean TOC yield of ~10.5 mmol m^{-2} y^{-1}.

In the Chubut River, ~2.5% is the average relative contribution of POC to total suspended sediment (TSS), whereas the mean carbon to particulate nitrogen (PN) ratio in TSS (POC/PN) is ~5, thus suggesting a meager proportion of soil-derived carbon and a dominant autochthonous origin (i.e. mostly phytoplankton) for the organic matter transported downriver. With the exceptional instance of the Gallegos River,[6] this condition is common in the remaining Patagonian rivers (Depetris et al. 2005).

Summing up, the Chubut River is a mesotrophic water body (i.e. having a moderate amount of dissolved nutrients). Runoff was identified as the most important variable controlling the organic load (i.e. TOC) which is exported from Patagonia to the SW Atlantic Ocean's coastal zone (i.e. ~115 10^9 g y^{-1}). The Chubut River is expected to supply ~3.5% of such load (Depetris et al. 2005).

4 Sediments

Sediments in fluvial systems can be conveyed in suspension or as bed load along the riverbed. The term total suspended sediment (TSS) usually denotes solids coarser than 0.45 μm. Bed load is difficult to measure and is usually assumed that it represents a relatively small fraction of the total sediment load (e.g. ~10%, Milliman and Meade 1983), although it may be considerably higher in steep mountainous streams or somewhat lower in larger meandering rivers (Milliman and Farnsworth 2011). In any case, the flux of sediments to coastal oceans is taken as an image of the physical denudation of continents (Milliman and Farnsworth 2011, and references therein).

4.1 TSS Yield and Transport

The instantaneous discharge and TSS concentration in the Chubut River are non-linearly correlated, as measured at the Los Altares gaging station (http://bdhi.hidricosargentina.gob.ar/) (Fig. 13). The statistical analysis of the TSS data shows a significant log-normality and, hence, its geometric mean is ~196 mg L^{-1} (N = 317

[5] DIC = $(CO_2^*) + (HCO_3^-) + (CO_3^{2-})$, where $(CO_2^*) = (CO_2) + (H_2CO_3)$.

[6] Mean POC/PN ≈ 10, thus suggesting a dominant origin in the terrestrial environment.

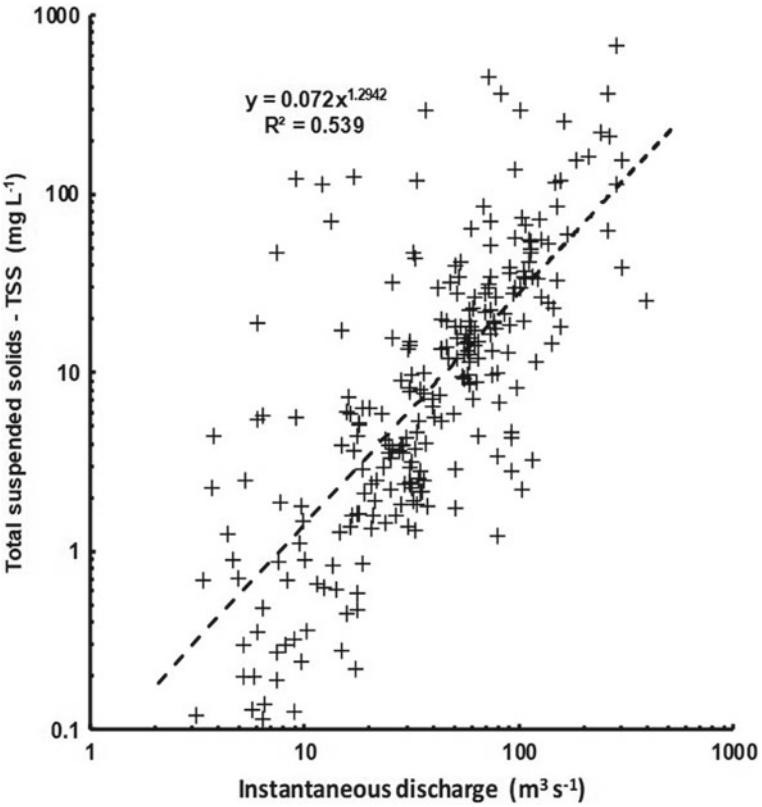

Fig. 13 Chubut River at Los Altares. Nonlinear relationship between instantaneous discharge and TSS concentration. Notice that some storm events may determine TSS concentrations ~1 g L^{-1}. Both axes are logarithmic

measurements). The lower quartile (i.e. 25% of the data is below) is ~71 mg L^{-1}, whereas the upper quartile (i.e. 75% of the data lies below) is ~443 mg L^{-1}. Clearly, the Chubut River is subjected to sporadic storm events that trigger very high TSS concentrations (e.g. over 2 g L^{-1}).

On the basis of the above calculated Q_g at Los Altares (i.e. ~36 m^3 s^{-1}) it is possible to compute a mean sediment transport rate of ~222.5 10^3 T y^{-1} or 610 T d^{-1}. It is possible, however, that during torrential storms the daily transport exceeds 7000 T. The resulting mean sediment yield at Los Altares is ~14 T km^2 y^{-1} (i.e. a measure of relatively low denudation). It is worth mentioning that a significant portion of the sediment load generated in the upper basin is retained at the Florentino Ameghino reservoir lake and—given the scarce vegetation cover, and the bare and loosened sediment outcrops that predominate in the lower valley-, more sediment is likely eroded,

added to the sediment load that bypasses the dam, and consequently transferred downstream, to the coastal zone.[7]

Pasquini et al. (2005) studied the nature of weathering, denudation, and the provenance of river bed sediments in the Chubut River system. A rating curve computed with data collected at the city of Trelew (i.e. ~25 km upstream the mouth) allowed to approach the mean TSS concentration. The equation [TSS (mg L^{-1}) = $0.8493Q^{1.3856}$] delivered a concentration range that fluctuated between ~80 and ~190 mg L^{-1} for the most frequent discharges at that particular gaging station.

The denudation rate computed at the time for the total Chubut drainage basin was ~25 T km^2 y^{-1}; the use of empirical models developed by Ludwig and Probst (1998) supplied denudation rates that fluctuated between 19 and 32 T km^2 y^{-1}. The Chubut River supplies an estimated ~3% of the TSS exported from Patagonia to the SW Atlantic coastal zone (Depetris et al. 2005).

4.2 The Geochemical Signature of Sediments

Another finding was that the materials removed from the drainage basin and exported to the coastal zone are barely modified by chemical weathering (i.e. the mean **chemical index of alteration**—or **CIA**—of riverbed material is ~55, relatively close to 47, the mean value calculated by McLennan (1993) for the Earth's Upper Continental Crust—UCC-) and exhibit a typical chemical and mineralogical signature characteristic of volcanic arcs. Hence, in spite of flowing toward a passive margin, the sediment bed load retains a geochemical signature typical of active margins, as Potter (1994) pointed out. Moreover, Pasquini (2000), and Pasquini et al. (2005) highlighted the features indicative of repeated weathering, supporting the view that, in the Chubut River drainage basin, most materials may have passed at least twice through the exogenous cycle (i.e. sedimentary recycling). Gaiero et al. (2004) probed into the significance of the **rare earth elements** (**REE**) signature in Patagonian wind- and river-borne sediments as provenance tracers.

Figure 14 shows the upper continental crust (UCC)-normalized REE extended diagrams (i.e. *spidergrams*) of Chubut River bed and suspended sediments (TSS) (Pasquini et al. 2005). Bed sediments are more depleted in light REE (i.e. LREE, La–Gd) than the TSS and have a conspicuous Eu anomaly, similar to the one exhibited by a typical Andean andesite (i.e. Average Andean Arc—AAA-). The REE of TSS exhibit a flatter pattern, a slightly depleted in LREE and enriched in heavy REE (i.e. HREE, Tb–Lu), and most plot above the Sample/UCC line. In general, they resemble the post-Archean Australian shale (PAAS), with a barely discernible Eu anomaly. Figure 14 ultimately shows the fractionation of the source rocks into a coarser fraction, transported along the channel bed and which, due to meager chemical weathering, is close to the dominant andesite. The finer size-fractions (i.e. TSS)

[7] The Los Altares gaging station is 230 km upstream from the city of Trelew and over 250 km from the estuary.

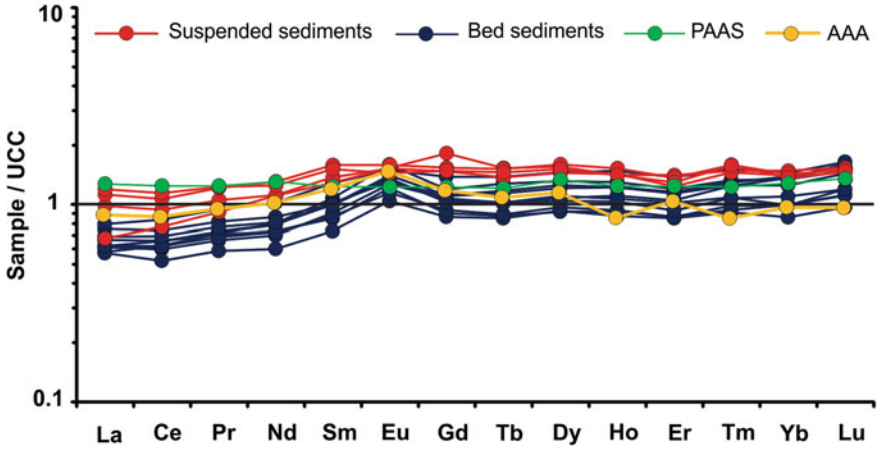

Fig. 14 Rare earth element *spider diagrams* (i.e. or *spidergrams*) of Chubut River bed and suspended sediments, normalized to the upper continental crust (UCC). Bulk bed sediments are similar to a typical Andean andesite, whereas TSS resemble an average mudstone. Post-Archean Australian Shales (PAAS) from McLennan (1989), Average Andean Arc (AAA) from http://www.geokem.com/

represents the ultimate weathering product, which is enriched in REE in general (i.e. the higher specific surface area results in a higher adsorption), but in HREE in particular, and resembles typical mudstones (e.g. PAAS).

5 Summary and Final Comments

The Chubut is a medium size river, typical of Patagonia in several aspects: its active catchments are near the Andes, where it receives most of the atmospheric precipitations; it crosses eastbound the arid and wind-swept plateau, and annually delivers a rather limited freshwater volume (i.e. ~1.1 km^3) to the SW Atlantic. In operation since 1963, the Florentino Ameghino dam supplies hydroelectric power (46.9 MW) and irrigation, which mainly supports the intensive agricultural activities that take place in the lowermost valley. Human impact is, hence, mostly localized in the river's lower reach where two important cities—Trelew and Rawson—are located.

In the Chubut River upper catchments, atmospheric precipitations (i.e. rain- and snowfall) occur between May and August (austral fall and winter), when ~62% of the total annual water volume is supplied to the drainage basin (Moyano and Moyano 2013). Accordingly, the discharge regime shows a mixed behavior in the upper gaging stations (i.e. Nacimiento, El Maitén, and Los Altares), accounted for by rainfall/snowfall in the (austral) winter months, and snow/ice melt, starting in September. The effect of the mountainous rain shadow—and the resulting aridity—is shown in the specific water yield, which varies from 11.6 L s^{-1} km^{-2} (Nacimiento),

to 13.5 L s^{-1} km^{-2} (El Maitén), down to 2.2 L s^{-1} km^{-2} (Los Altares). The specific water yield becomes even lower at Valle Inferior (1.1 L s^{-1} km^{-2}). The decrease in water yield is not only attributable to the increase of surface area, but also to the amplified consumptive use of water (i.e. water removed from the river that is evaporated, transpired by plants, incorporated into products or crops, consumed by humans or livestock, or otherwise removed from the Chubut River).

The Chubut's drainage basin is subjected to a *weathering-limited* denudation regime. Therefore, the mineral debris produced by erosion is scantily weathered and the mass of dissolved phases exported to the ocean is, hence, moderate. TZ^+ fluctuates between *medium dilute* and *medium mineralized* water-type ($1.5 < TZ^+ < 3.0$ meq L^{-1}). *Dilute*-type waters ($0.375 < TZ^+ < 0.75$ meq L^{-1}) are common in mountainous tributary streams, as well as in the antecedent rivers crossing the Andes and flowing towards the Pacific coast. Glacial oligotrophic lakes, also pertaining in such drainage, display *very dilute* concentrations ($0.185 < TZ^+ < 0.375$ meq L^{-1}). *Dilute* and *very dilute* waters are of the HCO_3^-–Ca^{2+}—type, often with SO_4^{2-} as a subsidiary chemical species (i.e. possibly the result of subglacial pyrite oxidation). Downstream, in *medium dilute* or *medium mineralized* water-types, Na^+, SO_4^{2-}, and Cl^- become more important components. The analysis of different water-mixing scenarios shows that: (a) the products of silicate weathering are ubiquitous; (b) given the abundance of glaciers in the headwaters, sulfide oxidation in subglacial conditions is likely to occur, generating H_2SO_4 that attacks limestone and other rocks; (c) the information supplied by strontium isotopes indicates that it is linked with Ca^{2+} concentrations and it is mainly supplied by limestone dissolution; (d) a comparison with the analysis performed in the Sierra Nevada (USA) (Garrels and Mackenzie 1967) suggests variable time of contact between water and rock.

The REE geochemical signature of bed and suspended sediments shows the fractionation between coarse rock debris, sparsely attacked by chemical weathering processes, and the fine size-fraction (i.e. TSS), which is the final product of weathering processes, and bears a geochemical resemblance to typical mudstones.

References

Bouza PJ, Saín C, Videla L, Dell'Archiprete P, Cortés E, Rua J (2017) Soil-geomorphology relationships in the Pichiñán uraniferous district, central region of Chubut Province, Argentina. In: Rabassa J (ed), Advances in geomorphology and quaternary studies in Argentina. Springer Earth System Sciences, Switzerland, pp 77–99

Calmels D, Gaillardet J, Brenot A, France-Lanord C (2007) Sustained sulfide oxidation by physical erosion processes in the Mackenzie River basin: climatic perspectives. Geology 35(11):1003–1006

Carson MA, Kirkby NJ (1972) Hillslope form and processes. Cambridge University Press

Chillrud SN, Pedrozo FL, Temporetti PF, Planas HF, Froelich PN (1994) Chemical weathering of phosphate and germanium in glacial meltwater streams: Effects of subglacial pyrite oxidation. Limnol Oceanogr 39(5):1130–1140

Davis JC (1986) Statistics and data analysis in geology. J Wiley & Sons, New York

Depetris PJ, Gaiero DM, Probst J-L, Hartmann J, Kempe S (2005) Biogeochemical output and typology of rivers draining Patagonia's Atlantic seaboard. J Coast Res 21:835–844
Depetris PJ, Pasquini AI (2008) Riverine flow and lake level variability in southern South America. Eos 89(28):254–255
Depetris PJ, Pasquini AI, Lecomte KL (2014) Weathering and the riverine denudation of continents. Springer, Dordrecht
Drever JI (1997) The geochemistry of natural waters. Prentice-Hall, Upper Saddle River
Gaiero DM, Depetris PJ, Probst J-L, Bidart SM, Leleyter L (2004) The signature of river-and wind-borne materials exported from Patagonia to the southern latitudes: a view from REEs and implications for paleoclimatic interpretations. Earth Planet Sci Lett 219:357–376
Gaiero DM, Probst J-L, Depetris PJ, Bidart SM, Leleyter L (2003) Iron and other transition metals in Patagonia river borne and windborne materials: geochemical control and transport to the southern South Atlantic Ocean. Geochim Cosmochim Acta 67:3606–3623
Gaiero DM, Probst J-L, Depetris PJ, Leleyter L, Kempe S (2002) Riverine transfer of heavy metals from Patagonia to the southwestern Atlantic Ocean. Reg Environ Chang 3(1–3):51–64
Gaillardet J, Dupré B, Louvat P, Allègre CJ (1999) Global silicate weathering and CO_2 consumption rates deduced from the chemistry of large rivers. Chem Geol 159:3–30
Garrels RM, Mackenzie FT (1967) Origin of the chemical compositions of some springs and lakes. In: Gould RF (ed) Equilibrium concepts in natural water systems. American Chemical Society, Washington DC, pp 222–242
Hernández MA, Ruiz de Galarreta VA, Fidalgo F (1983) Geohydrological diagnosis applied to the lower valley of Chubut River. Ciencia Del Suelo 1(2):83–91 (in Spanish)
Hirsch RM, Slack JR (1984) A nonparametric trend test for seasonal data with serial dependence. Water Resour Res 20:727–732
Kendall MG (1975) Rank correlation methods. Griffin, London
Killops S, Killops V (2005) Introduction to organic geochemistry. Blackwell, Malden
Langmuir D (1997) Aqueous environmental geochemistry. Prentice Hall, Upper Saddle River
Ludwig W, Probst J-L (1998) River sediments discharge to the ocean: present-day controls and global budgets. Am J Sci 298:265–295
Marsal D, Merriam DF (2014) Statistics for geoscientists. Elsevier, Amsterdam
McLennan SN (1989) Rare earth elements in sedimentary rocks; influence of provenance and sedimentary processes. Rev Mineral Geochem 21:169–200
McLennan SN (1993) Weathering and global denudation. J Geol 101:295–303
Meybeck M (2005) Global occurrence of major elements in rivers. In: Drever JI (ed), Surface and groundwater, weathering and soils. Elsevier, Amsterdam
Milliman JD, Farnsworth KL (2011) River discharge to the coastal ocean. A global synthesis, Cambridge
Milliman JD, Meade RH (1983) World-wide delivery of river sediment to the ocean. J Geol 91:1–21
Moyano CH, Moyano MC (2013) Hydrological study of the Chubut River. Upper and middle basin. Contrib Cient Gæa 251:149–164 (in Spanish)
Pasquini AI (2000) Geoquímica de sedimentos fluviales en una cuenca árida de alta latitud: el río Chubut, Patagonia, Argentina. Doctoral dissertation. Universidad Nacional de Córdoba, Argentina (in Spanish)
Pasquini AI, Depetris PJ (2007) Discharge trends and flow dynamics of South American rivers draining the southern Atlantic seaboard: An overview. J Hydrol 333:385–399
Pasquini AI, Depetris PJ, Gaiero DM, Probst J-L (2005) Material sources, chemical weathering and physical denudation in the Chubut River basin (Patagonia, Argentina): implications for Andean rivers. J Geol 113:451–469
Perdue EM, Ritchie JD (2005) Dissolved organic matter in freshwaters. In: Drever JI (ed) Surface and groundwater, weathering and soils. Elsevier, Amsterdam, pp 273–318
Piper A (1944) A graphic procedure in the geochemical interpretation of water analyses. Am Geophys Union Trans 25:914–923

Potter PE (1994) Modern sands of South America: composition, provenance and global significance. Geol Rundsch 83:212–232

Rapela CW, Pankhurst RJ (2020) The continental crust of Northeastern Patagonia. Ameghiniana 57(5):480–498

Sastre AV, Santinelli NH, Otaño SH, Ivanissevich ME (1998) Water quality in the lower section of the Chubut river, Patagonia, Argentina. Verh Internat Verein Limnol 26:951–955

Scapini M del C, Orfila JD (2001). Características químicas de las aguas superficiales del Chubut. http://www2.medioambiente.gov.ar/sian/chubut/trabajos/super.htm. Accessed on 29 Apr 2020 (in Spanish)

Subsecretaría de Recursos Hídricos (2002) Atlas Digital de los Recursos Hídricos Superficiales de la República Argentina, CD-Rom, Buenos Aires (in Spanish)

Torres AI, Andrade CF, Moore WS, Faleschini M, Esteves JL, Niencheski LFH, Depetris PJ (2018) Ra and Rn isotopes as natural tracers of submarine groundwater discharge in the Patagonian coastal zone (Argentina): an initial assessment. Environ Earth Sci 77(4):145–154

Tranter M (2005) Geochemical weathering in glacial and proglacial environments. In: Drever JI (ed) Surface and groundwater, weathering and soils. Elsevier, Amsterdam, pp 189–205

Hydrochemical Characteristics of Mid-Low Sections of North Patagonia Rivers, Argentina

Camilo Vélez-Agudelo, Daniel E. Martínez, Orlando M. Quiroz-Londoño, and Marcela A. Espinosa

Abstract The chemical composition of water in the mid-low sections of the three main rivers of Patagonia (Colorado, Negro and Chubut rivers) is an important proxy for the understanding of the water cycle in the region. River water samplings were done in summer and winter campaigns at Colorado (15 sites), Negro (18 sites) and Chubut (17 sites). Hydrochemical variables: pH, conductivity, salinity, and ion concentrations were measured. The data processing included regular hydrochemical diagrams, multivariate statistical analysis and saturation indexes calculation. The three rivers have two different sections: one inland section having the continental hydrochemical fingerprint and an estuarine section, with a markedly seawater mixing effect. Most water samples of the inland sites belong to the Mg^{2+}–Ca^{2+}–HCO_3^- type in the Negro and Chubut rivers and to the Ca^{2+}–SO_4^{2-} type in the Colorado River. In contrast, the prevailing hydrochemical facies was the Na–Cl type at estuarine sites. In general, rock weathering was the main hydrogeochemical process controlling chemistry composition of rivers, being the dissolution of gypsum, carbonate and silicate minerals the primary contributors. The inland section has a different composition for each river, which is related to differences in the rock-composition at the sources and chemical reactions during downstream flow. The Colorado River also showed the highest average values in salinity, conductivity and dissolved ions. Basin geology and brackish discharges from Curacó River during the high rainfall season contributed to explain the ionic concentration in Colorado River, in particular the excess of calcium and sulfate.

Keywords Major ions · River · Hydrochemistry · Patagonia

C. Vélez-Agudelo · D. E. Martínez (✉) · O. M. Quiroz-Londoño · M. A. Espinosa
Instituto de Geología de Costas y del Cuaternario, Universidad Nacional de Mar del Plata/CIC, CC 722 7600 Mar del Plata, Argentina
e-mail: demarti@mdp.edu.ar

Instituto de Investigaciones Marinas y Costeras, CONICET, Universidad Nacional de Mar del Plata, Mar del Plata, Argentina

A. I. Torres and V. A. Campodonico (eds.), *Environmental Assessment of Patagonia's Water Resources*, Environmental Earth Sciences,
https://doi.org/10.1007/978-3-030-89676-8_7

1 Introduction

Climatic change and human pressures increasingly stress the water resources worldwide (WWAP 2019). The challenge is greater in semiarid and arid areas, not only due to the predominant water scarcity but also to the increased vulnerability of their aquatic ecosystems (Huang et al. 2017; Wu et al. 2013). In these regions, the supply of easily accessible freshwater resources is found in dryland rivers, having their headwaters in areas of higher elevation. These fluvial environments are heterogeneous and complex systems whose hydrological dynamic occur on a small spatial and temporal scale (Davies et al. 2016). The chemical composition of surface waters in dryland rivers is characterized by the strong interaction between factors such as basin geology, hydroclimatic regimen, groundwater inputs, and biological activities (Sheldon and Fellows 2010). At a local scale, external factors such as soil erosion and the discharge of domestic and agricultural sewage also strongly affect the chemical balance of fluvial waters.

Hydrogeochemical studies are recognized as powerful tools to insight the processes and interactions that determine the composition and evolution of river systems (Hem et al. 1990; Hua et al. 2020; Jiang et al. 2020). The hydrochemical composition of rivers is indicative of the predominating processes of the drainage area and its linked environmental conditions are applied since the pioneer work of Gibbs (1970). In a broad sense, such studies enable to analyze the water–sediment interactions (ion exchange, dissolution–precipitation), to establish possible water mixtures (seawater intrusion, contribution from different aquifers), and to define sources and contamination processes (Carol and Kruse 2012; Li et al. 2019). Although hydrochemical studies have been effectively and widely applied to the assessment of surface water quality around the world, their potential in management matters remains still overlooked in Patagonia.

Compared with other continental landmass of the Southern Hemisphere, the Patagonia steppe has characteristics that make it unique in the region. In geological terms, this ancient basement is characterized by a varied lithology, structure and age (Coronato et al. 2008). This vast territory is also crossed by several dryland rivers, recording in the chemistry of its waters the effects on the environmental differences in the regional gradient. Among the eight main fluvial systems, Colorado, Negro and Chubut rivers account for about 78% of the drainage basin of Argentine Patagonia (Pasquini and Depetris 2007). These rivers support most of the economic, social and cultural activities of the region since they are the only available and stable water source for the surrounding communities. However, the rivers are currently threatened by moderate to intense human impacts because unsustainable agricultural practices, oil extraction and transportation, the expansion of urban areas, salinization of soils, use of agrochemicals and sewage effluents insufficiently treated of domestic and industrial activities (Abrameto et al. 2017; Brunet et al. 2005; Isla et al. 2015).

Up to now the hydrochemical studies of Patagonia rivers are either scarce or based only in a few samples, so further investigations are required (Brunet et al. 2005; Depetris 1980; Depetris et al. 2005; Gaiero et al. 2003). As the Colorado, Negro and

Chubut rivers flow through a large semiarid to arid region, these fluvial systems are strategically crucial to support both, biodiversity conservation and sustainable use of water resource from northern Patagonia. Hence, it is essential to have a comprehensive and extensive analysis of the hydrochemistry processes that take place in this arid region in order to develop suitable and efficient management strategies of their water resources.

In this context, a hydrochemical survey performed at several sampling points in the mid-low sections of the Colorado, Negro and Chubut rivers during summer and winter seasons is presented. The specific research questions intended to be addressed by the current study include: (i) What are the general hydrochemical characteristics of rivers? (ii) Are there spatial and temporal variations in the chemical composition among rivers? (iii) What are the main dominant processes controlling the hydrogeochemistry on a local scale? The main goal is to characterize the water composition and to analyze environmental factors that constrain the evolution of each river water composition.

2 Regional Setting and Previous Studies

Patagonia is the southernmost portion of Argentina (Fig. 1) representing about a third part of the country's territory. In this vast and diverse region, the Andes Cordillera plays an essential role in controlling the climate (Coronato et al. 2008). The moist air coming from the Pacific Ocean is lifted as it moves over the mountain range, producing heavy rainfalls on the western side. When the westerlies winds reach the eastern side of Patagonia, they become warmer and drier and the precipitation decreases abruptly (Paruelo et al. 2007). This strong west-east rainfall gradient creates two climatic and phytogeographic units: Andean Patagonia to the west and extra-Andean plateau drylands extending eastwards. A wet-temperate forest characterizes the first (about 700 mm year^{-1}), while a dry to semiarid climate (200 mm year^{-1} or less) prevails over the plateau. This last region is a large and heterogeneous environment that represents more than 60% of Patagonia region (Coronato et al. 2017; Depetris et al. 2005).

In addition to its aridity, the plateau drylands show a winter-summer thermal amplitude ranging from 5 to 16 °C, a highly evaporative condition and the intensity and persistence of the westerly winds exert a strong influence on the erosive processes that affect the extra-Andean region (Garreaud et al. 2013; Mazzoni and Vázquez 2009).

The geology of the Patagonia plateau (Fig. 2) exhibits a diverse lithology usually dominated by basalts, andesites, rhyolites and the well-known occurrence of pebbles or *rodados patagónicos* i.e. rounded rock fragments generated by erosion during water transport (Gaitán et al. 2020; Zambrano and Urien 1970). Tectonic, volcanism and past glaciations shaped diverse landforms, including elevated tablelands, hilly ranges, terraced levels, dune fields and fluvioglacial valleys that descend in elevation from the Andean sector towards the Atlantic coast (Hernández et al. 2008).

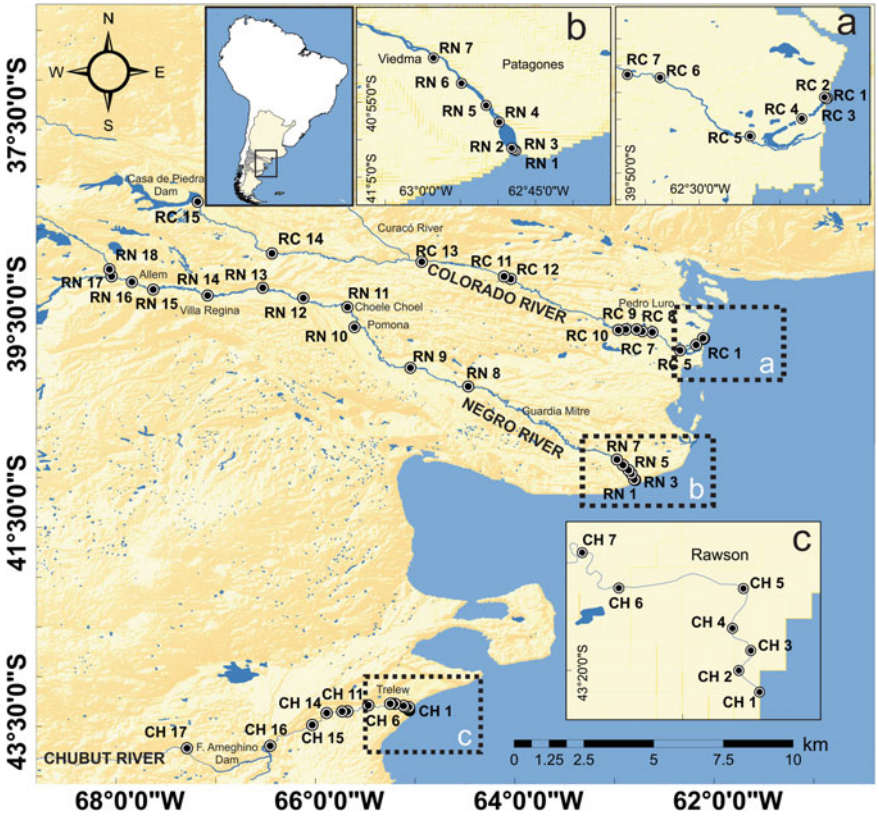

Fig. 1 Map of north Patagonia showing the location of sampling sites at the Colorado, Negro and Chubut rivers

The Colorado, Negro and Chubut rivers cross the northern Patagonia through wide fluvial valleys characterized by high cliffs. These watercourses originate on the eastern slope of the Andes and flow in a NW–SE direction until they reach the South Atlantic Ocean. As these rivers run through the arid tableland eastward, they gradually acquire allochthonous conditions and become more meandering, allowing the development of highly diverse riparian zones which are dynamic on a spatial and temporal scale (Paruelo et al. 2007).

While the Negro and Chubut rivers show a pluvio-nival regime due to the rainfall and snowfall contributions at the headwaters, the Colorado River is fed mostly by snowmelt (Coronato et al. 2008). It should be noted that the Atlantic Ocean exerts a moderate effect in temperature and precipitation in some areas of northeastern Patagonia (Gaitán et al. 2020).

The Negro River starts from the confluence of the Limay and Neuquén rivers at 635 km from the coast. This river displays a mean annual discharge of 900 $m^3\ s^{-1}$ (1951–2012), the greatest flow of Patagonia. Discharges of the Colorado

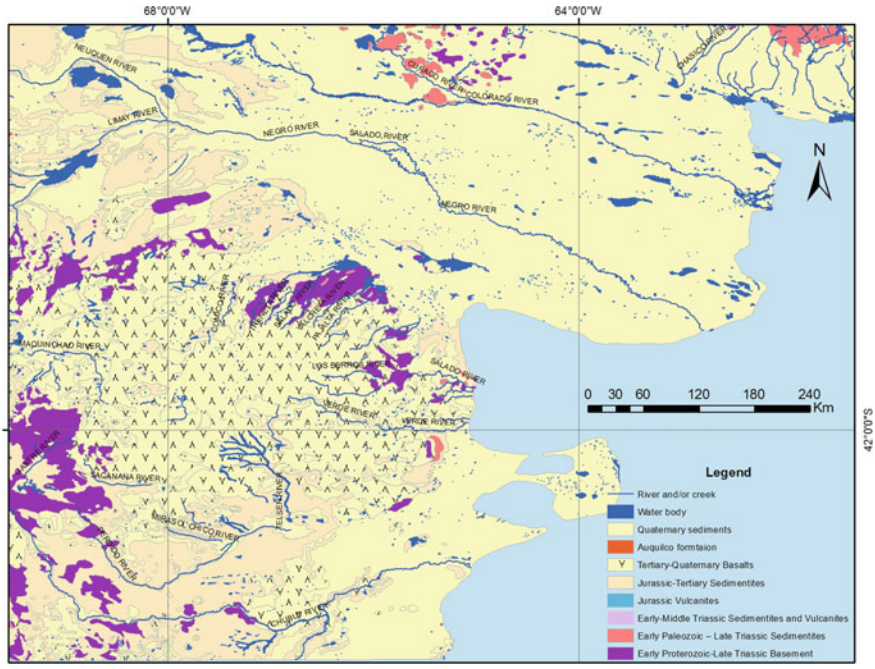

Fig. 2 Geological map of the study area

and Chubut rivers are about 155 $m^3\ s^{-1}$ (1940–2016) and 48 $m^3\ s^{-1}$ (1943–2016), respectively. At the Colorado River, the increase in discharge takes place at the end of the southern winter (due to snowmelt), reaching its highest values in spring and gradually decreasing towards the end of summer (Fig. 3). Meanwhile, the Negro and Chubut rivers show two peaks of flood discharges: one during the autumn and winter rainfalls and another one in spring due to snowmelt in the Andes (Pasquini et al. 2005; Romero and González 2016).

Climatic factors and the construction of several dams in the middle basins, have caused a downward trend of discharges at these rivers (Barros et al. 2015). Dams provide hydroelectric generation, land irrigation and water supply for human consumption at a provincial and national scale.

3 Materials and Methods

3.1 Sample Collection and Chemical Analysis

Fifty sampling sites were selected at the lower and middle basins from Colorado (15), Negro (18) and Chubut (17) rivers, covering a broad environmental gradient

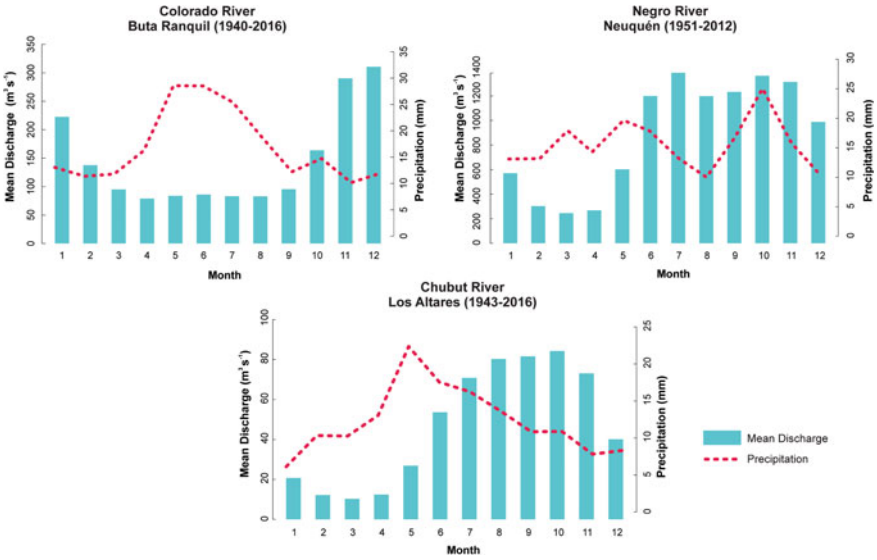

Fig. 3 Hydrographs showing the average discharges and precipitation of the north Patagonian rivers. Database of Colorado and Chubut rivers was taken from the National Water Information System of Argentina. Hydrological information of Negro River was modified from Romero and González (2016)

and fluvial morphology (Fig. 1). In addition, these sampling sites also were selected on the basis of some land-use activities characterizing each rivers section: intensive irrigation agriculture, livestock farms, mining and urban areas. In each site, physical and chemical variables of surface water were measured twice (during summer and winter) between the 2014 and 2015. It was not possible to measure in field and collect samples during austral winter in sites close to the outlet (RC1, RC2, RC3 and RC4) of the Colorado River, because diversion towards the main channel of the river, to prevent flooding, caused the complete dry up of the northern branch of the delta.

A Horiba U-10 water quality analyser was used to measure in situ pH, salinity (‰), conductivity (μS cm^{-1}), and water temperature (ºC). Major ions (HCO_3^-, Cl^-, SO_4^{-2}, NO_3^-, Na^+, K^+, Ca^{2+} and Mg^{2+}), and additional chemical variables as total hardness and silica (SiO_2) were analysed in the laboratory according to standardized methods (APHA 1998) including the corresponding detection limits (DL): chloride following Mhor method (DL 0.1 mg L^{-1}), sulfate by turbidimetry (DL 1 mg L^{-1}), calcium (DL 0.5 mg L^{-1}) and magnesium (DL 1 mg L^{-1}) by complexometric titrations with EDTA, sodium (DL 0.2 mg L^{-1}) and potassium (DL 0.1 mg L^{-1}) by flame spectrometry, bicarbonate (DL 0.5 mg L^{-1}) by potentiometric titrations, total silica by means of silico-molybdate method (DL 0.2 mg L^{-1}) and nitrate by a spectrophotometer Hach DREL 2800 method (DL 0.5 mg L^{-1}).

Water samples were collected in polypropylene bottles and kept refrigerated until the laboratory analysis. For nitrate analysis, water samples were preserved by acidification with HCl at pH < 2. Electroneutrality balances were done in order to check

the quality of the results, and in all the cases the error was below 10%, being below 5% in about 90% of the samples.

3.2 Preprocessing Data and Numerical Methods

The seasonal variation (winter–summer) of the physical and chemical variables was explored using beanplot analysis (Kampstra 2015). This graphical technique is an alternative way to compare univariate data into each river and among rivers. Furthermore, Kruskal-Wallis test followed up by Dunn's test were applied to identify significant differences among rivers. Principal Component Analysis (PCA) based on a correlation matrix was undertaken to reduce dimensionality of the whole dataset and identify meaningful variables that influence the chemical signature of surface waters in rivers. Prior to this analysis, environmental data (except for the pH) were log-transformed (log + 1) due to their skewed distribution. In order to eliminate the effect of tides both, the descriptive and ordination analyses, were conducted with the complete data set (50 sites) and without the estuarine sites (38 sites).

Major ion composition was analysed from typical diagrams such as the Gibbs diagram (Gibbs 1970) and Piper-Hill diagrams (Piper 1944). Ionic ratios of major elements were used to analyse the relative concentration of the different ions and their interaction, as well as to determine the types of hydro-geochemical processes controlling the chemical composition of rivers. Moreover, the chemical processes explaining the hydrochemical evolution were treated with the support of the PHREEQC code (Parkhurst and Appelo 1999). All descriptive and ordination analyses were performed with the statistical software R version 3.2.2 (R Development Core Team 2015), using additional packages such as "vegan" version 2.3-0 (Oksanen et al. 2015), and "beanplot" version 1.2 (Kampstra 2015).

4 Results

4.1 General and Seasonal Variability

Statistical analysis results of physical and chemical variables measured in the study area are presented in Tables 1, 2 and 3. Although only one sampling is not enough to characterize the seasonal behavior of a river, the availability of many sampling sites allows performing a comparison on the distribution of values comparing summer against winter campaigns.

The hydrochemical analyses provided a clear distinction among the middle basin sites and those located at the estuarine sites of the rivers (Fig. 4). Surface water temperature exhibited the same seasonal pattern in the three rivers. Although this

Table 1 Statistical summary of physical and chemical variables measured in summer (complete data set)

	Chubut River					Colorado River					Negro River				
	Min	Mean	Max	SD	CV	Min	Mean	Max	SD	CV	Min	Mean	Max	SD	CV
pH	8.7	9.1	9.4	0.2	2.4	7.4	8.4	9.4	0.7	8.1	7.5	8.8	9.6	0.5	5.1
Conductivity (mS cm^{-1})	0.2	3.8	26.8	8.3	215.5	0.1	4.2	20.1	6.3	151.4	0.1	1.5	10.2	3.0	204.3
Temperature (°C)	17.0	19.1	20.8	1.4	7.1	20.0	22.7	27.5	2.1	9.1	20.9	22.0	25.0	0.9	4.3
Salinity (‰)	0.0	2.2	16.5	5.1	232.3	0.5	2.3	12.1	3.8	163.9	0.0	0.7	5.6	1.7	233.8
Hardness (mg L^{-1})	141.3	501.0	2104.0	609.6	121.7	395.0	822.6	2110.0	607.0	73.8	93.5	300.9	1256.0	311.5	103.5
SiO_2 (mg L^{-1})	3.2	12.4	22.2	5.3	42.6	6.6	11.6	23.2	5.0	43.3	4.8	14.1	40.7	10.2	72.3
HCO_3^- (mg L^{-1})	23.0	168.3	278.0	56.1	33.3	113.6	233.6	387.0	87.7	37.6	55.6	123.3	248.5	51.8	42.0
Cl^- (mg L^{-1})	25.5	1113.7	8630.0	2429.2	218.1	148.0	994.1	5065.0	1752.8	176.3	18.2	432.0	2471.0	832.9	192.8
SO_4^{2-} (mg L^{-1})	18.0	155.1	960.0	296.2	191.0	225.0	559.3	1770.0	517.0	92.4	13.0	55.0	224.0	55.2	100.4
NO_3^- (mg L^{-1})	0.3	2.3	5.3	1.7	75.8	0.3	2.5	10.4	2.8	112.4	0.3	2.8	10.9	2.4	86.7
Ca^{2+} (mg L^{-1})	5.0	105.2	700.0	216.8	206.1	75.0	166.3	780.0	190.1	114.3	2.0	36.0	208.0	65.4	181.7
Mg^{2+} (mg L^{-1})	26.0	57.2	187.0	40.9	71.6	38.4	97.7	343.0	79.2	81.1	16.8	50.6	176.0	38.9	76.8
Na^+ (mg L^{-1})	6.0	564.6	4800.0	1311.8	232.3	87.0	536.9	2650.0	905.3	168.6	2.0	211.4	1200.0	412.1	194.9

(continued)

Table 1 (continued)

	Chubut River					Colorado River					Negro River				
	Min	Mean	Max	SD	CV	Min	Mean	Max	SD	CV	Min	Mean	Max	SD	CV
K^+ (mg L^{-1})	0.6	7.4	66.0	16.1	218.2	1.0	55.4	600.0	155.0	279.5	0.3	7.3	55.0	14.3	195.4

Min minimum, *Max* maximum, *SD* standard deviation, *CV* coefficient of variation (%)

Table 2 Statistical summary of physical and chemical variables measured in winter (complete data set)

	Chubut River					Colorado River					Negro River				
	Min	Mean	Max	SD	CV	Min	Mean	Max	SD	CV	Min	Mean	Max	SD	CV
pH	7.6	9.2	10.4	0.6	6.6	7.6	8.4	8.9	0.4	4.6	7.5	8.0	8.8	0.4	4.8
Conductivity (mS cm^{-1})	0.2	0.8	6.4	1.6	192.2	1.4	1.9	2.1	0.3	13.5	0.1	3.7	28.3	8.4	230.3
Temperature (°C)	5.8	8.0	10.0	1.2	15.6	5.1	7.3	10.8	1.9	25.4	6.5	8.6	9.4	0.7	8.0
Salinity (‰)	0.0	0.4	3.3	0.9	219.3	0.6	0.8	0.9	0.1	15.1	0.0	2.1	17.1	5.0	242.2
Hardness (mg L^{-1})	97.5	160.1	474.0	96.7	60.4	417.0	622.7	1000.0	205.7	33.0	99.0	660.9	6513.0	1509.2	228.4
SiO_2 (mg L^{-1})	9.0	14.6	34.8	5.8	39.5	2.6	6.3	10.0	2.7	42.2	2.0	3.6	6.9	1.2	34.0
HCO_3^- (mg L^{-1})	99.4	189.0	298.0	57.8	30.6	106.0	151.4	220.0	36.0	23.8	60.6	97.2	212.1	35.5	36.5
Cl^- (mg L^{-1})	10.9	210.3	1418.0	371.9	176.8	183.0	285.0	337.0	53.6	18.8	17.2	924.4	9406.0	2440.8	264.0
SO_4^{2-} (mg L^{-1})	21.0	43.2	124.0	29.3	67.7	228.0	461.8	670.0	142.7	30.9	17.0	260.4	1770.0	504.9	193.9
NO_3^- (mg L^{-1})	0.1	4.1	22.5	5.7	139.5	0.5	4.0	8.5	3.0	73.9	0.5	6.1	14.1	4.2	68.4
Ca^{2+} (mg L^{-1})	2.0	9.8	32.0	8.8	89.1	70.0	115.9	182.0	32.9	28.4	6.0	85.2	574.0	160.9	189.0
Mg^{2+} (mg L^{-1})	19.2	32.9	94.5	18.7	57.0	22.0	80.0	160.8	53.9	67.4	15.6	107.5	1323.1	304.0	282.8
Na^+ (mg L^{-1})	12.0	136.3	800.0	210.4	154.4	50.0	177.8	370.0	95.4	53.7	7.0	485.3	4400.0	1204.3	248.1

(continued)

Table 2 (continued)

	Chubut River					Colorado River					Negro River				
	Min	Mean	Max	SD	CV	Min	Mean	Max	SD	CV	Min	Mean	Max	SD	CV
K^+ (mg L^{-1})	0.6	5.4	30.0	7.9	146.1	2.8	4.7	8.5	2.2	45.6	0.2	20.5	220.0	57.1	278.4

Min minimum, Max maximum, *SD* standard deviation, *CV* coefficient of variation (%)

Table 3 Results of the Kruskal–Wallis test and the Dunn's multiple comparisons test among rivers in relation to the physical and chemical variables measured in the inland sites

	Kruskal–Wallis Test		Dunn's Test		
	H	*p* value	CH–RC	CH–RN	RC–RN
pH	27.5	***	***	***	ns
Conductivity (mS cm^{-1})	46.1	***	***	**	***
Temperature (°C)	7.7	*	*	**	ns
Salinity (‰)	60	***	***	ns	***
Hardness (mg L^{-1})	46	***	***	ns	***
SiO_2 (mg L^{-1})	17.9	***	*	*	ns
HCO_3^- (mg L^{-1})	29.5	***	***	ns	***
Cl^- (mg L^{-1})	40.5	***	***	ns	***
SO_4^{2-} (mg L^{-1})	47	***	***	ns	***
NO_3^- (mg L^{-1})	5.6	ns	ns	*	ns
Ca^{2+} (mg L^{-1})	46.3	***	***	ns	***
Mg^{2+} (mg L^{-1})	24.9	***	***	ns	***
Na^+ (mg L^{-1})	44.4	***	***	ns	***
K^+ (mg L^{-1})	31.3	***	***	ns	***

CH Chubut river, *RC* Colorado river, *RN* Negro River
ns non-significant, *p*, significance level: * $p \leq 0.05$; ** $p \leq 0.01$; *** $p \leq 0.001$

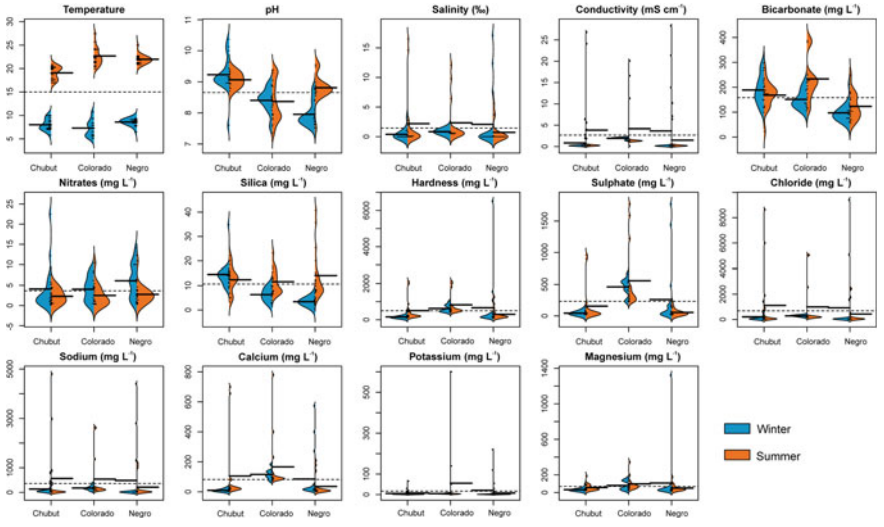

Fig. 4 Beanplots of physical and hydrochemical variables measured in the Colorado, Negro and Chubut rivers. The dotted line is the overall mean for each variable, while the solid line indicates the mean value in each season

variable showed similar values in the three rivers during winter, the mean temperature of the Chubut River during summer was statistically lower compared to those recorded in the other rivers. Salinity, conductivity, total hardness and the water ionic concentration increase as rivers flow towards the outlet. According to the pH values, the surface water of rivers ranged from slightly basic to basic with an average value of about 8.6. The Chubut River had the highest average pH value (9.1 ± 0.4) ($p = 1 \times 10^{-6}$), whereas the Colorado and Negro rivers showed similar average pH values (8.3 ± 0.5). However, the Negro River exhibited a significant seasonal difference in pH values ($p > 0.05$), with an average of 8.6 in summer and 7.8 in winter. In both seasons, this river also showed the highest pH values in the outlet sampling sites (RN1, RN2 and RN3).

The analysis excluding the samples belonging to the estuarine zone of the rivers allows a better observation of the seasonality in the variable's behavior (Fig. 5). The Colorado River showed the highest values of salinity, conductivity, total hardness and major ionic content. These variables also had a significant seasonal behavior in this river with higher concentrations in winter than in summer ($p = 0.04$). According to the hardness scheme (Durfor and Becker 1964), the Negro and Chubut rivers were categorized as hard waters (average total hardness of 180.8 mg L^{-1} and 164.9 mg L^{-1}, respectively), while the Colorado River was considered as very hard water (average total hardness of 576.1 mg L^{-1}). Comparatively, the Negro River had the lowest average concentrations of bicarbonate irrespective of the season (123.3 mg L^{-1} in summer and 97.2 mg L^{-1} in winter). In Colorado and Negro rivers the concentrations of this variable increased in summer and decreased in winter, but this seasonal trend

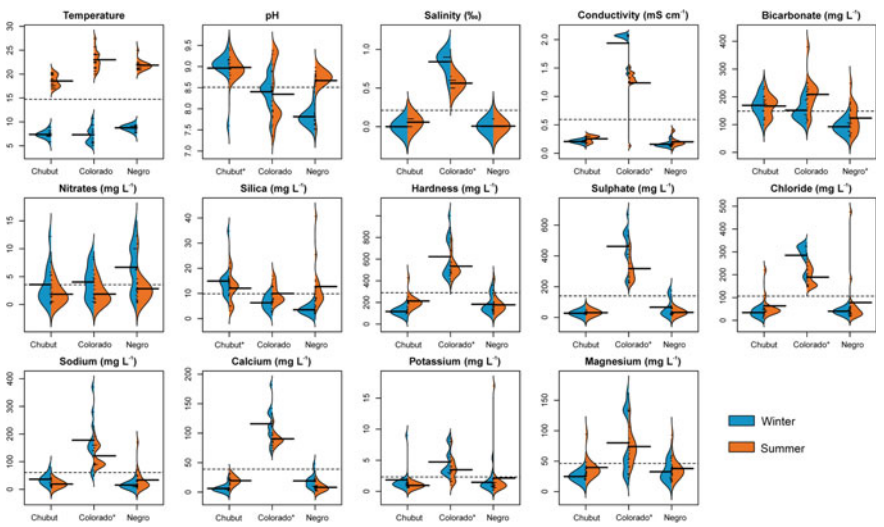

Fig. 5 Beanplots of physical and hydrochemical variables measured in inland areas (without estuarine sites). Asterisk (*) denotes the river that shows significant differences ($\alpha = 0.05$) based on Kruskal–Wallis and Dunn post hoc statistical tests

was only significant in the Colorado River ($p = 0.03$). Such seasonal pattern in the bicarbonate concentrations of the Colorado River was shown as inversely related to the behavior of major dissolved ions in the same river.

Nitrate concentrations varied from 0.3 mg L^{-1} to 8.5 mg L^{-1} in the Colorado River, from 0.3 mg L^{-1} to 14.1 mg L^{-1} in the Negro River and from 0.1 mg L^{-1} to 12.2 mg L^{-1} in the Chubut River. As for this variable, the statistical analyses did not show significant differences among rivers ($p = 0.06$). Although an apparent seasonal pattern in nitrate content in the three rivers occurs, with high mean values in winter and low concentrations in summer, the Kruskal–Wallis test indicated that these seasonal variations of nitrate were significant only in the Negro River ($p = 0.02$). Finally, the Chubut River showed high silica content with average values of 14.9 mg L^{-1} and 12.1 mg L^{-1} in winter and summer, respectively. Meanwhile, the Colorado and Negro rivers showed a slightly seasonal trend for this variable, with high values in summer and low values in winter.

The first two components of the PCA ordination explained 64.9% and 70.8% of the total variation in the summer and winter complete data, respectively (Fig. 6a, b). In both cases, the first axis explains the greatest amount of variation describing

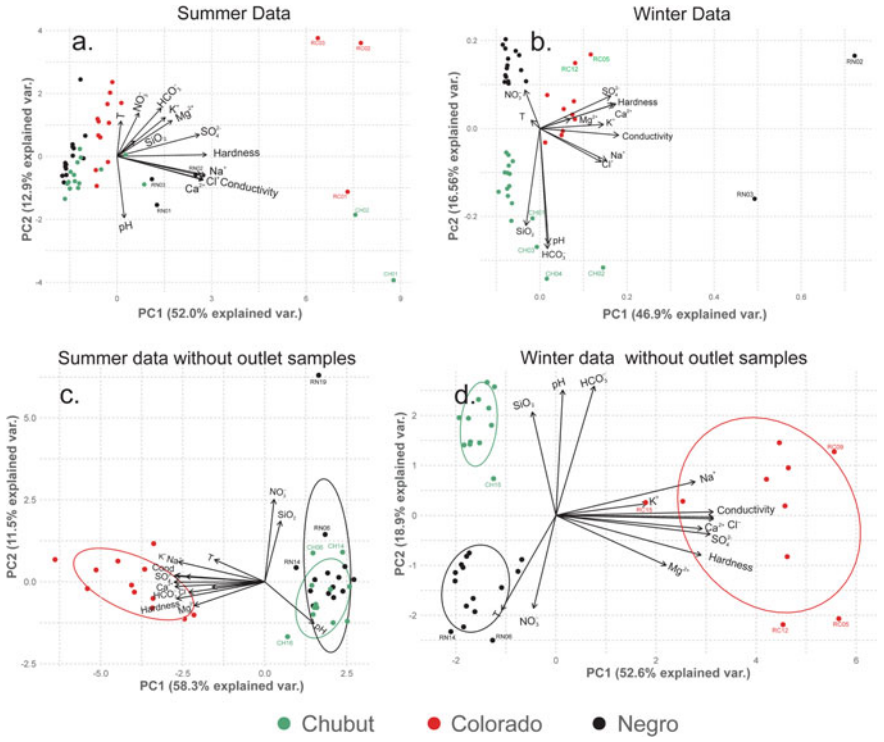

Fig. 6 Principal component analysis of physical and chemical data (summer and winter) with all sampling sites and without outlet sites

an ionic gradient that is highly correlated with conductivity, salinity, hardness, Cl^-, SO_4^{2-}, Na^+, Ca^{2+}, Mg^{2+} and K^+.

Considering only the freshwater sites of the three rivers (without the outlet sampling sites), the PCA showed that the first two axes capture up to 69.8% and 71.5% of the total variance in summer and winter data, respectively (Figs. 6c, d). However, seasonal differences regarding the ordination of data occurs as it can be observed from the figures. In summer data (Fig. 6c), the first axis was highly correlated with conductivity, salinity, total hardness, HCO_3^-, Cl^-, SO_4^{2-}, Na^+, Ca^{2+}, Mg^{2+} and K^+. Sites from the Colorado River showed a strong linear relationship with this component.

The second component was mainly associated with pH and SiO_2 as well as with the sampling sites of the Negro and Chubut rivers. Except for HCO_3^-, the first component of the winter data (Fig. 6d) was also related to conductivity, salinity, total hardness and major ions. Likewise, this ionic gradient was also associated with the sampling sites of the Colorado River. The second axis was mainly associated with pH, SiO_2, NO_3^- and HCO_3^-. Sites from the Chubut River were positively correlated with pH, SiO_2 and HCO_3^-, while the group of the Negro River sites exhibited moderate and direct correlation with NO_3^-.

4.2 Rivers Hydrogeochemistry

The samples taken in the Colorado, Negro and Chubut rivers have been plotted in Gibbs' diagrams (Fig. 7) (Gibbs 1970) in order to identify dominating processes in the determination of the composition of surface waters.

In Fig. 7 it is possible to observe that no water samples plot in the area assigned to precipitation dominance. Most of the samples are in the zone of water–rock interaction domain and displacing along a line parallel to the x axis, out of the fields described by Gibbs (1970). Samples from the Colorado River are disposed along to the zone indicated as corresponding to evaporation processes. Other samples from the three rivers are also towards the extreme of the evaporation zone, but they are those corresponding to the rivers' estuaries, being the result of seawater mixing.

The major ion composition of the three rivers was represented in two Piper diagrams, separating winter and summer samplings (Fig. 8). The Chubut River water is of the Mg^{2+}–Ca^{2+}–HCO_3^- type, evolving towards Na–Cl waters. The Colorado River belongs to the Ca^{2+}–SO_4^{2-} hydrochemical facies (Back 1960) with a Na–Cl–SO_4^{2-} member, close to seawater composition. The Negro River is mostly of the Mg^{2+}–Ca^{2+}–HCO_3^- type in summer, and divided into Mg^{2+}–Ca^{2+}–HCO_3^- and Mg^{2+}–Ca^{2+}–SO_4^{2-} types in winter, with a Na–Cl extreme member. In all the cases, the Na–Cl members correspond to the samples closer to the rivers' outlets to the Atlantic Ocean.

Cross sections representing the dissolved ion contents from the outlets towards inland show a strong increase of the anions Cl^- and SO_4^{-2} (Fig. 9a) and all the cations, but mostly Na^+ (Fig. 9b). At the continental area the contents of the different

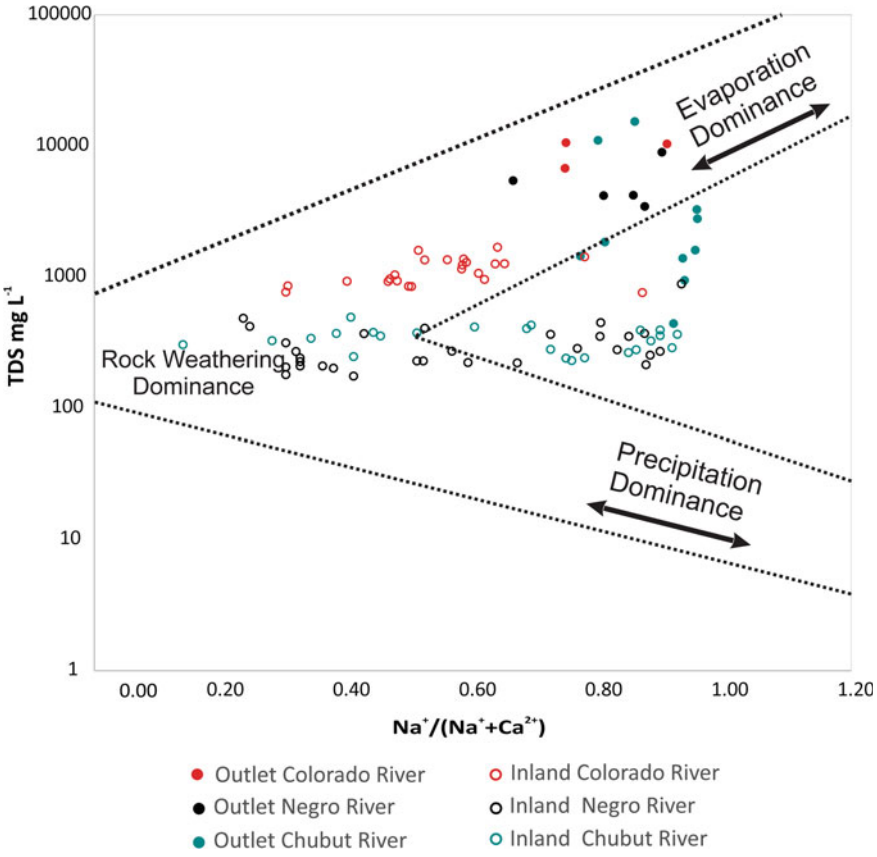

Fig. 7 Gibbs diagram showing major processes controlling surface water chemistry in the Colorado, Negro and Chubut rivers

ions are quite homogeneous, with an observable SO_4^{-2}, Cl^-, Na^+ and Ca^{+2} increase in the Colorado River, downstream point RC13.

The Piper diagram (Fig. 8), and the distribution of ion concentrations along the course, allows to differentiate a typical river section and an estuarine section for each river. The estuarine section can be defined by the point where the chloride and sodium contents increase several times compared to the previous site, resulting in Na–Cl water types.

The quite homogeneous composition of river waters upstream the estuarine zones (Figs. 8 and 9) indicates few changes regarding the water entering from the source areas. It is strengthened by the absence of significant tributaries in the considered river sections, with the exception of the occasional discharge of the Curacó River in the Colorado River. The hydrochemical fingerprint of each river shown in the Piper diagrams can be related to the rock source interaction through ionic ratios, their graphical representation and the equilibria against dominating minerals.

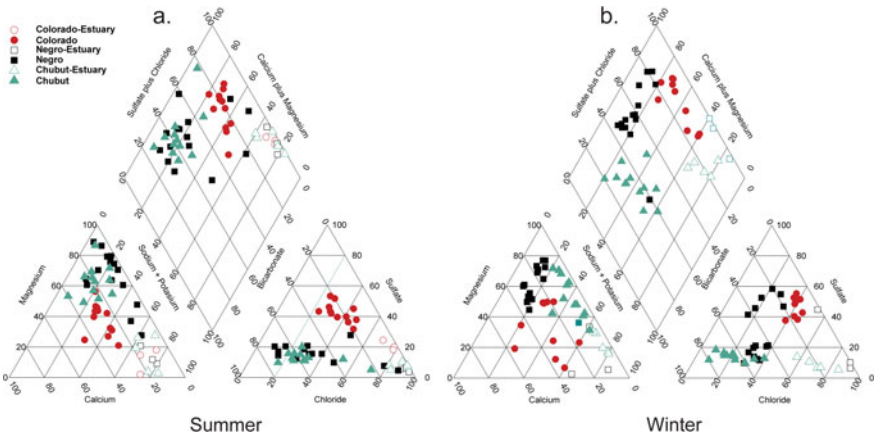

Fig. 8 Piper diagrams for summer **a** and winter **b** sampling periods

In order to have a first approximation of the rock source for the dissolved ions, HCO_3^-/SiO_2 ratios can be used as indicative of the main source of dissolved carbon species. If the mentioned ratio is >10 carbonate weathering is the assumed source, while if the ratio is < 5 it is considered to be a consequence of silicate weathering. All the samples explain their HCO_3^- sources by carbonate weathering, with the exception of samples RC05, RCH17 with rations assigned to silicate weathering.

Saturation indexes (SI) calculated using PHRREQC (Parkhurst and Appelo 1999) showed that 50% of the samples have a $SI_{calcite}$ between −0.5 and 0.5, which is considered the equilibrium fringe. About 25% of the samples are subsatutared in calcite, being mostly samples of the Negro River, and the other 25% is supersaturated, mostly in a low degree (IS < 1). High supersaturation (values up to 10) is observed in samples belonging to the estuary of the Chubut River.

$IS_{dolomite}$ shows equilibrium for 25% of the samples, and a similar proportion of sub-saturated samples. Dolomite supersaturated is observed in about 50% of the samples. IS_{gypsum} indicates subsaturation in all cases.

The Na^+/Cl^- ratio is often used to identify processes involving saline intrusions in arid and semiarid regions (Yang et al. 2016). In general, if the Na^+/Cl^- relationship is about 1 it is assumed that sodium comes mostly from halite dissolution. Figure 10a shows that almost all water samples belonging to inland sites in the studied Patagonia rivers not only showed a low Na^+/Cl^- ratio but also were plotted along the line 1:1. This means that, regardless of the season, the dissolution of halite is the main source of Na^+ in the freshwater sites of rivers. Moreover, samples at the estuarine sections are represented above this line, corresponding to a Na^+/Cl^- value of 0.86, typical of seawater.

The dissolution of carbonates (calcite and dolomite) and sulphate (gypsum) minerals are the dominant hydrogeochemical processes occurring in surface waters of rivers if the ratio $Ca^{2+}+Mg^{2+}$ against $HCO_3^-+SO_4^{2-}$ is close to 1 (Li et al. 2016). As it can be seen from Fig. 10b, most water samples of the Negro and Chubut rivers

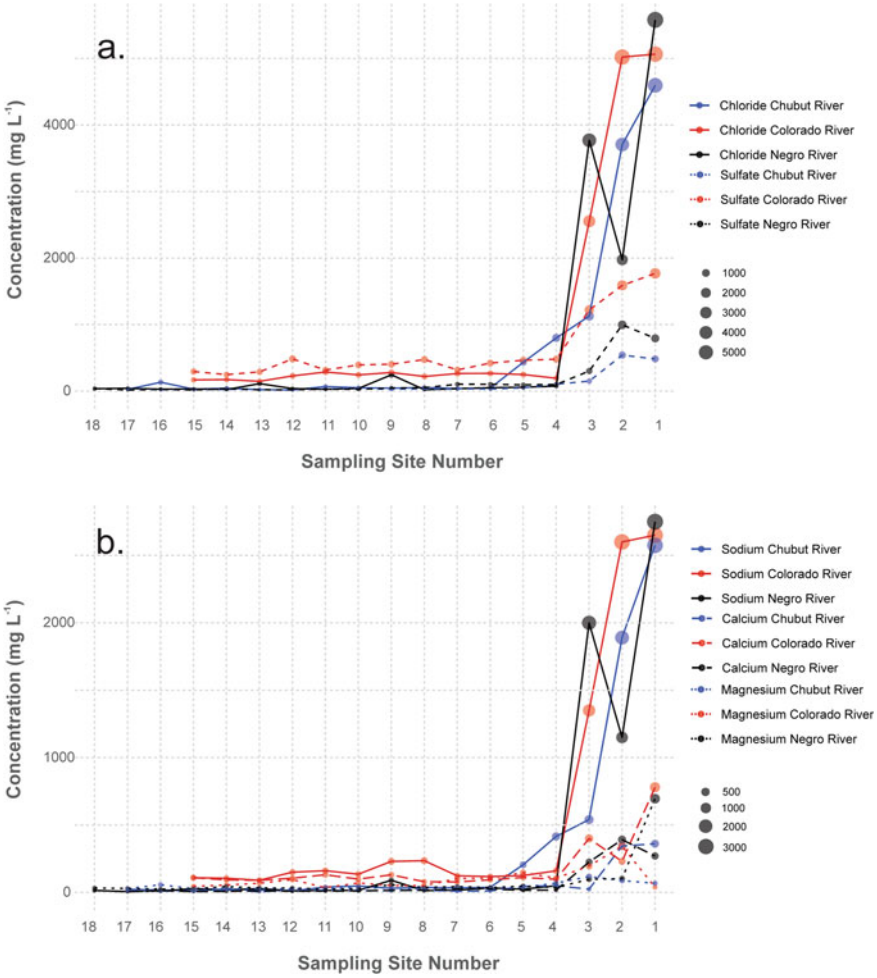

Fig. 9 Average winter-summer contents from river discharge at the inland towards the Ocean (point 1) **a** for anions chloride and sulfate, and **b** cations sodium, calcium and magnesium

showed low ratios and fall close to the line. Meanwhile, samples of the Colorado River were plotted above or below the 1:1 line. These trends suggest that the weathering of carbonate, silica and sulphate rocks is the main controlling factor of the chemical composition of Patagonia rivers. Dedolomitazion processes of the *rodados patagónicos*, which cover most of the surface of these basins, were identified in previous studies (Baumann et al. 2019).

Similarly, there is a linear relationship between Ca^{2+} and $SO_4{}^{2-}$ when the dissolution of gypsum is the main source of these ions. However, water samples should be plotted along the 1:1 line if Ca^{2+} and $SO_4{}^{2-}$ originate from the dissolution of gypsum. Figure 10c shows that most inland water samples of the Negro and Chubut

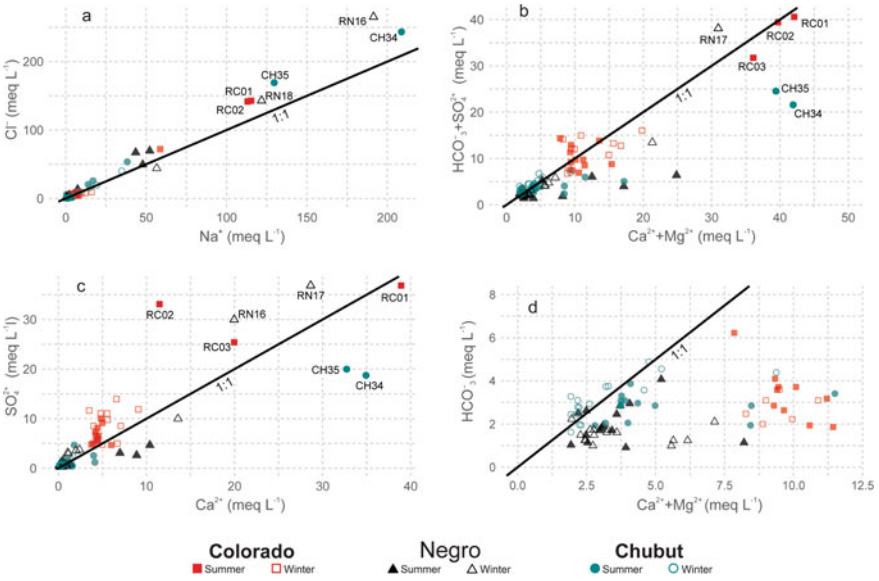

Fig. 10 Major ion ratios

rivers fall on the lower limit of the line, but the ionic ratio do not show a linear relationship, indicating that the dissolution of gypsum is not the main source of SO_4^{2-} in these rivers. Meanwhile, the water samples of the Colorado River deviate from the expected 1:1 line, displaying an excess of SO_4^{2-} over Ca^{2+}.

When the dissolution of dolomite and calcite controls the concentration of Ca^{2+}, Mg^{2+} and HCO_3^-, water samples should plot between the 1:1 line of the diagram. Figure 9d showed that most samples of the Negro and Chubut rivers were cluster below the 1:1 line, displaying a slightly excess of Ca^{2+} and Mg^{2+}. This fit of the HCO_3^- against $Ca^{2+} + Mg^{2+}$ contents to the 1:1 line likely can result from the mentioned dolomite dissolution, which is a typical consequence of the previously mentioned dedolomitazion process (Baumann et al. 2019), taking place at those basins. On the other hand, most water samples of the Colorado River were plotted to the right of the 1:1 line indicating an excess of Ca^{2+} and Mg^{2+} over HCO_3^- (Fig. 10d). This suggests that the dissolution of gypsum or silicates (anorthite and calcium montmorillonite), besides dolomite, may be the main sources of Ca^{2+} and Mg^{2+} in the Colorado River.

The minimum, maximum and average values of calcite saturation indexes for each river are shown in Table 4. Clear differences are observed between Negro River, on a side, and Colorado and Chubut rivers on the other side, which are expressing the differences in the main constraints for each water chemistry. Despite in average the three rivers are in the range of ± 0.5 $SI_{calcite}$, which can be indicating equilibrium dominating conditions, the negative average value for the Negro River is the result

Table 4 Calcite saturation indexes minimum, maximum and average values for each river, calculated with PHREEQC software (Parkhurst and Appelo 1999)

River	Minimun	Maximin	Average
Colorado	−0.161	1.070	0.529
Negro	−0.978	0.817	−0.549
Chubut	−0.083	1.240	0.385

of waters that are always subsaturated in calcite, with the only exception of the site RN01 which is affected by seawater in the river outlet.

Samples of the other two rivers are dominated by slightly supersaturated values. It can be a consequence of the analytical error, 0.5 of uncertainty in pH measurement implies 0.5 units of $SI_{calcite}$ (Appelo and Postma 1993). However, the dominance of low positive values should be interpreted as indicative of an overlapping of processes with different reaction kinetics, capable of producing the observed values. Typically, the gypsum dissolution increases the Ca^{+2} contents and leads calcite to precipitate, but this precipitation is kinetically slower that the gypsum dissolution (Appelo and Postma 1993).

5 Discussion

The physical and chemical variables measured in this study show clear differences in the Colorado, Negro and Chubut rivers, reflecting contrasting environmental conditions and external pressures across their watersheds. Of main river fluvial systems that flows through the plateau steppe, the Colorado River has the highest conductivity due to the geological features of its basin and the sporadic inputs of brackish water from the Curacó River, which in turn has connections with ENSO events (Gaiero et al. 2003; Isla and Toldo 2013). During periods of either high precipitation or snowmelt runoff from the Andean Mountains, the salinized waters accumulated in a variety of inland saline wetlands of the Curacó River are discharged into the Colorado River. This behavior also explains the Ca^{2+}-SO_4^{2-} dominating water type, because the headwaters of the river are located at the Andes at southern Mendoza province, where the Auquilco Formation is outcropping (Nullo et al. 2005; Weaver 1931). These marine sequences belong to the Lotena Group in the Neuquén Basin, and lithologically they are evaporites composed mainly by thick banks of gypsum and anhydrite, stratified, sometimes laminated or nodular (Narciso et al. 2004). In addition, the upper and middle valley of the river is characterized by Holocene lacustrine deposits containing evaporite minerals rich in sulfate sodium (Folguera et al. 2015). The erosion of these materials mostly by the wind effect can also play a pivotal role on the supply of sulfate to the river, explaining the sulfate excess over calcium (Fig. 7c) in waters of the Colorado River. On the other hand, the inter-annual hydrological dynamics clearly explain the seasonal variability of conductivity, salinity, total

hardness, and dissolved ions in the Colorado River. Ionic concentration decreases in summer when the highest flows occur, and increases in winter due to the decrease in the river flow. Recently, some studies indicate a significant decrease in the flow of the Colorado River since 2010, leading to a critical increase in the concentration of dissolved ions in the river (COIRCO 2017). These recent changes in the water quality affect the functioning of the river aquatic ecosystem, and have a strong impact on the productive, economic and social development of the region (Lurman et al. 2007).

Due to the recorded pH ranges, it can be stated that bicarbonate is the carbon species dominating the dissolved inorganic carbon in the rivers. Lithology, river discharge, temperature fluctuation, and biogeochemical processes play a pivotal role controlling the spatial and temporal trends of inorganic carbon content in most natural waters (Cai et al. 2008). A study conducted by Brunet et al. (2005) shows that the Colorado, Negro and Chubut rivers show the highest values of inorganic carbon compared with other Patagonia rivers. They argue that the occurrence of lakes and dams in the upper and middle basins seem to enhance the exchanges between river waters and atmospheric CO_2. In the same way, the low concentrations of bicarbonate recorded in the Negro River are likely linked with its high discharge, which is about ten and twenty times greater than that of the Colorado and Chubut rivers, respectively. This trend is consistent with previous studies indicating that the inverse correlation between the inorganic carbon content and river discharge is due to a simple dilution effect controlled by the precipitation and evaporation balance in the drainage basin (Cai et al. 2016; He and Xu 2018).

Negro and Chubut rivers are both of the Mg^{2+}–Ca^{2+}–HCO_3^- water type, but the HCO_3/SiO_2 ratio indicates some differences in the composition origin. The points located upstream of the Chubut River have a ratio >10, indicating that the water source is the weathering of silicates, basaltic and andesitic rocks at the headwaters. On the other hand, the composition of the Negro River probably has the same rock source composition, but the dams located upstream of the study section favor the silica precipitation lowering the HCO_3/SiO_2 ratio. In both rivers, water is equilibrated with calcite along the courses, being the reaction controlling the dissolved ion contents. The $SI_{calcite}$ values in Table 4 reflect the importance of the higher discharge of the Negro River, diluting the solution and sustaining the slightly undersaturated conditions. The lower discharge of the Chubut River put the $SI_{calcite}$ values in equilibrium values, according to the chemical reactivity of the *rodados patagónicos* (Baumann et al. 2019). On the other hand, Colorado River $SI_{calcite}$ is mostly supersaturated due to the mentioned discharge of Ca^{+2} from gypsum dissolution and the slower kinetic of calcite precipitation.

It is worth mentioning that the Colorado and Negro rivers show a noticeable seasonal variation in the bicarbonate concentration, with average values higher in summer, when the river flows are also higher, than in winter. This fluctuation might be partially explained by the annual thermal regime rather than due to variations in river flows. Biological respiration and decomposition processes of aquatic organisms tend to be higher as the water warms up in summer months, which increases the bicarbonate levels in the water (Cole 2013). Moreover, high salinity in the Colorado River during winter involves the increase of Ca^{+2}. As a consequence of the Ca^{+2}

increase the ionic activity product of Ca^{+2} and HCO_3^- equals the calcite equilibrium constant, resulting in calcite precipitation which controls the dissolved total inorganic carbon. In the Chubut River this temporal pattern in the bicarbonate concentrations is not clearly observed.

The concentration of nitrates in the analysed rivers indicates anthropogenic inputs and nutrient-enrichment in some extent, but for now the nitrate values are less than 13 mg L^{-1}, which is the maximum level allowed for protection and development of aquatic biological communities (CWQG 2012). The analysis seems to reveal that the Negro River has a moderate relationship with the nitrate content, particularly in winter when the river discharge is the lowest. It should be highlighted that the Negro River basin is the most extended hydrographic system of Patagonia, and is considered one of the most important agricultural and processing areas of Argentina. As a consequence, this river receives a large amount of sediments and agrochemicals such as fertilizers and pesticides (Isla et al. 2010; Miglioranza et al. 2013). In fact, some studies already indicate a strong trend of nitrate increasing towards the Lower Valley of the Negro River which are caused mainly by industrial inputs, sewage treatment plants discharge and agrochemicals runoff from Guardia Mitre, Zanjon Oyuela, Viedma and Carmen de Patagones (Abrameto et al. 2017). These results provide critical information indicating the need to develop a holistic and integrated approach in order to improve the monitoring programs in the river since nitrate pollution is one the major threats in arid/semiarid aquatic ecosystems worldwide (Cook et al. 2010).

6 Conclusions

The hydrochemical characteristics of the northern Patagonia rivers are a consequence of the weathering of silicate volcanic rocks located at the headwaters in the Andes, but strongly modified and conditioned by processes taking place during runoff in the extra-Andean zone. HCO_3^-/SiO_2 indexes indicate how the main processes move from silicate dissolution to carbonates equilibrium downflow and the important control of hydrological features in the different composition of rivers. Being carbonates equilibrium a dominant constraint, due to widespread distribution of the carbonatic cement of the *rodados patagónicos*, calcite saturation index variations are indicators of the other processes explaining variations among rivers. Moreover, the effect of seawater mixing is the main hydrochemical constraint at estuarine outlet sections. Discharge of the Negro River is several times higher than the others, and the dilution effect leads to unsaturated values and a Mg^{2+}–Ca^{2+}–HCO_3^- water type. In the case of the Chubut River, the water type is the same, but the lower discharge allows to sustain the calcite equilibrium along the studied section. On the other side, the Colorado River waters are of the Ca^{2+}–SO_4^{2-} type due to contributions of gypsum dissolution in the Upper Basin and by irregular brackish discharges from the Curacó River. This discharge of high Ca^{2+} contents, and the differences into reactions kinetic, results in slight carbonate supersaturation. Then, the effect of amount of discharge

and specific contributors establish the main hydrochemical differences at the inland area. Close to the outlet, estuarine behavior has been observed at the three rivers, and the chemical composition becomes of the Na–Cl type, and Cl^- contents indicate a seawater mixing proportion of about 25%. Significant seasonal differences were only observed with higher values in summer in the case of the pH of the Negro River, salinity in the Colorado River, Cl^- in Negro and Colorado rivers. These variations can be related to higher surface water evaporation during summer. Although it is preliminary, the hydrochemical information achieved from this study will be useful to understand the predominating processes that underlie the chemical composition in north Patagonia rivers. Revealing the main ion sources and the primarily controlling factors are key topics for developing effective management strategies of water resources in arid and semiarid regions like Patagonia.

Acknowledgements The authors wish to acknowledge F. Isla, R. Fayó, J. Bedmar and M. Taglioretti for their assistance with field sampling, and G. Bernava for hydrochemical analysis. This study was funded by the Agencia Nacional de Promoción Científica y Tecnológica ANPCyT (grant number PICT 1146/16).

References

Abrameto M, Torres M, Ruffini G (2017) Nutrients distributions in an estuary of the Argentine coast. WIT Trans Ecol Environ 216:277–283

APHA, American Public Health Association. (1998) Standard methods for the examination of water and wastewater. Water Environment Federation, Washington

Appelo CAJ, Postma D (1993) Geochemistry, groundwater and pollution. Balkema, The Netherlands

Back W (1960) Hydrochemical facies and ground-water flow patterns in Northern Atlantic Coastal Plain. AAPG Bull 44:1244–1245

Barros VR, Boninsegna JA, Camilloni IA, Chidiak M, Magrín GO, Rusticucci M (2015) Climate change in Argentina: trends, projections, impacts and adaptation. Wiley Interdisciplinary Reviews. Clim Chang 6:151–169

Baumann GO, Vital M, Glok-Galli M, Grondona S, Massone H, Martinez DE (2019) Hydrogeochemical modeling and dedolomitization processes in the Patagonian Boulders and Patagonia Formation in the eastern Patagonia, Argentina. Environ Earth Sci 78:1–16

Brunet F, Gaiero D, Probst J, Depetris PJ, Gauthier Lafaye F, Stille P (2005) δ13C tracing of dissolved inorganic carbon sources in Patagonian rivers (Argentina). Hydrol Process 19:3321–3344

Cai W-J, Guo X, Chen C-TA, Dai M, Zhang L, Zhai W, Lohrenz SE, Yin K, Harrison PJ, Wang Y (2008) A comparative overview of weathering intensity and HCO_3^- flux in the world's major rivers with emphasis on the Changjiang, Huanghe, Zhujiang (Pearl) and Mississippi Rivers. Cont Shelf Res 28:1538–1549

Cai Y, Shim M, Guo L, Shiller A (2016) Floodplain influence on carbon speciation and fluxes from the lower Pearl River, Mississippi. Geochim Cosmochim Acta 186:189–206

Carol ES, Kruse EE (2012) Hydrochemical characterization of the water resources in the coastal environments of the outer Río de la Plata Estuary, Argentina. J South Am Earth Sci 37:113–121

COIRCO, Comité Interjurisdiccional del Río Colorado (2017) Análisis estadístico de los parámetros fisicoquímicos, metales y metaloides. Estación piloto "Buta Ranquil". Universidad Nacional del Sur, Argentina (in Spanish)

Cole JJ (2013) The carbon cycle: with a brief introduction to global biogeochemistry. In: Weathers KC, Strayer DL, Likens GE (eds) Fundamentals of ecosystem science. Academic Press, New York, pp 109–135

Cook PL, Aldridge K, Lamontagne S, Brookes J (2010) Retention of nitrogen, phosphorus and silicon in a large semi-arid riverine lake system. Biogeochemistry 99:49–63

Coronato A, Coronato F, Mazzoni E, Vázquez M (2008) The physical geography of Patagonia and Tierra del Fuego. Dev Quat Sci 11:13–55

Coronato A, Mazzoni E, Vázquez M, Coronato F (2017) Patagonia. Una síntesis de su geografía física. Ediciones Universidad Nacional de la Patagonia Austral, Santa Cruz, Argentina (in Spanish)

CWQG, Canadian Water Quality Guidelines for the Protection of Aquatic Life (2012) Nitrate Ion. Canadian Council of Ministers of the Environment, Winnipeg

Davies J, Barchiesi S, Ogali CJ, Welling R, Dalton J, Laban P (2016) Water in drylands: adapting to scarcity through integrated management. IUCN, Gland, Switzerland

Depetris PJ (1980) Hydrochemical aspects of the Negro river, Patagonia, Argentina. Earth Surf Process 5:181–186

Depetris PJ, Gaiero DM, Probst JL, Hartmann J, Kempe S (2005) Biogeochemical output and typology of rivers draining Patagonia's Atlantic seaboard. J Coast Res 21:835–844

Durfor CN, Becker E (1964) Public water supplies of the 100 largest cities in the United States. US Government Printing Office, Washington

Folguera A, Etcheverría M, Zárate M, Miranda F, Faroux A, Getino P (2015) Hoja Geológica 3963-I, Río Colorado. Provincias de La Pampa, Buenos Aires y Río Negro. Instituto de Geología y Recursos Minerales, Servicio Geológico Minero Argentino, Buenos Aires (in Spanish)

Gaiero DM, Probst J, Depetris PJ, Bidart SM, Leleyter L (2003) Iron and other transition metals in Patagonian riverborne and windborne materials: geochemical control and transport to the southern South Atlantic Ocean. Geochim Cosmochim Acta 67:3603–3623

Gaitán JJ, Bran DE, Oliva GE (2020) Patagonian Desert. In: Goldstein M, DellaSala D (eds) Encyclopedia of the world's biomes. Elsevier, pp 163–180

Garreaud R, Lopez P, Minvielle M, Rojas M (2013) Large-scale control on the Patagonian climate. J Clim 26:215–230

Gibbs RJ (1970) Mechanisms controlling world water chemistry. Science 170:1088–1090

He S, Xu YJ (2018) Freshwater-saltwater mixing effects on dissolved carbon and CO_2 outgassing of a coastal river entering the northern Gulf of Mexico. Est Coast 41:734–750

Hem JD, Demayo A, Smith RA (1990) Hydrogeochemistry of rivers and lakes. In: Wolman MG, Rigss HC (eds) The geology of North America. Geological Society of America, USA, pp 189–231

Hernández MA, González N, Hernández L (2008) Late cenozoic geohydrology of extra-Andean Patagonia, Argentina. Dev Quat Sci 11:497–509

Hua K, Xiao J, Li S, Li Z (2020) Analysis of hydrochemical characteristics and their controlling factors in the Fen River of China. Sustain Cities Soc 52:101827

Huang J, Li Y, Fu C, Chen F, Fu Q, Dai A, Shinoda M, Ma Z, Guo W, Li W, Zhang L, Liu Y, Yu H, He Y, Xie Y, Guan X, Ji M, Lin L, Wang S, Yan H, Wang G (2017) Dryland climate change: recent progress and challenges. Rev Geophys 55:719–778

Isla F, Espinosa M, Rubio B, Escandell A, Gerpe M, Miglioranza K, Rey D, Vilas F (2015) Avulsion at a drift-dominated mesotidal estuary: the Chubut River outlet, Patagonia, Argentina. J Hydrol 529:632–639

Isla F, Miglioranza K, Ondarza P, Shimabukuro V, Menone M, Espinosa M, Quiroz Londoño M, Ferrante A, Aizpún J, Moreno V (2010) Sediment and pollutant distribution along the Negro River: Patagonia, Argentina. Int J River Basin Manag 8:319–330

Isla F, Toldo E (2013) ENSO impacts on Atlantic watersheds of South America. Quat Environ Geosci 4:34–41

Jiang Y, Gui H, Yu H, Wang M, Fang H, Wang C, Fang H, Chen C, Zhang Y, Huang Y (2020) Hydrochemical characteristics and water quality evaluation of rivers in different regions of cities: a case study of Suzhou city in northern Anhui Province, China. Water 12:950

Kampstra P (2015) Beanplot: visualization via beanplots. R package version 1.2. https://cran.r-project.org/package=beanplot. Accessed 15 June 2020
Li P, Zhang Y, Yang N, Jing L, Yu P (2016) Major ion chemistry and quality assessment of groundwater in and around a mountainous tourist town of China. Expos Health 8:239–252
Li Z, Xiao J, Evaristo J, Li Z (2019) Spatiotemporal variations in the hydrochemical characteristics and controlling factors of streamflow and groundwater in the Wei River of China. Environ Pollut 254:113006
Lurman D, Aragón M, Sánchez R, Ancía V (2007) Variables a considerar para una estimación de las pérdidas económicas por causa de la salinización del río Colorado y su cuantificación. CORFO-INTA 1:1–11 (in Spanish)
Mazzoni E, Vázquez M (2009) Desertification in Patagonia. In: Latrubesse E (ed) Geomorphology of natural and human-induced disasters in South America. Elsevier, Amsterdarm, pp 351–377. https://doi.org/10.1016/S0928-2025(08)10017-7
Miglioranza KS, Gonzalez M, Ondarza PM, Shimabukuro VM, Isla FI, Fillmann G, Aizpún J, Moreno VJ (2013) Assessment of Argentinean Patagonia pollution: PBDEs, OCPs and PCBs in different matrices from the Río Negro basin. Sci Total Environ 452:275–285
Narciso V, Santamaría G, Zanettini J (2004) Hoja Geológica 3769-I, Barrancas. Provincias de Mendoza y Neuquén. Instituto de Geología y Recursos Minerales, Servicio Geológico Minero Argentino, Buenos Aires (in Spanish)
Nullo FE, Stephens G, Combina A, Dimieri L, Baldauf P, Bouza P, Zanettini JC, Leanza HA (2005) Hoja Geológica 3569-III/3572-IV Malargüe, provincia de Mendoza. Servicio Geológico Minero Argentino. Instituto de Geología y Recursos Minerales, Buenos Aires (in Spanish)
Oksanen J, Blanchet FG, Kindt R, Legendre P, Minchin PR, O'Hara RB, Simpson GL, Solymos P, Stevens MMH, Wagner H (2015) Vegan: community ecology package. R package version 2.3-0. https://cran.r-project.org/package=vegan. Accessed 16 June 2020
Parkhurst DL, Appelo C (1999) User's guide to PHREEQC (Version 2): A computer program for speciation, batch-reaction, one-dimensional transport, and inverse geochemical calculations. Water-Resour Invest Rep 99–312
Paruelo JM, Jobbágy EG, Oesterheld M, Golluscio RA, Aguiar MR (2007) The grasslands and steppes of Patagonia and the Río de la Plata plains. In: Veblen T, Young K, Orme A (eds) The physical geography of South America. Oxford University Press, New York, pp 232–248
Pasquini AI, Depetris PJ (2007) Discharge trends and flow dynamics of South American rivers draining the southern Atlantic seaboard: an overview. J Hydrol 333:385–399
Pasquini AI, Depetris PJ, Gaiero DM, Probst J-L (2005) Material sources, chemical weathering, and physical denudation in the Chubut River basin (Patagonia, Argentina): implications for Andean rivers. J Geol 113:451–469
Piper AM (1944) A graphic procedure in the geochemical interpretation of water analyses. Eos, Tran Am Geophys Union 25:914–928
R Development Core Team R (2015) Language and environmental for statistical computing. R Foundation for Statistical Computing: Viena, Austria. www.r-project.org. Accessed 15 June 2020
Romero P, González M (2016) Relación entre caudales y precipitación en algunas cuencas de la Patagonia norte. Rev Geol Apl Ingen Ambiente 36:7–13 (in Spanish)
Sheldon F, Fellows CS (2010) Water quality in two Australian dryland rivers: spatial and temporal variability and the role of flow. Mar Fresh Res 61:864–874
Stiff HAJ (1951) The interpretation of chemical water analysis by means of patterns. J Pet Technol 3:15–13
Weaver CE (1931) Paleontology of the Jurassic and Cretaceous of west central Argentina. University of Washington press, Seattle
Wu G, Li L, Ahmad S, Chen X, Pan X (2013) A dynamic model for vulnerability assessment of regional water resources in arid areas: a case study of Bayingolin, China. Water Resour Manage 27:3085–3101
WWAP, World Water Assessment Programme (2019) The United Nations world water development report 2019: leaving no one behind. UNESCO, Paris

Yang Q, Li Z, Ma H, Wang L, Martín JD (2016) Identification of the hydrogeochemical processes and assessment of groundwater quality using classic integrated geochemical methods in the Southeastern part of Ordos basin, China. Environ Pollut 218:879–888

Zambrano J, Urien C (1970) Geological outline of the basins in Southern Argentina and their continuation off the Atlantic shore. J Geophys Res 75:1363–1396

Hydrochemistry of Patagonian Wet Meadows (*Mallines*) Under Different Geological Frames

María del Pilar Alvarez, Eleonora Carol, María Paz Pasquale Pérez, Edoardo Melendi, and Esteban Villalba

Abstract Surface water resources of Extra-Andean Patagonia are scarce, being the large rivers that cross the entire territory from the Andean cordillera to the Atlantic coast the main water supply for human activities. However, the large part of the area without permanent watercourses has small springs that give rise to wetlands known as *mallines* (wet meadows), of great environmental relevance due to the ecosystem services they provide. These wet meadows are sustained by groundwater, which gives them great variations in hydrochemical characteristics. These variations result from groundwater interaction with rocks and sediments through which it flows. To reflect this variability, four areas with wet meadows in different geological frames are described within Extra-Andean Patagonia, distributed according to the major geo-geomorphological regions: one sector in northern Patagonia, within the Mountain Sector of the Neuquén Embayment (Domuyo area); another in the coastal sector, associated with the Patagonian Tableland (Península Valdés), one on the center associated with the Somún Curá Massif (Carri Laufquen sector); and the fourth in southern sector, associated with the Deseado Massif.

Keywords Wetlands · Groundwater · Hydrogeochemistry · Arid zones · Extra-Andean Patagonia

M. del P. Alvarez (✉)
Instituto Patagónico Para el Estudio de los Ecosistemas Continentales, CCT-CONICET CENPAT, Puerto Madryn, Argentina
e-mail: alvarez@cenpat-conicet.gob.ar

Universidad Nacional de La Patagonia San Juan Bosco, Puerto Madryn, Argentina

E. Carol (✉) · M. P. Pasquale Pérez · E. Melendi · E. Villalba
Centro de Investigaciones Geológicas, CONICET, Universidad Nacional de La Plata, La Plata, Argentina
e-mail: eleocarol@fcnym.unlp.edu.ar

A. I. Torres and V. A. Campodonico (eds.), *Environmental Assessment of Patagonia's Water Resources*, Environmental Earth Sciences,
https://doi.org/10.1007/978-3-030-89676-8_8

1 Introduction

"*Mallín*" is an aboriginal term pertaining to the Mapuche nation language that denotes flooded areas with herbaceous ground cover (Ruiz Leal 1972; Wilhelm de Moesbach 1980). According to the definition of **wetland** provided by the RAMSAR Convention, *mallines* are a particular type of wetland denominated wet meadows (Canevari et al. 1999). In wetlands, water is the primary factor controlling the environment and associated plant and animal life, whereas its presence is determined by the geomorphological emplacement (Brinson and Malvárez 2002).

From the physiographic approach, two contrasting sectors can be distinguished in Patagonia: (1) the Patagonian Andes in the west sector and (2) the Extra-Andean Patagonia, extending east from the central sector to the Atlantic Ocean. The main feature of Extra-Andean Patagonia is the presence of extensive plains of different origins and ages, placed at different levels. This relief is occasionally interrupted by the appearance of rocky cliffs, lava plains (plateaus), and low mountain hills (Bouza and Bilmes 2020). This physiographic division is also accompanied by changes in climatic conditions. The Andes Cordillera strongly affects the regional climate by blocking the disturbances from westerly flow, therefore it gives rise to the precipitation over this area and influences wind patterns and precipitation in the whole region (Insel et al. 2010; Coronato et al. 2008). Uplift on the West side of the Andes leads to hyper humid conditions, while downslope subsidence dries the eastern plains leading to arid and highly evaporative conditions (Garreaud et al. 2013), resulting in a strong West–East gradient of precipitation across the region (Barros et al. 1979). On the West side of the Andes, the amount of annual rainfall exceeds 2000 mm while eastward the total annual precipitation decreases exponentially (Fig. 1), where most of the central portion of Patagonia receives less than 200 mm per year.

This distribution of precipitation is responsible for the abundance of lakes and rivers in the Andean sector, while in the Extra-Andean sector the main surface water manifestations are reduced to those rivers with Andean **headwaters** and Atlantic discharge (Fig. 1). In this context, *mallines* acquire vital importance as water sources for the sustenance of local fauna and the supply of local inhabitants (Epele et al. 2018). In Extra-Andean Patagonia, it is possible to find, with variations in their hydrological and hydrochemical characteristics, *mallines* in the different geological-geomorphological settings.

For this chapter, four areas with wet meadows in different geological frames are described within Extra-Andean Patagonia, distributed according to the major geological-geomorphological regions (Bouza and Bilmes 2020): one sector in northern Patagonia, within the Mountain Sector of the Neuquén Embayment (Domuyo area); another in the coastal sector, associated with the Patagonian Tableland (Península Valdés), one on the center associated with the Somún Curá Massif (Carri Laufquen sector); and the fourth in the southern sector, associated with the Deseado Massif (Fig. 1).

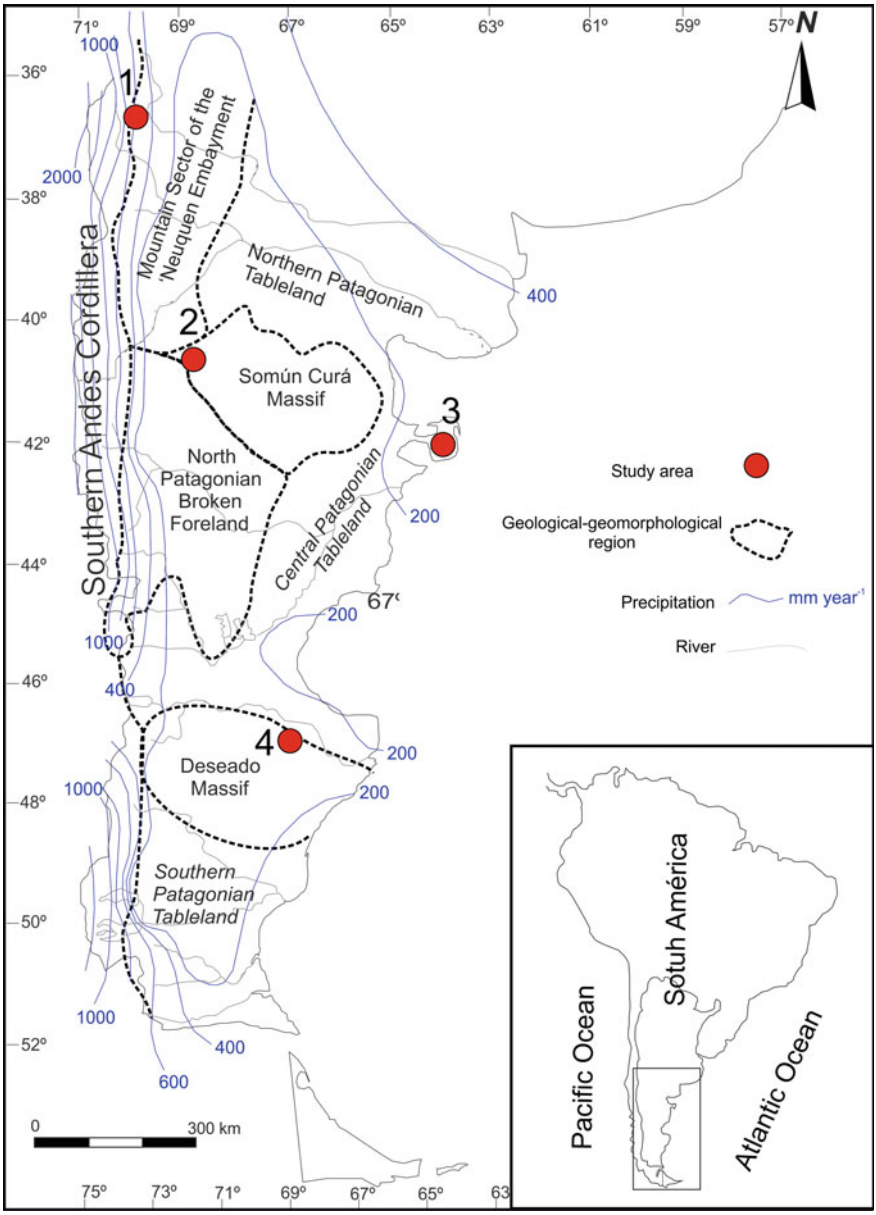

Fig. 1 Argentinean Patagonia map showing the regional annual rain distribution, the main geological-geomorphological units, and the location of the study sites. 1. Domuyo, 2. Península Valdés, 3. Carri Laufquen, 4. Deseado Massif

2 Wet Meadows in the Mountain Sector of the Neuquén Embayment. Domuyo Sector

The Mountain Sector of the Neuquén Embayment (Bracaccini 1970), includes two range systems with N-S orientation where the Domuyo volcano is located, which is the highest peak in Patagonia. The Domuyo Natural Protected Area is located in the north of Neuquén, Argentina (Fig. 2), and comprises an area dominated by Cenozoic volcanism (Brousse and Pesce 1982; Zanettini 2001; Miranda et al. 2006; Galetto et al. 2018). Within the Domuyo Natural Protected Area, the Domuyo Geothermal Field takes place, characterized by the presence of geothermal manifestations composed of aqueous solutions of high temperature, which result from ascending convective circulation of groundwater mainly of **meteoric origin**, through fissure systems and permeable layers (Panarello et al. 1992; Chiodini et al 2014; Tassi et al. 2016). This region presents mountainous relief with steep valleys carved by both glacial and fluvial processes (Zanettini 2001), where wet meadows formed related to small courses in the headwaters and lower basin sectors of streams crossing the area. The ones found in the headwaters of intermontane streams are associated with springs (Fig. 2a, b). Draining water infiltrates when it passes through the more permeable uncosolidated sediments, which are derived from mass removal processes. This, in turn, generates a shallow groundwater flow in the wet meadows area.

When both groundwater and surface water reach the slopes of the fluvial valleys, water cascades in the streams (Fig. 2b, c). The wet meadows located in the down basin of the intermontane streams are mostly developed on reliefs with gentle slopes, favouring a large areal extension over the fluvial plains (Fig. 2c, d). These originate when the gullies intercept the water table generating a groundwater discharge zone that drains in an indirect manner.

In the middle basin sector of the streams, a **geothermal water** area is developed (Fig. 2a). Geothermal waters have an average temperature of 66.5 °C with immature shallow water characteristics (according to Giggenbach 1986) and typically sodium chloride facies, with electrical conductivity (EC) values between 1485 and 9610 μS cm^{-1} and pH between 7.17 and 8.8. These geothermal waters present contrasting physicochemical characteristics with respect to the springs that support the wet meadows, mainly those located in the headwaters sector. The groundwater that sustains the wet meadows in the headwaters sector has calcium bicarbonate facies and has a mean temperature close to 11 °C, low EC with values between 21 and 118 μS cm^{-1} and neutral pH. Conversely, groundwater that sustains the down basin wet meadows is of sodium chloride type with temperature and EC considerably higher than those previously described, reaching an average temperature of 21 °C and an EC variation between 347 and 1741 μS cm^{-1}, although no significant differences are observed in relation to pH values.

The δ^2H versus δ^{18}O isotopic relationship shows that water of the *mallines* follows a trend similar to that of the local meteoric line established for the locality of San Rafael, Mendoza, located about 300 km from the study area (Hoke et al. 2013). For their part, the geothermal discharges deviate from the meteoric line with a clear trend

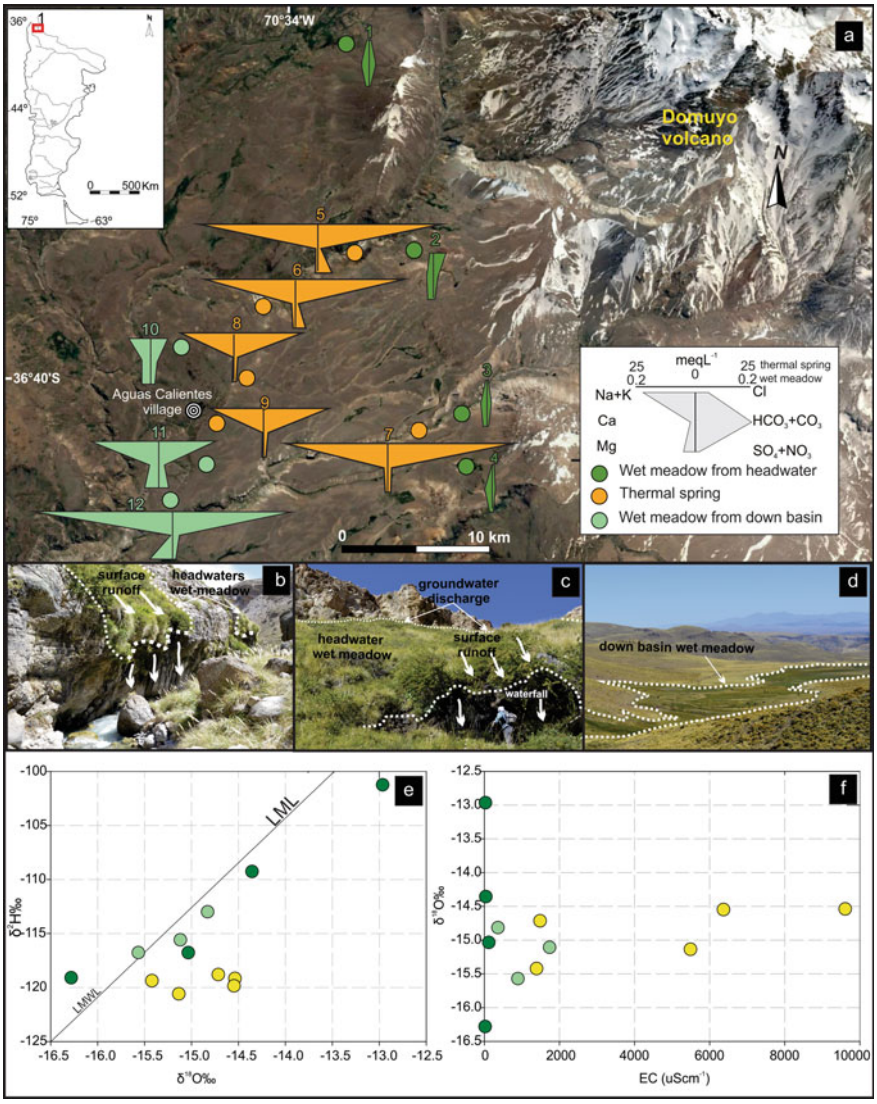

Fig. 2 Satellite image of the study area of the Domuyo sector with the sampling points and Stiff diagrams in each of them (**a**). Photographs of *mallines* of headwaters (**b**, **c**) and the lower basin (**d**). Bivariate diagrams of environmental isotopes (**e**) and in relation with electrical conductivity (**f**). LML: local meteoric line is $\delta^2H‰ = 29\ \delta^{18}O‰ + 11.75$ (Hoke et al. 2013)

towards an isotopic enrichment in $\delta^{18}O$ without recording considerable variations in $\delta^{2}H$ (Fig. 2e).

These isotopic signals show different processes within the study area, the NE and E sectors of the high summits constitute the hydrological recharge area where precipitations are composed mainly of snow, which is dominant during winter and accumulate forming mantles (Bran et al. 2002). During spring and summer, the snow-melting water partly runs off through the valleys of intermontane streams, while another part infiltrates the fractures and pores of rocks. This recharge due to rainwater seepage is evidenced in the isotopic content of all the samples from wet meadows which are located around the local meteoric line. On the other hand, thermal spring's water samples show enrichments in $\delta^{18}O$ compared to $\delta^{2}H$, a typical trend of geothermal environments (Clark 2015). Since this deviation occurs from the meteoric line (Fig. 2e) it is interpreted that geothermal water result from the interaction between meteoric waters that infiltrate and igneous bodies in cooling and/or magmatic set chambers, which supply heat as defined in previous studies that analyzed the origin of geothermal water (Panarello et al. 1992; Chiodini et al. 2014; Tassi et al. 2016).

A joint analysis of the geological-geomorphological, chemical and isotopic characteristics shows clear differences between the headwater and lower basin wet meadows (Villalba et al. 2020). Wet meadows from headwaters are associated with springs located near the areas of groundwater recharge. If analyzed at a regional scale, it can be seen that they are aligned along a NNW-SSE to N-S (Fig. 2a) due to a structural control given by a regional fault called Manchana Covunco Fault (Galetto et al. 2018). This structure gives rise to an abrupt topographic change that intercepts the water table, causing groundwater to discharge in form of springs which supports wet meadows located in the headwaters area of the streams. Isotopic signal, similar to the composition of meteoric water, indicates that these headwater areas are recharged by snowmelt, which also leaves its mark on water temperature with an average of 11 °C. The high slopes at headwaters and the short paths of the groundwater flow mean that the interaction of water with rocks and sediments is not sufficient for it to acquire an important quantity of salts (Tóth 1999), which would explain its low EC. Trends in the increase of the ionic content without isotopic enrichment are evidenced by the incorporation of salts product of dissolution or alteration of minerals in the rocks (Clark 2015). This dissolution would be mainly associated with carbonates and would be responsible for the presence of calcium bicarbonate type **chemical facies** that characterize these wet meadows. In wet meadows of down basin areas, the slopes are less steep and groundwater discharge is frequently close to river valleys in sectors of gullies that intercept the water table. The higher temperature, salinity, sodium chloride facies are similar to those of thermal springs, which probe that a geothermal influence is present in the water chemistry of these wet meadows (Villalba et al. 2020). This influence is also evidenced in the isotopic signal and in the relationship $\delta^{18}O$ versus EC (Fig. 2f). Although, wet meadows water still corresponds to freshwater as seen in the EC values measured, indicating that the influence of geothermal water is not that pronounced.

3 Wet Meadows in the Patagonian Tablelands. Península Valdés Sector

The regional geomorphology of the tableland landscape is a succession of old fluvial and **glacifluvial** terrace levels constituted by aggradational surfaces of sandy-gravel deposits (Fidalgo and Riggi 1970; Funes et al. 2017). These terrace levels are developed, in the Península Valdés, over marine Cenozoic sediments constituted by sandstones, coquinas, pelites, and tuffs (Haller et al. 2005). In sectors, these plains are interrupted by endorheic basins and discontinuously covered by aeolian deposits assigned to the Late Glacial/Holocene period (Trombotto 1998; Bouza et al. 2017). The Quaternary, which partially covers these geological units, is formed by colluvial, alluvial, aeolian, and lagoon deposits, the latter coming from small temporary and shallow depressions (pans).

In the southern sector of the Península Valdés, there are two endorheic basins, carved on these terraces, whose depressions reach values of −40 and −10 m a.s.l. In their lower sectors there are two salt ponds, Salina Grande and Salina Chica, and on the pediments of the endorheic basins at a topographic level close to the salt ponds wet meadows are found. To the south of the endorheic basins, covering the tablelands, is an eolian field with vegetation-stabilized dunes and active dunes (Fig. 3a). The *mallines* that develop on the southern flank of the endorheic basins (Figs. 3b, c, d) are the result of the intersection of the topography with the aquifer found in the Tertiary sediments (Alvarez et al. 2010, 2020).

Groundwater in the southern sector associated with the aeolian fields is of low salinity, with EC less than 2000 $\mu S\ cm^{-1}$ and pH between 7.3 and 8.3 and of sodium chloride bicarbonate to chloride sodium type. In contrast, groundwater in the tablelands without aeolian deposits above them, such as those found north of the Salinas Grande and Chica, are **brackish**, with EC greater than 20,000 $\mu S\ cm^{-1}$, neutral to slightly alkaline pH and sodium chloride to sodium chloride sulfate type (Fig. 3a). In turn, the **springs** that feed the *mallines* located on the southern slopes of the endorheic depressions have EC between 1500 and 2500 $\mu S\ cm^{-1}$ south of the Salina Grande salt pond and 4500 $\mu S\ cm^{-1}$ south of the Salina Chica salt pond and pH between 7.2 and 8.4, all of chloride sodium type.

The δ^2H versus $\delta^{18}O$ isotopic relationship shows that the water of the dune fields and the wet meadows follow a trend similar to that of the local meteoric line established for the locality of Puerto Madryn, Chubut, located about 100 km from the study area (Alvarez et al. 2020), indicating a local recharge from rainwater (Fig. 3e). When analyzing the relationship between $\delta^{18}O$ and EC, it is observed that while the water of the dunes maintains low conductivity values, the *mallines* show an increase in EC without isotopic variation with respect to the water of the dunes, which would indicate salt dissolution processes (Fig. 3f). For their part, groundwater from the salt ponds follows a trend similar to the local meteoric line but with an isotopic enrichment in both $\delta^{18}O$ and δ^2H, and in the case of the groundwater from the tablelands a deviation from the LML to lower values in δ^2H (Fig. 3e). In this case, in the salt ponds, the

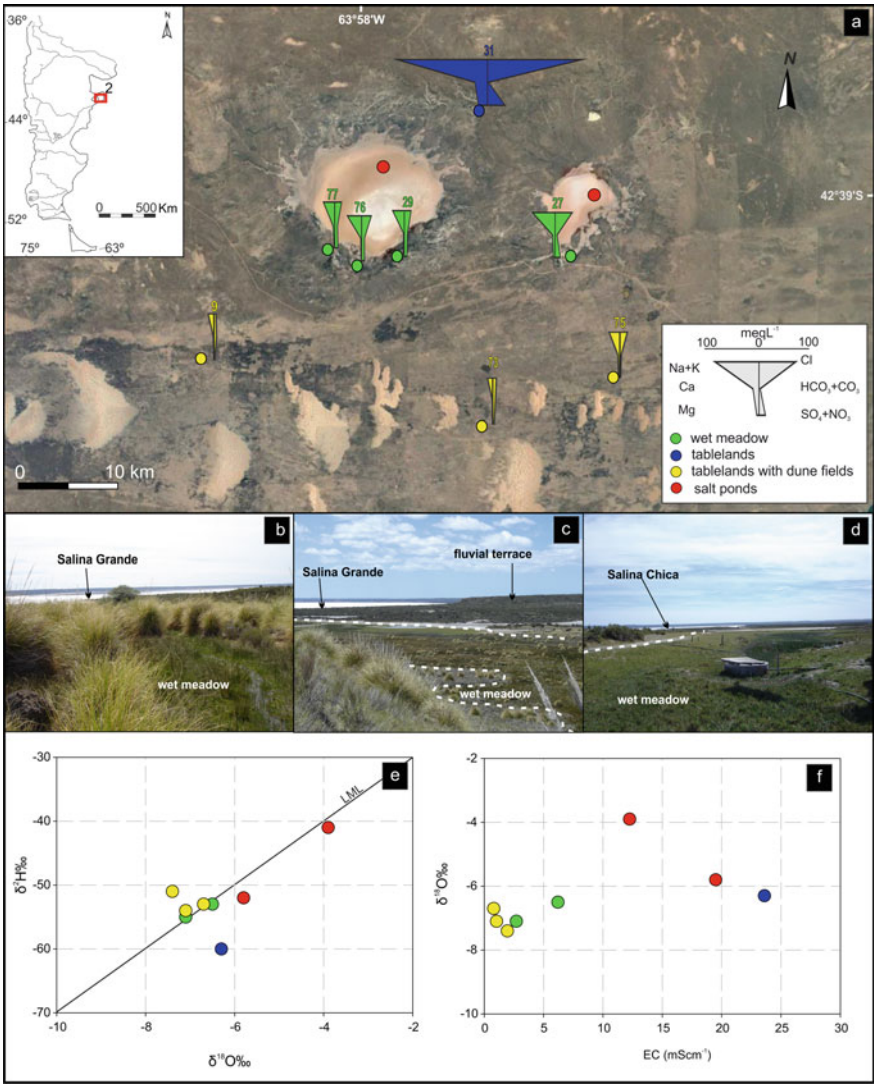

Fig. 3 Satellite image of the study area of the Península Valdés sector with the sampling points and Stiff diagrams in each of them (**a**). Photographs of *mallines* (**b**–**d**) Bivariate diagrams of environmental isotopes (**e**) and in relation with electrical conductivity (**f**). LML: local meteoric line is $\delta^2H‰ = 7.26\ \delta^{18}O‰ - 2.53$ (Alvarez et al. 2020)

isotopic enrichment is accompanied by an increase in EC, indicating both salt dissolution and evaporation (Fig. 3f). Finally, in the case of the tablelands it can be seen that although the $\delta^{18}O$ value of groundwater is similar to that of the aeolian deposits, the EC is much higher, which would indicate salt dissolution processes. These isotopic signals together with the variation in chemical facies show different processes within

the study area. The dune sector of the tablelands, with bicarbonate water type and low saline content, constitutes the hydrological recharge area where precipitations infiltrate and recharge the aquifer. From there, groundwater flows towards the discharge area that occurs in the endorheic basins. In its path, groundwater dissolves salts, but since the distance between recharge and discharge is short, it does not reach high saline contents and low EC water *mallines* develop. From these *mallines* the water drains towards the salt ponds where it continues dissolving salts and is concentrated by evaporation.

4 Wet Meadows Associated with the Somún Curá Massif. Carri Laufquen Sector

One of the most important features of the Somún Curá Massif is the presence of basaltic plains constituting the actual positive relief, so comprising a dominant plateau landscape. This plateau landscape is composed of mafic lava flows and smaller volumes of silicic volcanic rocks associated with large shield volcanoes of late Oligocene to Early Miocene age (Ardolino and Franchini 1993; Kay et al. 2007). Between these dominant features, other aggradational and erosional units developed as pediment association levels, fluvial terraces and alluvial fan levels (moderns and relicts), alluvial plains, wet meadows (*mallines*), and **endorheic basins** (Bouza and Bilmes 2020). Related to, these basaltic plateaus is a system of two endorheic basins that contain the Carri Laufquen Chica and Carri Laufquen Grande playa lakes (Fig. 4a).

On the slopes of the basaltic plateaus, bordering the lakes, there are *mallines* (Fig. 4b) that present spatial differences in the water type. The *mallines* on the slopes of the plateau, bordering the Carri Laufquen Chica lake, have calcium/magnesium bicarbonate water type with EC that vary between 469 and 529 $\mu S\ cm^{-1}$ and pH between 7.93 and 7.99. On the other hand, the springs that give rise to the *mallines* located on the northern margin of the Carri Laufquen Grande lake are sodium sulfate type with higher salinity (EC between 919 and 1051 $\mu S\ cm^{-1}$), with more variable pH values (between 7.83 and 8.32). In both cases, water presents an isotopic signal similar to that of the local meteoric line (Fig. 4f) noting that in the samples of the northern margin the increase in salinity occurs without significant variations in the isotopic content (Fig. 4g) characteristic that evidences mineral dissolution processes (Clark 2015). Plateau areas are recharge zones where water infiltrates rapidly thanks to the secondary permeability provided by the fracture system that igneous plateaus generally have (González et al. 1999; Hernández et al. 2009). Water infiltrating makes a short and rapid flow towards the slopes of the lakes, giving rise to the formation of *mallines* and/or springs. This type of groundwater, which sometimes is subsurface can be reach by the inhabitants, constituting a typical source of water supply in Patagonia (Hernández et al. 2007). The rapid infiltration of rainwater or water from snowmelt and the short interaction time between the water and the basaltic rock, where it could

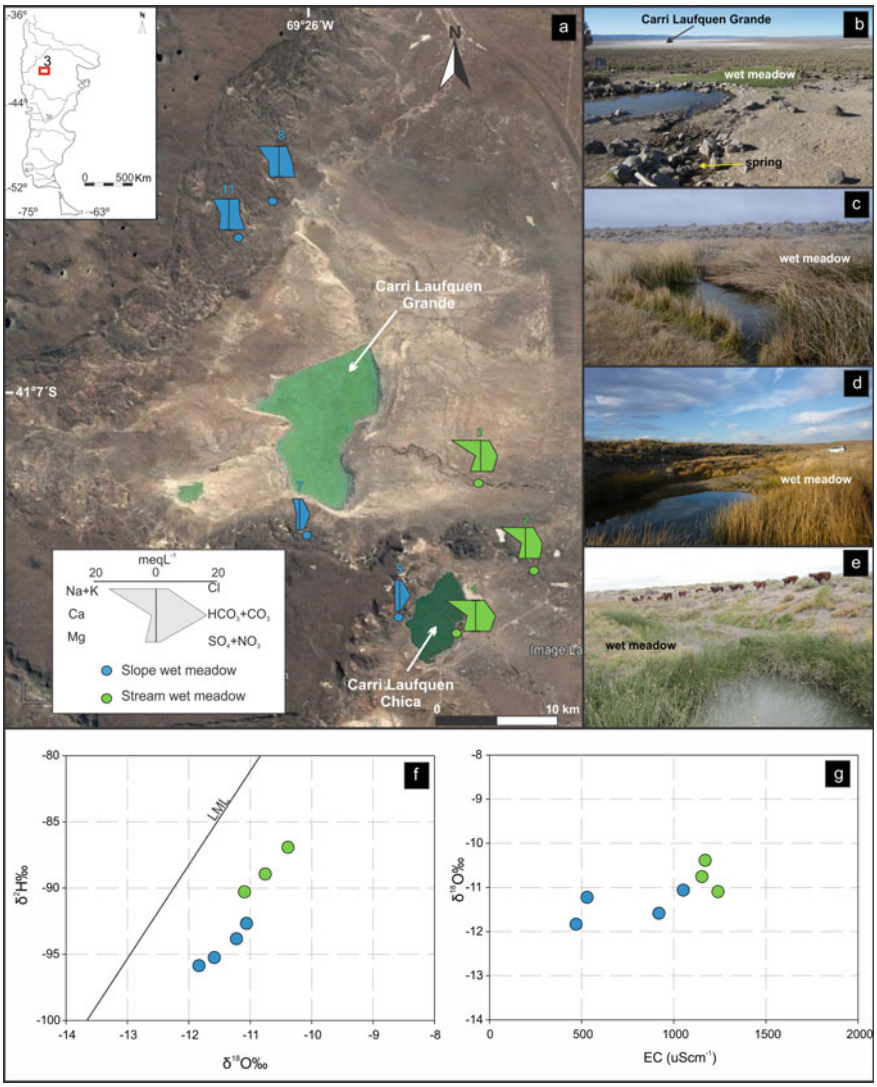

Fig. 4 Satellite image of the study area of the Carri Laufquen sector with the sampling points and Stiff diagrams in each of them (**a**) Photographs of *mallines* (**b**–**e**); Bivariate diagrams of environmental isotopes (**f**) and in relation with electrical conductivity (**g**) LML: local meteoric line is $\delta^2H‰ = 6.96\ \delta^{18}O‰ - 4.68$ (Dapeña and Panarello 2008)

acquire salts, give these waters characteristics of low salinity and calcic/magnesian bicarbonate (in the southern sector) and sodium sulfate (in the northern sector) facies, in all cases with EC below 1051 μS cm^{-1}. In the first ones, whose EC is lower, the dominant processes would be the alteration of basalts. In the case of the sodium sulfate water type, whose EC is slightly higher, they are found further away from

the edge of the plateau, being in contact with mass removal sediments and other sedimentary rocks. The alteration of minerals in these sediments and the presence of sulfate minerals typical of arid areas such as thenardite would add salts to the water, determining the presence of low-salinity sulfate facies (Pasquale Pérez et al. 2019).

In this area, *mallines* environments also develop in association with the Maquinchao stream (Fig. 4c–e), which is located between the Carri Laufquen Chica and Carri Laufquen Grande lakes. The water that sustains these *mallines* is sodium bicarbonate sulfate type with EC ranging between 1214 and 1580 $\mu S\ cm^{-1}$ and pH between 7.9 and 8.9. Isotopically presents a signal similar to that of the local rain showing a tendency to an increase in EC associated with the dissolution of sediment minerals (Figs. 4f, g). Hydrogeological studies conducted in the area (Pasquale Pérez et al. 2019), showed that the water in these sections of the streams has a strong dependence on groundwater inputs recognizing that there is a groundwater flow through them. In the Holocene sedimentary deposits associated with the stream *mallines*, local groundwater recharge occurs by infiltration of rainwater. Also, in these sediments, a groundwater circulation zone develops with a flow towards the Carri Laufquen Grande playa lake that also flows through the streams that intercept it. The water chemistry of the *mallines* associated with the Maquinchao stream and the nearby groundwater is very similar as a result of the fact that the stream is crossed by the groundwater flow (Pasquale Pérez et al. 2019). During its flow, groundwater dissolves minerals present in the sediment, mainly those of greater solubility.

5 Wet Meadows Associated with the Deseado Massif

The Deseado Massif is a geological province located in the southern edge of South America, characterized by its tectonic stability and its stable and sub-positive relief during the Paleozoic (Ramos 1999). The central area of the Deseado Massif where the *mallines* are described is characterized by the presence of basaltic plateaus laying on top of sedimentary rocks of subhorizontal stratification where steep areas of 150 m in altitude can be recognized, culminating in depressions forming small endorheic basins (Fig. 5). The basaltic plateau is composed of three levels of lava flows characterized by a vesicular texture and the presence of diaclases, which can be found filled with saline precipitates, mainly carbonates. Underlying the basalts are 30 m of medium to highly permeable sediments of psammitic granulometry. Below these are approximately 100 m of tuffaceous deposits in which thick paleosols and silicified levels develop, the latter of low to no permeability. The abrupt topographic change that occurs due to the escarpment causes the interception of the groundwater level, which is conditioned by the presence of impermeable formations giving rise to springs that support the wet meadows. The first level of springs is generated in contact with the paleosols and the second level of springs discharges at the base of the escarpment, where deposits of tuffs and reworked tuffs of low permeability outcrop. In some sectors the escarpment is free of debris, recognizing two zones of

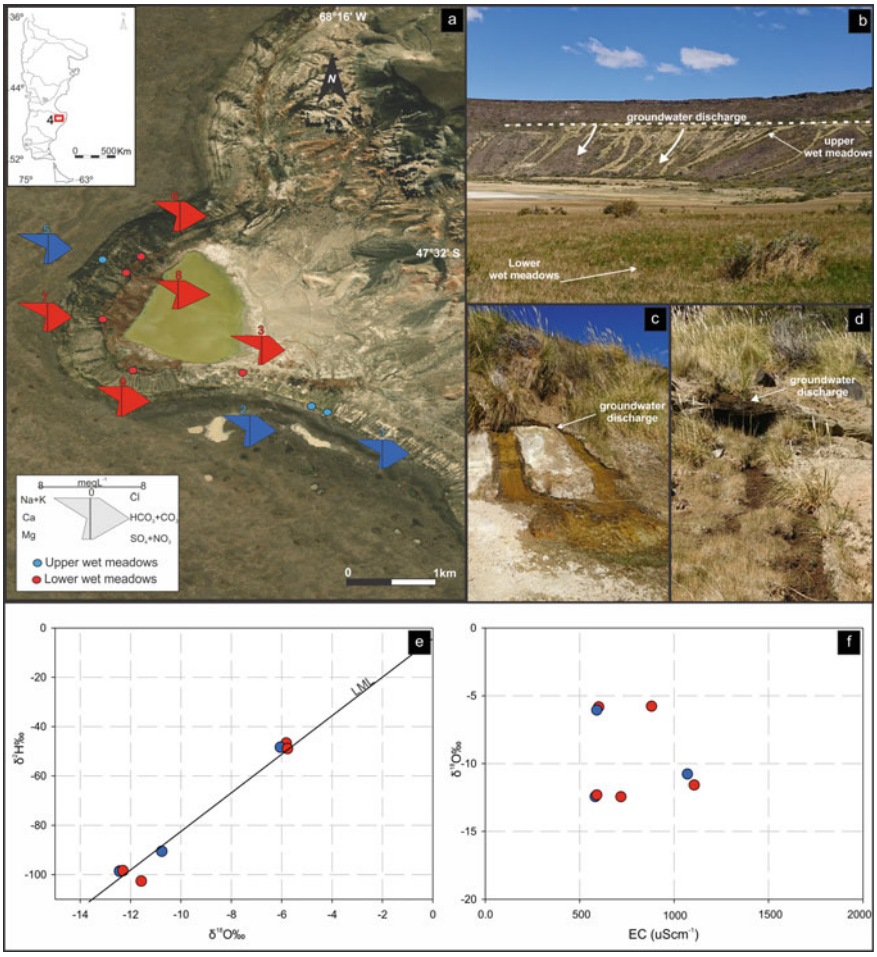

Fig. 5 Satellite image of the study area of the Deseado Massif sector with the sampling points and Stiff diagrams in each of them (**a**). Photographs of *mallines* (**b–d**). Bivariate diagrams of environmental isotopes (**e**) and in relation with electrical conductivity (**f**). LML: local meteoric line is $\delta^2H = 7.92\ \delta^{18}O + 1.22$ (Mayr et al. 2007)

groundwater discharge, one upper and one lower. While in other sectors the escarpment presents abundant mass removal deposits where, although it seems to maintain the two groundwater discharge sectors, the lower one is covered by these sediments. Groundwater discharge flows on the surface forming small streams that drain towards the depressed areas forming transitory lagoons (Figs. 5a–d). The spring water that sustains the wet meadows is sodium bicarbonate with EC less than 1000 μS cm^{-1}and an average pH of 8.7 (Fig. 5a). The $\delta^{18}O$ and δ^2H values in the upper and lower wet meadows samples are similar, being located in the δ^2H versus $\delta^{18}O$ plot close to

the local meteoric line (Fig. 5e). Although these samples have low EC, there is an increasing trend with no variation in the isotopic values (Fig. 5f).

The analysis of the geological and geomorphological characteristics along with the water chemistry highlights the processes and factors that regulate the hydrochemistry of the wet meadows. Water infiltrates through the basalts and is stored in the underlying sediments until, due to lithological controls often related to impermeable levels, it discharges on the slopes of the plateau forming springs. The upper wet meadows, associated with aquifers lodged in the sandy deposits underlying the basalts, discharge as a result of a permeability change caused by the clay levels. In these wet meadows, water is of low salinity and the incorporated ions derive from the interaction with the silicates (especially plagioclases) that compose the basalt (Melendi et al. 2020).

Since plagioclases are mainly calcic in these basalts (Panza 2001), it is expected that their incongruent hydrolysis generates calcic bicarbonate water (Appelo and Postma 2005). However, water in wet meadows is dominantly sodium bicarbonate, and this change is due to ion exchange processes where clayey sediments release Na^+ to water and adsorb Ca^{2+} ions (Melendi et al. 2020). In the lower wet meadows, water chemistry is similar, although there is a tendency for a slight increase in EC, which is associated with dissolution processes of evaporite salts precipitated in sediment pores and fractures (Melendi et al. 2020). Salt accumulation and efflorescent crusting in the **unsaturated zone** (Vengosh 2003; Cartwright et al. 2009; Scanlon et al. 2009), and fracture surfaces (Kamai et al. 2009; Weisbrod et al. 2000), are common in many arid zones. In addition, aqueous-soluble solutes present in aeolian dust constitute in arid areas with strong windy playa lakes, as in this case, an important input of salts that are dissolved by rainfall and incorporated into groundwater in recharge zones (Mahowald et al. 2003). The water of the lower wet meadows would add to the processes described above the dissolution of salts, although in low percentages, since its EC is also low.

6 Perspective and Future Work

Different geological and geomorphological settings were described as conditioning factors of the water flow and chemistry that sustain wet meadows, showing the variability of these wetland environments in Patagonia. Additionally, for similar geological settings, variations in water chemistry may occur depending on the rock type and structures through which groundwater flows. An example of this last characteristic are the differences observed between the *mallines* in basaltic plateaus of the Somún Curá Massif area and the Deseado Massif.

This shows that within Patagonia the *mallines* would present a great diversity due to the geological and geomorphological controls that determine the dynamics and chemistry of the water that sustains them. Given this diversity and the lack of hydrological studies of these wetland environments, especially with respect to groundwater, future lines of work will be oriented towards expanding hydrological

studies of wet meadows in different geological settings in Patagonia. Given the relevance of the ecosystem services that wet meadows provide to local inhabitants, such as drinking water supply, livestock, and native fauna feeding, these studies will be of vital importance for the development of rural populations in Patagonia, mainly in the Extra-Andean sector where arid conditions are marked and there is a scarcity of freshwater suitable for human consumption.

Acknowledgements This study was funded by the Consejo Nacional de Investigaciones Científicas y Técnicas (National Council for Scientific and Technological Research) by means of their grants P-UE CONICET No. 22920160100044, PUE 22920160100083CO and PIP No. 11220200102386CO by the Swiss National Science Foundation (SNF 200021_155927) and by the Universidad Nacional de la Patagonia (National University Patagonia: PIP No. 800 201702 00037 UP).

References

Alvarez MP, Funes DS, Dapeña C, Bouza PJ (2020) Origin and hydrochemical characteristics of groundwater in the Northeastern Patagonia, Argentina: the relationship with geomorphology and soils. Environ Earth Sci 79(22):1–14

Alvarez MP, Weiler N, Hernández MA (2010) Linking geomorphology and hydrodynamics: a case study from Peninsula Valdes, Patagonia Argentina. Hydrogeol J 18:473–486

Appelo C, Postma D (2005) Geochemistry, groundwater and pollution. AA Balkema, The Netherlands

Ardolino AA, Franchini M (1993) El vulcanismo cenozoico de la Meseta de Somuncurá, Provincias de Río Negro y Chubut. XII Congreso Geológico Argentino, Mendoza, Actas IV, pp 225–235

Barros V, Scian B, Mattio H (1979) Mapas de precipitación de la Provincia de Chubut. CENPAT. Recursos Hídricos de Chubut, Rawson (in Spanish)

Bouza PJ, Bilmes A (2020) Landscapes and geology of Patagonia: an introduction to the land of reptiles. In: Morando M, Avila LJ (eds) Lizards of Patagonia Springer. Springer, Switzerland, pp 59–83

Bouza PJ, Bilmes A, del Valle HF, Rostagno CM (2017) Late Cenozoic landforms and landscape evolution of Península Valdés. In: Bouza PJ, Bilmes A (eds) Late Cenozoic of Península Valdés, Patagonia, Argentina. Springer Earth System Sciences, Heidelberg, pp 105–129

Bracaccini IO (1970) Rasgos tectónicos de las acumulaciones mesozoicas en las provincias de Mendoza y Neuquén, República Argentina. RAGA 25(2):275–284

Bran D, Ayesa J, López C (2002) Áreas ecológicas de Neuquén. Informe Laboratorio de Teledetección-SIG No 4-INTA-EEA. San Carlos de Bariloche (in Spanish)

Brinson MM, Malvárez AI (2002) Temperate freshwater wetlands: types, status, and threats. Environ Conserv 29(2):115–133

Brousse R, Pesce AH (1982) Cerro Domo: Un volcán Cuartario con posibilidades geotérmicas. Provincia del Neuquén. In: Proceedings, 5th Congreso Latinoamericano de Geología. Buenos Aires. Servicio Geológico Nacional, Subsecretaría de Minería, vol 4, pp 197–208 (in Spanish)

Canevari P, Blanco DE, Bucher EH, Castro G, Davidson I (1999) Los humedales de la Argentina. Clasificación, situación actual, conservación y legislación. Wetlands Int Publ 46

Cartwright I, Hall S, Tweed S, Leblanc M (2009) Geochemical and isotopic constraints on the interaction between saline lakes and groundwater in southeast Australia. Hydrogeol J 17:1991–2004

Chiodini G, Liccioli C, Vaselli O, Calabrese S, Tassi F, Caliro S, D'alessandro W (2014) The Domuyo volcanic system: an enormous geothermal resource in Argentine Patagonia. J Volcanol Geotherm Res 274:71–77

Clark I (2015) Groundwater geochemistry and isotopes. CRC Press

Coronato AM, Coronato F, Mazzoni E, Vázquez M (2008) The physical geography of Patagonia and Tierra del Fuego. Dev Quat Sci 11:13–55

Dapeña C, Panarello HO (2008) Isotope composition of precipitation in Bariloche city, Río Negro. Argentina. In: VI South American symposium on isotope geology, San Carlos de Bariloche, Río Negro, Argentina

Epele LB, Manzo LM, Grech MG, Macchi P, Claverie AÑ, Lagomarsino L, Miserendino ML (2018) Disentangling natural and anthropogenic influences on Patagonian pond water quality. Sci Total Environ 613:866–876

Fidalgo F, Riggi JC (1970) Consideraciones geomórficas y sedimentológicas sobre los Rodados Patagónicos. RAGA 25:430–443 (in Spanish)

Funes DS, García M, Bucher J, Lopez M, Bilmes A, Delía L, Franzese J, Bouza P (2017) Análisis de la evolución geomorfológica del NE de Chubut: nuevos aportes pedogenéticos al estudio de los abanicos aluviales de la Formación Eizaguirre. XX Congreso Geológico Argentino, Tucumán, Argentina (in Spanish)

Galetto A, García V, Caselli A (2018) Structural controls of the Domuyo geothermal field, Southern Andes (36 38′ S), Argentina. J Struct Geol 114:76–94

Garreaud R, Lopez P, Minvielle M, Rojas M (2013) Large-scale control on the Patagonian climate. J Clim 26(1):215–230

Giggenbach WF (1986). Graphical techniques for the evaluation of water/rock equilibration conditions by use of Na, K, Mg and Ca contents of discharge waters. In: Proceedings of 8th New Zealand geothermal workshop, pp 37–44

González P, Coluccia A, Franchi M (1999) Geología y Recursos Minerales de la Hoja 4169-III 'Ingeniero Jacobacci' (Provincia de Río Negro). Escala: 1:250.000. Servicio Geológico Minero Argentino. Boletín N8 311. Buenos Aires (in Spanish)

Haller MJ, Meister C, Monti AJ, Weiler N (2005) Hoja Geológica 4366-II, Puerto Madryn, provincia de Chubut. Dirección Nacional del Servicio Geológico. Buenos Aires (in Spanish)

Hernández M, Gonzalez N, Hernandez L (2009) Regiones Áridas. Procesos diferenciales de recarga y casos ejemplo de Argentina. In: Carrica J, Hernandez M, Mariño E (eds) Recarga de Acuíferos. Aspectos generales y particularidades en regiones áridas. La Plata: Edulp (in Spanish), pp 345–350

Hernández M, Hernandez L, Gonzalez N (2007) Ocurrencia de manantiales poligénicos en Patagonia extra-andina austral. Sector central de la Provincia de Santa Cruz, Argentina. Actas del V Congreso Argentino de Hidrogeología. Paraná. Entre Ríos (in Spanish), pp 285–391

Hoke GD, Aranibar JN, Viale M, Araneo DC, Llano C (2013) Seasonal moisture sources and the isotopic composition of precipitation, rivers, and carbonates across the Andes at 32.5–35.5 S. Geochem Geophys Geosyst 14(4):962–997

Insel N, Poulsen CJ, Ehlers TA (2010) Influence of the Andes Mountains on South American moisture transport, convection, and precipitation. Clim Dyn 35(7–8):1477–1492

Kamai T, Weisbrod N, Dragila MI (2009) Impact of ambient temperature on evaporation from surface-exposed fractures. Water Resour Res 45:W02417

Kay SM, Ardolino AA, Gorring ML (2007) The Somuncura large igneous province in Patagonia: interaction of a transient mantle thermal anomaly with a subducting slab. J Petrol 48(1):43–77

Mahowald NM, Bryant RG, del Corral J, Steinberger L (2003) Ephemeral lakes and desert dust sources. Geophysical Res Lett 30(2):1074

Mayr C, Lücke A, Stichler W, Trimborn P, Ercolano B, Oliva G, Ohlendorf C, Soto J, Feye M, Haberzettl S, Janssen S, Schäbitz F, Schlesera G, Wille M, Zolitschka B (2007) Precipitation origin and evaporation of lakes in semi-arid Patagonia (Argentina) inferred from stable isotopes (δ18O, δ2H). J Hydrology 334(1–2):53–63

Melendi E, Tanjal C, Borzi G, Raigemborn M, Carol E (2020) Hydrodynamic and hydrochemistry of wet meadows and shallow lakes in areas of the patagonian basaltic plateaus, Argentina. Sci Total Environ, 744140897

Miranda F, Folguera A, Leal PR, Naranjo JA, Pesce A (2006) Upper Pliocene to lower Pleistocene volcanic complexes and upper Neogene deformation in the south-central Andes (36°30′–38° S). Spec Papers Geol Soc Am 407:287

Panarello H, Sierra JL, Pedro G, D'Amore F (1992) Isotopic and geochemical study of the Domuyo Geothermal field, Neuquén, Argentina (No. IAEA-TECDOC-641)

Panza JL, Genini A, Franchi M (2001) Hoja Geológica 44769-IV, Monumento Natural Bosques Petrificados. Provincia de Santa Cruz. Instituto de Geología y Recursos Minerales, Servicio Geológico Minero Argentino, Buenos Aires (in Spanish)

Pasquale Pérez MP, Carol E, Álvarez M, Eymard I, Bilmes A, Ariztegui D (2019) Hidroquimica del agua superficial y subterránea de los alrededores de las lagunas Carri Laufquen. Actas de la V Reunión Argentina de Geoquímica de la Superficie 290–293

Ramos V (1999) Las provincias geológicas del territorio argentino. In: Segemar (ed) Geología Argentina. Instituto de Geología y Recursos Minerales (in Spanish), Buenos Aires, pp 41–396

Ruiz Leal A (1972) Los confines boreal y austral de las provincias Patagónica y Central respectivamente. Bol Soc Argent Bot 13:89–118 (in Spanish)

Scanlon BR, Stonestrom DA, Reedy RC, Leaney FW, Gates J, Cresswell RG (2009) Inventories and mobilization of unsaturated zone sulfate, fluoride, and chloride relatedto land use change in semiarid regions, southwestern United States and Australia. Water Resour Res 45:W00A1

Tassi F, Liccioli C, Agusto M, Chiodini G, Vaselli O, Calabrese S, Caselli A (2016) The hydrothermal system of the Domuyo volcanic complex (Argentina): a conceptual model based on new geochemical and isotopic evidences. J Volcanol Geotherm Res 328:198–209

Tóth J (1999) Groundwater as a geologic agent: an overview of the causes, processes, and manifestations. Hydrogeol J 7(1):1–14

Trombotto D (1998) Paleo-permafrost in Patagonia. Bamberger Geographische Schriften Abreviado 15:133–214

Vengosh A (2003) Salinization and saline environments. Treatise Geochem 9:612

Villalba E, Tanjal C, Borzi G, Páez G, Carol E (2020) Geogenic arsenic contamination of wet-meadows associated with a geothermal system in an arid region and its relevance for drinking water. Sci Total Environ 137571

Weisbrod N, Nativh R, Adar KM, Ronend D (2000) Salt accumulation and flushing in unsaturated fractures in an arid environment. Ground Water 38(3):452–461

Wilhelm de Moesbach E (1980). Diccionario Español de Mapuche. Siringa Libros (in Spanish), Neuquén

Zanettini JC (2001) Hoja Geológica 3772-II Las Ovejas, Provincia del Neuquén. Servicio Geológico Minero Argentino, Instituto de Geología y Recursos Minerales (in Spanish)

The Main Hydrological Features of Patagonia's Santa Cruz River: An Updated Assessment

Andrea I. Pasquini, Nicolás J. Cosentino, and Pedro J. Depetris

Abstract Patagonia's Santa Cruz River exhibits the second largest discharge in the region (i.e. ~23 km^3 y^{-1}) and an outstanding runoff (i.e. ~1500 mm y^{-1}). Several glaciers with accumulation zones in the Southern Patagonia Ice field calve into two large proglacial lakes, Argentino (~1400 km^2) and Viedma (~1100 km^2), which are the main Santa Cruz River water sources. Trend analyses of the 1955–2020 discharge series have shown a previously undetected positive trend, possibly established during the last decade. The months with significantly increased discharge (i.e. August–December) suggest that the augmented water volume is supplied by snow/ice melt determined by the current global climate change. Harmonic analysis led to discard the previously suggested connection with the Southern Annular Mode, but reinforced the earlier evidence of an operating remote connection with El Niño Southern Oscillation, which possibly influences river discharge by promoting the ice-dam rupture mechanism which periodically operates in the Perito Moreno glacier.

Keywords Discharge series · Trend analysis · Harmonic analysis · ENSO · SAM · Perito Moreno glacier · Lake Argentino

A. I. Pasquini (✉)
Escuela de Geología, Facultad de Ciencias Exactas, Físicas y Naturales, Universidad Nacional de Córdoba, Córdoba, Argentina
e-mail: apasquini@unc.edu.ar

Centro de Investigaciones en Ciencias de la Tierra, Consejo Nacional de Investigaciones Científicas y Técnicas and Universidad Nacional de Córdoba, Córdoba, Argentina

N. J. Cosentino
Instituto de Geografía, Facultad de Historia, Geografía y Ciencia Política, Pontificia Universidad Católica de Chile, Santiago, Chile

Núcleo Milenio Paleoclima, Santiago, Chile

P. J. Depetris
Academia Nacional de Ciencias, Córdoba, Argentina

A. I. Torres and V. A. Campodonico (eds.), *Environmental Assessment of Patagonia's Water Resources*, Environmental Earth Sciences,
https://doi.org/10.1007/978-3-030-89676-8_9

1 Introduction

Abundant water supplied by glaciers, **proglacial-glacial lakes**, and plentiful atmospheric precipitations in the upper catchments, turns the Santa Cruz into one of Patagonia's main high-runoff rivers. The **headwaters**, directly connected with the Southern Patagonia Ice field (SPI) through several glaciers, constitute a clear manifestation of Nature's wonder. Since the beginning of the twentieth century, the unusual characteristics of the Perito Moreno glacier, which calves into Lake Argentino (i.e. one of Santa Cruz River's main water sources), have been a major focus of attention. Moreover, the Santa Cruz is one of the world's few rivers flowing south of 36° S and, hence, probing into its hydrology supplies valuable climatic information on that particular part of the globe.

The ongoing climate crisis has triggered scientific interest, seeking to identify hydrological changes connected with all the intervening features (e.g. glaciers' dynamics, climate change, discharge time series evolution). Some years ago, the hydrological behavior of the Santa Cruz River was examined, inferring through its discharge variability the occasional quasi harmonic periodicity of the Perito Moreno glacier's closure-rupture sequence (Depetris and Pasquini 2000; Pasquini and Depetris 2011). The analysis showed that the discernible sequence suggested a coherent teleconnection between discharge deviations from the monthly means, with the **El Niño Southern Oscillation** (ENSO) phenomena in the Pacific and, possibly, with the location of the Pacific anticyclone. Moreover, it was also documented that several other Patagonian lakes located north of 50° S showed an ENSO signature in their seasonally adjusted or deseasonalized[1] water level fluctuations (Pasquini et al. 2008).

The purpose of this chapter is to revisit the main hydrological features of Patagonia's Santa Cruz River, updating previous data and findings, particularly probing into low frequency processes.

2 Geographical Features

Patagonia lies between the semi-permanent subtropical high pressure and subpolar low pressure zones. Surface air moving towards the pole from the subtropical high zone results in strong westerly winds which, in the south shift poleward in summer and equatorward in winter. The drainage basin of the eastward-flowing Colorado River (~38° S) defines a transition zone between the subtropical summer rain regime (in the north) and the mid-latitude winter rain regime that dominates in Patagonia (Mancini et al. 2005). The main characteristics of the Holocene climate for such region were described by Mancini (1998, 2002). Glaciers, which are reliable long-term indicators of climate change, generally show a significant recession in Patagonia, which has commonly been associated with the combined effect of decreasing precipitation

[1] i.e. stripping data time series of its seasonality.

and increasing temperatures (Masiokas et al. 2008; Pabón-Caicedo et al. 2020 and references therein).

The SPI (i.e. 49° to 51° S) occupies 12,200 km^2 along the Chile-Argentina Andean border and has about 139 outlet glaciers that calve into fjords in the Pacific side, and into lakes on the eastern side of the Andes (Masiokas 2020). Several glaciers calve in the Argentino and Viedma lakes, both in the **headwaters** of the Santa Cruz River basin (Fig. 1a): e.g. Perito Moreno, Viedma, Ameghino, Uppsala, Mayo, and Onelli. Although it is not the largest, the Perito Moreno owes its notoriety to the damming-rupture sequence which, with uneven regularity, exhibits its terminus. It clearly is a major feature in the Santa Cruz River drainage basin. According to several authors (e.g. Stuefer et al. 2007, and references therein), the Perito Moreno glacier (Fig. 1b, c) is about 30 km-long, reaches a width of about 4 km in the valley, covers an area of 259 km^2, and extends from the continental divide (Pietrobelli peak, ~2950 m a.s.l.) down to Lake Argentino (~187 m a.s.l.). The snout ends in calving cliffs with heights of 50–80 m (Rott et al. 1998).

The climate in the Andean **headwaters** is cold and humid, subjected to strong westerlies which supply abundant Pacific humidity. At Lake Argentino location the mean temperature in (austral) summer is 12.7 °C (i.e. in January) and 1.2 °C in July. The lake modulates the temperatures (i.e. recorded maximum and minimum ambient

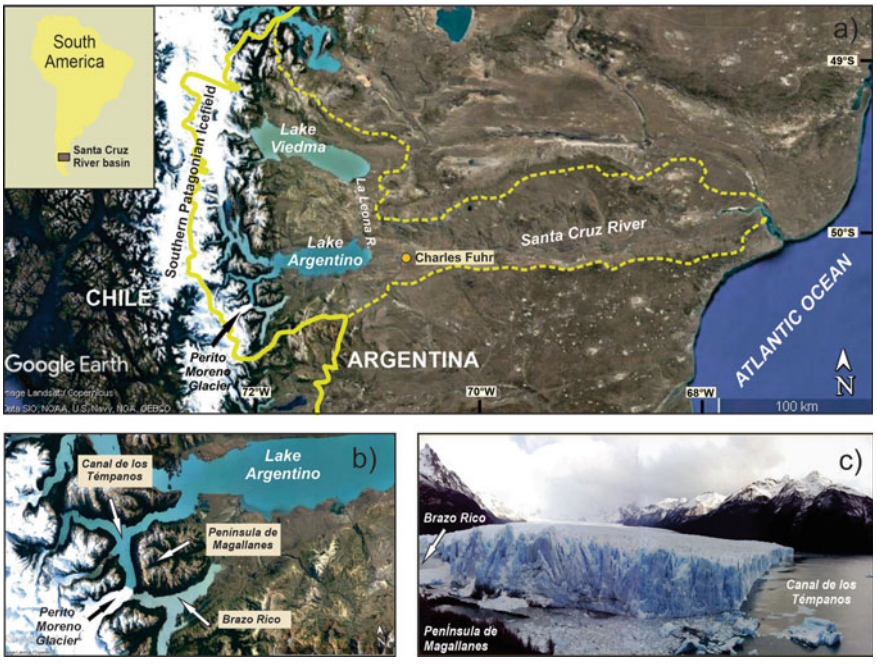

Fig. 1 The Santa Cruz River drainage basin. **a** Image of the Santa Cruz River drainage basin; **b** Amplified image depicting the location of the Perito Moreno Glacier and Lake Argentino; **c** Photograph of the Perito Moreno glacier terminus

temperatures are ~28.5 °C, −10 °C, respectively). In the mountainous region—but outside the SPI—, atmospheric precipitations fluctuate in the 900–2000 mm y^{-1}, whereas they reach 500 mm in the pre-Andean territory. Less than 100 km east of the Andes and governed by a pronounced rain-shadow, precipitations decrease to 200 mm y^{-1}. The average specific annual net accumulation of the Perito Moreno glacier (i.e. over the SPI) was established in 5540 ± 500 mm water equivalent, which is deemed one of the highest accumulations worldwide. Considering that part of the precipitation is surely lost as runoff, the average annual precipitation could be of the order of 7000–8000 mm (Rott et al. 1998).

Unlike the Perito Moreno which, up to now, seems in a stable situation (e.g. Minowa et al. 2015), the Viedma (i.e. 70 km-long, and a surface area of ~1100 km^2) is a retreating glacier, like the Ameghino, Uppsala, and all the other main glaciers in the area.

Lake Argentino (Fig. 1) is a prominent attribute in the Santa Cruz River hydrologic system (i.e. ~50° S 73° W, 187 m a.s.l.). The ultra-oligotrophic lake is among the largest lakes in Patagonia and it is, as well, the southernmost lake of the extended chain of Patagonian glacial/**proglacial lakes** (i.e. the geomorphologic result of 26 glacial-interglacial cycles that occurred during the Quaternary (Pasquini et al. 2008 and references therein), bordering the austral Andes along the eastern seaboard. It has a mean depth of 150 m although it reaches about 500 m in certain areas. Its surface area is close to 1400 km^2 and its volume has been estimated in about 220 hm^3. Fed by several streams and rivers (e.g. La Leona, Centinela, Mitre), the lake's drainage basin is ~17,000 km^2. The Santa Cruz River is the only exit of Lake Argentino, after receiving the discharge of La Leona River, the outlet of Lake Viedma (1100 km^2), which in this manner is connected with the Argentino (Fig. 1a). In an earlier contribution, it was shown that deseasonalized discharge anomalies of La Leona and Santa Cruz rivers, are not significantly correlated (Depetris and Pasquini 2000). Other smaller lakes, included in the drainage basin, are Burmeister, Quiroga, and del Desierto.

The Santa Cruz River[2] (Fig. 2) is the lowermost member of the SPI-Lake Argentino-Lake Viedma-Santa Cruz River hydrological network[3] (Fig. 1a). It is 385 km long, crosses eastward the Patagonian plateau, and delivers its noteworthy mean discharge (i.e. mean of 727 $m^3\ s^{-1}$ for the period 1956–2020 at the Charles Fuhr gauging station)[4] into a 2 km-wide estuary (i.e. shared with Chico River), in the SW Atlantic Ocean. According to Argentina's *Subsecretaría de Recursos Hídricos*, its drainage basin has a surface area of ~29,686 km^2; its mean water-surface slope is about 0.48 m km^{-1}; the mean maximum water discharge (~1200 $m^3\ s^{-1}$) occurs in March and the mean minimum flow (~300 $m^3\ s^{-1}$) in September. Its mean annual water yield is about 46.8 L $s^{-1}\ km^{-2}$ of deep-blue water, whereas its mean total suspended sediment concentration is about 23 mg L^{-1} (i.e. roughly fluctuating between ~ 10 and ~ 35 mg L^{-1}). Finally, its mean total dissolved solids

[2] http://www.hidricosargentina.gov.ar/Indice-argentino.html.

[3] 48°56′–50°50′ S, and 68°33′–73°35′ W.

[4] The drainage basin upstream Charles Fuhr is 15,550 km^2, and runoff is 1474 mm y^{-1}.

Fig. 2 Photograph of the Santa Cruz River, downstream from the Lake Argentino inflow. In the background, facing west, the Andes Cordillera

concentration is about 100 mg L^{-1} (i.e. near the mouth, oscillating between ~75 and ~140 mg L^{-1}) (Depetris et al. 2005).

2.1 ENSO and SAM

Several workers have researched into the significance of ENSO and/or Southern Annular Mode (SAM) in the southern latitudes, in general, or particularly in Patagonia (e.g. Jones and Widmann 2003; Fitzharris et al. 2007; Kastner et al. 2010; Ohlendorf et al. 2013; Masiokas et al. 2019). The broad characteristics of each event-type and, what appears to be, their mutual relationship are herein briefly reviewed.

There are changes in the Pacific Ocean and its overlying atmosphere that occur in an oceanic-atmospheric cycle known as the ENSO. This periodic event is the Earth's most important source of interannual climate variability, exerting deep worldwide effects. It refers to variations in the temperature of the surface of the tropical eastern Pacific Ocean (i.e. El Niño and La Niña) and in air surface pressure in the tropical western Pacific. The two variations are coupled: the warm oceanic phase (i.e. El Niño) goes together with high air surface pressure in the western Pacific, whereas the cold phase (i.e. La Niña) accompanies low air surface pressure in the western Pacific. (e.g. Philander 1990). ENSO references are numerous (e.g. McPhaden et al. 2020 and references therein).

The SAM or Antarctic Oscillation (AAO) is a high-frequency mode of atmospheric variability of the southern hemisphere. In contrast with ENSO, which owes its existence to coupled ocean/atmosphere interactions in the tropical Pacific, the annular modes are controlled by internal atmospheric dynamics in the middle latitudes. SAM may be defined as the normalized difference in the zonal mean sea-level

pressure between 40° S and 65° S. The sea level pressure pattern associated with SAM is a nearly annular pattern with a large low pressure anomaly centered on the South Pole and a ring of high pressure anomalies at mid-latitudes. In a positive SAM event the belt of strong westerly winds contracts towards Antarctica; this results in a significant cooling over Antarctica and much of Australia, and a significant warming over the Antarctic Peninsula, Argentina, Tasmania and the South of New Zealand. Due to the southward shift of the storm track, the positive phase of AAO is also associated with anomalously dry conditions over southern South America, New Zealand and Tasmania. Anomalously wet conditions occur over much of Australia and South Africa (Gillett et al. 2006). In contrast, a negative SAM event reflects an expansion of the belt of strong westerly winds towards the equator (e.g. Gillet et al. 2006; Silvestri and Vera 2009).

It has been argued that ENSO and AAO appear to have some degree of correlation which may eventually complicate the possibility of distinguishing the effect of each mechanism (Bertler et al. 2006). Climate research in southern latitudes (e.g. Fogt and Bromwich 2006) supplied valuable information to understand the ENSO/SAM connection. Fogt et al. (2011a, b) established that ENSO impact in the South Pacific is strongly dependent on the SAM phase: significant South Pacific teleconnections are recognized when ENSO events occur with a weak SAM or when El Niño (La Niña) occurs with a negative (positive) SAM phase. A direct linkage was found between this modulation in the South Pacific ENSO teleconnection and the interaction of the anomalous ENSO and AAO transient eddy momentum fluxes. During El Niño/SAM(−) and La Niña/SAM(+) combinations, the anomalous transient momentum fluxes in the Pacific operate to strengthen the circulation anomalies in middle latitudes, altering the circulation in such a way so as to maintain the ENSO teleconnections. In El Niño/SAM(+) and La Niña/SAM(−) cases, the anomalous transient eddies oppose each other at mid latitudes and reduce the magnitude of the high latitude ENSO teleconnection (Fogt et al. 2011a, b).

3 Data and Methods

The Santa Cruz River discharge time series (record period 1955–2020) at Charles Fuhr gauging station (Fig. 1a) and Brazo Rico gauge height time series (record period 1992–2020) were obtained from the web page of Argentina's *Subsecretaría de Recursos Hídricos*.[5] Data series were deseasonalized ($[x_d]$) by subtracting each monthly mean ($[x_i]$) from the overall mean for that specific month $[x_n]$: $[x_d] = [x_i] - [x_n]$.

Data time series of the Southern Annular Mode, AAO, or Southern Hemisphere Annular Mode (SHAM) was downloaded from http://www.jisao.washington.edu/aao/#data. Similarly, ENSO's Multivariate Index (**MEI, v. 1**) was obtained from

[5] http://www.hidricosargentina.gov.ar/sistema_sistema.php.

the corresponding National Oceanic and Atmospheric Administration (NOAA) web page.[6]

The significance of river discharge monthly trends was assessed with the **seasonal Kendall test** (Hirsch et al. 1982). The seasonal Kendall test has been accepted as one of the most robust techniques available to disclose and estimate linear trends in environmental data (Hess et al. 2001). Like the Mann–Kendall test (Mann 1945; Kendall 1975), it is a non-parametric tool that detects monotone trends in time series (e.g. Burn and Hag Elnur 2002; Yue et al. 2002).

Natural periodicities of multi-decadal climatological and river discharge time series were assessed by auto spectral analysis, while possible governing factors of river discharge were analyzed through cross-spectral analysis. To improve the spectrum's signal-to-noise ratio, the Blackman-Tukey method was employed, based on dividing the time series into eight segments with 50% overlap (Blackman and Tukey 1958; Welch 1967). Preceding spectral analysis, all-time series were detrended based on a least-squares linear fit to the data. The specialized literature offers numerous contributions on the theoretical aspects of Fourier harmonic analysis, and examples of their use to examine the structure underlying time-series (e.g. Cosentino et al. 2020; Labat 2005; Lau and Weng 1995; Torrence and Compo 1998).

4 River Discharge Dynamics

4.1 Mean Hydrograph and Discharge Time Series

The Santa Cruz River reaches maximum mean discharge in March (i.e. over 1300 $m^3\ s^{-1}$), which results of atmospheric precipitations and snow/ice-melt. The largest lakes in the basin (i.e. Argentino and Viedma) probably have a modulating effect, delaying peak discharges. Lowest mean discharges occur in September–October, exceeding 300 $m^3\ s^{-1}$ (Fig. 3).

The Santa Cruz River currently discharges 22.9 $km^3\ y^{-1}$ (i.e. mean discharge 727 $m^3\ s^{-1}$) into the SW Atlantic Ocean. The available discharge time series (1955–2020), at the Charles Fuhr gauging station, shows a remarkable seasonality (Fig. 4a). Some departures from the regular pattern are mostly determined by the floods occurring as a consequence of the sporadic rupture of the ice dam, which the Perito Moreno's terminus produces with some regularity.

The uppermost drainage basin lies **upstream** the Charles Fuhr gauging station. It includes ~52% of the total drainage basin area (i.e. the active basin). There are no significant tributaries **downstream** the gauging station. The specific discharge at the Charles Fuhr gauging is ~47 L s^{-1} km^{-2} whereas its runoff, 1474 mm y^{-1}, is among the highest in Patagonia. Figure 4b shows the deseasonalized Santa Cruz

[6] https://psl.noaa.gov/enso/mei/.

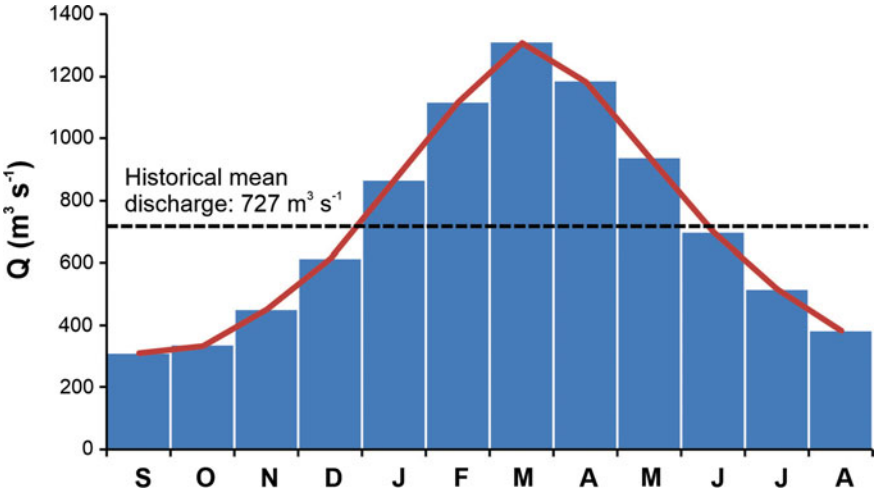

Fig. 3 Santa Cruz River mean annual hydrograph for the 1955–2020 record period. Total annual water discharge is ~23 km^3

River discharge time series. The most pronounced positive and negative departures from the historical mean are evident since 1955 until 1990.

4.2 Trends

The Mann–Kendall test is a distribution-free (i.e. non-parametric) test which seeks to statistically assess if there is a monotonic upward or downward trend (i.e. the trend may or may not be linear) of the variable of interest over time. A monotonic upward (downward) trend means that the variable consistently increases (decreases) through time.

The test (Fig. 5a) shows a statistically significant upward trend ($p < 0.05$) for the 1955–2020 discharge series. Earlier investigations (Pasquini and Depetris 2007; Depetris and Pasquini 2008) did not show a statistically significant trend for the 1955–2003 series. It must be concluded, then, that the significant positive trend has developed during the last decades. Undoubtedly, Fig. 5b shows a noticeable positive trend for the last two decades (2000–2020), exhibiting larger statistical confidence ($p < 0.001$) than the 1955–2020 series.

The hydrological data was also scrutinized by means of the **seasonal Kendall test**. The purpose of the seasonal Kendall test is to check for a monotonic trend of the variable of interest when the data collected over time are presumed to change in the same direction (i.e. up or down) for one or more seasons/months. The results (Table 1) show that during several months (i.e. July–November) of an average year, mean monthly discharges have increased significantly in the Santa Cruz River at the

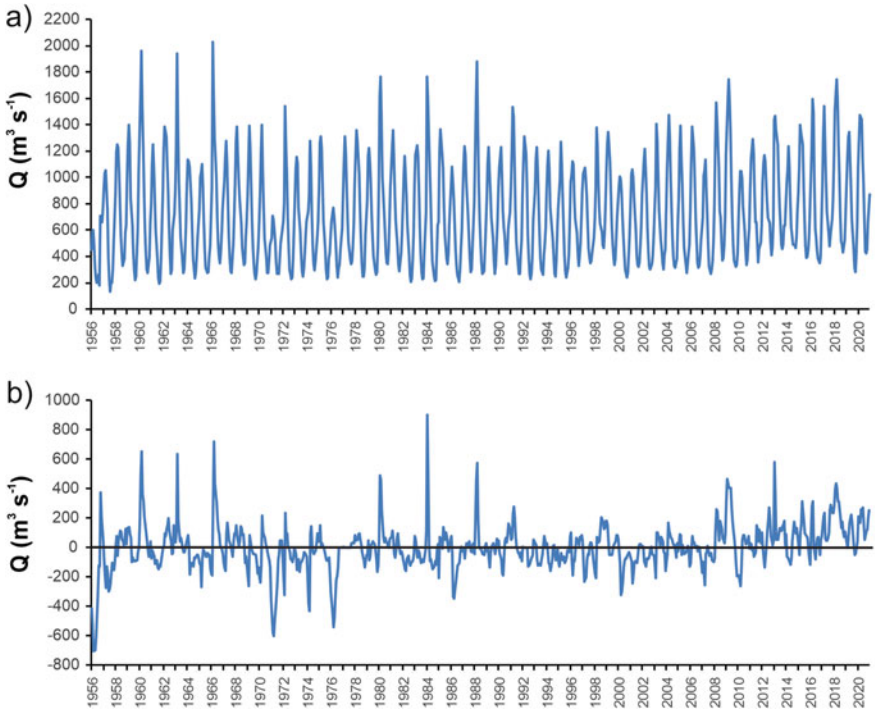

Fig. 4 **a** Santa Cruz River mean monthly discharge time series at Charles Fuhr gauging station. Mean monthly discharge has increased ~16% since 1955; **b** Sixty-five-year-long deseasonalized discharge series of the Santa Cruz River at the Charles Fuhr gauging station. Positive departures are usually associated with glacier's ice dam collapses

Charles Fuhr gauging station. This means that flow increases appreciably during low discharge months, probably due to the amplified contribution of snow-/ice melt and groundwater supply.

4.3 The Connection Between Glacier's Collapse and River Discharge

The Perito Moreno glacier flows towards the Peninsula Magallanes and, periodically, the ice terminus reaches the ground (Fig. 1b), separating Brazo Rico from the main lake. Hence, the water level rises several meters during many months. The ice dam eventually collapses spectacularly, frequently in March (i.e. end of austral summer and month of maximum precipitation), thus producing a **jökulhlaup** (i.e. outburst flood). Although this flooding is moderated by the size of Lake Argentino, it nonetheless produces a discernible signal in the Santa Cruz River

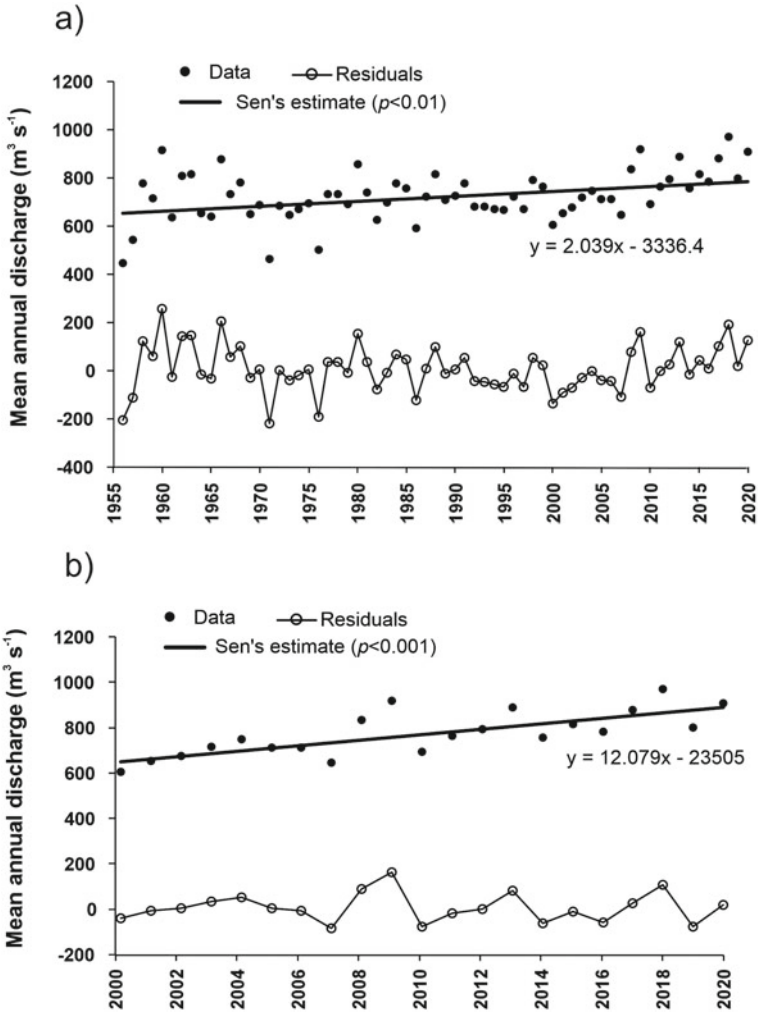

Fig. 5 **a** Mann–Kendall trend test of the 1955–2020 Santa Cruz River discharge time series; **b** The same treatment for the 2000–2020 discharge time series. The trend is significant ($p < 0.001$)

discharge series. Probing into Perito Moreno's closure-rupture dynamics, Fig. 6a shows the damming-rupture events that occurred during the last sixteen years at Brazo Rico; its gauge level shows a seasonal variability when its connection with Canal de los Témpanos and Lake Argentino is open (i.e. it mostly fluctuates between 1 and 3 m). Gauge readings show that when the ice-blocking takes place, the water level increases markedly until seepage underneath the ice dam begins, the breach enlarges and, subsequently, the remnants of the ice dam collapse. Figure 6b shows the detail of a typical damming-rupture event, with the gauge increase at Brazo Rico, the commencement of its drainage underneath the glacier's terminus, and the final

Table 1 Santa Cruz River seasonal Kendall non-parametric trend analysis

	N	Kendall t	*p* value
January	65	1.908	0.028201
February	65	1.404	0.080156
March	65	1.438	0.075212
April	65	1.059	0.144861
May	65	1.313	0.094517
June	65	1.665	0.048006
July	65	*3.448*	*0.000283*
August	65	*3.895*	*0.000049*
September	65	*4.722*	*0.000001*
October	65	*4.173*	*0.000015*
November	65	*1.880*	*0.030079*
December	65	*1.806*	*0.035454*
All	780	*3.587*	*0.000167*

Numbers in italic are statistically significant

moment of ice dam collapse, about four days afterwards. Figure 6b also shows the Santa Cruz River discharge response. Damming-rupture events are clearly visible in the deseasonalized Santa Cruz River discharge time series (Fig. 4b). Most damming-rupture events triggered significant jökulhlaups although a few produced a much less obvious discharge increase. Moreover, during the last decades, most collapsing events have been coincidental with El Niño events.

Perito Moreno's process is similar to the one observed at the sea-reaching Hubbard glacier, in Alaska, where ice has blocked Russell Fjord repeatedly (e.g. Calkin et al. 2001). Such events were followed by glacial outburst floods that have left discernible evidence in the adjacent marine sedimentary record (Willems et al. 2011).

4.4 Harmonic Analysis

In an early investigation of the Perito Moreno glacier-Lake Argentino—Santa Cruz River system, and in subsequent revisits to the subject matter (Depetris and Pasquini 2000, 2008; Pasquini and Depetris 2007, 2011; Pasquini et al. 2008) the harmonic behavior of the Santa Cruz River discharge series was explored, understanding that the glacier's damming-rupture sequence shows its hydrological impact on the river's deseasonalized discharge time series. Indirectly, it was pursued the exploration of the role of climate in the short term, high-frequency glacial dynamics.

The initial investigation (Depetris and Pasquini 2000) showed that the apparent sequence determined by periodic terminus collapses suggested a coherent teleconnection with ENSO and, possibly, with the variable location of the Pacific anticyclone. Moreover, subsequent research found out that several other glacial lakes located

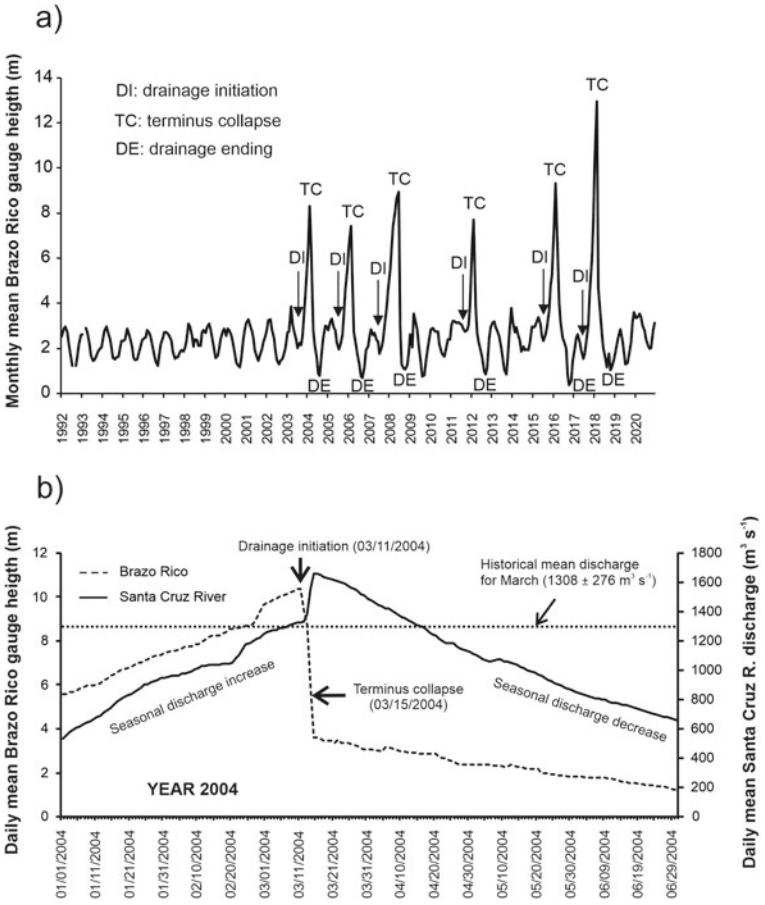

Fig. 6 **a** Lake Argentino's Brazo Rico gauge height variability showing the Perito Moreno's last recorded snout collapses; **b** Detailed example of the snout collapse recorded in 2004. It took about four days for the completion of the ice dam collapse, estimating the water volume delivered during one month in ~0.4 km^3. About thirty days after the ice dam collapse the river returned to its usual seasonal discharge

north of 50º S, in the Patagonian Andes, showed a significant ENSO signature in their deseasonalized water level fluctuations (Pasquini et al. 2008).

The subject matter was revisited about ten years later (Pasquini and Depetris 2011), using a longer discharge time-series. More significant statistical corroboration became evident in support of the teleconnection existing between ENSO and the Santa Cruz River hydrological dynamics. Moreover, results hinted that SAM could play a role in an ENSO/SAM combined mechanism.

In this opportunity, an expanded Santa Cruz River discharge time series (i.e. 1955–2020) is herein explored by means of harmonic analysis. The squared coherency between SAM and the Santa Cruz River discharge series presented the difficulty

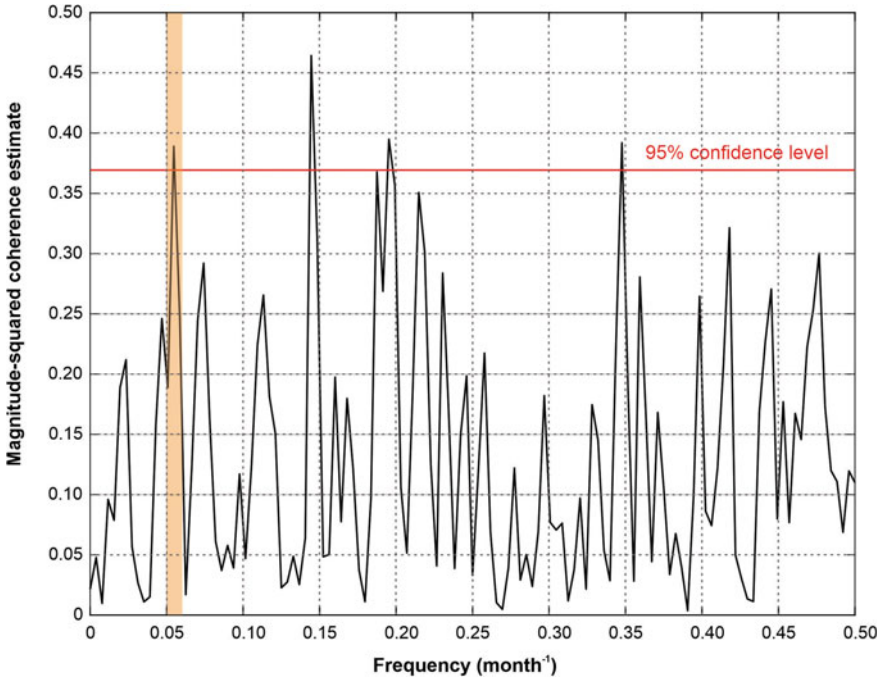

Fig. 7 Squared coherence (Fourier harmonic analysis) between the Santa Cruz River deseasonalized discharge time series and the MEI. The line of 95% confidence level is shown in the figure. The colored box corresponds to a significant frequency of 0.05–0.06 month^{-1} (i.e. ENSO-like periodicity of 20–18 month)

that the spectral density estimates in both series are small or intermediate resulting, therefore, in spurious coherency values.

The square coherence estimate between the selected ENSO index (i.e. **MEI, v.1**) and the deseasonalized Santa Cruz River discharge time series resulted in a significant ($p < 0.05$) peak, in the vicinity of the 0.05 month^{-1} **frequency** (Fig. 7). This analysis, then, corroborates previous findings in the sense that there is a strong cyclical component in the neighborhood of the 20-month period, which is coherent with ENSO oscillations. It is important to underline here that the damming-collapsing sequence recorded at the Perito Moreno glacier's terminus has followed a two-year periodicity during the last decades.

5 Concluding Comments

The Santa Cruz River has the second largest mean discharge among Patagonia's rivers (i.e. ~23 km^3 y^{-1}). The analysis of its flow dynamics by means of the Mann–Kendall trend test shows that, in contrast with previous findings (e.g. Pasquini and Depetris

2011), the river is now evidencing a statistically significant ($p < 0.05$) increasing trend meaning, therefore, that discharges began exhibiting a positive trend during the last decade. Furthermore, digging deeper into the characteristics of the process by means of the seasonal Kendall test showed that the discharge increase is determined by enhanced flow recorded during the months of snow-/ice melt. Clearly, this is distinct evidence of the effect of global climate change.

Previous investigations hinted that the Santa Cruz River deseasonalized discharge might be connected simultaneously with SAM and ENSO, in a type of oscillation, which impacted on the river discharge dynamics (Pasquini and Depetris 2011). Harmonic analysis did not show at this time a substantial connection between SAM and the Santa Cruz River discharge series, probably because SAM has shown a robust long-term trend towards a more positive state over recent decades (Sen Gupta and McNeil 2012). Fourier's squared coherence, however, proved significant at ENSO-like frequencies, thus reinforcing further earlier findings (Pasquini and Depetris 2011).

It seems clear that the dynamics of the glacier plays a role in the harmonic behavior of the Santa Cruz River. Moreover, the Perito Moreno glacier is not openly retreating when most of the other glaciers in the region show clear signs of such behavior in a climate change scenario. It follows, then, that the discussion on the factors affecting the Perito Moreno glacier's peculiar behavior appears to be still open.

References

Bertler NAN, Naish TR, Oerter H, Kipfstuhl S, Barrett PJ, Mayewski PA, Kreutz K (2006) The effects of joint ENSO-Antarctic oscillation forcing on the McMurdo Dry Valleys, Antarctica. Antarctic Sci 18:507–514

Blackman RB, Tukey JW (1958) The measurement of power spectra from the point of view of communications engineering—part I. Bell Syst Tech J 37:185–282

Burn DH, Hag Elnur MA (2002) Detection of hydrologic trends and variability. J Hydrol 255:107–122

Calkin PE, Wiles GC, Barcaly DJ (2001) Holocene coastal glaciations of Alaska. Quat Sci Rev 20:449–461

Cosentino NJ, Gaiero DM, Torre G, Pasquini AI, Coppo R, Arce JM, Vélez G (2020) Atmospheric dust dynamics in southern South America: A 14-year modern dust record in the loessic Pampean region. Holocene 30(4):575–588

Depetris PJ, Gaiero DM, Probst J-L, Hartmann J, Kempe S (2005) Biogeochemical output and typology of rivers draining Patagonia's Atlantic seaboard. J Coas Res 21:835–844

Depetris PJ, Pasquini AI (2000) The Hydrological signal of the Moreno Glacier damming of Lake Argentino (Southern Andean Patagonia): the ENSO connection. Global Planet Change 26:367–374

Depetris PJ, Pasquini AI (2008) Riverine flow and lake level variability in Southern South America. EOS Trans Am Geophys Union 89(28):254–255

Fitzharris B, Clare GR, Renwick J (2007) Teleconnections between Andean and New Zealand glaciers. Global Planet Change 59:159–174

Fogt RL, Bromwich DH (2006) Decadal variability of the ENSO teleconnection to the high-latitude South Pacific governed by coupling with the Southern Annular Mode. J Clim 19:979–997

Fogt RL, Bromwich DH, Hines KM (2011) Understanding the SAM influence on the South Pacific ENSO teleconnection. Clim Dyn 36:1555–1576
Fogt RL, Bromwich DH, Hines KM (2011) Erratum to: understanding the SAM influence on the South Pacific ENSO teleconnection. Clim Dyn 37:2127–2128
Gillett NP, Kell TD, Jones PD (2006) Regional climate impacts of the Southern Annular Mode. Geophys Res Lett 33(23):1–4
Hess A, Iyer H, Malm W (2001) Linear trend analysis: a comparison of methods. Atmos Environ 35:5211–5222
Hirsch RM, Slack JR, Smith RA (1982) Techniques of trend analysis for monthly water quality data. Water Resour 20:107–121
Jones JM, Widmann M (2003) Instrument- and tree-ring-based estimates of the Antarctic oscillation. J Clim 16:3511–3524
Kastner S, Enters D, Ohlendorf C, Haberzettl T, Kuhn G, Lücke A, Mayr C, Reyss J-L, Wastegård S, Zolitschka B (2010) Reconstructing 2000 years of hydrological variation derived from laminated proglacial sediments of Lago del Desierto at the eastern margin of South Patagonian Ice Field, Argentina. Global Planet Change 72:201–214
Kendall MG (1975) Rank correlation methods. Griffin, London
Labat D (2005) Recent advances in wavelet analyses: part 1. A review of concepts. J Hydrol 314:275–288
Lau K-M, Weng H-Y (1995) Climate signal detection using wavelet transform: how to make a time series sing. Bull Am Meteorol Soc 76:2391–2404
Mancini MV (1998) Vegetational changes during the holocene in extra-Andean Patagonia, Santa Cruz province, Argentina. Palaeogeogr Palaeoclimatol Palaeoecol 138:207–219
Mancini MV (2002) Vegetation and climate during the holocene in southwest Patagonia, Argentina. Rev Palaeobot Palynol 122:101–115
Mancini MV, Paez MM, Prieto AR, Stutz S, Tonillo M, Vilanova I (2005) Mid-Holocene climatic variability reconstruction from polen records (32°–52° S, Argentina). Quat Int 132:47–59
Mann HB (1945) Nonparametric tests against trend. Econometrica 13:245–259
Masiokas MH, Cara L, Villalba R, Pitte P, Luckman BH, Toum E, Christie DA, Le Quesne C, Mauget S (2019) Streamflow variations across the Andes (18°–55° S) during the instrumental era. Sci Rep 9:17879
Masiokas MH, Rabatel A, Rivera A, Ruiz L, Pitte P, Ceballos JL, Barcaza G, Soruco A, Bown F, Berthier E, Dussaillant I, MacDonell S (2020) A review of the current state and recent changes of the Andean cryosphere. Front Earth Sci 8:1–27
Masiokas MH, Villalba R, Luckman BH, Lascano ME, Delgado S, Stepanek P (2008) Twenty-century glacier recession and regional hydroclimatic changes in northwestern Patagonia. Global Planet Change 60:85–100
McPhaden MJ, Santoso A, Cai W (2020) El Niño southern oscillation in a changing climate. American Geophysical Union/Wiley, Washington, DC
Minowa M, Sugiyama S, Sakakiraba D, Sawagaki T (2015) Contrasting glacier variations of Glaciar Perito Moreno and Glaciar Ameghino, Southern Patagonia Icefield. Ann Glaciol 56:26–32
Ohlendorf C, Fey M, Gebhardt C, Haberzettl T, Lücke A, Mayr C, Schäbitz F, Wille M, Zolitschka B (2013) Mechanisms of lake-level change at Laguna Potrok Aike (Argentina)—insights from hydrological balance calculations. Quat Sci Rev 71:27–45
Pabón-Caicedo JD, Arias PA, Carril AF, Espinoza JC, Fita Borrel L, Goubanova K, Lavado-Casimiro W, Masiokas M, Solman S, Villalba R (2020) Observed and projected hydroclimate changes in the Andes. Front Earth Sci 8:1–29
Pasquini AI, Depetris PJ (2007) Discharge trends and flow dynamics of South American rivers draining the southern Atlantic seaboard: an overview. J Hydrol 333:385–399
Pasquini AI, Depetris PJ (2011) Southern Patagonia's Perito Moreno Glacier, Lake Argentino, and Santa Cruz River hydrological system: an overview. J Hydrol 405:48–56
Pasquini AI, Lecomte KL, Depetris PJ (2008) Climate change and recent water level variability in Patagonian proglacial lakes, Argentina. Global Planet Change 63:290–298

Philander SG (1990) El Niño, La Niña, and the southern oscillation. Academic Press, San Diego
Rott H, Stuefer M, Siegel A, Skvarca P, Eckstaller A (1998) Mass fluxes and dynamics of Moreno Glacier, Southern Patagonia Icefield. Geophys Res Lett 25:1407–1410
Sen Gupta A, McNeil B (2012) Variability and change in the ocean. In: Henderson-Sellers A, McGuffie K (eds) The future of the world's climate. Elsevier Science, Amsterdam, pp 141–165
Silvestri G, Vera C (2009) Nonstationary impacts of the southern annular mode on southern hemisphere climate. J Clim 22:6142–6148
Stuefer M, Rott H, Skvarca P (2007) Glaciar Perito Moreno, Patagonia: climate sensitivities and glacier characteristics preceding the 2003/2004 and 2005/2006 damming events. J Glaciol 53:3–16
Torrence C, Compo GP (1998) A practical guide to wavelet analysis. J Am Meteorol Soc 79:61–78
Welch P (1967) The use of fast Fourier transform for the estimation of power spectra: a method based on time averaging over short, modified periodograms. IEEE Trans Audio Electroacoust 15(2):70–73
Willems BA, Powell RD, Cowan EA, Jaeger JM (2011) Glacial outburst flood sediments within disenchantment Bay, Alaska: Implications of recognizing marine jökulhlaup deposits in the stratigraphic record. Mar Geol 284:1–12
Yue S, Pilon P, Cavadias G (2002) Power of the Mann-Kendall and Spearman' rho test to detecting monotonic trends in hydrological series. J Hydrol 259:254–271

The Role of Sediments and Phosphorus in the Evaluation of Water Resources Quality in Patagonia

Pedro Temporetti, Guadalupe Beamud, José León, Leandro Rotondo, Mayra Cuevas, and Fernando Pedrozo

Abstract Among the processes of anthropogenic contamination of aquatic environments, eutrophication is one of the most studied. Phosphorus is a key nutrient in eutrophication and, in many cases, the limiting nutrient in various water bodies. Furthermore, sediments from an aquatic environment can be considered as an "environmental information bank". They play an important role in the nutrient cycle in lakes since nutrients are transported to the bottom by sedimentation and can return to the water column by various mechanisms which are sometimes extremely complex. The aim of this chapter is to summarize 30 years of research carried out by the Water Quality Group (INIBIOMA, CONICET-UNComahue) on sediments from several lake environments in Argentinian Patagonia and their role in aquatic resource assessment. A total of 11 water bodies in the region were analyzed, considering different physical and chemical parameters, always applying the same methodology (in field and laboratory). The results show that (1) pH is one of the main parameters that influence the P exchange between sediments and the water column; (2) texture, chemical composition, and mineralogy are essential to understand sediment genesis and transport mechanisms; (3) three gradients determine the distribution of the studied environments: (a) North–South geographic gradient, (b) pH gradient and (c) trophic gradient; (4) the use of sediment bioassays with native algae is a particularly useful tool for rapidly evaluating the anthropic impact on water bodies; and (5) sediment studies allow obtaining information on, for example, contaminated and uncontaminated areas and distribution patterns of contaminants, and should be included in monitoring programs.

Keywords Sediments · Phosphorus · Water resources · Patagonia

P. Temporetti (✉) · G. Beamud · L. Rotondo · M. Cuevas · F. Pedrozo
Instituto de Investigaciones en Biodiversidad y Medioambiente, Centro Regional Universitario Bariloche-UNComahue, CCT-Patagonia Norte, CONICET, San Carlos de Bariloche, Argentina
e-mail: temporettipf@comahue-conicet.gob.ar

J. León
Centro de la Región Semiárida, Instituto Nacional del Agua. Villa Carlos Paz, Córdoba, Argentina

A. I. Torres and V. A. Campodonico (eds.), *Environmental Assessment of Patagonia's Water Resources*, Environmental Earth Sciences,
https://doi.org/10.1007/978-3-030-89676-8_10

1 Introduction

For more than 80 years, since the first works by Einsele (1936, 1938) and Mortimer (1941, 1942), lake sediments have been considered in limnology studies. The growing interest in sediment studies has clearly been triggered by the problems caused by anthropogenic contamination of water bodies.

In aquatic systems, sediments are made of organic and inorganic substances, including particulate material washed from the basin (allochthonous material), as well as material originated from the same water body (autochthonous material). In this sense, sediment composition is highly influenced and controlled by the composition of the rocks from which they derive either by erosion and/or weathering processes, and the type of basin (Golterman 2004). These processes are affected by many factors, such as climate, relief, biota, time, and anthropic factors like land-use conditions.

Sediments from an aquatic environment can be considered as an "environmental information bank" (Håkanson and Jansson 1983) because they provide much information regarding, for example, which areas are contaminated, as well as the dispersion patterns of different polluting substances, supplying relevant data at different levels (e.g. local and regional). Eutrophication is one of the most studied processes of contamination in aquatic environments (Wetzel 2001; Golterman 2004). It is defined as the excess of nutrients (mainly phosphorus (P) and nitrogen (N)), and organic matter that causes an increase in biological production (Sinke 1992; Wetzel 2001). The effects of this process on water bodies are numerous, among which are worth highlighting the decrease in water column transparency and dissolved oxygen concentration, the appearance of toxic algal species and, in very severe cases, fish mortality (Smith et al. 2006b).

Phosphorus is a key nutrient in eutrophication processes, and frequently the limiting nutrient in various water bodies (Elser et al. 2007; Zhongyao et al. 2020). Moreover, water column nutrient concentration is the main parameter considered for the trophic classification of water bodies (OECD 1982; Horne and Goldman 1994; Wetzel 2001; Schindler et al. 2008). The trophic state of aquatic environments is determined using physical (e.g. transparency) and chemical parameters [e.g. total phosphorus concentration (PT), soluble reactive phosphorus (PRS), and chlorophyll a (Chl-a)] (OECD 1982; Horne and Goldman 1994; Cunha et al. 2013). However, these parameters usually present seasonal fluctuations, hindering the trophic classification of water bodies (Maasen et al. 2005).

Several studies have related the P concentration in surface sediments with its concentration in the water column (Lee-Hyung et al. 2003; Smith et al. 2006a; McDaniel et al. 2009), supported by the concept that trophic state can be substantially influenced by P release from sediments (Carey and Rydin 2011). In this sense, sediments play an important role in the nutrient cycle in lakes since nutrients are transported to the bottom by sedimentation and can be returned into the water column by various (physical, chemical and biological) mechanisms, sometimes extremely

complex (Forsberg 1989). Håkanson and Jansson (1983) proposed that this recirculation can be very important when the involved elements are essential nutrients such as P and N, a phenomenon known as *internal load* in the specialized literature (Ryding and Forsberg 1976; Larsen et al. 1981; Boström et al. 1982; Golterman et al. 1983; Håkanson and Jansson 1983; Søndergaard et al. 2003; Jeppesen et al. 2005). This load represents a problem in the lake restoration process, even when the pollutant source has been eliminated (Boström et al. 1982; Carpenter 2005). Consequently, the knowledge of the sediment state and function is essential to predict the effects of different nutrient loads released to the environment and is necessary to plan the restoration of impacted water bodies.

Argentinian Patagonia comprises the southern portion of the Province of Mendoza, parts of the provinces of La Pampa and Buenos Aires, and the provinces of Chubut, Neuquén, Río Negro, Santa Cruz, Tierra del Fuego, Argentinian Antarctica, and Southern Atlantic Islands. This region is the largest in Argentina, with an area of 930,638 km^2. It can be divided into two sub-regions (Matteucci 2012b): (a) **Patagonian Andes**, with poorly developed soils, derived mainly from volcanic ash, and rich in allophones. This sub-region contains the largest and deepest glacial lakes of South America (over 300 lakes of different sizes), many of which are the sources of the longest Patagonian rivers that feed large reservoirs located on the Patagonian plateau (Quirós and Drago 1999). The vast majority of these water bodies are chemically poor (low ions and nutrients concentration) and, in general, dominated by silica (Pedrozo et al. 1993). (b) **Patagonian steppe**, with typically alkaline soils with high salt content, negative water balances and evaporation dominance. It is a complex landscape, mainly characterized by a basaltic plateau and tectonically uplifted pebble fans (Iriondo 1989). The allochthonous-exoreic rivers originating in the Andes can cross this arid region and feed large artificial lakes. Furthermore, some large depressions in Patagonia contain permanent natural and artificial lakes, while others have temporary waters with evaporitic deposits in central areas (Quirós and Drago 1999).

The first studies on lake sediments in the Patagonian region date back to 1990, when phosphorus retention in sediments from different lentic water bodies in the Nahuel Huapi National Park and in the Patagonian plateau was studied in response to the anthropic influence (Temporetti 1990). Since then, the number of studies on lake sediments in this region has increased considerably, addressing different aspects of the effect of anthropic activities on the aquatic environments (Temporetti 1998; Temporetti and Pedrozo 2000; Diaz et al. 2001, 2015; Temporetti et al. 2013, 2014a, b, 2019; Ribeiro Guevara et al. 2003, 2005a, b, 2009, 2010; Cabrera et al. 2016, 2020; León et al. 2017; Juncos et al. 2017; Williams et al. 2017).

The aim of this chapter is to summarize 30 years of research carried out by the Water Quality Group (INIBIOMA, CONICET-UNComahue) on sediments from lake environments in the Patagonian region and their role in aquatic resource assessment.

1.1 Study Area

The studied water bodies are located between 33° and 50° S and 68° and 72° W (Fig. 1). According to Quirós and Drago (1999), the aquatic environments of this region have been classified as warm monomictic, with a stratification period during summer. The climate in the Patagonian region is continental, classified as humid cold temperate in the mountains to arid in the steppe (Speck et al. 1982; Matteucci 2012a). Rain periods occur mainly between late winter and early spring. Due to moisture loss from the prevailing western winds, a strong annual west–east precipitation gradient is observed, ranging from 2700 mm y^{-1} on the Argentina/Chile border (altitude 1020 m a.s.l.) to 500 mm y^{-1} in the Patagonian steppe (800 m a.s.l.) in a distance of only 100 km. The annual average temperature varies between 8.0 °C at high altitudes (above 2000 m a.s.l.) and 20.0 °C in protected valleys, and between 7.5 and 12.5 °C in the Patagonian steppe. The studied environments are seven lakes, five reservoirs and two shallow lakes. Table 1 shows the geographic coordinates, morphometric data, physical and chemical parameters, and the trophic classification of the 14 environments. These environments include two very marked gradients: (a) **pH**, ranging from 2.5 in Lake Caviahue, a naturally acidic environment, to 9.2 in

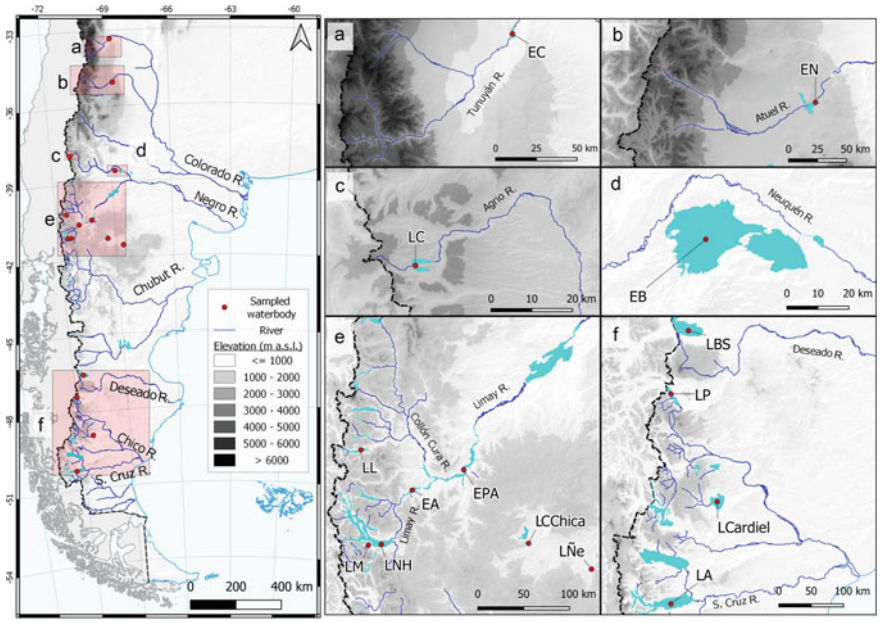

Fig. 1 Study area: **EC** = Reservoir El Carrizal; **EN** = Reservoir El Nihuil; **LC** = Lake Caviahue; **EB** = Reservoir Los Barreales; **LL** = Lake Lacar; **EA** = Reservoir Alicura; **EPA** = Reservoir Piedra del Aguila; **LM** = Lake Moreno; **LCChica** = Lagoon Cari-Laufquen Chica; **LÑe** = Lagoon Ñe-Luan; **LNH** = Lake Nahuel Huapi; **LBS** = Lake Buenos Aires; **LP** = Lake Pueyrredón; **LCardiel** = Lake Cardiel; **LA** = Lake Argentino

Table 1 Geographic position, morphometric data, physical and chemical parameters, trophic classification, and Eutrophication History for the 15 analyzed lakes. In brackets the acronyms for each water body. Water EC: Electric conductivity of water

	Geographic location	Altitude (ma.s.l.)	Area (km^2)	Maximum depth (m)	Secchi disk (m)	Water pH	Water EC ($\mu S\ cm^{-1}$)	Trophic classification	Eutrophication history
Reservoir El Carrizal [(1)] (EC)	33° 17′ 55.0″ S	786	31	40	1.4	8.1	1265	Mesotrophic	Man made reservoir for irrigation and hydropower generation
	68° 43′ 20.0″ W								Sparsely vegetated basin. Population: 10,000 inhabitants
Reservoir El Nihui[(1)] (EN)	35° 04′ 21.0″ S	1251	75	17	> 3	8.3	1283	Mesotrophic	Man made reservoir for hydropower generation. Sparsely vegetated basin
	68° 41′ 13.7″ W								Small urban settlements. Agricultural use of the land
Lake Caviahue[(2)] (LC)	37° 52′ 17.0″ S	1650	922	90	3.6	2.5	1259	Eutrophic	Naturally acidic lake of volcanic origin. Sparsely vegetated basin
	71° 00′ 53.0″ W								Stable population of 1000 inhabitants, which increases in tourist seasons

(continued)

Table 1 (continued)

	Geographic location	Altitude (ma.s.l.)	Area (km^2)	Maximum depth (m)	Secchi disk (m)	Water pH	Water EC ($\mu S\ cm^{-1}$)	Trophic classification	Eutrophication history
Reservoir Los Barreales[3] (EB)	38° 33′ 03.0″ S	422	407	120	3.3	8.0	265	Mesotrophic	Reservoir of anthropic origin flood attenuation, located in Vaca Muerta
	68° 49′ 21.0″ O								Basin, one of the five producing oil fields in Argentina. Sparsely vegetated basin
Lake Lácar[4] (LL)	40° 09′ 37.8″ S	625	49	279	25	7.7	60	Oligotrophic	Deep glacial lake. Wooded basin. City of 25,000 inhabitants. Tourist destination
	71° 21′ 47.3″ W								Discharge of effluents with different degrees of treatment
Reservoir Alicura[5] (EA)	40° 35′ 09.0″ S	705	65	115	6.9	7.4	36.0	Oligotrophic	Reservoir of anthropic origin. The main uses of this environment are:

(continued)

Table 1 (continued)

	Geographic location	Altitude (ma.s.l.)	Area (km^2)	Maximum depth (m)	Secchi disk (m)	Water pH	Water EC ($\mu S\ cm^{-1}$)	Trophic classification	Eutrophication history
	70° 45′ 09.0″ W								Power generation and intensive trout farming (1132 Tn y^{-1})
Reservoir Piedra del	40° 11′ 25.0″ S	592	285	120	6.4	7.0	50.0	Oligotrophic	Reservoir of anthropic origin. The main uses of this environment are:
Aguila[5] (EPA)	69° 59′ 30.0″ W								Production of electrical energy and intensive trout aquaculture (42 Tn y^{-1})
Lake Moreno[6] (LM)	41° 04′ 33.0″ S	778	164	100	12.5	7.0	35.9	Oligotrophic	Deep glacial lake. Basin forested. Little village of 800 inhabitants. Tourist destination
	71° 30′ 22.0″ W								Without effluent treatment. Fish farming center (50 Tn y^{-1})

(continued)

Table 1 (continued)

	Geographic location	Altitude (ma.s.l.)	Area (km^2)	Maximum depth (m)	Secchi disk (m)	Water pH	Water EC ($\mu S\ cm^{-1}$)	Trophic classification	Eutrophication history
Lagoon Cari-Laufquen	41° 13′ 04.6″ S	150	5	5	0.3	8.4	440	Eutrophic	Shallow lagoon of wind origin. Sparsely vegetated basin
Chica (LCChica)	69° 25′ 54.3″ W								No nearby urban settlements. Livestock-related land use
Lagoon Ñe-Luan (LÑe)	41° 30′ 15.9″ S	1000	0.6	15	0.7	8.2	324	Eutrophic	Shallow lagoon of wind origin. Sparsely vegetated Basin
	68° 37′ 32.3″ W								No nearby urban settlements. Livestock-related land use
Lake Nahuel Huapi[7] (LNH)	41° 05′ 25.0″ S	764	529	438	20	7.3	34	Oligotrophic	Deep glacial lake. 3 cities on its coasts:

(continued)

Table 1 (continued)

	Geographic location	Altitude (ma.s.l.)	Area (km^2)	Maximum depth (m)	Secchi disk (m)	Water pH	Water EC ($\mu S\ cm^{-1}$)	Trophic classification	Eutrophication history
	71° 20′ 08.0″ W								SC de Bariloche (130,000 inhabitants.), Villa la Angostura (15,000 inhabitants.) and Dina Huapi (6000 inhabitants). The main activity is tourism
Lake Buenos Aires[8] (LBS)	46° 18′ 14.0″ S	200	1892	550	3.3	7.8	77	Oligotrophic	Deep glacial lake. Very wide and partially wooded basin
	71° 42′ 57.1″ W								No significant human activity. Livestock-related land use
Lake Pueyrredón[8] (LP)	47° 26′ 20.2″ S	112	320	280	8.0	8.3	174	Oligotrophic	Deep glacial lake. Very wide and partially wooded basin

(continued)

Table 1 (continued)

	Geographic location	Altitude (ma.s.l.)	Area (km^2)	Maximum depth (m)	Secchi disk (m)	Water pH	Water EC ($\mu S\ cm^{-1}$)	Trophic classification	Eutrophication history
	71° 55′ 18.4″ W								No significant human activity. Livestock-related land use
Lake Cardiel[8] (LCardiel)	48° 48′ 38.6″ S	300	460	491	1.3	9.2	4512	Eutrophic	Shallow lake of wind origin. Sparsely vegetated basin
	71° 11′ 57.9″ W								No urban settlements. Livestock-related land use
Lake Argentino[8] (LA)	50° 07′ 40.1″ S	187	1466	500	2.0	7.5	40	Oligotrophic	Deep glacial lake. Very wide and partially wooded basin
	72° 06′ 51.9″ W								City of 20,000 inhabitants. Important tourist center. Livestock-related land use

Data from: (1) León et al. (2017), (2) Pedrozo et al. (2001), (3) Rotondo et al. (2020), (4) Temporetti et al. (2009), (5) Othaz Brida (2021), (6) Queimaliños et al. (2012), (7) Alonso et al. (2006), (8) Alemanni (2006) and (9) Pedrozo et al. (2006)

Lake Cardiel, an alkaline environment; and (b) **altitude**, ranging from 1650 m a.s.l. (Lake Caviahue) up to 112 m a.s.l. (Lake Pueyrredón).

1.2 Methodology

Sediment cores were collected between 1990 and 2019, at least once at each sampling site using a 6 cm diameter Uwitec-type extractor or an Ekman-Birge dredger in most cases. All samples were extracted at depths ranging from 5 to 20 m except for Lake Caviahue (90 m). The first 10 cm of the sediment column were considered in the analysis of all samples. In situ, pH and redox potential (Eh) were measured with specific and temperature-adjusted electrodes. The storage and conservation of the samples were carried out in accordance with APHA (1999). In the laboratory, samples were oven-dried at 60 °C, homogenized in a ceramic mortar, and sieved through a 500 μm mesh (Newark, ASTM Nº 36 USA Standard Series Sieves) to remove the least reactive coarse fraction. All performed analyses followed standardized analytical recommendations: (a) **Texture**: sieving method (2.00, 1.00 and 0.25 mm USA Standard Series Sieves) and densimeter (0.05 to 0.002 mm and < 0.002 mm) according to Forsythe (1985). (b) **Nutrients**: TP (Total Phosphorus): a sediment fraction was digested with SO_4H_2 and 30% hydrogen peroxide (H_2O_2) (Carter 1993). After digestion, the dissolved P was determined by the Murphy and Riley method (1962) and Total Nitrogen (TN) and Total Carbon (TC) by automatic Thermo-Flash 1112 analyzer. (c) **Elemental composition**: by SEM–EDX microanalysis (Philips 515-EDAX Genesis 2000) (Last 2001b; Saarinen and Petterson 2001). (d) **Mineralogy:** by X-ray diffraction (PANalycal Empyrean Diffractometer). (e) **Phosphorus fractionation**: following the recommendations by Hieltjes and Lijklema (1980), discriminating the labile fraction (P-Labile) (extracted with 1 M NH_4Cl), the fraction bound to Al/Fe oxy-hydroxides (P-Al/Fe) (extracted with 0.1 M NaOH), the fraction bound to calcium compounds (P-Ca) (extracted with 0.5 M HCl) and the organic fraction (P-OM) (calculated as the difference between the sediment TP and the sum of the previous mentioned fractions). (f) **Phosphorous fixing isotherms**: Batch experiments were performed by measuring dissolved P in a mixture of dried sediment and a set of increasing P concentration solutions (0.0, 1.7, 2.7, 3.7, 4.5, 5.5, 8.5, 10.0 mg P L^{-1} prepared from a 1000 mg L^{-1} PO_4^{3-} Merck Certipur® solution). Sediment aliquots (*ca.* 0.2 g) were put in centrifuge tubes (50 mL), filled with PO_4^{3-} solution (10 mL), and placed in the dark at room temperature (20 °C) for 48 h with periodic mixing (2 h in orbital shaker). The supernatant was filtered (through a 0.45 μm pore size) and analyzed for P (Murphy and Riley 1962). The maximum P adsorption capacity of the sediment (Pmax, mg g^{-1}) was estimated using the linearized Langmuir equation (Langmuir 1997):

$$1/\text{Pads} = 1/(\text{KL} \cdot \text{Pmax})\ \text{Pdis} + (1/\text{Pmax})$$

where Pads (mg g^{-1}) is the net P adsorbed to sediment estimated by mass difference of dissolved P between initial and final solutions after 48 h, KL (mg L^{-1}) is a constant related to the binding energy of P to the sediment, and Pdis (mg L^{-1}) is the P concentration remaining in solution after 48 h (Sposito 2008). Furthermore, the phosphorus retention coefficient (PRC) by sediments for each site was calculated as a percentage of the Pmax difference, estimated from the Langmuir equation, and the TP in sediments.

2 Effect of pH in P Adsorption Dynamics in Sediments

The factors that influence P exchange between sediments and the water column can be physical (temperature, wind action, etc.), chemical (pH, dissolved oxygen, nitrates, sulfates, etc.) and biological (bioturbation, bacterial activity, etc.) (Boström et al. 1982; Golterman 2004). In any of the compartments of the waterbody (water, sediment, water–sediment interface, interstitial water), pH is one of the factors that affect P release, and it has been one of the most studied (Jin et al. 2006; Wang et al. 2005; Wu et al. 2014). An increase in pH can release P bound to Fe and Al complexes due to site-specific competition between hydroxyl ions and P bound to these metal (hydro)oxides (Anderson 1974; Kim et al. 2003; Li et al. 2016). In this sense, pH is an important parameter in controlling P availability in sediments. The pH in lake sediments often varies because of specific microbial processes or changes in environmental conditions (Wang et al. 2005). Most of the studies to demonstrate the relationship between pH and P release/retention in lake sediments were carried out in laboratory tests, where a pH gradient is simulated by adding solutions of hydrochloric acid or sodium hydroxide. However, there are very few studies on the adsorption of phosphate by sediments with different pH values in natural systems (Ding et al. 2016). In a recent contribution, Temporetti et al. (2019) evaluated the pH effect on P dynamics (release/adsorption) in sediments in a river system with a natural pH gradient (from 1.5 to 6.7): the Agrio River, Neuquén province. The authors observed that, while TP concentration in water decreased with increasing pH, an inverse relationship occurred in sediments. On the other hand, the results also indicated that the phosphorus retention capacity was greater at low pH and decreased with increasing pH (Fig. 2), affecting the retention capacity of sediments from the upper part of the river, where the pH was more acidic. This P retention capacity varied according to the time of year, possibly due to several factors such as variations in river water level, temperature gradient, oxide precipitation (mainly as Fe and Al oxyhydroxides), the presence of algae and bacteria that consume dissolved nutrients and the formation of complexes with organic matter in sediments. Although the results of the different fractions of P in sediments showed the existence of an alternation in P control in relation to the variation in pH (Fe/Al at pH < 5.5 and Ca at pH > 5.7). According to Golterman (2004), increase in pH causes a change towards the co-precipitation of $CaCO_3$-P and a decrease in Fe(OOH)-P, while the decrease in pH produces the opposite effect. It was demonstrated that sediment P control of all

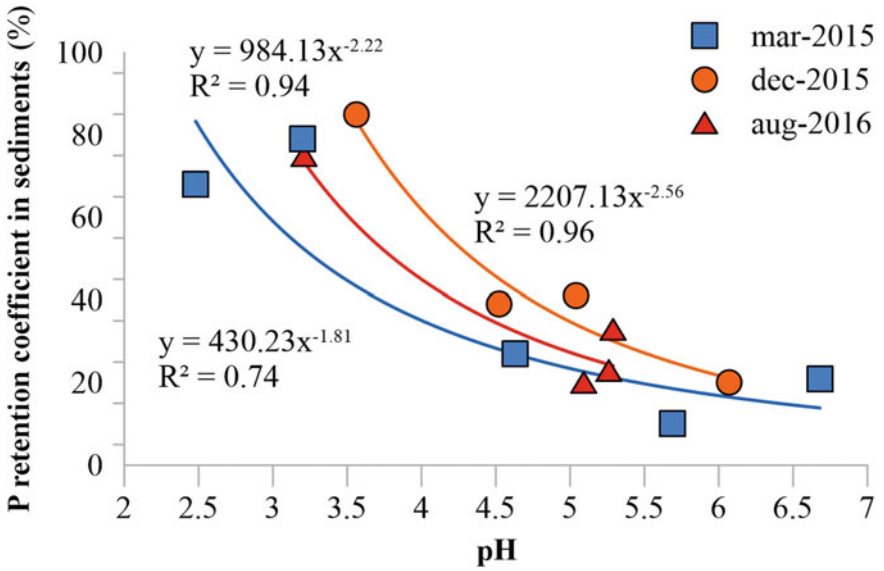

Fig. 2 Variation of phosphorus retention coefficient (PRC) with the pH gradient in sediments of Agrio River. Modified from Temporetti et al. (2019)

the system was regulated by Fe/Al oxyhydroxides and, to a lesser extent, by organic matter (OM) and not by Ca, as it occurs in alkaline pH sediments.

3 Texture, Chemical Characterization and Mineralogy

According to Lewis (1984), the three basic descriptors of sediments are texture, structure, and composition. The first involves the general physical appearance of sediments or rocks (Last 2001a) Besides, texture can provide information about sediments such as origin, transport mechanisms and environmental conditions within the basin. Knowing the textures of lake sediments is necessary because it enables us to understand their capacity to fix pollutants, among other things. Sediment structure enables us to comprehend their chemical properties and the behavior of the chemical substances inside them (Boyle 2001) by describing the elemental composition and understanding the interactions between different parts of the environment. Finally, like texture and structures, sediment mineralogical analysis is essential to adequately describe the material (Lewis 1984), in order to comprehend the genesis of sediments in a lake basin, to decipher transport mechanisms, and to infer limnological, hydrological and climate conditions (Last 2001b). According to Last (2001b), from a mineral origin perspective, there are three different types of minerals in most water bodies: (a) **Allochthonous or detrital minerals**, those which are introduced into the environment through surface currents, erosion from the coast, sheet

flooding, mass movement, or wind activity; (b) **Autochthonous minerals**, which are those inorganic components that originate within the water column, either by inorganic or biologically induced chemical precipitation; and (c) **Autigenic minerals**, those which originate from the diagenetic alteration of the sediment that is already deposited (secondary minerals) or by chemical reactions within the interstitial water of the sediment (primary or secondary minerals). According to Xiao et al. (2013), minerals are often important as very effective absorbents of environmental pollutants. Consequently, in order to better understand the interaction of phosphorus with sediments, it is necessary to study the characteristics of phosphorus adsorption by the sediment mineral matrix.

The sediments of the studied Patagonian environments were dominated (average = 69%) by a sand fraction (2 > sand > 0.05 mm), the reservoirs located at the south of Mendoza (El Carrizal and El Nihuil) and the lagoons of the Patagonian plateau (Carrilafquen Chica and Ñe-Luan) being the environments with the lowest percentages. The silt fraction (0.05 > silt > 0.002 mm) was 24.5% on average for all the environments, turning out to be the main fraction in the environments mentioned above. The clay fraction (< 0.002 mm) represented 19.3% on average in the sediments from El Carrizal and El Nihuil, and 13.2% on average in those from Carrilafquen Chica and Ñe-Luan lagoons, while it was present in a very low proportion (1.0% on average) in sediments from the rest of the environments. Following the textural classification established by the USDA (United States Department of Agriculture 1999), the sediments of the studied environments can be classified as: (a) Loam-Silt Loam, at southern Mendoza and the Patagonian Plateau and (b) Sand-Loamy Sand, at the Andean Patagonian region and southern Patagonia (Fig. 3a). The multivariate Principal Component Analysis (PCA) was used to display a graphical ordination of textural data, in order to highlight similarities or differences between the water bodies, and to verify an environmental gradient (Fig. 3b). The PCA showed that

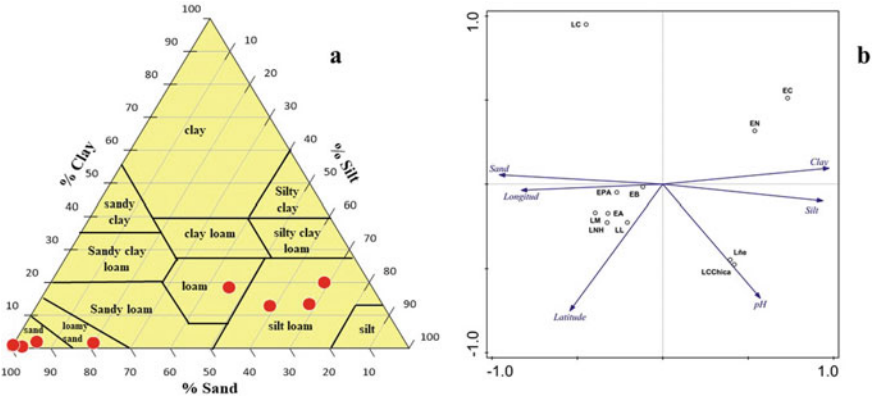

Fig. 3 **a** Textural classification triangle of the sediments from the studied environments. **b** PCA of textural variables performed on sediment samples from the studied environments. Both axes explain 98% of the total variance of the data

the more alkaline environments presented a higher percentage of silt and clay than the acid and neutral pH environments, which correlated significantly ($p < 0.05$). Both axes explained 85% of the total variance of the data. The sands presented a negative correlation ($r = -0.62$) while the silts and clays presented a positive correlation ($r = 0.67$ and $r = 0.72$, respectively). According to Wang et al. (2005), the finer textures have greater pollutant adsorption capacity and suspension potential. Therefore, the sediment with a higher proportion of clay and silty textures could be more contaminated. On the other hand, Wang et al. (2020) studied the adsorption of two pollutants in the sediments of a river in China, evaluating the effect of particle size, humic acids, pH and temperature. The authors found a significant interaction between particle size and pH, observing that the adsorption capacity of pollutants increased with the interaction between these two variables, arguing that pH can change the configuration of the deposited particles favoring adsorption. In this sense, an increase of pH would cause an increase in negative charges on the surface of the sediment.

The chemical composition of the sediments of all the studied environments (Table 2) was dominated by silicon oxides (SiO_2) with an average content of 61.4% (73.3–55.3%) followed by aluminum oxides (Al_2O_3) with concentrations ranging between 11.5% in Lake Caviahue and 22.5% in Lake Lácar. Overall, the mineralogy was dominated by quartz (SiO_2), a stable mineral and a main component of clays. In general, from the performed PCA (Fig. 4), we can identify a first gradient (axis 1) given by pH and SiO_2 that clearly separates Lake Caviahue from the rest of the

Table 2 Average pH values in water and chemical composition of sediments of the analyzed water bodies. The acronyms for each water body are defined in Table 1

	Water	SiO_2	Al_2O_3	Fe_2O_3	CaO	MgO	Na_2O	K_2O	TiO_2
	pH	(%)	(%)	(%)	(%)	(%)	(%)	(%)	(%)
EC	8.1	58.9	17.9	4.8	9.5	3.3	2.9	2.2	0.6
EN	8.3	59.0	17.9	4.9	9.9	3.0	2.6	2.1	0.5
LC	2.5	73.3	11.5	2.4	1.1	0.7	2.6	0.9	1.3
EB	8.0	55.3	18.4	8.9	5.3	2.9	2.8	3.2	1.2
LL	7.7	57.0	22.5	9.0	3.7	2.5	3.4	1.1	0.8
EA	7.4	–	–	–	–	–	–	–	–
EPA	7.0	–	–	–	–	–	–	–	–
LM	7.0	63.5	15.1	10.3	2.9	1.6	2.0	1.7	0.7
LCChica	8.4	56.6	17.4	7.0	7.4	4.0	1.4	1.4	0.8
LÑe	8.2	62.3	20.7	7.5	3.2	3.1	0.7	1.4	0.8
LNH	7.3	–	–	–	–	–	–	–	–
LBS	7.8	62.6	19.7	6.3	2.2	2.4	3.2	2.3	0.8
LP	8.3	60.0	20.9	6.6	0.6	1.2	1.5	3.9	0.7
LCardiel	9.2	65.4	17.3	5.7	2.7	3.3	3.2	1.7	0.8
LA	7.5	62.6	19.7	6.3	2.2	2.4	3.2	2.3	0.8

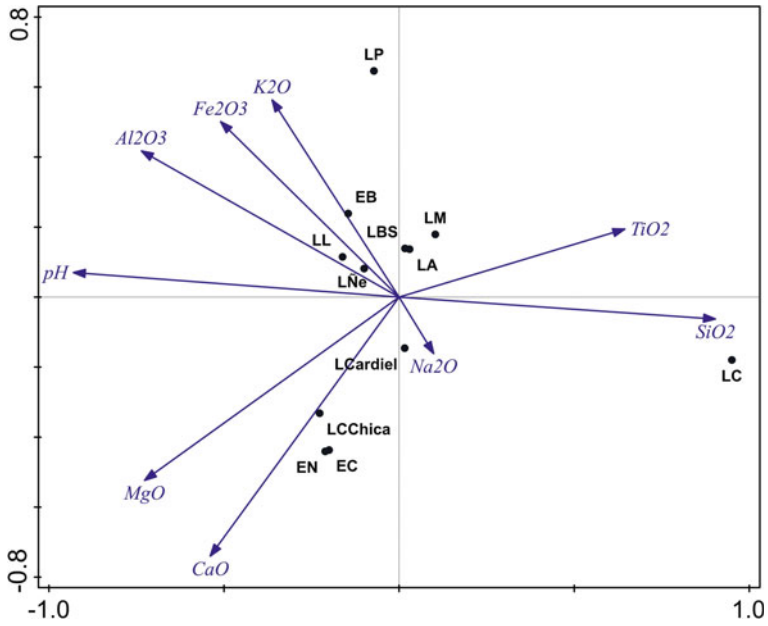

Fig. 4 PCA of chemical variables performed on sediment samples from the studied environments. Both axes explain 61.06% of the total variance of the data. The acronyms for each water body are defined in Table 1

studied environments, while a second gradient (axis 2) was linked to pH with the oxides of Fe, Al, Ca, K and Mg. Both axes explained 61.1% of the total variance of the data.

Certain distinctive peculiarities could be observed in some of the studied environments:

(a) The environments of Southern Mendoza (El Carrizal and El Nihuil reservoirs) were characterized by the presence of CaO as the third most important component of sediments with an average concentration of 9.7%. In this sense, León et al. (2017) found that the chemical composition of sediments from these two environments was characterized by calcium enrichment compared to the chemical composition of the Earth's continental crust and suspended material transported by rivers of South America, North America, Africa, Asia, and Europe. This was in accordance with the basin lithology, which is characterized by deposits rich in gypsum and calcite (Sruoga et al. 2005; Ramos et al. 2010), suggesting an endogenous formation of calcium minerals (León and Pedrozo 2015).

(b) For the rest of the water bodies located in the North–South geographic gradient, iron oxides (Fe_2O_3) were the third most important component of the sediments with an average concentration of 7.0% (between 5.7 and 10.3%).

(c) For the acidic environment Lake Caviahue, Temporetti et al. (2013) found that SO_3 was important in the chemical composition of lake sediments, with concentrations varying between 3.4 and 6.1%.

Regarding the mineralogical composition, the analysis of Lake Caviahue sediments showed that the predominant minerals were andesite ($(Na, Ca)(Si,Al)_4O_8$), albite ($Na(Si_3Al)O_8$), anorthite ($Na(Al_2Si_2O_8$) and cristobalite (SiO_2), indicating the volcanic origin of this sediments (Temporetti et al. 2013). According to Pesce (1989), the predominant rocks in this area are andesitic and pyroclastic lavas related to the dynamics of Andean volcanism. Furthermore, Murad and Rojík (2003) showed the relationship of pH with the mineralogy by studying the effect on drainage water of abandoned mines in the Czech Republic. These authors found a direct relationship between pH variation and mineral precipitation. In this sense, Temporetti et al. (2019) studied the Agrio River sediments in a natural pH gradient ranging from 1.7 to 6.7 from the river headwaters to 50 km downstream. They found a greater mineral diversity in this gradient. In sites where the pH varied between 2.8 and 4.9, the minerals associated with Fe such as magnetite, pigeonite, and iron and calcium silicates were predominant. On the other hand, minerals associated with aluminum compounds, such as anorthite and Al and Na silicates, predominated in sites from Agrio River where the pH varied between 5.4 and 6.7, although, in this case, pH would not control the crystallization of these minerals. These results were reflected in the formation of coatings found along this gradient (Fig. 5) and coincided with those reported by Parker et al. (2008), who observed orange coatings of hydrated ferric oxide ($Fe_2O_3.xH_2O$; HFO) and others of white hydrated aluminum oxide ($Al_2H_2O_4$; HAO) on rocks along the pH gradient of the Agrio River.

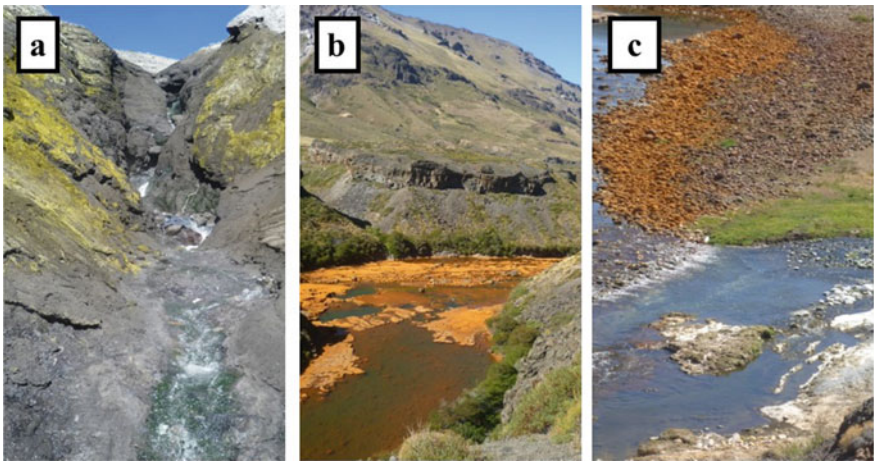

Fig. 5 Photographs of the rocks coatings taken at three different sites of Agrio River. **a** Sulfur coatings in the river headwater (water pH = 1.77); **b** iron coating downstream Agrio River Cascade (water pH = 4.11), and **c** aluminum coating in the confluence of Agrio (water pH = 5.30) and Ñorquín (water pH = 7.00) rivers

Moreover, for El Carrizal and El Nihuil reservoirs, León et al. (2017) observed that sediment mineralogy reflected the richness of calcium in the system, and the most abundant identified minerals (14%) were calcium carbonates and phosphates. Furthermore, these authors found that the amount of P-containing minerals was relatively high, mainly Ca phosphates and hydrated Al and Fe phosphates (11% and 3%, respectively).

4 Phosphorus and Its Fractions

In most of the aquatic environments of the Patagonian region, the main contamination problem is linked to eutrophication. It is an environmental issue of great global concern. In this sense, it is necessary to know not only the total amount of nutrients in the sediment, mainly P, but also the main sediment phases to which this nutrient is associated. Data on phosphorus fractionation enables the evaluation of the bioavailable fraction, which can contribute to the trophic state of the system (Pardo et al. 2003). On the other hand, in aquatic systems, the highest amount of P associated with sediments can be found linked to Fe/Al(OOH) or $CaCO_3$ (Golterman 2004). In addition, a considerable amount of phosphate is present as organic P, most of which is in the solid phase and a little portion in solution like inorganic P.

The analysis of TP concentration and its fractions in sediments of the studied water bodies can be carried out by considering three approaches: (a) **North–South geographic gradient**: TP concentration decreases southwards (Fig. 6a). From the data analysis, a negative ($r = -0.56$) and significant ($p < 0.05$) correlation was found between the latitude and TP concentration in sediments. This is probably related to the fact that the studied environments located south of 42° S have a very low anthropogenic pressure. (b) **pH gradient**: when analyzing P fractions, we observed that in environments with acidic and neutral pH, P control was associated with P bound to Fe/Al oxyhydroxides (Fig. 6b). However, this control begins to reverse when pH exceeds 7.0. As pH increases, P control is associated with bonding to Ca compounds (Fig. 6c). Although correlation analysis only showed a negative ($r = -0.95$) and significant ($p < 0.05$) correlation between the environments and the P bound to Fe/Al oxyhydroxides, the PCA indicated the existence of a gradient linked to the pH in the studied environments. Similar results were observed by Temporetti et al. (2019) when they analyzed the sediments of The Agrio River which shows a natural pH gradient. (c) **Trophic gradient**: when analyzing the content of P-labile (Fig. 6d), which is the one that is released more quickly into the water column (internal load) and is readily available for algal growth, it is observed that oligotrophic water bodies present lower P-labile concentrations than mesotrophic and eutrophic water bodies. In this case, the effect of the geographic gradient is less noticeable for the oligotrophic water bodies than for the mesotrophic and eutrophic studied water bodies. The performed PCA showed this gradient, and a negative ($r = -0.83$) and significant ($p < 0.05$) correlation was found between the studied water bodies and their meso-eutrophic condition.

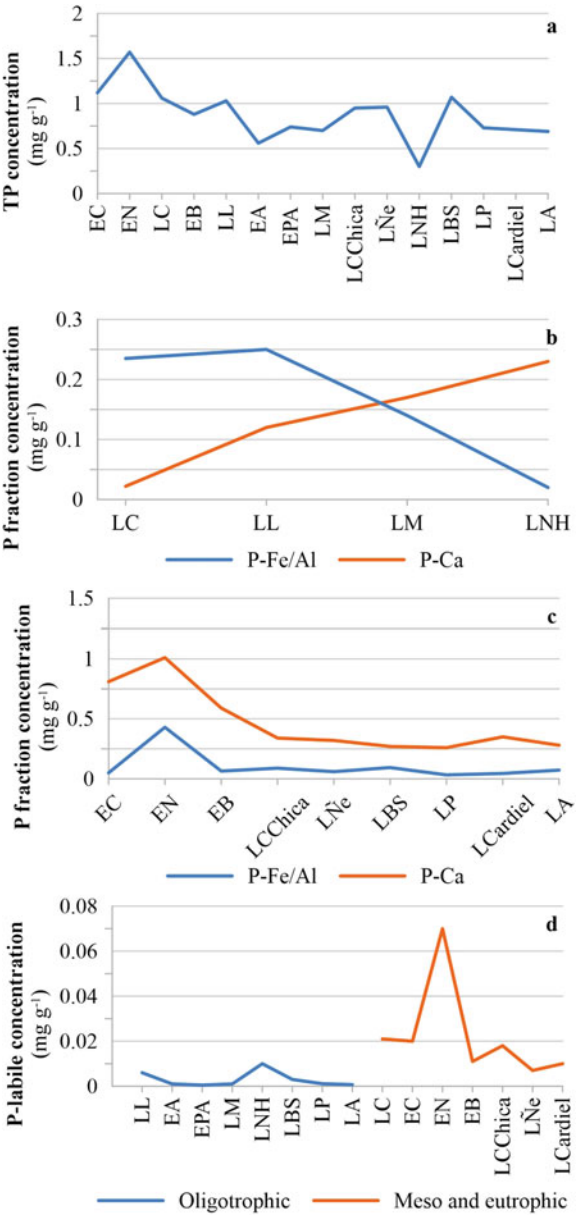

Fig. 6 **a** Variation of TP concentration in sediment samples from the studied environments. **b** Variation of P concentrations bound to iron and aluminum oxyhydroxides (P-Fe/Al) and calcium compounds (P-Ca) in sediments from acidic and neutral studied environments. **c** Variation of P concentrations bound to iron and aluminum oxyhydroxides (P-Fe/Al) and calcium compounds (P-Ca) in sediments from alkaline studied environments. **d** Variation of the P-labile concentration in relation to the trophic state of the studied environments. The acronyms for each water body are defined in Table 1

In an aquatic environment, P distribution in the sediment profile may indicate that the potentially mobile P may be represented by the difference between TP concentration in sediment surface and TP concentration at the stabilization depth (Carey and Rydin 2011). This potentially mobile P will eventually be released into the water column (Boström et al. 1982; Rydin 2000) and is mainly associated with iron and organic matter (Rydin 2000). According to Carey and Rydin (2011), the depth pattern of TP distribution in lake sediments can vary significantly between oligotrophic and eutrophic systems, which may explain the differences between low and high levels of nutrients in environments of different trophic states. Temporetti et al. (2014b) evaluated this hypothesis in the sediments of eight Patagonian environments such as lakes, lagoons and reservoirs. The results showed that oligotrophic lakes tend to accumulate P, whereas eutrophic lakes tend to release this nutrient into the water column. On the other hand, they observed that certain parameters of interstitial water and sediments were significantly correlated with the trophic state of the studied environments; in particular: (a) soluble reactive phosphorus (SRP) concentration in pore water, (b) P-labile fraction concentration, (c) TP depth distribution pattern, and (d) metal/P ratio (MPS). In the study mentioned above, only reservoir El Nihuil was classified as mesotrophic, presenting a homogeneous sediment TP distribution pattern that was intermediate between oligotrophic and eutrophic environments. In this case, sediments could be enriched with phosphorus, but they would be close to saturation, showing a homogeneous pattern of TP depth distribution. On the other hand, these authors observed that oligotrophic environments had a positive linear slope while eutrophic environments had a negative linear slope. However, some exceptions to these patterns were detected: (a) Lake Lácar, an oligotrophic environment which should have shown a positive linear slope but actually presented a negative linear slope; and (b) Lake Caviahue, an eutrophic environment (according to P concentration in water) presented a positive linear slope characteristic of oligotrophic environments. Finally, Temporetti et al. (2014b) concluded that, to define the trophic state of aquatic environments both, sediments, and interstitial water, could be considered more comprehensive parameters than the typical water column parameters. By considering the sediment TP distribution pattern, it is possible to determine if P fixation or sediment release into the water column is occurring.

5 Phosphorus Fixation/Release Capacity

Sediment TP content in aquatic environments depends on factors such as physicochemical conditions, chemical and textural composition, sedimentation rates, and diagenetic processes (Anshumali and Ramanathan 2007; Li et al. 2007). The balance between P fraction associated with sediments and that dissolved in the water column is determined by redox conditions (Boström et al. 1982; Sinke 1992; Katsev et al. 2006), adsorption processes, solubility in the mineral phase and mineralization of OM (Kaiserli et al. 2002), among other parameters.

According to Li et al. (2007), particulate OM sedimentation, anaerobic bacteria activity and dissolved oxygen decrease at the sediment surface produce reduced compounds that cause a decrease in redox potential. In turn, this decrease triggers the release of electrons that can be transferred to the oxidizing components (e.g. iron, aluminum and manganese oxides). These reduced compounds dissolved in the water column can decrease P adsorption capacity. Besides, the products of the reduction reactions [e.g. organic anions, ammonium ($N\text{-}NH_4^+$) and elemental sulfur (S)] compete with P for adsorption sites in sediments, generating phosphorus release into the water column (Koski-Vähälä et al. 2001). In sediments, P sorption mechanisms are generally studied through empirical models that describe the characteristics of these processes, such as Freundlich and Langmuir isotherms (Langmuir 1997; Limousin et al. 2007). Isotherm tests have been widely used to estimate P adsorption in soils (Tunesi et al. 1999), in river sediments (Lin et al. 2009), lake and reservoir sediments (Wang et al. 2009), and in purified solid media (Freeman and Rowell 1981; Yagi and Fukushi 2012; Perassi and Borgnino 2014; Abdala et al. 2015).

León et al. (2017) studied two reservoirs with naturally high sulfate waters in Southern Mendoza (El Nihuil and El Carrizal) to assess the effect of this anion concentration on geochemical processes acting upon P bonding and speciation in sediments. These authors observed that only El Carrizal sediments adjusted to a typical Langmuir isotherm, while El Nihuil sediments adjusted to a steeper slope that changed from positive to negative. These authors concluded that this last pattern was established as a result of initial adsorption at low concentrations of dissolved P and co-precipitation of P bound to carbonates at higher concentrations of P. The percentage of dissolved P after the test carried out with El Nihuil sediments reservoir was low (18%) compared to that of El Carrizal sediments (69%), which suggests that the co-precipitation of P in the first reservoir may be occurring at higher rates than in the second reservoir.

Furthermore, P fixation isotherms were used to determine the sorption capacity of natural sediments and those affected by intensive salmonid farming in Lake Moreno and reservoir Alicura (Temporetti et al. 1991; Temporetti 1998). The results of P uptake kinetics by natural sediments from both environments confirmed that the dominant processes were regulated by equilibrium reactions and that is the reason why they could be described by the Freundlich and Langmuir isotherms. These sediments are receiving part of the phosphorus entering the basin. Phosphorus fixing capacity was lower in Moreno sediments than in Alicura sediments; this could be due to the fact that the dominant texture in Lake Moreno was sand, while the silty fraction predominated in reservoir Alicura. The predominance of the Ca as a control mechanism for P precipitation over the organic matter-iron mechanism agrees with the results obtained by Shulka et al. (1971), who observed that calcareous sediments retained more phosphorus than non-calcareous sediments. On the other hand, Temporetti (1998) observed in the reservoir Alicura, that the sediments in the area affected by fish farming, compared with sites located upstream and downstream of it, had a high P content that exceeded its fixation capacity, releasing P into the water column (Fig. 7). Othaz Brida (2021) used P sorption experiments to estimate P adsorption capacity in sediments from three reservoirs in Patagonia. In two of them

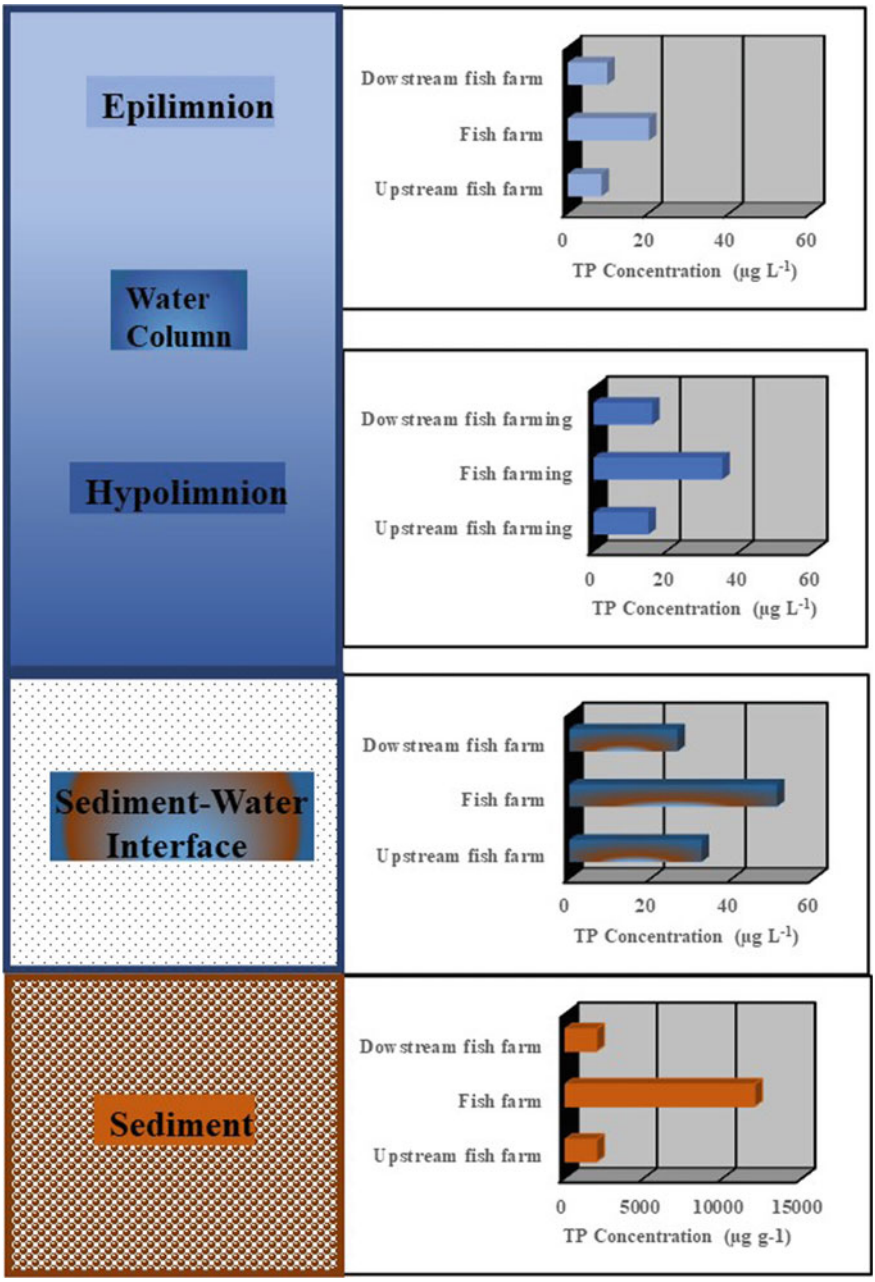

Fig. 7 Decreasing pattern of TP concentration from sediments to epilimnion at three stations in Reservoir Alicura: upstream of fish farm, fish farm and downstream fish farm

(Alicura and Piedra del Águila), since the 1990s and promoted by the administrations of Neuquén and Río Negro provinces, salmonid farms have been installed for intensive farming. Currently, its production is concentrated mainly in reservoir Alicura, where seven companies are operating with a total production of 1200 tons y^{-1}, and in Piedra del Águila there are operating three companies with a total production of 100 tons y^{-1}. The results showed that: 1) although the two reservoirs have an adequate P adsorption capacity, Alicura sediments (in the main body of the reservoir) presented a lower P fixation capacity (1026 $\mu g\ g^{-1}$ d.w., 43%) than Piedra del Águila sediments (1268 $\mu g\ g^{-1}$ d.w., 57%). Additionally, evaluations carried out on sediments under Alicura breeding cages showed, in all cases, that sediments are saturated or close to saturation (CFI 2013), highlighting the impact generated by the higher aquaculture production in this reservoir.

Antonuk (2010) and Temporetti et al. (2014a) used P adsorption capacity to determine the saturation degree of sediments affected by sewage discharge into Lake Lácar. These authors evaluated the sediment quality (P contribution) of the eastern bay of the lake, affected by the discharge of residual waters. They compared sites within the bay with a control site located in the center of the lake and away from the bay. For all the evaluated sites, the results of the performed isotherms adjusted for both, Freundlich and Langmuir isotherms. From this last equation, the authors estimated that the maximum P fixation capacity to the sediment was 17% within the bay and 36% for the control site. These percentages indicated that the sediments within the bay are almost saturated, which may cause a release of nutrients from sediments into the water column.

6 Bioassays with Sediments

By definition, a bioindicator is any species or group of species whose function, population, or condition can reveal the qualitative state of the environment (Ospina Álvarez and Peña 2004). In the case of biological indicators, the presence or absence of certain species constitutes a unit of measurement for the qualitative conditions of a water body. Once an aquatic ecosystem is characterized, the presence and quantity of certain species could directly and accurately indicate the concentrations of specific pollutants (Ptacnik et al. 2008). The most widely used techniques to assess the bioavailability of nutrients and the toxicity of contaminated sediments are **phytoplankton** bioassays (Aksmann and Tukaj 2004; Ramadass et al. 2016). Due to short generation times, the use of planktonic algae as indicators is useful given its rapid response to a contamination process. Quantitative variation in phytoplankton communities is the first response to aquatic environmental changes, and an increase or decrease in algae abundance can be observed depending on the type of damage. Furthermore, qualitative changes can also be observed in phytoplankton communities since new species can colonize the environment while others can decrease and occasionally disappear (Ptacnik et al. 2008). Autochthonous phytoplankton populations are widely used

as bioassays to determine nutrient limitation and resource competition (Tilman and Kilham 1976; Goldman 1978; Tilman et al. 1986; Reynolds 1992).

Diaz et al. (2001) used bioassays with native phytoplankton to assess the response of this communities to the addition of nutrients generated by the intensive production of cage trout in reservoir Alicura. Bioassays were carried out by using sediments affected and unaffected by fish farming, with water and phytoplankton from the environment. These authors found that both, algal biomass, and fresh weight, as well as chlorophyll-a content showed the highest concentrations in bioassays with contaminated fish farming sediments, increasing biomass up to 700% compared to bioassays with uncontaminated sediments. On the other hand, they also observed that nutrient concentrations released from the contaminated sediments to the water in the bioassays increased considerably after 15 days of incubation. These authors concluded that the main consequences of aquaculture activities in the reservoir are an increase in nutrient concentrations, algae density, and phytoplankton biomass due to the release of nutrients from the sediments into the water column. Similar results were obtained by Temporetti (1998), who used algal bioassays to evaluate the effect of contaminated sediments by fish farms in Lake Moreno.

Rotondo et al. (2021) worked in reservoir Los Barreales, located in the most important oil basin of Argentinian Patagonia, Vaca Muerta, and they used bioassays to evaluate the response of phytoplankton and the nutrient availability from contaminated sediments with increasing doses of polycyclic aromatic hydrocarbons (PAHs). On the other hand, they determined the use of native algae from this environment as bioindicators of PAH contamination in sediments. These authors carried out four different bioassays that allowed them to evaluate: (a) the effect of sediment contamination on nutrient availability in solution; (b) the effect of sediment contamination on phytoplankton to highlight the presence of one or more indicator species; (c) the response of an algae species as a potential indicator of sediment contamination; and (d) the response of an algae species to water contamination. To carry out these bioassays, they used water, algae, and sediment from the reservoir, and contaminated the sediments with increasing concentrations (0 (basal), 50, 100, 250, 500, and 1000 ppm) of Phenanthrene (Ph), Anthracene (An), Pyrene (Py) or Benzo(a)anthracene (Ba). The main obtained results showed that PAH contamination of sediments from reservoir Los Barreales modified the release of nutrients into the water column, and also affected the growth of the dominant species of phytoplankton *Scenedesmus quadricauda* at concentrations of at least 50 ppm Ba, 250 ppm Ph, and 1000 ppm Py. The results indicated that bioassays with native algae species from the reservoir were useful in detecting the effect of PAH contamination on sediments and constitute the first approach to create a rapid monitoring tool for assessing the effect of oil spills on the hydrocarbon formation of Vaca Muerta.

7 Conclusions

In this chapter, we evaluated different parameters related to the sediments of eleven aquatic environments of Argentinian Patagonia with different characteristics and degrees of anthropic impact. The main conclusions are:

(1) pH is one of the main parameters that influence P exchange between sediments and the water column. It was demonstrated that the P adsorption capacity in sediments decreases with increasing pH.
(2) Parameters such as texture, chemical composition and mineralogy are essential to understand sediment genesis and transport mechanisms, and to infer limnological, hydrological and climatic conditions from past events.
(3) Three gradients determine different degrees of approach to the distribution of the studied environments: (a) **North–South geographic gradient**, with a tendency to decrease the TP concentration in sediments. (b) **pH gradient**, which determined that, in general, sediment P control in environments with acidic and neutral pH is by Fe/Al oxyhydroxides, while in environments with slightly alkaline to alkaline pH, sediment P control is by Ca compounds. (c) **Trophic gradient**, which determined that P more readily available for algal growth (P-labile) is lower in oligotrophic environments than in mesotrophic and eutrophic environments.
(4) The study of different P fractions, as well as P adsorption/release capacities from sediments, was essential to define the control mechanisms of this nutrient in sediments. Furthermore, understanding these mechanisms will make it possible to evaluate their internal load, necessary when assessing the degree of eutrophication of a water body and/or the carrying capacity of water bodies. This information is important to carry out any productive activity in any aquatic environment.
(5) The use of sediment bioassays with native algae is a particularly useful tool for rapidly evaluating the anthropic impact on water bodies, enabling the detection of algal species sensitive to the presence of specific contaminants.
(6) Sediment studies are a tool for obtaining information on, for example, contaminated and uncontaminated areas, and contaminant distribution patterns. In this sense, these studies should be included when defining monitoring programs since, in many cases, sediment parameters are usually more stable than those measured in the water column, which can present daily or seasonal fluctuations.

References

Abdala DB, Northrup PA, Arai Y, Spearks DL (2015) Surface loading effects on orthophosphate surface complexation at the goethite/water interface as examined by extended X-ray Absorption Fine Structure (EXAFS) spectroscopy. J Colloid Interface Sci 437:297–303

Aksmann A, Tukaj Z (2004) The effect of anthracene and phenanthrene on the growth, photosynthesis, and SOD activity of the green alga Scenedesmus armatus depends on the PAR irradiance and CO_2 level. Arch Environ Cont Toxic 47(2):177–184

Alemanni E (2006) Estado trófico del lago Nahuel Huapi en relación con el crecimiento poblacional urbano en San Carlos de Bariloche. Informe Final Universidad Nacional del Comahue (in Spanish)

Anderson JM (1974) Nitrogen and phosphorus budgets and the role of sediments in six shallow Danish Lakes. Arch Hydrobiol 74:527–550

Anshumali A, Ramanathan L (2007) Phosphorus fractionation in surficial sediments of Pandoh lake, lesser Himalaya, Himachal Pradesh, India. Appl Geochem 22:1860–1871

Antonuk L (2010) Influencia de la descarga de líquidos cloacales sobre los sedimentos de la cubeta Oriental del Lago Lácar. Universidad Nacional del Comahue (in Spanish), Tesis de grado

APHA, American Public Health Association. (1999) Standard methods for the examination of water and wastewater. American Public Health Association, Washington, D.C.

Boström B, Jansson M, Forsberg C (1982) Phosphorus release from lake sediments. Arch Hydrobiol Beih Erg Limnol 18:5–59

Boyle JF (2001) Inorganic geochemical methods in palaeolimnology. In: Last WM, Smol JP (eds) Tracking environmental change using lake sediments. Phys Geochem Methods, Dordrecht, Netherlands, pp 82–141

Cabrera JM, Diaz MM, Schultz S, Temporetti P, Pedrozo F (2016) Iron buffer system in the water column and partitioning in the sediments chemical phases of the naturally acidic lake Caviahue, Neuquén, Argentina. J Volcanol Geother Res 318:19–26

Cabrera JM, Temporetti PF, Pedrozo FL (2020) Trace metal partitioning and potential mobility in the naturally acidic sediment of Lake Caviahue, Neuquén Argentina. Andean Geol 47(1):46–60

Carey C, Rydin E (2011) Lake trophic status can be determined by the depth distribution of sediment phosphorus. Limnol Oceanogr 56:2051–2063

Carpenter S (2005) Eutrophication of aquatic ecosystems: Bistability and soil phosphorus. PNAS 102:10002–10005

Carter M (1993) Soil sampling and methods of analysis. Canadian Society of Soil Science. Canada: Lewis Pub

CFI, Federal Investment Council, COPADE, UNCo (2013) Caracterización técnica-ambiental de sitios en uso y potenciales para la producción acuícola en el embalse Alicura. Calidad de agua y sedimentos por sitio. https://copade.neuquen.gob.ar/Pub.Detalle.aspx?Id=4879 (in Spanish). Accessed 2 Mar 2020

Cunha D, Fernandes G, Calijuri M, Lamparelli MC (2013) A trophic state index for tropical/subtropical reservoirs (TSI-tsr). Ecol Engineer 60:126–134

Diaz M, Mora V, Pedrozo F, Nichela D, Baffico G (2015) Evaluation of native acidophilic algae species as potential indicators of polycyclic aromatic hydrocarbon (PAH) soil contamination. J Appl Phycol 27(1):321–325

Diaz MM, Temporetti P, Pedrozo F (2001) Response of phytoplankton to enrichment from cage fish farm waste in Alicura Reservoir (Patagonia, Argentina). Lakes & Reservoirs Res Manag 6:151–158

Ding S, Wang Y, Wang D, Li YY, Gong M, Zhang C (2016) In situ, high-resolution evidence for iron-coupled mobilization of phosphorus in sediments. Sci Rep 6:24341

Einsele W (1936) Uber die beziehungen des eisenkreislaufszum phosphatkreislauf im eutrophen see. Arch Hydrobiol 29:664–686

Einsele W (1938) Uber chemische und kolloidchemische vorgange in eisen-phosphat-systemen unterlimnochemischen und limnogeologischen gesichtspunkten. Arch Hydrobiol 33:361–387

Elser JJ, Bracken ME, Cleland EE, Gruner DS, Harpole WS, Hillebrand H, Smith JE (2007) Global analysis of nitrogen and phosphorus limitation of primary producers in freshwater, marine and terrestrial ecosystems. Ecol Lett 10(12):1135–1142

Forsberg C (1989) Importance of sediments in understanding nutrient cyclings in lakes. Hydrobiologia 176(177):61–75

Forsythe W (1985) Física de suelo. Manual de laboratorio. Instituto Interamericano de Cooperación para la Agricultura, San José, Costa Rica
Freeman JS, Rowell DL (1981) The adsorption and precipitation of phosphate onto calcite. J Soil Sci 32(1):75–84
Goldman JC (1978) The use of natural phytoplankton populations in bioassay. Mitt Int Ver Limnol 21:364–371
Golterman HL (2004) The chemistry of phosphate and nitrogen compounds in sediments. Kluwer Academic Publishers, London
Golterman HL, Sly PG, Thoma RL (1983) Study of the relationship between water quality and sediment transport. UNESCO, USA
Håkanson L, Jansson M (1983) Principles of lake sedimentology. Springer, Heidelberg
Hieltjes AH, Lijklema L (1980) Fractionation of inorganic phosphates in calcareous sediments. J Environ Qual 9(3):405–407
Horne AJ, Goldman ChR (1994) Limnology. McGraw Hill Inc., New York
Iriondo M (1989) Quaternary lakes of Argentina. Palaeogeogr Palaeoclimatol Palaeoecol 70:81–88
Jeppesen E, Jeppesen E, Søndergaard M, Jensen JP, Havens KE, Anneville O et al (2005) Lake responses to reduced nutrient loading–an analysis of contemporary long-term data from 35 case studies. Freshw Biol 50(10):1747–1771
Jin X, Wang S, Pang Y, Wu FC (2006) Phosphorus fractions and the effect of pH on the phosphorus release of the sediments from different trophic areas in Taihu Lake, China. Environ Pollut 139:288–295
Juncos R, Campbell L, Arcagni M, Daga R, Rizzo A, Arribere M, Ribeiro Guevara S (2017) Variations in anthropogenic silver in a large Patagonian lake correlate with global shifts in photographic processing technology. Environ Pollut 233:685–694
Kaiserli A, Voutsa D, Samara C (2002) Phosphorus fractionation in lake sediments: Lakes Volvi and Koronia N. Greece. Chemosphere 46:1147–1155
Katsev S, Tsandev I, L'Heureux I, Rancourt DG (2006) Factors controlling long-term phosphorus efflux from lake sediments: Exploratory reactive-transport modelling. Chem Geol 234:127–147
Kim LH, Choi E, Stenstrom MK (2003) Sediment characteristics, phosphorus types and phosphorus release rates between river and lake sediments. Chemosphere 50:53–61
Koski-Vähälä J, Hartikainen H, Tallberg P (2001) Phosphorus mobilization from various sediment poolin response to increased pH and silicate concentration. J Environ Qual 30:546–552
Langmuir D (1997) Aqueous environmental geochemistry. Prentice Hall, Pearsson
Larsen K, Shults L, Malneg A (1981) Summer internal phosphorus supplies in shagawa lakes Minnesota. Limnol Oceanogr 26(4):740–754
Last W (2001) Textural analysis of lake sediment. In: Last WM, Smol JP (eds) Tracking environmental change using lake sediments. Kluwer Academic Publishers, Dordrecht, Netherlands, pp 41–81
Last W (2001) Mineralogical analysis of lake sediment. In: Last WM, Smol JP (eds) Tracking environmental change using lake sediments. Kluwer Academic Publishers, Dordrecht, Netherlands, pp 143–187
Lee-Hyung K, Choi E, Stenstrom MK (2003) Sediment characteristics, phosphorus types and phosphorus release rates between river and lake sediments. Chemosphere 50(1):53–61
León JG, Pedrozo FL (2015) Lithological and hydrological controls on water composition: evaporite dissolution and glacial weathering in the south central Andes of Argentina (33°–34° S). Hydrol Process 29:1156–1172b
León JG, Pedrozo FL, Temporetti PF (2017) Phosphorus fractions and sorption dynamics in the sediments of two Ca-SO_4 water reservoirs in the central Argentine Andes. Int J Sediment Res 32:442–451
Lewis DW (1984) Practical sedimentology. Hutchinson Ross Publishing Company, New York
Li M, Liu J, Xu Y, Qian G (2016) Phosphate adsorption on metal oxides and metal hydroxides: a comparative review. Environ Rev 24(3):319–332

Li Q, Zhang W, Wang X, Zhou Y, Yang H, Ji G (2007) Phosphorus in interstitial water induced by redox potential in sediment of dianchi lake China. Pedosphere 17(6):739–746
Limousin G, Gaudet JP, Charlet L, Szenkect S, Barthes V, Krimissa M (2007) Sorption isotherms: a review on physical bases, modelling and measurement. J Appl Geochem 22(2):249–275
Lin C, Wang Z, He M, Li Y, Liu R, Yang Z (2009) Phosphorus sorption and fraction characteristics in the upper, middle and low reach sediments of the Daliao river systems, China. J Haz Mat 170:278–285
Maasen S, Uhlmann D, Roske I (2005) Sediment and porewater composition as a basis for the trophic evaluation of standing waters. Hidrobiologia 543:55–70
Matteucci S (2012a) Ecorregión Bosques Patagónicos. In: Morello J, Matteucci S, Rodríguez A, Silva M (eds) Ecorregiones y complejos ecosistémicos argentinos. Orientación Gráfica Editora (in Spanish), Buenos Aires, pp 489–547
Matteucci S (2012b) Ecorregión estepa patagónica. In: Morello J, Matteucci S, Rodríguez A, Silva M (eds) Ecorregiones y complejos ecosistémicos argentinos. Orientación Gráfica Editora (in Spanish), Buenos Aires, pp 549–654
McDaniel M, Marshall D, Mark B, Todd VR (2009) Relationships between benthic sediments and water column phosphorus in Illinois streams. J Environ Qual 38(2):607–617
Mortimer CH (1941) The exchange of dissolved substances between mud and water in lake. J Ecol 29:280–329
Mortimer CH (1942) The exchange of dissolved substances between mud and water lakes. J Ecol 30:147–201
Murad E, Rojík P (2003) Iron-rich precipitates in a mine drainage environment: Influence of pH on mineralogy. Am Mineral 88:1915–1918
Murphy J, Riley JP (1962) A modified single solution method for the determination of phosphate in natural waters. Analyt Chim Acta 27:31–35
OECD, Organization for Economic Cooperation and Development (1982) Eutrophication of waters, monitoring, assessment and control. Organization for Economic Co-operation and Development, París
Ospina Alvarez N, Peña EJ (2004) Alternativas de monitoreo de calidad de aguas: Algas como bioindicadores. Acta Nova 2(4):513–517 (in Spanish)
Othaz Brida A (2021) Dinámica de nutrientes en cinco embalses en cadena en la cuenca del río Limay, Norpatagonia Argentina. Tesis Maestría. Universidad Nacional del Comahue (in Spanish)
Pardo P, Rauret G, López-Sánchez JF (2003) Analytical approaches to the determination of phosphorus partitioning patterns in sediments. J Environ Monit 5:312–318
Parker SR, Gammons CH, Pedrozo FL, Wood SA (2008) Diel changes in metal concentrations in a geogenically acidic river: river Agrio, Argentina. J Volcanol Geotherm Res 178:213–223
Pedrozo F, Chillrud S, Temporetti P, Diaz M (1993) Chemical composition and nutrient limitation in rivers and lakes of Northern Patagonian Andes (39.5°-42° S; 71°W). Verh Internat Verein Theoret Angew Limnol 25:207–214
Pedrozo F, Kelly L, Diaz M, Temporetti P, Baffico G, Kringel R et al (2001) First results on the water chemistry, algae and trophic state of an Andean acidic lake system of volcanic origin in Patagonia (Lake Caviahue). Hidrobiologia 452:129–137
Perassi I, Borgnino L (2014) Adsorption and surface precipitation of phosphate onto $CaCO_3$-montmorillonite: Effect of pH, ionic strength and competition with humic acid. Geoderma 232:600–608
Pesce AH (1989) Evolucion volcano-tectonic del complejo efusivo copahue-caviahue y su modelo geotérmico preliminar. RAGA 44:307–327 (in Spanish)
Ptacnik R, Lepistö L, Willén E, Brettum P, Andersen T, Rekolainen S, Carvalho L (2008) Quantitative responses of lake phytoplankton to eutrophication in northern Europe. Aquat Ecol 42(2):227–236
Queimaliños C, Reissig M, Diéguez MC, Arcagni M, Ribeiro Guevara S, Campbell L et al (2012) Influence of precipitation, landscape and hydrogeomorphic lake features on pelagic allochthonous

indicators in two connected ultraoligotrophic lakes of North Patagonia. Sci Total Environ 427–428:219–228
Quirós R, Drago E (1999) The environmental state of Argentinean lakes: An overview. Res Manag 4:55–64
Ramadass K, Megharaj M, Venkateswarlu K, Naidu R (2016) Sensitivity and antioxidant response of Chlorella sp. MM3 to used engine oil and its water accommodated fraction. Bull Environ Contam Toxicol 97(1):71–77
Ramos VA, Aguirre Urreta MB, Alvarez PP, Coluccia A, Giambiagi LB, Pérez D, Tunik Vujovich G (2010) Geologic sheet 3369-III cerro Tupungato (1: 250.000). Servicio Geológico Minero Argentino, Buenos Aires. Instituto de Geología y Recursos Minerales (in Spanish)
Reynolds CS (1992) Eutrophication and management of planktonic algae: what Vollenweider couldn't tell us. In: Sutcliffe DW, Jones JG (eds) Eutrophication: research and application to water supply. Freshw Biol Assoc., Ambleside, pp 4–29
Ribeiro Guevara S, Arribére M, Bubach D, Vigliano P, Rizzo A, Alonso A, Sánchez R (2005a) Silver contamination on abiotic and biotic compartments of Nahuel Huapi National Park lakes, Patagonia, Argentina. Sci Total Environ 336:119–134
Ribeiro Guevara S, Meili M, Rizzo A, Daga R, Arribére MA (2010) Sediment record of highly variable mercury inputs to mountain lakes in Patagonia during the past millennium. Atms Chem Phys 10:3443–3453
Ribeiro Guevara S, Pérez Catán S, Marvin-DiPasquale M (2009) Benthic methylmercury production in lacustrine ecosystems of Nahuel Huapi National Park, Patagonia, Argentina. Chemosphere 77:471–477
Ribeiro Guevara S, Rizzo A, Sánchez R, Arribére M (2003) ^{210}Pb fluxes in sediment layers sampled from northern Patagonia lakes. J Radioanal Nucl Chem 258(3):583–595
Ribeiro Guevara S, Rizzo A, Sánchez R, Arribére M (2005b) Heavy metal inputs in northern Patagonia lakes from short sediment core analysis. J Radioanal Nucl Chem 265(3):481–493
Rotondo L, Temporetti P, Mora V, Diaz M, Beamud G, Baffico G, Pedrozo F (2021) Effects of sediment contamination by PAHs on nutrients and growth of *Scenedesmus quadricauda*. Environ Earth Sci 80:66
Rydin E (2000) Potentially mobile phosphorus in lake erken sediment. Wat Res 34(7):2037–2042
Ryding SO, Forsberg C (1976) Sediments as a nutrients sources in shallow polluted lakes. In: Golterman H (ed) Interactions between sediments and freshwater. Junk, The Hague, pp 227–235
Saarinen T, Petterson G (2001) Image analysis techniques. In Last WM, Smol JP (eds) Tracking environmental change using lake sediments. Geochemical methods. Kluwer Academic Publishers, Dordrecht, Netherlands, pp 23–39
Schindler D, Hecky RE, Findlay DL, Stainton MP, Parker BR, Paterson MJ, Beaty KG, Lyng M, Kasian EM (2008) Eutrophication of lakes cannot be controlled by reducing nitrogen input: Results of a 37-year whole ecosystem experiment. PNAS 105:11254–11258
Shulka S, Syers J, Williams J, Armstrong D, Harris R (1971) Sorption of inorganic phosphorus by lake sediments. Soil Sci Soc Amer Proc 35:244–249
Sinke JC (1992) Phosphorus dynamics in the sediment of an eutrophic lake. Ph.D. Thesis. University of Wageningen, The Netherlands
Smith DR, Warnemuende EA, Haggard BE, Huang C (2006) Changes in sediment–water column phosphorus interactions following sediment disturbance. Ecol Eng 27(1):71–78
Smith VH, Joye SB, Howarth RW (2006b) Eutrophication of freshwater and marine ecosystems. Limnol Oceanogr 51(1 part 2):351–355
Søndergaard M, Jensen JP, Jeppesen E (2003) Role of sediment and internal loading of phosphorus in shallow lakes. Hydrobiologia 506(1–3):135–145
Speck NH, Sourrille EH, Wijnhoud S, Minist E, Vofkheimer W, Menendez JA (1982) Sistemas fisiográficos de la zona de Ingeniero Jacobacci-Maquinchao. INTA (in Spanish), Bariloche
Sposito G (2008) The chemistry of soils. Oxford University Press, Oxford

Sruoga P, Etcheverría M, Folguera A, Repol D, Zanettini J (2005) Geologic sheet 3569-I: Volcán Maipo, province of Mendoza (1: 250.000). Servicio Geológico Minero Argentino, Buenos Aires. Instituto de Geología y Recursos Minerales (in Spanish).

Temporetti P (1990) Retención de fósforo en sedimentos de diferentes cuerpos de agua lénticos del Parque Nacional Nahuel Huapi y de la Meseta Patagónica: Respuesta a la influencia antrópica. Centro Regional Universitario Bariloche, Universidad Nacional del Comahue (in Spanish), Tesis de Grado

Temporetti P (1998) Dinámica del fósforo en cuerpos de agua con cría intensiva de salmónidos. Centro Regional Universitario Bariloche, Universidad Nacional del Comahue (in Spanish), Tesis Doctoral

Temporetti P, Pedrozo F (2000) Phosphorus release rates from sediments affected by fish farming. Aquac Res 31:447–455

Temporetti P, Antonuk L, Pedrozo F (2014a) Características de los sedimentos de la Bahía Oriental del Lago Lácar afectado por la descarga de aguas residuales. Ecol Austral 24:294–303

Temporetti P, Beamud G, Pedrozo F (2014b) The trophic state of Patagonian Argentinean lakes and their relationship with distribution in depth of phosphorus in sediments. Int J Environ Res 8:671–686

Temporetti P, Beamud G, Nichela D, Baffico G, Pedrozo F (2019) The effect of pH on phosphorus sorbed from sediments in a river with a natural pH gradient. Chemosphere 228:287–299

Temporetti P, Snodgrass K, Pedrozo F (2013) Dynamics of phosphorus in sediments of a naturally acidic lake (Lake Caviahue, Patagonia-Argentina). Int J Sediment Res 28(1):1–15

Tilman D, Kiesling R, Sterner R, Kilham SS, Johnson FA (1986) Green, bluegreen and diatom algae: Taxonomic differences in competitive ability for phosphorus, silicon and nitrogen. Arch Hydrobiol 106:473–485

Tilman D, Kilham SS (1976) Phosphate and silicate uptake and growth kinetics of the diatoms *Asterionella formosa* and *Cyclotella meneghiniana* in batch and semicontinuous culture. J Phycol 12:375–383

Tunesi S, Poggi V, Gessa C (1999) Phosphate adsorption and precipitation in calcareous soils: The role of calcium ions in solution and carbonate minerals. Nutr Cycling Agroecosyst 53(3):219–227

USDA, United States Department of Agriculture (1999) Soil taxonomy. A basic system of soil classification for making and interpreting soil surveys. Agriculture Handbook N° 436. USDA, USA

Wang S, Jin X, Panga Y, Zhao H, Zhou X (2005) The study of the effect of pH on phosphate sorption by different trophic lake sediments. J Colloid Interface Sci 285:448–457

Wang Y, Shen Z, Niu J, Liu R (2009) Adsorption of phosphorus on sediments from the Three-Gorges Reservoir (China) and the relation with sediment compositions. J Haz Mat 162:92–98

Wang X, Chen A, Chen B, Wang L (2020) Adsorption of phenol and bisphenol A on river sediments: Effects of particle size, humic acid, pH and temperature. Ecotoxicol Environ Saf 204: 111093

Wetzel R (2001) Limnology. Academic Press, San Diego

Williams N, Rizzo A, Arribére M, Añón Suárez D, Ribeiro Guevara S (2017) Silver bioaccumulation in chironomid larvae as a potential source for upper trophic levels: a study case from northern Patagonia. Environ Sci Pollut Res 25(2):1921–1932

Wu Y, Wen Y, Zhou J, Wu Y (2014) Phosphorus release from Lake sediments: effects of pH, temperature and dissolved oxygen KSCE. J Civil Eng 18(1):323–329

Xiao Y, Zhu XL, Cheng H, Li K, Lu Q, Liang D (2013) Characteristics of phosphorus adsorption by sediment mineral matrices with different particle sizes. Water Sci Eng 6(3):262–271

Yagi S, Fukushi K (2012) Removal of phosphate from solution by adsorption and precipitation of calcium phosphate onto monohydrocalcite. J Coloid Interf Sc 384(1):128–136

Zhongyao L, Soranno PA, Wagner T (2020) The role of phosphorus and nitrogen on chlorophyll a: evidence from hundreds of lakes. Wat Res 11:6236

A Hydrological and Biogeochemical Appraisal of Patagonia's Río Gallegos

Pedro J. Depetris, Diego M. Gaiero, and Nicolás J. Cosentino

Abstract The Gallegos is the southernmost river of continental Patagonia. It has the smallest drainage basin of all the main rivers in the region. Moderate atmospheric precipitations (~500 mm y^{-1} in the uppermost catchments) determine discharge maxima in austral winter (rainfall/snowfall) and spring (snowmelt), delivering ~0.573 km^3 y^{-1} of freshwater (i.e. ~57 L m^2 y^{-1}) into an ample estuary in the SW Atlantic Ocean. The Gallegos stands out among the remaining Patagonian rivers for its connection (~18-month significant squared coherency) with the Southern Annular Mode, and due to its biogeochemistry, which appears affected by groundwater and debris, both associated to some degree with Eocene bituminous coal beds. The relevant factors seem to be: (a) the marked prevalence of NO_3^-–N among nutrients (N:P = 50:1–60:1); (b) the mean DOC concentration (~500 μmol L^{-1}), higher than all remaining Patagonian rivers (mean of ~300 μmol L^{-1}), and linked to river discharge; (c) high DIC, correlated with high pCO_2 (probably groundwater-supplied); (d) mean POC/PN molar ratio of ~8:1 (the highest in Patagonia's rivers), leading to infer a terrigenous source with some planktonic contribution. High DOC concentrations (~1000 μmol L^{-1}) are associated with low $\delta^{13}C_{DIC}$ (~−11 per mil), probably controlled by carbonate dissolution. Mean TOC in the Gallegos River is ~700 μmol L^{-1}, 70% of which is accounted for by DOC.

P. J. Depetris (✉)
Academia Nacional de Ciencias, Córdoba, Argentina
e-mail: pedro.depetris@anc-argentina.org.ar

D. M. Gaiero
Escuela de Geología, Facultad de Ciencias Exactas, Físicas y Naturales, Universidad Nacional de Córdoba, Córdoba, Argentina

Centro de Investigaciones en Ciencias de la Tierra, Consejo Nacional de Investigaciones Científicas y Técnicas y Universidad Nacional de Córdoba, Córdoba, Argentina

N. J. Cosentino
Instituto de Geografía, Facultad de Historia, Geografía y Ciencia Política, Pontificia Universidad Católica de Chile, Santiago, Chile

Núcleo Milenio Paleoclima, Santiago, Chile

A. I. Torres and V. A. Campodonico (eds.), *Environmental Assessment of Patagonia's Water Resources*, Environmental Earth Sciences,
https://doi.org/10.1007/978-3-030-89676-8_11

Keywords Hydrology · Biogeochemistry · Organic components · Nutrients · DOC · River sediments

1 Introduction

Without taking into account the main rivers draining the island of Tierra del Fuego (i.e. Grande, San Martín, Cullen, Chico, Fuego, and Ewan), the Gallegos is the Patagonia's southernmost river. It owes its name to Blasco Gallegos, a member of Ferdinand Magellan's expedition, which sailed the southern seas in the sixteenth century.

In terms of drainage basin area, the east-flowing Gallegos River is the smallest Patagonian river, ranking behind the Coyle (or Coig) River, its neighbor to the north. However, the Gallegos stands out among other Patagonian rivers due to a harmonic connection with the Southern Annular Mode (SAM), and to the presence in its drainage basin of subbituminous/bituminous coal-bearing beds of presumed Eocene age (i.e. 51º32′ S, 72º19′ W, Río Turbio Fm.). This chapter seeks primarily to explore a set of characteristics, probing into the impact which, apparently, they force on the main hydrological and biogeochemical features of the Gallegos River.

1.1 Geographic Characteristics

The binational Gallegos River (Fig. 1) drainage basin (51º17′–52º09′ S, 68º56′–72º22′ W), along with the less noticeable Chico River (i.e. inflowing from the southeast, with which the Gallegos shares the wide Atlantic estuary), drain the southernmost portion of Argentina's Santa Cruz Province as well as a portion of Chile's Región de Magallanes y de la Antártica Chilena. It has a drainage basin area of ~9554 km^2 (SSRH 2002). Climate in the region is temperate-cold; mean annual temperature is ~6 ºC. Annual atmospheric precipitations (i.e. rain and snowfall) reach ~500 mm in the upper catchments and ~300 mm in the central and eastern reaches. Atmospheric precipitations are concentrated in (austral) autumn and winter. Relative humidity in July (austral winter) reaches 80% in the entire drainage basin, and oscillates between 60 and 70% in January (in the western and eastern regions), and between 50 and 60% in the central area. Strong western and southwestern winds sweep the region, affecting evapotranspiration. High river flow occurs between August and November, triggered by high atmospheric precipitations occurring in the wintertime, and snow/ice melt for the duration of springtime.

The Turbio River (i.e. Spanish for turbid, murky) is the main **headwater** tributary. It flows initially to the south, bordered by the Andes (to the west) and the Cordillera Chica to the north and east. Several Chilean rivers join the main stem in the upper and middle stretch (e.g. Rubens, Penitente, and El Zurdo rivers). The Gallegos is 300 km

Fig. 1 Southernmost portion of Argentina's Santa Cruz Province, at the southern extreme of continental Patagonia. The city of Río Gallegos is the provincial capital. The map is framed between ~50º to ~53º S, and ~69º to ~73º W. Yacimientos Río Turbio situates the coal mine operation. Gauging stations: **A** Puente Blanco; **B** Toma de Agua

long; the lower 45 km are impacted by large oceanic tides, which reach variations of up to 13 m at the estuary.

In the western region, the Andean Cordillera exhibits a decreasing altitude towards the south. The dominant forest is typical of the Strait of Magellan region, where *guindo* (*Nothofagus betuloides*) predominates among deciduous species, as well as *lenga* (*Nothofagus pumilio*) and *ñire* (*Nothofagus antartica*), among the perennial trees. A steppe of low bushes and grasses prevail in the extra-Andean eastern slope. Most representative soils belong in the mollisols order.

The geology of Gallego's upper catchments is dominated by Pliocene-Recent basaltic rocks and glacial and glacial/fluvial sediments with a predominant basaltic mineral signature, and Quaternary sediments of varied grain-size. Water samples from the Gallegos River exhibited a mean $^{87}Sr/^{86}Sr$ composition of 0.704863 ± 0.000129, which is slightly higher than the mean composition found in local basaltic rocks ($^{87}Sr/^{86}Sr = 0.703267 \pm 0.000091$) (Brunet et al. 2005 and references therein).

The Rio Turbio coal deposit, currently mined (51º32 S, 72º19 W) (Río Tubio Fm., Eocene), is deemed an extension of the Loreto Fm. (i.e. Magellan Basin). Its reserves are estimated in 750 million tons of low-sulfur subbituminous-bituminous coal (e.g. Brooks et al. 2006).

1.2 Methodology

The field and laboratory techniques employed to analyze river water and sediment samples obtained during the European Commission-funded PARAT Project (Contract CI1*-CT94-0030) were described in Depetris et al. (2005).

The hydrological information was obtained from the data base operated by Argentina's *Secretaría de Infraestructura y Política Hídrica*,[1] and processed with standard statistical software.

Natural periodicities of multi-decadal river flow time series were evaluated by auto spectral analysis, while possible controlling factors of river discharge were analyzed through cross-spectral analysis. To improve the signal-to-noise ratio of the spectrum, the Blackman-Tukey method was used, based on dividing the time series into eight segments with 50% overlap (Blackman and Tukey 1958; Welch 1967). Prior to spectral analysis, all series were detrended based on a least-squares linear fit to the data.

2 Hydrological Features

Constrained by the Andean mountainous chain, the shallow Turbio River (i.e. with sources at 51°20′ S, Dorotea mountain range) is the main tributary in the uppermost headwaters of the Gallegos River drainage basin (Díaz et al. 2016). To the best of our knowledge, there are no extended and continuous discharge records along its course. In the Gallegos, the uppermost gauging station with a recent continuous record is located at Puente Blanco (51º53′39″ S, 71º35′46.6″ W),[2] about 190 km **upstream** the estuary.

Figure 2 shows a markedly asymmetrical statistical discharge distribution that fits to a log-normal model (Chi-square = 8.72, d.f. = 2; $p < 0.01$). The geometric mean ± standard deviation is 19.1 ± 2.35 $m^3\ s^{-1}$ (1993–2021), whereas the arithmetic mean discharge is 28.2 $m^3\ s^{-1}$ for the same period. Earlier discharge measurements for 1993–2000 exhibited a higher mean discharge: 34.2 $m^3\ s^{-1}$. The estimated runoff[3] at Puente Blanco is ~160 mm y^{-1} and the specific water yield is ~140 L $m^2\ y^{-1}$.

Figure 3 shows the synthetic hydrograph of Gallegos River at Puente Blanco gauging station. Maximum discharge is coherent with maximum rainfall/snowfall (Jul.–Aug.) and with snow-ice spring melting (Sep.–Oct.).

The graph in Fig. 4 shows the Gallegos discharge time series as well as the corresponding deseasonalized data series (1993–2020) determined for the upper reaches. Discharge data (Q) stripped from its seasonal components (i.e. deseasonalized) shows a significant ($p < 0.05$) negative trend: its mean annual discharge has decreased about 15 $m^3\ s^{-1}$ over the last ~27 years, whereas its mean deseasonalized discharge has reached about −8.3 $m^3\ s^{-1}$ during the same period (i.e. ~40% of its current geometric mean discharge).

River discharge is generally influenced by cyclic trends and changing atmospheric circulation patterns, such as **El Niño-Southern Oscillation** (**ENSO**) (e.g. Yang et al.

[1] http://bdhi.hidricosargentina.gob.ar.

[2] https://snih.hidricosargentina.gob.ar/.

[3] Also known as overland flow.

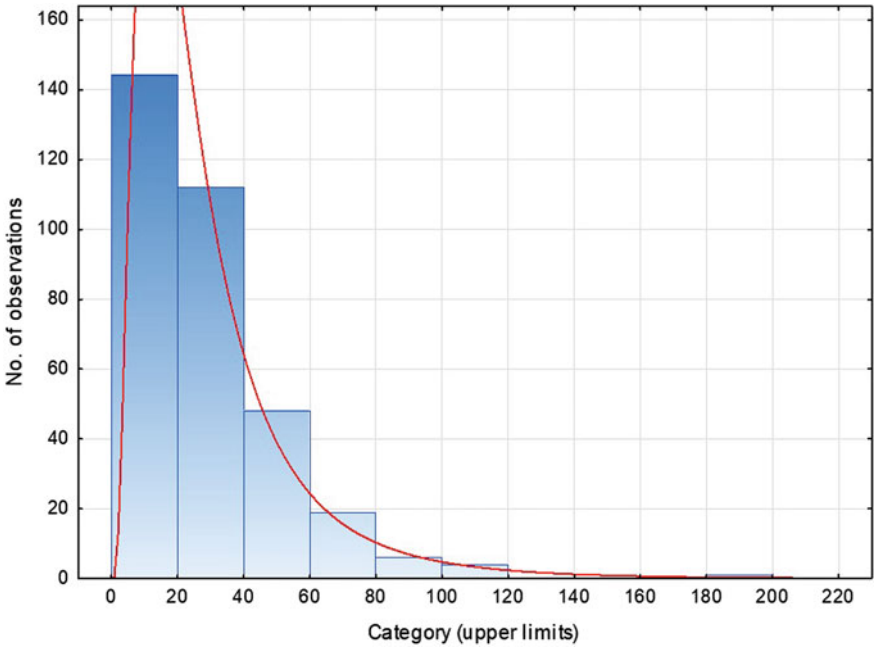

Fig. 2 Log-normal distribution of instantaneous discharges (N = 166) of Gallegos River, measured at Puente Blanco gauging station (3.02.1993–29.01.2021)

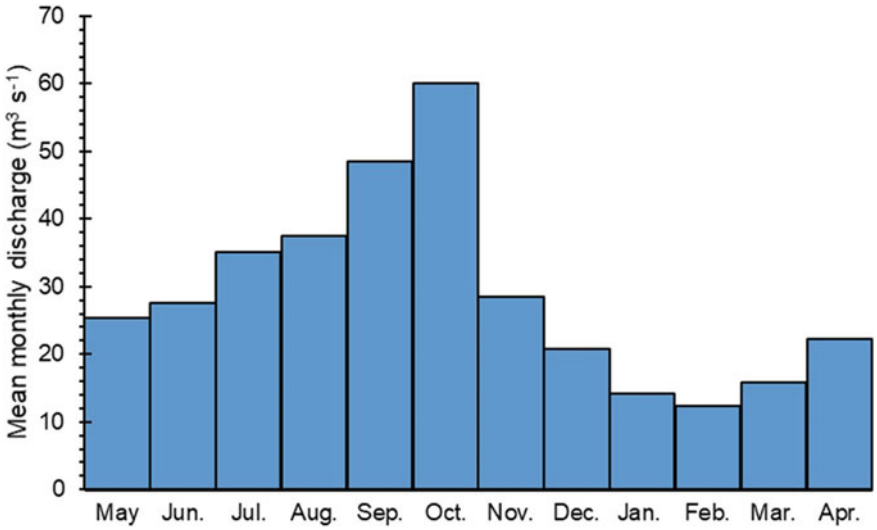

Fig. 3 Gallegos River synthetic hydrograph determined at the upstream Puente Blanco gauging station (station 2818). Highest discharges in the upper reaches (~60 m^3 s^{-1}) are controlled by snow/ice melt (i.e. spring)

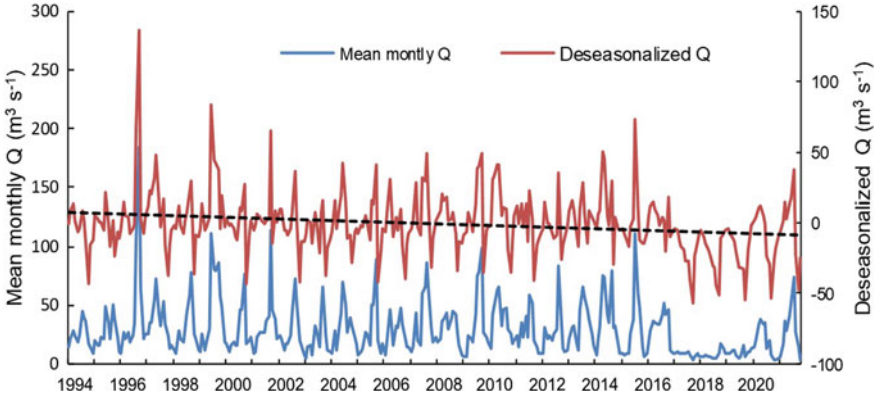

Fig. 4 The Gallegos River at Puente Blanco. The graph shows the mean monthly discharge, along with the corresponding deseasonalized Q time series (1993–2020). The slope of the regression line ($y = -0.0486x + 7.8587$) is significantly different from cero ($p < 0.05$)

2018) or the Southern Annular Mode (SAM)[4] (e.g. Marshall 2003; Gillett et al. 2006). As a climate driver, the SAM affects southern latitudes (i.e. south of ~50º–60º S). When in positive phase, the westerly wind belt driving the Antarctic Circumpolar Current intensifies and contracts towards Antarctica. In its negative phase, SAM expands towards the Equator. The negative phase will usually be more frequent if coincidental with El Niño events.

Contrasting with Patagonia,—where the impact of SAM is insufficiently known—its effect on Australian climate has been thoroughly researched[5] (e.g. Hendon et al. 2007). It refers to the (non-seasonal) N–S displacement of westerlies that almost constantly blow in the mid- to high-latitudes of the southern hemisphere. The time frame separating positive and negative events is fairly random, usually ranging between a week and a few months. The effect that the SAM has on rainfall varies greatly depending on season and region.

Figure 5 compares, for the period 1994–2020, the variability of SAM with the deseasonalized Gallegos River time series. A cursory inspection of the graph shows that some—but not all—positive or negative SAM departures coincide with corresponding positive or negative departures in the deseasonalized discharge time series. Clearly, both series do not exhibit a significant correlation and, hence, it is not possible to infer a consistent effect of SAM on precipitations by means of parametric statistics.

Spectrum analysis is related with the exploration of cyclical patterns of data, and may prove fruitful in the exploration of deseasonalized Gallegos discharges and SAM variability. The aim of the analysis is to decompose a complex time series with cyclical components into a few underlying sinusoidal functions of particular wavelengths. Performing spectrum analysis on a time series allows to identify the

[4] SAM is also known as the Antarctic Oscillation (AAO). It is defined as a low-pressure belt surrounding Antarctica.

[5] http://www.bom.gov.au/climate/sam/.

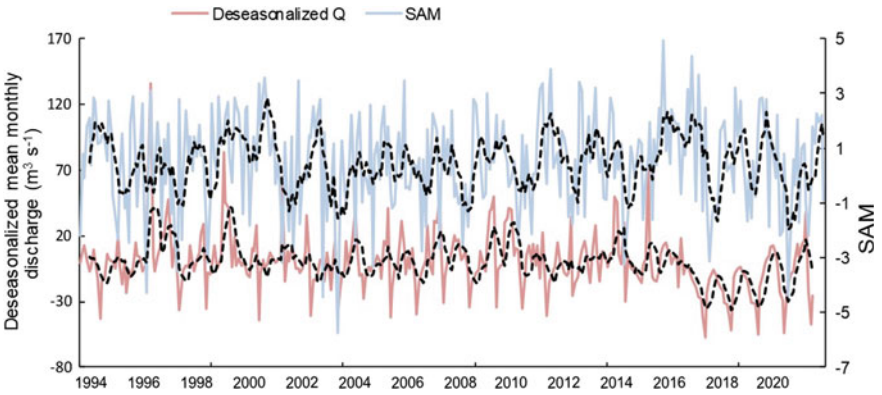

Fig. 5 Comparison of SAM and Gallegos River mean monthly deseasonalized discharge series (at Puente Blanco). Some positive (negative) SAM departures are coherent with positive (negative) deseasonalized discharges. Broken lines are fitted moving averages (period = 5)

wave lengths and importance of underlying cyclical components. As a result, a few recurring cycles of different lengths in the time series may become evident, which at first looked like random noise (e.g. Figure 5).

Fourier harmonic analysis is helpful in exploring the relationship that is likely to exist between both time series in the 1994–2020-time interval. The first step was to explore the harmonic characteristics of SAM by means of its auto spectral analysis (Fig. 6). The power spectral density is high and significant ($p < 0.05$) in the neighborhood of the 20-month period. This is a key feature when probing into the coherency with Gallegos' deseasonalized discharge.

Cross-spectrum analysis is an expansion of the auto spectral analysis to the simultaneous analysis of two series. The purpose of cross-spectrum analysis is to uncover the correlations between two series at different frequencies. The result is the squared coherency, which can be interpreted similarly to the squared correlation coefficient (i.e. the coherency value is the squared correlation between the cyclical components in the two series at the respective frequency).

Fourier's square coherency was employed to analyze the association existing between SAM and the Gallegos River deseasonalized discharge time series for the interval 1994–2020. Figure 7 shows the square coherence spectrum between both variables. A significant ($p < 0.05$) peak is identifiable for the ~18-months period. It is coincidental with the peak identified in SAM's auto spectral analysis, meaning that in the Gallegos' discharge time series, there are recurring hydrological features, stripped from the seasonal component, which correlate with SAM, with ~18 months' time periodicity (i.e. ~0.05 frequency).

As mentioned above, the time frame separating SAM's positive and negative events is quite random, and it may reach high-frequency values, which may range

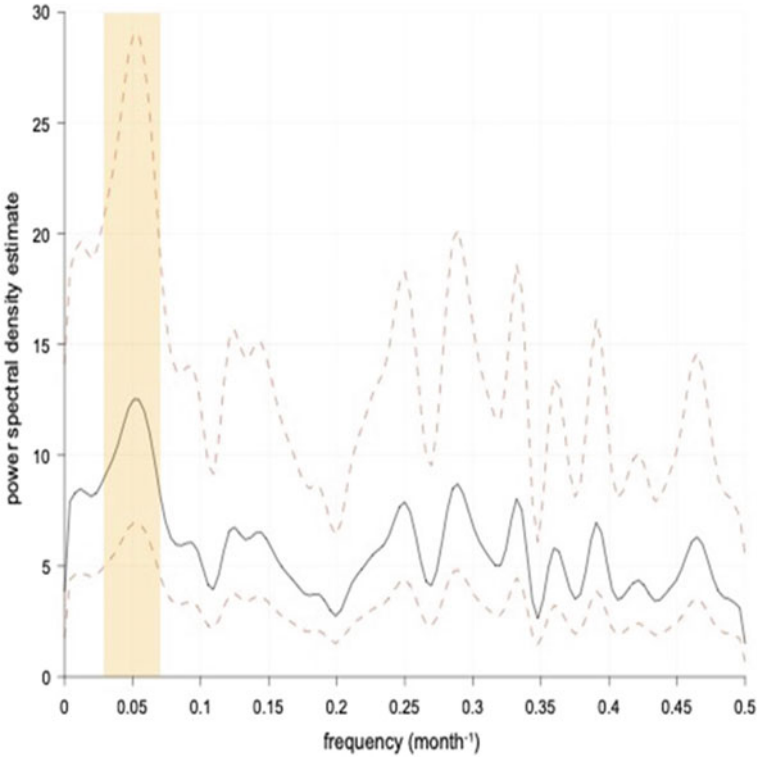

Fig. 6 The auto spectral analysis of SAM shows a 95%-significant periodicity of ~20 months (light brown box). The power spectral density best estimate is shown in black, while the 95%-confidence interval is shown in dashed red lines

between a week and a few months. It might occur, then, that both variables are associated with short-period or high-frequency (i.e. ~0.33–0.34) deseasonalized hydrological events. It may be a seasonal-like signal that persists in deseasonalized data. It is difficult, however, to assign a physical meaning to the 2.9–3.0-month period peak observable in Fig. 7.

The Gallegos' water discharge shows a significant flow variation, at Toma de Agua, near the city of Río Gallegos (Fig. 8). The geometric mean discharge ± standard deviation = 15.5 ± 1.71 $m^3\ s^{-1}$. The river flow displays a decrease (i.e. with respect to Puente Blanco), replicated in the hydrograph, that can be attributed to several causes, including strong evapotranspiration and the consumptive use of the resource. The current mean (arithmetic) discharge at Toma de Agua is 18.2 $m^3\ s^{-1}$ (2016–2020); the specific water yield at the Gallegos' mouth is 57 L $m^2\ y^{-1}$.

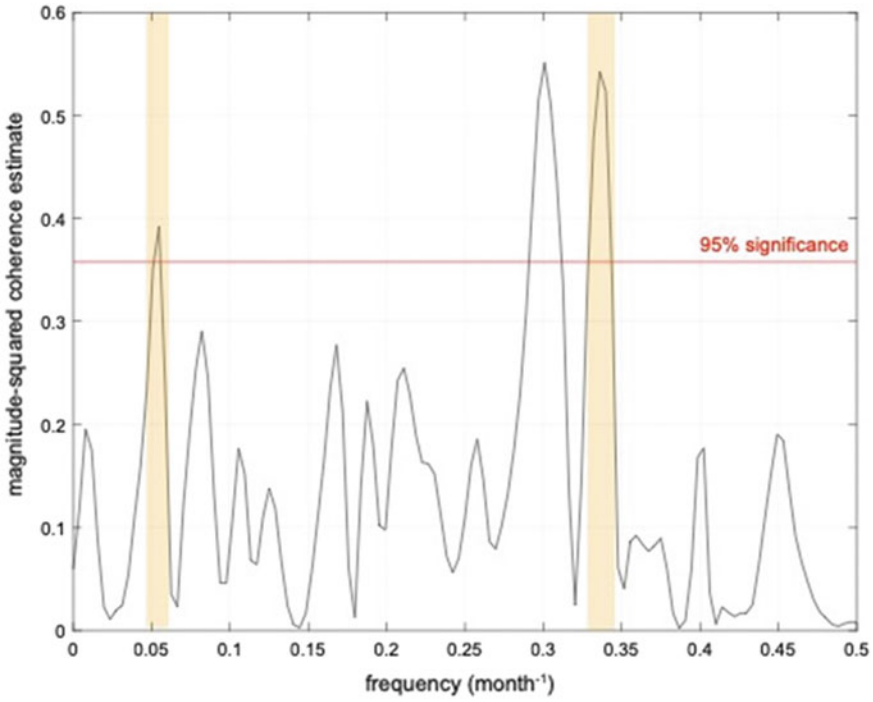

Fig. 7 Gallegos River at Puente Blanco. The squared coherence calculated with Fourier harmonic analysis shows the relationship between the time series of SAM and deseasonalized Q, with two 95%-significant periodicities of 2.9–3.0 and ~18 months (light brown boxes), that also show strong relative peaks in the cross power spectral density estimate (not shown). The 95% significance level for the magnitude-squared coherence estimates was computed using a bootstrap method

3 Biogeochemical Evaluation

The Gallegos' main physicochemical parameters portray an Andean river subjected to a **weathering-limited denudation** (Carson and Kirkby 1972), basically governed by physical processes, with chemical weathering playing a subordinate role. The geochemical aspects of the Gallegos River were surveyed by the PARAT Project, between September 1985 and April 1998. The main physicochemical characteristics can be summarized as follows: pH frequently drops below neutrality (7.07 ± 0.54), and water conductivity is low (112.2 ± 4.67 μS cm^{-1}), with ΣZ^+ (i.e. $\Sigma Z^+ = 2Ca^{2+} + 2Mg^{2+} + Na^+ + K^+$) fitting in the medium dilute category ($0.75 > \Sigma Z^+ > 1.5$ meq L^{-1}) (Meybeck 2005). The most frequent order of decreasing abundance among cations is $Na^+ > Ca^{2+} > Mg^{2+} > K^+$, whereas among anions is $HCO_3^- > Cl^- > SO_4^{2-}$. Lee et al. (2013) investigated a set of southern Patagonian rivers, including one sample from the Gallegos. Recent studies have shown that glacial sediments (Quaternary), prevailing in the drainage basin, regulate the material contribution to

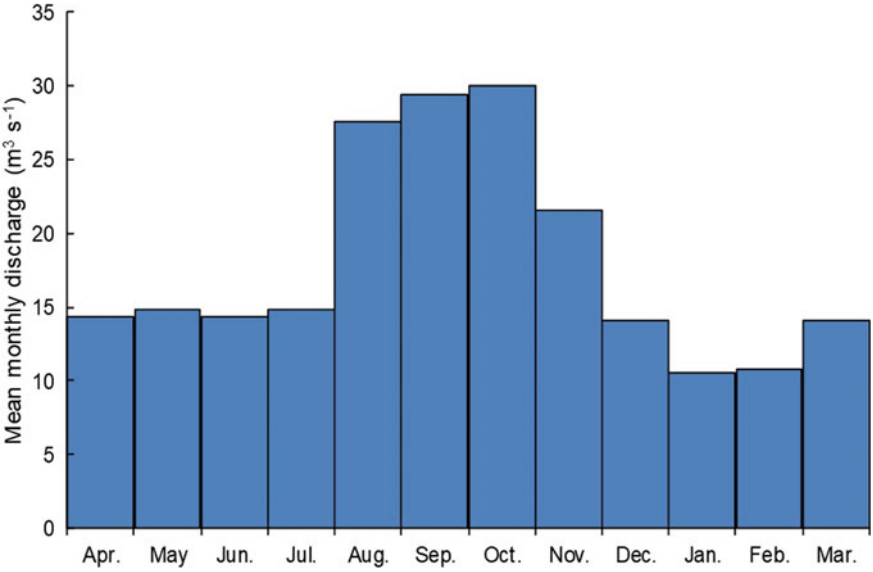

Fig. 8 Gallegos River mean synthetic hydrograph (2016–2020) determined near the estuary, at Toma de Agua (station 2838). High discharges are determined by winter precipitations (August) and snow/ice melt (September–October)

the dissolved and particulate load, balancing the output between silicates, evaporitic and carbonate rocks (Gaiero et al. submitted).

3.1 Dissolved Components

Nutrients are chemical elements essential for the development of plant and animal life. In oceans, rivers and lakes, nutrients are needed for the growth of algae that form the basis of an intricate food web sustaining the entire aquatic ecosystem. Nitrogen and phosphorous are the most conspicuous nutrients in rivers and lakes, whereas silicon and several other micronutrients also play a role in primary biological production.

Nitrogen is released during organic matter decomposition, largely as ammonium (NH_4^+). It can be adsorbed onto negatively charged organic coatings on soil particles or clay mineral surfaces. Ammonium is also taken up by algae or plants, or converted to nitrite (NO_2^-) through nitrification, which is oxidized further to nitrate (NO_3^-), a process usually catalyzed by bacteria. Nitrate is soluble and it is not retained in soils. Consequently, NO_3^- supplied by rainwater, or derived from the oxidation of soil organic matter and animal wastes, will wash out of sediment or regolith/soils into rivers.

In natural waters, dissolved inorganic phosphorous (DIP) exists largely as a number of dissociation products of H_3PO_4. Phosphorous is usually retained in soils (e.g. by adsorption onto soil particles) or regolith. Phosphate is usually in sediments as insoluble $FePO_4$ (i.e. under reducing conditions) and, therefore, DIP can be returned to the water column associated with Fe(III) reduction to Fe(II). Phosphorous may be supplied, as well, by the dissolution/hydrolysis of phosphate minerals, such as the apatite group (i.e. $Ca_5(PO_4)_3(F,Cl,OH)$).

The Gallegos River showed a wide-ranging concentration variability in NO_3^-–N. Between Sep. 1995 and Apr. 1998 the river was sampled sporadically at the Güer Aike site (i.e. near the outfall into the estuary). During the sampling period, high and low concentrations fluctuated 100-fold, between ~92 and 0.97 μmol L^{-1}, whereas NO_2^-–N exhibited, as expected, much lower concentrations (12.80–1.16 μmol L^{-1}) during the same period. The markedly low concentrations of DIP (1.69–0.02 μmol L^{-1}) reflected the meager DIP supply received either from point or non-point sources. Hence, the approximate N:P dissolved ratio in the Gallegos apparently remained in the 50:1–60:1 range throughout the hydrological year, regardless of the water flow level. The high NO_3^-–N concentrations and the resulting, equally high N:P ratio, can only be explained by the contribution of groundwater, which dissolved phases may be supplied by coal-bearing beds and mudstones, containing nitrogen but only traces of phosphorous.[6] It must be added that, in comparison with the remaining Patagonian Rivers, the Gallegos is the river that showed the highest nitrogen concentrations in the set (Depetris et al. 2005).

Table 1 shows the concentrations of several chemical variables (i.e. also sampled at Güer Aike) of significance in biogeochemical reactions. Silicon, also a nutrient, is used—for example—by diatoms and radiolarian to build their exoskeletons and hence, also plays a significant biogeochemical role. The mean silicon oxide (SiO_2) concentration found was 243.2 μmol L^{-1} (i.e. 14.6 mg L^{-1}) and also exhibited a constrained variability (i.e. the coefficient of variation is ~10%). Silicon originates solely from weathering reactions, and its inherently low concentrations may be modulated further by biological consumption.

Figure 9 shows the variability of dissolved organic carbon (DOC) and $\delta^{13}C_{DIC}$ against Gallegos River discharge. In contrast with other examples, where DOC is diluted by swelling river flow, DOC concentrations in the Gallegos increase significantly, thus suggesting an allochthonous source for the dissolved organic carbon: a four-fold increase in discharge, from 20 to 80 m^3 s^{-1}, generates an almost three-fold increase in DOC concentration.

In contrast, $\delta^{13}C_{DIC}$ decreases with increasing discharge and DOC. The latter could contribute to decrease $\delta^{13}C_{DIC}$, as shown for the St. Lawrence River (Barth and Veizer 1999). Moreover, high discharge determines a more negative $\delta^{13}C_{DIC}$, which could mean a change in the supplying source.

DIC concentrations in fresh water bodies are controlled by lithology, water temperature, flow variations, and biogeochemical processes (e.g. organic matter oxidation).

[6] Río Turbio subbituminous-bituminous coal (geometric) mean composition on a dry, ash-free basis, is ~56.6% carbon, ~0.97% nitrogen, ~0.68% sulphur, and ~0.02% phosphorous (Brooks et al. 2006).

Table 1 Dissolved biogeochemical parameters determined in the Gallegos River at Güer Aike

Date	pH	Q ($m^3 s^{-1}$)	TDS (mg L^{-1})	SiO_2 (µmol L^{-1})	$Fe_{diss.}$ (µmol L^{-1})	DOC (mmol L^{-1})	DIC (mmol L^{-1})	pCO_2 (µatm)	$\delta^{13}C_{DIC}$ (per mil)
Sep. 1995	6.96	105	98.3	185	n.d	1.06	1.10	6907	−11.1
May 1996	6.90	54	76.4	266	0.23	0.57	0.85	6395	n.d
Sep. 1996	6.65	53	80.4	258	0.23	0.59	1.23	13,051	−5.5
Dec. 1996	7.44	14	106.1	248	0.09	0.22	1.00	2299	−5.7
Dec. 1997	6.41	18	85.5	252	0.27	0.59	1.47	18,427	−6.2
Apr. 1998	8.05	25	137.3	261	0.17	0.30	1.25	763	−6.4
G.M	**7.05**	**35**	**95.4**	**243.2**	**0.19**	**0.49**	**1.13**	**5153**	**−7.0**

G.M. geometric mean
n.d. not determined

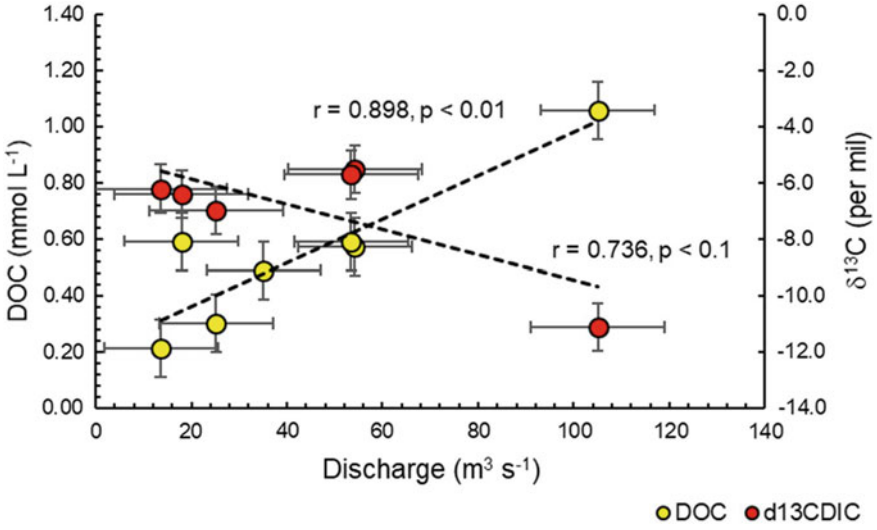

Fig. 9 Scatter graph showing DOC and $\delta^{13}C_{DIC}$ variation as a function of Gallegos River discharge. Significant correlations support a cause-effect relationship between the variables and river flow. Error bars are the standard error of the mean. Data from Brunet et al. (2005)

Brunet et al. (2005) studied the provenance of dissolved inorganic carbon (DIC) in Patagonian rivers. Their data, included in Fig. 10, points to an interesting aspect.

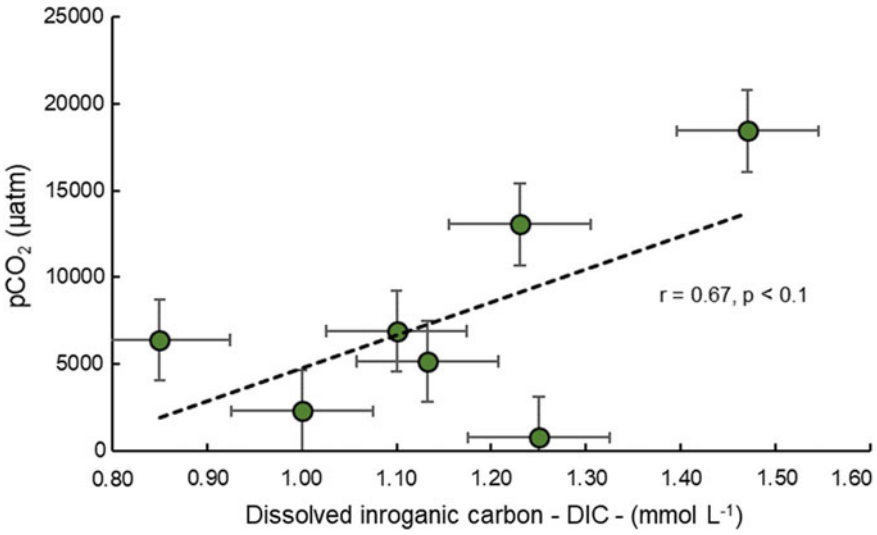

Fig. 10 Variability of DIC and pCO_2 in the Gallegos River. Error bars are the standard error of the mean. Data from Brunet et al. (2005)

One feature in which the Gallegos diverges from most Patagonian rivers is that a significant proportion of DIC is accounted for by H_2CO_3 (i.e. high pCO_2). Hence, high DIC may be linked to a significant groundwater supply or to waters circulating under snow/ice, in the mountainous upper reaches.

Iron is an indispensable micronutrient of **phytoplankton**. Iron plays an important role in many biological processes such as nitrogen assimilation, N_2 fixation, photosynthetic and respiratory electron transport, and porphyrin biosynthesis. Consequently, the regulation effects of Fe should be considered besides nitrogen and phosphorus when dealing with the processes of river and lake **eutrophication**. There are several sources of Fe, including the above mentioned reduction of Fe(III) to Fe(II). Among them, pyrite (FeS_2) is the most common sulfide mineral on the Earth's surface, and it plays an important part in geochemistry, as well as in biology and environmental processes. The maximum SO_4^{2-} concentration that can be attained by sulfide oxidation in surface waters saturated with O_2 is ~400 μeq L^{-1} although subglacial waters may increase three-fold this concentration (Tranter 2005).

The Río Turbio coal has a mean of 0.3 ± 0.31% pyritic sulfur, and 0.5 ± 0.23% organic sulfur (Brooks et al. 2006). When exposed to air, pyrite is oxidized, whether by natural processes or anthropogenic activities, forming sulfuric acid in the presence of humidity (e.g. Campos dos Santos et al. 2016):

$$FeS_2(s) + 7/2O_2 + H_2O = Fe^{2+} + 2SO_4^{2-} + 2H^+$$

Stumm and Morgan (1996) described the following reactions: Fe^{2+} endures oxygenation to Fe^{3+}, which is subsequently hydrolyzed to $Fe(OH)_3(s)$, liberating more acidity and coating mineral grains in the streambed.

$$Fe^{3+} + 3H_2O = Fe(OH)_3(s) + 3H^+$$

Pyrite can reduce Fe^{3+} and $FeS_2(s)$ is again oxidized. Acidity is released along with additional Fe^{2+}, which can again reenter the reaction cycle and drive it further:

$$FeS_2(s) + 14Fe^{3+} + 8H_2O = 15Fe^{+2} + 2SO_4^{2-} + 16H^+$$

$$Fe^{2+} + 1/4O^2 + H^+ = Fe^{3+} + 1/2H_2O$$

This set of reactions can explain Fig. 11, where increasing SO_4^{2-} concentrations are accompanied by decreasing Fe concentrations due to a series of feedback chemical mechanisms—described above—which tend to precipitate $Fe_3(OH)(s)$, removing Fe from the solution.

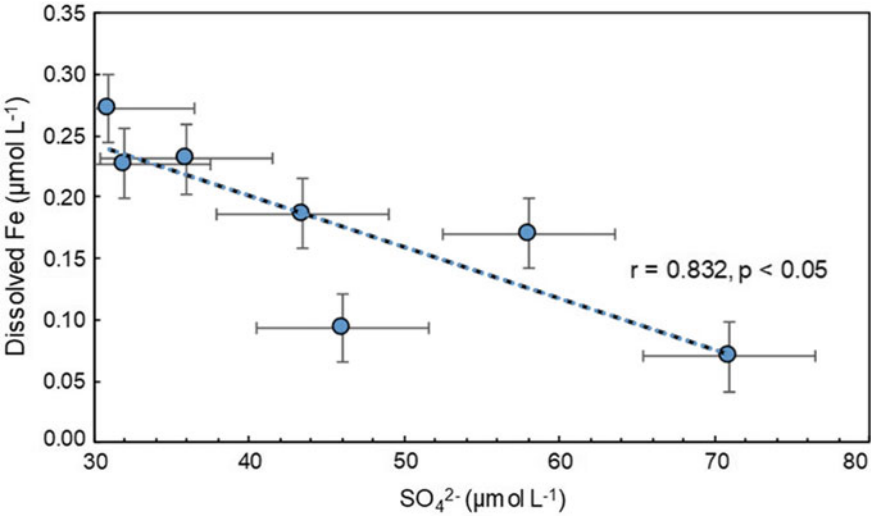

Fig. 11 Decreasing concentrations trends of SO_4^{2-} and Fe in the Gallegos River. See text for explanations. Error bars are the standard error of the mean

3.2 Particulate Organic Constituents

Particulate organic debris transported by rivers supplies important information on a series of important biogeochemical processes taking place within drainage basins. Depetris et al. (2005) have probed into the biogeochemical typology and output of all the main Patagonian rivers and the information collated in that particular project for the Gallegos Rivers is examined here in more detail. Figure 12 shows an illustrating image of a typical sample of the dark Gallegos' bed load sediment.

Table 2 shows mean values and fluxes, expressed in molar masses, as determined in the Gallegos River within the framework of the PARAT Project. The geometric mean of total suspended solids (TSS) was 25 mg L^{-1}, whereas its concentrations varied between 5 and 60 mg L^{-1} during the period of sampling. Between 6.5 and 9% of TSS was accounted for by organic matter.

It is clear from Table 2 that most of the carbon transported in suspension by the river was organic, in as much the difference between the mean total particulate carbon (PC) and the mean organic fraction (POC) is about 120 mol L^{-1} (~35%). Such proportion of the particulate phases is probably accounted for by carbonates, which have been identified as significant in the carbon-bearing Río Turbio beds (Brooks et al. 2006).

The concentration of POC (Table 2) is among the noteworthy concentrations in Patagonian rivers and the Gallegos' mean concentration is only exceeded by the Deseado and Chico rivers, with mean POC concentrations in the neighborhood of 380 µmol L^{-1}. The nearby Coyle River, draining marshes and peat bogs, showed a mean POC concentration of ~50 µmol L^{-1} (Depetris et al. 2005).

Fig. 12 Image of a typical bed sediment sample of the Gallegos River collected at a point bar. The mostly silt and sand grain-size sample includes large coal fragments (i.e. ~0.5–1.0 cm)

Table 2 Gallegos River organic particulate matter: means and fluxes

Variables	G.M. (μmol L^{-1})	Mass (Kmol y^{-1})	Yield (mol km^{-2} y^{-1})
PC	332	10.5	1.10
POC	215	6.8	0.71
PN	28	0.9	0.09
DOC	491	15.5	1.62

G.M. geometric mean

C/N ratios in the range 4:1–10:1 are typically from marine (i.e. phytoplankton) sources, whereas higher ratios are to be expected to come from a terrestrial source because vascular plants from land-dwelling sources tend to have C/N ratios greater than 20. The mean POC/PN molar ratio in the Gallegos River is ~8:1, which leads to interpret a terrigenous source with some planktonic contribution. The Gallegos has the largest mean POC/PN ratio of all the Patagonian rivers, most of which point to a dominating autochthonous source (i.e. 4:1–5:1) (Depetris et al. 2005). It is worthwhile to highlight the significance of DOC over all the other forms of carbon (i.e. mean DOC/POC $\approx$ 2.3), which stands out among all the other Patagonian water bodies. The largest rivers in Patagonia (e.g. Negro, Santa Cruz, Chubut) exhibit DOC/POC < 2.0 (Depetris et al. 2005).

The world average total organic carbon (i.e. TOC = DOC + POC) concentrations in rivers fluctuates in the range of 730–880 μmol L^{-1}. On a global scale, the mean concentrations of DOC and POC are 400–480 μmol L^{-1} and 330–400 μmol L^{-1}, respectively (Perdue and Ritchie 2005). In the Gallegos, mean TOC is 706 μmol L^{-1}, below the global range. On the other hand, average DOC concentration in the

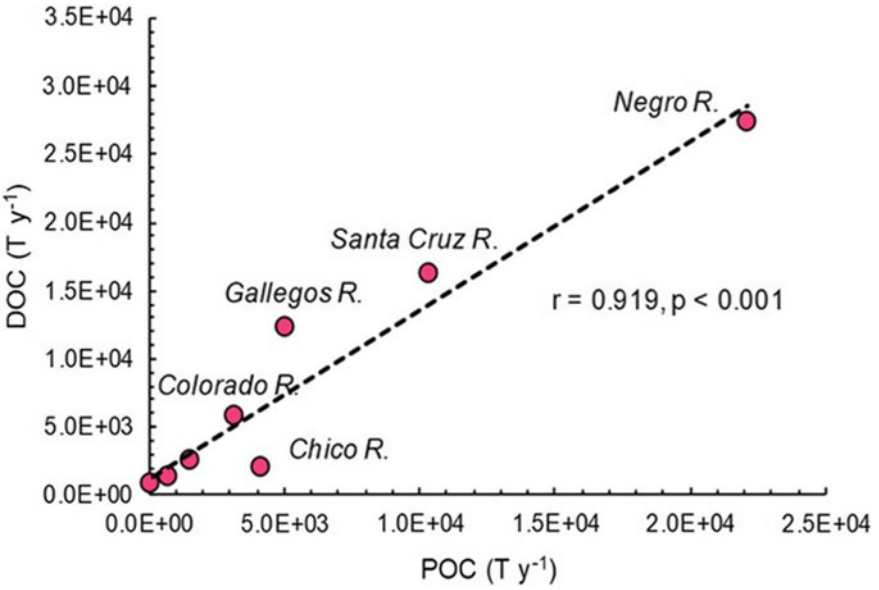

Fig. 13 Mass transport rates of POC and DOC in Patagonian rivers. The Negro and Santa Cruz have the highest discharges in Patagonia's riverine set (Depetris et al. 2005)

Gallegos is somewhat higher than the most frequent global values. Mean POC, in contrast, is lower.

Patagonian rivers export to the SW Atlantic Ocean about 47.4 Gg y^{-1} of POC and about 67.8 Gg y^{-1} of DOC. The Gallegos River supplies about 11% of POC and about 18% of DOC supplied to the Patagonian coastal zone. Figure 13 shows the high covariance of both transport rates as well as the significance of high discharge (Depetris et al. 2005). Clearly, the relevance of both, the Negro and Santa Cruz rivers, is mainly determined by their high discharge, even though the Gallegos River exhibits higher organic carbon concentrations.

4 Final Observations

The Gallegos is the southernmost river of continental Patagonia. It delivers ~0.573 km^3 y^{-1} of freshwater into an ample estuary in the SW Atlantic Ocean. The water specific yield at the mouth is 57 L m^2 y^{-1} and discharge peaks occur in August due to (austral) winter precipitations, and in September–October owing to snow/ice-melt occurring in the southern spring. Annual atmospheric precipitations are moderate and climate change is seemingly affecting the Gallegos River mean discharge: deseasonalized discharge data shows a significant ($p < 0.05$) negative trend. Its mean monthly discharge has decreased ~15 m^3 s^{-1} over the last ~27 years,

whereas its deseasonalized monthly discharge also shows a significant decrease of about $-8.3\ m^3\ s^{-1}$ during the same period (i.e. ~40% of its current mean discharge).

The Gallegos River discharge time series at Puente Blanco appears to be connected with the southern atmospheric pressure variability. Fourier harmonic analysis shows that the deseasonalized flow series is coherent with the SAM (a.k.a. Antarctic Oscillation, AAO) with significant peaks at 18 and 3 months. It is interesting to point out that the negative discharge trend exhibited by Gallegos' discharge trend does not appear to be associated with SAM's variability although there is a significant coherency between both variables.

Nutrients do not reach high concentrations in the Gallegos, as it happens in most Patagonian rivers. Several factors, however, suggest that the coal-bearing beds, which are being mined at Río Turbio, play a significant role in supplying dissolved and particulate matter to the river, thus affecting its biogeochemical characteristics.

Nitrogen, which is the factor limiting biological productivity in most Patagonian water bodies, is the most conspicuous nutrient in the Gallegos River. NO_3^-–N may reach almost 100 $\mu mol\ L^{-1}$ and the N:P ratio may be in the 50:1–60:1 range. This is an indication that dissolved nitrogen is likely supplied by N-rich groundwater, in contact with coal strata or with organic-rich mudstones. Likewise, the Gallegos has the highest DOC concentrations in Patagonian waters (e.g. mean concentrations of 500 $\mu mol\ L^{-1}$), which tend to increase with increasing discharge and shows an inverse relationship with $\delta^{13}C$ (i.e. $\delta^{13}C$ is possibly connected with the alkalinity supplied by carbonate dissolution). Additionally, DIC is significantly correlated with pCO_2, which concentration is possibly governed by groundwater. All these aspects reinforce the scenario of Río Turbio coal as a factor to consider in the riverine biogeochemistry.

Another interesting aspect is the dynamics of SO_4^{2-}. Río Turbio's is a low-sulfur bituminous coal but, according to Brooks et al. (2006), it has some pyritic sulfur (i.e. 0.1–0.8%) and organic sulfur (i.e. 0.3–0.8%). The opposite correlation of SO_4^{2-} with dissolved Fe, is probably governed by the precipitation of (oxy)hydroxides and further suggests the partial significance of a coal-related source for dissolved phases of biogeochemical meaning.

The mean POC/PN molar ratio in the Gallegos River (i.e. ~8:1), is the highest C/N in Patagonia's riverine TSS, most of which exhibit a prevailing autochthonous source (i.e. ~4:1–5:1) (Depetris et al. 2005). This feature leads to infer for the Gallegos a phytoplankton source with some terrigenous contribution.

Mean TOC in the Gallegos River is ~700 $\mu mol\ L^{-1}$. This figure falls in the lower end of the riverine TOC global scenario (Perdue and Ritchie 2005). The DOC/POC mean ratio is ~2.3, because DOC supplies ~70% of TOC and its mean concentration in the Gallegos is higher than the most frequent DOC concentrations, on a global basis (e.g. Perdue and Ritchie 2005). This further supports the image that the coal-bearing beds supplies, likely via groundwater, the important DOC concentrations exhibited by the Gallegos River.

Patagonian rivers export to the SW Atlantic Ocean ~115 Gg y^{-1} of TOC, with an average DOC/POC ratio 1.4:1. The Gallegos River supplies about 11% of POC and about 18% of the DOC contributed by rivers to the Patagonian coastal zone (Depetris et al. 2005).

References

Barth JAC, Veizer J (1999) Carbon cycle in the St Lawrence aquatic ecosystem at Cornwall (Ontario), Canada: seasonal and spatial variations. Chem Geol 159:107–128

Blackman RB, Tukey JW (1958) The measurement of power spectra from the point of view of communications engineering–part I. Bell Syst Tech J 37:185–282

Brooks WE, Finkelman RB, Willett JC, Torres IE (2006) World quality inventory: Argentina. In: Karlsen AW, Tewalt SJ, Bragg LJ, Finkelman RB (eds) World coal quality inventory: South America. US Geological Survey, Washington DC, pp 27–47

Brunet F, Gaiero D, Probst J-L, Depetris PJ, Gauthier, Lafaye F, Stille P (2005) ™13C tracing of dissolved inorganic carbon sources in Patagonian rivers (Argentina). Hydrol Proc 19:3321–3344

Campos Dos Santos E, De Mendonça Silva JC, Anderson Duarte H (2016) Pyrite oxidation mechanism by oxygen in aqueous medium. J Phys Chem C 120(5):2760–2768

Carson MA, Kirkby NJ (1972) Hillslope form and processes. University Press, Cambridge

Depetris PJ, Gaiero DM, Probst J-L, Hartmann J, Kempe S (2005) Biogeochemical output and typology of rivers draining Patagonia's Atlantic seaboard. J Coast Res 21(4):835–844

Díaz B, Monserrat MC, Tiberi PE, Mardewald G, Hofmann C, Caparrós L, Mattenet F, Zerpa D, Billoni SL, Martínez L (2016) Surface–water hydrology of the Río Gallegos watershed (South of Santa Cruz province, Argentina). Techn Report-UNPA 8(3):136–161 (in Spanish)

Gillett NP, Kell TD, Jones PD (2006) Regional climate impacts of the Southern Annular Mode. Geophys Res Lett 33:1–4

Hendon HH, Thompson DWJ, Wheeler MC (2007) Australian rainfall and surface temperature variations associated with the Southern Hemisphere Annular Mode. J Clim 20:2452–2467

Lee B, Han Y, Huh Y, Lundstrom C, Siame LL, Lee JI, Park B-K, Aster, team. (2013) Chemical and physical weathering in south Patagonia rivers: a combined Sr-U-Be isotope approach. Geochim Cosmochim Acta 101:173–190

Marshall GJ (2003) Trends in the Southern Annular Mode from observations and reanalyzes. J Clim 16:4134–4143

Meybeck M (2005) Global occurrence of major elements in rivers. In: Drever JI (ed) Surface and groundwater, weathering and soils. Elsevier, Amsterdam, pp 207–223

Perdue EM, Ritchie JD (2005) Dissolved organic matter in freshwaters. In: Drever JI (ed) Surface and groundwater, weathering and soils. Elsevier, Amsterdam, pp 273–318

SSRH (2002) Acta digital de los recursos hídricos superficiales de la República Argentina, CD-Rom, Buenos Aires (in Spanish)

Stumm W, Morgan JJ (1996) Aquatic chemistry. Chemical equilibria and rates in natural waters. Wiley-Interscience, New York

Tranter M (2005) Geochemical weathering in glacial and proglacial environments. In: Drever JI (ed) Surface and groundwater, weathering and soils. Elsevier, Amsterdam, pp 189–205

Welch P (1967) The use of fast Fourier transform for the estimation of power spectra: a method based on time averaging over short, modified periodograms. IEEE Trans Audio Electroacoust 15(2):70–73

Yang S, Li Z, Yu J-Y, Hu X, Dong W, He S (2018) El Niño-Southern Oscillation and its impact in the changing climate. Ntl Sci Rev 5(6):840–857

Vertical Electrical Sounding Applied to Hydrolithological Interpretations in the Fuegian Steppe, Argentina

Candela Gorza, Claudio Lexow, Juan F. Ponce, Andrea Coronato, Ramiro López, and María Laura Villarreal

Abstract The aim of this chapter is to present the main hydrolithological features of an area of the northern region of Tierra del Fuego province, based on geoelectrical analyses. The surface geology is dominated by the Carmen Silva Formation (middle Miocene), composed by two members deposited on marine environments, from marginal to deltaic, and sands and gravels corresponding to Middle Pleistocene glaciofluvial fans. The geomorphological characteristics are represented by strongly-dissected low hills, plateaus, valleys and closed depressions which host semi-permanent shallow lakes. The geoelectrical prospecting allowed us to differentiate several layers based on resistivity. The shallow ones would agree with the upper member of the Carmen Silva Formation as well as the glaciofluvial deposits, and would be the unconfined aquifer. The deeper ones would correspond to the lower member of such formation and would form an aquitard.

Keywords Aquifer · Hydrolithology · Geoelectrical surveys · Fuegian steppe

C. Gorza (✉) · J. F. Ponce · A. Coronato · R. López
Centro Austral de Investigaciones Científicas—CONICET, Bernardo Houssay 200, C.P. 9410 Ushuaia, Tierra del Fuego, Argentina
e-mail: gorzacandela@conicet.gov.ar

C. Lexow
Centro de Geología Aplicada, Agua y Medio Ambiente -CIC- Universidad Nacional del Sur. Comisión de Investigaciones Científicas, Bahía Blanca, Argentina

Departamento de Geología, Universidad Nacional del Sur, Bahía Blanca, Argentina

J. F. Ponce
Universidad Nacional de Tierra del Fuego, Antártida e Islas del Atlántico Sur. Instituto de Ciencias Polares, Ambiente y Recursos Naturales, Tierra del Fuego, Fuegia Basket 251, Ushuaia, Argentina

M. L. Villarreal
Departamento de Geografía y Turismo, Universidad Nacional del Sur, Bahía Blanca, Argentina

A. I. Torres and V. A. Campodonico (eds.), *Environmental Assessment of Patagonia's Water Resources*, Environmental Earth Sciences,
https://doi.org/10.1007/978-3-030-89676-8_12

1 Introduction

The geoelectrical methods are based on electrical conductivity or **resistivity** of rocks and sediments, and they allow to determine the thickness of a strata sequence. They are used for groundwater exploration, due to this property in the presence of water. The Vertical Electrical Sounding (VES) is a simple and relatively accessible geophysical prospecting method that allows to obtain a distribution curve of resistivity vs. depth.

Although this geoelectrical methods are used in different regions for groundwater prospecting (e.g. López Vazques 2011; Mársico et al. 2013; Perdomo et al. 2011, 2013a, b), they have not been applied in the studied area in order to survey the characteristics and behavior of the groundwater systems. The available information on groundwater close to the study area is scarce, where the work of Kruse et al. (2017) on Río Grande city (Fig. 1) stands out. Most previous works refer to the characteristics of the surface catchment areas, either lacustrine or fluvial (Iturraspe and Urciuolo 2000, 2002; Quiroga et al. 2014, 2017; Quiroga et al. 2014; Villarreal et al. 2014; Villarreal and Coronato 2015, 2017; among others).

The Fuegian steppe represents the main livestock area of Tierra del Fuego, Antártida e Islas del Atlántico Sur province. Although there are shallow lakes, most of them contain salty waters, not suitable for animal consumption (Mariazzi et al. 1987; Crosta et al. 2014). The surface catchment areas of the region have numerous streams, but with a very low flow, and in many cases, only functional in spring (Quiroga et al. 2014). Therefore, there is a need to have alternative water sources to facilitate livestock activity.

The aim of this chapter is to present the hydrolithological features of an area in the Fuegian steppe, based mainly on a series of VES. The information presented here is expected to contribute with the understanding of the hydrogeological system of an area of northern Tierra del Fuego.

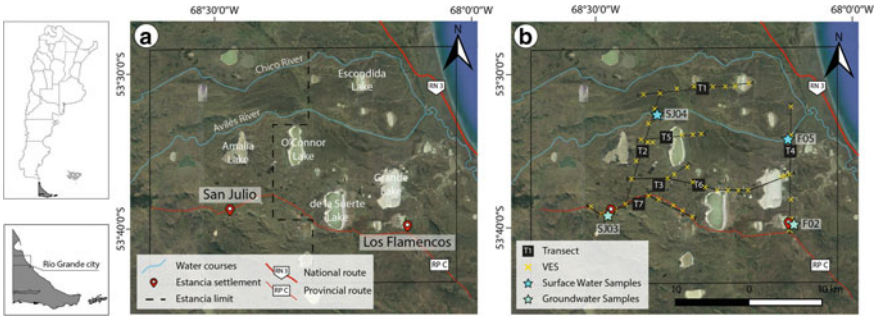

Fig. 1 **a** Location of the studied area in the northern of Tierra del Fuego province, Argentina, **b** Location map of the transects and water samples. VES: Vertical Electrical Sounding

2 Study Area

The study area is located in the province of Tierra del Fuego, Antártida e Islas del Atlántico Sur, Argentina, at 34 km northwest of Río Grande city (Fig. 1a). It has an area of approximately 700 km^2, and is largely included in the area of Estancias (Ea), Los Flamencos (LF) and San Julio (SJ).

The climate for this region was defined by Coronato et al. (2008) as sub-humid oceanic cold with an aridity index of 0.75. Its main feature is the intensity and permanence of wind prevailing from the NW-W-SW. The mean temperature during austral summer is 10 °C (January) and −1 °C in austral winter (July). Such annual variation determines one of the highest continentality indices for the Isla Grande de Tierra del Fuego (Tukhanen 1992). The mean annual precipitation of the region was pointed out to be below 400 mm (Tukhanen 1992), including snowfalls from April to September. Seasonal ground freezing occurs in the upper 30 cm between May and August. At a regional scale, the southwest sector receives 410 mm per year, whereas the northeast is the least rainy area with 320 mm per year. Such progressive decrease in the rainfall data defines a diminishing southwest-northeast gradient at a rate of 2 mm km^{-1} (Quiroga 2018).

The dominant vegetation in the steppe is represented by *Festuca gracillima* (coirón), *Empetrum rubrum* (murtilla), *Chiliotrichium diffusum* (mata negra), *Hordeum comosum* (cola de zorro) as well as different species of *Poa*. In grazing areas, endemic plant species of cold environments and nutrient-lacking soils such as *Bolax gummifera* and *Azorella trifurcata* are found (Moore 1983; Collantes et al. 1989). *Hieracium pilosella* represents the most conspicuous and disseminated invasive species in the study area (Villarreal et al. 2014).

The geology of the area (Fig. 2) is dominated by marine sediments from the Carmen Silva Formation (middle Miocene) (Codignotto and Malumián 1981). Most of the outcrops are found in the west of the study area. It is formed by two members: the lower one made of claystones and sandy limestones from marginal marine environments, and the upper one made of limestones and sandstones with conglomerate banks, of a **deltaic** origin (Malumián and Olivero 2006). Above these sediments, a gravel level of varied thickness, covered by aeolian deposits composed by fine sands and silty clays occurs (Coronato 2014). In the Ea. SJ settlement nearby area and above Carmen Silva Formation, outcrops of Castillo Formation (De Ferrariis 1938) of middle Miocene age (Codignotto and Malumián 1981) are found. They are composed of conglomerates and conglomeratic sandstones from fluvial environments (Malumián and Olivero 2006). Several levels of sands and gravels of **glaciofluvial** fans (middle Pleistocene) (Bujalesky et al. 2001) are found in the northern area, which form smooth slope lands to the east. The rest of the area is covered by fluvial, lacustrine and aeolian deposits (late Pleistocene-Holocene).

The topography is represented by deeply dissected hills, low round-shaped and plateau-like whose maximum heights reach 320 m a.s.l. (Coronato 2007) (Fig. 3). The lower areas are characterized by abundant pans or deflation basins where semi-permanent shallow lakes are formed seasonally (Villarreal and Coronato 2017). These

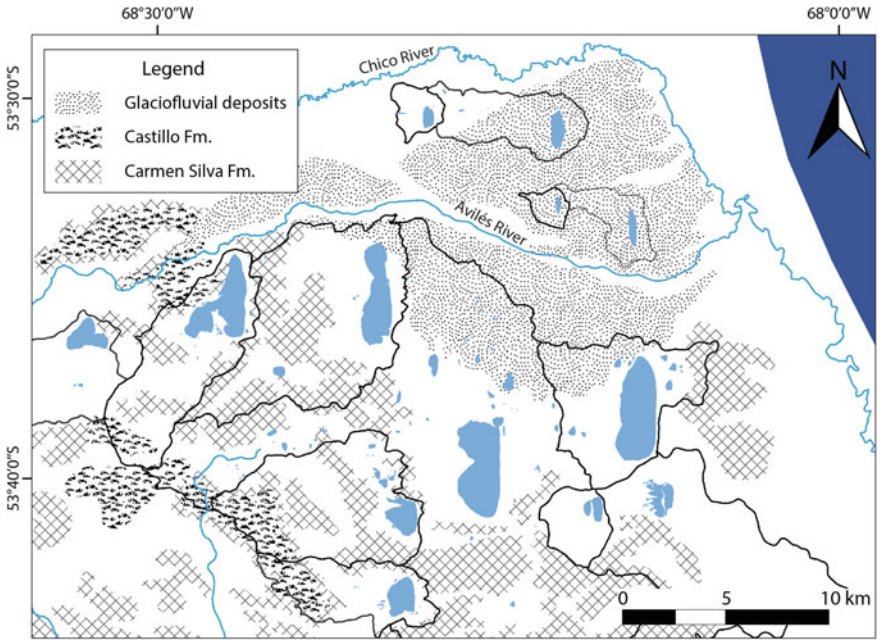

Fig. 2 Distribution of the main lithology units

shallow and ephemeral lakes are the center of **endorheic basins** and have no permanent superficial affluents or discharge runoff (Iturraspe and Urciuolo 2002), however they gather the runoff from precipitation. The pans which contain the shallow lakes vary in size from 3 to 207 km^2 (Villarreal and Coronato 2015), according to their development on glaciofluvial deposits, marine deltaic sediments or marine-proximal continental sediments (Fig. 3). Their water content depends on the soil-vegetation association and is highly sensitive to evaporation, mainly during summer when temperatures are the highest and winds blow frequently and intensively (Iturraspe and Urciuolo 2000). The water saline content, together with the turbidity, make these shallow lakes not suitable for human or cattle consumption. Mariazzi et al. (1987) carried out limnological studies in one of these lakes where the dissolved contents of sodium, phosphorus, manganese and iron stand out, whereas Crosta et al. (2014) observed halite superficial crystallization on the dry bottom of Escondida Lake along periods of water deficiency (October–November). In general, the valleys dissecting the hills are wide and flat-bottomed, with narrow and shallow streams. Most of the streams are ephemeral and of a pluvio-nival regime and form the endorheic drainage basins network where several shallow lakes are found (Coronato 2014). Although their mean low discharge, Avilés (0.035 m^3 s^{-1}; Quiroga et al. 2014) and Chico (3 m^3 s^{-1}; Urciuolo and Iturraspe 2010) rivers are the main surface water courses in the region. Their headwaters are located in the western Chilean area of Tierra del

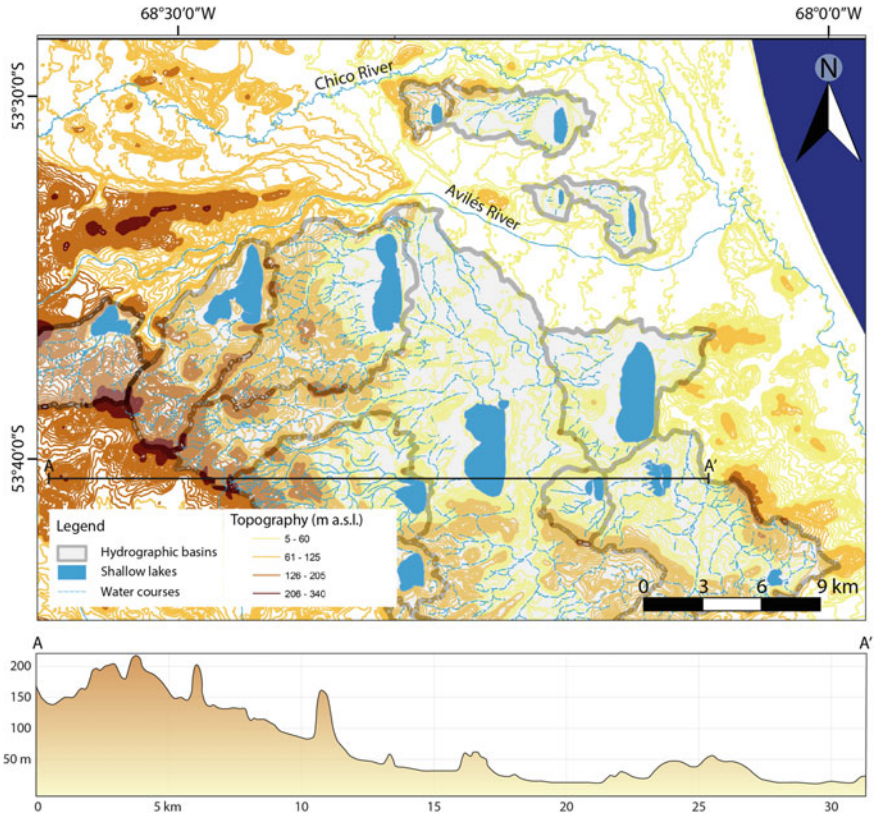

Fig. 3 Hydrographic basins and topographic map

Fuego and they flow with a W-E direction, being part of an exorheic basin including the Avilés River as a tributary branch of the Chico River (Fig. 1a).

3 Methodology

Fieldwork consisting in hydrological and geophysical surveys was carried out in order to determine the main units and hydrolithological features of the study area during spring–summer seasons from 2017 to 2019. In April 2018, two surface water samples from the middle and lower sections of the Avilés River; and two groundwater samples, one from spring water collected in a tank in the Ea. SJ settlement and another one from a drilling well in the Ea. LF settlements were collected (Fig. 1b) using PVC bottles and stored at 4° C. They were analyzed in laboratory (LANAQUI-CERZOS-CONICET) in order to determine the major and some minor ions concentrations (Na^+, Mg^{2+}, K^+, Ca^{2+}, Cl^-, SO_4^{2-}, HCO_3^-, CO_3^{2-}, $N–NO_3^-$ and As), as well as

pH and electrical conductivity (EC). Besides this, a groundwater level measurement was carried out in a second drilling well.

The **geophysical survey** was carried out through VES in seven transects. The VES is an indirect geoelectrical method based on the rocks and sediments conductivity or resistivity**,** which allows to determine thickness of layers, as long as the sequence is horizontal and the contrast between layers is noticeable enough. The employed equipment was a Digital Geometer Resistivimeter MPX-400 formed by a transmitting module which sends direct current, a receptor module which operates resistivity and spontaneous potential, together with a 12 V battery. Both modules must be connected to each other and to the battery (Fig. 4). Two current electrodes (AB, iron made) to inject electricity into the ground and two potential electrodes (MN, copper made) for potential difference measurements complete the equipment. The electrodes are buried along a straight line according to the Schlumberger configuration where the further from each other, the deeper. The difference in the measured potential leads to the apparent resistivity value (ohm.m), which allows to build a new curve in agreement with the distance of the current electrodes (AB).

Every sounding was geographically referenced using a Trimble R8s Global Positioning System, including the height measurement. The VES were strategically located on the ground according to the geological, geomorphological and accessibility characteristics, making transects which allowed us to correlate data and generate geoelectrical sections.

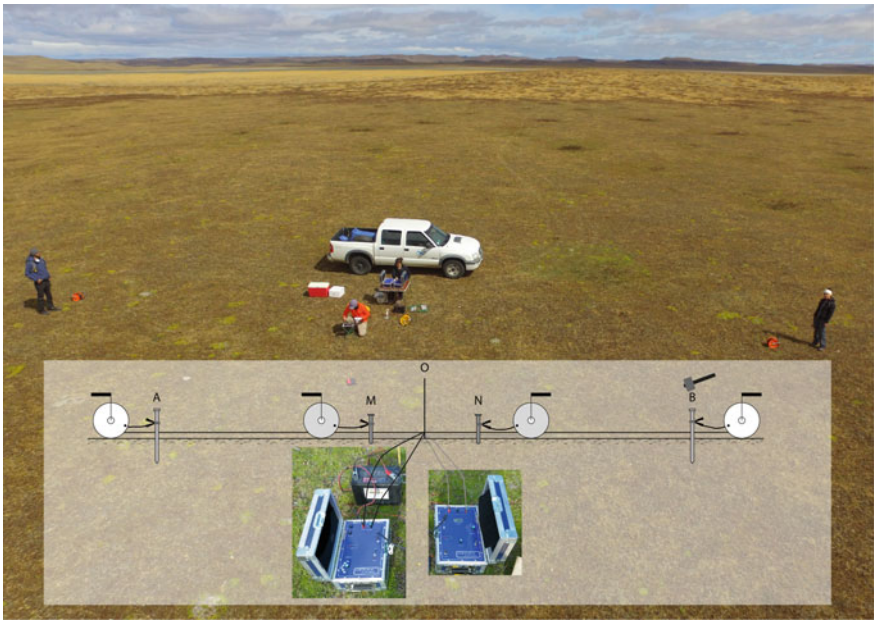

Fig. 4 Vertical Electrical Sounding fieldwork and its operation scheme

The methodology proposed by Zohdy (1989) was used for the inversion process. The field apparent resistivity data are digitized in a rate of 6 dots per logarithmic decade, then processed with Zohdy (1973) software. Such geoelectric cuts resistivity values were gathered in groups to define layers that may be geologically and hydrolithologically correlated.

The **geoelectric cuts** for each VES were gathered in transects (Fig. 1b), which allowed the construction of geoelectric sections. A first correlation was carried out according to the resistivity ranges which allowed gathering the layers in different units on the basis of the available geological data. The units may be outlined in transects that represent geoelectrical sections, where the geology and geomorphology of the sector are both correlated.

4 Results and Analysis

4.1 Geoelectrical Resistivity

Transect 1: It is located in the north of the study area and it is 13.5 km long (Fig. 5a). From west to east the VES are 58, 57, 56, 20, 12, 11, 55 and 54. The geoelectric section shows a series of layers with resistivity over 30 Ω.m (Units 3a and 4a), west of Escondida Lake. These layers define a deposit of a maximum thickness of 35 m

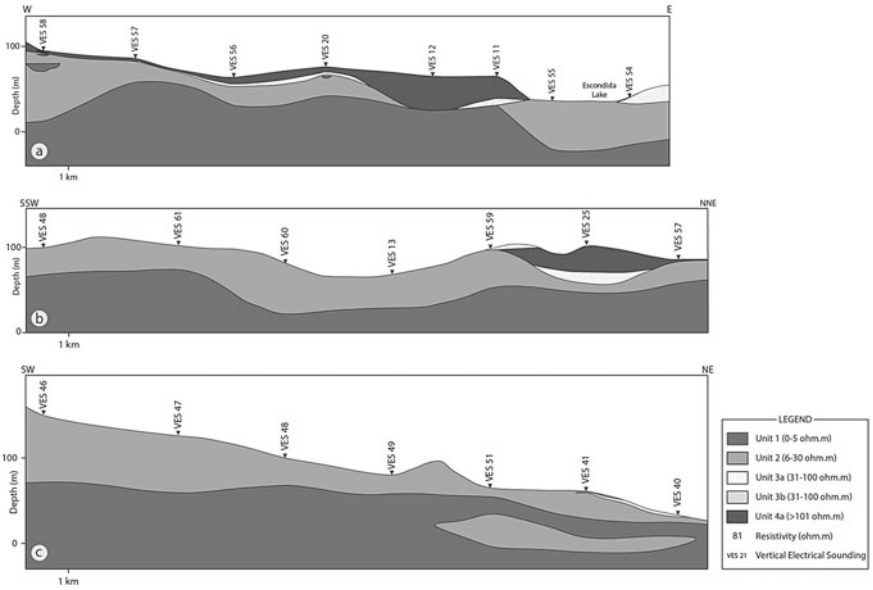

Fig. 5 **a** Transect 1, **b** Transect 2, **c** Transect 3

(VES 12). Another layer is defined below this one, with resistivity between 6 and 30 Ω.m (Unit 2).

Finally, the lowest layer is identified, with a low resistivity (below 5 Ω.m). In VES 58 and 20 small lenses interspersed with Unit 2 may be observed.

Transect 2: It is located in the west of the study area, between Amalia and O´Connor lakes and it is 14.8 km long (Fig. 5b). From south-southwest to north-northeast the VES are 48, 61, 60, 13, 59, 25 and 57. In VES 48, 61, 60 and 13 only two layers are defined: the upper one, 30 to 50 m thick, with resistivity up to 30 Ω.m (Unit 2); below a layer with resistivity lower than 5 Ω.m (Unit 1).

To the north-northwest, in VES 59, 25 and 57, Units 3a and 4a are observed over those previously described. They present resistivity over 30 Ω.m. They both express their maximum thickness in VES 25 (15 and 30 m, respectively).

Transect 3: It is a southwest-northeast oriented transect, south of Amalia and O´Connor lakes with a length of 14.8 km (Fig. 5c). It is represented by VES 46, 47, 48, 49, 51, 41 and 40. The transect presents an upper layer whose thickness varies from 90 m to almost 5 m, from southwest to northeast. The resistivity ranges from 6 to 30 Ω.m (Unit 2). Below, another layer with resistivity lower than 5 Ω.m is found all along the transect (Unit 1).

Between VES 51 and 40, to the northeast of the section, a lens with up to 30 Ω.m resistivity intersperses with the previous layer. The maximum thickness recorded is 37 m at 30 m depth. Finally, in the northeast tip of the transect, between VES 41 and 40, a 1 to 2 m thick superficial layer from Unit 3b is observed, whose resistivity ranges from 40 to 60 Ω.m.

Transect 4: It is located east of the study area, with a north–south orientation, and is 15.9 km long (Fig. 6a). It is represented by VES 53, 52, 3, 24, 10, 9, 8 and 22. This transect mostly presents two layers: the lower one, with resistivity lower than 5 Ω.m

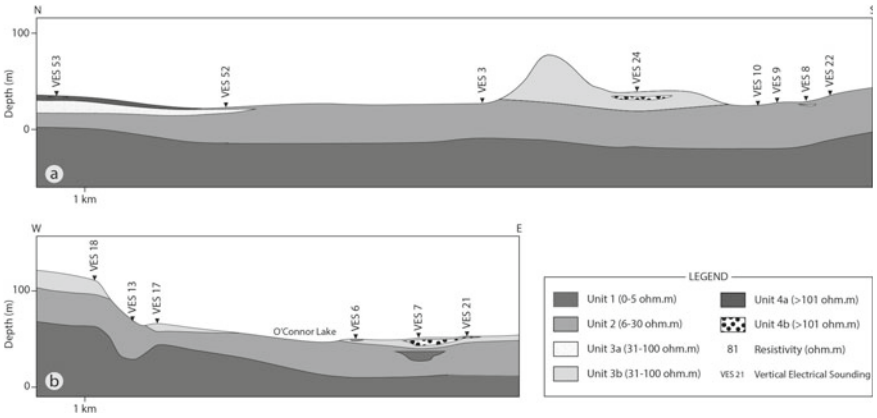

Fig. 6 **a** Transect 4, **b** Transect 5

at around 35–40 m deep (Unit 1), and the upper one with resistivity up to 30 Ω.m and 20 to 40 m thick (Unit 2).

Other two units overlying the previous ones are found to the north. The surface layer presents a maximum thickness of 5 m and resistivity up to 230 Ω.m (Unit 4a), whereas Unit 3a is below this one, with a thickness ranging from 4 to 13 m and resistivity between 37 and 68 Ω.m.

Finally, VES 24 presents resistivity higher than 30 Ω.m in the layers of the upper 20 m (Units 3b and 4b). They do not occur in the adjacent VES, except for VES 8 where a small lens is observed at 3 m depth, with a resistivity of 42 Ω.m which represents Unit 3b.

Transect 5: It is located in the center of the study area, west–east oriented and crosses O´Connor Lake (Fig. 6b). It is 7.7 km long and lies along VES 18, 13, 17, 6, 7 and 21. It is mainly formed by three layers. The lower one is at 50 m deep, corresponding to Unit 1, with resistivity below 5 Ω.m. Right over is Unit 2 with resistivity between 6 and 30 Ω.m, from 5 to 20 m depth. Unit 3b emerges in a layer from 5 to 20 m thick with resistivity ranging from 31 to 100 Ω.m.

VES 7 and 21 are east of the transect, where a lens from Unit 4b is observed at 1 m depth, interspersed in Unit 3b. It presents resistivity higher than 101 Ω.m and has a thickness from 1 to 8 m. Finally, in VES 7, a 10 m thick lens from Unit 1 is found at 13 m depth, within Unit 2.

Transect 6: It is located in the center of the study area; it is 21 km long and is west–east oriented (Fig. 7a). It is formed by VES 61, 51, 37, 36, 35, 34, 33, 32, 1, 2 and 3.

An interspersed series of layers of Units 1 and 2 repeats four times to the west, with thicknesses from 10 to 30 m, whereas only two appear to the east: the upper one with a thickness of 30 m and resistivity between 6 and 30 Ω.m, and the lower

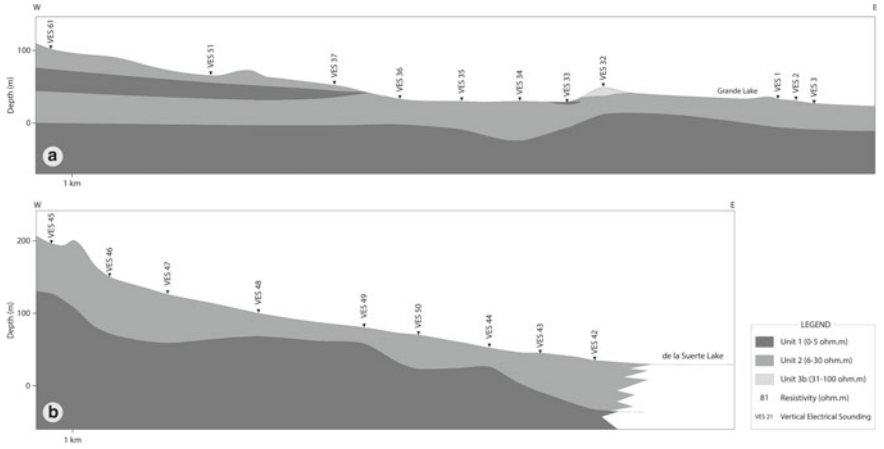

Fig. 7 **a** Transect 6, **b** Transect 7

one with resistivity below 5 Ω.m at 30 m depth. A layer of around 15 m thickness, with resistivity ranging from 31 to 100 Ω.m is found in VES 32 and corresponds to Unit 3b.

Transect 7: It is located on Provincial Route C, in the southwest of the study area and is 15 km long (Fig. 7b). It is formed by VES 45, 46, 47, 48, 49, 50, 44, 43 and 42.

Two layers occur all along, the lowest one with resistivity below 5 Ω.m (Unit 1), between 20 and 75 m depth, and the upper one with resistivity between 6 and 30 Ω.m (Unit 2) and a thickness between 20 and 75 m.

4.2 Hydrochemistry

According to Table 1, in the highest area (sample SJ03), groundwater presents an EC of 460 μS cm^{-1} (Ea. SJ) and corresponds to the sodium bicarbonate type, whereas in the topographically lowest sectors (Ea. LF—LF02), groundwater presents higher EC values that reach 1110 μS cm^{-1}, and is classified as sodium chloride.

Moreover, sampling carried out in the middle (SJ04) and lower (LF05) catchment sections of Avilés River resulted in sodium bicarbonate and sodium bicarbonate/chloride water types respectively, with EC values of 330 and 370 μS cm^{-1} respectively, and pH 8.

Table 1 Water samples analyses results

Samples	LF02	SJ03	SJ04	LF05
pH	8.2	7.6	8.0	8.1
EC (μS cm^{-1})	1110	460	330	370
Na^+ (mg L^{-1})	225.0	59.5	46.6	55.4
Mg^{2+} (mg L^{-1})	0.8	6.5	10.1	6.4
K^+ (mg L^{-1})	9.6	7.4	6.7	5.9
Ca^{2+} (mg L^{-1})	2.5	21.0	27.1	13.9
Cl^- (mg L^{-1})	195.0	40.4	33.6	63.9
$SO_4{}^{2-}$ (mg L^{-1})	30.9	10.2	24.2	15.0
$HCO_3{}^-$ (mg L^{-1})	288	190	140	115
$CO_3{}^{2-}$ (mg L^{-1})	Free	Free	Free	Free
N–NO_3– (mg L^{-1})	0.59	0.45	0.41	0.32
As (mg L^{-1})	<0.01	<0.01	<0.01	<0.01

5 Discussion: *Lithological and Hydrolithological Interpretations*

A synthesis of the lithological interpretation of the SEVs transects is shown in Table 2.

The geoelectrical prospecting by VES allowed to get indirect information of the subsoil down to 100 m depth. The superficial geological, hydrological and geomorphological information led to the elaboration of the conceptual model of a system with two different hydrolithological units: the lowest one identified in depths varying from 5 to 90 m, of an **aquiclude or aquitard** (Unit 1), and the top one formed by the **unconfined aquifer**, an aquitard and the non-saturated portion zone (Units 2, 3a, 3b, 4a, 4b).

The **lithological** characteristics and the low resistivity recorded (0 to 5 Ω.m) in the lowest hydrolithological unit (LHU) allow us to infer layers of low (aquitard) to null (aquiclude) water transmission, as well as high salinity waters.

The upper hydrolithological unit (UHU) would be formed by both aquitards and aquifer layers. The first ones would be represented by the middle-**hydraulic conductivity** deposits (limestones) which belong to the upper member of the Carmen Silva Formation. On the other hand, the aquifers would be formed by sandstones with conglomerate banks from the same formation, as well as the quaternary sand and gravel sediments corresponding to different levels of glaciofluvial fans, both with resistivity recorded from 31 to above 100 Ω.m.

Table 2 Resistivity and lithology of the proposed units

Unit	Resistivity (ohm.m)	Lithology	Possible geological formation	Hydrolithological assumptions
1	<5	Claystones/sandy-limestones	Lower member of Carmen Silva Formation	Lowest hydrolithological unit (LHU)
2	6–30	Limestones	Upper member of Carmen Silva Formation	Upper hydrolithological unit (UHU)
3a	31–100	Sands	Quaternary glaciofluvial fan	
3b	31–100	Sandstones	Undifferentiated quaternary sediments	
4a	>101	Gravels	Quaternary glaciofluvial fan	
4b	>101	Conglomerates	Undifferentiated quaternary sediments	

Although the UHU presents resistivity values above 100 Ω.m, they are still low according to its lithology, which could be due to the presence of high salinity groundwater.

In general terms it may be stated that the **water table** is found at a shallow depth in the topographically depressed sectors. This is confirmed by the geoelectric results and the measurement of the water table in Ea. LF.

This preliminary hydrolithological model coincides partially with the one presented by Kruse et al. (2017) for the city of Río Grande (15 m a.s.l.), where the top unit is characterized as a shallow aquifer with high hydraulic conductivity, related with marine pleistocene and holocene gravels and sands. On the contrary, for the deepest hydrolithological unit, the authors recognize certain levels corresponding to a semi-confined aquifer with interspersion of high and low hydraulic conductivity layers.

6 Conclusions

The geoelectrical survey provided indirect information which reaches approximately 100 m depth and allowed to elaborate a conceptual model based on the correlation between layers of a similar resistivity and geological formations that occur in the area. The altimetric location and geomorphology of the outcrops allowed to adjust the conceptual model as a system composed by interspersions of sediments of low, middle and high hydraulic conductivity. The shallow ones would agree with the upper member of the Carmen Silva Formation as well as the glaciofluvial deposits, and would be the unconfined aquifer identified as the upper hydrolithological unit. The deeper ones would correspond to the lower member of such formation and would form an aquitard identified as the lowest hydrolithological unit.

The regional groundwater flow direction is inferred from west to east given by the topographic relationship with rivers and shallow lakes, some water table measurements and the groundwater samples analyses.

The fragility of the hydrolithological system, mainly conditioned by the lithological and climatic characteristics of the area, makes the exploitation of the groundwater resources a matter that must be properly planned in order to grant its sustainability, for which it is essential to deepen several aspects of the hydrogeological studies in the region, such as exploration drilling wells, hydraulic pumping tests and more groundwater samples analysis.

Acknowledgements This study was supported by Consejo Nacional de Investigaciones Científicas y Técnicas (P-UE 22920160100077CO). We want to thank managers and staff from Estancias Los Flamencos and San Julio for allowing us to develop all our activities, as well as the staff from Estación Astronómica Río Grande for welcoming and providing us accommodation throughout field work.

References

Bujalesky GG, Coronato A, Isla FI (2001) Ambientes glacifluviales y litorales cuaternarios de la región del río Chico, Tierra del Fuego, Argentina. RAGA 56(1):73–90 (in Spanish)

Codignotto JO, Malumián N (1981) Geología de la región al norte del paralelo 54°S de la Isla Grande de Tierra del Fuego. RAGA 36(1):44–48 (in Spanish)

Collantes MB, Anchorena J, Koremblit G (1989) A soil nutrient gradient in Magellanic Empetrum heathlands. Vegetatio 80(2):183–193

Coronato A (2007) El paisaje de Tierra del Fuego. In: Godoy Manríquez CJ (ed) Patagonia total, antártida e islas malvinas. Barcel Baires Ediciones (in Spanish), Buenos Aires, pp 601–615

Coronato A (2014) Territorios fueguinos: fisonomía, origen, evolución. In: Oría J, Tívoli A (eds) Cazadores de mar y tierra. Estudios recientes en arqueología fueguina. Editora Cultural Tierra del Fuego (in Spanish), Ushuaia, pp 43–63

Coronato A, Coronato F, Mazzoni E, Vázquez M (2008) The Physical Geography of Patagonia and Tierra del Fuego. Dev Quaternary Sci 11:13–55

Crosta S, Villareal ML, Coronato A (2014) Formación de cristales de halita en la laguna Escondida, norte de Tierra del Fuego. In Massone H, Miglioranza K (eds) Actas III Reunión argentina de geoquímica de la superficie. UNMdP-IIMYC-CONICET, Argentina (in Spanish), Mar del Plata, pp 16

De Ferrariis C (1938) Una reunión de geólogos de YPF y el problema de la terminología estratigráfica. In: Fossa Mancini E, Feruglio E, Yussen de Campana JC (eds) Boletín de informaciones petroleras (in Spanish), pp 43–44; 94–95

Iturraspe R, Urciuolo A (2000) Clasificación y caracterización de las cuencas hídricas de Tierra del Fuego. In: Proceedings of the XVIII congreso nacional del Agua, Río Hondo, Argentina (in Spanish)

Iturraspe R, Urciuolo A (2002) Ciclos deficitarios en el régimen de sistemas lagunares de la estepa fueguina. In: Proceedings of the XIX congreso nacional del Agua, Villa Carlos Paz, Argentina (in Spanish)

Kruse E, Lofiego R, Laurencena P, Deluchi M, Carretero S (2017) Condiciones hidrogeológicas en la zona de Río Grande (Tierra del Fuego). In: Proceedings of the XX congreso geológico argentino, San Miguel de Tucumán, Argentina (in Spanish)

López Vazques G (2011) Investigación hidrogeológica en salares con la aplicación del método geoeléctrico. Salar de Olaroz, Cauchari, Departamento Susques, Jujuy, Argentina. In: Proceedings of the VII congreso argentino de Hidrogeología, V Seminario Hispano-Latinoamericano sobre temas actuales de la hidrología subterránea. Hidrogeología regional y exploración hidrogeológica, Salta (in Spanish)

Malumián N, Olivero EB (2006) El grupo Cabo Domingo, Tierra del Fuego: Bioestratigrafía, paleoambientes y acontecimientos del Eoceno-Mioceno marino. RAGA 61(2):139–160 (in Spanish)

Mariazzi A, Conzonno VH, Ulibarrena J, Paggi JC, Donadelli JL (1987) Limnological investigation in Tierra del Fuego—Argentina. Biol Acuat 10:80

Mársico D, Díaz E, Dalla Costa O, Aceñolaza B (2013) Los sondeos eléctricos verticales aplicados a la prospección de las aguas termales en la provincia de Entre Ríos. VIII Congreso Argentino de Hidrogeología. VI Seminario Hispano-Latinoamericano sobre termas actuales de la hidrología subterránea. La Plata, Argentina (in Spanish)

Moore DM (1983) Flora of Tierra del Fuego. Missouri Botanical Garden, USA

Perdomo S, Ainchil JE, Kruse EE, Nigro J, Tessone M, Lagos SR, Pensa M (2013a) Resistividad eléctrica y cargabilidad del acuífero puelche en La Plata, provincia de Buenos Aires. VIII Congreso Argentino de Hidrogeología. VI Seminario Hispano-Latinoamricano sobre temas actuales de la hidrología subterránea. La Plata, Argentina (in Spanish)

Perdomo S, Carretero S, Ainchil JE, Kruse EE (2011) Imágenes de resistividad eléctrica en lentes de agua dulce de la zona costera oriental de la provincia de Buenos Aires. VII Congreso Argentino

de Hidrogeología. V Seminario Hispano-Latinoamericano sobre temas actuales de la hidrología subterránea. Salta, Argentina (in Spanish)

Perdomo S, Carretero SC, Kruse EE, Ainchil JE (2013b) Identificación de la intrusión salina en Santa Teresita (Prov. Buenos Aires), mediante la aplicación de métodos eléctricos. VIII Congreso Argentino de Hidrogeología. VI Seminario Hispano-Latinoamericano sobre temas actuales de la hidrología subterránea. La Plata, Argentina (in Spanish)

Quiroga D (2018) La incidencia de los agentes naturales y antropogénicos en la evolución geomorfológica de la región Río Chico—Río Grande, Tierra del Fuego. Tesis doctoral. Universidad Nacional del Sur, Bahía Blanca (in Spanish)

Quiroga D, Gil V, Coronato A (2014) Morfometría y geomorfología de la cuenca del río Avilés, Tierra del Fuego, Argentina. Aportes al conocimiento de las condiciones de escurrimiento en territorios semiáridos. Cuat Geomor 28(1–2), 63–80 (in Spanish)

Quiroga D, Gil V, Coronato A (2017) Quantitative geomorphology applied to fluvial dynamic in Aviles and Moneta basins, Tierra del Fuego, Southern Argentina. Environ Earth Sci 76(5):188

Tuhkanen S (1992) The climate of Tierra del Fuego from a vegetation geographical point of view and its ecoclimatic counterparts elsewhere. Acta Bot Fenn 145:1–64

Urciuolo A, Iturraspe R (2010) Informe Hidrológico Cuenca Río Chico. Secretaría de Desarrollo Sustentable y Ambiente, Dirección General de Recursos Hídricos (in Spanish), Tierra del Fuego

Villareal ML, Coronato A (2015) Caracterización morfométrica de lagunas interiores del norte de Tierra del Fuego. VI Congreso Argentino de Cuaternario y Geomorfología, Ushuaia (in Spanish)

Villarreal ML, Coronato A (2017) Characteristics and nature of pans in the semiarid temperate-cold steppe of Tierra del Fuego. In: Rabassa J (ed) Advances in geomorphology and quaternary studies in Argentina. Springer, The Netherlands, pp 203–224

Villarreal ML, Coronato A, Mazzoni E, López R (2014) Mantos eólicos y lagunas semipermanentes de la Estepa Fueguina (53°S), Argentina. Rev Soc Geol Esp 27(2):81–96 (in Spanish)

Zohdy AR (1973) A computer program for the automatic interpretation of schlumberger sounding curves over horizontally stratified media geological survey. Department of Commerce, Springfield, USA

Zohdy AR (1989) A new method for the automatic interpretation of schlumberger and wenner sounding curves. Geophysics 54(2):245–253

Water Quality Assessment in Urban Watersheds of Tierra del Fuego: A Perspective from the Integrated Water Resources Management

Soledad Diodato, Yamila Nohra, Gerardo Noir, Julio Escobar, Romina Mansilla, and Alicia Moretto

Abstract Water quality deterioration is one of the most challenging environmental problems in the world. Land use change like urbanization has several impacts on the presence, utilization and management of water resources. The Province of Tierra del Fuego, Southernmost Patagonia, Argentina, is not exempt from the challenges that happen at a global scale. Several problems derived from the high pressure that natural resources are subjected to are evident. Therefore, the generation of information is of great relevance within the Integrated Water Resources Management (IWRM) framework with an Ecosystem Approach (EA). Water Quality of five relevant watersheds of Tierra del Fuego from the Río Grande and Ushuaia cities was systematically monitored during the period 2008–2019, assessing physicochemical and microbiological parameters. The Canadian Council of Ministers of the Environment Water Quality Index was applied to simplify and facilitate the transmission of the generated information to diverse actors. Although downstream sampling sites presented fair to poor water quality, headwaters from water intakes remains of good quality. It is necessary to implement IWRM with an EA as a way of preserving environmental and population health.

Keywords Urbanization · Water quality monitoring · Río Grande · Ushuaia · Water sources

S. Diodato (✉) · J. Escobar · R. Mansilla · A. Moretto
Centro Austral de Investigaciones Científicas, CONICET, Ushuaia, Argentina
e-mail: sdiodato@conicet.gov.ar

S. Diodato · R. Mansilla · A. Moretto
Instituto de Ciencias Polares, Ambiente y Recursos Naturales, Universidad Nacional de Tierra del Fuego, Ushuaia, Argentina

Y. Nohra · G. Noir
Dirección General de Recursos Hídricos, Secretaría de Ambiente, Ministerio de Producción y Ambiente de Tierra del Fuego, Ushuaia, Argentina

A. I. Torres and V. A. Campodonico (eds.), *Environmental Assessment of Patagonia's Water Resources*, Environmental Earth Sciences,
https://doi.org/10.1007/978-3-030-89676-8_13

1 Introduction

Water, as a vital resource for the life and the development of the society, must be managed for the benefit of the entire population, since it is a scarce resource in time and space, it has low costs, sometimes does not have legal protection measures and it is subjected to the vulnerability of pollution. This fact implies that the local government authorities have to assume the responsibilities related to its management, conservation, control and regulation of its appropriate use. If there is or will be a water crisis there will also be a development crisis; therefore, water management has to do with how this vital natural resource is managed (Al Radif 1999).

Worldwide, there is a competition for the multiple uses of water due to population, energy and agricultural demands. As the population increases and the economy grows, the need for water provision and the pressure on water resources increases (Giri and Qiu 2016). In essence, water management is a conflict management, which allows focusing on several interests related to the quantity and quality of water; and involving the design and use of practical and effective mechanisms to solve the future conflicts (Martínez Valdes and Villalejo García 2018).

During the recent decades, river water quality and the different problems related to the presence, utilization and management of water resources have been matter of constant concern (Al Radif 1999; Zamparas and Zacharias 2014; Chittoor Viswanathan and Schirmer 2015). Direct and indirect impacts of urbanization and agricultural activities degrade water quality, as the consequence of land use change (Yu et al. 2013; Giri and Qiu 2016; Miller and Hutchins 2017). Agricultural activities involve the use of increasing amounts of fertilizers, pesticides, herbicides, and dairy manures in croplands to fulfill the food demand of human population and some of them enter into the nearest water bodies (Giri and Qiu 2016). Urbanization increases impervious surfaces such as parking lots, roads, and sidewalks, resulting into an increase in runoff which creates an additional pathway for the transportation of pollutants from landscape into water bodies (Wilson and Weng 2010; Glińska-Lewczuk et al. 2016).

As a consequence of urbanization, a great number of rivers and streams are highly contaminated due to the anthropogenic activities such as industrial and sewage disposal (Almeida et al. 2007; Zagarola et al. 2017; Granitto et al. 2021). The problem increases when the depurating capacities of these aquatic systems are significantly reduced in relation to the amount and kind of contaminating substances received (Almeida et al. 2007; Oliva González et al. 2014). In this sense, river pollution endangers water reserves and the ecosystem services related to it. Therefore, every problem associated with the lack of water and the deterioration of its quality constitutes an important issue for the twenty-first century.

The Integrated Water Resources Management (IWRM) is defined as "a process which promotes the coordinated development and management of water, land and related resources, in order to maximize the resultant economic and social welfare

in an equitable manner, without compromising the sustainability of vital ecosystems" (GWP 2000). This approach promotes moving from fragmentation to integration, from the mere exploitation of the resource to the conservation and rational use of it, from the management of supply to the management of demand, from paternalism to participation, from centralization to decentralization, from infrastructure management to efficient administration (Martínez Valdes and Villalejo García 2018).

The Province of Tierra del Fuego (TDF), Southernmost Patagonia, Argentina (Fig. 1a), is not exempt from the problems that happen at a global scale. For many years, the Fuegian community has been concerned about local water resources, which led in 2016 to the enactment of the Framework Law for the Integrated Water Resources Management N° 1126. The goal of this regulation is to build and promote an IWRM, in order to overcome threats, and to reduce vulnerability to scarcity or deterioration in water quality. These problems derive from the high pressure that the basins' natural resources are subjected due to the development of activities that impact them. This holistic concept is developed worldwide and is used to explore new forms of relationships between water and society within the Ecosystem Approach (EA) (IPBES 2019; Noir 2019). In this context, the generation of information is of great relevance within the framework of what is established by IWRM with an EA: the forests, peatlands, glacial environments and wetlands of TDF play a fundamental role due to the ecosystem services they provide for the conservation of the quantity and quality of water (Zagarola et al. 2014; Mrotek et al. 2019).

In TDF, 97% of the total population (127,205 inhabitants, INDEC 2010) is concentrated in the urban areas, in the cities of Río Grande, Ushuaia, and Tolhuin. The city of Río Grande is crossed by the largest basin of TDF. The Grande River watershed (GR) is a binational basin located in the southern portion of Argentina and Chile. Its importance lies in its large size and the magnitude of its annual average flow (40 m^3 seg^{-1}), receiving important tributaries in the Argentine sector of TDF (Iturraspe and Urciuolo 2000). Also, it is the basin with the greatest number of uses in the province (drinking water, tourism, animal husbandry, fishing, oil activity, etc.), as well as the one that involves several social actors related to the different water uses. The GR is the drinking water source of Río Grande city, with the water intake located a few kilometers above the city. Also, the touristic and recreational use of water in the middle and lower basins has acquired great importance since numerous ranches have diversified their activities towards agrotourism and the establishment of fishing preserves (Urciuolo et al. 2009). Given its characteristics and ecological importance, this sector of 220 km of coast was incorporated into the Provincial System of Protected Natural Areas through the creation of the "Atlantic Coast Reserve" (1992; https://whsrn.org/es/whsrn_sites/costa-atlantica-de-tierra-del-fuego/), assigning it the category of Coastal Natural Reserve. In addition, since 1992 it constitutes a site of the Western Hemisphere Shorebird Reserve Network and a wetland of international importance declared a RAMSAR site (SAyDS 2009). The GR flows into the protected marine coastal zone constituting an estuary, where the city of Río Grande is located. The significant urban and industrial expansion of the city based on economic promotion laws of the 1970s, has caused changes in land use, as well as situations that altered the water quality of the estuary such as human settlements in the riverside

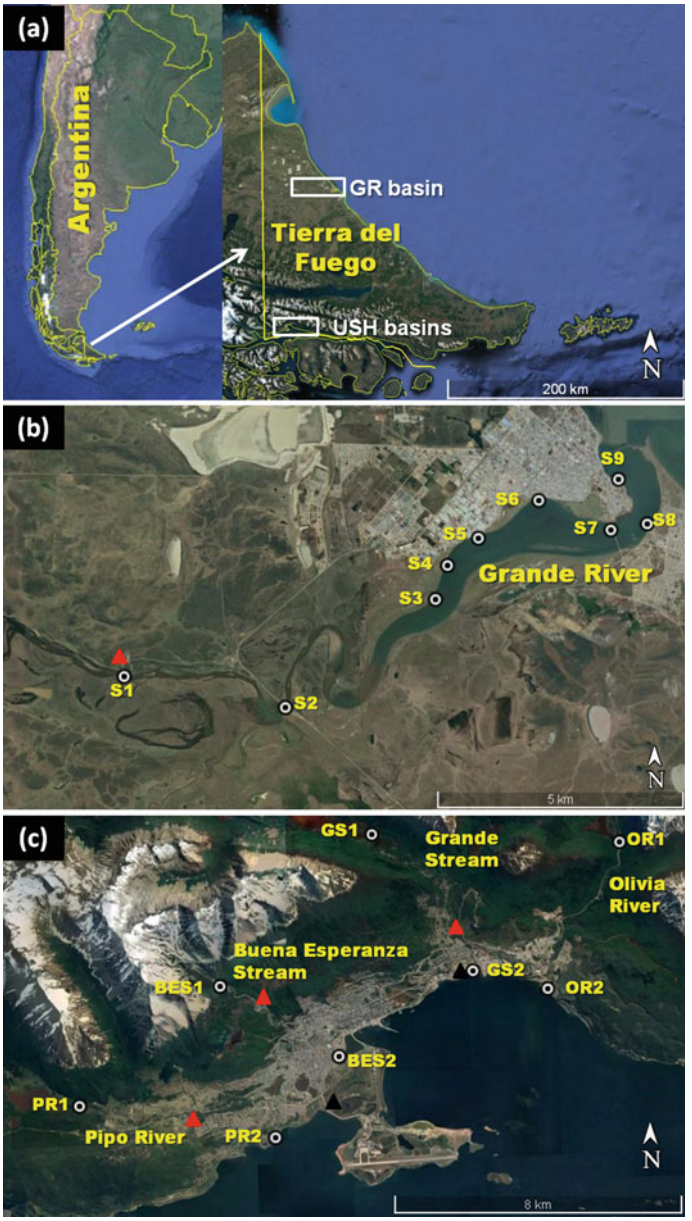

Fig. 1 Maps showing the location of the study area in Tierra del Fuego, Argentina (**a**), and the sampling sites at Grande River basin (**b**; S1–S9), and at four watersheds in Ushuaia city (**c**): Buena Esperanza Stream upstream (BES1) and downstream (BES2); Grande Stream upstream (GS1) and downstream (GS2), Olivia River upstream (OR1) and downstream (OR2), and Pipo River upstream (PR1) and downstream (PR2). Red triangles indicate drinking water treatment plants, and black triangles indicate wastewater treatment plants

and flooded areas, effluent discharges without treatment, and presence of solid wastes on the banks. In this way, the anthropogenic impact on the wetland has generated severe changes in the landscape of this relevant site (Lofiego et al. 2009), which also constitutes an environment of great importance for the inhabitants of Río Grande city.

The city of Ushuaia is defined by four main watersheds: Buena Esperanza Stream (BES), Grande Stream (GS), Olivia River (OR), and Pipo River (PR) (Iturraspe and Urciuolo 2000). Although each water course presents particular characteristics and defined uses, the major problem they have been subjected to is the negative consequences of urbanization. The population has exponentially increased in the last decades (from 7000 inhabitants in 1970 to approximately 60,000 in 2010; INDEC 2010). The main reason for this population growth was the promulgation of the Argentinian National Law N° 19,640 of industrial promotion and customs benefits, which motivated immigration from the central and northern provinces of Argentina. These facts led to substantial changes in land use, mainly due to the need for space for urban and industrial settlements. The urban expansion was not largely accompanied by the development of the necessary infrastructure to provide services such as drinking water and sewers to all the population. Therefore, the degradation of fluvial watersheds that cross the city and consequently, the coastal system of Ushuaia city has been subjected to the impact of raw sewage effluents (Amin et al. 2011; Zagarola et al. 2017; Diodato et al. 2018, 2020; Granitto et al. 2021).

Evaluation of limnological parameters can be considered an essential tool in the study of environmental problems, contributing to the knowledge of the main functioning mechanisms of aquatic ecosystems, assisting in water quality management, with a substantial role in the monitoring and recovery of water bodies, mainly regarding eutrophication control (Almeida et al. 2007; Akkoyunlu and Akiner 2012; Poonam et al. 2013; Oliva González et al. 2014; Glińska-Lewczuk et al. 2016). The information that provides the evaluation of limnological parameters are comprehensible for scientists; however, this type of information should also be meaningful to managers and decision makers who want to know about the state of their local water bodies. For this reason, water quality indexes (WQI) were designed with the aim of creating a mean of communicating water quality issues (CCME 2001).

One of the most commonly used indexes was developed in 2001 by the Canadian Council of Ministers of the Environment (CCME): the CCME Water Quality Index (CCME WQI). This index has been used widely worldwide to evaluate the water quality in rivers and other water bodies (Akkoyunlu and Akiner 2012; Bilgin 2018; Gikas et al. 2020; Hossain and Patra 2020). The CCME WQI offers several advantages over other methods, including compliance with different legal requirements and different water uses, eligibility for water quality assessment in specific areas, flexibility in the selection criteria, and tolerance for missing data. On the other hand, it does not require a huge number of different water quality parameters for its development and validation (CCME 2001). The index incorporates three elements: *scope*—the number of parameters not meeting water quality guidelines; *frequency*—the number of times these guidelines are not met; and *amplitude*—the amount by which the guidelines are not met (CCME 2017). The index produces a number

between 0 (worst water quality) and 100 (best water quality) and is divided into five descriptive categories to simplify its presentation: “poor”, “marginal”, “fair”, “good”, and “excellent”.

The CCME WQI can be used to track changes at one site over time and comparisons among sites. If used for the latter purpose, care should be taken to ensure that there is a valid basis for comparison. Sites should be compared when the same parameters and guidelines, time periods and numbers of samples are used. Otherwise, each site should be measured against its ability to meet relevant guidelines (CCME 2001, 2017; Hossain and Patra 2020).

In the present study, the hydrographic basin is the scale of study. Moreover, they are the geographic spaces where groups and communities share activities, socialize and work, based on the availability of renewable and non-renewable natural resources. Based on the foregoing, we can conclude that in hydrographic basins it is possible to identify real-scale solutions to problems to water situations and risks, which is why they constitute the ideal territories to carry out IWRM (Noir 2019).

Although past and current uses of the watersheds differ among them, monitoring physicochemical and microbiological parameters of water quality over time will provide a better characterization of our natural resources. Therefore, the aim of this study was to assess the water quality of five hydrological basins of TDF with different degrees of anthropogenic impact along each watershed and between watersheds. The CCME WQI was applied to compare upstream and downstream sites in each course, providing simplified information to decision makers and stakeholders. On the other hand, and related to water quality and different uses of the basins, a perspective from the IWRM is also provided. These results may be useful for the development of local and regional mitigation and remediation programs regarding the deterioration of water quality with different uses along freshwater courses.

2 Study Area

Tierra del Fuego watersheds can be classified and characterized into four groups of basins or water zones. In the present study, we evaluate water quality from two of them: central or transition basins, and southern or mountain range basins (Iturraspe and Urciuolo 2000).

The GR basin belongs to a transition basin located in the central steppe-forest zone called ecotone (Fig. 1b; Iturraspe and Urciuolo 2000). The total area of the basin is 8580 km^2, but only 3780 km^2 correspond to the Argentine territory (Table 1; Iturraspe et al. 2007). The GR flows from west to east, receiving tributaries from the south and from the north. Before discharging into the Atlantic Ocean and constituting an estuary, the river makes a long bend to the south around gravel beach barriers on which the GR is built (Isla and Bujalesky 2004). In GR’s outer estuary, the mean tidal range is 4.16 m. The climate is semi-arid, and mean annual rainfall varies from 600 mm in the southern springs of the basin to 330 mm in Río Grande city at sea level. Strong winds prevail from the west, which are of great intensity in

spring and summer. The floods appear in early spring, which mainly depend on local precipitation, with the lowest water level in autumn and early winter due to freezing temperatures in the soil and riverbeds (Koremblit and Forte Lay 1991). The landscape is highly variable, undulating with low slopes and marked meanders in the river course. Forests that grow in this zone are deciduous; they are represented mostly by *Nothofagus antarctica* (ñire), followed by *N. pumilio* (lenga). These forests take up the hills and the highest places, whereas the low zones and the wide and not very deep valleys are occupied by herbaceous vegetation, predominantly the gramineous one (Iturraspe and Urciuolo 2005). The GR basin stands out for the extension, diversity and uniqueness of its wetlands (Anchorena et al. 2009), which, outside the thaw period, acquire importance as regulatory storages.

The southern or mountain range basins comprise the area delimited between the northern part of the Fuegian Andes and the Beagle Channel. The orography responds to structural features that have resisted the intense glacial activity, basically erosive. The transversal and longitudinal valleys of the Fuegian Andes (Andorra, Cañadón del Toro, Pipo, Olivia, Carbajal-Tierra Mayor, and Beagle Channel) show the effect of Pleistocene glacier erosion (Rabassa et al. 2000). The tributary valleys were occupied by multiple valley glaciers, ranging from 20 to 30 km in length, with smaller, single valley glaciers (Rabassa et al. 2000). Forest is the absolutely dominant vegetation in this mountainous landscape, covering the mountain hillsides until 500–600 m a.s.l. Beyond that height, there are only peat bog patches and high mountain thin vegetation adjacent to the forest, In higher altitudes, it's only possible to find nude rocks, glaciers, semi-permanent snows and little high lakes (Iturraspe and Urciuolo 2005; Strelin and Iturraspe 2007). The main watersheds that cross Ushuaia city are BES, GS, OR and PR, which belong to southern or mountain range basins (Fig. 1c; Table 1).

The BES basin springs in the Martial mountains at 1340 m a.s.l. and it flows into the Encerrada Bay after a 7 km way in which it crosses the urban area of the city (Urciuolo and Iturraspe 2005). Its waters are hyposaline, slightly bicarbonated, of great transparency and with a moderately high Fe content; although its turbidity increases during floods due to sediment drag (Iturraspe et al. 2007). There is no

Table 1 Hydrological characteristics of five watersheds of Tierra del Fuego (Argentina): Grande River (GR), Buena Esperanza Stream (BES), Grande Stream (GS), Olivia River (OR) and Pipo River (PR). Data from Iturraspe et al. (2009), Zagarola et al. (2017) and Granitto et al. (2021)

Watershed	Area (Ha)	Mean annual flow (m^3 s^{-1})	River length (km)	Urbanized area* (%)
GR	868,000	40.00	240.00	2.9
BES	1656	0.37	6.97	68.0
GS	12,538	3.20	18.31	18.1
OR	20,924	5.40	41.59	7.0
PR	15,900	3.70	11.60	28.3

*Percentage of the total river length

agricultural or livestock activity within this basin. A water treatment plant is located at 110 m a.s.l., which contributes 20% of the raw water that is purified there (Huelin Rueda 2008). Above that point, there are small water intakes for tourist settlements such as hotels, cabins and mountain huts, and downflow the treatment plant begins the densely urbanized area. Through the urban area, the stream crosses house settlements with different degrees of consolidation. In its middle and lower sections, the stream receives the majority of pluvial and sewage discharges, urban water runoff and water from urban peat bogs, before draining into Encerrada Bay.

GS is located in the Andorra Valley, where peat bogs, lagoons and glaciers compose the natural landscape (Urciuolo and Iturraspe 2011). In 2009, the middle section of the Andorra Valley basin was declared a RAMSAR site called "Vinciguerra Glacier and associated peatlands" (https://rsis.ramsar.org/es/ris/1886). This condition led to stop urbanization planning in the sector and the exploitation of peat. The RAMSAR site, limits to the west with the Tierra del Fuego National Park where the headwaters of GS are located. These protected areas favor the preservation of the 72% of the GS basin, which is relevant because this stream is the main source of drinking water in the city providing approximately 80% of the raw water in the treatment plants (Huelin Rueda 2008). Moreover, it is a direct water source that supplies some of the precarious houses of the area and the irrigation of crops in small farms in the valley (Urciuolo and Iturraspe 2005). Over the years, the urbanization in this sector has been planned, building social neighborhoods and single-family homes, although untreated domestic discharges have been detected (Amin et al. 2011; Diodato et al. 2018, 2020; Granitto et al. 2021). Crossing the urban area, GS flows into the eastern part of Ushuaia city and discharges in Ushuaia Bay, Beagle Channel. In the lower basin, GS crosses a zone occupied by different industries (plastic and electronic manufactures), a petrol station, and the municipal slaughterhouse, whose spills have been occasionally dumped into the stream during the last years. Close to the outlet, a secondary sewage treatment plant is under construction and would begin operating at the end of 2021.

The OR defines the East boundary of the urban area of Ushuaia city. It occupies the Carbajal bottom Valley, where a large wetland of 672 ha is made up of peat bogs and lagoons, and is influenced by allochthonous drainages (Urciuolo and Iturraspe 2011). There is an active peat extraction. The low slope of the catchment determines a fair runoff regime and marked meanders in the river course, draining into the coast of Ushuaia Bay. The capacity of self-purification of this stream is low, especially in winter when the low temperatures and the reduction of flow rates are combined. In addition, surface freezing hinders water oxygenation during part of the year (Urciuolo and Iturraspe 2005). In its middle section, this course is a possible source of drinking water for the city. Moreover, this basin provides valuable environmental services, especially in terms of hydrological regulation (Noir 2019). In its lower section, the urbanization is reduced, but several economic and productive activities are settled: the current sanitary landfill, a concrete plant, a quarry, a fish farming station, a hazardous wastes treatment plant with a pyrolytic oven, and a small bottled water venture.

The upper section of the PR is away from the principal urban area and belongs to a protected area under the preservation of the Tierra del Fuego National Park.

Leaving this restricted area, the newest drinking water treatment plant of the city is located (recently opened in 2017), supplying drinking water to the western sector of the city. In the 1990s, the middle section of this watershed was used as a quarry for the extraction of solid material for the construction of the international airport and a sanitary landfill operated there without any type of aquifer protection. In the last 10 years, large urbanization projects such as neighborhoods have been developed in this sector, joining the already urban urbanization near the outlet of the PR into Golondrina Bay.

3 Materials and Methods

3.1 Sampling Sites and Experimental Design

Nine sampling sites were selected along the GR (S1–S9; Fig. 1b; Table 2) taking into account different characteristics such as the degree of occupation, the development of socio-economic activities, and the presence of wastewater discharges, among others. Most of the sites were located on the north riverside, because there is where most of the pollutants could accumulate, according to river dynamics. In Ushuaia watersheds, two sites were sampled for each watershed: one site upstream before urbanization (labelled by adding number "1") and the other site close to the outlet in the coast of Beagle Channel (labelled by adding number "2") (Fig. 1c; Table 2).

Water samples were collected between 2008 and 2014 in the GR, and between 2009 and 2019 in Ushuaia watersheds (BES, GS, OR and PR) with a frequency between 2 and 4 months, and taking into account the tidal regime for downstream sites, since salinity conditions could influence chemical determinations. In all cases, subsurface water samples were taken and at a distance of about 1.5 m from the river bank with a horizontal Niskin bottle. After collection, samples were kept refrigerated (4 °C) and processed as quickly as possible. In all samples from the GR, 12 parameters were registered to characterize the water quality: pH, electrical conductivity (EC), salinity (SAL), total dissolved solids (TDS), 5-day biochemical oxygen demand (BOD_5), chemical oxygen demand (COD), turbidity (TURB), orthophosphate (PO_4^{3-}), nitrate (NO_3^-), nitrite (NO_2^-), total coliforms (TC) and fecal coliforms (FC). In water samples from Ushuaia watersheds, 10 parameters were evaluated: pH, EC, TDS, BOD_5, PO_4^{3-}, ammonium (NH_4^+), NO_3^-, NO_2^-, TC and FC. Determinations were performed using the procedures recommended in APHA (2017). The list of the examined parameters with their units, used abbreviations and applied analytical methods are shown in Table 3.

Table 2 General characteristics of the studied sampling sites in Tierra del Fuego watersheds, geographical locations and site descriptions

Watershed	Sampling site	Geographical coordinates		Site description
		Latitude (S)	Longitude (W)	
Grande River (GR)	S1	−53.829605°	−67.843270°	50 m upstream the water intake
	S2	−53.835158°	−67.792277°	Bridge of GR and National route No 3
	S3	−53.814860°	−67.745440°	Old channel from industrial zone
	S4	−53.809104°	−67.741318°	New channel from industrial zone
	S5	−53.804100°	−67.730430°	Pluvial discharge next to industrial zone
	S6	−53.797243°	−67.709829°	Direct discharges from neighbourhoods
	S7	−53.802862°	−67.689083°	Point in the bridge near direct discharges
	S8	−53.802041°	−67.676338°	Small dock in south riverbank
	S9	−53.793543°	−67.685823°	Dock located at the mouth of the GR where small ships moor
Buena Esperanza Stream (BES)	BES1	−54.798361°	−68.371000°	Mountain area (800 m a.s.l.) located before the drinking water treatment plant and surrounded by *Nothofagus* spp. forests
	BES2	−54.819083°	−68.324306°	High degree of urbanization including direct sewage discharges. It discharges into Encerrada Bay
Grande Stream (GS)	GS1	−54.759721°	−68.304928°	Natural area surrounded by *Nothofagus* spp. forests and peatlands; upstream the urbanization
	GS2	−54.795701°	−68.257813°	Next to an industrial area and influenced by urban settlements along its course. It discharges into Ushuaia Bay
Olivia River (OR)	OR1	−54.762667°	−68.194444°	Area surrounded by *Nothofagus* spp. forests

(continued)

Table 2 (continued)

Watershed	Sampling site	Geographical coordinates		Site description
		Latitude (S)	Longitude (W)	
	OR2	−54.799194°	−68.226611°	Low degree of urbanization. Area receiving leaches from the sanitary landfill, an aggregate quarry and a small fish farm. It discharges into Ushuaia Bay
Pipo River (PR)	PR1	−54.829778°	−68.427083°	Area surrounded by *Nothofagus* spp. forests, outside the National Park boundary
	PR2	−54.836333°	−68.352783°	Middle degree of urbanization. It discharges into Golondrina Bay

3.2 Legal Framework

The assessment of surface freshwater quality was based on standards established by national and international guidelines. The implemented national normative derives from the Water Quality Guidelines for the Protection of Aquatic Life in Surface Freshwater established in the resolution No 1333/93 of the Environmental law No 55 from Tierra del Fuego province (https://desarrollosustentable.tierradelfuego.gob.ar/wp-content/uploads/2017/04/Decreto-N%C2%BA1333-93.pdf). Two international guidelines were applied when national regulations did not establish the standards for some of the studied parameters. In this case, guidelines from the Chilean National Commission for Environment (CONAMA-Chile) and the Canadian Council of Ministers of the Environment (CCME) were applied (CONAMA Guide for the Establishment of Secondary Environmental Standards for Surface Continental and Marine Waters, and Canadian Water Quality Guidelines for the Protection of Aquatic Life, respectively).

3.3 Data Analysis

All the data were processed in order to determine mean and median values, standard deviations, and maximum and minimum values and were graphically displayed as boxplots using the software Statistica 7.0.

Table 3 List of physicochemical and microbiological parameters measured in the sampling sites, their units, and the applied methodological techniques. For parameter´s abbreviations see the text

Watershed	Parameter	Unit	Applied analytical techniques
Grande River (GR)	pH	–	In situ measurements with multiparametric probe HORIBA W-23XD and HANNA HI 9813-5
	EC	mS cm^{-1}	
	SAL	PSU	
	TDS	mg L^{-1}	
	TURB	NTU	
	BOD_5	mg L^{-1}	SM 5210 D; incubation and respirometric measurements with BODTrak from HACH
	COD	mg L^{-1}	SM5220 D; colorimetric method
	PO_4^{3-}	mg L^{-1}	4500-P E; ascorbic acid method
	NO_3^-	mg L^{-1}	4500-NO_3 E; cadmium reduction method
	NO_2^-	mg L^{-1}	4500-NO_2 B; colorimetric method
	TC	MPN 100 mL^{-1}	9221 B/C/E; incubation and multi-tube fermentation technique
	FC	MPN 100 mL^{-1}	
Ushuaia watersheds (BES, GS, OR and PR)	pH	–	In situ measurements with multiparametric probes HORIBA W-23XD and HANNA HI 9813-5, and conductivity meter HANNA HI8733
	EC	mS cm^{-1}	
	TDS	mg L^{-1}	
	BOD_5	mg L^{-1}	SM 5210 D; incubation and respirometric measurements with BODTrak from HACH
	PO_4^{3-}	mg L^{-1}	4500-P E; ascorbic acid Method
	NH_4^+	mg L^{-1}	SM 4500-NH_3 F; phenate method
	NO_3^-	mg L^{-1}	4500-NO_3 E; cadmium reduction method
	NO_2^-	mg L^{-1}	4500-NO_2 B; colorimetric method
	TC	MPN 100 mL^{-1}	9221 B/C/F; incubation and multi-tube fermentation technique with 24 h-Colitag™ (CPI International) substrate
	FC	MPN 100 mL^{-1}	

3.4 Calculation of CCME WQI

CCME WQI was computed using the method of CCME (2001). This method was developed to protect aquatic life and assess water quality by applying local or international guidelines in order to compare these standard permissible values with the observed values. In this case, the selected guidelines for comparison purposes came from the local and international normative (see Sect. 9.3.2).

The mathematical formulation of CCME WQI is shown in (Eq. 1) (CCME 2001):

$$CCME\ WQI = 100 - \left(\frac{\sqrt{F_1^2+F_2^2+F_3^2}}{1.732}\right) \tag{1}$$

where F_1 represents the percentage of variables that do not meet their objectives at least once during the time period under consideration (failed variables), relative to the total number of measured variables (see Eq. 2); F_2 represents the percentage of failed individual tests that do not meet their objectives (see Eq. 3); F_3 is an asymptotic capping function that scales the normalized sum of the departures from objectives (*nse*) to yield a range between 0 and 100, and the constant, 1.732, is a scaling factor (see Eq. 4):

$$F_1 = \left(\frac{Number\ of\ failed\ variables}{Total\ number\ of\ variables}\right) \times 100 \tag{2}$$

$$F_2 = \left(\frac{Number\ of\ failed\ tests}{Total\ number\ of\ tests}\right) \times 100 \tag{3}$$

$$F_3 = \left(\frac{nse}{0.01\,nse + 0.01}\right) \tag{4}$$

The *nse* variable is, expressed as:

$$nse = \frac{\sum_{i=1}^{n} departure_i}{\#\ of\ tests} \tag{5}$$

The collective amount by which individual tests are out of compliance is calculated by summing the departures of individual tests from their objectives and dividing by the total number of tests (Eq. 5).

For the cases in which the test value must not exceed the objective:

$$departure_i = \left(\frac{Failed\ Test_i}{Objective_j}\right) - 1 \tag{6a}$$

For the cases in which the test value must not fall below the objective:

$$departure_i = \left(\frac{Objective_j}{Failed\ Test_i} \right) - 1 \tag{6b}$$

For the cases in which the objective is zero:

$$departure_i = Failed\ Test_i \tag{6c}$$

As a result of the calculations, CCME WQI was evaluated as "poor" (0–44), "marginal" (45–64), "fair" (65–79), "good" (80–94), and "excellent" (95–100) (CCME 2001).

4 Results and Discussions

4.1 Spatial Variation of Water Quality Parameters in Grande River

The spatial variation of physicochemical and microbiological parameters in nine sites from the GR is shown in Figs. 2 and 3. Mean pH values in all sites were similar and near the neutrality (mean values between 7.25 and 7.67). Mean values of EC, SAL and TDS showed a similar trend in each site due to its common origin: lower values were found in S1 (means of 0.15 mS cm^{-1}, 0.10 PSU and 87.24 mg L^{-1}, respectively), which were increasing towards the mouth of the river. Maximum values were reached in S9, which corresponded to approximately 100 times those found in S1 (means of 15.70 mS cm^{-1}, 9.93 PSU and 8121.89 mg L^{-1}, respectively). This gradual increase in EC, SAL and TDS can be explained due to the dynamics of the estuary and the intrusion of seawater in each tidal cycle. S9 is the closest site near the coast where the GR inlet is controlled by macrotides and high-energy waves (Bujalesky 2007). Despite the fact that precautions were taken during sampling to avoid the influence of seawater, estuarine parameters fluctuate in relation to the tide. The wind effect is very important during some days and during slack water (Isla and Bujalesky 2004).

BOD_5 mean values were consistently below 10 mg L^{-1} in all sites, although some extreme values were recorded in sites with industrial influence (S3–S5; up to 46 mg L^{-1}) and urban inputs (S6–S9; up to 39 mg L^{-1}). COD mean values varied between 30 mg L^{-1} (S2) and 128 mg L^{-1} (S9), with intermediate values in sites with industrial influence. Maximal COD values were registered in S9, according to the presence of ships that moored in the dock. Extreme values registered in 2012 in almost all sites were related to a devastating fire in the industrial park near the riverbank, where approximately 2000 tanks with disused, highly flammable petroleum, degreasers and

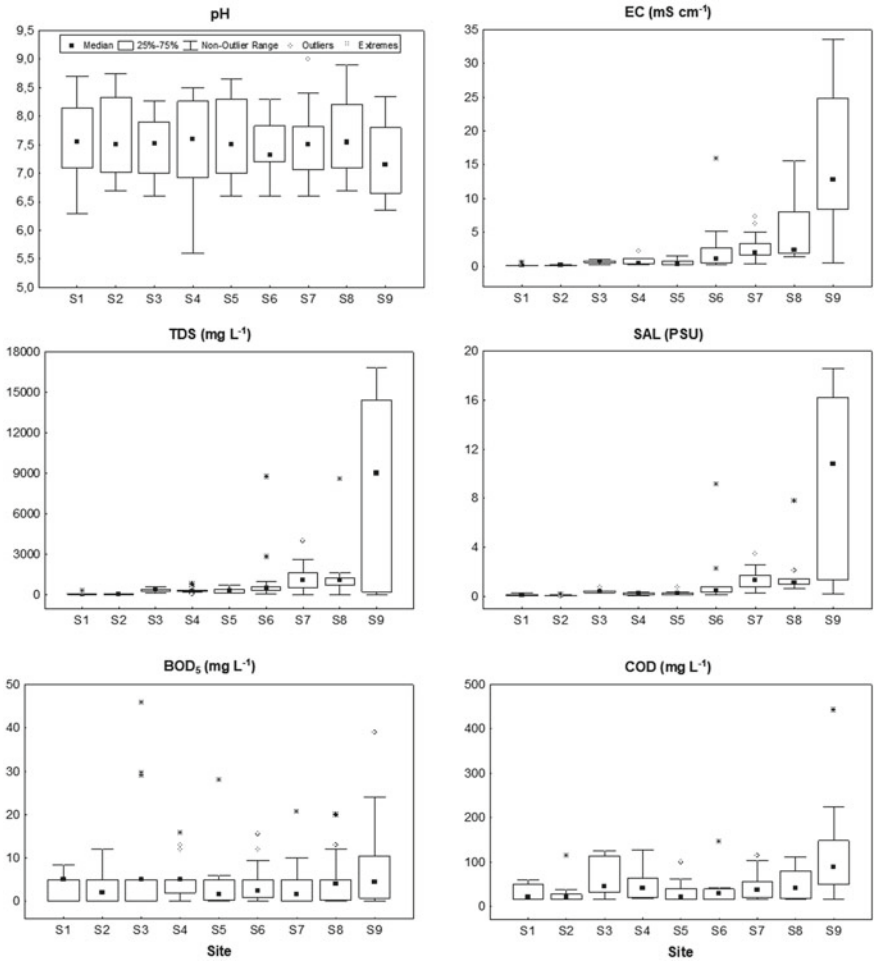

Fig. 2 Boxplots representing the variation of pH, electrical conductivity (EC), total dissolved solids (TDS), salinity (SAL), 5-day biochemical oxygen demand (BOD_5) and chemical oxygen demand (COD) in water samples collected in Grande River watershed (S1–S9)

other fuels burned. TURB mean values were higher in sites with urban influence, ranging from 40 to 76 NTU.

The concentration of dissolved nutrients in water samples did not reflect severe problems of N and P contamination. PO_4^{3-} values were close to the detection limit (0.5 mg L^{-1}), although maximal values were registered in sites S5–S9 (2.0 to 2.7 mg L^{-1}), which are associated with urban influence and wastewater discharges. NO_3^- mean values were higher in those sites near the coast (up to 10.4 mg L^{-1}) compared to those sites located upstream with lower seawater influence. Nevertheless, they did not exceed the values established by the international normative (13 mg L^{-1}).

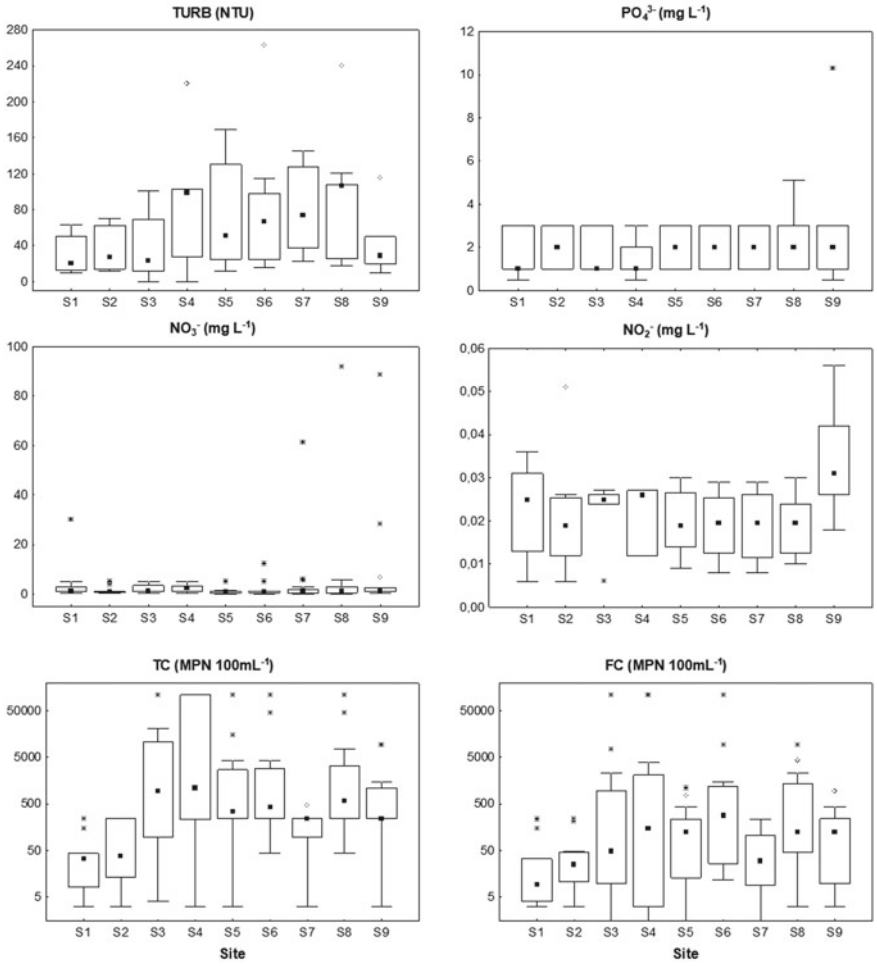

Fig. 3 Boxplots representing the variation of turbidity (TURB), orthophosphate (PO_4^{3-}), nitrate (NO_3^-), nitrite (NO_2^-), total coliforms (TC) and fecal coliforms (FC) in water samples collected in Grande River watershed (S1–S9). Note the different scale of the y-axis (log scale) in TC and FC

NO_2^- values recorded in this study (from 0.01 to 0.06 mg L^{-1}) were within the range suggested by the literature (Chapman 1996) and they did not exceed the standard values established by the national normative (0.06 mg L^{-1}). Lower concentrations of dissolved nutrients could be due to the tidal dynamics to which the estuary is subjected. This fact allows the constant dilution of the pollutants that enter the river through wastewater discharges.

The presence of coliform bacteria and especially fecal coliforms is widely used as an indicator of contamination, particularly due to the contribution of human and animal fecal matter (Chapman 1996; Pommepuy et al. 2006). By themselves,

coliform bacteria are not a threat to health; however, the detection of *Escherichia coli*, a fecal coliform, is used to indicate the potential presence of other possibly harmful pathogens (viruses, bacteria, gastrointestinal parasites, among others) and transmittable by water (Haile et al. 1999; Pommepuy et al. 2006). In the present study, it was observed that TC and FC concentrations were the lowest in S1 and S2. Those found values (means below 100 and 60 MPN 100 mL^{-1} of TC and FC, respectively) allow inferring the existence of diffuse contamination in the upper basin, probably due to the presence of livestock. From S3 towards S9, TC and FC concentrations increased in agreement with the urbanization gradient. In these sites, high concentrations of *Pseudomonas aeruginosa* and *Enterococcus* spp. were also found in water samples (data not shown).

4.2 Spatial Variation of Water Quality Parameters in Ushuaia Watercourses

Water quality parameters registered in Ushuaia watersheds are shown in Figs. 4 and 5. Mean pH values ranged between 6.68 (PR1) and 7.34 (OR2); remaining near neutrality in all sites. EC values were within the range established for most freshwaters (0.01 and 1 mS cm^{-1}; Chapman 1996), but they were higher in downstream sites respect to upstream sites, mainly in BES and GS. A similar trend was registered in TDS. Both parameters increased as a function of increasing urbanization which is in agreement with the findings of Zagarola et al. (2017), Albizzi et al. (2021) and Granitto et al. (2021). BOD_5 mean values were below 5 mg L^{-1} in all sites except in BES2, where it was 54 mg L^{-1} with an extreme value of 112 mg L^{-1}.

In Ushuaia watersheds, nutrient inputs fundamentally come from two sources: in upstream sites, *Nothofagus* spp. forests contribute through litter-fall (Frangi et al. 2005; Amin et al. 2011); while in the downstream sections of the watercourses, the main nutrient provision comes from untreated sewage discharges (Torres et al. 2009; Gil et al. 2011; Diodato et al. 2018, 2020; Albizzi et al. 2021; Granitto et al. 2021). In general, dissolved nutrients increased its concentrations from upstream to downstream sites, in agreement with the contribution of urban inputs to the watercourses. $PO_4{}^{-3}$ values ranged between 0.05 and 15.30 mg L^{-1} with the highest mean concentrations in BES2 (2.82 ± 2.23 mg L^{-1}) and PR2 (3.23 ± 5.93 mg L^{-1}), exceeding the level established by the international normative (0.05 mg L^{-1}; CCME). Among N compounds, $NH_4{}^{+}$ mean values exceeded the national normative (0.05 mg L^{-1}) only in BES2 (10.49 mg L^{-1}) and GS2 (0.29 mg L^{-1}). Respect to $NO_3{}^{-}$, BES and GS presented higher mean values than OR and PR watersheds, although they did not exceed allowed values established by the international normative (13 mg L^{-1}; CCME). $NO_2{}^{-}$ was higher in BES2 (0.17 mg L^{-1}) than in the other sites, exceeding the national normative (0.06 mg L^{-1}).

It is possible that TC and FC were the most indicative parameters of urban inputs in Ushuaia watersheds. The highest mean values of FC were observed in downstream

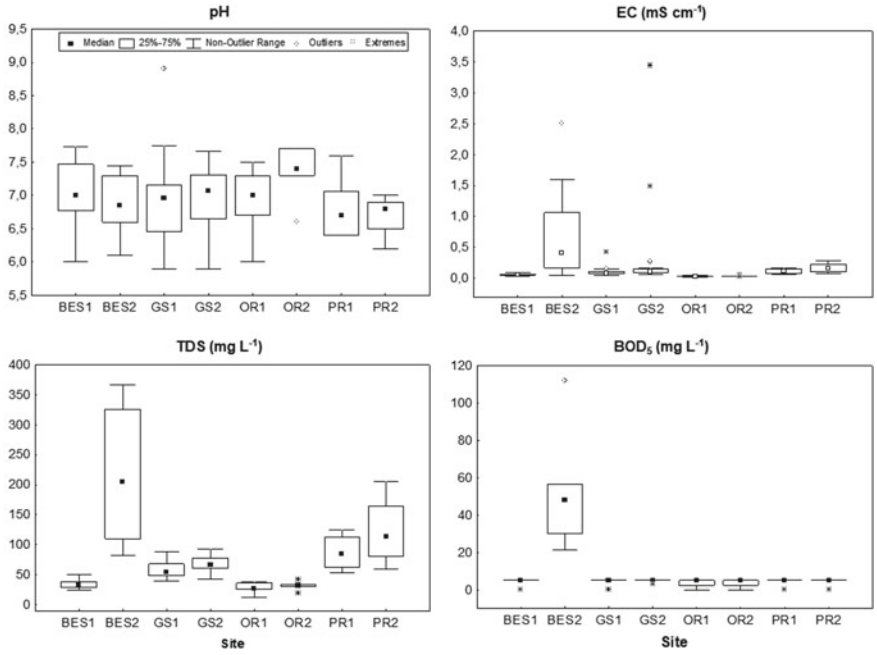

Fig. 4 Boxplots representing the variation of pH, electrical conductivity (EC), total dissolved solids (TDS) and 5-day biochemical oxygen demand (BOD_5) in water samples collected in Ushuaia watersheds: Buena Esperanza Stream upstream (BES1) and downstream (BES2); Grande Stream upstream (GS1) and downstream (GS2), Olivia River upstream (OR1) and downstream (OR2), and Pipo River upstream (PR1) and downstream (PR2)

sites of BES, GS and PR basins (BES2: 211,324 MPN 100 mL^{-1}, GS2: 22,249 MPN 100 mL^{-1} and PR2: 38,506 MPN 100 mL^{-1}), all of them above the national legislation (2000 MPN 100 mL^{-1}), and in agreement with Albizzi et al. (2021) and Granitto et al. (2021). FC values found in upstream sites were detected in small quantities and related to the presence of wild animals like beavers and horses. On the other hand, the total coliform/*Escherichia coli* (TC/EC) ratio has been used to define the origin of coliform bacteria (fecal or natural origin). As the ratio approaches 1, the probability of a fecal origin is higher (Haile et al. 1999; Evanson and Ambrose 2006). In this study, the calculated TC/EC ratios in all sites, except at PR1, were near 1, which indicates an increased probability of human fecal contamination. At PR1, this ratio was approximately 53, indicating a natural origin probably caused by the proliferation of fecal indicator bacteria in sediments (Evanson and Ambrose 2006).

Taking into account all water quality parameters, the most notable differences between upstream and downstream sites within each watershed were observed in the BES basin. The highest amounts of EC, TDS, BOD_5, PO_4^{3-}, NH_4^+, NO_3^-, NO_2^-, TC and FC were registered in BES2, the downstream site that flows into Encerrada Bay. Moreover, the most marked differences in the analyzed chemical properties of fluvial sediments of Ushuaia watersheds have been registered in the same site, which had the

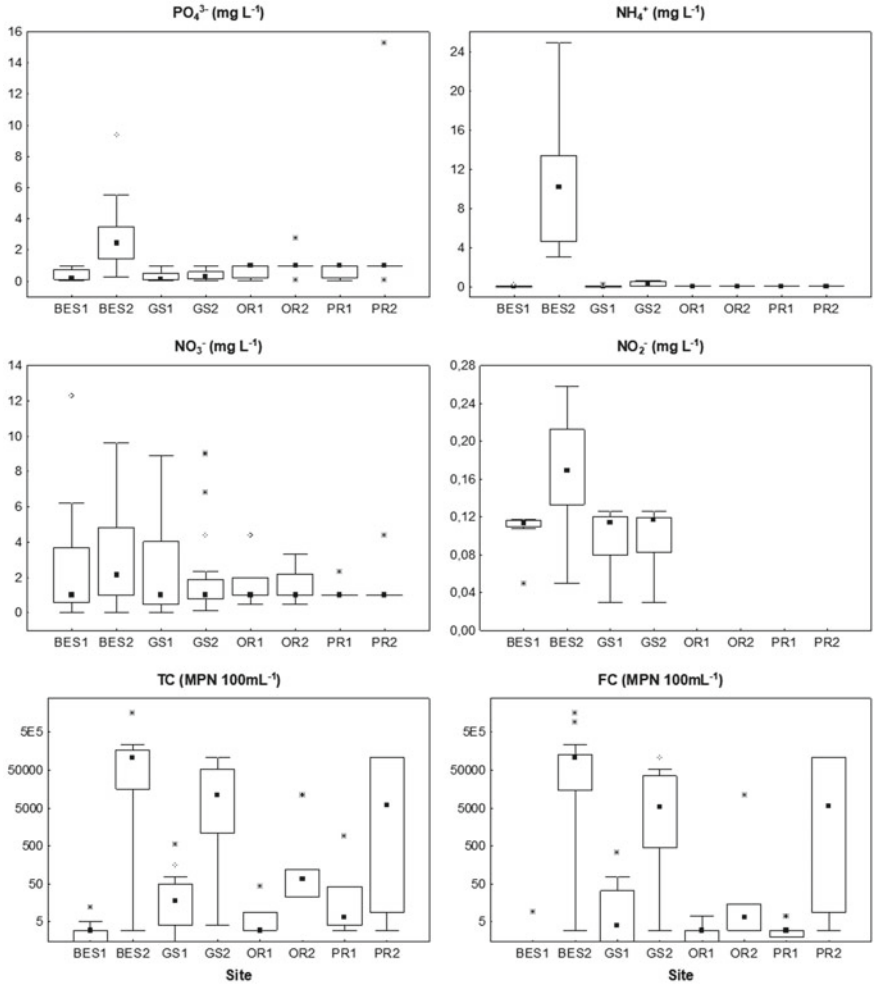

Fig. 5 Boxplots representing the variation of orthophosphate (PO_4^{3-}), ammonium (NH_4^+), nitrate (NO_3^-), nitrite (NO_2^-), total coliforms (TC) and fecal coliforms (FC) in water samples collected in Ushuaia watersheds: Buena Esperanza Stream upstream (BES1) and downstream (BES2); Grande Stream upstream (GS1) and downstream (GS2), Olivia River upstream (OR1) and downstream (OR2), and Pipo River upstream (PR1) and downstream (PR2). Note the different scale of the y-axis (log scale) in TC and FC

lowest mean pH values and the highest mean concentrations of organic carbon, total nitrogen, and soluble reactive phosphorous (Diodato et al. 2020). Several factors are related to this fact: BES is the watershed most affected by urban discharges and has the least mean water flow (0.37 $m^3\ s^{-1}$), which is aggravated by the fact that it covers a larger urbanized area in comparison to GS, OR, and PR (Table 1). The opposite situation occurs in GS which presents 10 times more water flow and consequently,

the dilution effect is more relevant (Diodato et al. 2018). Dilution is a physical process directly related to water discharge, since with lower water discharge, the dilution power of pollutants decreases. The relative influence of the hydrology and morphology of the watersheds must be taken into account since they could explain larger vulnerability to the impacts of urbanization (Granitto et al. 2021).

4.3 CCME WQI Results

The following nine parameters were used for the index calculation: pH, EC, TDS, BOD_5, COD, NO_3^-, NO_2^-, TC and FC for GR (n = 144 including all samplings between 2008 and 2014), and pH, EC, TDS, BOD_5, NH_4^+, NO_3^-, NO_2^-, TC and FC for Ushuaia watercourses (n = 98 including all samplings between 2009 and 2019). The CCME WQI results are shown in Fig. 6. The water quality ranged between "good" (WQI = 87) and "poor" (WQI = 33) in GR, and between "good" (WQI = 93) and "poor" (WQI = 22) in Ushuaia watersheds.

Specifically in GR, water quality decreased gradually from S1 to S9. S1 is located upstream the water intake of the drinking water treatment plant and presented "good" quality (WQI = 81). S2 is 3.5 km from S1 and also presented "good" quality (WQI = 87). S3, S4 and S5 are sites with high industrial influence, and the estimated water quality was "marginal" in S3 (WQI = 47) to "poor" quality in S4 and S5 (WQI = 40 and 33, respectively). S6–S9 presented "poor" water quality (mean WQI = 35), mainly related to urban influence due to the presence of direct wastewater discharges into the river and the presence of several neighbourhoods in the riverbank without the provision of essential services (drinking water and sewers). Lofiego et al. (2009) calculated for the same sites of GR the WQI proposed by the National Sanitation Foundation (Brown et al. 1970), arriving to similar results in downstream sites of GR. However, they found a worse water quality in S1 and S2, which reinforces the idea of using a unique WQI for comparison purposes between sites and times.

The CCME WQI values estimated for Ushuaia watersheds were in agreement with the results obtained in the spatial variation of physicochemical and microbiological parameters. All upstream sites (BES1, GS1, OR1, and PR1) presented "good" water quality (mean WQI = 92.5), which is of great importance because they are the sources of drinking water to the local population. However, "poor" water quality was found in PR2 (WQI = 43), GS2 (WQI = 41) and BES2 (WQI = 22). OR2 presented "fair" water quality (WQI = 78) showing that there is no marked evidence of degradation of the watercourse by organic inputs. This information is totally relevant because the riverbanks of OR will soon be urbanized owing to the growth need of the city. Granitto et al. (2021) calculated the Fuegian WQI (F_WQI), which includes periphytic chlorophyll-*a*, and they found F_WQI values higher than 76 at all sites of the PR basin, indicating a very good water quality during 2018–2019. This could be due to the fact that PR only receives occasional contributions of wastewater from the overflow of a near pumping station, and does not have a mixed sewage system. Therefore, pluvial and sewage effluents are separated. On the other hand, they

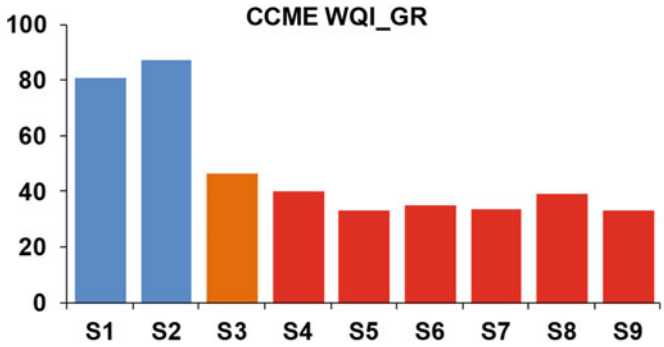

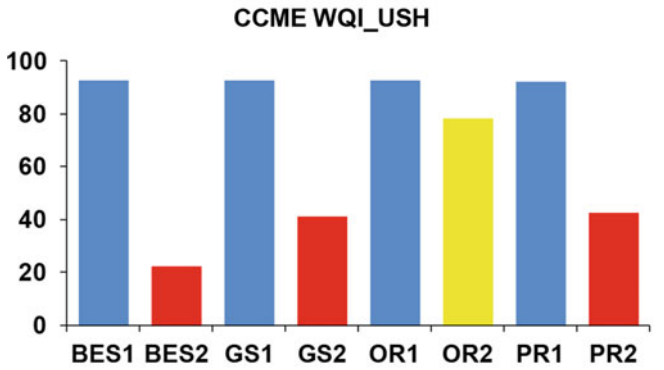

CCME WQI		
EXCELLENT	95-100	The water quality is not under any threat and it is not degraded and close to natural levels.
GOOD	80-94	The water quality is not under a little threat and it is rarely seen under desired levels.
FAIR	65-79	The overall water quality is protected;however, it is under threat in some cases and sometimes not in the desired conditions
MARGINAL	45-64	The water quality is frequently under threat and degradation and often not in the desired conditions.
POOR	0-44	Water quality departs from its desirable level.

Fig. 6 CCME water quality index results for Grande River (GR, S1–S9) and Ushuaia (USH) watersheds: Buena Esperanza Stream upstream (BES1) and downstream (BES2); Grande Stream upstream (GS1) and downstream (GS2), Olivia River upstream (OR1) and downstream (OR2), and Pipo River upstream (PR1) and downstream (PR2). Classification table of CCME WQI values (CCME 2001) are also presented

found that at BES and GS the F_WQI showed broader variation between upstream and downstream sites, in agreement with the present study.

4.4 The Integrated Water Resources Management (IWRM) in Tierra del Fuego Basins: Threats and Affected Functions and Services

The hydrographic basins are the territories where the hydrological cycle occurs, being a natural and ideal unit of development planning. Watershed ecosystems provide goods and services to human populations, including protecting water sources, mitigating the effects of natural disasters by regulating runoff, protecting other resources such as fishing, protecting urbanized areas, among others. The quality and quantity of these services are affected by both, natural phenomena and human activity. The actors involved within the basin must adopt behavior in order to promote the conservation and management of ecosystems, improving life quality and their sustainability, trying to have a positive attitude towards the environment, and without harming the activities they carry out in the basin. This balance is a goal that must be achieved, although obstacles and difficulties are always present. The protection and good management of the middle and upper basins will benefit the entire ecosystem (Noir 2019). Several threats on the different ecosystems of the basins and the effects generated on their functions and services were identified by Noir (2019), and are listed in Table 4.

In the analyzed watersheds, there is a great diversity of actors that operate in a divided and uncoordinated way, primarily regarding the use of the different ecosystems. Since most of the actors are linked to the political and institutional sphere, the system is weakened, showing an evident lack of management policies for the administration of provincial water resources.

The lower sectors of the basins are the most disturbed and present the greatest environmental problems, where the most densely populated areas are concentrated and several activities are carried out. These bad practices threaten the natural conditions of the ecosystems. It is necessary to work on water and land use planning to reduce risks, avoid conflicts, and promote activities within a social, economic and environmental sustainability framework.

The hydro-environmental management must be based on the strategic guidelines of each basin within the framework of IWRM with an EA. It must define urgent actions aimed at generating information, education and dissemination, land use planning, water risks management, inter-institutional coordination, and applicable regulations.

Ecosystem management requires the coordination of the actors and depends on the availability of scientific information generated for decision-making. It is essential to promote the strengthening of the technical structures of the local authorities and academic institutions to create knowledge and to improve inter-institutional coordination for the execution of public policies.

Table 4 Threats and affected functions and/or services of the different ecosystems of Tierra del Fuego (TDF)

Ecosystem	Threats	Affected functions and/or services
Watercourses	– Exploitation of wetlands – Peat extraction	– The aesthetics of the landscape and the services related to recreation and ecotourism – Cultural function related to artistic and spiritual inspiration, raising the cultural heritage and identity in the region – Drinking water supply for the population of Ushuaia and Río Grande cities, and for the touristic infrastructure – Economic condition through job increase in tourism companies and water treatment plants – Water provision in appropriate amounts for hydroelectric use – Biodiversity
	– Quarry mining activity and aggregate washing – Sanitary landfill and hazardous waste operating companies – Container's transport and storage companies – Fuel and lubricant dispensing companies – Concrete production plant – Sewage treatment plant	– Sports and recreational activities linked to the use of hydrobiological resources – Ecological services such as habitat maintenance for local species – Generation of gases and toxic leachates – Adequate water provision to the aquaculture station in OR: eggs incubation destined to watercourse repopulation for sport fishing – Water provision for companies that produce beverages such as bottled water, juices and beer production – Adequate provision of water for irrigation and cattle beverage
	– Changes in land use (urbanization of Ushuaia and Río Grande cities) – Irregular clearing	– Sports and recreational activities linked to the use of hydrobiological resources – Ecological services such as habitat maintenance for local species – Adequate provision of water for aquaculture
	– Bad practices in touristic and recreational activities – Activity of invasive species: *Castor canadensis* and *Didymosphenia geminata*	– Sports and recreational activities linked to the use of hydrobiological resources – Ecological services such as habitat maintenance for local species – Adequate provision of water for irrigation, aquaculture – Provision of drinking water for the population

(continued)

Table 4 (continued)

Ecosystem	Threats	Affected functions and/or services
	– Non-point contamination from livestock activity	– Sports and recreational activities linked to the use of hydrobiological resources – Water provision for companies that produce beverages such as bottled water, juices and beer production – Adequate provision of water for irrigation, aquaculture – Provision of drinking water for the population and touristic infrastructure
	– Climate change	– Provision of water for hydroelectric power generation projects – Water provision for the production of drinking water – Adequate provision of water irrigation, aquaculture
Wetlands: peatlands, lagoons, floodplains and estuary	– Peat exploitation – Wetland drainage for the construction of roads or trails – Urbanizations of wetlands – Expansion of the urban area in Ushuaia and Río Grande cities – Effluent discharges on peat bogs and the estuary – Non-compatible recreational activities (trips in trucks, motorcycles, ATVs, etc.)	– Hydrological regulation capacity, slowing water flow in times of water excesses – Freshwater reservoir for different uses – Soil stabilization and erosion reduction in the basin – Sediment retention and improvement of water quality – Reduction of water risks in extreme water events – Biogeochemical regulation in nutrient cycling – Climate change mitigation – Climate regulation by organic matter accumulation and control of atmospheric emissions – Transformation and degradation of pollutants – Recreation and ecotourism – Cultural heritage and identity; artistic and spiritual inspiration – Organic carbon storage in peatlands – Socio-economic function through job increases in tourism companies – Habitat provision and refuge to avifauna – Conservation of biodiversity for flora and fauna species – Scientific and historical function about the evolution of the climate, vegetation, volcanic eruptions, and other environmental aspects

(continued)

Table 4 (continued)

Ecosystem	Threats	Affected functions and/or services
Glaciers and Andean tundra	– Climate change	– Feeding the river systems of the basin – Water storage and regulation of the hydrological cycle of the basin – Water availability in the basin for different uses – Climate evolution for scientific research – Recreational and touristic activities – Relevance of the landscape in a pristine area – Socio-economic function through job increases in tourism companies
Forests	– Irregular occupations and illegal clearings – Changes in land use for unplanned urban and tourist developments – Deterioration of the forest due to the presence of cattle – Clearing for quarrying activity – Clearing to generate areas for container storage – Expansion of the urban area of Ushuaia city – Activity of the invasive species C*astor canadensis* – Forest fires	– Hydrological regulation in water collection and storage – Availability of water for different uses – Protection that reduces erosive power, improving water quality – Reduction of risks facing extreme rain events – Cultural function; enjoyment of the landscape through recreation and tourism – Socio-economic function through job increase in tourism companies – Development of recreational spaces

5 Conclusions

The systematic and continuous study of the water quality of five watersheds of Tierra del Fuego showed that unplanned urbanization and the lack of specific regulations (or failure to comply) are the main problems that Rio Grande and Ushuaia cities are facing today. The implementation of the CCME WQI is an applicable and simple tool to transmit the information to the different actors in order to improve the environmental problems we are subjected to. Severe alterations of the studied watersheds were also determined, which responded to changes in land use and to the development of authorized and unauthorized anthropogenic activities. These activities, carried out without urban planning and ignoring water management guidelines are of environmental importance for the conservation of the ecosystems of Tierra del Fuego. In this sense, it is necessary to implement short and medium-term measures to solve these problems to preserve the health of this relevant environment and the associated population.

Acknowledgements We would like to thank the Guest Editors, Dr. Américo Torres and Dr. Verena Compodonico for providing us the opportunity to participate in this special issue. Also we want to thank to the technical teams of the Dirección General de Recursos Hídricos from Secretaría de Ambiente, Ministerio de Producción y Ambiente of Tierra del Fuego. We want to specially thank two anonymous reviewers for their valuable comments on the manuscript.

References

Akkoyunlu A, Akiner M (2012) Pollution evaluation in streams using water quality indices: a case study from Turkey's Sapanca Lake Basin. Ecol Indic 18:501–511

Al Radif A (1999) Integrated water resources management (IWRM): an approach to face the challenges of the next century and to avert future crises. Desalination 124:145–153

Albizzi A, Diodato S, González Garraza G (2021) El uso de bioensayos crónicos en *Daphnia magna* para la evaluación ambiental de un arroyo urbano en Tierra del Fuego (Argentina). Ecol Austr 31:277–288 (in Spanish)

Almeida C, Quintar S, González P, Mallea M (2007) Influence of urbanization and tourist activities on the water quality of the Potrero de los Funes River (San Luis—Argentina). Environ Monit Assess 133:459–465

Amin O, Comoglio L, Spetter C, Duarte C, Asteasuain R, Freije R, Marcovecchio J (2011) Assessment of land influence on a high latitude marine coastal system: Tierra del Fuego, southernmost Argentina. Environ Monit Assess 175:63–73

Anchorena J, Collantes M, Rauber R, Escartín C (2009) Humedales de la Cuenca del Río Grande Tierra del Fuego, Argentina. Dirección General de Recursos Hídricos. SDSyA Tierra del Fuego (in Spanish)

APHA, American Public Health Association (2017) Standard methods for the examination of water and wastewater. American Public Health Association, Washington, DC

Bilgin A (2018) Evaluation of surface water quality by using Canadian council of ministers of the environment water quality index (CCME WQI) method and discriminant analysis method: a case study Coruh River Basin. Environ Monit Assess 190:554

Brown R, Mc Clleland N, Deininger R, Tozer R (1970) A water quality index—do we dare? Water Sew Works 117(10):339–343
Bujalesky G (2007) Coastal geomorphology and evolution of Tierra del Fuego (Southern Argentina). Geol Acta 5(4):337–362
CCME, Canadian Council of Ministers of the Environment (2001) Canadian water quality guidelines for the protection of aquatic life: CCME Water Quality Index 1.0. Winnipeg. https://ccme.ca/en. Accessed 27 Oct 2020
CCME, Canadian Council of Ministers of the Environment (2017) Canadian water quality guidelines for the protection of aquatic life: CCME Water Quality Index, User's Manual 2017 Update, Winnipeg. https://ccme.ca/en/res/wqimanualen.pdf. Accessed 27 Oct 2020
Chapman D (1996) Water quality assessments—a guide to use of biota, sediments and water in environmental monitoring. UNESCO/WHO/UNEP, Cambridge
Chittoor Viswanathan V, Schirmer M (2015) Water quality deterioration as a driver for river restoration: a review of case studies from Asia, Europe and North America. Environ Earth Sci 74:3145–3158
Diodato S, Comoglio, L., Moretto, A., Marcovecchio, J. (2018). Dinámica e impacto de la eutrofización por aportes urbanos en las cuencas hídricas y zona costera de la ciudad de Ushuaia, Tierra del Fuego. In E. M. Abraham, R. D. Quintana, G. Mataloni (Eds.), *Agua+Humedales*. Buenos Aires: UNSAM EDITA (in Spanish).
Diodato S, González Garraza G, Mansilla R, Moretto A, Escobar J, Méndez-López M, Gómez-Armesto A, Marcovecchio J, Nóvoa-Muñoz JC (2020) Quality changes of fluvial sediments impacted by urban effluents in Ushuaia, Tierra del Fuego, southernmost Patagonia. Environ Earth Sci 79:481
Evanson M, Ambrose R (2006) Sources and growth dynamics of fecal indicator bacteria in a coastal wetland system and potential impacts to adjacent waters. Water Res 40:475–486
Frangi J, Barrera M, Richter L, Lugo A (2005) Nutrient cycling in *Nothofagus pumilio* forests along an altitudinal gradient in Tierra del Fuego, Argentina. For Ecol Manage 217:80–94
Gikas G, Sylaios G, Tsihrintzis V, Konstantinou I, Albanis T, Boskidis I (2020) Comparative evaluation of river chemical status based on WFD methodology and CCME water quality index. Sci Tot Environ 745:140849
Gil M, Torres AI, Amin O, Esteves JL (2011) Assessment of recent sediment influence in an urban polluted subantarctic coastal ecosystem. Beagle Channel (Southern Argentina). Mar Pollut Bull 62(1):201–207
Giri S, Qiu Z (2016) Understanding the relationship of land uses and water quality in twenty first century: a review. J Environ Manage 173:41–48
Glińska-Lewczuk K, Gołaś I, Koc J, Gotkowska-Płachta A, Harnisz M, Rochwerger A (2016) The impact of urban areas on the water quality gradient along a lowland river. Environ Monit Assess 188:624
Granitto M, Diodato S, Rodríguez P (2021) Water quality index including periphyton chlorophyll-a in forested urban watersheds from Tierra del Fuego (Argentina). Ecol Indic 126:107614
GWP, Global Water Partnership (2000) Towards water security: a framework for action. Technical Advisory Committee. Stockholm, Sweden: Global Water Partnership
Haile R, White J, Gold M, Cressey R, McGee C, Millikan R et al (1999) The health effects of swimming in ocean water contaminated by storm drain runoff. Epidemiology 10:355–363
Hossain M, Patra K (2020) Water pollution index—a new integrated approach to rank water quality. Ecol Indic 117:106668
Huelin Rueda P (2008) Ordenación hidrológico-forestal de la cuenca del arroyo de Buena Esperanza. Tierra del Fuego (Argentina), Degree Thesis. Universidad Politéctica de Madrid (in Spanish)
INDEC, Instituto Nacional de Estadística y Censos República Argentina (2010) Censo Nacional de Población, Hogares y Viviendas. https://www.indec.gob.ar/indec/web/Nivel4-CensoProvincia-999-999-94-014-2010. Accessed 10 May 2021
IPBES, Intergovernmental Science-Policy Platform on Biodiversity and Ecosystem Services (2019) In: Díaz S, Settele J, Brondízio E, Ngo H, Guèze M, Agard J et al (eds) Summary for policymakers

of the global assessment report on biodiversity and ecosystem services of the IPBES. IPBES secretariat, Bonn, Germany, pp 1–56
Isla F, Bujalesky G (2004) Morphodynamics of a gravel-dominated macrotidal estuary: Rio Grande. Tierra Del Fuego. RAGA 59(2):220–228
Iturraspe R, Urciuolo A (2000) Clasificación y caracterización de las cuencas hídricas de Tierra del Fuego. Actas XVIII Congreso Nacional del Agua, Termas de Río Hondo, Santiago del Estero, Argentina (in Spanish)
Iturraspe R, Urciuolo A (2005) IMCG mires and peatlands field symposium Tierra del Fuego. Field Guide. Argentina
Iturraspe R, Urciuolo A, Guerrero Borges V, Gaviño Novillo M, Collado L, Sarandón R, Burns S (2007) Report on basin response for Argentina. Argentina: Subsecretaría de Recursos Naturales de Tierra del Fuego—Universidad Nacional de La Plata. Deliverable D18 EPIC ORCE
Iturraspe R, Urciuolo A, Iturraspe R, Camargo S (2009) Vulnerabilidad de las cuencas hídricas ante la recesión de los glaciares en Tierra del Fuego. Actas XXII Congreso Nacional del Agua, Puerto Madryn, Chubut, Argentina (in Spanish)
Koremblit G, Forte Lay J (1991) Contribución al estudio agroclimático del norte de Tierra del Fuego (Argentina). An Inst Patagon Ser Cs Nat 20(1):125–134 (in Spanish)
Lofiego R, Noir G, Urciuolo A, Iturraspe R (2009) Evaluación hidro-ambiental del estuario del Río Grande de Tierra del Fuego. XXII Congreso Nacional del Agua, Trelew, Chubut, Argentina (in Spanish)
Martínez Valdes Y, Villalejo García V (2018) The integrated water resources management: a nowadays need. Ing Hidrau Amb 39(1):58–72
Miller J, Hutchins M (2017) The impacts of urbanisation and climate change on urban flooding and urban water quality: a review of the evidence concerning the United Kingdom. J Hydrol Reg Stud 12:345–362
Mrotek A, Anderson C, Valenzuela A, Manak L, Weber A, Van Aert P, Malizia M, Nielsen E (2019) An evaluation of local, national and international perceptions of benefits and threats to nature in Tierra del Fuego National Park (Patagonia, Argentina). Environ Conserv 46(4):326–333
Noir G (2019) Lineamientos de un plan de gestión para el desarrollo sostenible de la cuenca del río Olivia, provincia de Tierra del Fuego, Argentina. Master Thesis, Universidad Nacional del Litoral, Argentina (in Spanish)
Oliva González S, Almeida C, Calderón M, Mallea M, González P (2014) Assessment of the water self-purification capacity on a river affected by organic pollution: application of chemometrics in spatial and temporal variations. Environ Sci Pollut Res 21:10583–10593
Pommepuy M, Hervio-Heath D, Caprais M, Gourmelon M, Le Saux J, Le Guyader F (2006) Fecal contamination in coastal areas: an engineering approach. In: Colwell B (ed) Oceans and health: pathogens in the marine environment. Springer, New York, pp 331–359
Poonam T, Tanushree B, Sukalyan C (2013) Water quality indices-important tools for water quality assessment: a review. Int J Adv Chem 1(1):15–28
Rabassa J, Coronato A, Bujalesky G, Salemme M, Roig C, Meglioli A, Heusser C, Gordillo S, Roig F, Borromei A, Quattrocchio M (2000) Quaternary of Tierra del Fuego, Southernmost South America: an updated review. Quatern Int 68–71:217–240
SAyDS, Secretaría de Ambiente y Desarrollo Sustentable (2009) Sitios RAMSAR de la Argentina. Grupo de Trabajo de Recursos Acuáticos. https://www.argentina.gob.ar/ambiente/agua/humedales/sitiosramsar/tierradelfuego. Accessed 12 May 2021
Strelin J, Iturraspe R (2007) Recent evolution and mass balance of Cordón Martial glaciers, Cordillera Fueguina Oriental. Glob Planet Change 59:17–26 (in Spanish)
Torres AI, Gil M, Amin O, Esteves JL (2009) Environmental characterization of an eutrophicated semi-enclosed system: nutrient budget (Encerrada Bay, Tierra del Fuego Island, Patagonia, Argentina). Water Air Soil Pollut 204:259–270
Urciuolo A, Iturraspe R (2005) Ordenamiento hídrico de las cuencas de fuentes aptas para provisión de agua potable a la ciudad de Ushuaia. Anales XX Congreso Nacional del Agua, Mendoza, Argentina (in Spanish)

Urciuolo A, Iturraspe R (2011) Glaciares de Tierra del Fuego. Ciudad Autónoma de Buenos Aires, Argentina: Dunken (in Spanish)
Urciuolo A, Iturraspe R, Lofiego R, Noir G (2009) Estrategias para el ordenamiento hidro-ambiental de la cuenca binacional del río Grande de Tierra del Fuego. Anales XXII Congreso Nacional del Agua, Trelew, Argentina (in Spanish)
Wilson C, Weng Q (2010) Assessing surface water quality and its relation with urban land cover changes in the Lake Calumet area, Greater Chicago. Environ Manage 45:1096–1111
Yu D, Shi P, Liu Y, Xun B (2013) Detecting land use-water quality relationships from the viewpoint of ecological restoration in an urban area. Ecol Eng 53:205–216
Zagarola J, Anderson C, Veteto J (2014) Perceiving Patagonia: an assessment of social values and perspectives regarding watershed ecosystem services and management in southern South America. Environ Manage 53:769–782
Zagarola J, Martínez Pastur G, Lopez M, Anderson C (2017) Assessing the effects of urbanization on streams in Tierra del Fuego. Ecol Austr 27:45–54
Zamparas M, Zacharias I (2014) Restoration of eutrophic freshwater by managing internal nutrient loads. A review. Sci Total Environ 496:551–562

Disturbances in Freshwater Environments of Patagonia: A Review

Rodolfo Iturraspe

Abstract Patagonia has the attraction of being a wild region, very sparsely populated that involves a great variety of pristine landscapes. However, the contrasting social and environmental changes that this territory evidenced over the past century are, likewise, distinctive features, as well as spontaneous devastating natural events. Taking into account that rivers and lakes are demonstrative of the environmental status resulting from shifts occurring in their respective drainage basins, the purpose of this chapter is to present a review on the state of knowledge on several kinds of changes and disturbances affecting freshwater environments in Patagonia and to discuss their effects. The chapter structure consists of two axes: natural changes caused by volcanism, and human-made changes: invasive species, climate change, and land-use/land-cover changes. The extremely extensive scope of the focused subject, due to the diversity of elements involved, and the great dimension of the territory, does not allow this work to be of exhaustive character, but it represents a first document consisting of a compendium on the effects of disturbances in Patagonian freshwaters, rarely analyzed together. The results reflect a good recovery response of aquatic ecosystems to severe disturbances of natural origin, and scattered changes of human origin, many of them irreversible, whose effects tend to increase over still healthy ecosystems.

Keywords Freshwater · Aquatic ecosystems · Disturbances · Water availability · Invasive species · Patagonia

R. Iturraspe (✉)
Universidad Nacional de Tierra del Fuego, Antártida e Islas del Atlántico Sur, Ushuaia, Argentina
e-mail: riturraspe@untdf.edu.ar

Instituto de Ciencias Polares, Ambiente y Recursos Naturales, Ushuaia, Argentina

A. I. Torres and V. A. Campodonico (eds.), *Environmental Assessment of Patagonia's Water Resources*, Environmental Earth Sciences,
https://doi.org/10.1007/978-3-030-89676-8_14

1 Introduction

Hydrological systems are critical for aquatic and terrestrial biota, as well as for the population and the development of the region, notably in the wide and dry extra-Andean steppe.

Patagonia is exposed to two oceans, is part of two countries, and includes high mountains, wide plateaus dissected by long rivers, islands, and endless shores. However, the major landscape component is the Andes, not in extent, but both in function and dynamic. The great function of the Andes is the production of water, and its dynamic is evident through its tectonic activity, volcanism, glacier behavior, erosion, landslides, torrential floods, and other processes.

Freshwater environments are subjected to disturbances and permanent stressors, those of natural origin, and those resulting from human activities.

Explosive volcanic eruptions represent the extreme manifestation of natural disturbances. Pyroclastic flows, tephra falls, lava flows, lahars and dense sediment flows are destructive volcanic forms that may involve multiple mechanisms, such as the impact force, abrasion, heating, and deposition of materials (Crisafully et al. 2015).

An important question in ecology is how ecosystems respond to and recover from environmental stressors, such as volcanic eruptions (Bunbury 2008). Authors such as Dorava and Milner (1999) asserted that these severe disturbances lead to recovery through primary succession at affected sites. However, Crisafulli et al. (2015) sustained that volcanic disturbances rarely result in the complete annihilation of the biota, and survivorship is the general rule, ranging from most of the biota persisting to only a few individuals surviving in isolated refugia. Several authors described short-term biota recovery in highly impacted freshwater ecosystems, as Dorava and Milner (1999), for the Drift River, where macroinvertebrates recovered five years after powerful eruptions in the Cook Inlet region.

Alien species, non-native, non-indigenous, foreign, exotic, "means a species, subspecies, or lower taxon occurring outside of its natural range (past or present) and with dispersal potential and includes any part, gametes or propagule of such species that might survive and subsequently reproduce" (IUCN 2000). A big majority of exotic species are not capable of increasing and spreading outside of their native range (Primack 2006).

An alien species becomes an invasive alien species when it is established in natural or semi-natural ecosystems or habitat, is an agent of change, and threatens native biological diversity (IUCN 2000). Biological invasions can modify biogeochemical cycles, and cause loss of biodiversity and the transmission of new diseases in the ecosystem.

Changes in land use and land cover produce direct hydrological shifts. Land cover alterations affect seepage and evapotranspiration (Mustard and Fisher 2005) that modify the terms of the water balance. Increased rates in soil erosion and sediment load are additional effects that alter biota and trophic chains. The expansion of agricultural use in arid and semi arid areas generates the greatest extractive use of water. The most striking effect of water diversion worldwide has been the almost

total drying out of the Aral Sea, which until 1960 was the fourth-largest inland water body (Micklin 2010).

Stream pollution by residual pesticides and fertilizers may result from agricultural practices. The expansion of agriculture and urban growth has led to great losses of **wetlands** worldwide (Lin and Yu 2018), inducing the increase of exotic species and the reduction of native species. Cities are sources of contamination to nearby freshwater environments. Pollutant potential of cities depends on the population size and the industrial development, but the addition of factors such as poverty, underdevelopment, and urban informality defines the most critical environmental conditions for freshwaters linked to urban zones.

Climatic change projections reveal increasing temperatures under all scenarios. Changes in rainfall present higher uncertainty levels, and it is assumed that they will not be uniform (Barros et al. 2015). Freshwater environments fed by snow and glaciers will be exposed to hydrological changes due to ice retreat and snowpack storage reduction.

That is the global environmental context for freshwaters in Patagonia, where the Andes is the major area of water recharge for main streams and lakes in the region. The long rivers that cross the eastern slope to reach the Atlantic Ocean (Fig. 1) constitute an oasis in the arid-semiarid steppes that allow the settlement of human populations and their development.

The chapter aims to present a review of the effects on freshwater environments in Patagonia related to volcanism, invasive species, climate change, and land-use/land-cover changes, through a revision of the knowledge, and to discuss the suitability of ecosystems for their recovery. While a disturbance is a relatively discrete event in time that disrupts ecosystem, community, or population structure, and changes resources, substrate availability, or physical environment (Crisafulli et al. 2015), permanent environmental disruptions acting over ecosystems are those caused by land-use changes or invasive species. These changes should be analyzed jointly to the effects of disturbances when they represent common stressors acting on the same ecosystem.

Major natural disturbances in water environments have their origin at the Andes, where current freshwater ecosystems are the natural result of catastrophic events that occurred in the past, as part of its gradual evolutionary process. On this basis, the hypothesis to validate sustains that the effects of natural devastating events on freshwater ecosystems in Patagonia generate transitory disturbances, which does not determine the complete annihilation of the biota and that allow the recovery of the aquatic ecosystem in the short or medium term. On the other hand, certain changes of human origin can produce permanent shifts in freshwater ecosystems, which had never occurred before, and they can lead to the extinction of species and profound transformations.

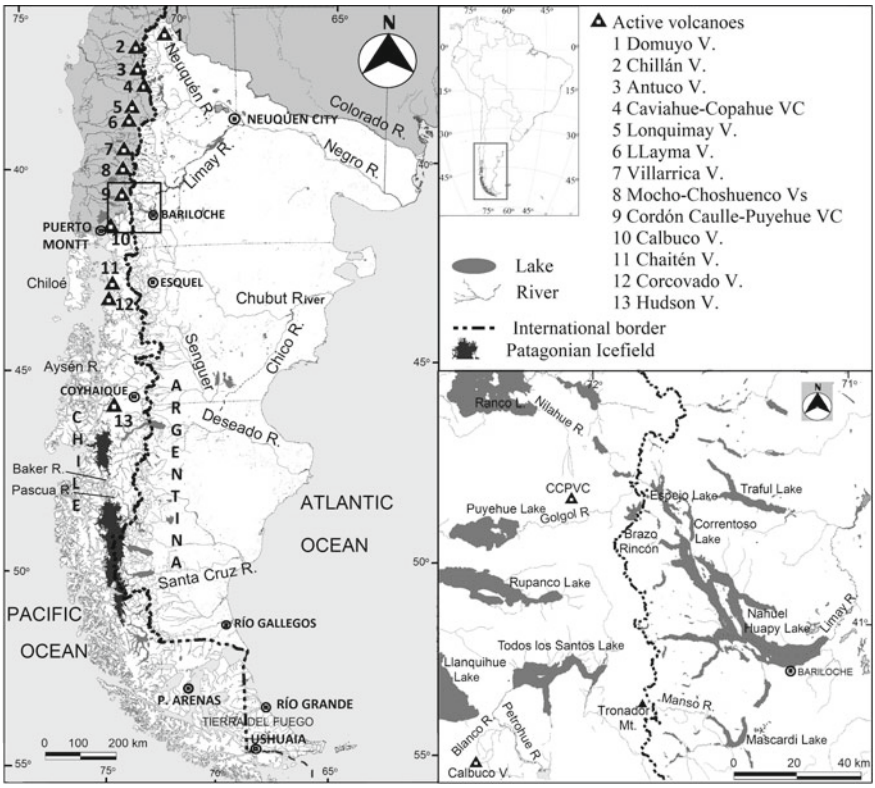

Fig. 1 Study area with detail of the Nahuel Huapí lake area

2 Impacts of Volcanic Eruptions on Freshwaters

In the last decades, volcanoes shocked the Patagonian landscape through eruptions that caused alterations in the morphology, hydrology, water quality, and biology of terrestrial and aquatic ecosystems. The Hudson in 1991, Chaitén in 2008, Cordón Caulle-Puyehue in 2011, Copahue-Caviahue in 2000 and later manifestations, and Calbuco in 2015, produced explosive events with severe widespread ashfalls and serious damages in surrounding areas caused by pyroclastic fluxes and lahars. Figure 1 shows their location, as well as other active volcanoes. Chilean and Argentine scientists had the opportunity to investigate the scope of the immediate disturbances on ecosystems in the short term, as well as their evolution. For the mentioned cases, physical, chemical, and biological changes focused on freshwater environments are explained below.

2.1 Physical Changes Produced by Volcanic Eruptions Affecting Freshwaters

2.1.1 Hudson Eruption, 1991

In August 1991, the Hudson Volcano generated one of the largest Plinian explosive eruptions of the twentieth century, producing 4.3 km^3 bulk volume of tephra deposits that reached the Atlantic coast. Ashes that fell into the Buenos Aires-General Carreras Lake drifted to the shore changing the beach composition. Tephra filled small lakes, depressions, and streambeds; winds remobilized them for several years (Inbar et al. 1995).

The Ibáñez River, at the foot of the Hudson volcano, was seriously affected. Ash covered the valley floor, changing the fluvial morphology and the hydraulic flow. Braided and parallel channels with ash banks replaced the main course covered by ashes. Most biota temporarily disappeared in the bottom valley. The lower river section still shows an unsteady channel system with erosive-cumulative behavior in floods/medium waters (Chávez Barría 2016). At present, bottom oscillations maintain a level up one meter above the pre-eruption bed level. The solid load, 30 years after the eruption, remains over the original rate.

2.1.2 Copahue-Caviahue Volcanic Complex Eruption, 2000

Historical Copahue eruptions were characterized by their high frequency and low magnitude; however, between July and October 2000, the largest and longest eruptive cycle occurred, although it was of a lesser potency, concerning the other volcanic activities explained in this chapter. The main related hazards were ash fall, acid rain, scoriaceous bombs, and small-volume mudflows (Naranjo and Polanco 2004). The more affected by tephra deposition were the Caviahue Lake and Village, as well as the upper basin of the Agrio River, a tributary of the Neuquén River.

2.1.3 Chaitén Eruption, 2008

The Chaitén event evidences the heavy disastrous consequences of ash deposition by reducing the drainage capacity in the fluvial area. The Chaitén Volcano (42.83º S, 72.65º W) and the homonymous town are connected by a steep valley of 10 km long. The Blanco River is the main course, which joins the Chaitén River 6 km **upstream** of the town (Fig. 2).

On May 2, 2008, it began a large and unexpected plinian eruption, consisting of a two-week explosive phase with ash emission that generated 1 km^3 bulk tephra deposits (Major and Lara 2013). Tephra plumes were dispersed downwind across Argentina, loading riverbeds and their respective basins. Ulloa et al. (2016) presented details about strong morphologic changes in channels of the Blanco, Amarillo and

Fig. 2 Chaitén town and Volcano. Left: image from 2001. Right: the same area after 2009, one year after the eruption, where the impact of the eruption on the forest is evident, as well as ash deposits on the Blanco, Amarillo and Rayas river valleys. Images from Google earth

Rayas rivers, close to the volcano (Fig. 2). The eruption devastated the vegetation in the proximal areas and severely damaged at least 480 km^2 of the forest. Tree mortality is evident in the Amarillo River Valley, located 18 km SW of the crater (personal observation 2015). Ten days after the fine ash accumulation in the Blanco River basin, an intense, but not exceptional rainfall generated a flow of volcanic sediments, which ran over the entire width of the valley floor, starting a lahar that remobilized ashes. The alluvium reached the Chaitén town in the mudflow phase, with 7 m aggradation over the original channel. Its avulsion towards the town largely devastated it (Pierson et al. 2013). Fortunately, the authorities had evacuated the population the previous days. The event destroyed the fluvial ecosystem, the riparian vegetation, and a great forest extension; as well, it resulted in notable shifts in the landscape and river hydrology.

2.1.4 Cordón Caulle-Puyehue Volcanic Complex Eruption, 2011

The Cordón Caulle-Puyehue Volcanic Complex (CCPVC), located at the **headwaters** of the Bueno River basin, is composed of multiple craters under different activity patterns. The last large-scale eruption began on June 4, 2011, with a plinian explosive phase that generated a column of 15 km height. Ash and gas emissions lasted eight months, causing many disturbances in Chile and Argentina (Rovira et al. 2013). Ashes circled the globe and interrupted the air traffic in the Southern Hemisphere.

The Nilahue stream, which runs through the north slope of the CCPVC (Fig. 1) was affected by pyroclastic flows and lahars. The fluvial morphology changed severely, and the water temperature raised to 45 °C, resulting in fish mortality, including 4.5 million fishes from a factory. Streams transported pumice to the lakes, where they covered the banks, forming reservoirs over 100 m wide (Rovira et al. 2013).

The Nahuel Huapi Lake (NHL) is a deep and ultraoligotrophic water body, whose branches extend to the W and NW, collecting the flow of the headwater network. From the lake outlet starts the Limay River, affluent of the Negro River. The basin reaches

the international limit, only 20 km leeward of the CCPVC. The Acantuco River is the closest NHL tributary to the volcano. Just after the eruption, it showed deactivated sections and extensive channel modifications by ash deposition (15–30 cm). Thirty months after the eruption, dead riparian vegetation did not yet reestablish in several sectors, and both turbidity and sediment load remained over the normal rates. Ash remobilization by aeolian and fluvial agents increased habitat instability in the closest streams (Lallement et al. 2016).

2.1.5 Calbuco Eruption, 2015

The basaltic andesitic eruption of Calbuco Volcano started suddenly in April 2015, with a high-intensity explosive phase. Two main sub-plinian pulses deposited five tephra layers, mostly northeast of the volcano, totalizing 0.28 km^3 bulk tephra (Romero et al. 2016). A pyroclastic flow took the course of the Blanco River, affluent of the Petrohué River, along 7.5 km from the volcano, filling the bottom valley and destroying the vegetation.

A previous eruption in 1961 reached a similar magnitude, producing a principal lahar over the Tepú River (affluent of the Llanquihue Lake) and a secondary one in the Blanco River.

Before 2015, the Blanco River had reached, a quasi-equilibrium state (Zingaretti 2019). The later eruption caused similar fluvial processes to those already described for the Ibáñez River. Figure 3 shows the Blanco River in 2014 in a quasy-equilibrium state, and successive changes after 2015 demonstrating the current unsteady morphology of the riverbed.

2.2 Water Quality Changes

Large tephra amounts in rivers and lakes, by direct deposition during eruptions, or by subsequent removal, modified physical and chemical conditions of waters. The increase in total suspended solids (TSS) is the common effect, which leads to increased turbidity and decreased luminosity. Chemical changes in freshwaters produced by volcanic activity depend on the eruption characteristics and the composition of the emitted material. Changes in pH, increased concentration of silica, metals, trace elements, and toxic elements linked to volcanism such as mercury and arsenic, are frequent. Below is a brief overview of volcanic activity's effects on the chemistry of aquatic ecosystems based on evidence.

The Caviahue-Copahue Volcanic Complex (CCVC) presents a **hydrothermal magmatic system**, which is composed of: a hot and acidic lake, located in the active crater of the Copahue volcano, two hot acidic creeks that arise from the eastern volcano's flank to form the Agrio River, and nearby **hydrothermal manifestations** (Agusto et al. 2012).

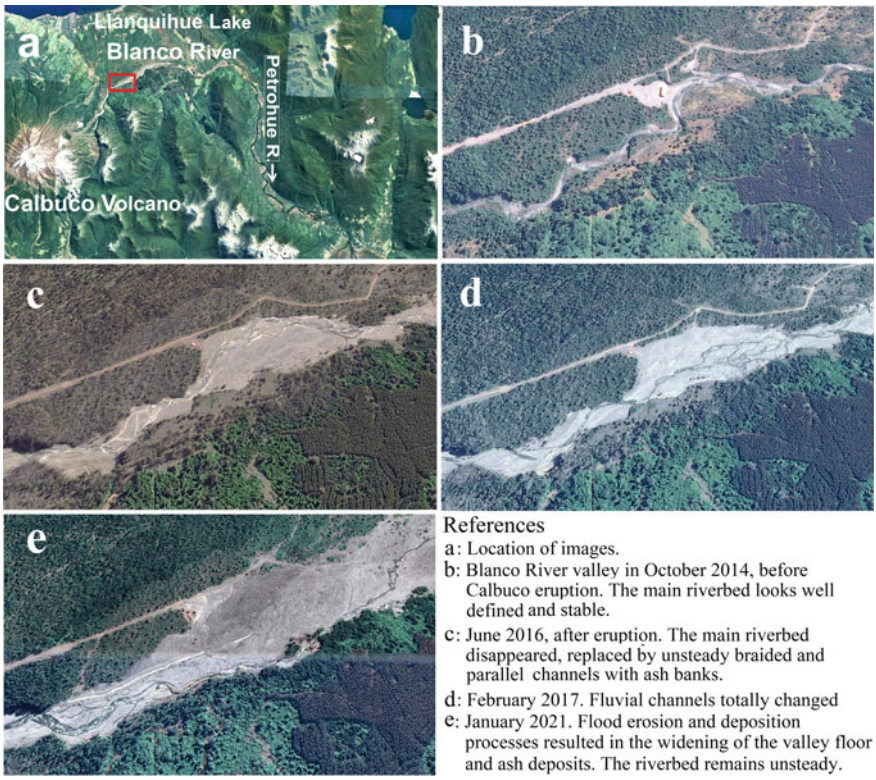

Fig. 3 Morphological changes in the Blanco river valley caused by the 2015 Calbuco eruption

Chemical determinations of waters from the Lomín River, Agrio River, and Caviahue Lake during the eruption, indicated pH values from 2.5 to 4.4; 56–57% SiO_2 and high fluorine contents, from 3.3 mg L^{-1} to 8.4 mg L^{-1} (Naranjo and Polanco 2004). Fluorine is a highly electronegative and reactive element, and the observed values exceeded the limit for human consumption established by the Argentinian Alimentary Code. Waters are of the calcic-sulfide and magnesium-sulfide types. **Geothermal** features dissipate along the Agrio River, **downstream** of Caviahue Lake.

The NH Lake basin exposition to the 2011 CCPVC eruption plume affected surface water quality at varying intensities, depending on the distance to the crater. Under normal conditions, the stream's features of the NH basin are rushing flow, oxygen saturated, low salinity, slightly alkaline, and transparent. Western streams show greater flows, less bottom sediments, and higher total dissolved solids (TDS) values compared to those of the eastern side. River's features changed after the eruption, notably in the western streams, showing TDS values 33 to 68% higher than those measured pre-eruption (Lallement et al. 2016).

Immediately after the CCPVC event, in lakes Espejo, Correntoso, and NH (Fig. 1), TSS increased 28 fold, from about 0.5 to 14 mg L^{-1}. Six months later, TSS levels

were diminished but remained 2–8 times higher than pre-eruption values, and the light extinction coefficient (Kpar) was 1.5 to 2.5 fold higher than the pre-eruption values that were in the range 0.10–0.15 m^{-1} (Modenutti et al. 2013). For several sites along the NH Lake, Pérez Catán et al. (2016) reported that element contents between the water column and pore water evidenced the potential dissolution. Many physicochemical transformations occurred after the pyroclastic material entered the water body, such as pH changes from 3.2 to 8.1, the electrical conductivity increased from 28.9 to 457 $\mu s\ cm^{-1}$, and redox potential increased from 171 to 591 mV. Maximum measured concentrations of F, Al, and Hg were 600, 40, and 0.038 $\mu g\ L^{-1}$ respectively, which were lower than the toxicity limit for aquatic life according to EPA (2021).

Geochemical interactions promote the initial state recovery, thus the physicochemical parameters stabilized one year after the eruption.

Ashfall from the 2008 Chaitén eruption notably affected Los Alerces National Park area and its surroundings, where rivers reached high TSS values in the water column in May–June 2008, which persisted high in the following months. In western streams, TSS fluctuated between 20 and 236 fold higher than pre-eruption values. Ash resuspension and remobilization continued even 20 months after. Glass was the main ash constituent with minor amounts of andesine, quartz, and cristobalite. Chemical elements that exhibited higher enrichment factors included As, Cs, Sb, Bi, Th, U, Pb, Cd, Zn, and Sr. Some of these elements detected in leachates are potentially toxic (Miserendino et al. 2012).

2.2.1 Arsenic

Arsenic (As) is a toxic element, whose presence is linked to Andean volcanism. In Patagonia, highest As rates in water are registered close to geothermal processes in volcanoes, thus decreasing from the Andes to the Atlantic coast. Domuyo and Copahue volcanoes are the main As sources in Northern Patagonia. The highest As concentration in water was found in the Domuyo Volcano (Colorado River basin), which flows up from rocks as hot **springs**, in variable values, from no detectable to 950 $\mu g\ L^{-1}$ and a mean value of 303 $\mu g\ L^{-1}$ (Lamela et al. 2019).

Copahue volcano is also an important contributor of As. Total As levels decrease significantly after the Caviahue Lake (50 $\mu g\ L^{-1}$ in the lake outlet to 25 $\mu g\ L^{-1}$ 7 km downstream). Cyanobacteria, algae, and mollusks have major As rates than fishes and birds. Surface waters in the Limay River basin do not present significant As concentrations, but Juncos et al. (2016) reported As increases in the NH Lake after the 2015 CCPCV eruption, as well as great As variations in **phytoplankton** (3.9–64.8 $\mu g\ g^{-1}$ dry weight, d.w.) and small zooplankton (4.3–22.3 $\mu g\ g^{-1}$ d.w.). The observed As accumulation pattern was: primary producers (phytoplankton) > scrapper mollusks (9.3–15.3 $\mu g\ g^{-1}$ d.w.) > filter feeding mollusks (5.4–15.6 $\mu g\ g^{-1}$ d.w.) > omnivorous invertebrates (0.4–9.2 $\mu g\ g^{-1}$ d.w.) > zooplankton (1.2–3.5 $\mu g\ g^{-1}$ d.w.) > fish (0.2–1.9 $\mu g\ g^{-1}$ d.w.). Juncos et al. (2016) reported As biodilution in the whole food web, and salmonids food chains, feeding on fish prey. Biomagnification resulted in

the food chain of creole perch, feeding on benthic crayfish. Only in the short term, the As increase in biota was more evident in zooplankton and planktivorous fish.

2.2.2 Mercury

Mercury (Hg) is a toxic element, present in rivers, lakes, soils, and groundwater. Hg deposition from the atmosphere is the widespread global source of Hg in water, mainly caused by human pollution. Wildfires release to the atmosphere the bioaccumulated Hg in the forests by years, reactivating the cycle of transport and deposition. Patagonian lakes and streams are far away from punctual Hg emissions of human origin, but volcanic eruptions are frequently natural sources of Hg by tephra or gas emanations. Chemical Hg forms in the water column and sediments are strongly related to its effects on living organisms.

Soto Cárdenas et al. (2018) reported the highest Hg rates in Brazo Rincón, the western branch of NH Lake, close to the CVPCC. Total Hg determined in November 2013 ranged from 17 to 363 ng L^{-1}, with a very low MeHg:THg ratio. It was lower in lakes (0.12%) than in streams (>0.21%). These levels were similar to those found in typical highly human-contaminated areas.

Arcagni et al. (2017) detected high Hg inorganic rates in plankton of the NH Lake, reaching 260 mg g^{-1} THg mostly inorganic, and very low MeHg values. In contrast to MeHg, THg is inefficiently transferred and hence is not biomagnified. Arcagni et al. (2017) remarked a differential THg bioaccumulation between benthic and pelagic taxa. In the benthic-littoral zone, THg in native fish increased as the trophic level increased, but salmonids presented lower THg rates than both, their diet and native fish, which positioned in the lowest trophic levels.

Daga et al. (2016) reported a sequence of 1600 years Hg deposition in lacustrine sediment layers of Futalaufquen Lake, located 75 km west of the Chaitén volcano. The Lake received significant ashfalls from the Chaitén eruption in 2008. The Hg peak on the top of the sediment core corresponds to the 2008 Chaitén event; showing a Hg accumulation rate two times higher than that of the underlying layer. Volcanic eruptions and irregular anthropogenic fire episodes explained most Hg accumulations in the last 300 years.

2.3 Biologic Effects

Due to the 2011 CCPVC event, phytoplankton biomass increased at least 4 times its pre-eruption values in lakes of the NH National Park, due to the combination of Phosphorus (P) increase with a lowering of light intensity caused by suspended ashes (Modenutti et al. 2013).

In the same area, Balseiro et al. (2014) analyzed the effects over pelagic microcrustaceans. At the subcellular level, ash exposition reduced the performance because organisms derived energy to compensate for cellular damages. At the organismic

level, zooplankton reduced its survival and fecundity due to ash ingestion. At the ecosystem level, shifts in the light-nutrient ratio in the water column were observed, which reduced the photo-inhibition on producers by light decreasing. The increase in P augments the producer level. Volcanic ashes caused a mismatch in the trophic food web with an increase in the producers and a decrease in the herbivores. The recovery of pre-eruption conditions demanded between one to three years.

In the nearest streams to the volcano, Chironomid densities were still high eight months after the eruption, varying between 33 and 100% of total macroinvertebrate densities (Lallement et al. 2016).

In the most impacted western streams, ash-choked channels from the initial ash deposition killed numerous fishes. Immediately after the eruption, the absence of both benthic and drift fauna was absolute, and after eighteen months, Trichoptera was still absent. Exposed streams to moderate ash loads showed a drop of fish densities due to the decrease of benthic fauna. Thirty months after the eruption, environmental changes were still occurring due to ash remobilization and transport. However, salmonids were progressively recolonizing the affected streams (Lallement et al. 2016).

The normal zooplankton composition in the nearby Chilean lakes to CCPVC, dominated by larval forms of copepods, followed by adult stages of calanoids copepods and to a lesser extent ciclopoids, evidenced, after the eruption, a marked decrease of cladocerans in Ranco Lake and notably in Puyehue Lake, where they completely disappeared.

After the 2008 Chaitén eruption, macroinvertebrate density and richness diminished rapidly in affected streams of the Upper Futaleufú River (Argentina) by the eruptive plume, showing still low values in March 2010. At least 25 taxa resulted significantly affected, being Trichoptera the order with a higher number of affected taxa (Miserendino et al. 2012). Habitat deterioration, food quality diminution, and interferences with breathing mechanisms were the causes of the increase in mortality.

3 Alien Invasive Species Disturbances

It is widely recognized that the introduction of species represents a major cause of biodiversity loss and alteration of freshwater ecosystems. Established invasive species are very difficult to control, and many times impossible to eradicate (Reid et al. 2012).

Competition for habitat or food, and predation on local species are the main and common related processes and eventually shared with habitat alteration or disease transmission, even with negative consequences for the native species. The issues related to invasive species in freshwater ecosystems, particularly salmonids, “didymo”, and beavers, are below examined.

Table 1 First introductions of salmonids in different zones of Patagonia

Location	Date	Specie	References
North Patagonia, Arg.	1904–1905	Brook trout (*Salvelinus fontinalis*), lake trout (*S. namaycush*), rainbow trout/steelhead (*Oncorhynchus mykiss*), landlocked salmon (*Salmo salar sebago*)	Pascual et al. (2007)
Santa Cruz, Arg.	1906–1910	Brook trout, lake trout, rainbow trout, landlocked salmon chinook (*Oncorhynchus tshawytscha*), sockeye (*O. nerka*), coho (*O. kisutch*), sea trout (anadromous brown trout, *Salmo trutta*) Atlantic salmon (*Salmo salar*)	
Aysén region	1968	Rainbow trout, brown trout	Correa and Hendry (2012)
Tierra del Fuego (TDF) Chile TDF (Argentina)	1927 1935–1937	*Salmo trutta*	O'Neal (2008)

3.1 Salmonids

In the first decade of the twentieth century, Argentinean national authorities trusted the initiative to establish feral salmonids, for sport fishing and aquaculture purposes. Table 1 shows the initial introductions of the different species in Patagonia. They succeed without having a baseline neither ecological studies that evaluated impacts on ecosystems. There is practically no information related to the native fish community's composition before salmonid's introduction, neither about its trophic relationships (Pascual et al. 2007; Macchi et al. 1999).

From fifteen introduced species in Patagonia, eleven have established self-sustaining populations. Of those, salmonids are dominant. Rainbow trout, brown trout, and brook trout are widely distributed, being trout the most common species in Patagonia. Anadromy is limited to rainbow trout, brown trout, and chinook salmon (Pascual et al. 2007).

The native Patagonian freshwater fish fauna is composed of only 26 species (Pascual et al. 2007) of which *Galaxias platei* (puyén[1] grande) is the most widely distributed.

Piscivorous salmonids, preying mainly on *G. platei*, are likely the main cause of this species declining in Patagonia. It is hard to specify the real magnitude of the effect of introduced fishes on native species since additional factors also have

[1] Puyén in Argentina, Puye in Chile.

negative incidence on them. However, consistent evidence explained below supports the determinant role of alien fish on native fish declining.

In lakes and reservoirs of the Limay River basin, the same salmonids species showed different levels of piscivory in different water bodies, with higher rates related to the bottom organism reduction. *G. maculatus* was observed as the major prey category among fishes, without strong effects over this species abundance (Macchi et al. 1999).

Although trout and galaxiids can coexist in Patagonian lakes, the ecological niche of *G. platei* has been restricted through predation and competition. That could lead to the collapse of local populations in the long-term, through the depletion of *G. platei* recruits and juveniles (Ortiz Sandoval et al. 2016).

Samplings performed in 11 large lakes and 105 streams, from 13 main water basins of Chile (39° to 52°S), evidenced that *Salmo trutta* and *O. mykiss* accounted for more than 60% of total fish abundance and more than 80% of the total biomass, while 40% of the sampled streams did not have native fish (Soto et al. 2006). In the lakes, the authors verified a delay in changing to piscivory of *G. platei* in trout environments. It is a negative impact on the *G. platei* trophic ecology, reflected in their nitrogen signature and trophic level.

A survey on 25 lakes in the Aysén Region (Chile) revealed a strong negative relationship between the abundance index of *G. platei* and salmonids (Correa and Hendry 2012).

Frequent fish escapes from hatcheries involve negative consequences. Since the 1980s, the marine cage culture of salmonids in Chile has grown sharply. Chinook salmon (*O. tshawytscha)*, which was the last farmed species, had invaded almost every major basin in Patagonia (Cussac et al. 2016). Fernández et al. (2010) informed chinook salmon's findings at the Lapataia estuary (Beagle Channel) of a different parental source from that established for the population at the Upper Santa Cruz River Basin. Later, Nardi et al. (2019) confirmed the presumption of chinook invasion in the main rivers of TDF, through a detection method based on environmental DNA.

Alien species sometimes also introduce parasites and diseases. *Cyprinus carpio* is a globally distributed freshwater fish species, present in the Neuquén River (Argentina). Waicheim et al. (2014) reported 6 microparasites species in 33 examined fishes captured in the Ingeniero Ballester dam, being three of them likely introduced with the carp: *Dactylogyrus extensus*, *Pseudacolpenteron sp.* and *Bothriocephalus sp.*

Moreover, fish introduction increased the phytoplankton similarity in lakes of the Patagonian Plateau, from 39 to 49°S. Cyanobacteria dominates only in lakes with introduced fishes. *Daphnia* spp. elimination likely favored cyanobacteria proliferation due to nutrient rebalance, inducing decreasing water quality (Reissig et al. 2006).

3.2 Didymo

Didymosphenia geminata (DG) is a diatom native to the Northern Hemisphere that in a short term invaded Patagonian rivers by intense blooms, mostly in oligotrophic freshwater systems, covering rocks and gravels on the bottom of benthic and lotic environments.

The first South American occurrence of a DG bloom occurred in April 2010, at the Espolón River in Palena, Chile, followed by another event upstream, in Futaleufú River, in Argentina (Sastre et al. 2010). However, the species have been already in Chile since the 1960s, in the Sarmiento Lake, Magallanes, as well as in Los Cisnes River, Aysén (Asprey et al. 1964), and in the Mejillones River (Rivera and Gebauer 1989).

Despite the efforts of the Chilean and Argentine authorities to control the expansion, in less than 18 months after the first bloom, DG had spread in twenty rivers of Los Lagos and Aysén Region (Chile), as well as in four rivers of the Chubut and Neuquén provinces, in Argentina (Reid et al. 2012). In 2013, DG was detected in the Grande River, TDF.

Didymo spreading is attributed to algal rests introduced through foreign fisherman's equipment. Wildlife vectors may also play a role in DG dispersal. *Neovison vison* is also an alien species that has semi-aquatic habits and high territorial mobility, with the potential to facilitate DG dispersal across terrestrial barriers. Birds are also possible vectors.

Patagonian rivers and lakes are widely recognized for their highly scenic and pristine quality; however, DG presence degrades the visual landscape perception, with negative implications in tourist and recreational activities.

Physical changes resulting from DG proliferation produced increased algal biomass, fine sediment trapping, and hydrodynamic changes. DG induces biogeochemical processes within its mats, as pH changes and Phosphorus uptake (Reid and Torres 2014). Alterations in the habitat of benthic species might cause shifting in food chains, however, studies in the Upper Limay River indicate no evidence of modifications in the abundance of microcrustaceans such as *Aegla* sp. and *Samastacus* sp. caused by DG proliferation (Añón Suárez and Albariño 2020).

3.3 Beaver Invasion in Tierra del Fuego

In 1946, when a few beavers (*Castor canadensis*) transported to TDF, Argentina, from Canada, were released in the Fagnano Lake, nobody could imagine the magnitude of the ecological impact that this act would imply a few years later. Indeed, the beaver expansion in TDF was an extraordinarily successful biological invasion. Although most papers referred to a precursor group of 25 couples, Pietrek and Fasola (2014) demonstrated that only 20 individuals composed this group.

C. canadensis is a big rodent with semi-aquatic habits. As a survival strategy, they build dams using branches and trunks from the riparian vegetation, adding mud as impervious material. In the lack of *Nothofagus* trees, beavers use shrubs and reeds. Dams include a lodge, underwater accessible. The lack of predators and competitors, food abundance, human absence, and stream density, were favorable features for its naturalization and rapid expansion. Beavers invaded not only TDF but also the adjacent islands, reaching many times the continent.

Molina et al. (2018) reported 56 beaver activity findings in the continent, south of the Magallanes region, mainly in the San Juan River basin, where beavers reached the headwaters. The oldest continental evidence was in 1968, near the mouth of this river. Frequent findings have been reported since 1994. The northernmost sighting was in the Hollemberg River, 19 km south of Puerto Natales. However, beavers have not established populations in the continent.

Drainage systems shifts and destruction of riparian vegetation by cutting and flooding are direct impacts of *C. canadensis* on freshwater environments. The geomorphological features of the river valleys influence the dam extension which tends to expand over time. Recent buildings show low height, raising the water level in around 0.50 m, but sediment deposition by flow speed reduction forces beavers to augment the water level in the dam. Elevated impoundments have also the function to extend the aquatic access to new riparian sectors. Some dikes can reach over 1.50 m height. Beaver buildings require continuous care and material supplying, which means permanent local alterations.

In contrast with prevailing deep-oligotrophic lakes, beavers build shallow reservoirs rich in organic matter (OM). Beaver dam area in the Argentine side of TDF represents 0.42% of the total area (Henn et al. 2016). The increase on the evaporation and infiltration linked to the dam's areas has low signification at a basin level, then runoff decreasing is negligible.

Regarding dam's effects on the drainage regime, the water volume kept by dams during floods is in general insignificant, because of the lower relative dam area and their low specific storage, since these buildings normally remain full. However, flood attenuation by beavers might be more reliant on flood retard rather than on water volume retention. Successive dam cascades (Fig. 4a) dissipate flow energy, reducing the flow velocity along the stream, and mitigating the intensity of regular flood peaks. The asynchronous flow peak convergence of goodly and poorly dam-controlled streams might also contribute to ordinary peak flood mitigation at the lower river section. This mitigation is not effective in extreme events, which frequently cause beaver dams to collapse.

Failures of a beaver's reservoir with high positional energy may cause damage in inhabited zones. In the Pipo River valley, nearby Ushuaia city, a beaver impoundment located near the top of the Susana Mount (400 m a.s.l.) failed, after heavy rains occurred on November 1, 2002. It released abruptly water and sediments that cascaded 300 m, resulting in a dangerous mud-trunks torrent. This happened again in May 2007.

C. canadensis regularly colonized peatlands. *Nothofagus* trees can reach only dwarf tall on them, except in gallery forests, along streams through these wetlands

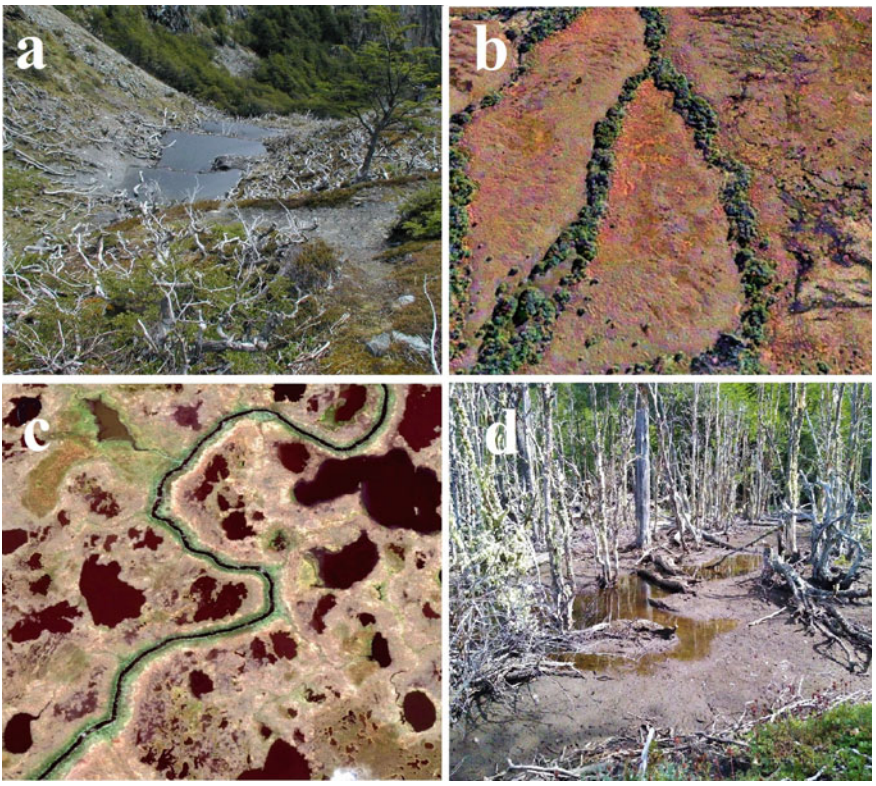

Fig. 4 Effects of beaver activity. **a** Successive dams dissipate flow energy in the upper streams. **b** Gallery Forest (GF) in a natural state on peatlands in Península Mitre, eastern TDF, Argentina; **c** GF degraded by *C. canadensis*. The forest disappeared, remaining only grasses. **d** Dead trees and sediment accumulation in an empty beaver dam after its failure

(Fig. 4a). Riversides are differential environments in peatland landscapes, whose soils include fluvial sediments and present deeper **water table** levels than the bog lawn. These features favor contrasting riparian vegetation, which includes trees vulnerable to beavers and proper grasses for the beaver's diet (Fig. 4a, c).

The inundation of a bog sector kills vegetation, inhibits C accumulation, and favors OM decomposition. Moreover, impoundments implicate unsteady changes in the affected patches, since its local influence is transitory. Dam permanency depends on the colony's jobs. Great floods, colony relocation, and human interferences are factors that lead to its ruin, and the beginning of new local shifts (Fig. 4d).

Sphagnum-raised bogs usually include natural **ponds** that play the surface-water retention function. Most of these ponds are naturally unlinked, but beavers connect them, through channels that they build to move through the bog, modifying the hydrological features. Moreover, such channels drain the peat-saturated layer, lowering the water table level and shifting the anoxic condition that inhibits OM decomposition.

Thus, beavers might induce peatland degradation processes. In contrast with dams, which cause unsteady changes, channels can modify features of peatlands hydrology for a long period of time.

C. canadensis transforms lotic in lentic systems by stream damming, resulting in sediment and OM retention, which shifts the physic-chemical characteristics of waters and the benthic fauna composition (Lizarralde et al. 1996; Vila et al. 1999). Beaver ponds are sources of nutrients and C, with higher levels of organic than inorganic nitrogen. The effects induced by these rodents are major factors influencing the processes of nutrient transformation in TDF streams (Lizarralde et al. 1996).

Naturally, heterotrophic Fuegian rivers show intensification in the heterotrophy of the periphytic community because of beavers activity, likely related to the increasing water turbidity and OM retention (García and Rodríguez 2018).

The rapid water temperature increase during insolation hours, due to the shallow depth of waters, dark hue, and stagnation, along with the OM abundance incorporated from the flooded **riparian zone**, are favorable conditions for the development of invertebrates, which are the food base of many birds and fishes (Sielfeld and Venegas 1980). Vila et al. (1999) found a positive correlation between beaver activity and benthic fauna abundance, and Arismendi et al. (2020) reported, higher macroinvertebrate densities in colonized streams, mainly of Diptera, followed by Amphipoda taxas.

In the Cóndor River (western TDF), the presence of *G. maculatus*, which is the most common TDF native species (Moorman et al. 2009), and beaver impoundment abundance, link positively. However, the frequency of puye below dams suggests that these barriers might be fragmenting these populations (Vila et al. 1999).

In beaver-influenced streams, trout has a wider dietary breadth with Diptera and Amphipoda as the prey items provide most of the energy, whereas in no colonized streams it is Trichoptera. The highest growth in trout populations occurs in sympatry with *C. canadensis*. The trout growth rate was on average 14% higher in streams in sympatry than in allopatry (Arismendi et al. 2020). Beavers enhanced puye trophic web and thereby increased the abundance of that species, mitigating in this way the salmonid's impact (Moorman et al. 2009).

In streams of the Cabo de Hornos Archipelago, beaver environments increased both, in abundance and secondary production, three to five-fold no colonized ones, but richness, diversity, and the number of functional feeding groups dropped by half. Thus, while a generally positive link between diversity and ecosystem function is frequent in a variety of systems, this can be decoupled by responding to alternative mechanisms (Anderson and Rosemond 2007).

4 Climate Change Effects on Freshwaters

The significant glacier recession occurring since the beginning of the twentieth century, along the Andes, as well as in the main mountain systems of the world, is the clearest signal of climate change (CC) at a global level.

Negative CC impacts are evident in Patagonia. Linear trend data analyses reveal a highly significant tendency towards drier and warmer conditions over the 1912–2002 period in NW of Patagonia (Masiokas et al. 2008) that persists in the present. Due to the reduction in precipitation in the Northern Andes, rivers located north 42° S registered a strong negative flow trend, which in some cases led to reductions by half (Barros et al. 2015).

Multimodel-projections indicate for Patagonia higher temperatures and slightly lower rainfall, both with increasing tendencies towards the end of this century; that represents a trend towards greater aridity for all scenarios. The most affected area corresponds to the upper basins of the Colorado and Neuquén rivers (Barros et al. 2015).

Seasonal snow accumulation, which depends on both precipitation and temperature, is also a proper CC indicator that shows a general negative trend. In the upper basins of Northern Patagonia, the reduction in precipitation is indicated as the main cause. For the Aysén River basin, Pérez et al. (2018) report a -20.01 km^2 y^{-1} trend in snow cover, related to both, a $+0.07$ °C y^{-1} temperature trend and a 8.66 mm y^{-1} decreasing precipitation. In Brunswick Peninsula (Magallanes Region), the average snow extent decreased 19% in 1972–2016, compared to 1958–1972. It is attributed to a $+$ 0.71 °C warming registered in Punta Arenas, during April-September (austral winter) for the same period (Aguirre et al. 2018).

Global warming implies the weakening of the snowpack stability, and the rise of its altitudinal lower limit, resulting in water storage reduction at a basin level. The shift from the combined nival-pluvial to a pluvial streamflow regime would be a consequence of global warming. Winter floods might increase in frequency and intensity, and summer water scarcity might increase in severity.

These problems are present in a framework of greater pressures on water resources due to population growth and productive development. Irrigation concentrates water demands in spring–summer seasons when water availability becomes critical.

The Patagonian Andes contain the greatest glacier area of South America. Glaciers reach their largest development between 46° S and 52° S, in the Patagonian Icefields that feed greater Patagonian rivers: the Baker and Pascua in Chile, and the Santa Cruz in Argentina. Ice melting recharges many Patagonian rivers, but this water contribution tends to decrease linked to the glacier area reduction.

Miserendino et al. (2018) assert that glacier-fed streams seem vulnerable to global warming, and warned that the functioning of the related ecosystems could be altered. Endemic elements could disappear at the upper segments being replaced by other species.

4.1 Lake Changes

Glacier's dynamics causes substantial physical changes in glacial lakes, such as the new lake's development and the ice-dammed lake emptying.

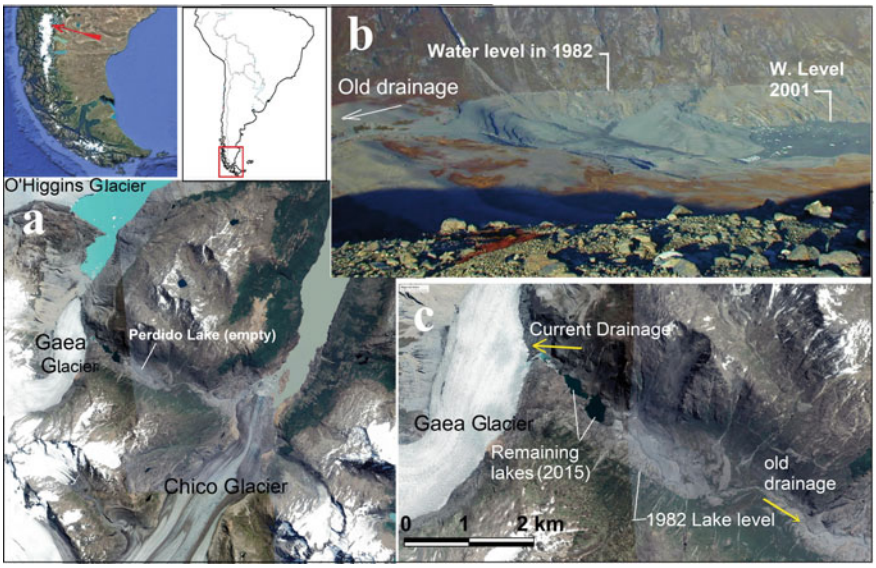

Fig. 5 Emptying of Perdido Lake. **a**, **c** current state. **b** View from the west in 2001. Images from Google earth

Glacier retreat during the twentieth century resulted in the formation of many small and medium lakes, such as the Ventisquero Negro Lake (41°12′ S, 71°50′ W), contiguous to the Manso Glacier's front. This began in the 1990s, after a rapid ice retreat (Masiokas et al. 2010). The lake still expands amid the recessive glacier front and the main moraine ridges, inducing ecological shifts in the Mascardi Lake, located 17 km downstream. Sedimentation in the new lake reduces the incoming sediment load to the Mascardi Lake, increasing its water transparency and altering the autotroph distribution in the water column (Bastidas et al. 2017).

Iturraspe and Strelin (2002) reported the gradual emptying of the Perdido Lake[2] (48°59′ S, 73°07′ W), at the eastern Southern Patagonian Icefield (SPI), Chile, between Chico and O'Higgins glaciers (Fig. 5a). A third glacier, the Gaea, dammed the lake, which drained towards the Chico glacier valley (Fig. 5b, c). Ice-dam shrinkage allowed the sub-glacial flow towards the O'Higgins Lake; thus in 1986, Perdido Lake dropped 41 m below its level registered in 1982, finishing its outlet towards the Chico Valley. In 2001, the level dropped another 20 m, diminishing its area to 40% of the original extension. In February 2013, a sudden release resulted in the lake segmentation and its surface reduction to 23 ha (8% of the surface that it had in 1982).

The Greve Lake (49°03′S, 73°59′W) was generated by the Pio XI Glacier advance, blocking in 1926 a wide valley to form a 195 km^2 glacial lake. Pio XI is the largest glacier in South America and one of the very few in expansion. The valley occlusion

[2] Appellation given by the author due to the lack of an official lake name.

barely gave the colonists, who had settled shortly before, time to leave (De Agostini 1945). At present, a moderate glacier advance persists, and the lake level is controlled by the drainage through a northern col towards the Témpano Fiord. The glacier advance generated drastic changes in the Greve Valley hydrology, as well as in the preceding lotic and terrestrial ecosystems, which became a new great 150 m depth lentic system of doubtful hydrological and ecological stability.

4.2 Glacial Lake Outburst Floods

Glacial lake outburst floods (GLOFs) are torrential events caused by the sudden drainage of a glacial lake. Ice retreating, ice thinning, moraine-dam failures, subglacial tunnels progress, or a combination of these processes, resulting in the rapid discharge of greater water volumes. GLOFs motivate hazards and violent disturbances, especially in the lack of large lakes able to mitigate its effects.

One of the best-known GLOF examples is the periodic occlusion of the Rico Arm of the Argentino Lake by the Perito Moreno glacier causing the level rise of the Rico Arm over the Argentino Lake. The water pressure generates tunnels or subglacial drainage whose development determines the spectacular ice collapse releasing the Rico discharge.

In 2009, the moraine that dammed the Ventisquero Negro Lake collapsed, at the foot of Tronador Mount, Argentina, causing a GLOF in the Manso Superior River Valley. The flood was attenuated at Mascardi Lake (Fig. 1), where the sediment load produced a transitory decrease in water transparency (Bastidas et al. 2017).

CC affected the stability of glaciers in Southern Chile producing an increase in the GLOFs frequency. For instance, in 1977, the failure of the moraine-dammed Engaño Lake (46°27′ S, 72°58′ W) caused a GLOF aggravated by carrying large woody debris transport. This surge destroyed houses settled in the valley and produced damages in Bahía Murta town, at the shore of General Carreras Lake (Iribarren Anacona et al. 2015).

In Torres del Paine National Park (Magallanes Region), in the summers of 1982 and 1983, Paine River floods raised levels of local lakes, inundated roads, and damaged riverside installations. These torrents resulted from rapid evacuations of a transitory supra-glacial lake on the Dickson and Frías glaciers (Peña and Escobar 1983).

These glaciers ended in a transverse valley where they blocked the drainage. Most of the Frias flows towards the NE, to the Argentino Lake, but the Dickson retreat allowed, around 2005 year, a new flow-path towards the SW. Thus, the Payne River system captured the entire Frías outflow, changing its discharge from the Atlantic to the Pacific slope.

In the Baker basin, powerful and recurrent GLOFs occurred during the last years, due to the periodic emptying of the Cachet Dos Lake that is dammed by Colonia Glacier (Fig. 6). Twenty-one GLOFs occurred between 2008 and 2017, producing floods that duplicated the maximum annual flow (Jacquet et al. 2017).

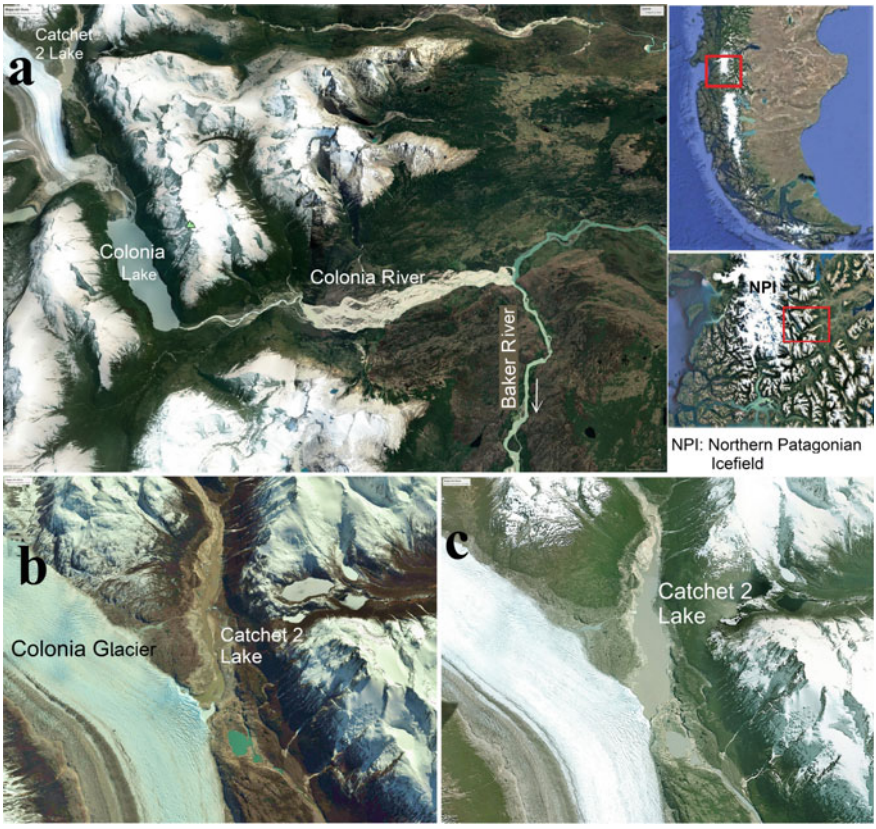

Fig. 6 Colonia river GLOF area. **a** General setting and geomorphological shifts in the Colonia riverbed due to recurrent GLOFs from Catchet 2 Lake. **b** Catchet 2 Lake after its subglacial drain. **c** Lake storage recovering after a new glacier blockage. Images from Google earth

Although Colonia Lake mitigates effects, specific locations evidenced > 40 m incision. Active channel migration and cut-bank erosion removed terraces (Jacquet et al. 2017). GLOFs shifted not only the Baker hydrology but also the conveyance system, which could be affecting the fluvial ecosystem functioning. The normal state of macroinvertebrates in the Baker River system observed in 2006, before the GLOFs sequence (Moya et al. 2009), suggested the recovering of a previous GLOF event occurred in 1960, however, there is scarce information on the effects of the current GLOFs sequence over invertebrates in this river.

5 Land Use and Land Cover Changes

5.1 Urban Land Use

Rainwater drainage systems in urban centers facilitate a fast and direct discharge into a collector water body. Hence, cities are spots of all kinds of elements, which concentrations are not present naturally in freshwater ecosystems, such as heavy metals, hydrocarbons, phosphates, nitrogen, mercury, arsenic, etc. Although most Patagonian cities have wastewater treatment systems, they often do not cover the entire urban area.

Many drainage systems collect both rainwater and wastewater fluxes, which is inconvenient for the discharge treatment. It results in the biological contamination of the receiving water body. The level of wastewater treatment for final discharges varies notably in different cities. Urbane streams from the city of Ushuaia (TDF) collected wastewaters until 2016, when a court order instructed the Province and the Municipality to improve the sewage system and remedy the environment. These watercourses acted as receptors of human activities and became emitters to the coastal system. Nutrients still remained in bottom sediments four years after that direct wastewater discharge ended (Diodato et al. 2020). Likewise, wastewater discharges from the drainage system of Río Grande city (TDF), produced organic and bacteriological pollution on the shores of the estuary of the Grande River (Lofiego et al. 2009).

Organic pollution is the common result of urban sewage discharges. Further contamination types depend on industrial activities. In developed cities, industries are in a proper sector, and pollutant factories usually perform wastewater treatments by themselves. However, discharges do not always meet the environmental requests, and official controls are often deficient.

The pollutant load correlates with the number of inhabitants living in the urban area. In Argentine Patagonia, the conglomerate of Neuquén-Cipolletti-Plottier cities (Fig. 7) is the highest urban concentration, with about 400,000 residents in 2018 (Pérez 2018). The largest city in Chilean Patagonia is Puerto Montt (213,117 inhabitants, 2017 census). Both populations relate to intermediate cities and moderate pollutant potential.

Urban effluents generate increasing fluvial contamination levels. Wastewaters are treated, but sewage-treatment plants have shown poor performance during some periods. Clandestine discharges end up in highly contaminated streams parallel to the main channel, such as Los Milicos channel, which joins the Neuquén River, and the Durán Stream (both marked in Fig. 7), which crosses the Neuquén city and pours into the Limay River. These channels collect effluents from precarious urban areas and animal farms, as well as diverse industrial wastewater that discharges right in the rivers (Pérez 2018).

The rapid growth of some Patagonian cities resulted in land-use changes that have implied severe wetland loss. The industrial development of Río Grande city (TDF-Argentina) attracts immigration, which produced an explosive urban expansion in

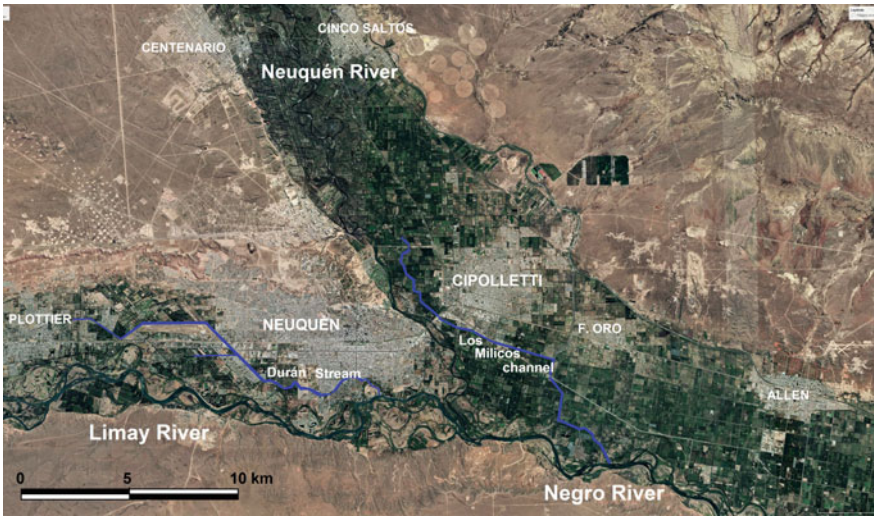

Fig. 7 The confluence of Limay and Neuquén rivers, where the main cities, productive farms, and oil activity are settled

1972–2020 through a conditioned process by housing crisis, social vulnerability, and informal land occupation. The urban expansion affected coastal and continental wetlands, over which 1/3 of the current urban area is consolidated (Iturraspe et al. 2021).

Ushuaia city grew up as well as Río Grande city, transforming forest and some peatland areas in urban soils and modifying stream courses. On the other hand, Peri-urban areas of Puerto Montt (Chile), suffered strong changes, losing lakes, "hualves" and peatlands, which were drained and filled to be urbanized. An innovative Supreme Court's decision ordered the proprietary of the Llantén Wetland, to protect it, revoking the permission of the municipality for its urbanization (Rojas Quezada 2019).

5.2 Effects of Intensive Agriculture

In Argentine Patagonia, agriculture needs irrigation, due to the water deficit in the extra-Andean region. Therefore, this productive activity has been concentrated in the main fluvial valleys, reaching its maximum development after dam construction. Floods control by dams resulted in the occupation of the flood valleys for fruit crops. The intensive agricultural activity has implied changes in the aquatic systems in terms of water quality, and runoff flow reduction due to the significant water demands for irrigation. The use of pesticides is causing disturbances in the Negro River, while water scarcity affects most notably the Colorado River.

The Valleys of Neuquén, Limay and Negro rivers (Argentina) integrate an important fruit productive area, with about 120,000 ha of crops fed by a vast irrigation net, complemented by drains that return irrigation excess.

Macchi et al. (2018) analyzed pesticide concentrations in drainage waters discharging to the Neuquén River, in combination with macroinvertebrates biomonitoring in the irrigation channels. Chlorpyrifos was the most frequently detected pesticide (61%), followed by azinphosmethyl (44%) and carbaryl (21%). The highest monthly concentration occurred in spring–summer: azinphosmethyl (0.4 μg L^{-1}-Nov/2009), chlorpyrifos (0.6 μg L^{-1}-Nov/2010) and carbaryl (2.6 μg L^{-1}-Feb/2010). Chlorpyrifos affected the richness and abundance of macroinvertebrate assemblages.

Downstream the Neuquén-Limay confluence, Miglioranza et al. (2013) reported the presence of endosulfan, organochlorine pesticides (OCPs), polychlorinated biphenyls (PCBs), and polybrominated diphenyl ethers (PBDEs) in soils, sediments, suspended particulate matter, stream waters and **macrophytes**, which indicate the impact of agriculture on the **watershed**.

In 2006, an extraordinary flood of the Negro River inundated valley farms and mobilized soil contaminants to the fluvial ecosystem. The pollutants detected in rainbow trout increased in most cases one order of magnitude, according to pre and post-flood samples. DDTs and PCBs were the main compounds in fish, with concentrations in muscle above the maximum allowed for human consumption (Ondarza et al. 2012).

The Colorado River constitutes the water source for irrigation of 158,800 ha. The snowfall decrease in the upper basin, very noticeable since 2010, has caused constraints in water availability at the lower basin, where the flow is regulated by the Casa de Piedra dam. During drought periods, the water authority has reduced or suspended the water supply for irrigation, releasing from the dam only the necessary flow for supplying populations and ecological requirements.

In the early twentieth century, the Desaguadero River, fed by the Andean streams located in the North of Patagonia, emptied into the Colorado River with the name of Curicó River. The water diversion for irrigation upstream of Patagonia, caused its flow reduction until it turned disconnected from the Colorado River, becoming an **endorheic** stream. That causes the salinization of lakes and lowlands in its terminal section. This situation generated conflicts between provinces, where La Pampa province was the most affected. In addition, in 1980, an unexpected and occasional Curicó's reactivation impacted the Colorado River by discharging water with a saline concentration three times higher than seawater.

The Musters-Colhué Huapí Lake system, located in the southern Chubut province, Argentina, has undergone strong hydrological shifts due to the combined effects of climate change, irrigation, and water supply to the local population and urban centers outside the basin. The lakes are fed by the Senguer River, whose flow regime depends on the snow precipitation in the upper basin. The river discharges into the Bajo Sarmiento, where these lakes and Sarmiento town are located. This system is currently endorheic, but about one century ago the Colhué-Huapí Lake (CHL)

discharged, likely intermittently, towards the Chico River (Scordo et al. 2017), which is a tributary of the Chubut River.

The Senguer River naturally recharged both lakes, through a wide alluvial fan, in which Sarmiento town has developed since the end of the nineteenth century, becoming a significant agricultural-livestock productive center. Sarmiento's farms are located in the windy steppe, hence its strength has been based on irrigation, fed from the Senguer River. This context led to managing water distribution, prioritizing the supply for the population, the irrigation, and the storage of the Musters Lake, from which an aqueduct supplies water to 350,000 inhabitants of urban settlements in the region. That was detrimental to the storage of CHL, whose recharge through the Falso Senguer stream is subjected to the availability of domestic wastewater (Scordo et al. 2017). The CHL is only 2 m depth, then its extension is very susceptible to storage changes. Its area of ~720 km^2 has been reduced in the recent decades, and it almost disappeared in the drought of 2016.

The historical Senguer's average flow in Bajo Sarmiento is 48.1 $m^3\ s^{-1}$, but between 2010 and 2020 it reduced to 37.4 $m^3\ s^{-1}$ (obtained from Servicio Nacional de Información Hídrica). Total water consumption in the summertime is estimated at 18.5 $m^3\ s^{-1}$ (Scordo et al. 2017), being not enough the remaining flow to support the evaporation rate from the full extension of both lakes. As the system is endorheic, the lake area reduction is the expected result from new negative terms added by consumptive water uses and inflow reduction.

Chiloé Island is the most important agricultural area in southern Chile. Family farm traditions date back to pre-Hispanic times, with potato varieties production as the local specialty. There are no reports on freshwater pollution related to this land use. Most environmental troubles concern the sea, and are being attributed to fish factories. Although precipitation reaches around 2000 mm y^{-1}, the local population affronts difficulties in the water provision during dry periods, which might be related to land-use changes in detriment of wetlands. Given the lack of glaciers and seasonal snow, wetlands provide irreplaceable ecosystem services on streamflow regulation. "Pomponales" is the local name for Sphagnum moss ecosystems with great capacity for water retention, described as secondary or anthropological peatlands by León et al. (2021). The moss fiber extraction for export has resulted in the degradation of these wetlands. Furthermore, the harvesting of "Tepual" wet forests to get wood as domestic fuel has also produced losses in the hydrological services that these humid ecosystems provide.

5.3 Forest Fires

Native forests were subjected to massive clearance in the Aysén Region (Chile). Since the beginning of the twentieth century, fires destroyed about three million hectares, particularly between 1936 and 1956, due to uncontrolled fires, set to create grazing lands. Fires reduced in Aysén the original forest area by half, resulting in widespread erosion (Quintanilla Pérez 2008).

There are no reports about the ecological effects that these fires produced in the short term, but it is widely accepted that large fires cause loss of native vegetation, runoff, and sediment load increase. The rise in total primary production, as well as shifts in the biogeochemical cycles and in biological communities assemblages, are ecological effects that can be assumed. Later land use change, more so than fire, significantly modified total nutrient stocks and isotopic N composition of plants and soils (Fajardo and Gundale 2015).

Forest fires, almost all of them of human origin, are recurrent in Patagonia, altering terrestrial and aquatic ecosystems, which increase in frequency and spread during dry, warm, and windy periods. Moreover, global warming will likely raise the fire hazard status.

5.4 Oil Exploitation

Oil exploitation involves important land use and land-cover changes. Oil deposits discovery caused the development of new towns in Patagonia. Oil camps, dense road networks, well's installations, auxiliary pools, pipelines, deposits, etc., involve land-cover changes and landscape transformations. Oil exploitation exposes soils and waters to recurrent environmental incidents, which comprise spills of hydrocarbons and **brackish** water from production and injection. Most spills occur in the terrestrial environment; however, heavy rains can activate its transport to water bodies. Although security measures are applied, any eventual oil spill in freshwater implicates a social-environmental disaster.

In 1997 and 1999 the water supply was interrupted for all uses in the Colorado River valley due to oil stains presence, caused by a flood that broke oil pipes installed on the riverbank (Dillon 2004). Until 1997, oil companies threw into the river drilling purge water with a saline concentration seven times higher than that of seawater.

Companies have enhanced security measures, and the state control has increased. However, oil spill events are frequent. In the Colorado River basin, for the 2011–2015 period, on average 1973 annual incidents were reported with environmental effects (COIRCO 2016). Corrosion or material failures were the main causes, originating 380 $m^3\ y^{-1}$ of oil spills and 5125 $m^3\ y^{-1}$ of production or injection of water spills. The total affected area was 3945 $m^2\ y^{-1}$, with no cases registered in fluvial environments; 3% in dry canyons, 8% in soils, and 89% in oil installations, which indicates the spill retention efficiency.

Monza et al. (2014) determined a low degree of contamination by hydrocarbons in the Neuquén River and identified sectors whose low levels of hydrocarbons of biogenic origin can be used as baseline.

6 Conclusions

Scarce biodiversity characterizes Patagonian freshwater ecosystems; however, its endemic species contribute to the global biodiversity, and the entire native biotic components play specific functions at different levels.

Volcanism is a regional feature in the matter of natural disasters. Despite the amazing magnitude that some eruptions reached, the evidence shows a recovery of the biota, tending to normalize after two or three years. In accordance with assertions of Crisafulli et al. (2015), and as it was hypothesized, no events resulted in the annihilation of the biota, and no turn back to a primary succession occurred. Lakes such as Nahuel Huapí provided fundamental refuges for fishes, allowing the later repopulation of damaged tributary streams. Riverbed morphology demanded more time to stabilize, as it was evidenced by the affected rivers by the Hudson and Calbuco eruptions.

The information on the response of aquatic environments affected by GLOFs is scarce, notably in altered riverbed sections. Like volcanic lahars and pyroclastic fluxes, GLOFs events transform the bottom valley morphology and the fluvial sediment transport, altering the habitat of benthic organisms.

GLOFs are extreme events not statistically represented in historical flow series. Therefore, stationary analysis of extreme flow peak's frequency, generally applied for hydraulic design, is unsuitable in basins with potential GLOF events. Moreover, the increase in the sediment load is a new feature to evaluate, especially for dam's design. Potential sediment mobilization in the first event occurrence seems to be higher than in later repetitions (Jacquet et al. 2017). GLOF threats implicate the convenience of the availability of GLOF's potential hazard maps.

Climate change involves uncertainties for future water availability in the Colorado and Negro rivers basins, where IPCC projections indicated the highest increase in temperature in Patagonia, threatening the seasonal snow stability.

Human outcomes tend to be permanent and increasing stressors. Introduced species, land-cover changes, and wetland's loss are some examples, which produce irreversible changes in freshwater environments.

The prospects for invasive species eradication are hard and uncertain. There is a lack of general social perception of salmonids as alien species. Moreover, no programs exist for native fish's protection, despite the advice of experts. Pascual et al. (2007) highlighted their calamitous state, not only due to exotic fishes but also for additional factors, such as aquatic contamination, habitat segmentation by dams, loss of riparian vegetation, volcanic ashfalls, GLOFs, fires, etc.

Beavers favored benthic environments and native fish, but also caused strong degradation of riparian forests. Argentina and Chile have signed in 2008 a collaborative agreement for the control and eradication of *Castor canadensis*. Successful eradication experiences in pilot basins have been performed in both countries. However, these efforts are far from attaining the beaver population control. Main drawbacks are the difficult access to colonized areas, the magnitude of the necessary financial and logistical resources, the beaver's heading habit, their reproductive rate, and

their ability to recolonize areas. At the present, the main success was avoiding their invasion to the continent.

Didymosphenia geminata produced the most successful invasion of a non-voluntary introduced species in aquatic ecosystems from Patagonia. Its expansion has prevailed over public campaigns and preventive actions to stop it. The opportunity to eradicate DG has likely passed, given its vast distribution, and the lack of precedents for the suppression of invasive aquatic microbial species from fluvial networks (Reid et al. 2012). Basualto et al. (2016) reported the expansion of *Gomphoneis minuta* in Chile, notably in Las Lajas River, Bío-Bío Region. This invasive alga, which visually can be confused with *D. geminata,* is present in confined colonies, in rivers of the Aysén Region, as well as in the Chubut River. It is advisable not to miss the chance to stop their expansion by the intervention on these spots.

Severe disturbances that forest fires generate have a natural recovery in the medium or long term. Nevertheless, many forest burnings gave rise to changes in land use that caused irreversible shifts in freshwater ecosystems.

Superposed disturbances demand special attention. The Baker River basin is an example of strong alterations, like catastrophic fires, the large eruption of the Hudson volcano, recurrent GLOFS, as well as didymo and salmonid biological invasions.

In rivers of the Northern Argentine Patagonia, different stressors dominate: increasing water demand, pesticide contamination, superimposed disturbances by urban discharges of the Neuquén conglomerate, biological invasions, habitat segmentation by dams, and uncertain future hydrological changes due to the effects of climate change. The irrigation-based agricultural development in the area has limitations. The Colhué Huapí drying out is, on a different scale, the Patagonian version of the Aral Sea drying out. The Colhué Huapí is not the only case in Patagonia. The disconnection of the Desaguadero-Curacó system from the Colorado River was also a result of intensive irrigation.

One examined case invalidates the generality of the hypothesis related to natural events. It is the formation of Lake Greve due to the Pio XI glacier advance, replacing the pre-existing fluvial ecosystem. Changes linked to glacier retreat are attributable to global warming, whose origin is human, but it has not been proven that the Pio XI anomalous behavior is due to global warming. The validation of the hypothesis requires excluding in its formulation the changes produced by the eventual expansion of glaciers, as well as the extensive lava flows, not present in the analyzed events.

The scientific advances in the last two decades related to the focused topics are remarkable. References cited in this chapter only represent a fraction of the available literature and approximately 90% of these works were published after 2000. Research has as well improved in quality and interdisciplinary scope. However, it is necessary to enhance the knowledge on some topics, such as inventory, composition, and distribution of native fish; ecological flow; limnology in glacial lakes; snowpack monitoring, and glacier contribution to runoff. The great Patagonian Baker, Pascua, and Santa Cruz rivers involve complex systems that include wetlands, large lakes, and glaciers. Dam projects on these rivers for hydropower have generated controversies. Studies on these freshwater ecosystems are still scarce; and the improved knowledge

on the ecological baseline would allow a better evidence-based understanding of pre- and post-dam changes, as well as the adaptive capacity of species.

It is highly recommended to strengthen the binational collaboration to efficiently respond to the environmental effects from huge natural events, as well as to plan the water management in transboundary basins and to promote joint investigations.

Most powerful natural disturbances in freshwater environments are not manageable, but these ecosystems are relatively resilient to these effects. Some changes of human origin are also unmanageable, like many of those associated with climate change. Manageable anthropological changes are usually severe, but they can be prevented or mitigated.

Many aquatic environments in Patagonia have ceased to be pristine to start a declining environmental process. However, they are still far from the levels of degradation easily observed outside of Patagonia. The future of Patagonian people is linked to that of the freshwater ecosystems, so their sustainable management is the challenge for the coming decades.

References

De Agostini A (1945) Andes Patagónicos. Kraft, Buenos Aires (in Spanish)

Aguirre F, Carrasco J, Sauter T, Schneider C, Gaete K, Garin E, Casassa G (2018) Snow cover change as a climate indicator in Brunswick Peninsula. Front Earth Sci 6(130):1–20

Agusto M, Caselli A, Tassi F, Dos Santos Afonso M, Vaselli O (2012) Seguimiento geoquímico de las aguas ácidas del sistema volcán Copahue-Río Agrio. RAGA 69(4):481–495 (in Spanish)

Anderson C, Rosemond A (2007) Ecosystem engineering by invasive exotic beavers reduces in-stream diversity and enhances ecosystem function in Cape Horn, Chile. Oecologia 154:141–153

Añón Suárez D, Albariño R (2020) Efecto del establecimiento del alga invasora *Didymosphenia geminata* sobre la abundancia de macrocrustáceos en el Río Limay superior, Patagonia, Argentina. Biol Acuat 34:1–12 (in Spanish)

Arcagni M, Rizzo A, Juncos R, Pavlin M, Campbell L (2017) Mercury and selenium in the food web of Lake Nahuel Huapí, Patagonia, Argentina. Chemosphere 166:163–173

Arismendi I, Penaluna B, Jara C (2020) Introduced beaver improve growth of non-native trout in Tierra del Fuego, South America. Ecol Evol 10(17):9454–9465

Asprey JF, Benson-Evans K, Furet JE (1964) A contribution to the study of South American freshwater phytoplankton. Gayana Bot 0:1–18

Balseiro E, Souza M, Olabuenaga I, Wolinsky L, Bastidas M, Laspoumaderes C, Modenutti B (2014) Effect of the Puyehue-Cordon Caulle Volcanic Complex eruption on crustacean zooplankton of Andean lakes. Ecol Austr 24(1):75–82

Barros V, Boninsegna J, Camilloni I, Chidiak M, Magrín G, Rusticucci M (2015) Climate change in Argentina: trends, projections, impacts and adaptation. Clim Chang 6(2):151–169

Bastidas M, Martyniuk N, Balseiro E, Modenutti B (2017) Effect of glacial lake outburst floods on the light climate in an Andean Patagonian lake: implications for planktonic phototrophs. Hydrobiology 816(1):39–48

Basualto S, Rivera P, Cruces F, Ector L, Ascencio E (2016) Didymosphenia geminata (Lyngbye) M. Schmidt y Gomphoneis minuta (Stone) Kociolek & Stoermer (Bacillariophyta), especies presentes en ríos de la VIII Región, Chile, formadoras de proliferaciones con aspecto muy similar. Gayana Bot 73(2):457–461 (in Spanish)

Bunbury J (2008) Effects of the White river Ash event and climate change on aquatic ecosystems in the southwest Yukon. Arctic 61(4):453–455 (in Spanish)

Chávez Barría PE (2016) Análisis de la dinámica del río Ibáñez en desembocadura, mediante la modelación en 2 dimensiones del flujo, transporte de sedimentos y morfodinámica de lecho. Tesis Magister. Univ Chile, Santiago, p 160 (in Spanish)
COIRCO, Comité Interjurisdiccional del Río Colorado. Estadística general de incidentes de todos los yacimientos hidrocarburíferos ubicados en la cuenca del río Colorado (2000–2015) https://www.coirco.gov.ar/centro-de-documentacion (2016). Accessed 12 March 2021 (in Spanish)
Correa C, Hendry A (2012) Invasive salmonids and lake order interact in the decline of puye grande *Galaxias platei* in western Patagonia lakes. Ecol Appl 22(3):828–842
Crisafulli C, Swanson F, Halvorson J, Clarkson B (2015) Volcano ecology: disturbance characteristics and assembly of biological communities. In: Sigurdsson H, Houghton B (eds) The encyclopedia of volcanoes. Academic Press, USA, pp 1265–1284
Cussac V, Habit E, Ciancio J, Battini M (2016) Freshwater fishes of Patagonia: conservation and fisheries. J Fish Biol 89(1):1068–1097
Daga R, Guevara S, Pavlin M, Rizzo A, Lojen S (2016) Historical records of mercury in southern latitudes over 1600 years: Lake Futalaufquen, Northern Patagonia. Sci Total Environ 553:541–550
Dillon B (2004) Riesgo, recurso hídrico y explotación de hidrocarburos. El caso especial de los derrames de petróleo en el Río Colorado, La Pampa, Argentina. Anuario 6:41–61 (in Spanish)
Diodato S, Garraza G, Mansilla R, Moretto A, Escobar J, Novoa J (2020) Quality changes of fluvial sediments impacted by urban effluents in Ushuaia, Tierra del Fuego, Southernmost Patagonia. Environ Earth Sci 79(20):1–14
Dorava J, Milner M (1999) Effects of recent volcanic eruptions on aquatic habitat in the Drift river, Alaska, USA: implications at other Cook Inlet region volcanoes. Environ Manage 23(2):217–230
EPA, Environmental Protection Agency (2021) National recommended water quality criteria, aquatic life criteria table. https://www.epa.gov/wqc. Accessed 20 May 2021
Fajardo A, Gundale M (2015) Combined effects of anthropogenic fires and land-use change on soil properties and processes in Patagonia, Chile. Forest Ecol Manage 357:60–67
Fernández D, Ciancio J, Ceballos S, Riva C, Pascual M (2010) Chinook salmon (Oncorhynchus tshawytscha, Walbaum (1792) in the Beagle Channel, Tierra del Fuego: the onset of an invasion. Biol Invasions 12(299):1–7
García V, Rodríguez P (2018) Efecto del castor en el metabolismo del perifiton y en variables limnológicas de ríos y arroyos fueguinos. Ecol Austr 28(3):593–605
Henn J, Anderson C, Pastur GM (2016) Landscape-level impact and habitat factors associated with invasive beaver distribution in Tierra del Fuego. Biol Invasions 18(6):1679–1688
Inbar M, Ostera H, Parica C, Remesal M, Salami F (1995) Environmental assessment of 1991 Hudson volcano eruption ashfall effects on southern Patagonia region Argentina. Environ Geol 25(2):119–125
Iribarren Anacona P, Mackintosh A, Norton K (2015) Reconstruction of a glacial lake outburst flood (GLOF) in the Engaño Valley, Chilean Patagonia: lessons for GLOF risk management. Sci Total Environ 527–528:1–11
Iturraspe R, Fank L, Urciuolo A, Lofiego R (2021) Efectos del crecimiento urbano sobre humedales costero-continentales del ambiente semiárido de Tierra del Fuego, Argentina. Inv Geogr 75:139–165 (in Spanish)
Iturraspe R, Strelin J (2002) Dinámica de procesos y geoformas vinculadas al retroceso del glaciar O'Higgins, Campo de Hielo Patagónico Sur, Chile. An Inst Patagonia 30:13–24 (in Spanish)
IUCN, International Union for the Conservation of Nature (2000) Guidelines for the prevention of biodiversity loss caused by Alien invasive species. https://portals.iucn.org/library/efiles/documents/Rep-2000-052.pdf. Accessed 27 May 2021
Jacquet J, McCoy S, McGrath D, Nimick D, Fahey M (2017) Hydrologic and geomorphic changes resulting from episodic glacial lake outburst floods: Rio Colonia, Patagonia, Chile. Geoph Res Lett 448:54–864
Juncos R, Arcagni M, Rizzo A, Campbell L, Arribére M (2016) Natural origin arsenic in aquatic organisms from a deep oligotrophic lake under the influence of volcanic eruptions. Chemosphere 144:2277–2289

Lallement M, Macchi PJ, Vigliano P, Suarez S (2016) Rising from the ashes: changes in salmonid fish assemblages after 30 months of the Puyehue-Cordon Caulle volcanic eruption. Sci Total Environ 541:1041–1051

Lamela P, Navoni J, Pérez R, Pérez C, Vodopivez C, Curtosi A, Bongiovanni G (2019) Analysis of occurrence, bioaccumulation and molecular targets of arsenic and other selected volcanic elements in Argentinean Patagonia and Antarctic ecosystems. Sci Total Environ 681:379–391

León C, Gabriel M, Rodríguez C, Iturraspe R (2021) Peatlands of Southern South America: a review. Mires Peat 27:1–29

Lin Q, Yu S (2018) Losses of natural coastal wetlands by land conversion and ecological degradation in the urbanizing Chinese coast. Sci Reports 8(1):1–10

Lizarralde M, Deferreri G, Alvarez S, Escobar J (1996) Effects of beaver (*Castor canadensis*) on the nutrient dynamics of the Southern Beech forest of Tierra del Fuego (Argentina). Ecol Austr 6(02):101–105

Lofiego R, Noir G, Urciuolo A, Iturraspe R (2009) Evaluación hidro-ambiental del estuario del río Grande de Tierra del Fuego. Actas 22 Congreso Nacional del Agua, Trelew, Argentina, pp 124–133 (in Spanish)

Macchi P, Cussac V, Alonso M, Denegri M (1999) Predation relationships between introduced salmonids and the native fish fauna in lakes and reservoirs in northern Patagonia. Ecol Freshwater Fish 8(4):227–236

Macchi P, Loewy R, Lares B (2018) The impact of pesticides on the macroinvertebrate community in the water channels of the Río Negro-Neuquén Valley North Patagonia. Environ Sci Pollut Res 25(11):10668–10678

Major J, Lara L (2013) Overview of Chaitén Volcano, Chile, and its 2008–2009 eruption. Andean Geo 40(2):196–215

Masiokas M, Luckman B, Villalba R, Ripalta A, Rabassa J (2010) Little Ice Age fluctuations of Glaciar Río Manso in the north Patagonian Andes of Argentina. Quat Res 73(1):96–106

Masiokas M, Villalba R, Luckman B, Lascano M, Delgado S, Stepanek P (2008) 20th-century glacier recession and regional hydroclimatic changes in northwestern Patagonia. Global Planet Change 60(1–2):85–100

Micklin P (2010) The past, present, and future Aral sea. Res Manage 15(3):193–213

Miglioranza K, Gonzalez M, Ondarza P (2013) Assessment of Argentinean Patagonia pollution: PBDEs, OCPs and PCBs in different matrices from the Río Negro basin. Sci Total Environ 452:275–285

Miserendino ML, Archangelsky M, Brand C, Epele L (2012) Environmental changes and macroinvertebrate responses in Patagonian streams (Argentina) to ashfall from the Chaitén Volcano. Sci Total Environ 424:202–212

Miserendino ML, Brand C, Epele L, Di Prinzio C, Omad G, Kustchker K (2018) Biotic diversity of benthic macroinvertebrates at contrasting glacier-fed systems in Patagonia Mountains: the role of environmental heterogeneity facing global warming. Sci Total Environ 622:152–163

Modenutti B, Balseiro E, Elser J, Navarro MB, Cuassolo F (2013) Effect of volcanic eruption on nutrients, light, and phytoplankton in oligotrophic lakes. Limnol Oceanogr 58(4):1165–1175

Molina R, Soto N, Tapia A (2018) Estado actual de la distribución del castor Castor canadensis Kuhl 1820 (Rodentia) en el área continental de la región de Magallanes Chile. An Inst Patagonia 46(3):7–15 (in Spanish)

Monza L, Loewy R, Savini M, Pechen A (2014) Sources and distribution of aliphatic and polyaromatic hydrocarbons in sediments from the Neuquén river, Argentine Patagonia. J Environ Sci Health A 48(4):370–379

Moorman M, Eggleston D, Anderson C, Mansilla A (2009) Implications of beaver *Castor canadensis* and trout introductions on native fish in the Cape Horn biosphere reserve Chile. Trans Amer Fish Soc 138(2):306–313

Moya C, Valdovinos C, Moraga A, Omero F (2009) Patrones de distribución espacial de ensambles de macroinvertebrados bentónicos de un sistema fluvial Andino Patagónico. Rev Chil Hist Nat 82(3):425–442

Mustard J, Fisher T (2005) Land use and hydrology. In: Gutman G, Janetos A, Justice C (eds) Land change science. Springer, Dordrecht, pp 257–276
Naranjo J, Polanco E (2004) The 2000 AD eruption of Copahue volcano, southern Andes. Rev Geol Chile 31(2):279–292
Nardi CF, Fernández D, Vanella F, Chalde T (2019) The expansion of exotic Chinook salmon (Oncorhynchus tshawytscha) in the extreme south of Patagonia: an environmental DNA approach. Biol Invasions 21(4):1415–1425
Ondarza P, Gonzalez M, Fillmann G, Miglioranza K (2012) Increasing levels of persistent organic pollutants in rainbow trout (Oncorhynchus mykiss) following a mega-flooding episode in the Negro river basin, Argentinean Patagonia. Sci Total Environ 419:233–239
O'Neal SL (2008) Lessons to learn from all-out invasion: life history of brown trout (Salmo trutta) in a Patagonian river. Master Thesis, Univ Montana, p 42
Ortiz Sandoval J, Górski K, Sobenes C, González J, Manosalva A, Elgueta A, Habit E (2016) Invasive trout affect trophic ecology of *Galaxias platei* in Patagonian lakes. Hydrobiologia 790(1):201–212
Pascual M, Cussac V, Dyer B, Soto D, Vigliano P, Ortubay S, Macchi P (2007) Freshwater fishes of Patagonia in the 21 century after hundred years of human settlement, species introductions and environmental change. Aquat Ecosyst Health Manage 10(2):212–227
Peña H, Escobar F (1983) Análisis de las crecidas del Río Paine-XII Región. Publ Int EH 83/7. Dirección General de Aguas, Santiago (in Spanish)
Pérez G (2018) La conurbación en torno a la ciudad de Neuquén. Universidad Nacional de La Plata, La Plata (in Spanish), Tesis Doctoral
Pérez T, Mattar C, Fuster R (2018) Decrease in snow cover over the Aysén river catchment in Patagonia Chile. Water 10(5):619
Pérez Catán S, Juarez N, Bubach D (2016) Characterization of freshwater changes in lakes of Nahuel Huapí National Park produced by the 2011 Puyehue-Cordón Caulle eruption. Environ Sci Pollution Res 23(20):20700–20710
Pierson T, Major J, Amigo A, Moreno H (2013) Acute sedimentation response to rainfall following the explosive phase of the 2008–2009 eruption of Chaitén volcano Chile. Bull Volcanol 75(5):1–17
Pietrek A, Fasola L (2014) Origin and history of the beaver introduction in South America. Mastozoo Neotr 21(2):355–359
Primack R (2006) Essentials of conservation biology. Sinauer Assoc, Sunderland
Quintanilla Pérez V (2008) Estado de recuperación del bosque nativo en una cuenca nordpatagónica de Chile, perturbada por grandes fuegos acaecidos 50 años atrás (44º–45ºS). Rev Geog N Grande 39:73–92 (in Spanish)
Reid B, Hernández K, Frangópulos M, Bauer G, Lorca M, Kilroy C, Spaulding S (2012) The invasion of the freshwater diatom *Didymosphenia geminata* in Patagonia: prospects, strategies, and implications for biosecurity of invasive microorganisms in continental waters. Conserv Lett 5(6):432–440
Reid B, Torres R (2014) *Didymosphenia geminata* invasion in South America: ecosystem impacts and potential biogeochemical state change in Patagonian rivers. Acta Oecol 54:101–109
Reissig M, Trochine C, Queimaliños C, Balseiro E, Modenutti B (2006) Impact of fish introduction on planktonic food webs in lakes of the Patagonian Plateau. Biol Conserv 132(4):437–447
Rivera P, Gebauer M (1989) Diatomeas chilenas en las Colecciones de Boyer, Cleve & Moeller, Schulze y Smith, depositadas en la Academia de Ciencias Naturales de Filadelfia, Estados Unidos. Gayana Bot 46:89–116 (in Spanish)
Rojas Quezada C (2019) Humedales Urbanos en Chile: El impacto en políticas públicas y en el desarrollo sostenible. In: Acevedo M (ed) Humedales Urbanos, historia de una ley pionera y ciudadana de protección ambiental. Ed Univ Valparaiso, Chile (in Spanish), pp 44–52
Romero JE, Morgavi D, Arzilli F, Daga R, Caselli A (2016) Eruption dynamics of the 22–23 April 2015 Calbuco Volcano (Southern Chile): analyses of tephra fall deposits. J Volc Geoth Res 317:15–29

Rovira A, Rojas C, Díez S (2013) Efectos de una erupción volcánica Andina: el caso del Cordón Caulle, Sur de chile (2011). In: Borsdorf A (ed) Forschen im Gebirge, investigating the mountains—Innsbruck. Austrian Academy of Sciences Press, Vienna, pp 288–304

Sastre V, Bauer G, Atesterán M (2010) Monitoreo de *Didymosphenia geminata*. Resultados muestreo 31 de Agosto, 2 y 7 de Septiembre de 2010. Informe Técnico N°5. Ministerio de Ambiente, Chubut. UNPSJB, Comodoro Rivadavia, Argentina (in Spanish)

Scordo F, Seitz C, Zilio M (2017) Evolución de los Recursos Hídricos en el "Bajo de Sarmiento" (Patagonia Extra Andina): Impactos Naturales y Antrópicos. An Inst Geosci 40:106–117 (in Spanish)

Sielfeld W, Venegas C (1980) Poblamiento e impacto ambiental de *Castor canadensis* en Isla Navarino, Chile. An Inst Pat 11:247–257 (in Spanish)

Soto D, Arismendi I, González J, Sanzana J, Jara F, Jara C, Guzmán E, Lara A (2006) Sur de Chile, país de truchas y salmones: patrones de invasión y amenazas para las especies nativas. Rev Chil Hist Nat 79(1):97–117 (in Spanish)

Soto Cárdenas C, Diéguez M, Queimaliños C, Rizzo A, Fajon V, Kotnik J, Horvat M, Ribeiro S (2018) Mercury in a stream-lake network of Andean Patagonia. Chemosphere 197:262–270

Ulloa H, Iroumé A, Picco L, Mohr C, Mazzorana B, Lenzi M, Mao L (2016) Spatial analysis of the impacts of the Chaitén volcano eruption (Chile) in three fluvial systems. J South Am Earth Sci 69:213–225

Vila I, Fuentes L, Saavedra M (1999) Ictiofauna en los sistemas límnicos de la Isla Grande, Tierra del Fuego Chile. Rev Chi Hist Nat 72(2):273–284 (in Spanish)

Waicheim A, Blasetti G, Cordero P, Rauque C, Viozzi G (2014) Macroparasites of the invasive fish, Cyprinus carpio, in Patagonia Argentina. Compar Parasit 81(2):270–275

Zingaretti V (2019) Evolución geomorfológica del río Blanco Este después de erupciones del Volcán Calbuco (sur Chile). Univ Austral Chile, Valdivia, Tesis Magister (in Spanish)

Glossary

Alunite a hydroxysulfate mineral with aluminum and potassium as main cations, usually found in hydrothermal systems.

Aquitard geological formation of a rather semipervious nature that transmits water at slower rates than an aquifer.

Aquiclude hydrogeologic unit which is porous and capable of storing water, but it does not transmit it at sufficient rates to furnish an appreciable supply for a well or spring.

Authigenic minerals minerals which originate from the diagenetic alteration of sediments that are already deposited (secondary minerals) or by chemical reactions within the interstitial water of sediments.

Autochthonous minerals minerals whose inorganic components originate within the water column, either by inorganic or biologically induced chemical precipitation.

Basaluminite a hydroxysulfate mineral with aluminum as the main cation, usually found in low pH systems related to rock and mine acid drainage or waters associated with active volcanic systems.

Benthic macroinvertebrate community benthic (meaning "bottom-dwelling") macroinvertebrates are small aquatic animals (>1 mm). They include, among others, aquatic insect larvae, snails, worms, flatworms, and crustaceans. Benthic macroinvertebrates are often found attached to rocks, vegetation, logs and sticks or burrowed into the sand and sediments at the bottom of aquatic environments such as streams, rivers lakes and wetlands.

Bioindicator any species or group of species (animals and plants) whose function may reveal the qualitative state of the environment.

Biotic monitoring patagonian stream (BMPS) biotic index based on macroinvertebrate communities (Miserendino and Pizzolón 1999). It is obtained from a table of 95 families of macroinvertebrates present in Patagonia which have different degrees of pollution sensitivity (scores 1–10). The total BMPS score ranges from 0 to >150. The criteria of water quality are discriminated as follows: > 150 very

A. I. Torres and V. A. Campodonico (eds.), *Environmental Assessment of Patagonia's Water Resources*, Environmental Earth Sciences,
https://doi.org/10.1007/978-3-030-89676-8

clean waters, 101–150: unpolluted waters, 61–100 probably incipient pollution or others kinds of perturbations, 36–60: probably polluted waters, 16–35 polluted waters, and <15: strongly polluted waters.

BOD_5 5-day biochemical oxygen demand. It is a water quality parameter that measures the quantity of biodegradable organic matter contained in water and is evaluated by measuring the oxygen consumed by the microorganisms involved in natural purification mechanisms.

Brackish water with a salt content higher than that of fresh water, with total dissolved solid contents between 1 and 10 g L^{-1}.

Caldera big size depression formed after a volcanic eruption. The magma chamber consists of large volumes of magma that can be withdrawn or erupted, after this magma removal the structural support above the chamber can collapse forming the caldera. Its size depends on the amount of magma that erupted and the volcanic eruption, and it may range from 2 to 50 km across.

Cassiterite an oxide mineral with tin as the main cation (SnO_2).

Chemical facies dominant chemical composition of water considering the major anions and cations.

CIA Chemical Index of Alteration, to evaluate the intensity of chemical weathering. It is defined as follows, where CaO* represents the CaO of the silicate fraction.$CIA = 100 \times [Al_2O_3/(Al_2O_3 + CaO* + Na_2O + K_2O)]$.

Clear waters streams or rivers waters with low suspended sediments contents.

Colloid a homogeneous system of molecules or particles disperse through a medium. In water environments they usually serve as transport vectors of diverse contaminants. Elements, complexes or molecules can be easily adsorbed onto colloids.

Deltaic pertaining to or like a delta. Deltaic environments are gradational to both fluvial and coastal environments.

Detrital minerals minerals which are introduced into the environment through surface currents, erosion from the coast, sheet flooding, mass movement, or wind activity.

Domes circular mounds that originate above the volcanic duct by the slow emplacement of viscous lava in a sector of a volcano.

Downstream in the direction in which a stream or river flows.

El niño-southern oscillation (ENSO) is a periodic fluctuation in sea surface temperature and the air pressure of the overlying atmosphere across the equatorial Pacific Ocean.

Endorheic basin a basin draining to some depression or pond within its area, from which water is lost only by evaporation. A basin without a surface outlet.

EPT richness the EPTr Index (Klemm et al. 1990) is a measure to assess water quality based on the richness of Ephemeroptera, Plecoptera and Trichoptera (aquatic invertebrates). It is widely used in Patagonia, and the water quality criteria are as follows: >10 without impact, 6–10 slightly impacted, 2–5: impacted and 0–1: strongly impacted.

Eutrophication when an aquatic ecosystem becomes overly enriched with minerals and nutrients (mostly forms of nitrogen or phosphorus), which induce

excessive growth of algae. The process may also result in oxygen depletion. Although the phenomenon can occur by natural causes over a long period of time, human activities can accelerate eutrophication by introducing extra nutrients through treatment plants, fertilizers, farms, untreated sewage, etc.

Evaporitic deposits minerals chemically precipitated from standing bodies of seawater (marine evaporites) or lake-waters (nonmarine evaporites) as a result of evaporative processes.

Exorheic basin fluvial system developed in a basin with sea connection.

Frequency (f) is defined as the number of cycles per unit of time: $f = 1/T$, where the period T is the time taken to complete one cycle of an oscillation.

Fumarole component of a hydrothermal system that corresponds to a vent which emits steam and gases.

Geoelectric cuts diagrams that show the different resistivity values of a vertical section in depth.

Geophysical survey any subsurface investigation technique that applies geophysical methods.

Geothermal system natural system characterized by having a heat source that leads to the mobilization of water through convective cells.

Geothermal water groundwater which has a temperature appreciably higher than that of the local average annual air temperature.

Glacieret ice or permanent snow mass with no evidence of displacement.

Glaciofluvial of glacial and fluvial origin.

Habitat condition index (HA) evaluation of habitat quality is critical to any assessment of ecological integrity and should be performed at each site at the time of the biological sampling. The "habitat condition index" incorporates all aspects of physical and chemical constituents along with the biotic interactions. This method ranks 10 river channel features (e.g. epifaunal substrate availability, embeddedness, sediment deposition, frequency of riffles, bank stability, etc.) from 0 to 20. A score of 200 points indicates that the river is natural and pristine and in its best possible condition (optimal: range: 150–200). Other judgement classes are defined as follows: sub-optimal (range: 100–150), marginal (range: 50–100), and poor (0–50).

Headwater it is the source of a stream.

Hydraulic conductivity a material property that describes the rate at which water can flow through pore spaces or fractures.

Hydrothermal manifestations/Geothermal manifestations/Thermal springs aqueous solutions of high temperature heated naturally under the Earth.

Hydrothermal system groundwater system which receives temperature and energy from a deep magmatic heat. Usually are evidenced in surface as fumaroles, mud and bubbling pools or geysers and can be used for geothermal energy.

Icecap unconfined, dome-shaped glacial ice mass that flows in all directions.

Internal load term used to describe P movement and recycling between lake sediments and the water column.

Jarosite a hydroxysulfate mineral with iron and potassium as main cations, usually found in hydrothermal systems.

Jökulhlaup is an Icelandic term. It refers originally to outburst floods, which are triggered by geothermal heating and, occasionally, by a volcanic subglacial eruption. It is now used to describe any large and abrupt release of water from a subglacial or proglacial lake.

Jurbanite a hydroxysulfate mineral with aluminum as the main cation. It usually occurs as a secondary mineral in systems related to rock and mine drainage.

Lithological relative to lithology.

Macrophytes aquatic plants growing in or near water. They may be either emergent (i.e. with upright portions above the water surface), submerged or floating.

Magmatic chamber large and deep subterranean reservoir of partially or total molten fluid located in the Earth crust, mostly stored beneath a volcano. The molten rock or magma is less dense than the surrounding rock, thus the fluid tends to ascend to the surface, developing a volcano.

MEI, v.1 the Multivariate ENSO Index (version 1) combines both, oceanic and atmospheric variables, facilitating ENSO assessment with a single index. Version 1 includes data recorded between 1950 and 2018.

Meltwater water derived from the natural melting of snow.

Meteoric origin the word "meteoric" (as in the sense of direct atmospheric origin) is used here to refer to rain or snow water.

Milky waters waters with a high load of suspended sediments, usually by glacier meltwater.

Molybdenite a sulfur mineral with molybdenum as the main cation.

Monomictic water body with a single period of thermal stratification during the summer.

Phreatic eruption steam-driven explosion that occurs when water beneath the surface is heated by magma or hot rocks. This intense heat may cause water to boil and flash to steam generating an explosion which involves steam, water, ash and rocks.

Phreatomagmatic eruption explosive eruption that involves magma and water which leads to concurrent ejection of steam and pyroclastic fragments. They usually tend to be explosive events.

Phytoplankton autotrophic (self-feeding) components of the plankton community, with photosynthetic capacity. Key part of ocean and freshwater ecosystems.

P-labile phosphorus bound to sediment, which is released more quickly into the water column and is readily available for algal growth.

Planktonic algae microscopic algae that live freely floating in the water column.

Pond an area filled with water, either natural or artificial, generally smaller than a lake. It may arise naturally in floodplains as part of a river system (connected), or be a somewhat an isolated depression.

Proglacial lake lake formed by the damming of a moraine during the retreat of a melting glacier, or by meltwater accumulated in an isostatic depression of the crust around the ice.

Pyrite oxidation redox chemical reaction affecting pyrite mineral, that produces sulfuric acid according to the following equation: $4FeS_{2\ (s)} + 15O_{2(aq)+}14H_2O_{(1)} \leftrightarrow 8SO^{2-}_{4\ (aq)} + 16H^{+}_{(aq)} + 3Fe(OH)_{3\ (s)}$.

Patagonian riparian forest quality index (QBRp) this index combines information from four additive metrics: total cover (proportion of the riparian area covered by trees and shrubs), structure (proportion of riparian vegetation composed of trees and shrubs separately), complexity and naturalness of vegetation (number of trees or shrub species and absence of introduced species, and other human impacts in riparian vegetation), and the degree of channel naturalness (e.g. bank modifications, dredging, etc.). It also takes into account differences in the geomorphology of the river from its headwaters to the lower reaches. The total QBRp score ranges from 0 points (extreme degradation) to 100 points (excellent quality, natural riparian forest).

Rare earth elements (REE) a group of seventeen chemical elements that occur together in the periodic table, represented by lanthanides (lanthanum–lutetium series), plus scandium and yttrium. They have many similar chemical properties.

Resistivity the electrical property of a material that determines the resistance of a piece of given dimensions. Is the reciprocal of conductivity.

Riparian buffer zone (also stream buffer) vegetated area (a "buffer strip") near a stream or water body, usually forested, which helps shade and partially protect the watercourse or waterbody from the impact of adjacent land uses.

Riparian integrity a property of riparian corridors, that is a site's relative ability to provide all the necessary ecological functions including: retaining sediment and nutrients, flood attenuation, bank stabilization and regulating stream temperature.

Schwertmannite a hydroxysulfate mineral with iron as the main cation, usually found in low pH systems related to rock and mine acid drainage or waters associated with active volcanic systems.

Seasonal Kendall test statistical non-parametric tool to detect monotone trends in time series.

Silicate hydrolysis chemical reaction or breaking down of silicates to form new minerals and dissolved products.

Soluble reactive phosphorous phosphorus fraction bioavailable for algae growth.

Springs groundwater discharge to the surface in small areas.

Stratovolcano a volcano with conical shape formed by lava and ejected materials during different volcanic events through thousands of years. They are usually characterized by summit craters and periodic intervals of explosive and effusive eruptions.

Transmissivity aquifer ability to transmit water throughout its entire saturated thickness.

Trophic gradient gradient productivity of aquatic ecosystems.

Trophic state productivity of aquatic ecosystems.

Unconfined aquifer aquifer whose upper water surface (water table) is at atmospheric pressure, and thus is able to rise and fall.

Unsaturated zone is the portion of the subsurface above the groundwater table. The soil and rock in this zone contains air as well as water in its pores.

Upstream river or stream sector that is close to the river basin headwaters.

Water table upper surface of the saturated zone.

Watershed fluvial basin of moderate dimensions.

Weathering set of physical, chemical and biological processes that breaks down the internal structure of minerals, modifying the chemical composition of the original material. Weathering occurs in situ, forming mineral species thermodynamically stable in Earth surface conditions.

Weathering-limited regime denudation regime limited by weathering. The material is removed at a faster rate than it is generated. Incipient weathering profiles and little or no development of soils are characteristic.

Wetlands *(mallines)* areas where water covers the soil, or is present either at or near the surface of the soil all year or for varying periods of time during the year, including during the growing season. Water saturation (hydrology) largely determines how the soil develops and the types of plant and animal communities living in and on the soil. Wetlands in Patagonia are locally named *mallines*, an aboriginal (Mapuche) word that means swampy area or lowland area where water accumulates.